Filmwise condensation on a horizontal tube in the presence of forced convection and non-condensing gas

Lee, Wah Cheng

FILMWISE CONDENSATION ON A HORIZONTAL TUBE IN THE PRESENCE OF FORCED CONVECTION AND NON-CONDENSING GAS

by

Wah Cheng LEE

A thesis submitted for the Degree of
Doctor of Philosophy
to the University of London

Department of Mechanical Engineering
Queen Mary College
University of London

February 1982

FILMWISE CONDENSATION ON A HORIZONTAL TUBE IN THE PRESENCE OF FORCED CONVECTION AND NON-CONDENSING GAS

by

Wah Cheng LEE

ABSTRACT

Accurate and repeatable heat-transfer data have been obtained for filmwise condensation from pure vapours (steam and Refrigerant 113) and vapour-gas (steam-air, steam-hydrogen, Refrigerant 113-air and Refrigerant 113-hydrogen) mixtures flowing vertically downward over single horizontal tubes. The tube surface could be viewed to ensure that the filmwise mode of condensation prevailed throughout all tests. Two copper tubes having diameters 12.5 mm and 25.25 mm were used. Surface temperatures at four positions were obtained from thermocouples embedded in the tube wall. The heat flux was obtained from coolant measurements which were checked against values obtained by condensate collection. The vapour mass flow rate was obtained from the electrical power input to the boiler. (The mass flow rate determination incorporated a correction for relatively small 'thermal losses' to the environment which were established by preliminary measurements in which all the vapour supplied to the test section was condensed and collected. Non-condensing gases could be supplied continuously via variable-aperture float-type flowmeters to the boiler. The working length ($\simeq$ 110 mm) of the condenser tube was located centrally in the cylindrical test section (152.4 mm). The vapour Reynolds number (based on the test section diameter) was generally greater than 2000. The mean vapour approach velocity over the working length was determined on the basis of a 'seventh power profile' in conjunction with the measured flow rate. The approximate ranges of the variables used were:- pressure (4 - 124 kPa), heat flux (12 - 466 kW/m^2), vapour velocity (0.3 - 26 m/s), gas mole (mass) fraction (0.1 % (0.02 %) - 35 % (32 %)). The vapour-gas combinations were chosen to give a wide range of Schmidt number (about 0.05 - 0.5).

For pure vapours, the results are in overall agreement with earlier data (mostly steam) at moderate approach velocities. While discrepancies exist at higher velocities, both the present and earlier results show satisfactory agreement with theory at low and moderate velocities. The vapour-gas data are in good agreement with the limited earlier measurements (steam-air only) and with theory. In particular, the theoretically predicted Schmidt number dependence was clearly established.

ACKNOWLEDGEMENTS

The author is deeply indebted to Dr. J.W. Rose, who initiated the project, for his guidance, supervision and encouragement during the course of this work.

Special thanks are due to Mr. C.A. Lodge and the technician staff, in particular Mr. J. Whiter, for their advice and help in modifying the apparatus. The author is also grateful to Mr. E. Ager and the secretarial staff for their assistance and support during the course of this work.

The author would also like to thank Dr. M.R. Nightingale for computing assistance and to colleagues and friends for their help and encouragement.

Finally, the author wishes to express sincere gratitude to his parents, brothers and sisters for their support and inspiration throughout his education and to his wife and sons for their love, patience and understanding.

LIST OF CONTENTS

LIST OF SYMBOLS

A	a function of the angle measured from the forward stagnation point and defined in equations 2.27 and 2.28
A_j (j=1 to 11)	constants defined in equation E.2.4
A_{ts}	cross-sectional area of the test section
A_{tt}	exposed area of the test condenser tube
a	constant defined in equation 2.51
a_1	constant defined in equation 2.41
B	$(W_\infty - W_i)/W_i$
B_m	$\omega - 1$
B_1	second virial coefficient for steam
B_2	$2P_s/RT$
b	constant defined in equation 2.51
b_1	constant defined in equation 2.41
C	function defined in eqn. 2.19b; constant defined in eqn. 2.54
C_x	constant defined in equation 2.19a
c	constant defined in equation 2.51
c_P	isobaric specific heat capacity
c_{Pcw}	isobaric specific heat capacity of cooling water
c_{Pf}	isobaric specific heat capacity of saturated liquid
c_{PL}	isobaric specific heat capacity of condensate
c_{Pn}	isobaric specific heat capacity of non-condensing gas
c_{Pv}	isobaric specific heat capacity of vapour or vapour-gas mixture
c_t	temperature correction factor defined in equation 4.1
D	binary diffusion coefficient
Dr	dimensionless number, $\rho_L \tau_F h_{fg} L_P^2/(\mu_L k_L \Delta T)$

d_i	inside diameter of test condenser tube
d_{ic}	inside diameter of test section
d_o	outside diameter of test condenser tube
d_{tc}	test condenser tube wall thermocouples location diameter
E	$(M_n - M_v)/(M_n - W_\infty(M_n - M_v))$
e	thermo-emf
e_j $(j = 1,2)$	thermo-emfs recorded by calibrated thermocouples
Fr	Froude number, U_∞/gd_o
Fr_L	Froude number, U_∞/gL_p
Fr_x	Froude number, U_∞/gx
Ga	Galileo number, $gd_o^3 / \nu_L{}^2$
G_w	dimensionless number defined in equation 2.6
G_w''	dimensionless number defined in equation 2.6
g	local gravitational acceleration
g^*	$g\ (1 - \rho_V/\rho_L)$
$g(B)$	function of B defined in equations 2.49 and 2.50
g_m	mass-transfer conductance defined in equation 2.56
g_m^*	value of g_m for zero mass transfer
H	phase change number, $c_{PL}\Delta T/h_{fg}$
H_c	phase change number, $c_{PL}\Delta T_c/h_{fg}$
h	difference in heights of the mercury columns of the manometer
h_{fg}	specific enthalpy of evaporation
h_{fg}'	modified specific enthalpy of evaporation, see equations 2.19
h_{f1}	specific enthalpy of condensate return at entry to the boilers

h_{f2}	specific enthalpy of condensate on the walls of the calming and test sections
h_{g2}	specific enthalpy of vapour at T_∞
h_{n0}	specific enthalpy of non-condensing gas at entry to the boiler
h_{n2}	specific enthalpy of non-condensing gas at T_∞
I_j(j=1 to 6)	electrical currents flowing through the standard resistors R_j(j=1 to 6)
K	dimensionless number defined in equation 2.24
k_L	thermal conductivity of condensate
k_t	thermal conductivity of copper
k_v	thermal conductivity of vapour or vapour-gas mixture
k_1	constant defined in equation 4.1
L	exposed length of the test condenser tube
L_p	height of plate
lr	air in-leakage rate, see Table 5.2
$\tilde{M}$	dimensionless number, $\dot{Q}'' d_o/\mu_L h_{fg}$
M_n	relative molecular mass of non-condensing gas
M_v	relative molecular mass of condensing vapour
M_1	relative molecular mass of constituent 1
M_2	relative molecular mass of constituent 2
$\dot{m}''$	condensation flux
$\dot{m}_A$	condensation rate obtained during thermal loss determination tests
$\dot{m}_B$	condensation rate obtained during thermal loss determination tests
$\dot{m}_a$	air in-leakage rate, see Table 5.2
$\dot{m}_{cc}$	collected condensate, see Appendix C

$\dot{m}_{cw}$	mass flow rate of cooling water
$\dot{m}_{c1}$	condensation rate obtained from condensate collection measurements
$\dot{m}_{c2}$	condensation rate obtained from coolant measurements
$\dot{m}_{n}$	mass flow rate of non-condensing gas
$\dot{m}_{v}$	mass flow rate of vapour or vapour-gas mixture
$\dot{m}''_{x}$	local condensation flux
N	dimensionless number, $c_{PL}\Delta T/(Pr_L\, h_{fg})$
n	constant defined in equation 2.18
Nu	average Nusselt number, $\dot{Q}''\, d_o/k_L\, \Delta T$
Nu_{Nu}	average Nusselt number based on the simple Nusselt theory, $\dot{Q}''_{Nu}\, d_o/k_L\, \Delta T$
Nu_x	local Nusselt number, $\dot{Q}''_x\, x/k_L\, \Delta T_x$
P	pressure
P_{at}	atmospheric pressure
P_c	critical pressure
$P_{n\infty}$	bulk partial pressure of non-condensing gas
P_o	= 101325 Pa
P_s	saturation pressure
P_{sti}	saturated steam pressure at the vapour-condensate interface
$P_{st\infty}$	bulk saturated steam pressure
P_∞	bulk pressure of vapour or vapour-gas mixture
Pr_L	Prandtl number of condensate, $c_{PL}\, \mu_L/k_L$
Pr_v	Prandtl number of vapour or vapour-gas mixture, $c_{Pv}\, \mu_v/k_v$
$\dot{Q}''$	heat-transfer flux
$\dot{Q}_a$	heat-transfer rate calculated from condensate collection measurements
$\dot{Q}_b$	heat-transfer rate calculated from coolant measurements

$\dot{Q}''_{calc}$	calculated heat flux
$\dot{Q}''_{calc1}$	calculated heat flux using equation 7.3, see Appendix F
$\dot{Q}''_{calc2}$	calculated heat flux using equation 7.13, see Appendix F
$\dot{Q}_{cw}$	heat-transfer to cooling water
$\dot{Q}''_{gas}$	heat-transfer flux in the presence of non-condensing gas
$\dot{Q}_{h}$	heater input power
$\dot{Q}_{loss1}$	thermal loss defined in equation 6.8
$\dot{Q}^{*}_{loss1}$	thermal loss defined in equation 6.6
$\dot{Q}_{loss2}$	thermal loss defined in equation 6.9
$\dot{Q}^{*}_{loss2}$	thermal loss defined in equation 6.7
$\dot{Q}''_{nogas}$	heat-transfer flux for pure vapour case based on same conditions as $\dot{Q}''_{gas}$
$\dot{Q}''_{Nu}$	heat-transfer flux based on the simple Nusselt theory
$\dot{Q}''_{obs}$	observed heat flux
$\dot{Q}''_{x}$	local heat-transfer flux
R	$\rho\mu$ - ratio, $(\rho_L\mu_L/\rho_V\mu_V)^{\frac{1}{2}}$; specific ideal-gas constant
R_j(j=1 to 6)	resistance of the standard resistors, defined in equation 6.5
R_n	specific ideal-gas constant of non-condensing gas
R_{st}	specific ideal-gas constant of steam
R_v	specific ideal-gas constant of vapour
r	radius
r_{tc}	test condenser tube wall thermocouples location radius
r_1	$1 / (Pr_L \cdot (h_{fg}/(c_{PL}\,\Delta T) + 0.354))$
Re_{TP}	two-phase Reynolds number, $U_\infty\, d_o/\nu_L$
$Re_{TP,x}$	local two-phase Reynolds number, $U_\infty x/\nu_L$
Re_v	Reynolds number of vapour or vapour-gas mixture, $U_\infty\, d_o/\nu_v$

$Re_{v,x}$	local Reynolds number of vapour or vapour-gas mixture, $U_\infty x/\nu_v$
S	dimensionless number, $\rho_L g h_{fg} L_P^3/(4\mu_L k_L \Delta T)$
Sc	Schmidt number, ν_v/D
Sh	Sherwood number, $\dot{m}'' d_o/(\rho_v D (1 - \omega))$
Sh_x	local Sherwood number, $\dot{m}''_x d_o/(\rho_v D (1 - \omega))$
T	thermodynamic temperature
T_{at}	ambient temperature
T^*_{at}	mean ambient temperature during thermal loss determination tests
T_c	critical temperature
T_{calc}	thermodynamic temperature calculated using equation B.1 for $e = (e_1 + e_2)/2$
T_{cw}	mean coolant temperature, $(T_{in} + T_{out})/2$
T_i	temperature at vapour-condensate interface, ($= T_\infty$ for pure vapour)
T_{in}	inlet temperature of cooling water
T_o	$= 288.15$ K
T_{obs}	thermodynamic temperature recorded by resistance thermometer during thermocouple calibration
T_{out}	outlet temperature of cooling water
T_r	reference temperature defined in equations 2.18a and 7.5
$T_{tc,j}$ (j=1, 4)	temperatures measured by the test condenser tube wall thermocouples
T_w	mean condensing-side wall surface temperature
$T_{wo,j}$ (j=1, 4)	local test condenser tube wall outside temperature
T_0	temperature of non-condensing gas at entry to the boiler
T_1	temperature of the condensate return at entry to the boiler

T_∞	bulk temperature of vapour or vapour-gas mixture
T_∞^*	mean vapour temperature during thermal loss determination tests
t	Celsius temperature, $= T - 273.15$
U	velocity, x-direction velocity in vapour boundary layer
$\bar{U}$	mean velocity of vapour or vapour-gas mixture over the whole test section
U_{cw}	mean cooling water velocity
$U_{L/2}$	velocity of vapour or vapour-gas mixture at $r = L/2$
U_o	velocity of vapour or vapour-gas mixture at $r = 0$
U_r	velocity of vapour or vapour-gas mixture at radius r
U_ϕ	local x-direction velocity
U_∞	bulk velocity of vapour or vapour-gas mixture
u_δ	x-direction velocity at the vapour-condensate interface
$\dot{V}$	volume flow rate
$\dot{V}_{ind}$	volume flow rate indicated by the gas flow meters
$\dot{V}_{i,c}$	volume flow rate indicated by the coolant flow meters in percent of maximum flow rate
V_j (j=1 to 6)	potential drop across the electric immersion heaters
V_{rj} (j=1 to 6)	potential drop across the standard resistors
v	y-direction velocity in the vapour boundary layer
v_f	specific volume of saturated liquid
v_g	specific volume of saturated vapour
v_o	y- direction velocity at $y = 0$
v_v	specific volume of vapour or vapour-gas mixture
W	mass fraction of non-condensing gas
$\tilde{W}$	mole fraction of non-condensing gas
W_{air}	air mass fraction
$\tilde{W}_{air}$	air mole fraction

W_∞	bulk mass fraction of non-condensing gas
$\tilde{W}_\infty$	bulk mole fraction of non-condensing gas
$W_{\infty 1}$	bulk mass fraction of non-condensing gas calculated from mass flow rate measurements
$\tilde{W}_{\infty 1}$	bulk mole fraction of non-condensing gas corresponding to $W_{\infty 1}$
$W_{\infty 2}$	bulk mass fraction of non-condensing gas calculated from the pressure and temperature measurements
$\tilde{W}_{\infty 2}$	bulk mole fraction of non-condensing gas corresponding to $W_{\infty 2}$
X	dimensionless number defined in equation 2.37
X_1	function of temperature defined in equation F.2.6
X_2	function of temperature defined in equation F.2.6
x	distance measured along the condensing surface
y	distance measured normal to the x-direction
z	$= Sh/\sqrt{Re_v}$
z_x	$= Sh_x/\sqrt{Re_{v,x}}$

<u>Greek symbols</u>

$\bar{\alpha}$	average vapour-side heat-transfer coefficient
$\alpha_{a,x}$	local vapour-side heat-transfer coefficient for the non-isothermal vertical plate theory
$\bar{\alpha}_{nosep}$	average vapour-side heat-transfer coefficient for the case when the vapour boundary layer does not separate
$\bar{\alpha}_{Nu}$	average vapour-side heat-transfer coefficient for the simple Nusselt theory

$\bar{\alpha}_{Nu,\dot{Q}}$	average vapour-side heat-transfer coefficient for the uniform wall heat flux "Nusselt-type" theory
$\bar{\alpha}_{\dot{Q}}$	average vapour-side heat-transfer coefficient for the uniform wall heat flux theory
$\bar{\alpha}_{sep}$	average vapour-side heat-transfer coefficient for the case when the vapour boundary layer separates at $\phi_s = 82^{\circ}$
$\bar{\alpha}_{Shek}$	average vapour-side heat-transfer coefficient according to the theory of Shekriladze and Gomelauri
α_x	local vapour-side heat-transfer coefficient
$\alpha_{x,Nu}$	local vapour-side heat-transfer coefficient according to the simple Nusselt theory
$\alpha_{x,\dot{Q}}$	local vapour-side heat-transfer coefficient for the uniform wall heat flux theory
α_{ϕ}	local vapour-side heat-transfer coefficient
β	suction parameter $((-v_o/U_\infty)\sqrt{Re_v})$; see also equation 2.51
β_x	suction parameter $((-v_o/U_\infty)\sqrt{Re_{v,x}})$; see also equation 2.48
γ	a constant defined in equation 2.18a
ΔP_{st}	far-to-near pressure difference for steam
ΔT	bulk-to-wall temperature difference
$\overline{\Delta T}$	area-averaged bulk-to-wall temperature difference, $\frac{1}{b-a}\int_a^b \Delta T \, dx$
ΔT_c	temperature drop across the condensate film, $(T_i - T_w)$
ΔT_{Nu}	bulk-to-wall temperature difference for the simple Nusselt theory
$\Delta T_{\dot{Q}}$	area-averaged bulk-to-wall temperature difference for the uniform wall heat flux theory
ΔT_x	local bulk-to-wall temperature difference
δ	condensate film thickness
δ_L	condensate film thickness at the bottom of the condensing plate of height L_F

$\delta \dot{Q}''_{obs}$	estimate of error in the observed value of $\dot{Q}''_{obs}$
δU_{∞}	estimate of error in the observed value of U_{∞}
Σv_i	diffusion volume
ϵ_o	interaction energy parameter
ζ	a function of the Schmidt number defined in equation 2.48
κ	Boltzmann's constant
μ	dynamic viscosity
μ_g	dynamic viscosity of saturated vapour
μ_L	dynamic viscosity of condensate
μ_v	dynamic viscosity of vapour or vapour-gas mixture
ν_L	kinematic viscosity of condensate
ν_v	kinematic viscosity of vapour or vapour-gas mixture
ξ_g	ratio of the bulk partial pressure of the non-condensing gas to the total bulk pressure
π_g	$\Delta P_{st}/P_{\infty}$
ρ	density
ρ_{Hg}	density of mercury
ρ_L	density of condensate
ρ_o	density of non-condensing gas at pressure P_o and temperature T_o
ρ_v	density of vapour or vapour-gas mixture
$\sigma(T_w)$	standard deviation of T_w
τ_F	shear stress for single-phase flow over an impermeable surface
τ_i	interfacial shear stress
$\bar{\tau}_i$	dimensionless interfacial shear stress, $\tau_i\sqrt{Re_v}/(\frac{1}{2}\rho_v U_{\infty}^2)$

τ_M	asymptotic shear stress defined in equations 2.5 and 2.29
ϕ	angle measured from the forward stagnation point
ϕ_s	value of ϕ at the separation point
ϕ_0	direction of approach of oncoming vapour measured from the vertical
ϕ_1	function defined in equation E.6.9
ϕ_2	function defined in equation E.6.9
ψ	a multiplication factor for τ_M
ω	ratio of the far-to-near mass fraction of non-condensing gas

Symbols not defined in the list above are defined in the text immediately following the place where they occur.

NOTE ON PRESENTATION

Graphs, diagrams and tables may be found at the end of the relevant Chapter unless they immediately accompany the text.

CHAPTER 1 - INTRODUCTION

Condensation occurs when a vapour comes into contact with a surface at a temperature lower than the saturation temperature. Often the condensing fluid and coolant are seperated by a solid wall. Sometimes, however, the two streams are allowed to come into contact. The latter process is known as direct-contact condensation. For the former case, there are two ideal modes of condensation of which filmwise condensation (i.e. when the condensate forms a continuous film on the solid surface) is the more common. The second mode of condensation is termed dropwise condensation because the condensate collects in growing droplets on the surface.

Condensers are found in many engineering applications, for example, in power generating (both land-based and marine) and distillation plants, and in the chemical and process industries. Owing to the fact that condensers are often large plant components of relatively high capital cost (eg. the price of a steam condenser for a 600 MW power station might typically be around £1 500 000) and the fact that current design methods are often based on empirical correlations, there is a need for accurate and adequate experimental data to ensure that such correlations are reliable. Furthermore, many fundamental heat-transfer problems associated with condensation have yet to be fully understood and reliable data are needed to guide and to validate theoretical models.

Nusselt /1,2 / was the first to present analytical solutions to the problem of laminar filmwise condensation. Nusselt considered the case of a stationary and pure (i.e. only one molecular constituent) vapour.

In many practical problems, however, relatively large vapour velocities occur. Also there may be more than one molecular species, eg. non-condensing gases in greater or lesser amounts will usually be present in the vapour.

The effects of vapour velocity and non-condensing gases are of primary interest in the present work. In recent years, significant theoretical progress has been made (although there remain several important areas of uncertainty) in both of these fields, but few reliable experimental data are available. The primary objective of the present work was to provide such data.

The geometry studied was that of vertical vapour downflow over a single horizontal condenser tube. Even for this relatively straight-forward geometry, considerable theoretical difficulties arise and, the problem cannot, at present, be said to be fully understood. It was felt that, before proceeding to the more complex cases of cross flow and condensation on bundles of tubes, it was necessary to resolve certain outstanding issues relating to the simpler case.

In the present work, strenuous efforts were made to obtain reliable and accurate measurements of the important parameters, i.e. vapour velocity, non-condensing gas content, vapour temperature, tube-wall temperature and heat-transfer rate. Data have been obtained, using two tube diameters, for a range of vapour velocities at atmospheric and sub-atmospheric pressures. Two condensing fluids have been used, both pure and in the presence of each of two non-condensing gases. The implications of these data for theoretical studies of the pure vapour and non-condensing gas problems are discussed.

CHAPTER 2 - LITERATURE SURVEY

2.1 Introduction

It is now known that there are two ideal modes of condensation. If the condensate tends to wet the condensing surface, and thereby forms a continuous liquid film, the process is termed filmwise condensation. If the condensate does not tend to wet the condensing surface, but instead collects in growing droplets on the surface, the process is termed dropwise condensation. In some cases, a mixture of these two ideal modes occur simultaneously.

This survey, and the present investigation are concerned only with filmwise condensation of non-metallic vapours. The interested reader is referred to recently-published comprehensive reviews and bibliographies / 3 - 6 / on dropwise condensation. The work of Stylianou / 3 / is concerned with dropwise condensation of non-metallic vapours while that of Niknejad /4 / examined both filmwise and dropwise condensation of metallic vapours. Wilmshurst / 5 / presented a general bibliography on condensation heat transfer while Tanasawa / 6 / indicated some of the possibilities of industrial applications of dropwise condensation.

Nusselt was the first to present analytical solutions /1,2 / for filmwise condensation of a pure vapour. Nusselt's work, however, does not cover the important effects of :-

i. significant vapour velocity and its associated drag on the condensate film;

ii. presence on non-condensing gas.

Interfacial resistance and vapour superheating (also excluded in the Nusselt model) are, in general, of lesser importance, but the former may be significant when condensing metallic vapours at low pressures, see for example /4, 7 /.

The effects of significant vapour velocity and non-condensing gas constitute the subject matter of this thesis. Previous investigations of the effects of these factors on condensation heat transfer are reviewed in some detail in this chapter.

2.2 Filmwise condensation of pure vapours

2.2.1 Theoretical developments

2.2.1.1 Stationary vapours

Nusselt was the first to present an analytical solution for heat transfer during filmwise condensation of a "stationary" saturated vapour on a plane vertical surface /1 / and on a horizontal tube /2 /. The principal assumptions were :-

i. the condensate film is laminar and its flow governed by gravitational and viscous forces;

ii. heat transfer through the condensate film is by conduction only;

iii. fluid properties are uniform;

iv. the condensing surface temperature is uniform.

The results,

$$\bar{\alpha}_{Nu} = 0.943 \left[\frac{k_L^3\, g\, h_{fg}\, \rho_L\, (\rho_L - \rho_v)}{\mu_L L_P\, \Delta T}\right]^{\frac{1}{4}} \qquad (2.1)$$

for the plane vertical surface, and

$$\bar{\alpha}_{Nu} = 0.728 \left[\frac{k_L^3 \, g \, h_{fg} \, \varrho_L \, (\varrho_L - \varrho_v)}{\mu_L \, d_o \, \Delta T} \right]^{\frac{1}{4}} \tag{2.2}$$

for the horizontal tube, have received substantial experimental confirmation / 8 – 12 / and have been widely used. In equations 2.1 and 2.2,

$\bar{\alpha}_{Nu}$	is the average vapour-side heat-transfer coefficient according to the simple Nusselt theory
k_L	is the thermal conductivity of the condensate
g	is the gravitational acceleration
h_{fg}	is the specific enthalpy of evaporation
ϱ_L	is the density of the condensate
ϱ_v	is the density of the vapour
μ_L	is the dynamic viscosity of the condensate
L_p	is the plate height
ΔT	is the mean vapour-to-wall temperature difference
d_o	is the tube outside diameter

Various workers have since sought to extend and refine the results of Nusselt's pioneering studies. In particular, Bromley /13 / and Rohsenow / 14 / extended the Nusselt analyses to account for subcooling within the liquid (i.e. the mean temperature of the condensate is below that of the condensate surface temperature). The results are in agreement with each other / 15 / and indicated that the value of h_{fg} in equations 2.1 and 2.2 should be replaced by h_{fg} $(1 + 0.68\, c_{PL}\, \Delta T/h_{fg})$, where c_{PL} is the isobaric specific heat capacity of the condensate. However, it should be noted that in most engineering applications, the value of $c_{PL}\Delta T/h_{fg}$ is small (typically less than 0.001) and hence the effects of condensate subcooling can often be neglected.

Sparrow and Gregg /16, 17 / treated the Nusselt problem by considering the condensate film on the basis of the boundary-layer equations. Inertia forces and convection within the condensate film were included. The governing partial differential equations were reduced to ordinary differential equations by means of similarity transformations. It was found that :-

i. for small values of $c_{PL}\Delta T/h_{fg}$, the results are in agreement with / 13 - 15/, fig. 2.1a;

ii. for Prandtl number (Pr_L) greater than unity, inertia effects are negligible for values of $c_{PL}\Delta T/h_{fg}$ less than 2.0, fig. 2.1b;

iii. for low values of Pr_L (i.e. liquid metals), inertia effects can be important when $c_{PL}\Delta T/h_{fg} > 0.001$; the deviation from Nusselt increasing with increasing $c_{PL}\Delta T/h_{fg}$ and with decreasing Pr_L, fig. 2.2a.

It is of interest to note that, in practical situations, the values of $c_{PL}\Delta T/h_{fg}$ for liquid metals /4 / has a maximum value of about 0.01. However, the values of $c_{PL}\Delta T/h_{fg}$ are generally less than 0.001, i.e. in the region where inertia effects are less important.

In the above analyses, it had been assumed that there was zero shear stress‡ on the condensate film at the vapour-condensate interface. Koh et. al. /18/ and Chen /19, 20/ included interfacial shear stress

---

‡The interfacial shear stress considered here results in "hold-up" of the condensate film, since the vapour remote from the condensing surface is "stationary". (Cases where the vapour is undergoing forced convection are considered later).

in their analyses of the Nusselt problem; this necessitated consideration also of the vapour boundary layer. In /18 - 20 /, both the condensate film and the vapour layer were treated on the basis of boundary-layer equations; appropriate conditions at the interface were applied. Koh et. al. adopted similarity transformation along the lines of Sparrow and Gregg /16, 17 / whereas Chen used the integral boundary-layer equations. Their results, which are in satisfactory agreement with each other, are:-

i. for $Pr_L \geqslant 1.0$, the effects of interfacial shear stress on heat transfer are small and steadily decrease with increasing Pr_L, figs. 2.2b and 2.3

ii. for low values of Pr_L (i.e. liquid metals), interfacial shear stress can substantially reduce heat transfer due to "hold-up" of the condensate film, figs. 2.2a and 2.3. As mentioned above, the values of $c_{PL}\Delta T/h_{fg}$ for liquid metals are generally less than 0.001, i.e. in the region where interfacial shear stress effects are less important.

All the preceeding analyses were obtained for the case of an isothermal condensing surface. Fujii et. al. /21 / however, treated the Nusselt problem for the case of uniform wall heat flux and obtained the following results,

$$\bar{\alpha}_{Nu,Q} = 0.943 \left[\frac{k_L^3 \, g \, h_{fg} \, \rho_L^2}{\mu_L \, \Delta T_Q \, L_P} \right]^{\frac{1}{4}} \qquad (2.3)$$

for the plane vertical surface, and

$$\bar{\alpha}_{Nu,Q} = 0.695 \left[\frac{k_L^3 \, g \, h_{fg} \, \rho_L^2}{\mu_L \, \Delta T_Q \, d_o} \right]^{\frac{1}{4}} \qquad (2.4)$$

for the horizontal tube. In equations 2.3 and 2.4,

$\bar{\alpha}_{Nu,Q}$ is the vapour-side heat-transfer coefficient for Nusselt-type uniform wall heat flux theory

ΔT_Q is the area-averaged vapour-to-wall temperature difference (i.e. $\Delta T_Q = \frac{1}{b-a}\int_a^b \Delta T_x \, dx$)

It is of interest to note that the expression for the mean vapour-side heat-transfer coefficient (i.e. the ratio of the heat flux to the area-averaged temperature difference, $\dot{Q}''/\Delta T_Q$) for the vertical plane surface case is the same as that obtained by Nusselt. For the horizontal tube, the value of the mean vapour-side heat-transfer coefficient is about 5 % lower than that given by the simple Nusselt theory.

2.2.1.2. Moving vapours

The above analyses all relate to the case where the vapour is "stationary". In many practical problems, however, relatively large vapour velocities are present. In recent years, various workers have attempted to include the effects of vapour velocity and its associated drag on the condensate film in their analyses. In such cases, it is, in general, necessary to include considerations of the vapour flow (and the relevant conservation equations) as well as that of the condensate film, and to match the mass flux, shear stress, temperature and velocity at the interface.

Horizontal plate

For the case of vapour flow parallel to a horizontal flat plate, Cess /22/ and Koh /23/ presented uniform-property boundary-layer solutions obtained by means of similarity transformations. Cess neglected the inertia and energy convection effects within the condensate film and assumed that the interfacial velocity was negligible in comparison with the free-stream vapour velocity. Koh, on the other hand, did not make these simplifications.

The results of Cess, fig. 2.4a, showed that for low condensation rates, the interfacial shear stress approaches the "frictional" shear stress for single-phase flow over an impermeable plate while at the other extreme, it approaches the asymptotic value, τ_M , given by:-

$$\tau_M = \dot{m}'' \; (U_\infty - u_\delta) \tag{2.5}$$

where $\dot{m}''$ is the condensation flux

U_∞ is the free-stream vapour velocity

u_δ is the streamwise velocity at the vapour-condensate interface.

In the work of Cess, it was assumed that $u_\delta = 0$. It may be noted that the asymptotic shear stress, τ_M , is only slightly lower than the actual value over most of the range of the abscissa (i.e. $\left[\frac{\varrho_L \mu_L}{\varrho_V \mu_V}\right]^{\frac{1}{2}} \cdot \left[\frac{c_{PL}\,\Delta T}{Pr_L\, h_{fg}}\right]$), fig.2.4a. This suggests that the asymptotic shear stress, τ_M, is a satisfactory approximation to the actual value in many cases. The heat-transfer result,

$$\frac{Nu_x}{\sqrt{Re_{TP,x}}} = \left[\frac{G_w''}{4} \cdot \frac{Pr_L}{R\;H}\right]^{\frac{1}{3}} \tag{2.6}$$

where Nu_x is the local Nusselt number, $\dot{Q}_x'' \, x/(k_L \Delta T_x)$

$Re_{TP,x}$ is the local two-phase Reynold's number, $U_\infty x \, \varrho_L/\mu_L$

G_w'' is found from Table 2.1 for given values of G_w, the suction parameter

$R = (\rho_L \mu_L / \rho_V \mu_V)^{\frac{1}{2}}$

$H = c_{PL} \Delta T / h_{fg}$

$\dot{Q}''_x$ is the local heat flux

x is the distance measured along the condensing surface,

is shown in fig. 2.4b. For small and large values of the abscissa, fig. 2.4b, Cess gave the following respective expressions:-

$$\frac{Nu_x}{\sqrt{Re_{TP,x}}} = 0.436\,(Pr_L/RH)^{\frac{1}{3}} \qquad (2.7)$$

$$\frac{Nu_x}{\sqrt{Re_{TP,x}}} = 0.5 \qquad (2.8)$$

Table 2.1 Relation between G''_w and G_w; reproduced from Cess /22 /

Table 1. Values of G''_w [4]

G_w	0	0·1	0·2	0·4	0·6	0·8	1·0	1·5	2	5	10
G''_w	0·332	0·369	0·406	0·483	0·563	0·645	0·729	0·945	1·169	2·590	5·049

Cess further suggested that the neglect of the inertia forces is permissible for $H/Pr_L \ll 30$ and that energy convection within the condensate film has negligible effect on the heat transfer for $H \ll 12$. These results are in general agreement with those for the stationary vapour case /13-17, 19, 20 /.

The results of Koh's analysis are in good agreement with those of Cess for low values of Pr_L (i.e. liquid metals), fig. 2.5a. For $Pr_L \geq 1.0$, the values of the Nusselt number obtained by Koh are significantly higher than those of Cess; the discrepancy becoming larger with increasing Pr_L and with increasing RH/Pr_L, fig. 2.5b. Koh attributed this to the fact that Cess neglected the convection terms in the energy equation for the condensate film. However, as mentioned above, in many engineering applications the value of H/Pr_L is generally less than 0.001 and for this range, Koh's results are in good agreement with those of Cess.

Shekriladze and Gomelauri /24/ greatly simplified the problem by taking, for the interfacial shear stress, the asymptotic value given by equation 2.5. With this simplification, it is no longer necessary to solve the vapour boundary layer. In addition, the simplifications, except $u_\delta = 0$, used by Cess /22 / were also invoked. For the case of uniform wall temperature, the authors obtained the following simple results for the local and average vapour-side heat-transfer coefficients:-

$$\alpha_x = \tfrac{1}{2}\sqrt{\left[\frac{N}{N+1}\right] \cdot \left[\frac{\rho_L\, h_{fg}\, U_\infty\, k_L}{\Delta T\, x}\right]} \tag{2.9}$$

$$\bar{\alpha} = \sqrt{\left[\frac{N}{N+1}\right] \cdot \left[\frac{\rho_L\, h_{fg}\, U_\infty\, k_L}{\Delta T\, L_p}\right]} \tag{2.10}$$

where α_x is the local vapour-side heat-transfer coefficient

$N = c_{PL}\Delta T/(Pr_L h_{fg}) = H/Pr_L$

Equation 2.9 can be rewritten as:-

$$\frac{Nu_x}{\sqrt{Re_{TP,x}}} = \tfrac{1}{2}\sqrt{\left[\frac{1}{1+N}\right]} \tag{2.11}$$

It is interesting to note that for high condensation rates, Cess's /22/ result (equation 2.8) corresponds to the result of Shekriladze and Gomelauri /24/ (equation 2.11) when $N << 1$. (This is generally true for non-metallic liquids). Thus, it is seen that for high condensation rates, the asymptotic shear stress, τ_M, is a satisfactory approximation to the actual value, τ_i. From the work of Cess /22/, it may be inferred that $\tau_i \simeq \tau_M$ except for very low condensation rates, fig. 2.4a. It may further be noted that Cess's assumption that $u_\delta << U_\infty$ is valid since equations 2.8 and 2.11 give the same result for $N << 1$.

Shekriladze and Gomelauri /24/ also considered the case of uniform wall heat flux, using the above assumptions together with $u_\delta = 0$, and obtained the following result for the local vapour-side heat-transfer coefficient:-

$$\alpha_{x,Q} = \sqrt{k_L^2 \, \rho_L \, U_\infty / (\mu_L \, x)} \tag{2.12}$$

It may be noted that the equation for the average vapour-side heat-transfer coefficient given by the authors contains errors. The corrected value is

$$\bar{\alpha}_Q = \frac{L_P \, \dot{Q}''}{\int_0^{L_P} \Delta T_x \, dx} = 1.5 \sqrt{k_L^2 \, \rho_L \, U_\infty / (\mu_L \, L_P)} \tag{2.13}$$

Vertical plate

Shekriladze and Gomelauri /24/ also considered the case of an isothermal vertical plate (Again, the effects of inertia forces and energy convection within the condensate film were neglected. In addition, the assumption $u_\delta << U_\infty$, i.e. $u_\delta \simeq 0$, was made). The following results were obtained:-

$$\alpha_x = \tfrac{1}{2} \left[\frac{k_L^2 \, \rho_L \, U_\infty}{\mu_L \, x} \right]^{\frac{1}{2}} \sqrt{\tfrac{1}{2} \left[1 + \sqrt{(1 + 16 \, Pr_L / (Fr_x H))} \right]} \tag{2.14}$$

$$\bar{\alpha} = \left[\frac{k_L^2 \, \rho_L \, U_\infty}{\mu_L \, L_P} \right]^{\frac{1}{2}} \frac{\sqrt{2} \left[2 + \sqrt{(1 + 16 \, Pr_L / (Fr_L H))} \right]}{3 \sqrt{\{1 + \sqrt{(1 + 16 \, Pr_L / (Fr_L H))}\}}} \tag{2.15}$$

where Fr_x, Fr_L are the Froude numbers U_∞^2 / gx and U_∞^2 / gL_P respectively

It is seen from the work of Cess /22/ that for very low condensation rates, the interfacial shear stress, τ_i, approaches that for single-phase flow over an impermeable surface, τ_F, while at the other extreme of high condensation rates, it approaches the asymptotic value for flow under strong suction, τ_M. For intermediate values of condensation rates, it was also seen that τ_M is a good approximation of τ_i, see fig. 2.4a. Mayhew et. al. /25, 26 / attempted to handle the isothermal vertical plate problem in an approximate way by assuming that the interfacial shear stress, τ_i, is given by a very simple interpolation formula thus,

$$\tau_i = \tau_F + \tau_M \qquad (2.16)$$

where τ_F is the shear stress for single-phase flow over an impermeable surface

τ_M is the asymptotic shear stress given by equation 2.5, with $u_\delta = 0$

Equation 2.16 is valid for both the limiting cases of small and large condensation rates. Proceeding along the lines of Nusselt /1, 2 / (except that the interfacial shear stress was present), the authors derived a quartic equation for the condensate film thickness at the bottom of the plate, δ_L,

$$S \left(\frac{\delta_L}{L_P}\right)^4 + \frac{1}{3} Dr \left(\frac{\delta_L}{L_P}\right)^3 + \frac{1}{4} Re_{TP} \left(\frac{\delta_L}{L_P}\right)^2 - 1 = 0 \qquad (2.17)$$

where $S = \dfrac{\rho_L g h_{fg} L_P^3}{4 \mu_L k_L \Delta T}$

$Dr = \dfrac{\rho_L \tau_F h_{fg} L_P^2}{\mu_L k_L \Delta T}$

The value of $\dfrac{\delta_L}{L_P}$ found from equation 2.17 was used to determine the average Nusselt number and the average vapour-side heat-transfer coefficient. The average Nusselt numbers found from equation 2.17

when Dr = 0 are in excellent agreement with those given by equation 2.15 (i.e. the result of Shekriladze and Gomelauri /24/), figs. 2.6. (It may be noted that equation 2.15 corresponds to the case Dr = 0, $\psi = 1$ in figs. 2.6, where ψ is a multiplying factor for τ_M).

South and Denny /27 / proposed an interpolation formula of the form,

$$\tau_i = (\tau_F^n + \tau_M^n)^{1/n} \qquad (2.18)$$

where n is a constant

for the interfacial shear stress; this is a marked improvement over the expression used by Mayhew and co-workers. For the range of the suction parameter (i.e. $\left[\frac{-v_o}{U_\infty}\right]\sqrt{Re_v}$) between 0 and 5, a value of n = 1.375 was found to give good agreement with the numerical results (obtained from the solution of finite difference analogues of the governing partial differential equations, see /28 /) for both the flat plate /29 / and stagnation point flow /30 /, fig. 2.7. However, in view of the fact that the contribution of τ_F to τ_i is small, (except for very low condensation rates), such interpolation formula to include τ_F in τ_i would only lead to a small difference in the heat transfer over the result found when using $\tau_i = \tau_M$.

Denny and Mills /28 / considered the case of the vertical plate and assumed that the interfacial shear stress is given by the asymptotic value, equation 2.5 with $u_\delta = 0$. The effects of prescribed longitudinal variation of the wall temperature and variable properties were included. Numerical solutions were obtained by solving the finite difference analogue of the governing partial differential equations. (The reliability of the numerical method was established by reproducing the uniform-property solutions of Sparrow and Gregg /16 / and Koh et. al. /18 /, see fig. 2.8a). In addition, closed-form analytical solutions based on the Nusselt assumptions (except for τ_i) were extended to include the case of a non-isothermal wall. In so doing, a reference temperature, T_r, for evaluating locally variable fluid properties in the form,

$$T_r = T_w + \gamma \Delta T_x \tag{2.18a}$$

where T_w is the condensing-side wall temperature

γ = 0.33 for water

ΔT_x is the local vapour-to-wall temperature difference

was used. The analytical result was expressed, to a good approximation, as

$$\frac{\alpha_{a,x}}{\alpha_x} = \left\{\left[\frac{2\Delta T_x}{\Delta \bar{T}} - 1\right]\left[\frac{1 + \sqrt{[1 + (16g^* x/(r_1 U_\infty^2))(\Delta\bar{T}/\Delta T_x)/(2 - \Delta\bar{T}/\Delta T_x)^2]}}{1 + \sqrt{[1 + (16g^* x/(r_1 U_\infty^2))]}}\right]\right\}^{\frac{1}{2}} \tag{2.19}$$

where $\alpha_{a,x}$ is the local vapour-side heat-transfer coefficient for the non-isothermal vertical plate case

α_x is the local vapour-side heat-transfer coefficient for the isothermal vertical plate case

$\Delta\bar{T}$ is the area-averaged vapour-to-wall temperature difference (i.e. $\frac{1}{b-a}\int_a^b \Delta T_x \, dx$)

$g^* = g\,(1 - \varrho_v / \varrho_L)$

$r_1 = 1 / (Pr_L \cdot (h_{fg} /(c_{PL}\,\Delta T) + 0.354))$

The values obtained from equation 2.19 were compared with the numerical calculations and it was found that, except for severe wall temperature variations, the difference between the two solutions was generally less than 2 %, fig. 2.8b. Further, on the basis of a comparison between the numerical solutions obtained from the finite difference analogue to the momentum conservation equation governing the vapour flow and those obtained when using $\tau_i = \tau_M$, it was concluded that the error in the heat transfer introduced by the asymptotic shear stress expression (i.e. equation 2.5) was less than 1 %, for values of the suction parameter, $-v_o\sqrt{Re_v}/U_\infty$, greater than 2.0. This is in good agreement with the solution of Cess /22 /, fig. 2.4a, where it was found that τ_M is a good representation for τ_i, except for very low condensation rates, and this lends good support to the simpler analysis of Shekriladze and Gomelauri /24 /.

Recently, Asano et. al. /31 / considered the case of the vertical plate and in the theoretical analysis assumed that the interfacial shear stress was the same as that for single-phase flow along an impermeable plate. Proceeding along the lines of Nusselt /1 /, the authors derived equations for the local and average vapour-side heat-transfer coefficients thus,

$$\alpha_x / \alpha_{x,Nu} = 1 + C_x \qquad (2.19a)$$

$$\bar{\alpha}/\bar{\alpha}_{Nu} = 1 + C \qquad (2.19b)$$

where α_x is the local vapour-side heat-transfer coefficient

$\alpha_{x,Nu}$ is the local vapour-side heat-transfer coefficient according to the simple Nusselt theory

$C_x = 0.679 \left\{(Pr_L/R^4) \cdot (h'_{fg} U_\infty^6/(g^3 c_{PL} \Delta T x^3))\right\}^{1/12}$

$\bar{\alpha}$ is the average vapour-side heat-transfer coefficient

$\bar{\alpha}_{Nu}$ is the average vapour-side heat-transfer coefficient according to the simple Nusselt theory

$$C = 1.02 \left\{(Pr_L/R^4) \cdot (h'_{fg} U_\infty^6/(g^3 c_{PL} \Delta T L_p^3))\right\}^{1/12}$$

$$h'_{fg} = h_{fg} + 3\, c_{PL}\, \Delta T / 8$$

It was noted earlier that the use of "dry friction" to represent the interfacial shear stress is correct only for very low condensation rates.

In the preceeding works for the vertical plate, the workers in each case have made assumptions regarding the interfacial shear stress. Jacobs /32 /, however, used an integral method to solve the two-phase boundary-layer equations, matching the mass flux, shear stress, temperature and velocity at the interface. Uniform fluid properties were assumed and, inertia and convection terms in the condensate momentum and energy equations were neglected. Unfortunately, an incorrect boundary condition for the vapour boundary layer, $v \to 0$ as $y \to 0$, rather than $\partial U/\partial y \to 0$ as $y \to \delta$, was used.

Fujii and Uehara /33 / solved the problem considered by Jacobs but used the correct boundary condition. In addition, the velocity profile of the vapour boundary layer was represented by a quadratic expression in y, the normal distance from the plate. For the limiting case of body force convection only, the analytical results agreed with those of Nusselt. For the other extreme limiting case of forced convection only, expressions for the local and average Nusselt numbers, which agreed with the numerical calculations to within 2 %, fig. 2.9a, were proposed as follows :-

for $RH/Pr_L \geq 10$,

$$Nu_x/\sqrt{Re_{TP,x}} = 0.5 \qquad (2.20)$$

$$Nu/\sqrt{Re_{TP}} = 1.0 \qquad (2.21)$$

for $RH/Pr_L < 10$,

$$Nu_x/\sqrt{Re_{TP,x}} = 0.450\ (1.20 + Pr_L/RH)^{\frac{1}{3}} \qquad (2.22)$$

$$Nu/\sqrt{Re_{TP}} = 0.90\ (1.20 + Pr_L/RH)^{\frac{1}{3}} \qquad (2.23)$$

Equation 2.22 agrees with Cess's /22/ approximate solutions to within 3 %.

For the case of combined body force and forced convection, an approximate expression, which agreed with the numerical calculations to within 2.5 %, was proposed,

$$Nu_x/\sqrt{Re_{TP,x}} = K\ (1 + (1/4K^4)\ (Pr_L/Fr_x H))^{\frac{1}{4}} \qquad (2.24)$$

where $K = 0.450\ (1.20 + Pr_L/RH)^{\frac{1}{3}}$

It was found that, for values of $RH/Pr_L \geq 10$, equation 2.24 agrees satisfactorily with the solution of Shekriladze and Gomelauri /24 / (who used the asymptotic value for the interfacial shear stress; equation 2.14), see fig. 2.9b. Average Nusselt numbers were obtained by integrating equation 2.24 numerically. The expression,

$$Nu/\sqrt{Re_{TP}} = 2\,K\,(1 + (\sqrt{2}/3K)^4\,(Pr_L/Fr_L H))^{\frac{1}{4}} \qquad (2.25)$$

was found to agree with the results obtained by integrating equation 2.24 to within 4 %, fig. 2.9c.

Horizontal tube

In the theoretical developments for the flat plate case (for forced vapour flow), the problem is complicated by the need to specify or evaluate the interfacial shear stress. For the case of the horizontal tube, the problem is further complicated by the fact that the vapour boundary layer separates from the condensing surface and that the separation point (i.e. at $\tau_i = 0$) varies with the "suction parameter" (i.e. $(-v_o/U_\infty)\sqrt{Re_v}$; see for example Schlichting /34 /, pages 362-390). Thus, for a "complete" solution of the vapour-side, it is necessary to solve the coupled two-phase governing conservation equations. However, most workers made simplifying assumptions for the interfacial shear stress and in such cases it is only necessary to consider the condensate film. For the rest of this section, it should be noted that, unless otherwise stated, the assumptions made in all cases considered are as follows:-

i. inertia and convection terms in the condensate film conservation equations are neglected;
ii. fluid properties are uniform;
iii. condensate film flow is laminar;

iv. beyond the separation point, the interfacial shear stress is taken as zero;

v. free-stream vapour flow is governed by potential flow theory.

In addition, except in the case of /35 /, the direction of the free-stream vapour flow is perpendicular to the tube axis.

Sugawara et. al. /36 / and Nicol and co-workers /37 - 40 / considered the drag on the surface of the condensate film was the same as that for single-phase flow over an impermeable tube, i.e. the effect of momentum transfer arising from condensation was neglected. On the basis of boundary-layer flow, the tangential shear stress, τ_F, distribution around the tube for single-phase flow (see / 34/) is given by:-

$$\tau_F = \frac{1}{\sqrt{2}} \cdot \frac{\rho_v U_\infty^2}{\sqrt{Re_v}} \cdot A \qquad (2.26)$$

where A is a function of the angle measured from the forward stagnation point.

Sugawara et. al. used Heimenz's / 41 / measurements of the static pressure distribution around a tube and obtained:-

$$A = 6.0222\, \phi - 2.1114\, \phi^3 - 0.4053\, \phi^5 \qquad (2.27)$$

Nicol and co-workers used the first six terms of the Blasius power series (see / 34/) thus,

$$A = 6.973\, \phi - 2.732\, \phi^3 + 0.292\, \phi^5 - 0.0183\, \phi^7 + 0.000043\, \phi^9 - 0.000115\, \phi^{11} \qquad (2.28)$$

The separation points (i.e. at $\tau_i = 0$) of the vapour boundary layer are respectively $\phi_s = 83.3^\circ$ and $\phi_s = 108.8^\circ$.

Sugawara et.al. /36 / considered the case of downward vapour flow only, whereas Nicol and co-workers considered the cases of downward /37 - 39 /, upward /37 - 39 / and horizontal /40 / vapour flow.

As was seen in the simpler cases of the flat plate, the asymptotic shear stress is a better representation of the interfacial shear stress (except for very low condensation rates). In view of this, the above works /36 - 40 / may be considered to be correct only for very low condensation rates.

On the same basis as in the earlier works of Mayhew et. al. /25, 26 /, Nobbs /42 / and Nobbs and Mayhew /43 / considered that the interfacial shear stress, τ_i , was given by equation 2.16. For the shear stress due to "friction", τ_F , the authors used the same expression as Nicol et. al. /37 - 40 /, i.e. equation 2.26 with A given by equation 2.28, while the asymptotic shear stress, τ_M, was taken as,

$$\tau_M = \dot{m}'' (2\, U_\infty \sin\phi - u_\delta) \simeq 2\, \dot{m}''\, U_\infty \sin\phi \qquad (2.29)$$

The authors considered the case of downward vapour flow only. The separation point was determined on the basis of an approximate analysis due to Prandtl /44 /, thus

$$\frac{-v_o}{U_\infty}\sqrt{Re_v} = 4.36\sqrt{-\cos\phi_s} \quad ; \quad \phi_s > \pi/2 \qquad (2.30)$$

where ϕ_s is the value of ϕ at the separation point.
It may be noted that, from equation 2.30, separation is completely suppressed for $(-v_o/U_\infty)\sqrt{Re_v} = 4.36$.

Recently, Morsy /45 / carried out experiments for air flowing over porous tubes for values of the suction parameter (i.e. $(-v_o/U_\infty)\sqrt{Re_v}$) up to 30. The results indicated that separation still occurred for values of $(-v_o/U_\infty)\sqrt{Re_v}$ significantly higher than 4.36. In particular, for $(-v_o/U_\infty)\sqrt{Re_v} = 25$, the separation point was found to occur at about $\phi_s = 130^o$. In a typical steam condenser, the values of $(-v_o/U_\infty)\sqrt{Re_v}$ might range between 1 and 5.

Shekriladze and Gomelauri /24/ assumed that the interfacial shear stress was given by the asymptotic value given by equation 2.29. This simplification meant that the interfacial shear stress is positive for values of ϕ between zero and π (i.e. vapour boundary-layer separation was inherently suppressed). On the basis of the approximate analysis of Prandtl /44 /, Shekriladze and Gomelauri argued that, under normal conditions, condensation was sufficient to prevent separation of the vapour boundary layer (cf. boundary layer suction). However, as seen above, separation of the vapour boundary layer may not be completely supressed under normal conditions. In the absence of body (i.e. gravitational) forces, the local and average vapour-side heat-transfer coefficients were found to be:-

$$\alpha_x = \sqrt{\left[\frac{k_L^2 \ \rho_L \ U_\infty}{\mu_L \ d_o}\right]} \cdot \frac{\sin\phi}{\sqrt{(1 - \cos\phi)}} \qquad (2.31)$$

$$\bar{\alpha} = 0.9\sqrt{\left[\frac{k_L^2 \ \rho_L \ U_\infty}{\mu_L \ d_o}\right]} \qquad (2.32)$$

In the presence of body and forced convection, a simple explicit expression cannot be obtained. However, using the above results and those of Nusselt, the authors proposed an interpolation formula for the average vapour-side heat-transfer coefficient, thus,

$$\bar{\alpha} = 0.64 \left[\frac{k_L^2 \rho_L U_\infty}{\mu_L d_o}\right]^{\frac{1}{2}} \left\{1 + \left[1 + 1.69 \frac{Pr_L}{Fr\ H}\right]^{\frac{1}{2}}\right\}^{\frac{1}{2}} \qquad (2.33)$$

Equation 2.33 agrees with the results for the limiting cases of body convection only (equation 2.2) and forced convection only (equation 2.32).

Equation 2.33 agrees satisfactorily with experimental results of Berman and Tumanov /46/, fig. 2.10a. However, the data at the higher vapour velocity end indicated that the experimental Nusselt numbers fall below those predicted by equation 2.33, fig. 2.10b. Shekriladze and Gomelauri probably suspected their assumption that separation does not occur. On the basis that separation would occur at $\phi_s = 82^\circ$ (minimum separation point, single-phase flow over an impermeable tube) and that the heat transfer beyond the separation point could be neglected (the heat transfer up to this point was assumed to be the same as that for flow without separation), the authors proposed a conservative formula, thus

$$\bar{\alpha}_{sep} = 0.65\ \bar{\alpha}_{nosep} \qquad (2.34)$$

where $\bar{\alpha}_{nosep}$ is given by equation 2.33
(Note: 35 % of the total heat transfer, for the no separation case, takes place beyond $\phi = 82^\circ$). The authors then noted that for vapour flow with separation point between $\phi = 82^\circ$ and $\phi = 180^\circ$, the average vapour-side heat-transfer coefficient should lie between the values given by equations 2.33 and 2.34, fig. 2.10b.

However, for $U_\infty = 0$, the value of $\bar{\alpha}_{sep}$ (equation 2.34) does not correspond to the simple Nusselt result (equation 2.2). Butterworth /47 / pointed out that a more satisfactory interpolation formula was obtained by applying the factor 0.65 to the forced-convection result only, thus,

$$\bar{\alpha}_{sep} = 0.416 \left[\frac{k_L^2\, \rho_L\, U_\infty}{\mu_L\, d_o}\right]^{\frac{1}{2}} \left\{1 + \left[1 + 9.467\, \frac{Pr_L}{Fr\, H}\right]^{\frac{1}{2}}\right\}^{\frac{1}{2}} \qquad (2.35)$$

Equation 2.35 agrees with both the limiting cases of body force convection only (equation 2.2) and forced convection only (with separation at $\phi_s = 82^{\circ}$, i.e. equation 2.34).

Denny and Mills /48 / extended the method of Shekriladze and Gomelauri /24 / to the case of combined gravity and forced convection. The analysis yielded an equation, for the local vapour-side heat-transfer coefficient, which is to be used in conjunction with tabulated functions. The solution was compared with numerical solutions of a finite difference analogue of the conservation equations. The comparison was made for the cases of water, butanol and ethanol. It was found that the difference between the two solutions was less than 2 % for $\phi < 140^{\circ}$. For $\phi > 140^{\circ}$, the numerical solutions indicated that the assumption of negligible inertia effects is not valid. As for the flat plate /28 /, it was concluded that the error in the heat transfer introduced by the use of the asymptotic shear stress expression (equation 2.29) was less than 1 % for values of the suction parameter, $-v_o\sqrt{Re_v}/U_\infty$, greater than 2.0.

Honda and Fujii /35 / extended the method of Shekriladze and Gomelauri

/24/ to include vapour flow directions which were neither vertically downwards nor perpendicular to the tube axis. Two special cases were analysed:-

i. on-coming vapour flow direction parallel with the vertical plane which includes the tube axis, fig. 2.11a;

ii. on-coming vapour flow direction parallel with a vertical plane perpendicular to the tube axis, fig. 2.11b.

When the physical situations corresponded to those considered by Shekriladze and Gomelauri, the results, for both cases, reduce exactly to those obtained by the latter workers. Also, when the vapour velocity is zero, the results agree with those of Nusselt.

In the preceeding works for the horizontal tube, the workers in each case have made an assumption regarding the interfacial shear stress. Fujii et. al. /49/ did not invoke such approximations, but used integral methods to solve the two-phase boundary-layer equations, matching the mass flux, shear stress, temperature and velocity at the interface. The velocity profile in the vapour boundary layer was approximated by a quadratic expression in y, the radial distance from the condensate surface. The assumed velocity profile is such that the shear stress at the condensate surface is always greater than zero, i.e. separation of the vapour boundary layer is inherently suppressed. For the limiting case of body force convection only, the numerical results for the average Nusselt numbers agree with those calculated from the simple Nusselt theory. For the limiting case of forced convection only, the numerical results for the average Nusselt numbers can be expressed by:-

$$\frac{Nu}{\sqrt{Re_{TP}}} = 0.90 \left(1 + \frac{Pr_L}{RH}\right)^{\frac{1}{3}} \quad ; \quad RH/Pr_L < 10 \qquad (2.36)$$

For values of $RH/Pr_L \geq 10$, equation 2.36 reduces to the result of Shekriladze and Gomelauri /24/ (equation 2.32), fig. 2.12a. For the case of combined body force and forced convection, an approximate expression for the average Nusselt number , which agreed with the numerical results to within 5 %, was proposed,

$$\frac{Nu}{\sqrt{Re_{TP}}} = X \left(1 + \frac{0.276}{X^4} \cdot \frac{Pr_L}{Fr\ H}\right)^{\frac{1}{4}} \qquad (2.37)$$

where $X = 0.90\ (1 + Pr_L/RH)^{\frac{1}{3}}$

For values of $RH/Pr_L \geq 10$, equation 2.37 reduces to the result of Shekriladze and Gomelauri for the no separation case (equation 2.33), fig. 2.12b.

Very recently, Fujii et. al. /50,51/ and Fujii /52/ solved the governing two-phase boundary-layer equations for the case of a vapour flowing normally to a horizontal tube at an angle ϕ_o from the vertical. In /50,51/, both the uniform wall surface temperature and the uniform wall heat flux cases were considered, while in /52/ an overall vapour-to-coolant analysis was presented, including a solution of the conduction equation in the tube wall subject to the condition that the convective heat-transfer coefficient inside the tube was uniform.

In all three analyses, the interfacial shear stress was estimated by the method suggested by Truckenbrodt /53/. Truckenbrodt solved the momentum integral equation for the related problem of flow over a surface with suction. The authors /50-52 / modified the method /53 / in order to obtain better agreement with the "exact" numerical solutions for flow over a surface with and without suction, of Terril /54 /. The essential difference between this and the earlier analysis /49 / (where the assumed vapour velocity profile within the boundary layer resulted in the suppression of the separation of the boundary layer) is that the separation point is determined.

In general, Fujii et. al. show that solutions‡ may be expressed in the form:-

$$\frac{Nu}{\sqrt{Re_{TP}}} = \psi_1 \left[\frac{\sqrt{Re_{TP}}}{Fr\tilde{M}} , \frac{\sqrt{Re_{TP}}}{R\tilde{M}} \right]$$

for the uniform wall heat flux case, and

$$\frac{Nu}{\sqrt{Re_{TP}}} = \psi_2 \left[\frac{Pr_L}{FrH} , \frac{Pr_L}{RH} \right]$$

for the uniform wall temperature case.

Numerical calculations were performed for two cases of the tangential velocity distributions around the tube at the "edge" of the vapour boundary layer. Fujii et. al. /50, 51 / considered velocity distributions (calculated

‡ It may be noted that each term containing $\bar{\tau}_i$ and $d\bar{\tau}_i/d\phi$ in the differential equations for the condensate film thickness, δ, in /50-51/ should be divided by 2, see /55 /.

from the measurements of static pressure distribution around a tube for flows, at moderate Reynolds numbers, with and without suction, of various workers /41, 56 - 58 /) and concluded that a distribution due to Roshko / 57 / and that of potential flow theory represented extreme cases, see fig. 2.13a.

Roshko's flow indicates :

$$U_\phi = U_\infty \,(1.762\,\phi - 0.314\,\phi^3 - 0.0338\,\phi^5) \qquad (2.38)$$

and potential flow theory gives :

$$U_\phi = 2\,U_\infty \sin\phi \qquad (2.39)$$

The numerical results‡ indicated that:-

i. the separation points in the case of potential flow are further back than those in the case of Roshko's flow and the local Nusselt numbers in the former case are higher, fig. 2.13b - 2.13d;

ii. the local Nusselt numbers for the front half of the tube for the case of uniform wall temperature are higher than those for the case of uniform wall heat flux;

iii. for the case of uniform wall heat flux, the values of $Nu/\sqrt{Re_{TP}}$, for Roshko's flow, is almost independent of the parameter $R\widetilde{M}/\sqrt{Re_{TP}}$ (i.e. the suction parameter), whereas for the potential flow case, $Nu/\sqrt{Re_{TP}}$ is considerably affected by the parameter $R\widetilde{M}/\sqrt{Re_{TP}}$, fig. 2.13e;

iv. for the case of uniform wall surface temperature, the dependence of $Nu/\sqrt{Re_{TP}}$ on the parameter RH/Pr_L for Roshko's and potential flows is about the same, fig. 2.13f. The values of $Nu/\sqrt{Re_{TP}}$ for the

‡ Calculations carried out by the present author using the corrected equations (see footnote on page 47) show that these conclusions remain valid.

uniform wall surface temperature case are significantly higher than those for the uniform wall heat flux case.

It is seen from fig. 2.13e that the $Nu/\sqrt{Re_{TP}} - \sqrt{Re_{TP}}/Fr\tilde{M}$ curves undulate over part of the range of the parameter $\sqrt{Re_{TP}}/Fr\tilde{M}$. Physical consideration suggests that the values of $Nu/\sqrt{Re_{TP}}$ should become independent of $\sqrt{Re_{TP}}/Fr\tilde{M}$ for high vapour velocities when the effect of vapour velocity overwhelms that of gravity. Fujii et.al. /50,51/ did not comment on this unlikely result.

It is interesting to note that, from fig. 6‡ of /50/ (i.e. fig 2.13f) when the uniform wall temperature results are compared with the earlier solution /49/ (no boundary layer separation and potential flow case only), for values of $RH/Pr_L = 0.1$, 1.0 and 10.0, the inclusion of the vapour boundary-layer separation in the numerical calculations increases the heat transfer. Fujii et. al. did not, however, comment on this unlikely result. This may be due to the fact that the authors used an incorrect equation for the condensate film (see footnote on page 47 and see also /55 /). For $RH/Pr_L = 10$ (see fig. 2.13f), the limiting value of $Nu/\sqrt{Re_{TP}}$ (i.e. for forced convection case only) is quite close to that given by the the earlier solution /49 / suggesting that at this value of RH/Pr_L, separation of the vapour boundary layer, as predicted by the method used, is essentially suppressed.

---

‡ It may be noted that the curve for $RH/Pr_L = 0.1$ for the theory of Fujii et. al. /49/ was plotted incorrectly in fig. 6 of /50 /. The limiting value of $Nu/\sqrt{Re_{TP}}$ in this case should be 2.0.

It is also interesting to note that the overall vapour-to-coolant analysis /52/ gave very similar results to those obtained from the simpler (with respect to /52/) uniform wall heat flux analysis, (cf. figs. 2.13e and 2.14). It may further be noted that the heat-transfer rate was found to be only weakly dependent on the direction of the oncoming vapour.

2.2.1.3 Summary

For the stationary non-metallic vapour case, it is seen that Nusselt's simple theory/1, 2 / is sufficiently accurate for predicting the vapour-side heat-transfer coefficient for both the vertical plate and the horizontal tube. Refinements to the simple theory by various workers /13 - 21 / to account for inertia and convection effects within the condensate film and the interfacial shear stress (due to "hold-up" of the liquid film) indicated that, for non-metallic fluids, these effects are generally negligible.

For the flowing non-metallic vapour case, the approximate analysis of Cess /22 / (which is in agreement with the exact analysis of Koh /23 /) indicated that, except for very low condensation rates, the asymptotic shear stress is a good approximation to the actual interfacial shear stress. For the horizontal plate, Shekriladze and Gomelauri /24/, who used the asymptotic shear stress expression for the interfacial shear stress, gave a simple result for calculating the vapour-side heat-transfer coefficient. For the vertical plate and the horizontal tube, Shekriladze and Gomelauri also gave simple results for calculating the vapour-side heat-transfer coefficient. For the last two geometries, Fujii and co-workers /33, 49 / also gave simple approximate algebraic expressions for calculating the vapour-side heat-transfer coefficient. For sufficiently high condensation rates (i.e. $RH/Pr_L \geq 10$), these expressions reduce to the corresponding Shekriladze results /24/. For the horizontal tube geometry, both analyses /24,49/ neglected the separation of the vapour boundary layer. The more recent analyses of Fujii and co-workers /50-52/, who modified the approximate method of Truckenbrodt /53 / to evaluate the interfacial shear stress distribution around the tube, indicated that at high vapour velocities and high condensation rates, the results of /24,49/ overestimate the vapour-side heat-transfer coefficients.

2.2.2 Experimental investigations

2.2.2.1 Stationary vapours

Much experimental work has been done for filmwise condensation of a pure saturated vapour on vertical surfaces and horizontal tubes. McAdams / 8 / compared the experimental results of a number of earlier (pre - 1950) investigators with the Nusselt theory and found that the observed vapour-side heat-transfer coefficient varied from 36 % below to 70 % above the theoretical predictions. The differences between the experimental and theoretical values can be attributed to one or more of the following:-

i. presence of non-condensing gas;

ii. presence of dropwise condensation;

iii. significant forced-convection effects;

iv. rippling, splashing and turbulence within the condensate film.

More recently, various workers / 9 - 12 / have obtained data, both for the vertical flat plate and for the horizontal tube, which is in good agreement with the Nusselt solutions. In these works extra care was taken to avoid the above-mentioned factors.

For the vertical flat plate case, Mills and Seban / 9 / and Slegers and Seban /10 / respectively, condensed steam and n-butyl alcohol on a copper plate (50 mm high, 20 mm wide, 112.5 mm thick) located within a glass bell jar, fig. 2.15. Temperatures within the plate were measured by thermocouples. In / 9 /, these thermocouples were arranged in a 3 x 3 matrix, fig. 2.16a, while in /10 / two columns of six thermocouples each, fig. 2.16b, were used. In both cases the heat flux was calculated from the measured temperature gradient of the plate and from condensate collection. In / 9 /, an additional estimate was obtained from coolant measurements. Table 2.2 below gives the experimental ranges used in these investigations. The measured heat fluxes compare well with each other and with the Nusselt theory.

Table 2.2 Experimental results of Mills and Seban / 9 / and Slegers and Seban /10 /

Investigator	fluid	$T_\infty/^oC$	ΔT /K	$\dot{Q}''$/ (kW/m^2)	$\dot{Q}''/\dot{Q}''_{Nu}$
/ 9/	steam	7.2 - 10.0	4.4 - 6.1	31.4 - 34.6	0.9 - 1.1
/10/	n-butyl alcohol	29.5 - 38.2	3.9 - 5.6	25.1 - 34.6	0.98 - 1.02

Magal /11 / condensed low-pressure steam on a horizontal stainless-steel tube (6.25 mm o.d.) located within a pyrex glass test section, fig. 2.17. The tube itself was used as a resistance thermometer in order to obtain a mean tube wall temperature. Heat flux was obtained from coolant measurements and by condensate collection. Measurements were made at an approximately constant heat flux of 33 kW/m^2 (by adjusting the coolant flow rate and temperature) for pressures in the approximate range 1.5 - 35 kPa. The measured heat fluxes are in good agreement with each other and with the Nusselt theory.

Recent verification of the Nusselt theory for filmwise condensation of steam flowing, at low velocity (0.5 to 1.2 m/s), vertically downwards over a horizontal tube was given by Chung /12 / who obtained local heat fluxes for the upper half of a stainless-steel tube (19 mm o.d. 12.5 mm i.d.) by means of five pairs of thermocouples embedded within the tube wall. The thermocouples were uniformly spaced around the upper half of the tube. The apparatus is shown in fig. 2.18a. Measurements were made for steam temperatures 38 - 62 °C and steam-to-wall temperature differences 1 - 8 K. The results, figs. 2.18b and 2.18c, indicated that the measured local heat fluxes for the upper half of the tube were within ± 10 % of Nusselts predictions. It may be noted that the ratio of the vapour-side heat-transfer coefficient given by Shekriladze and Gomelauri's equation (i.e. equation 2.33) to that of Nusselt (i.e. $\bar{\alpha}_{Shek}/\bar{\alpha}_{Nu}$) for a vapour velocity of 1.2 m/s and ΔT of 8 K is only about 1.08.

Thus, it is seen that recent experimental data (obtained under "Nusselt" conditions) have lent good support to the simple Nusselt theory.

2.2.2.2 Moving vapours

Horizontal plate

Mayhew and Aggarwal / 26 / experimented with steam condensing on a horizontal flat surface (50 mm wide, 150 mm long) which formed one side of a rectangular duct (100 mm by 25 mm cross section). To avoid air in-leakage, the experiments were carried out at pressures slightly above atmospheric. Measurements (for co-current steam and coolant flows) were made for wall temperatures and steam velocities of 343 to 351 K and 6 to 60 m/s respectively. These measurements were obtained for the cases of the horizontal, the inclined and the vertical plate. The results, fig. 2.6a, showed satisfactory agreement with the author's own theory (i.e. equation 2.17). It may be noted that the equation of Shekriladze and Gomelauri /24/ (i.e. equation 2.10) corresponds to the case $Dr = 0$, $\psi = 1$ in fig. 2.6a and that the experimental results indicated that equation 2.10 (which was derived using the assumption that the interfacial shear stress is given by the asymptotic shear stress) was conservative.

Vertical plate

Mayhew and Aggarwal /26 / also carried out experiments with steam flowing vertically downwards parallel to a vertical flat plate; the experimental ranges used in this case are already given above. Additional measurements were also obtained for counter current (steam and coolant) flows for vapour velocities up to 7 m/s. The results, fig. 2.6b, for co-current flow cases, are in satisfactory agreement with the author's own theory and with the Shekriladze and Gomelauri /24/ prediction (i.e. equation 2.15; which corresponded to the case $Dr = 0$, $\psi = 1$ in fig. 2.6b). It is interesting to note that the results for the counter-current flow cases are significantly higher than those predicted by the authors' own theory and are always higher than the corresponding stationary vapour ($Re_v = 0$) values. The authors attributed this to turbulence within the condensate film.

Recently, Asano et. al. /31 / condensed vertically downwards flowing steam, methanol, carbon tetrachloride and benzene on a vertical flat copper plate (17.6 mm wide, 49.8 mm long, 0.5 mm thick), see fig. 2.19a. The surface temperature was measured by two thermocouples soldered on the wall at 4.1 mm and 4.7 mm from the upper and the lower edges. The heat flux was determined by condensate collection and from coolant measurements; agreement between the two methods was better than ± 15 %. Measurements were obtained for vapour Reynolds numbers in the approximate range 300 to 17500. Comparison with the result of Shekriladze and Gomelauri /24 / is not possible as details of the original data given are insufficient.

Horizontal tube

Berman and Tumanov /46 / carried out experiments with downward-flowing steam condensing on a single horizontal tube (19 mm o.d., 500 mm long) placed in the fourth row of a bundle of diagonally arranged uncooled "dummy" tubes. The condensing tube wall temperature was measured using a resistance thermometer located in a 0.9 mm square groove helically machined on the outside of the tube. Special care was taken to avoid the presence of non-condensing gas and samples of the vapour taken from the steam chamber indicated an air mole fraction less than 0.017 %. The heat flux was determined from coolant measurements. Table 2.3 below gives the ranges of the variables used by Berman and Tumanov.

Table 2.3 Experimental variables used in Berman and Tumanov's tests / 46 /

Test series	$T_\infty/^\circ C$	$\Delta T/K$	$U_\infty/(m/s)$ (based on cross sectional area of the test chamber)
I	25	0.56–5.3	0.97–17.6
II	31.5	0.71–6.5	0.96–13.0
III	43	1.5 –9.3	0.84– 7.2
IV	80	2.1–12.1	0.26– 1.5

The results were satisfactorily correlated by:-

$$\bar{\alpha}/\bar{\alpha}_{Nu} = 1 + 0.0095\,Re_v^{\,11.8/\sqrt{Nu_{Nu}}} \qquad (2.40)$$

Gogonin and Dorokhov /59 / carried out experiments with downward-flowing Freon-21 condensing on a nickel tube (17 mm o.d., 520 mm long) located in a test chamber as shown in fig. 2.20a. The tube was used as a resistance thermometer in order to obtain a mean wall temperature. The heat flux was calculated from coolant measurements. Tests were carried out at a saturation pressure of 520 kPa. Measurements were obtained for vapour velocity 0 to 0.56 m/s and vapour-to-wall temperature difference 2 to 20 K. The results for stationary vapour agreed with those calculated using Nusselt's equation to within ± 10 %. The vapour-side heat-transfer coefficients for the moving vapour was found to increase with increasing vapour velocity, fig. 2.20b. It may be noted that the value of $\bar{\alpha}_{Shek}/\bar{\alpha}_{Nu}$ for a vapour velocity of 0.56 m/s and ΔT of 21 K is about 1.11 (cf. $\bar{\alpha}_{Shek}/\bar{\alpha}_{Nu} = 1.08$, for steam velocity of 1.2 m/s and ΔT of 8 K).

Nicol and co-workers carried out experiments using steam with upflow /37 - 39 /, downflow /37 - 39 / and horizontal flow /40 / using the apparatus shown in fig. 2.21a. The experimental aluminium-brass tube (19.05 mm o.d., 16.56 mm i.d., 143 mm long) was located within a rectangular test section (143 mm by 92.2 mm). The tube wall temperature was taken as the mean of local temperatures measured by twelve thermocouples. The heat flux was determined from coolant measurements. The approximate ranges of the variables used were:- pressure 14 to 50 kPa, steam-to-wall temperature difference 9 to 30 K, and vapour velocity 10 to 150 m/s. The results indicated that the vapour-side heat-transfer coefficient increases with increasing vapour velocity, fig. 2.21b. It may be noted that for steam velocity of 150 m/s and ΔT of 10 K, the value of

$\bar{\alpha}_{Shek}/\bar{\alpha}_{Nu}$ is about 6.2 while the corresponding observed value is about 1.95. Samples of the vapour taken from the test section (see /38 /) indicated that a significant amount of air (mass fraction up to 5 %) was present in the steam.

Nobbs and Mayhew /42, 43 / experimented with steam at near atmospheric pressure using the apparatus shown in fig. 2.22a. Two series of tests were carried out for the single tube; the tube wall temperature was measured by three thermocouples only for one series. The tube used was a copper tube of dimensions 19.05 mm o.d., 15.875 mm i.d. and 500 mm long. The heat flux was calculated from coolant measurements. Tests were performed at steam pressures of about 105 kPa to avoid air in-leakage. The approximate ranges of the experimental variables were:- steam-to-wall temperature difference 15 to 30 K, steam velocity 0.6 to 8 m/s. The results indicated that the vapour-side heat-transfer coefficient increases with increasing vapour velocity, fig. 2.22b. It may be noted that for a steam velocity of 8 m/s and ΔT of 27.6 K, the value of $\bar{\alpha}_{Shek}/\bar{\alpha}_{Nu}$ is about 2.28 while the corresponding observed value is about 1.86.

Recently Fujii et. al. /50,60 / carried out experiments with low-pressure steam in a horizontal steam flow using the apparatus shown in fig. 2.23 (see also /61 /). Measurements were obtained with two tubes of different diameters and different materials. In each case, the tube wall temperatures were measured by eight thermocouples. The heat flux was determined from coolant measurements. Table 2.4 gives the approximate ranges of the experimental variables used.

Table 2.4 Approximate ranges of the experimental variables used by Fujii et. al. /50, 60/

Series	tube material	tube dimensions	T_∞ / °C	ΔT / K	U_∞ / m/s
A	copper	37.7 mm o.d.	23.4	1.8	0.6
		30.3 mm i.d.	to	to	to
		500 mm long	36.1	7.2	15.1
B	brass	18.6 mm o.d.	32.1	5.1	21.6
		12.6 mm i.d.	to	to	to
		197 mm long	35.8	6.8	34.8
C	copper	37.2 mm o.d.	30.5	2.0	0.7
		30.3 mm i.d.	to	to	to
		97.5 mm long	38.3	8.1	79.9
D	brass	18.6 mm o.d.	21.2	3.2	4.4
		12.6 mm i.d.	to	to	to
		96.5 mm long	38.8	5.6	64.2

The results, figs. 2.13g and 2.13h, indicated that the vapour-side heat-transfer coefficient increases with increasing vapour velocity. For a steam velocity of 80 m/s and ΔT of 3 K, the value of $\bar{\alpha}_{Shek}/\bar{\alpha}_{Nu}$ is about 3.71 while the corresponding observed value is about 1.40.

Correlations and comparison for the horizontal tube

Recently, Berman / 62, 63/ re-analysed the data of Berman and Tumanov / 46/ (Table 2.3) using the steam velocity calculated on the basis of the narrow section between the tubes. (The steam velocities given in Table 2.3 will then be multiplied by 3.1). Comparisons, figs.2.24 and 2.25, were made with the data of Gogonin and Dorokhov /59 / for Refrigerant 21 and the steam data of Nicol and Wallace / 37/ and Nobbs /42 /. It was shown that these data can be represented by an equation of the form :

$$\bar{\alpha}/\bar{\alpha}_{Nu} = a_1 + b_1 \lg(FrH/Pr_L) \qquad (2.41)$$

where for series I, II and III /46 /;

$a_1 = 1.28$, $b_1 = 0.12$ for $0.01 \leq FrH/Pr_L \leq 1$

$b_1 = 0.21$ for $1 < FrH/Pr_L \leq 15$

for series IV /46 / and Refrigerant 21 /59 /;

$a_1 = 1.45$, $b_1 = 0.12$ for $0.01 \leq FrH/Pr_L \leq 1$

$b_1 = 0.28$ for $1 < FrH/Pr_L \leq 20$

for data of /42 /;

$a_1 = 1.45$, $b_1 = 0.16$ for $FrH/Pr_L \leq 1$

$b_1 = 0.28$ for $FrH/Pr_L > 1$

It was noted that the three different data sets /42, 46, 59 / are in satisfactory agreement while the values of $\bar{\alpha}/\bar{\alpha}_{Nu}$ of /37 / are substantially lower. It was suggested that the data of /37 / may contain some systematic errors. It was also noted that the available experimental results did not show any obvious dependence on the parameter RH/Pr_L as was indicated by the theoretical results of Fujii and co-workers /49-51 /, (see equations 2.36 and 2.37). It was further suggested that the differences between experiment and theory may be due to one or both of the following:-

i. presence of non-condensing gas in the experiments;

ii. assumption of no vapour-boundary separation in the theories /24, 49 /.

In their recent publications, Fujii and co-workers /50-52 / did not give any closed-form expressions from their numerical calculations but, on the basis of their theories (which suggested the important parameters) and their their experimental results for steam, proposed two alternative forms of semi-empirical correlations (see /50, 60 /):-

a. based on the uniform wall heat flux theory:-

$$Nu/\sqrt{Re_{TP}} = 0.91\ (\sqrt{Re_{TP}}/Fr\widetilde{M})^{0.26} \tag{2.42}$$

$$\text{for } 0.06 \leqslant \sqrt{Re_{TP}}/Fr\widetilde{M} \leqslant 200$$

and

$$Nu/\sqrt{Re_{TP}} = 0.615\ (\sqrt{Re_{TP}}/Fr\widetilde{M})^{\frac{1}{3}} \tag{2.43}$$

$$\text{for } \sqrt{Re_{TP}}/Fr\widetilde{M} > 200$$

b. based on the uniform wall temperature theory:-

$$Nu/\sqrt{Re_{TP}} = 0.96\ (Pr_L/FrH)^{0.2} \tag{2.44}$$

$$\text{for } 0.03 \leqslant Pr_L/FrH \leqslant 600$$

and

$$Nu/\sqrt{Re_{TP}} = 0.728\ (Pr_L/FrH)^{\frac{1}{4}} \tag{2.45}$$

$$\text{for } Pr_L/FrH > 600$$

Equation 2.43 is the Nusselt-type uniform wall heat flux result (i.e. equation 2.4) while equation 2.45 is the simple Nusselt result (i.e. equation 2.2). Equations 2.44 and 2.45 were compared with the steam data of Nicol and co-workers /39, 40 / and Nobbs and Mayhew /43 /, see fig. 2.13i. Good agreement was found to exist between these equations and the data of /43 /. The measurements of /39, 40 / fell below those predicted by equation 2.44. As noted earlier, these observations may contain some systematic errors.

2.2.2.3 Summary

For the stationary vapour case, it is seen that recent experimental measurements (both for the vertical flat plate and the horizontal tube), obtained under "Nusselt" conditions, have shown good agreement with the simple Nusselt theory. The difference between the earlier (pre - 1950) measurements and the theoretical predictions may be attributed to one or more of the following:-

i. presence of non-condensing gas;

ii. presence of dropwise condensation;

iii. significant forced-convection effects;

iv. rippling, splashing and turbulence within the condensate film.

For the flowing vapour case, the good agreement between the experimental measurements for the horizontal plate and the vertical plate and the simple results of Shekriladze and Gomelauri /24/ (who used the asymptotic shear stress to represent the interfacial shear stress) suggested that the assumptions used in the theoretical derivation are valid. For the horizontal tube, the recent experimental measurements of Nobbs and Mayhew /42, 43 / and Fujii et. al. /50,60/ indicated satisfactory agreement with the uniform-wall-heat-flux theory of Fujii et. al. /50,51/ and the overall vapour-to-coolant analysis of Fujii /52/. These observations indicated that the uniform-wall-temperature analyses, with /50,51 / and without /24,49 / consideration of the vapour boundary-layer separation, overestimated the vapour-side heat-transfer coefficient for the cases of high vapour approach velocities and high condensation rates. The results of Nicol and co-workers /37 - 40 / appeared to be out of line with those of the other investigators. However, the range of vapour approach velocities used in /37 - 40 / are much higher than those used by the other investigators.

2.3. Filmwise condensation from vapour-gas mixtures

2.3.1 Introduction

The previous section surveyed some of the work that has been done for the case when the vapour is saturated and pure (i.e. single constituent). In many practical situations, however, non-condensing gases are present in the condensing vapour; for example, in a steam condenser which operates at sub-atmospheric pressures, in-leakage of air inevitably occurs. It has long been known that the presence of non-condensing gases can lead to significant reduction in heat transfer during condensation.

During condensation from a vapour-gas mixture, the vapour that is to be condensed is transferred from the bulk to the condensate surface by convective flow, which also carries with it the non-condensing gases. At the interface, the vapour is "removed" by condensation leaving behind a gas-rich region in the vicinity of the interface. In steady state, the equilibrium gas composition at the interface is governed by diffusion in the presence of forced and/or free convection.

The buildup of the non-condensing gas at the interface causes a corresponding reduction in the partial pressure of the vapour at the interface. In turn, this reduces the saturation temperature at which condensation takes place, i.e. the interface temperature. The net effect is to lower the effective thermal driving force, $T_i - T_w$, thereby reducing the heat transfer.

2.3.2 Theoretical developments

In view of the fact that there are two constituents in the vapour-gas layer, it is therefore necessary to consider the vapour-gas layer in the theoretical developments. A general solution of the above problem, i.e. the determination of the vapour-gas layer temperature drop and the heat flux, requires simultaneous solution of the conservation equations (i.e. mass, momentum and energy) for both the condensate film and the vapour-gas layer, together with the conservation of species (i.e. diffusion equation) for the vapour-gas layer; applying appropriate boundary and interfacial compatibility conditions. Some workers have attempted detailed solutions along these lines while others have used simplifying assumptions.

In the case of stationary vapour-gas mixtures, the only geometry studied seems to have been that of the vertical flat plate, while for moving vapour-gas mixtures, the cases of the horizontal and the vertical plates and the horizontal tube have been considered.

2.3.2.1 Stationary vapour-gas mixtures

For the quiescent vapour-gas mixture case, Sparrow and Eckert /64 / and Sparrow and Lin /65 / presented boundary-layer analyses of laminar film condensation on an isothermal vertical plate. The governing partial differential equations were re-written as ordinary differential equations by means of a similarity transformation. In /64 /, the motion of the vapour-gas mixture was considered to result only from the downward motion of the condensate film, whereas in /65 /, free convection, arising from density differences associated with composition differences, was also included. With the exception that in /65 / the density variation was included in the "buoyancy term", both analyses assumed uniform fluid properties. These analyses indicated that:-

$$\dot{Q}''/\dot{Q}''_{Nu} = \psi(W_{\infty}, Sc, R, (H_c/Pr_L)) \qquad (2.46)$$

where $\dot{Q}''$ is the heat flux

$\dot{Q}''_{Nu}$ is the heat flux given by the simple Nusselt theory for the same bulk-to-wall temperature difference as $\dot{Q}''$

W_{∞} is the bulk gas mass fraction

Sc is the vapour-gas mixture Schmidt number

$R = (\rho_L \mu_L / \rho_v \mu_v)^{\frac{1}{2}}$

$H_c = c_{PL} \Delta T_c / h_{fg}$

Pr_L is the condensate Prandtl number

ΔT_c is the temperature drop across the condensate film (i.e. $\Delta T_c = T_i - T_w$)

It is interesting to note in /65 / that $\dot{Q}''/\dot{Q}''_{Nu}$ is independent of gravity. In both cases, numerical calculations were obtained for steam-air mixtures. Figs. 2.26a to 2.26c shows the variation of the interfacial concentration of the non-condensing gas and the partial pressure of the condensing vapour with the parameter H_c/Pr_L. It may be seen from the figures that the detrimental effect of the noncondensing gas increases with increasing Schmidt number and increasing values of R. Moreover, it is evident from figs. 2.26d and 2.26e that free convection is important when the vapour and the non-condensing gas have significantly different relative molecular masses and that its importance increases with increasing bulk gas mass fraction and increasing values of R.

Minkowycz and Sparrow /66 / elaborated on the analysis of /65 / by including also free convection arising from temperature differences. This necessitated the inclusion, in the analysis, of the energy equation for the vapour-gas layer. In addition, the analytical model included interfacial resistance, superheating, thermal diffusion and did not assume uniform properties in the condensate film and in the vapour-gas mixture. Heat transfer results for steam-air mixtures were obtained for a wide range of parameters including the bulk air mass fraction (W_∞), system pressure (P_∞), bulk-to-wall temperature differences (ΔT) and the degree of superheating. The results /66 /, see figs. 2.27a and 2.27b, indicated that the considerations formerly included in /65 / are the dominating factors and that the additional effects (except superheating which may be important, see fig. 2.27c) included in /66 / are generally less important.

The above solutions /64 - 66 / all require extensive computations; in the words of Minkowycz and Sparrow /66 /:- "even with a computer such as the CDC 1604, the time requirement was measureable in tens of hours". For the case considered by Sparrow and Lin /65 / (and shown by Minkowycz and Sparrow /66 / to include the important features), Rose /67 / presented an approximate integral uniform-property (except for density in the "buoyancy term") boundary-layer solution. Plausible velocity and concentration profiles for the vapour-gas boundary layers were used and it was assumed that these two layers had equal thicknesses. The result,

$$10 \frac{H_c}{Pr_L} Sc\, R^2 \left(\frac{\omega}{1-\omega}\right)^2 \left[\frac{20}{21} + \frac{1}{\omega} Sc\right]$$

$$+ \frac{8}{Sc} \left[\frac{Pr_L}{H_c}\right]^2 \frac{1}{R^2} (1-\omega)^2 \left[\frac{5}{28} \frac{H_c}{Pr_L} - \frac{E\,(W_i - W_\infty)}{3}\right]$$

$$= \frac{100}{21}\omega - 2(1-\omega) + 8\, Sc \qquad (2.47)$$

where $\omega = W_\infty / W_i$

$E = (M_n - M_v) / (M_n - W_\infty (M_n - M_v))$

W_i is the interfacial gas mass fraction

M_n is the relative molecular mass of the non-condensing gas

M_v is the relative molecular mass of the condensing vapour

for the vapour-gas layer was obtained by using the local condensation rate and interfacial velocity given by the Nusselt theory. Quite good agreement between the exact / 66/ and the approximate / 67/ solutions was obtained, fig. 2.28.

2.3.2.2 Moving vapour-gas mixtures

Horizontal plate

For the case when the vapour-gas mixture is flowing in a parallel direction to a horizontal plate, Sparrow and co-workers /68, 69 / solved the relevant two-phase conservation equations along the lines of their earlier solutions / 66/ for the stationary vapour-gas mixtures. Sparrow and co-workers /68, 69 / assumed that inertia forces and subcooling within the condensate film are negligible and that the condensate surface velocity is taken as zero when considering the vapour-gas layer. The authors also assumed uniform properties (a reference temperature was used when obtaining numerical results). Heat transfer results were obtained for steam-air mixtures for a wide range of operating conditions. It was shown that the detrimental effect of non-condensing gas for the moving vapour-gas mixture case is much less than the corresponding stationary vapour-gas mixture case, fig. 2.29. Physical consideration suggests that a moving vapour-gas mixture has a "sweeping" effect thereby resulting in a lower gas concentration at the interface (compared to the corresponding stationary vapour-gas mixture case). It is interesting to note that the ratio of the heat flux with gas to that without gas (i.e. $\dot{Q}''_{gas}/\dot{Q}''_{nogas}$ is independent of the vapour-gas mixture approach velocity. The results also indicated that interfacial resistance has a negligible effect on the heat transfer /68/ and that the effect of superheating was much less than the corresponding free convection case /69/.

Koh /70/ and more recently Fujii et. al. /71/ solved the problem considered by Sparrow and co-workers /68, 69/ but did not make the simplifying assumptions adopted in /68, 69/. Both /70, 71 / assumed uniform properties as did /68, 69/. Koh obtained numerical solutions for the ranges Sc = 0.5 and 1.0 and R $(=(\rho_L \mu_L/\rho_V \mu_V)^{\frac{1}{2}})$ = 10, 100 and 500 while Fujii et. al. used Sc = 0.2, 0.5, 1.0 and 1.5 and R = 100, 500 and 1000. Good agreement was found between the results of Koh and Fujii et.al., fig. 2.30a. Comparisons, see figs. 2.30b - 2.30c, between the approximate /68/ and the exact /71/ solutions indicated that, except for very high condensation rates and low values of R, good agreement was obtained, suggesting that the assumptions used in the approximate analyses are valid.

For the problem considered by Sparrow et. al. /68/, Rose /72/ used the heat-transfer results for flow over a flat plate with suction /73/ and obtained a simple expression giving the relationship between the vapour mass flux to the condensate surface and the composition at the interface thus,

$$\omega = (1 + \beta_x \, Sc \, (1 + 0.941 \, \beta_x^{1.14} \, Sc^{0.93}) / \zeta)^{-1} \qquad (2.48a)$$

or

$$z_x + 0.941 \, Sc^{-0.21} \, (1 - \omega)^{1.14} \, z_x^{2.14} - \zeta/\omega = 0 \qquad (2.48b)$$

where $\omega = W_\infty / W_i$

$\beta_x = (\dot{m}_x'' / \varrho_v U_\infty) \, Re_{v,x}^{\frac{1}{2}}$

$\zeta = Sc^{\frac{1}{2}} \, (27.8 + 75.9 \, Sc^{0.306} + 657 \, Sc)^{-1/6}$

$z_x = Sh_x Re_{v,x}^{-\frac{1}{2}} = \beta_x \, Sc/(1 - \omega)$

The results given by equation 2.48a were compared with the numerical solutions of Sparrow et.al. /68/ and very good agreement was found, see Table 2.5. The results given by equation 2.48b were compared with the exact numerical solutions of Koh /70 / and Fujii et.al. / 71, 74/, fig. 2.31 (see also /74a/). The good agreement between the exact / 70, 71, 74/ and approximate / 68, 72/ solutions indicated that the approximate equations are satisfactory and confirmed the validity of the simplifying assumptions used in the work of /68, 69, 72/.

Table 1. Condensation on a flat plate. Comparison of numerical solutions of Sparrow *et al* [3] for $Sc = 0.55$ with values given by equation (9)

β_x	ω	
	Sparrow	Equation (9)
0 025	0.951	0 951
0 05	0.905	0 905
0 075	0.863	0.863
0.1	0.823	0.824
0.125	0.787	0.788
0 15	0.752	0.753
0 175	0.720	0.721
0.2	0.690	0.691
0.225	0.662	0.663
0.25	0 635	0 637
0.3	0.587	0.588
0.35	0.543	0.545
0.5	0.438	0.439
0.75	0.319	0.318
1.0	0.241	0.240
1.5	0.149	0.149
2.0	0.100	0.100
2.5	0.0717	0.0713
3.0	0.0532	0.0532
5.0	0.0216	0.0217

Table 2.5 Reproduced from Rose /72 /

Vertical plate

Denny and co-workers / 29, 75/ considered the case of downward vapour-gas mixture flow parallel to a vertical flat plate. The governing conservation equations in the vapour boundary layer were solved numerically by means of finite difference methods using a forward marching technique. The liquid film was treated as in the Nusselt analysis except that at the condensate surface shear stress was present. In /29 /, numerical calculations were carried out for steam-air mixtures only whereas in /75 / steam-air, ammonia-air, Refrigerant 12-air, ethanol-air, butanol-air and carbon tetrachloride-air mixtures were considered. Table 2.6 gives the approximate ranges for which dimensionless heat transfer results, $\dot{Q}''/\dot{Q}''_{Nu}$ as a function of distance, x, were obtained. The results indicated that the effect of the non-condensing gas is most marked for low oncoming vapour velocities and large gas concentrations. It may be noted that as the oncoming velocity approaches zero the result asymptotically approaches that of Minkowycz and Sparrow /66 / (who considered the case of the stationary vapour-gas mixtures).

Table 2.6 Approximate ranges of variables used in the numerical calculations of Denny and co-workers /29, 75 /

Investigator	T_∞/K	ΔT/K	W_∞	U_∞/m/s
/29 /	311 - 373	3 - 22	0.001 - 0.1	0.03 - 3
/75 /	305 - 323	5 - 22	0.001 - 0.01	0.3 - 30

Recently, Asano et. al. /31 / treated the problem considered by Denny and co-workers / 29, 75/. The condensate film was treated as in the Nusselt analysis but assuming that the interfacial shear stress was the same as that for single-phase flow over an impermeable plate. The vapour-gas layer was solved, independently of the condensate film (i.e. the streamwise interfacial velocity was taken as zero when considering the vapour-gas layer), by means of a similarity transformation and the results are:-

$$Nu_x/Re_{v,x}^{\frac{1}{2}} = 0.332\ Pr_v^{\frac{1}{3}}\ g(B) \tag{2.49}$$

for the vapour-phase heat flux, and

$$Sh_x/Re_{v,x}^{\frac{1}{2}} = 0.332\ Sc^{\frac{1}{3}}\ g(B) \tag{2.50}$$

for the vapour-phase mass flux.

In equations 2.49 and 2.50, $g(B)$ is a function of the dimensionless mass-transfer driving force, $B\ (=(W_\infty - W_i)/W_i)$, and is given in Table 2.7.

(Note F(0) in the table is a dimensionless stream function).
Satisfactory agreement was found between the results /31 / and those of Denny and co-workers /29, 75 / for a vapour velocity of 0.3 m/s. However, the effect of such a low vapour velocity is small and the deviation from the stationary vapour-gas mixture result is also small.

Table 1 Function $g(B)$

$F(0)$	B	$g(B)$	$F(0)$	B	$g(B)$
0.00	0.0000	1.000	2.00	−0.8568	3.514
0.10	−0.1356	1.110	2.20	−0.8747	3.787
0.20	−0.2462	1.223	2.40	−0.8898	4.061
0.30	−0.3376	1.338	2.60	−0.9026	4.337
0.40	−0.4138	1.455	2.80	−0.9136	4.614
0.50	−0.4782	1.574	3.00	−0.9232	4.892
0.60	−0.5329	1.695	3.50	−0.9423	5.592
0.70	−0.5798	1.818	4.00	−0.9566	6.295
0.80	−0.6203	1.942	4.50	−0.9678	7.000
0.90	−0.6555	2.067	5.00	−0.9770	7.705
1.00	−0.6863	2.194	5.50	−0.9847	8.409
1.20	−0.7372	2.451	6.00	−0.9914	9.111
1.40	−0.7773	2.712	6.50	−0.9975	9.811
1.60	−0.8093	2.976			
1.80	−0.8354	3.244			

Table 2.7 Reproduced from Asano et. al. /31/

Horizontal tube

Denny and South /30 / treated the problem for the case of downward vapour-gas mixture flow over a horizontal tube. They considered only the forward stagnation point (i.e. uppermost point) of the tube. The governing partial differential equations were transformed by means of a similarity variable into ordinary differential equations which were then solved numerically, matching the conditions of mass flux, shear stress, temperature and velocity at the interface. Numerical results were obtained for steam-air mixtures for a wide range of conditions: vapour velocity 0.3 to 30.5 m/s, saturation pressure 6.5 to 100 kPa, bulk air mass fraction 0.01 to 0.15 and tube diameter 12.7 to 76.2 mm o.d.. The results indicated that the general trends are similar to those obtained by Minkowycz and Sparrow /66/ and also that the detrimental effect of non-condensing gas is less marked than in the latter case.

On the same basis as the horizontal plate case, Rose /72/ proposed an approximate equation for the mass transfer in a two-constituent boundary-layer flow over a porous tube,‡

$$Sh/\sqrt{Re_v} = 0.57\ Sc^{\frac{1}{3}}\ \xi(\beta, Sc) + \beta Sc \qquad (2.51)$$

where $Sh = \dot{m}'' d_o / \rho_v D(1 - \omega)$

$\xi(\beta, Sc) = (1 + a\ \beta^b\ Sc^c)^{-1}$

$\beta = (\dot{m}''/\rho_v\ U_\infty)\ Re_v^{\frac{1}{2}}$

and D is the binary diffusion coefficient of the mixture

$\omega = W_\infty/W_i$

a, b, c are constants of order unity

In addition the condition that the condensate surface is impermeable to the non-condensing gas gave,

$$Sh/\sqrt{Re_v} = \beta Sc/(1 - \omega) \qquad (2.52)$$

---

‡ It was assumed that the distribution of surface radial velocity in the mass transfer problem is the same as that in the heat transfer problem.

king a = b = c = 1, the following equivalent results were obtained:-

$$\omega = \{1 + 1.75\ Sc^{\frac{2}{3}}\ (1 + \beta Sc)^{-1} \qquad (2.53a)$$

$$\omega = \left\{1 + z^{-1} - \{1 + 2z^{-1} + z^{-2}(1 - 2.28Sc^{\frac{1}{3}})\}^{\frac{1}{2}}\right\}/2 \qquad (2.53b)$$

$$z = \{(1 + 2.28Sc^{\frac{1}{3}}\ (\omega^{-1} - 1))^{\frac{1}{2}} - 1\}/(2 - 2\omega) \qquad (2.53c)$$

$$\beta = (1 + 2.28Sc^{\frac{1}{3}}\ (\omega^{-1} - 1))^{\frac{1}{2}} - 1\ /2Sc \qquad (2.53d)$$

ere $z = Sh/\sqrt{Re_v}$

od agreement was found between equations 2.53 and the measurements r steam-air mixtures of Mills et. al. /76 / and Fujii et. al. /77 /, g. 2.32. It was suggested that in view of the good agreement and the mited comparison (steam-air mixtures only) made, further refinements the values a, b and c be postponed.

3.2.3 Summary

r the stationary vapour-gas mixture case, the only geometry studied emed to have been that of the vertical plate. For this case, the proximate solution of Rose /67 / showed good agreement with the exact merical results of Minkowycz and Sparrow /66 / suggesting that the proximations used in /67 / are valid. However, it may be noted that both solutions are only applicable to the cases where the relative molecular mass of the non-condensing gas is greater than that of the condensing vapour.

For the moving vapour-gas mixture case, the approximate numerical solutions of Sparrow and co-workers /68, 69 /, for the horizontal plate, indicated that the detrimental effect of the non-condensing gas is much less than the corresponding stationary vapour-gas mixture case. Moreover, the exact numerical solutions of Koh /70 / and Fujii et.al. / 71, 74/ for a wide range of operating conditions, are in good agreement with each other and with the approximate solution /68 / suggesting that the approximations used in / 68, 69/ are valid. For the problem considered by Sparrow et. al. /68 /, Rose /72 / obtained simple algebraic equations (i.e. equations 2.48) which are in good agreement with the approximate /68 / and the exact /70, 71, 74 / numerical results and which confirmed the validty of the simplifying assumptions used in the work of / 68, 69, 72/.

The vertical plate results of Denny and co-workers / 29, 75/ agreed satisfactorily with those of Asano et. al. /31 / for a vapour velocity of 0.3 m/s. In the limiting case of zero vapour velocity, the results of /29, 75 / approaches those of Minkowycz and Sparrow /66 / (for the case of stationary vapour-gas mixtures).

For the case of the horizontal tube, Rose /72 / obtained an approximate equation for the mass-transfer flux in the vapour-gas layer. This equation when combined with an appropriate equation for the condensate film (for example, equation 2.37) can be used to calculate the condensation rate (and therefore the heat-transfer flux) for given conditions in the bulk of the vapour-gas mixture and the outside wall of the tube.

2.3.3 Experimental investigations

2.3.3.1 Stationary vapour-gas mixtures

Vertical plate

Lack of reliable and accurate data for the case considered in the theories /64 - 66 / (i.e. condensation from a stationary vapour-gas mixture on a plane vertical plate) led the authors /65, 66 / to compare their numerical results with the experimental data for a horizontal tube obtained by Othmer / 78 / who condensed steam in the presence of air. Clearly, such a comparison of different geometries is unsatisfactory, although general agreement on a $\dot{Q}''/\dot{Q}''_{Nu}$ (where $\dot{Q}''_{Nu}$ is the Nusselt heat flux for the same ΔT as $\dot{Q}''$) basis between experiments and theories were found.

The vertical-plate data of Hampson / 79/ for steam-hydrogen mixtures and of Akers et. àl. / 80/ for ethanol and carbon tetrachloride in the presence of nitrogen and carbon dioxide were obtained under conditions where substantial forced convection was apparently present. In the case of / 79/, nitrogen was fed continuously to the apparatus and vented, along with excess steam, near to the bottom of the condensing surface. In the case of / 80/, the condensing plate was situated directly above the boiling liquid. Although a baffle, in the form of a disc, was fitted at the bottom of the test plate, this may not be adequate to prevent significant disturbance of the flow near the plate. The observed heat-transfer coefficients were substatially higher (in excess of 20 %) than those predicted by the theories / 65, 66/.

In view of the above, Slegers and Seban /81 / performed further experiments for condensation of steam, in the presence of air, on a vertical copper plate (50.8 mm wide, 127 mm high and 114.3 mm thick). The condensing plate was placed in a glass bell jar, fig. 2.15. A baffle and steam distributor was fitted over the boiler opening so as to avoid forced convection effects. The condensing plate surface temperature was evaluated by extrapolating the measured temperatures within the plate. (Two vertical rows of six thermocouples each were located at 25.4 mm and 50.8 mm from the condensing surface, fig. 2.16b. The mean temperature for each row was used to determine the mean temperature gradient). Measurements were obtained for steam temperatures of 60 °C, 46 °C and 27 °C, bulk-to-wall temperature differences up to 22 K, maximum heat flux of about 95 kW/m^2 and air mass fractions 0.0001 to 0.01. The observed heat fluxes (normalised with respect to Nusselt values for the same ΔT) were, on average, about 20 % higher than the theoretical predictions /66 /, figs. 2.33. This was attributed to forced flow despite the care taken to avoid this.

For the same geometry as /81 /, Al-Diwany and Rose /82 / obtained heat-transfer measurements for steam, at near atmospheric pressure, condensing in the presence of air, argon, neon and helium. The vertically-mounted copper plate (97 mm wide, 97 mm high, 12.5 mm thick) was located in a cylindrical glass steam chamber, fig. 2.34a. The vapour-gas mixture was passed into the steam chamber via flow straighteners which provided uniform flow of the mixture towards the condensing surface so as to obviate forced convection effects. The wall surface temperature was obtained by extrapolating the six measured temperatures within the plate. The heat fluxes were estimated from the temperature gradient within the plate. Measurements were obtained for bulk-to-wall temperature difference 5 - 80 K and gas mass fraction up to 0.4. The observed heat fluxes (normalised with respect to the Nusselt value for the same ΔT) for steam-air, steam-argon and steam-neon showed satisfactory agreement with the exact and the approximate theoretical solutions /66, 67 /, figs. 2.34b - 2.34g. The authors noted that the theories /66, 67 / do not apply for the case when $M_n < M_v$, i.e. steam-helium mixtures. It may be noted that for the latter case, the values of $\dot{Q}''/\dot{Q}''_{Nu}$ for given values of gas mass fractions are somewhat smaller than those for the other mixtures, cf. figs. 2.34b - 2.34g with figs. 2.34h and 2.34i.

Horizontal tube

Othmer /78 / introduced air for mole fractions of up to 11 % into quiescent steam condensing on the outside of a horizontal nickel-plated copper tube (75.2 mm o.d.), fig. 2.35. No provision was made for visual observation of the tube surface. The tube wall temperature was measured by thermocouples embedded in the tube wall by the nickel plating process. Measurements were obtained for steam temperature 100 - 110 $^{\circ}$C and bulk-to-wall temperature difference up to 40 K. The results indicated that the addition of 0.5 % air would decrease the vapour-side heat-transfer coefficients by 50 %.

Hampson /83 / condensed atmospheric-pressure steam on a horizontal copper tube in the presence of hydrogen. During the tests, the steam-hydrogen mixtures were vented continuously from the end plate of the condenser shell at the coolant outlet end suggesting that significant forced convection may have been present. The heat flux was evaluated from coolant measurements. Since the tube wall temperature was not measured, the vapour-side heat-transfer coefficient was estimated from the overall measurements by means of the "Wilson plot". Measurements were obtained for a wide range of tube diameters (6 mm to 25 mm o.d.), tube inclination (0° to 90°), heat fluxes (up to 630 kW/m^2) and hydrogen-steam ratio (0 - 0.05). The results, figs. 2.36, clearly demonstrate the detrimental effect of a non-condensing gas.

An experimental investigation was carried out by Provan / 84/ for steam condensing on a horizontal titanium tube (18.6 mm o.d.) in the presence of air and argon. The condensing tube was centrally located in a 152.4 mm i.d. glass cylinder and the steam-gas mixture was supplied to the test chamber via a perforated tube located above the test tube, fig. 2.37a; the holes in the tube were arranged so that the vapour did not eject directly on to the condensing tube. The heat flux was evaluated from the coolant measurements. The experiments were carried out at near atmospheric pressure and the maximum gas (both air and argon) mole fraction of about 0.06 was used. The results indicated that for equal gas content the reduction in the heat flux is of similar magnitude for both air and argon, fig. 2.37b.

More recently, Henderson and Marchello / 85/ obtained experimental data for steam-air and toluene-nitrogen mixtures condensing on a horizontal copper tube (28.6 mm o.d.) for pressures a little above that of the atmosphere. Twelve thermocouples were embedded at various intervals around and along the tube. Measurements were obtained for air and nitrogen mole fractions in the ranges 0.0064 to 0.251 and 0.0071 to 0.591 respectively. The vapour-side heat-transfer coefficients (normalised by the Nusselt values for the same ΔT), fig. 2.38, were found to be in good agreement with those of Othmer /78/ and a semi-empirical equation, which fitted both sets of data well, was given,

$$\bar{\alpha} = (1/\{1 + C\widetilde{W}_{\infty})) \bar{\alpha}_{Nu} \qquad (2.54)$$

where $\bar{\alpha}$ is the vapour-side heat-transfer coefficient

$\bar{\alpha}_{Nu}$ is the Nusselt heat-transfer coefficient for the same ΔT ($= T_{\infty} - T_w$)

$\widetilde{W}_{\infty}$ is the bulk gas mole fraction

C is a "fitted" constant given in Table 2.8 below.

Table 2.8 Value of C used in equation 2.54; reproduced from Henderson and Marchello /85 /

Table 1 Constants for Equation (10)

System	C	Percent Standard Deviation	Percent Noncondensable Range
Steam-air	0 51	9 2	0.64–25 1
Toluene-nitrogen	0 149	8.7	0.71–59.1
Benzene-nitrogen	0.076	14 3	7.1–20.3

(Note: Data for benzene-nitrogen were taken from Kirkbride /86 /).

2.3.3.2 Moving vapour-gas mixtures

Vertical plate

Recently Asano et. al. /31 / performed experiments, in turn, with vertically downward-flowing steam, methanol, benzene and carbon tetrachloride condensing, in the presence of air, on a vertical flat copper plate (17.6 mm wide, 49.8 mm high and 0.5 mm thick), fig. 2.19a. The surface temperature was measured by two thermocouples "soldered on the wall" at 4.1 mm and 4.7 mm from the upper and the lower edges. The heat flux was determined by condensate collection. The experiments were carried out at atmospheric pressure for the approximate ranges: bulk-to-wall temperature difference 0.5 to 20 K, air mass fraction 0.027 to 0.787 and vapour-phase Reynolds number 1106 to 7613. The results, fig. 2.19b, clearly demonstrate the detrimental effect of air.

Horizontal tube

Berman and Fuks /87/ carried out experiments, for a wide range of conditions, with flowing steam condensing, in the presence of air, on a horizontal tube (19 mm o.d., 522 mm long) located within a rectangular test section. Special precautions were taken to ensure that the apparatus remained leak-tight. The temperature of the tube wall was measured by means of a resistance thermometer located in a 0.9 mm x 0.9 mm spiral groove on the outside surface of the tube. The heat flux was evaluated from coolant measurements. Two series of experiments were performed and Table 2.9 gives the ranges of the variables used. It was found that for $Re_v > 350$, the results could be correlated to within ± 15 % by:-

$$\frac{\dot{m}'' d_o R_{st} T_\infty}{\Delta P_{st} D} = 0.47\, Re_v^{\frac{1}{2}}\, \pi_g^{\frac{1}{3}}\, \xi_g^{-0.6} \qquad (2.55)$$

where $\Delta P_{st} = P_{st\infty} - P_{sti}$

$\pi_g = \Delta P_{st}/P_\infty$

$\xi_g = P_{n\infty}/P_\infty$

Table 2.9 Range of experimental variables used by Berman and Fuks /87 /

Series	P_∞/kPa	ΔT/K	Re_v	$\tilde{W}_{air}$/%	$\dot{Q}''$/(kW/m^2)
1	9-91	4.5-66.0	425- 2760	0.01 -0.17	29-325
2	9-91	5.0-21.4	2310-11430	0.013-0.13	39-315

More recently, Mills et. al. /76 / carried out experiments with low-pressure, low-velocity, downward-flowing steam condensing, in the presence of air, on a copper-plated stainless-steel tube (19.1 mm o.d., 12.8 mm i.d., 76.1 mm long) using the apparatus shown in fig 2.18a. Considerable care was taken to minimise the possibility of contaminating the steam and to ensure a vacuum-tight apparatus. The tube wall temperature was measured by five thermocouples which were soldered into longitudinal grooves on the outside surface of the tube. The thermocouples were circumferentially spaced around the tube at 45° intervals. The heat flux was determined from condensate collection. Measurements were obtained for steam temperatures, bulk air mass fractions, oncoming vapour velocities and steam-to-wall temperature differences in the approximate ranges 307 to 333 K, 0.001 to 0.078, 0.277 to 0.88 m/s and 2.8 to 25.6 K respectively. The authors used the results of an analysis by Acrivos /88 /, for the boundary layers under strong suction, to correlate their results, see fig. 2.39, and obtained:-

$$g_m/g_m^* = (1 + (-1.18\ B_m/(1 + B_m)^{\frac{1}{2}})^{3/2})^{\frac{2}{3}} \qquad (2.56)$$

where $g_m = \rho_v U_\infty Sh/(Re_v Sc)$

$g_m^* = \rho_v U_\infty\ (0.43/(Re_v Sc) + 0.53/(Re_v^{\frac{1}{2}}\ Sc^{0.69}))$

$B_m = \omega - 1$

Rauscher et. al. /89 / performed experiments with low-pressure, low-velocity, downward flowing steam condensing, in the presence of air, on a horizontal copper-plated stainless-steel tube (19 mm o.d.) using the apparatus shown in fig. 2.18a. Considerable care was taken to minimise the possibility of contaminating the steam and to ensure a vacuum-tight apparatus. Five pairs of thermocouples were embedded in the tube wall and these were spread circumferentially around the tube wall at 45° intervals, fig. 2.40a. The thermocouples were calibrated as local heat flux meters which were used to determine the local heat flux around the tube. The local tube surface temperature was obtained from the measured local heat flux and the local temperature measured by the outermost wall thermocouple. In order to compare with the numerical results of Denny and South /30 /, data for the forward stagnation point were given. Measurments were obtained for the following approximate ranges:-

saturation temperature	37 to 66 $^{\circ}$C
bulk-to-wall temperature difference	1 to 17 K
bulk air mass fraction	0 to 0.07
on-coming vapour velocity	0.3 to 1.8 m/s

The experimental results were found to agree, to within ± 10 %, with the numerical solutions of Denny and South /30 /, fig. 2.40b. Moreover, it was also shown that the heat-transfer coefficient over the upper half of the tube is nearly constant, fig. 2.40c.

Very recently, Fujii et. al. / 52, 77 / carried out experiments with horizontal-flowing steam condensing, in the presence of air, on a horizontal tube using the apparatus shown in fig. 2.23. The tube used in these tests is the same one used in Series C of the pure steam tests, see Table 2.4. Measurements were obtained for the following approximate ranges:-

system pressure	37 - 85 kPa
saturation temperature	26.8 - 39.6 °C
bulk-to-wall temperature difference	5 - 15 K
vapour velocity	2.5 - 71 m/s
bulk air mass fraction	0 - 0.2
heat flux	30 - 110 kW/m^2

The results, together with those of Mills et. al. /76 /, were compared with the correlation of Berman and Fuks /87. / (see also / 90/) and the theoretically -based equation of Rose /72 / (i.e. equation 2.53c) in fig. 2.32. Good agreement was found with the equation of Rose / 72/ for the whole range of ω (i.e. W_∞/W_i) while it is evident that the correlation of /87, 90 / behaves incorrectly as $1/\omega$ approaches unity (i.e. low condensation rates or high gas mass fractions).

2.3.3.3 Summary

For the case of a stationary vapour condensing, in the presence of a non-condensing gas, on a vertical plate, the measurements, for steam-air, steam-argon, steam-neon and steam-helium mixtures, of Al-Diwany and Rose / 82/ are in good agreement with the approximate theoretical solution of Rose / 67/ (i.e. equation 2.47), which itself was in satisfactory agreement with more accurate numerical solutions /66 /. The measurements of /79-81 / which were higher than those predicted by the theory are thought to have been obtained in the presence of significant forced convection. For the case of the horizontal tube, the measurements of Othmer /78/, Hampson /83/, Provan /84/ and Henderson et. al. /85/ clearly show the detrimental effect of non-condensing gas. These measurements can be correlated satisfactorily by equation 2.54.

For the case of the moving vapour-gas mixtures, no data for the horizontal plate is apparently available in the literature. For the case of the vertical plate, the data of Asano et.al. /31 /, for steam-air, methanol-air, benzene-air and carbon tetrachloride-air mixtures, indicated similar general trends as those obtained by the above investigators (for the stationary vapour-gas mixtures case). For the horizontal tube case, limited data exists only for steam-air mixtures /52, 76, 77, 87, 89/. The data of Mills et. al. /76 / and Fujii et. al. /52,77 / agrees well with the theoretically-based equation of Rose /72 / (i.e. equation 2.53). It may be noted that the correlation of Berman and Fuks / 87, 90/ behaves incorrectly as W_i/W_∞ approaches unity (i.e. low condensation rates or high gas mass fraction).

2.4 Concluding remarks

It has been seen above that, for the case of a flowing pure vapour condensing on a horizontal tube, for low vapour velocities, the available data /42, 43, 50, 59, 60 / showed fair agreement with the uniform wall temperature theory /24, 49 - 51 / (see also footnote on page 48). However, in this region, the deviation from the Nusselt theory /2 / is small. With increasing vapour velocities, there is some evidence of departure from theory, and at very high vapour velocities, the discrepancies are large.

In addition, apart from the very low vapour velocity data of Gogonin and Dorokhov /59 /, all the other measurements were obtained for the case of steam only.

For the case of a flowing vapour condensing, in the presence of a non-condensing gas, on a horizontal tube, it appears that the limited data available /52, 76, 77, 87, 90 / are well represented by theory /72 /. However, it must be noted that these data are only for the steam-air case (i.e. essentially one Schmidt number).

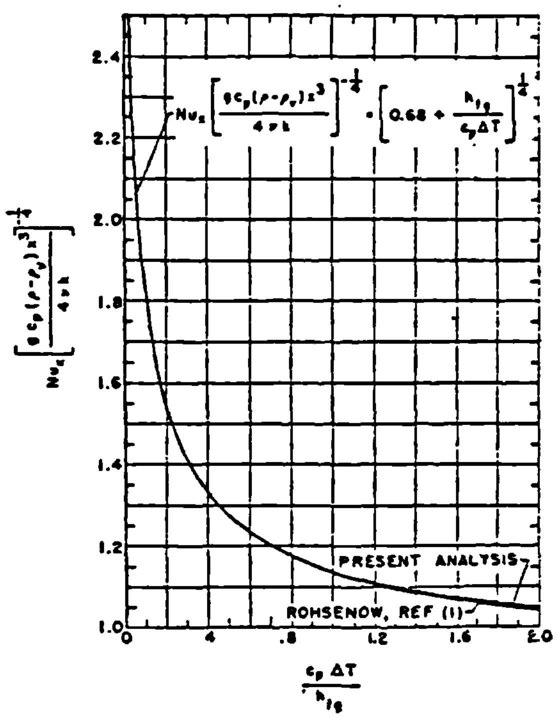

Fig. 2 Local heat-transfer results based on neglect of acceleration terms $\left(h_{avg} = \frac{4}{3} h_x\right)$

(a)

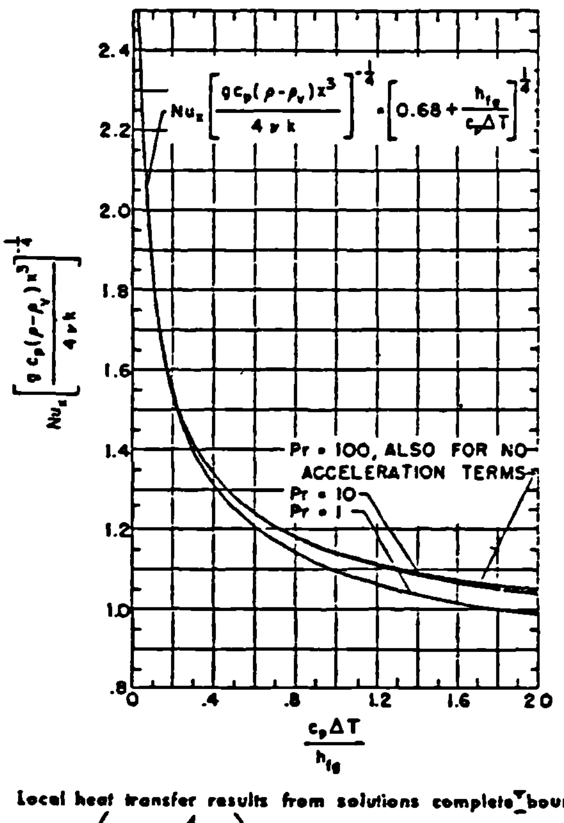

Fig. 5 Local heat transfer results from solutions complete boundary layer equations $\left(h_{avg} = \frac{4}{3} h_x\right)$

(b)

Figure 2.1 Reproduced from Sparrow and Gregg / 16/

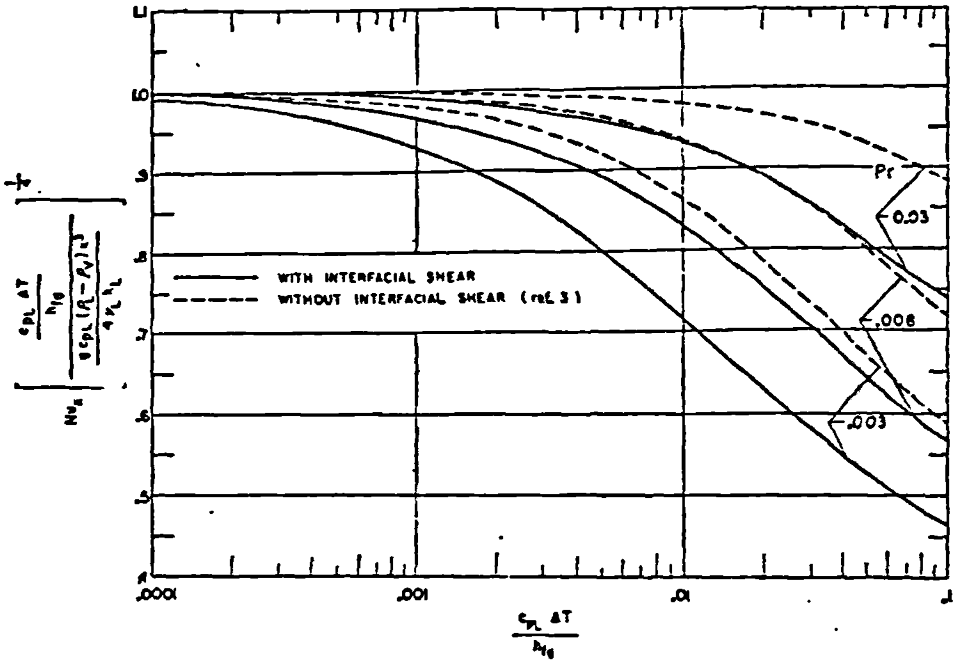

FIG. 3. Effect of interfacial shear stress on heat transfer, liquid metal range.

(a)

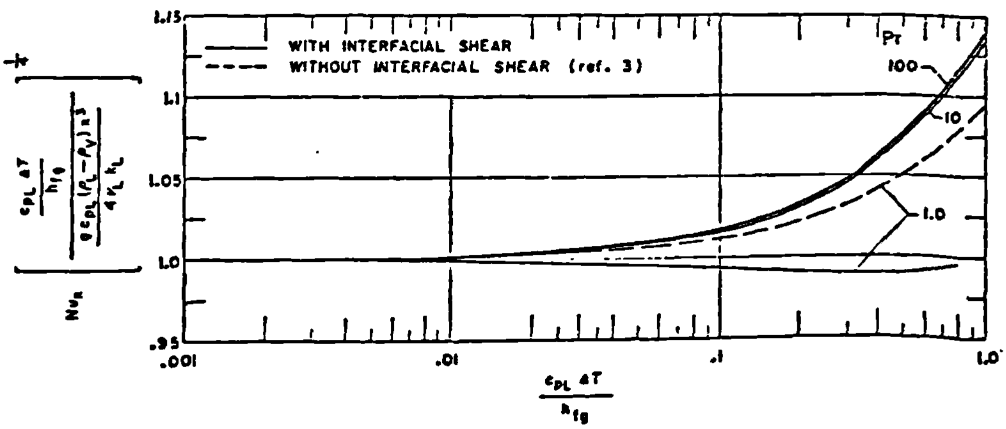

FIG. 2. Effect of interfacial shear stress on heat transfer, $Pr > 1$.

(b)

Figure 2.2 Reproduced from Koh et. al. /18 /

Figure 2.3 Reproduced from Chen /20 /

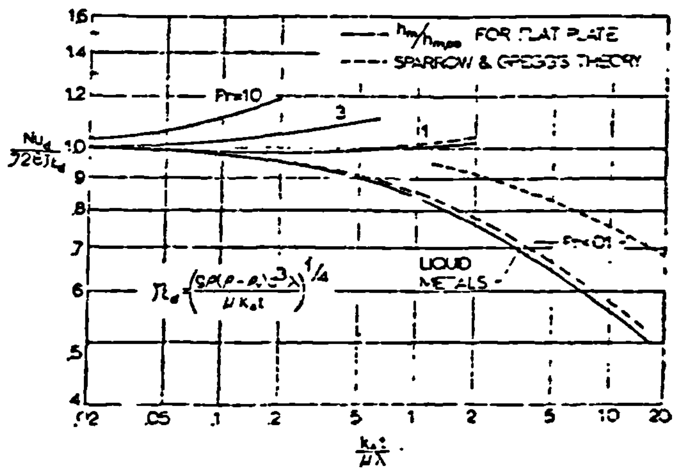

Fig. 5 Heat-transfer results for single horizontal tubes

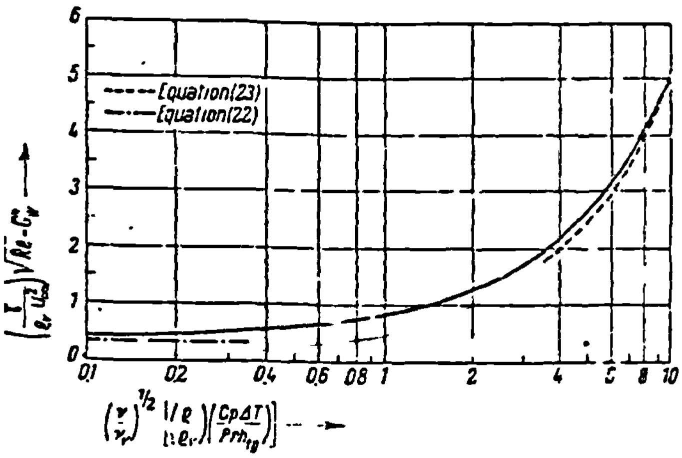

Figure 2
Variation of local shear stress.

(a)

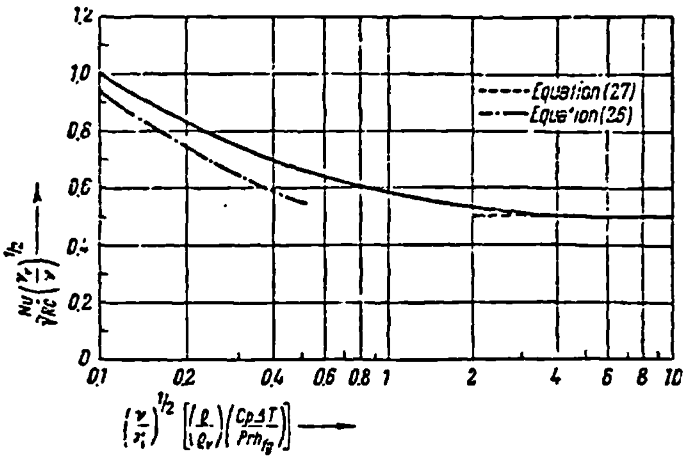

Figure 3
Variation of local Nusselt number.

(b)

Figure 2.4 Reproduced from Cess / 22 /

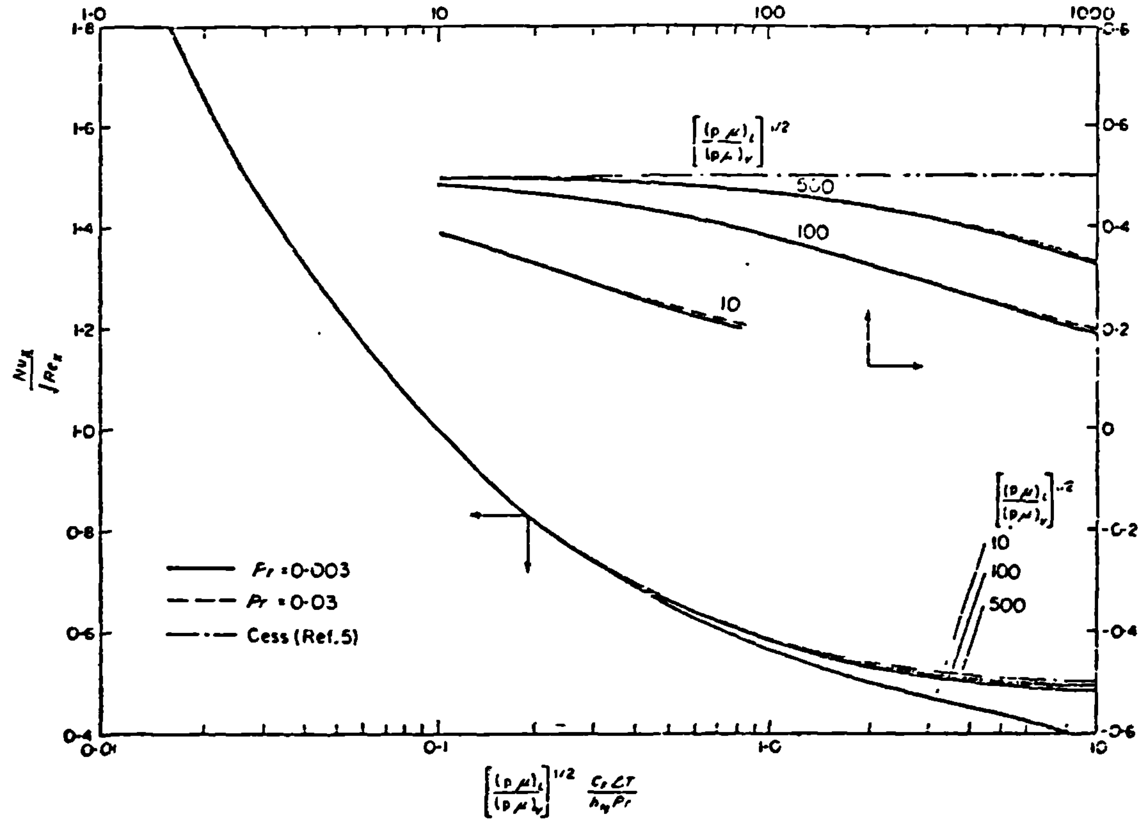

FIG. 8(a). Comparison of heat transfer between exact and approximate analysis (low Pr).
(a)

Figure 2.5 Reproduced from Koh / 23 /

Figure 2.5 (b)

Reproduced from

Koh /23 /

(continued)

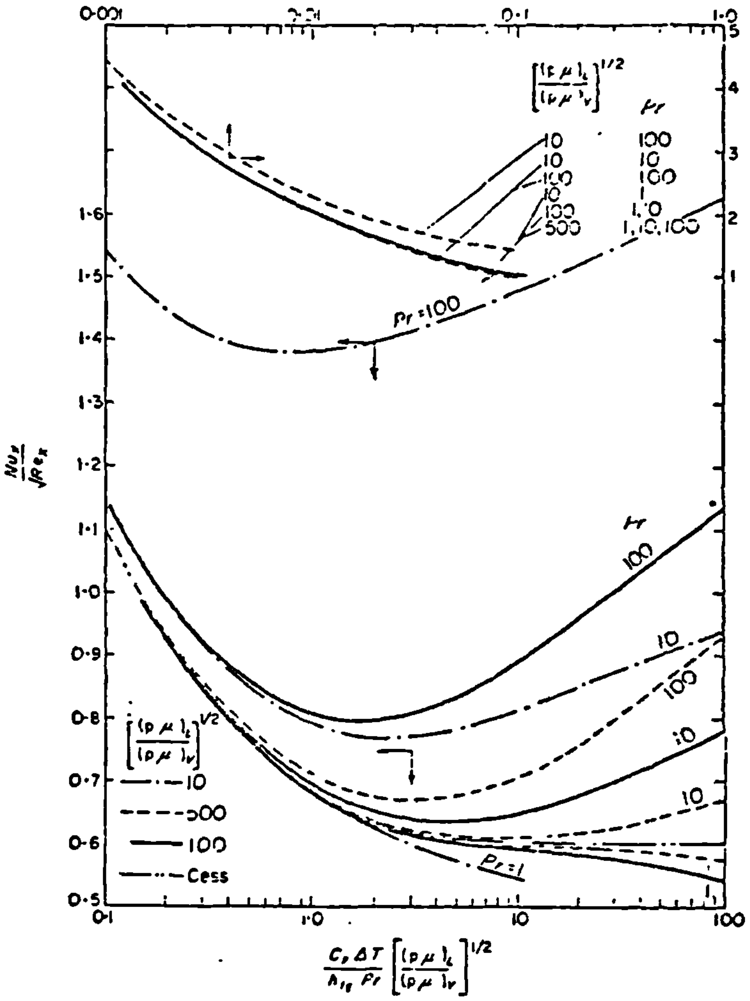

FIG. 8(b). Comparison of heat transfer between exact and approximate analyses (high Pr).

Figure 2.6 (a)

Reproduced from

Mayhew and Aggarwal /26 /

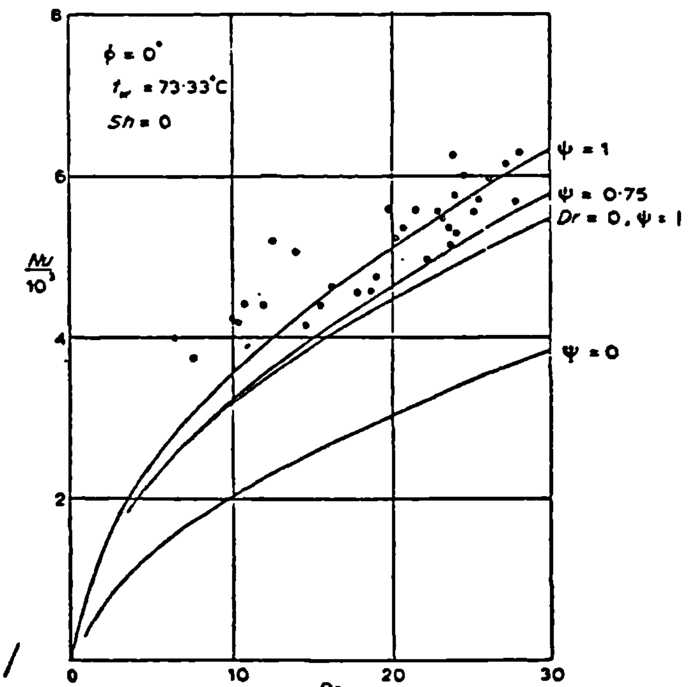

FIG. 1. Condensation on a horizontal plate with horizontal steam flow. (N.B. The scatter of experimental results in Figs. 1 and 2 is in part due to the fact that these results were obtained with various wall temperatures t_w lying mainly between 70°C and 78°C. The theoretical curves were computed for a nominal value of $t_w = 73{\cdot}33°C$. It was estimated that the variation of t_w in the range 70–78°C would account for a scatter band in Nu of about 200.)

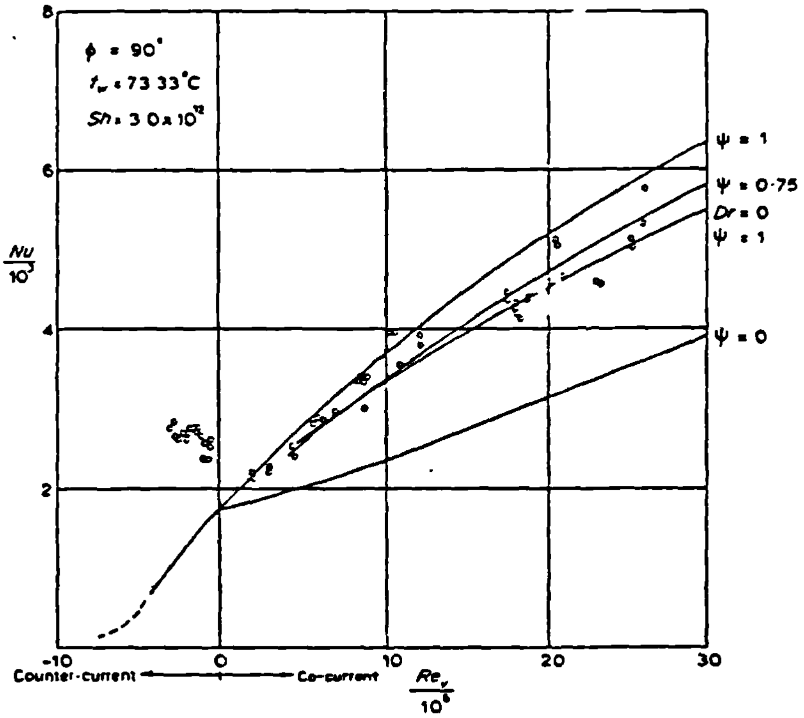

FIG. 2 Condensation on a vertical plate with counter-current and co-current steam flow.

Figure 2.6 (b) Reproduced from Mayhew and Aggarwal /26/ (continued)

Figure 2.7 Reproduced from Denny and South /27/

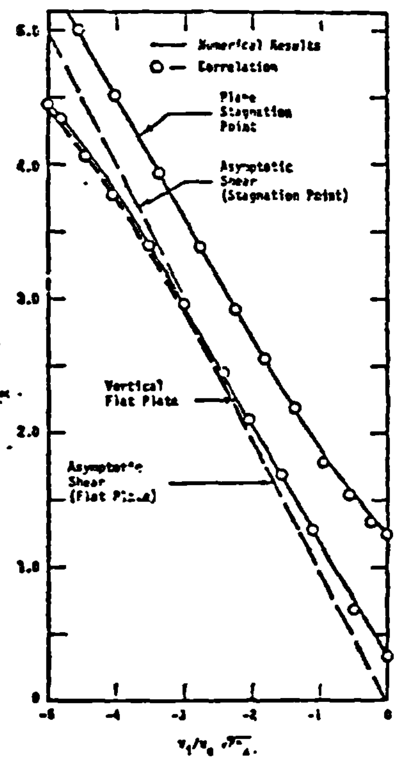

Fig. 2 Comparison of dimensionless shear correlation with numerical results for laminar film condensation down a vertical flat plate and a horizontal cylinder

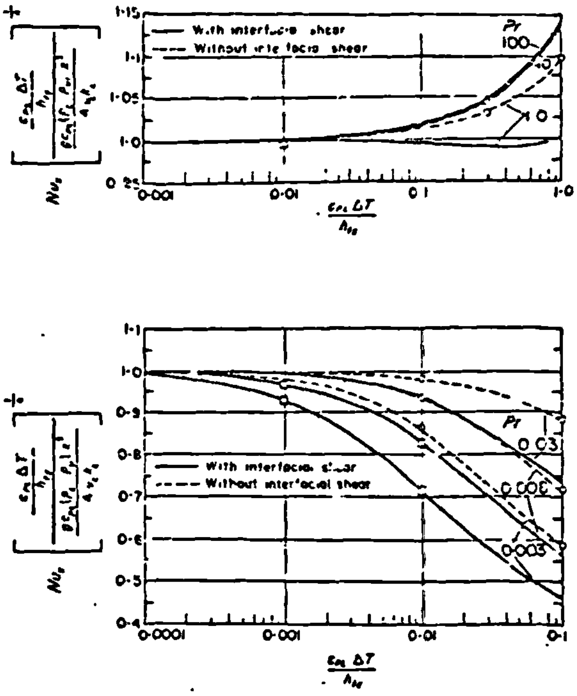

FIG. 2. Comparison of numerical solutions with similar solutions [2, 3] at zero vapor velocity. The numerical solutions with and without interfacial shear are represented by the symbols □ and ○ respectively.

(a)

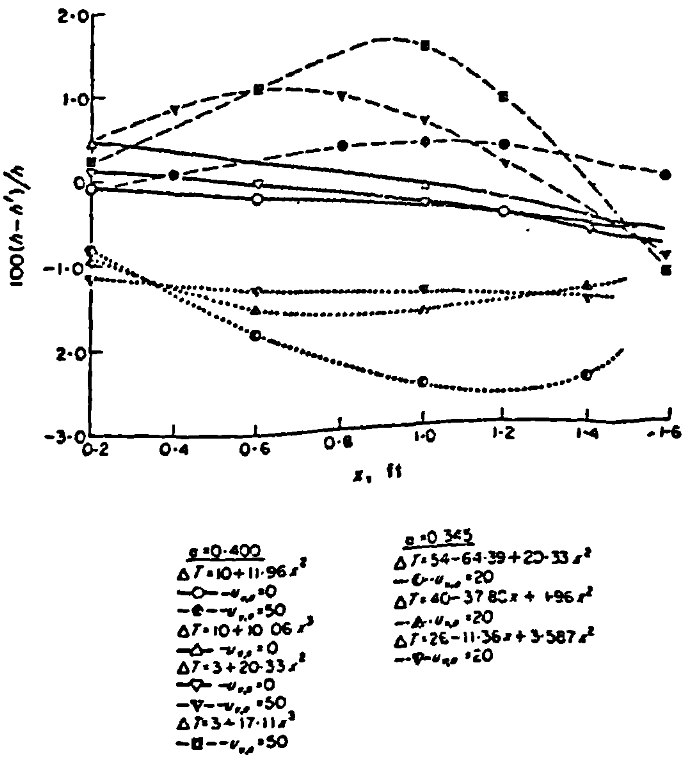

FIG. 4. Comparisons of equation (A.11) with the numerical results for condensation of water on a vertical nonisothermal wall.

(b)

Figure 2.8 Reproduced from Denny and Mills /28 /

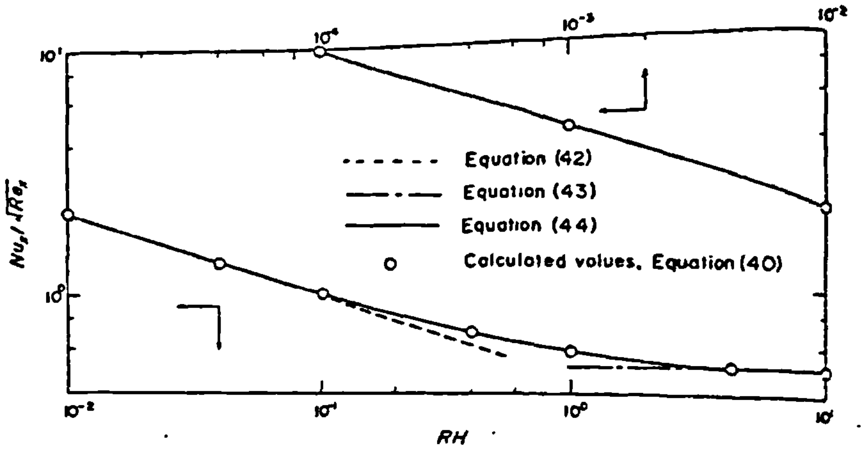

FIG. 2. Local coefficients of heat transfer in forced convection.

(a)

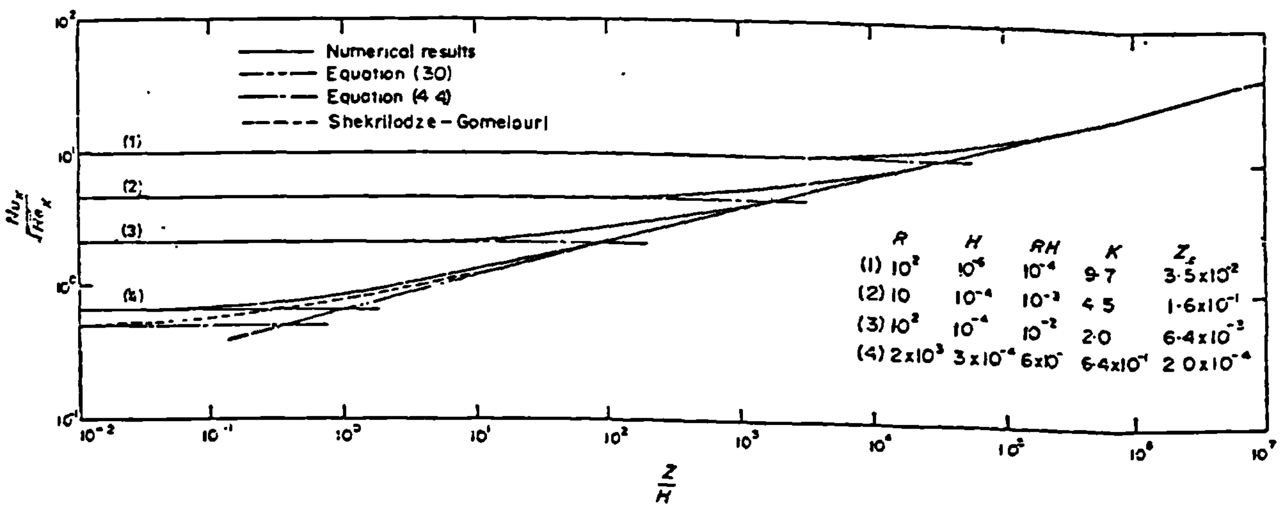

FIG. 3. Local coefficients of heat transfer in combined convection.

(b)

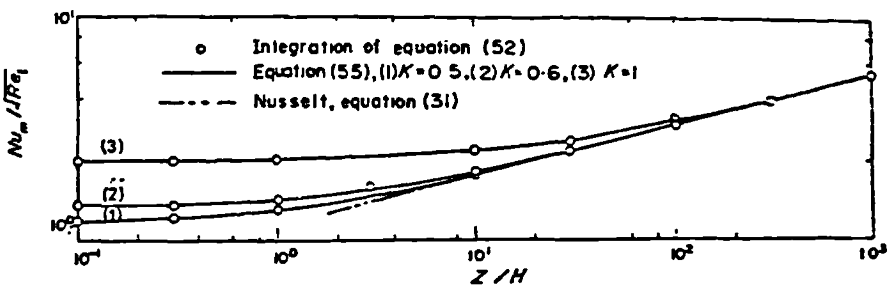

FIG. 4. Average coefficients of heat transfer in combined convection.

(c)

Figure 2.9 Reproduced from Fujii and Uehara /33 /

(a)

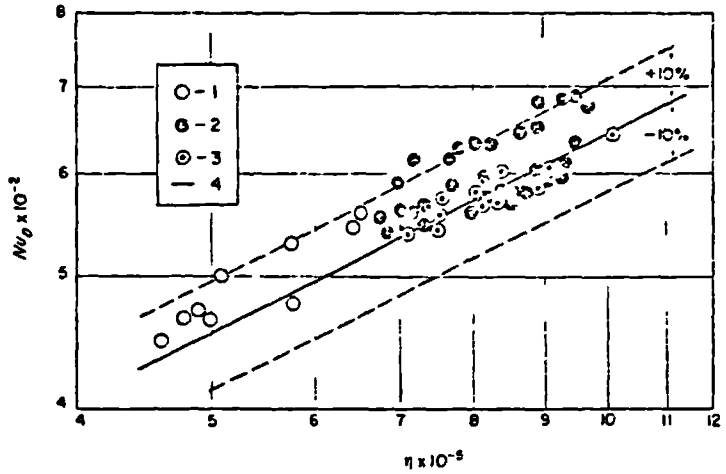

FIG. 5. Comparison of experimental data of Berman and Tumanov [14] with relation (28).
(1) P = 4·7 N cm², Δt = 7·4 degC, (2) P = 4·7 N cm², Δt = 2·5 degC; (3) P = 0·31 N/cm², Δt = 1·2 degC; (4) relation (28)

(b)

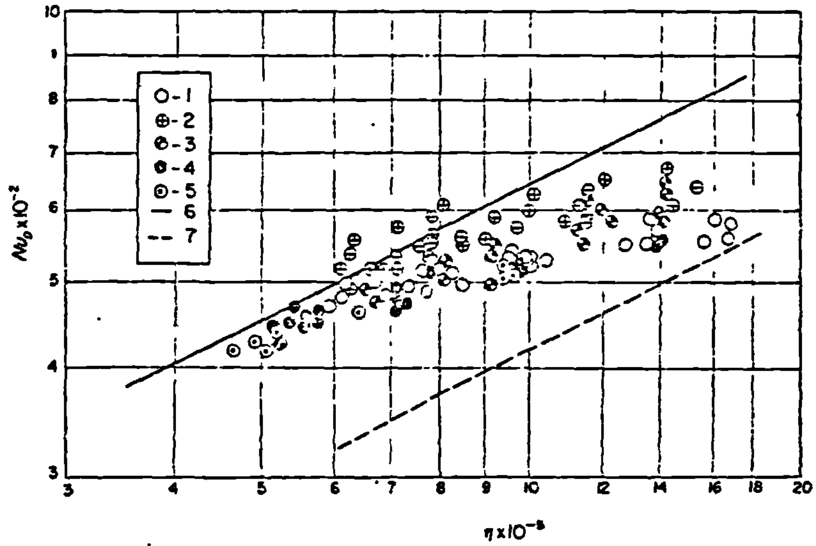

FIG. 6. Comparison of experimental data of Berman and Tumanov [14] with relations (28) and (29).
(1) P = 0·31 N/cm², Δt = 3·1 degC; (2) P = 0·86 N/cm², Δt = 2·2 degC; (3) P = 0·86 N/cm², Δt = 5 degC; (4) P = 0·86 N/cm², Δt = 6·4 degC; (5) P = 0·86 N/cm², Δt = 8·5 degC; (6) relation (28); (7) relation (29).

Figure 2.10 Reproduced from Shekriladze and Gomelauri /24/

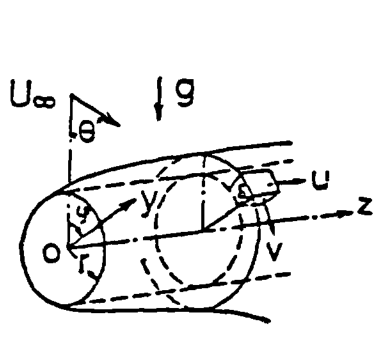

Fig.1 PHYSICAL MODEL AND COORDINATE SYSTEM

(a)

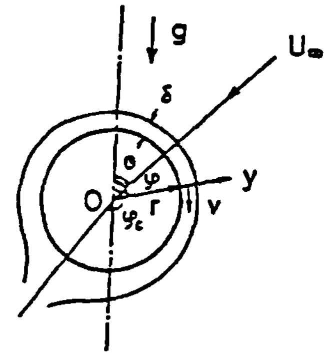

Fig.6. PHYSICAL MODEL AND COORDINATE SYSTEM

(b)

Figure 2.11 Reproduced from Honda and Fujii /35/

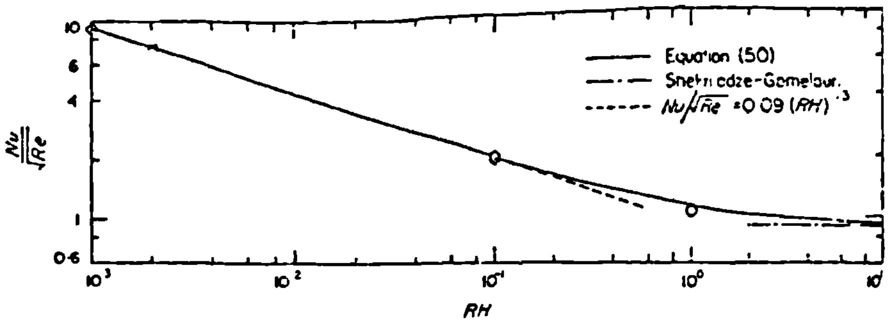

FIG. 5. Average Nusselt number in the case of large oncoming vapour velocity. Symbols correspond to those in Table 1 respectively.

(a)

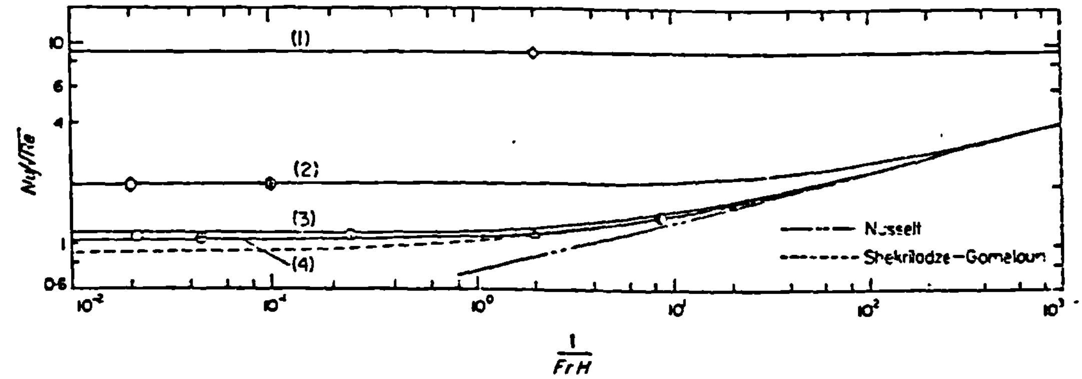

FIG. 6. Comparison between the numerical results and the values predicted by (53) on average Nusselt number. The curves (1), (2), (3) and (4) correspond to the cases of $RH = 10^{-3}, 10^{-1}$, 1 and 2 in (53) respectively. Symbols correspond to those in Table 1 respectively.

(b)

Figure 2.12 Reproduced from Fujii et. al. /49/

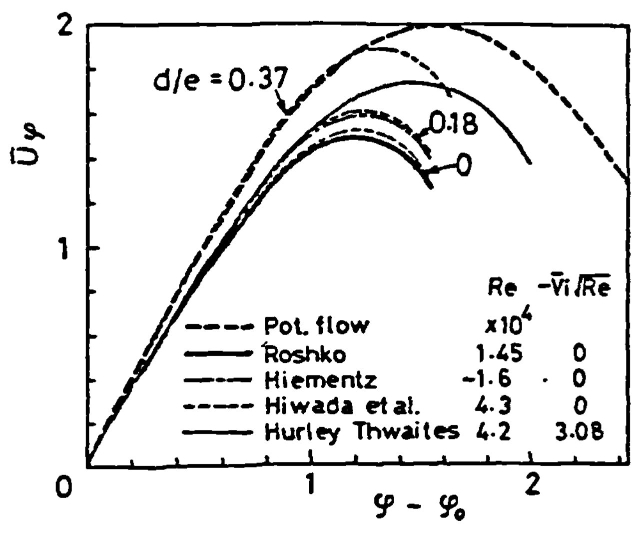

Fig.2 Comparison of distributions of mainstream velocity around a tube

Figure 2.13 (a) Reproduced from Fujii et. al. /50/

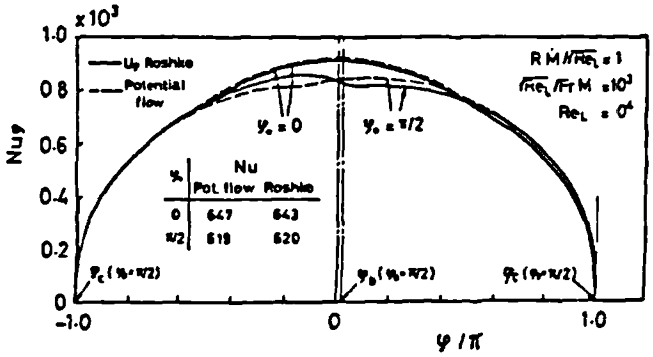

(a)

(b)

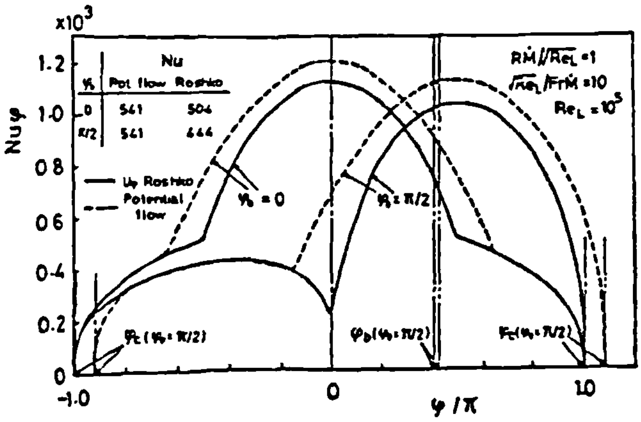

(b)

(c)

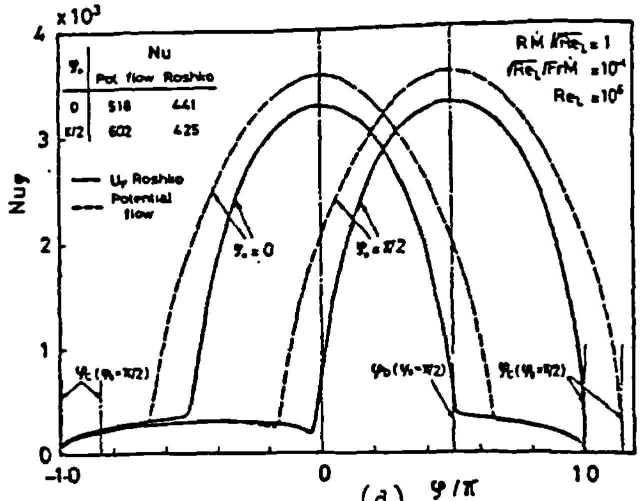

(d)

(c)

Fig.4 Circumferential distribution of local Nusselt number for uniform heat flux

(a) Body force convection
(b) Combined convection
(c) Forced convection

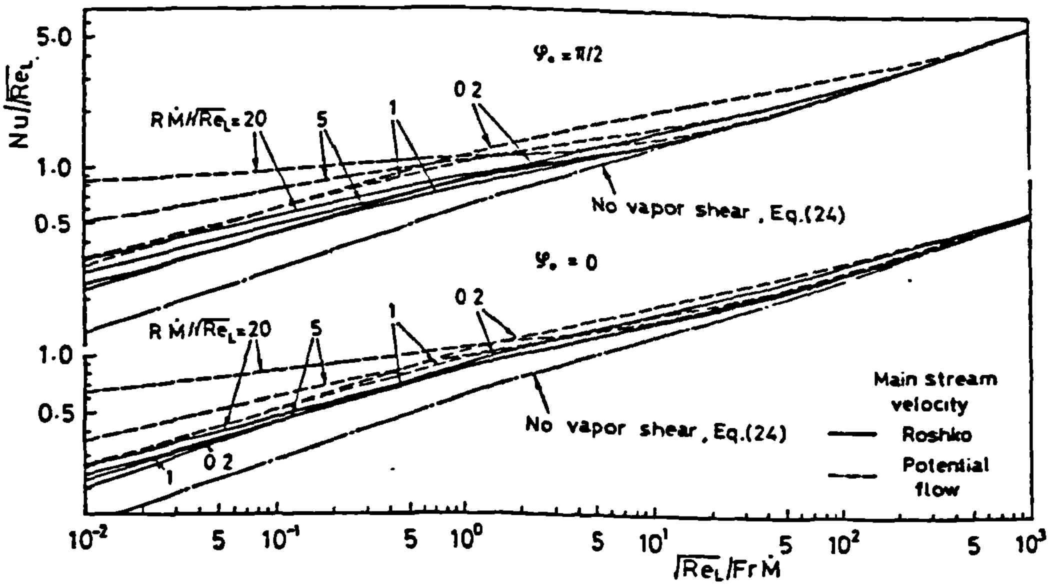

Fig.5 Relation between $Nu/\sqrt{Re_L}$ and $\sqrt{Re_L}/Fr\dot{M}$ for uniform wall heat flux and for downflow φ_0 = 0 and horizontal flow $\varphi_0 = \pi/2$

(e)

Figure 2.13 Reproduced from Fujii et. al. /50/ (continued)

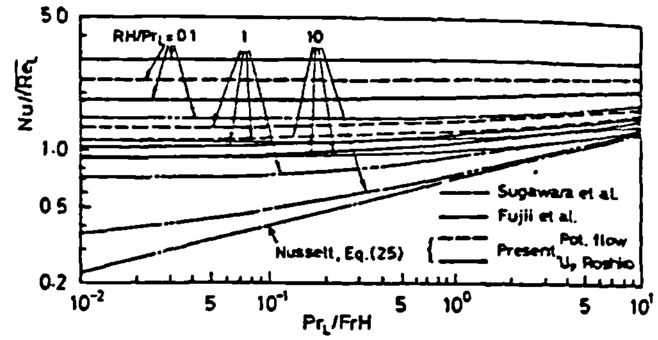

Fig.6 Relation between $Nu/\sqrt{Re_L}$ and Pr_L/FrH for uniform wall temperature and for downflow $\varphi_0 = 0$

(f)

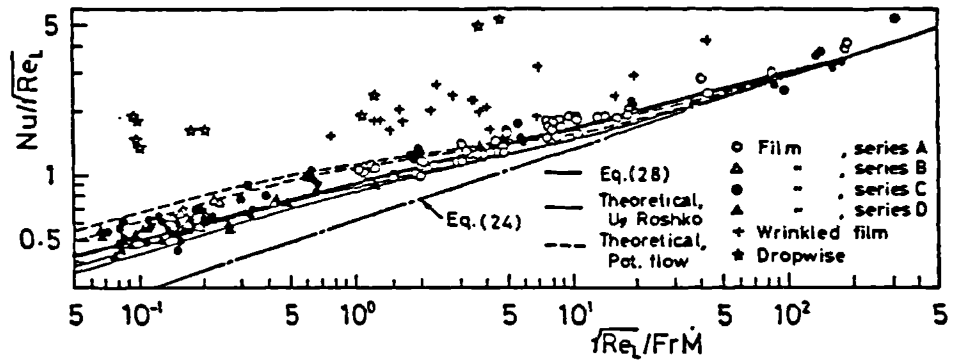

Fig.9 Comparison of experiment with theory for average heat transfer coefficient in the relation between $Nu/\sqrt{Re_L}$ and $\sqrt{Re_L}/FrM$

(g)

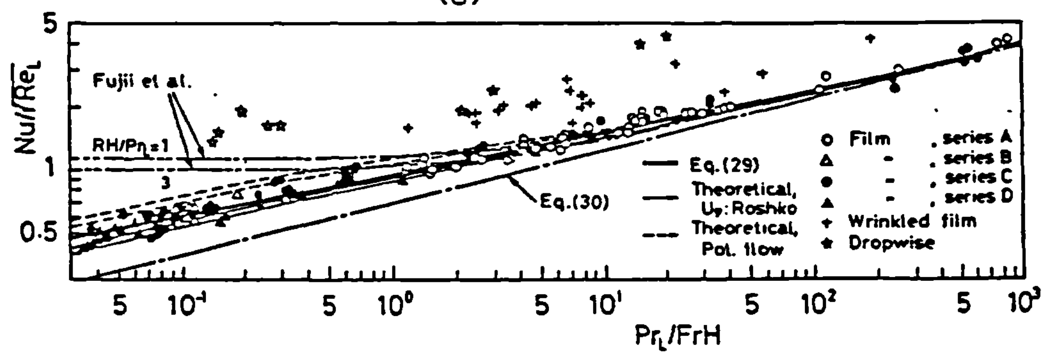

Fig.10 Comparison of experiment with theory for average heat transfer coefficient in the relation between $Nu/\sqrt{Re_L}$ and Pr_L/FrH

(h)

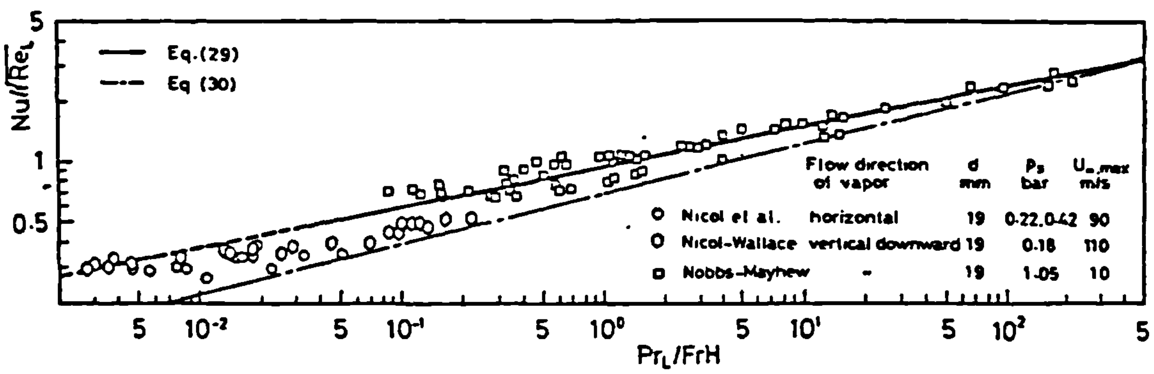

Fig.11 Comparison of the proposed experimental equations for average Nusselt number with experimental data hitherto reported

(i)

Figure 2.13 Reproduced from Fujii et. al. /50/ (continued)

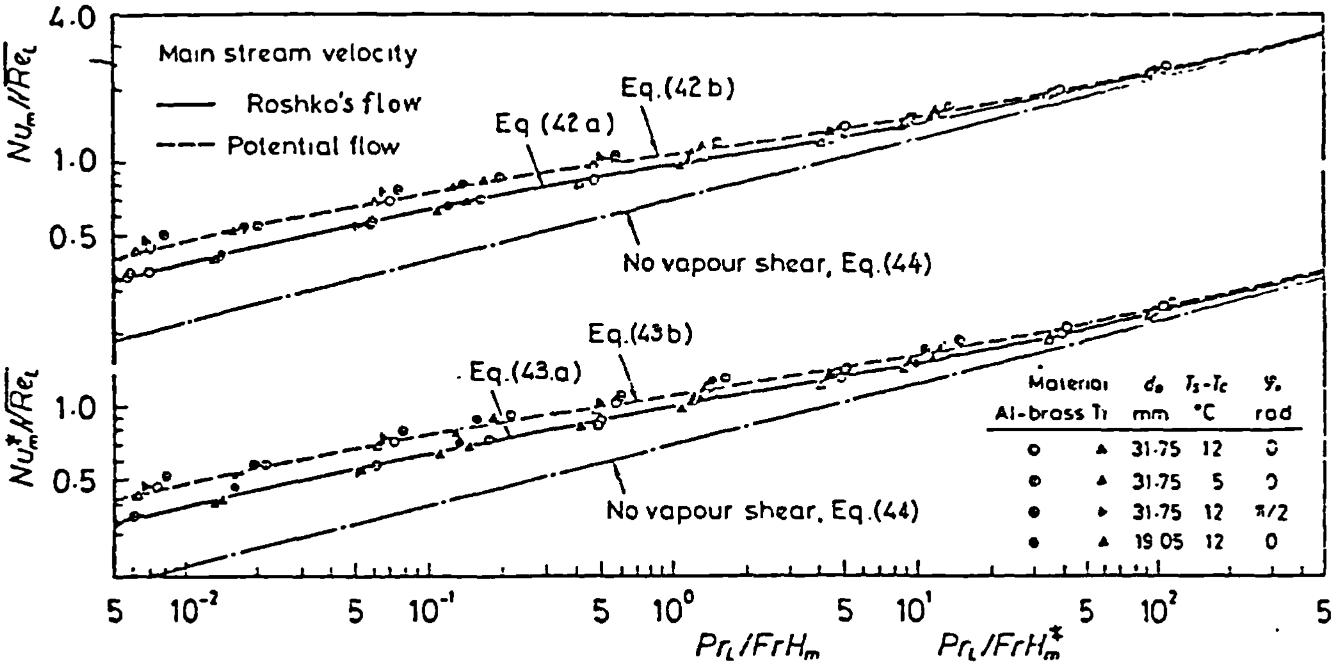

Fig. 7 Average Nusselt number for aluminium-brass and titanium tubes in common use[15]

Figure 2.14 Reproduced from Fujii /52/

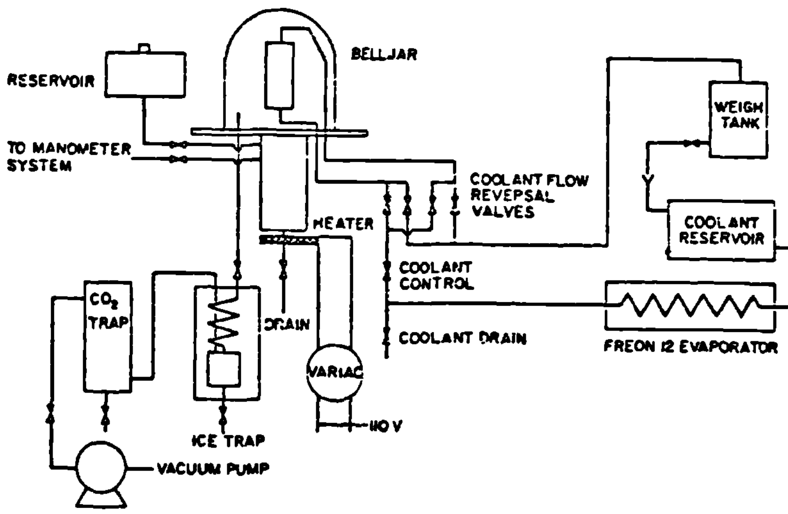

FIG. 1. Flow diagram of the experimental system.

Figure 2.15 (a) Reproduced from Mills and Seban / 9 /

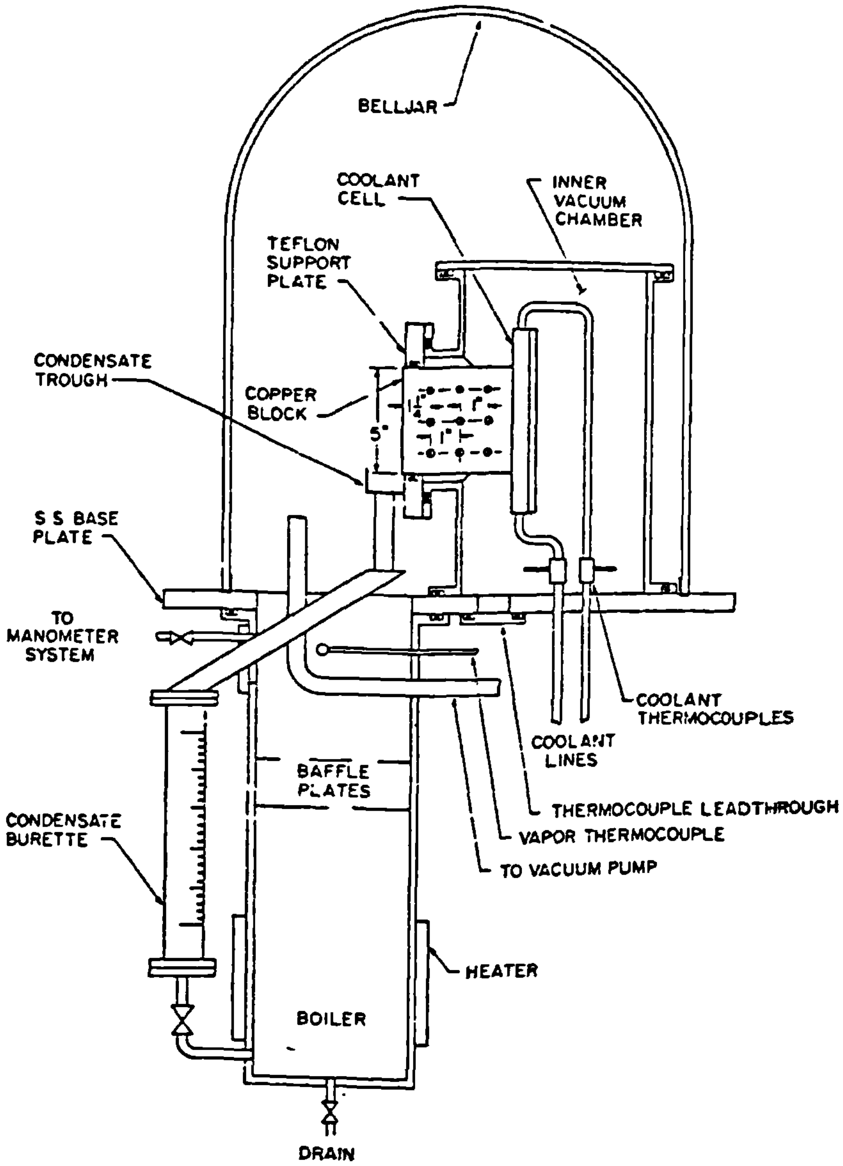

FIG. 2. Schematic drawing of the bell jar system.

Figure 2.15 (b) Reproduced from Mills and Seban /9 /
(continued)

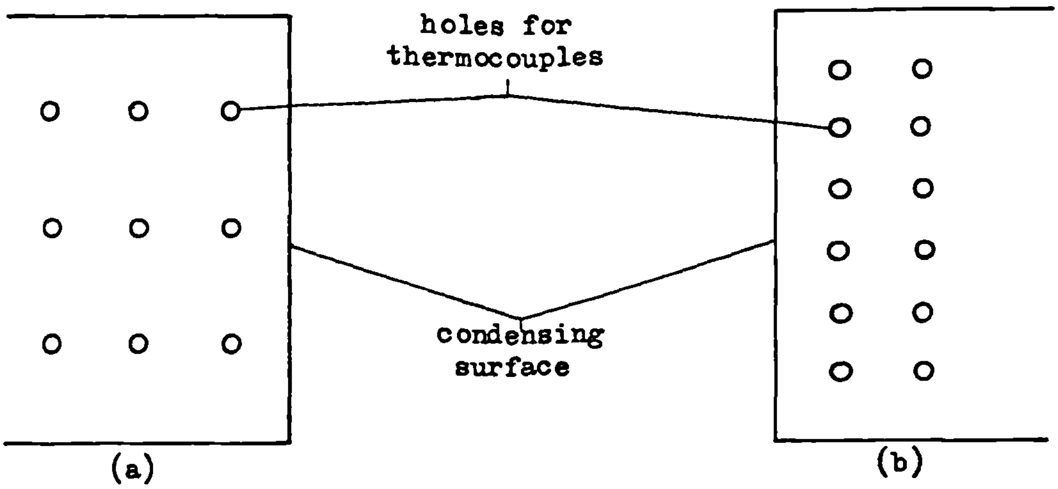

Figure 2.16 Arrangement of the wall thermocouples in the tests of (a) Mills and Seban / 9 /
(b) Slegers and Seban /10 /

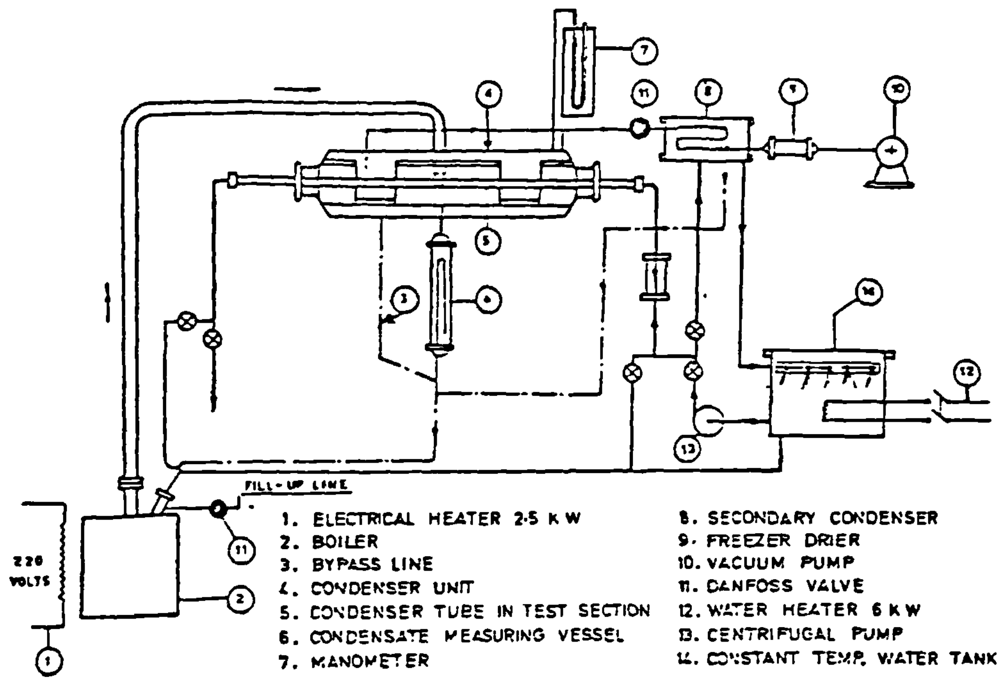

Fig. 2 — Schematic layout of apparatus

Figure 2.17 Reproduced from Magal /11 /

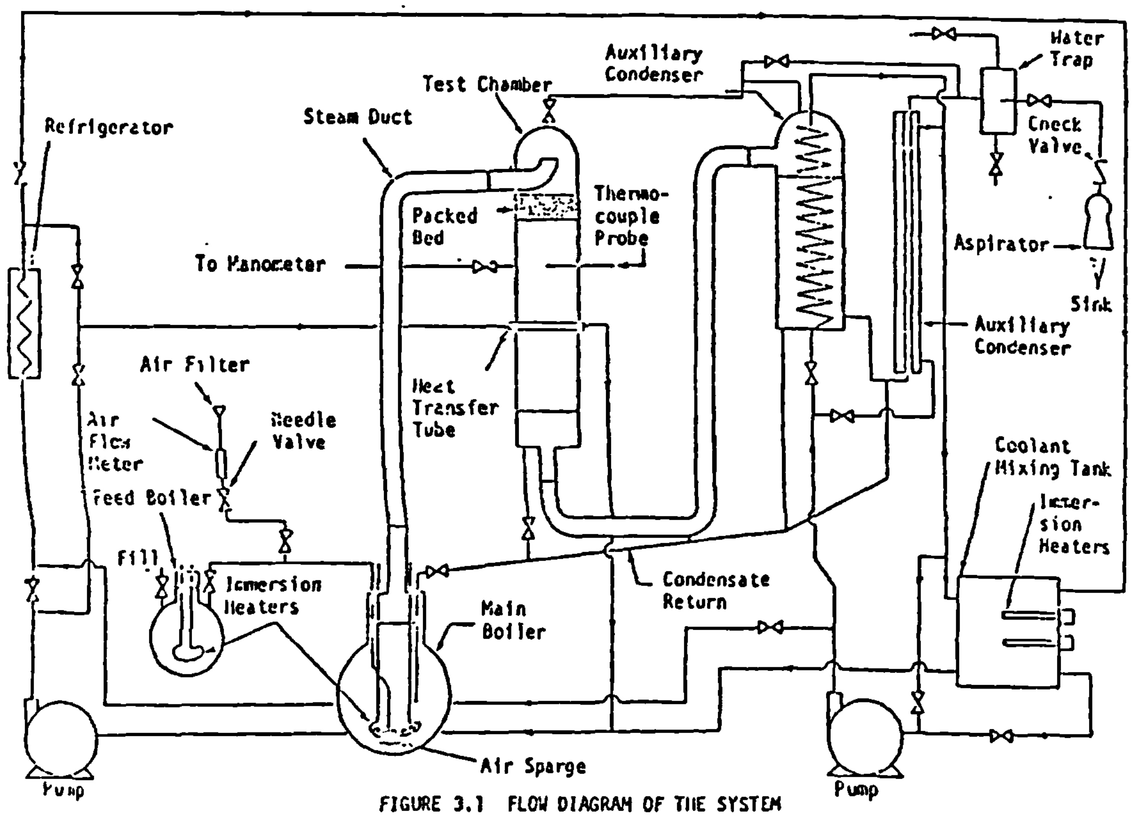

FIGURE 3.1 FLOW DIAGRAM OF THE SYSTEM

Figure 2.18 (a) Reproduced from Chung / 12/

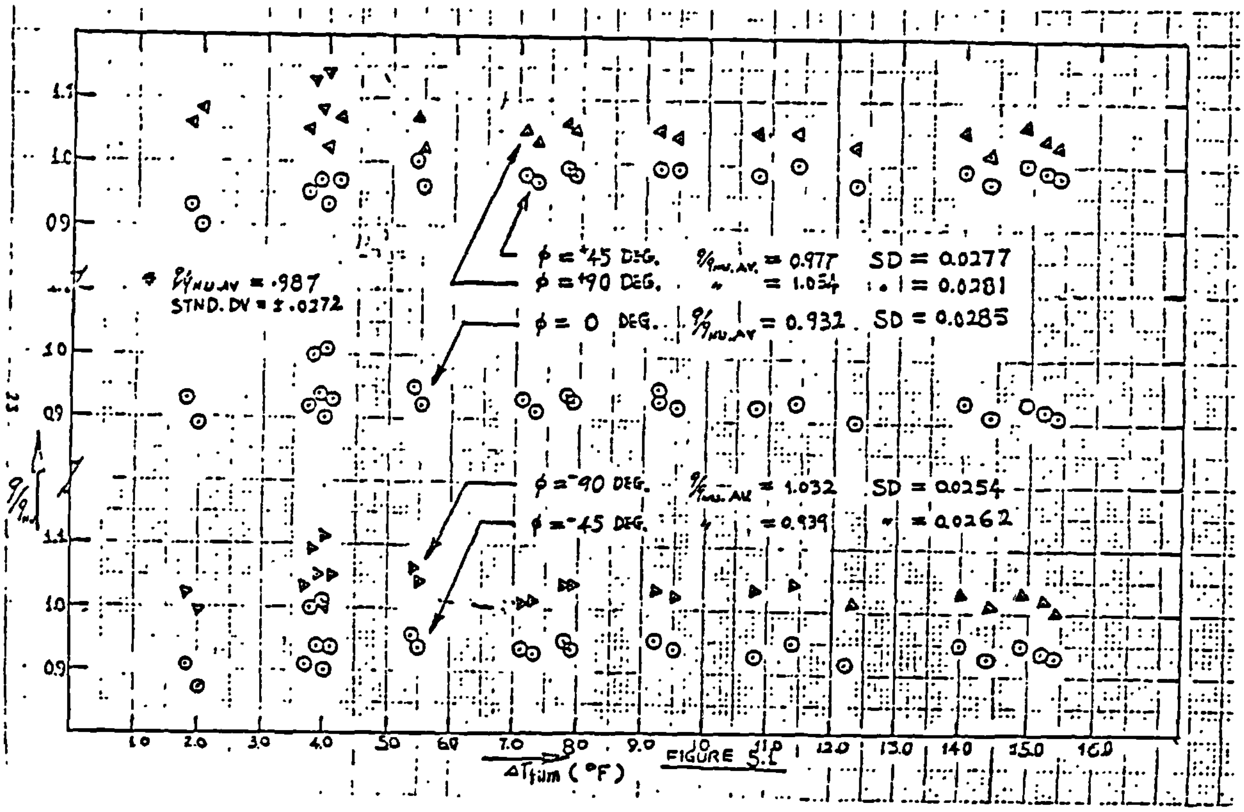

(b)

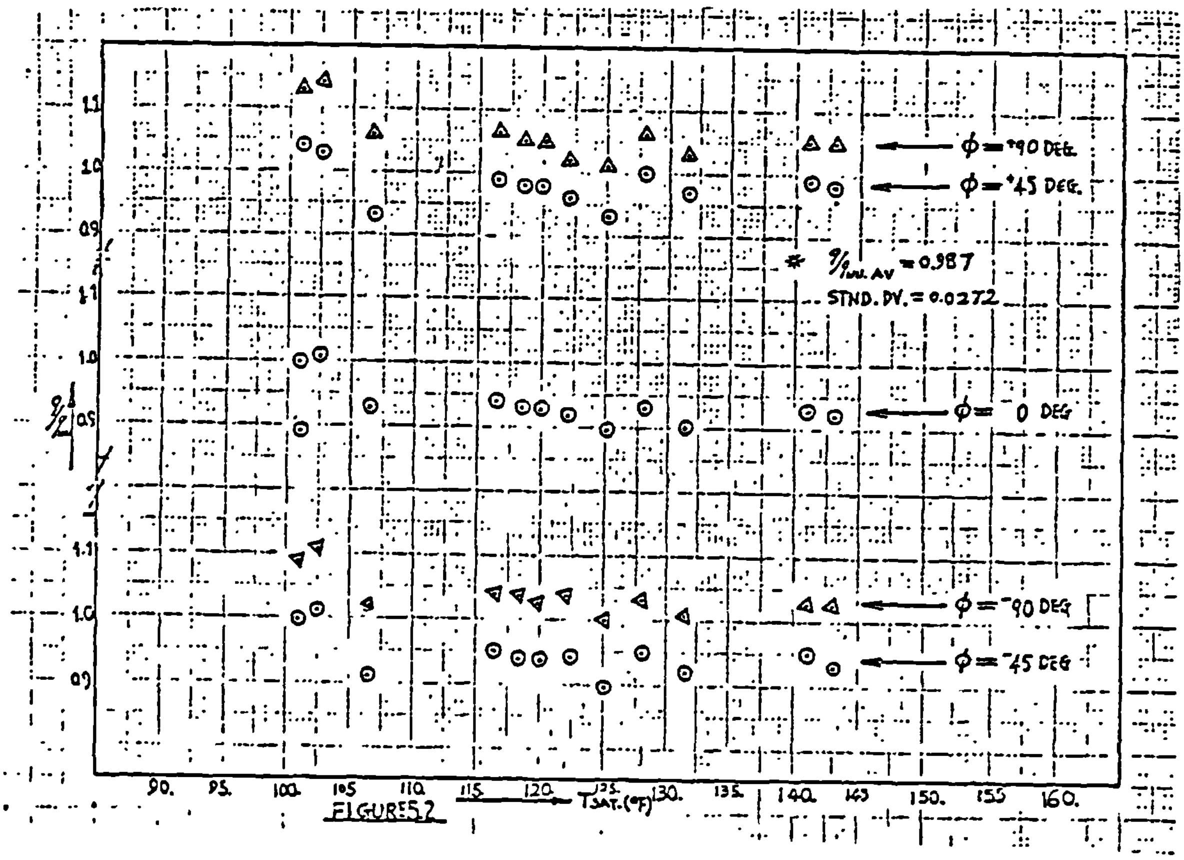

(c)

Figure 2.18 Reproduced from Chung / 12/ (continued)

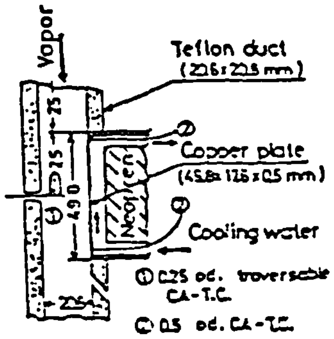

Fig. 2 Details of test section

(a)

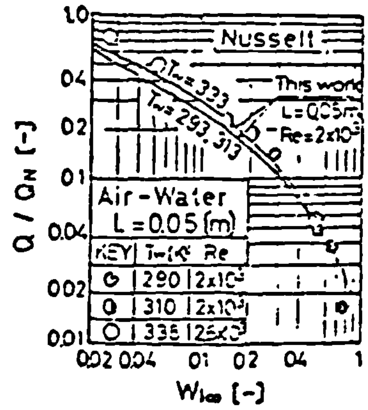

Fig. 10 Effect of noncondensable gas on the overall rate of heat transfer through condensate liquid film (wall heat flux); a comparison with theory

(b)

Figure 2.19 Reproduced from Asano et. al. / 31/

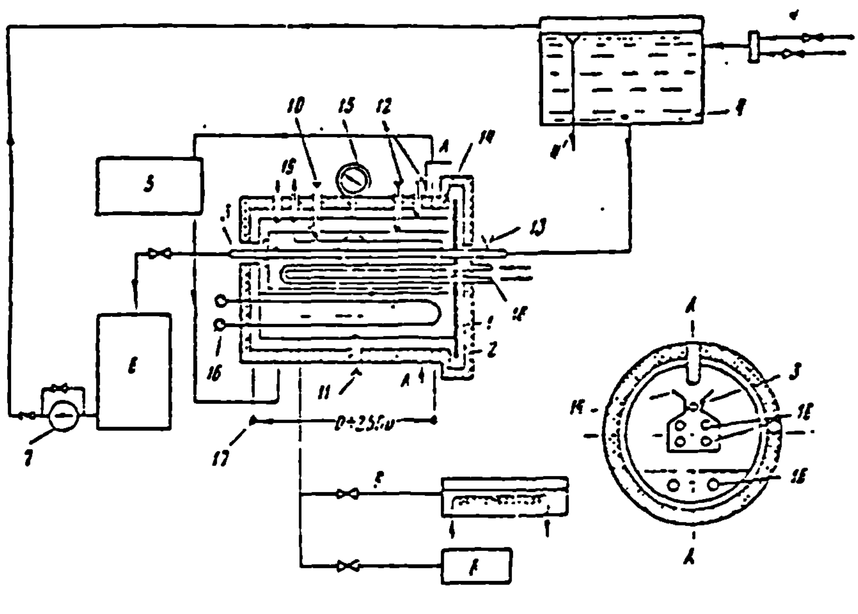

Fig. 2.

(a)

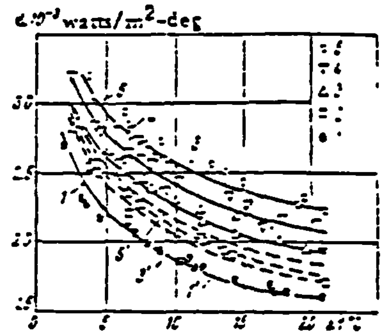

Fig. 3.

(b)

Figure 2.20 Reproduced from Gogonin and Dorokhov /59 /

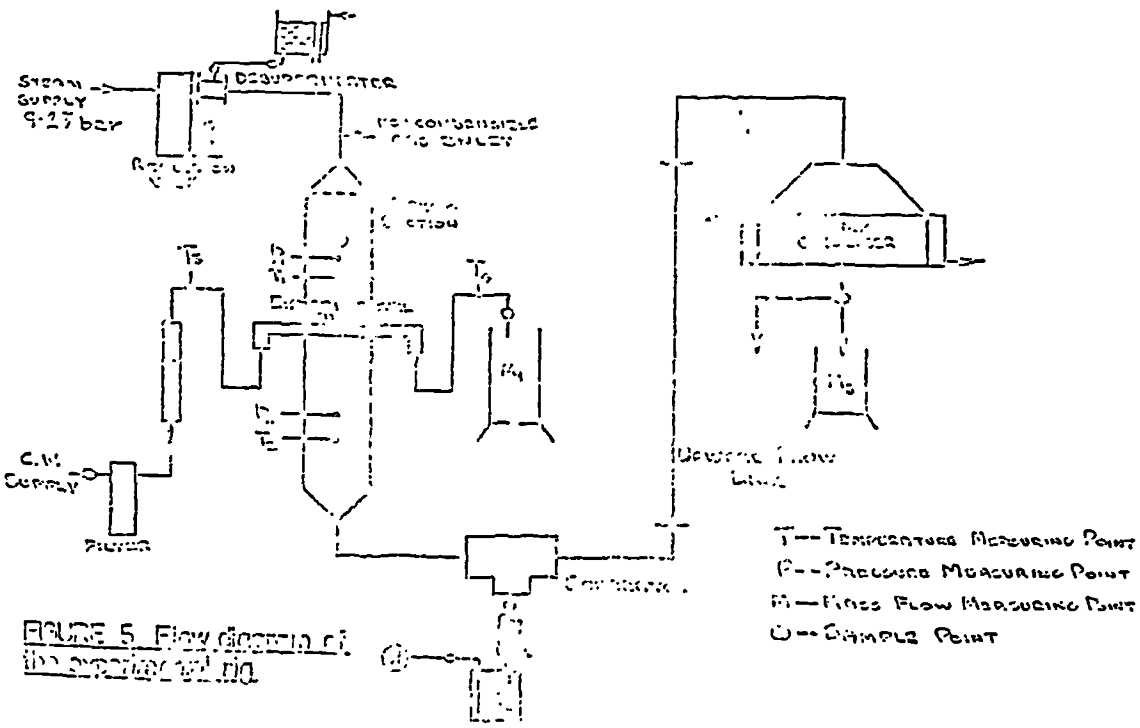

(a)

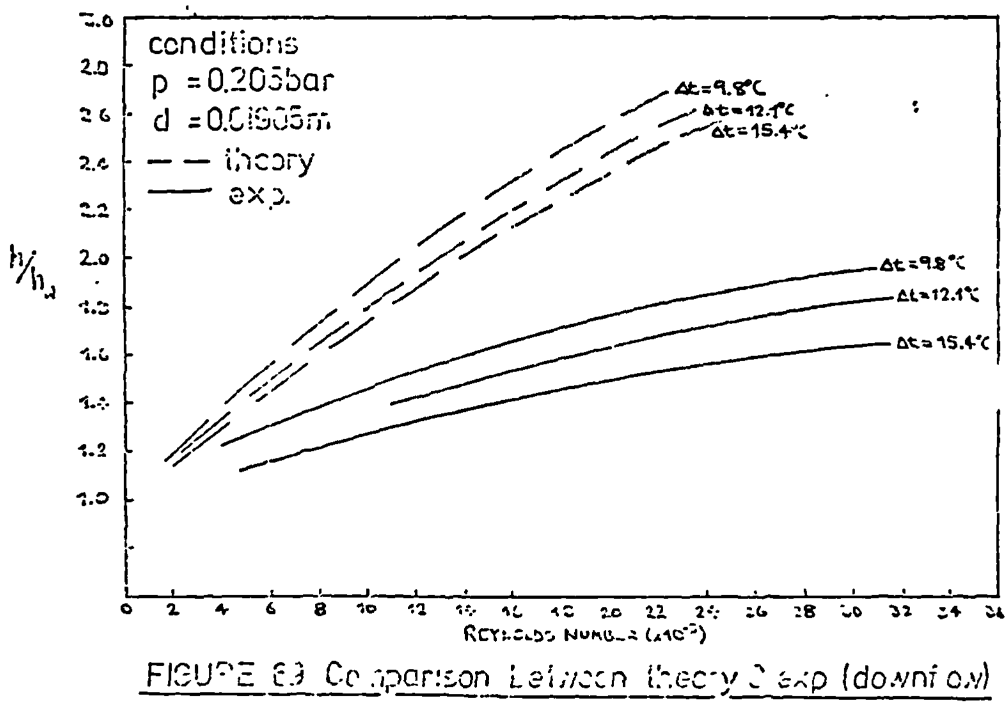

(b)

Figure 2.21 Reproduced from Wallace /38/

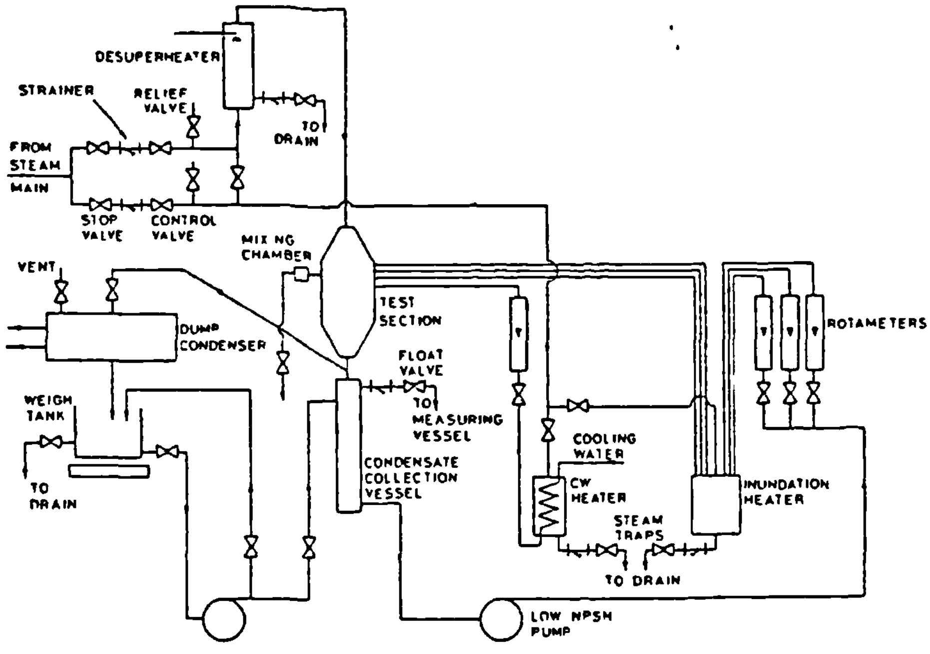

Fig. 8.4 Line Diagram of Rig

(a)

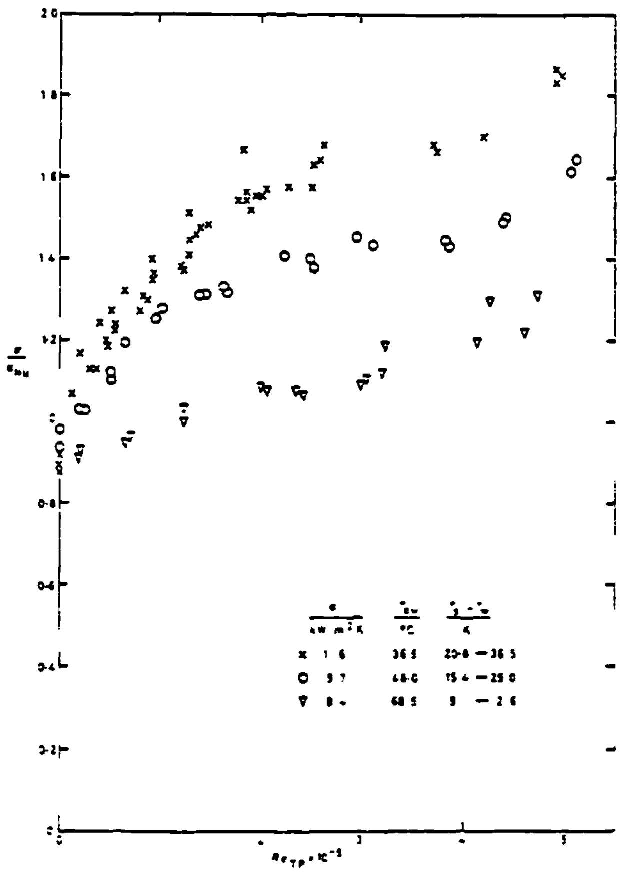

Fig. 8.8 Single Tube Tests with Constant Cooling Water Conditions

(b)

Figure 2.22 Reproduced from Nobbs and Mayhew /43

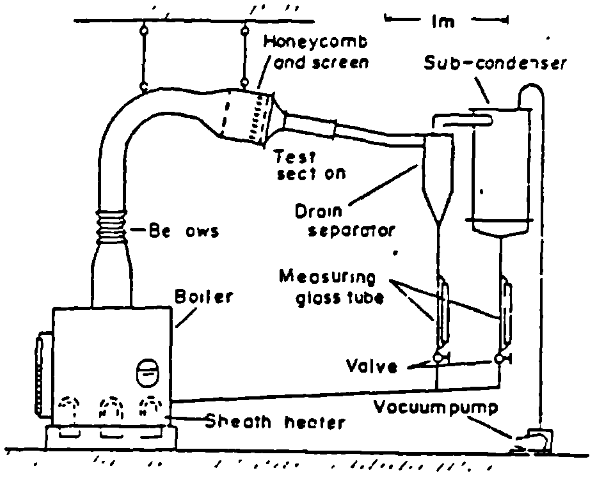

FIG. 1. A circulation loop of steam and the condensate.

Figure 2.23 Reproduced from Fujii et. al. /61/

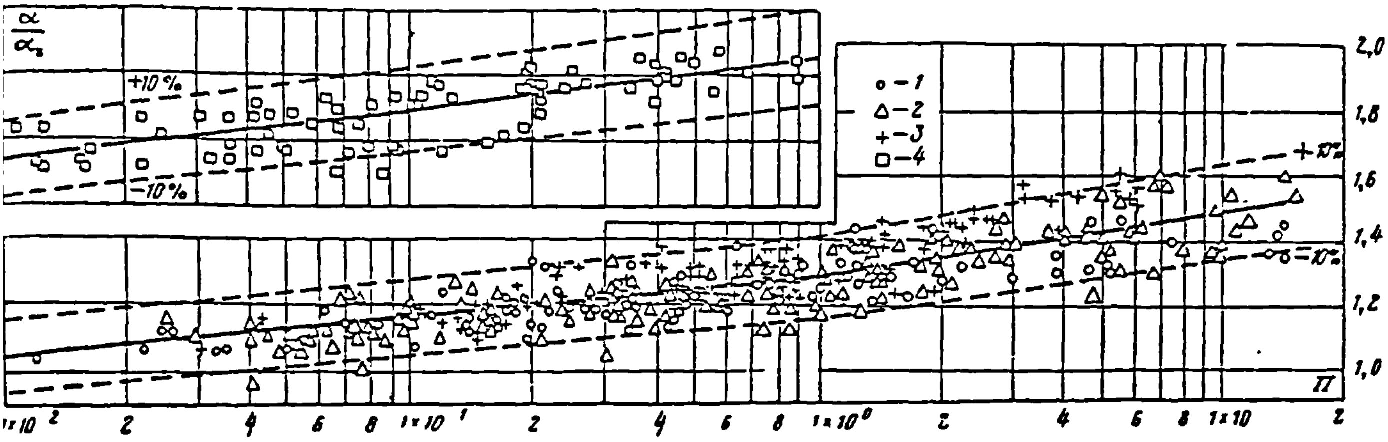

FIG. 1. Dependence of α/α_s on Π with condensation of steam.
est series I (steam pressure 0.032 bar); 2 – series II (0.046 bar); 3 – series III (0.086 bar); 4 – series IV (0.49 ba

Figure 2.24 Reproduced from Berman /62/

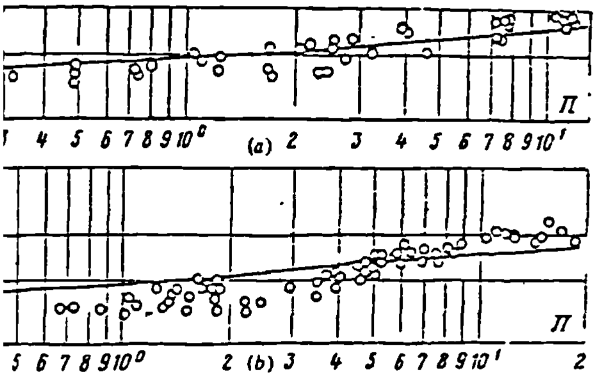

. Experimental dependences of α/α_s on Π.
es were plotted by equation (4). Experimental
) steam according to Ref. 22; b) freon-21 vapour
g to Ref. 23.

(a)

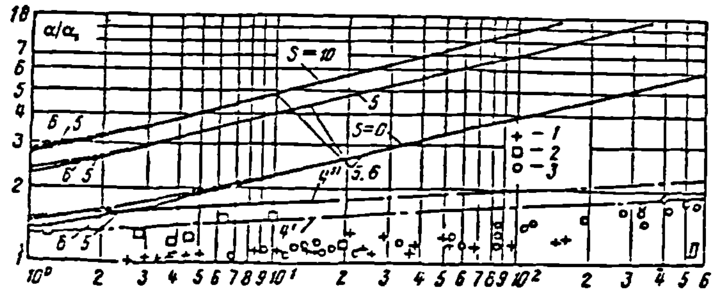

Figure 3. Experimental and calculated dependences of α/α_s on Π. 1) according to Ref. 16, p = 4.7–51 kPa; 2) according to experiments in Ref. 17, p = 4.8 kPa; 3) according to experimental data [12]; according to experimental equation (4): 4′) for p = 3.2–8.6 kPa; 4″) for p = 47 kPa; 5) curve calculated by equation (6); 6) by equation (8).

(b)

Figure 2.25 Reproduced from Berman /63/

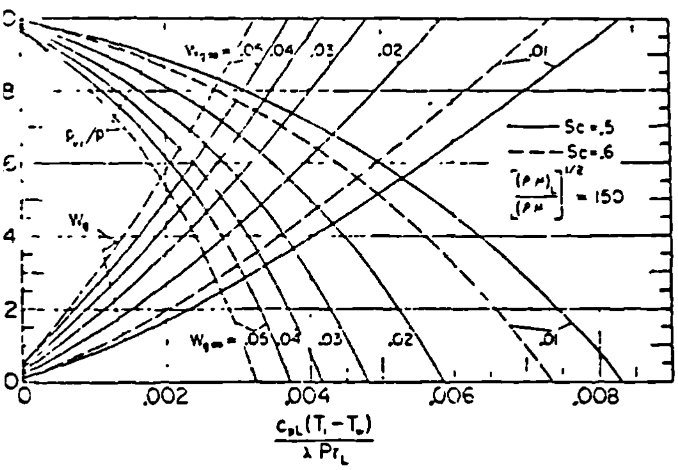

Fig. 2 Interfacial concentration of noncondensable gas and partial pressure of vapor $[(\rho\mu)_L/\rho\mu]^{1/2} = 150$

(a)

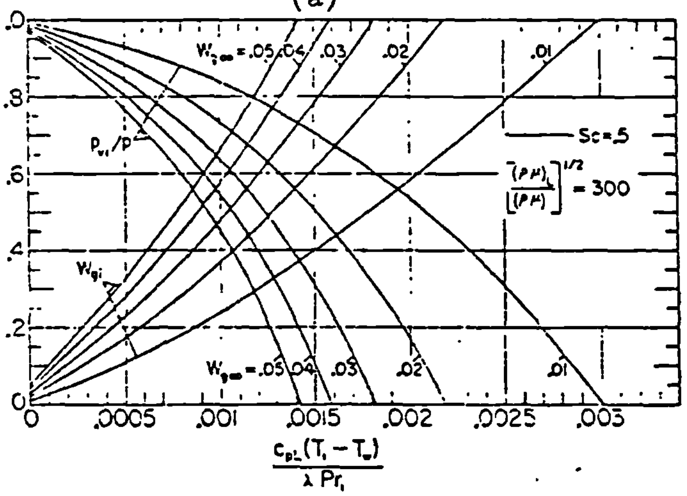

Fig. 3 Interfacial concentration of noncondensable gas and partial pressure of vapor $[(\rho\mu)_L/\rho\mu]^{1/2} = 300$

(b)

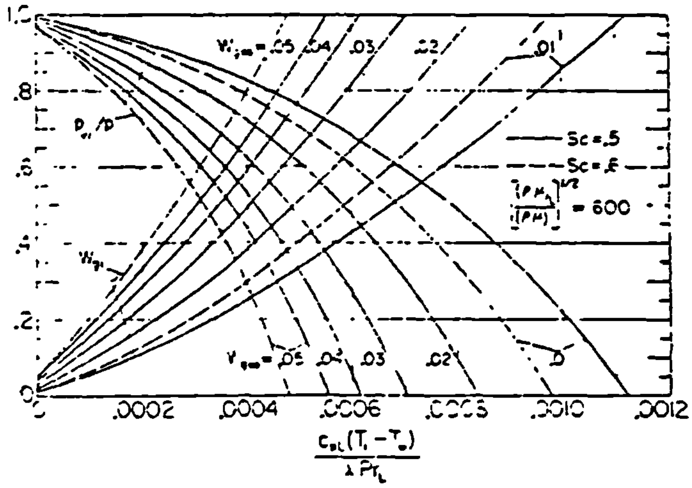

Fig. 4 Interfacial concentration of noncondensable gas and partial pressure of vapor $[(\rho\mu)_L/\rho\mu]^{1/2} = 600$

(c)

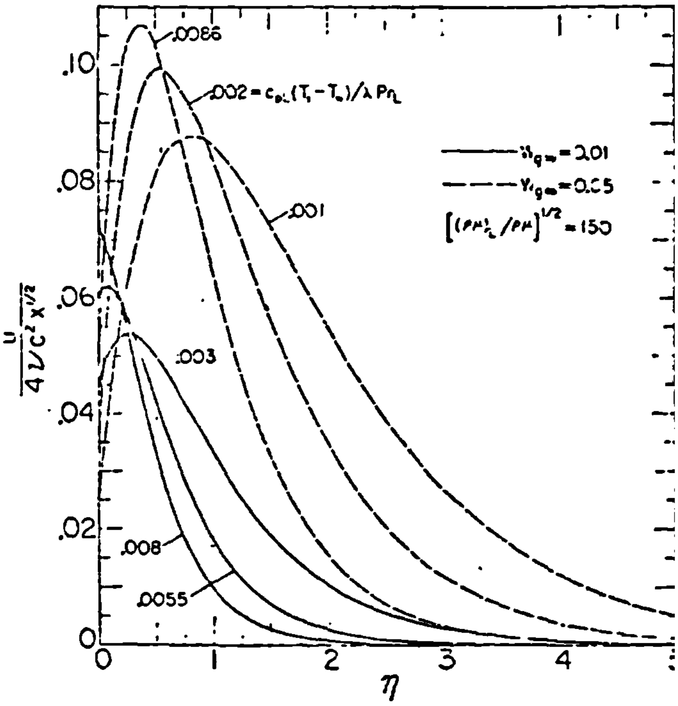

Fig. 8 Representative velocity profiles $[(\rho\mu)_L/\rho\mu]^{1/2} = 150$

(d)

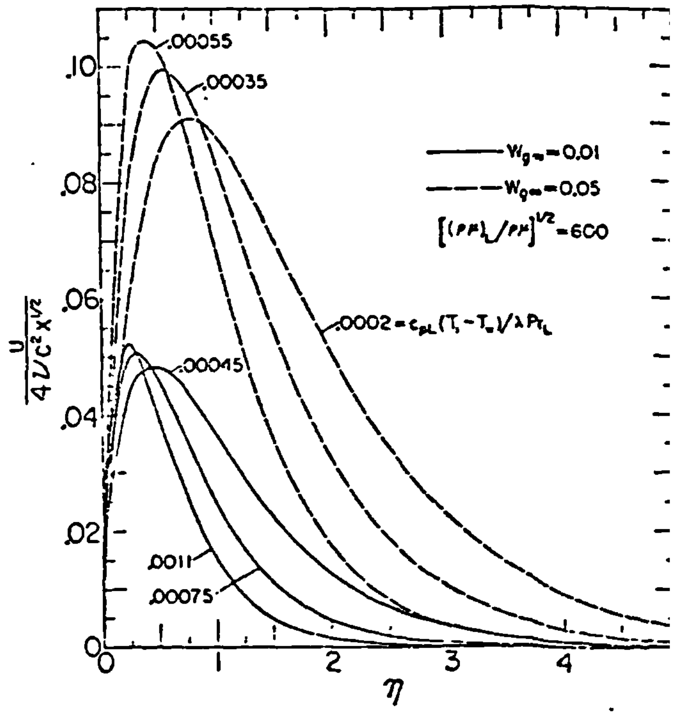

Fig. 9 Representative velocity profiles $[(\rho\mu)_L/\rho\mu]^{1/2} = 600$

(e)

Figure 2.26 Reproduced from Sparrow and Lin /65 /

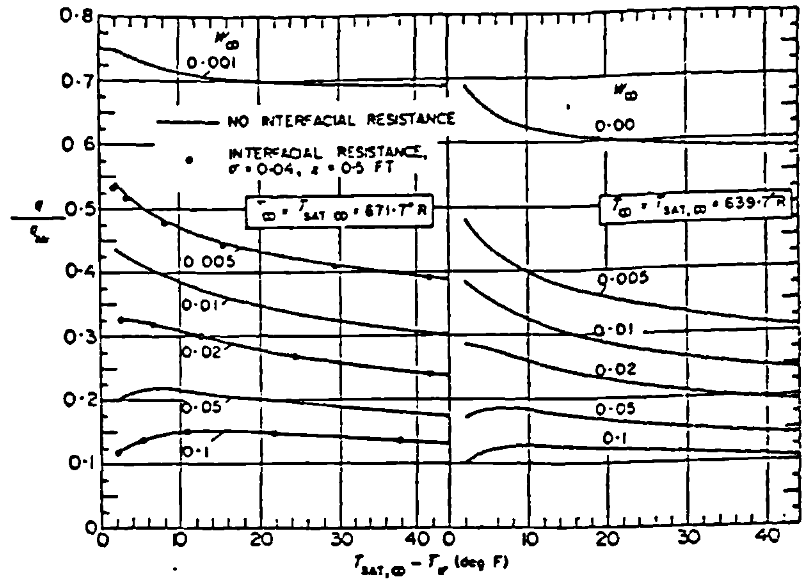

FIG. 1. Condensation heat transfer in the presence of a noncondensable gas, saturated bulk, $T_{sat,\infty}$ = 671·7°R and 639·7°R.

(a)

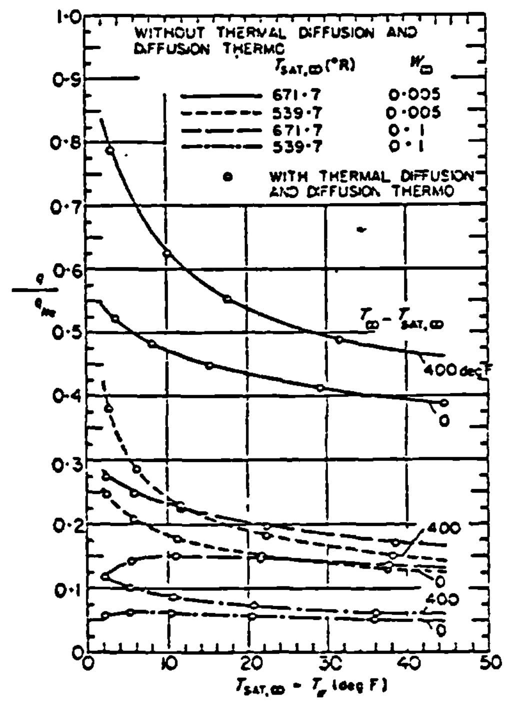

FIG. 9. Effect of thermal diffusion and diffusion thermo on condensation heat transfer.

(b)

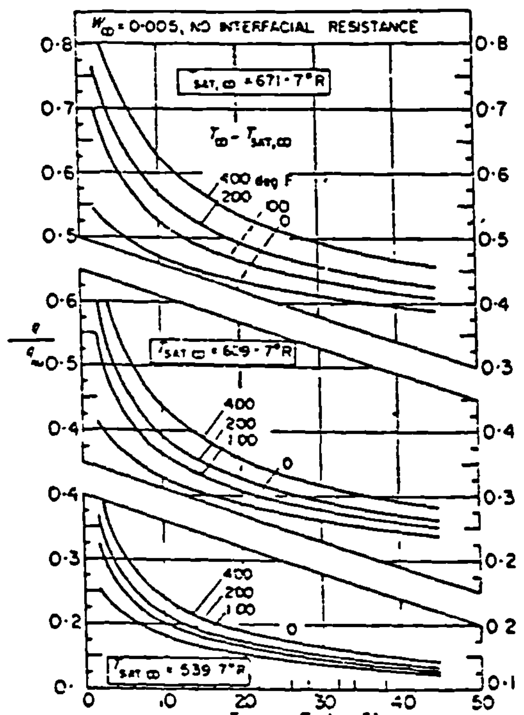

FIG. 3 Condensation heat transfer in the presence of a non-condensable gas, superheated bulk, W'_∞ = 0·005.

(c)

Figure 2.27 Reproduced from Minkowycz and Sparrow /66 /

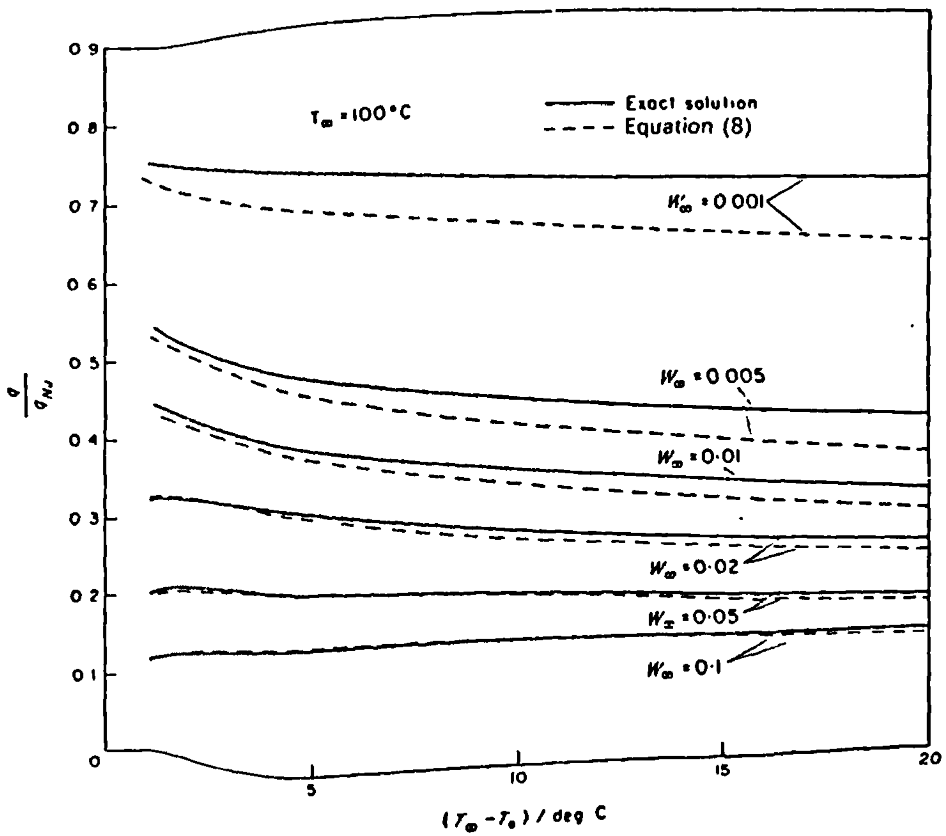

FIG. 3. Fractional reduction in heat transfer. Comparison of equation (8) with exact variable property solution [3].

Figure 2.28 Reproduced from Rose /67/

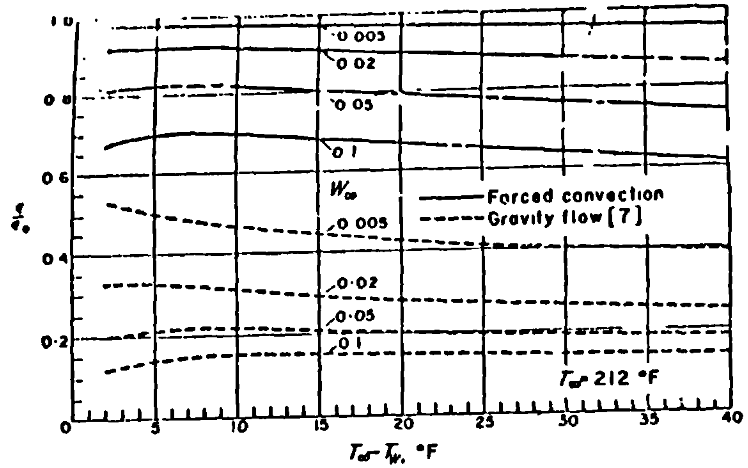

FIG. 4. Condensation heat transfer for steam air system, $T_\infty = 212°F$.

(a)

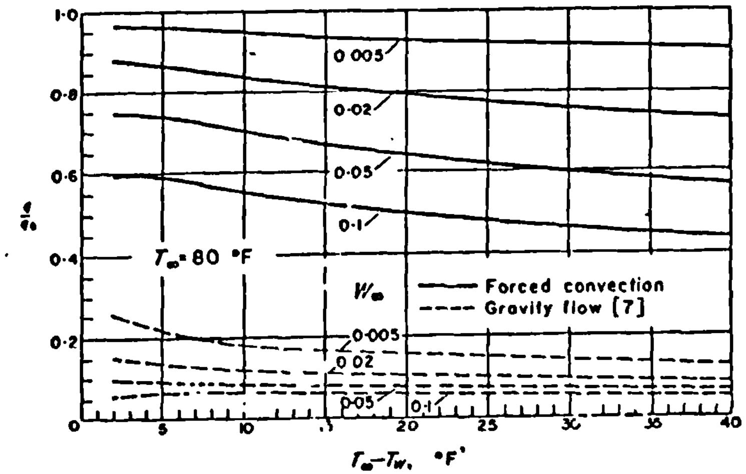

FIG. 8. Condensation heat transfer for steam-air system, $T_\infty = 80°F$.

(b)

Figure 2.29 Reproduced from Sparrow et. al. /68/

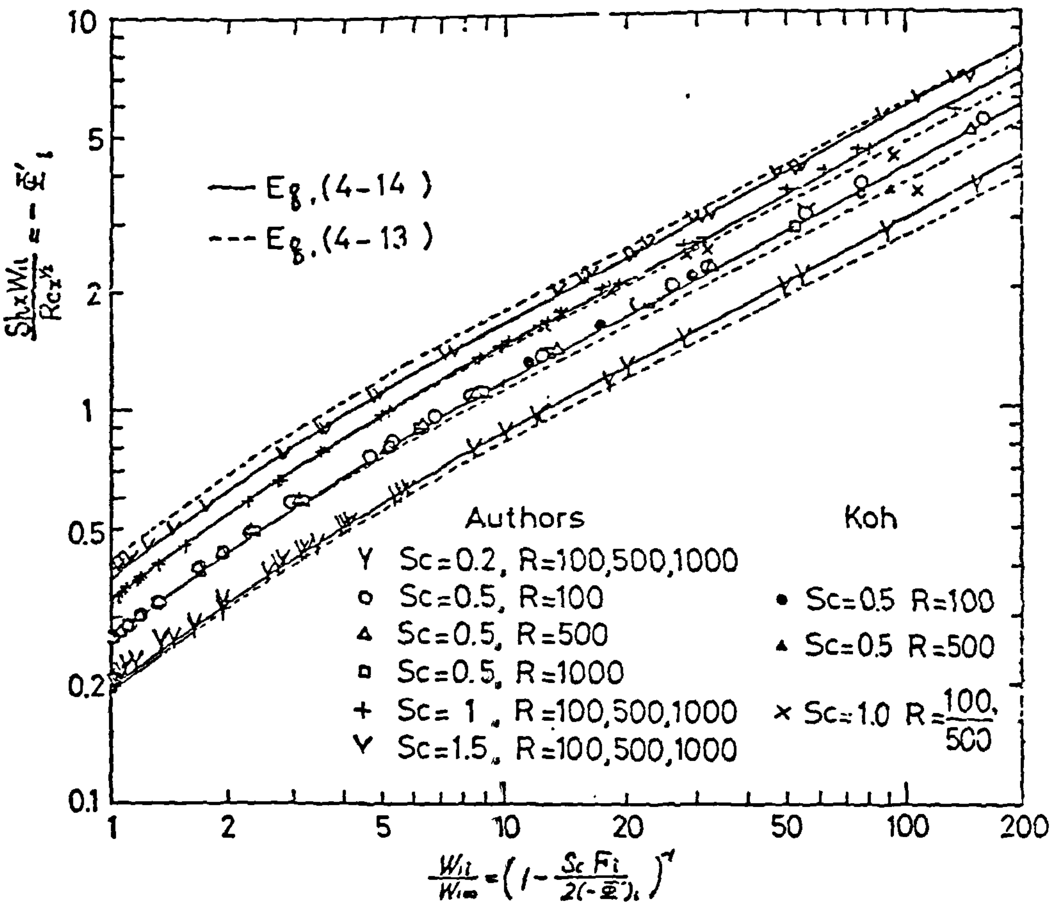

Fig. 2 Comparison of similarity solutions with correlation equations on relation between $Sh_x \bar{W}_{1i}/Re_x^{1/2}$ and $W_{1i}/W_{1\infty}$.

(a)

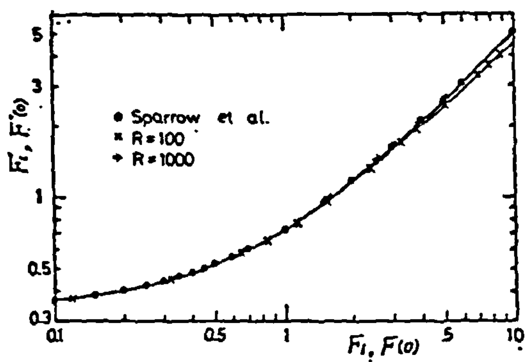

Fig. 9 Comparison of the present solutions with those of Sparrow et al.[2] on the variation of F_i'' with F_i or $F''(0)$ with $F(0)$.

(b)

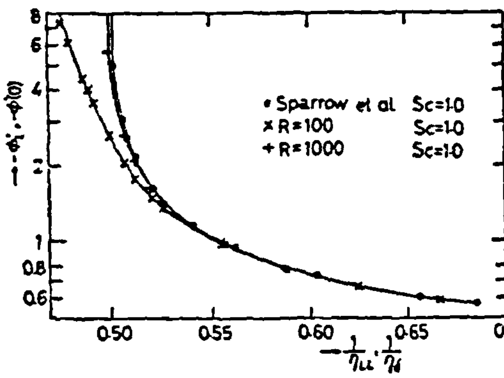

Fig. 10 Comparison of the present solutions with those of Sparrow et al[2], on the variation of Φ_i' with $1/\eta_{Li}$ or $\Phi(0)$ with $1/\eta_i$.

(c)

Figure 2.30 Reproduced from Fujii et. al. /71/

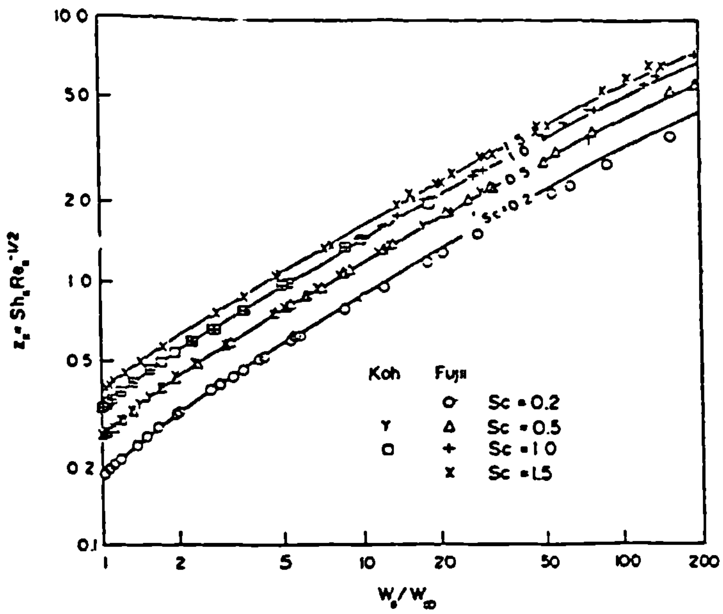

FIG. 2. Condensation on a horizontal plane surface. Comparison of numerical results of Koh [1] and Fujii *et al.* [2] with equation (10) (represented by the lines). *Note*: The accuracy of some of the data given in [2] has been improved [12]. Figure 2 incorporates the revised values.

Figure 2.31 Reproduced from Rose /72 /

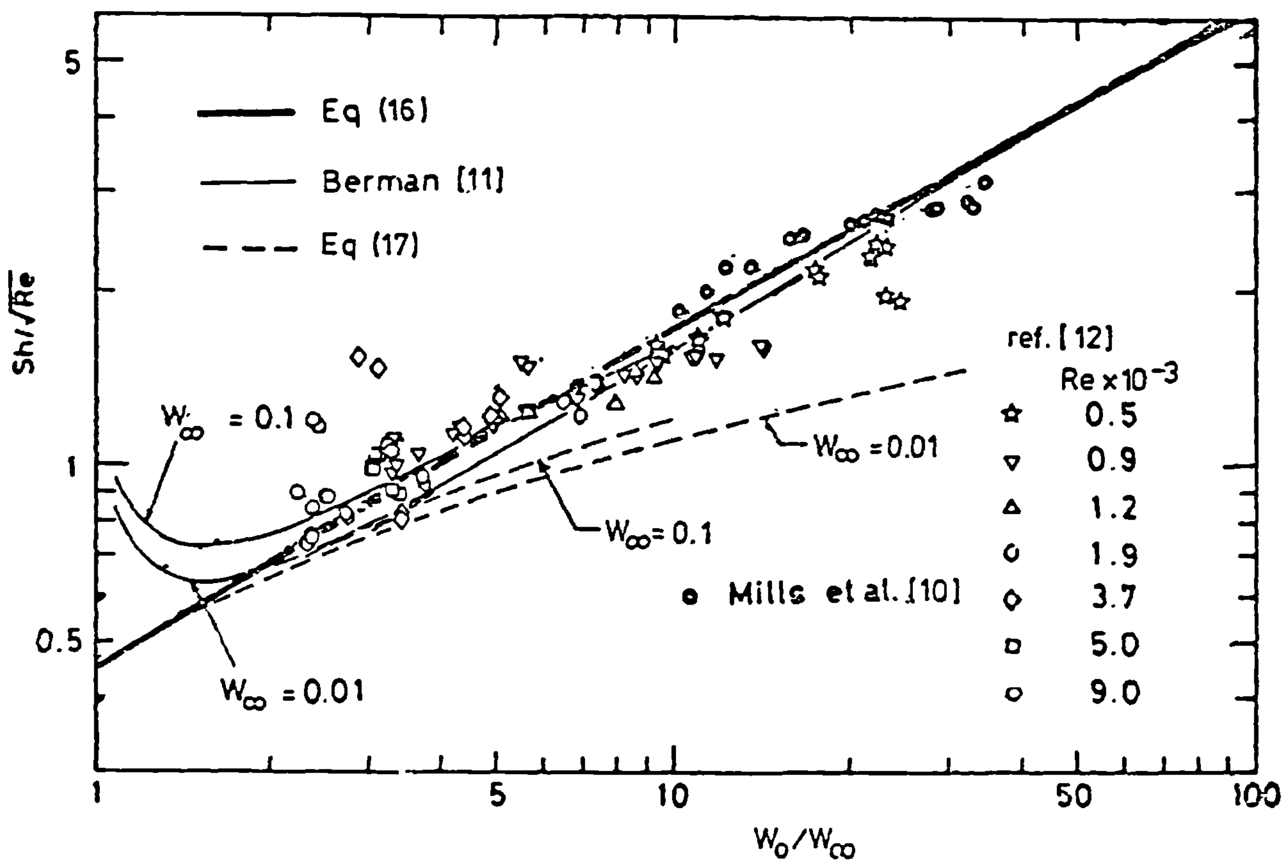

Fig.4 Condensation of steam on a horizontal tube in the presence of air. Comparison of experimental data with various calculation methods.

Figure 2.32 Reproduced from Rose /74a/

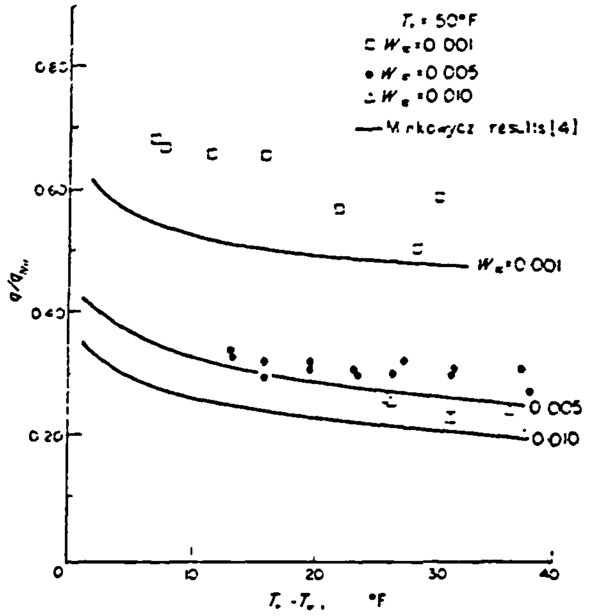

FIG. 2. Average heat flux measurements on condensing air–steam mixtures at constant vapor temperature.

(a)

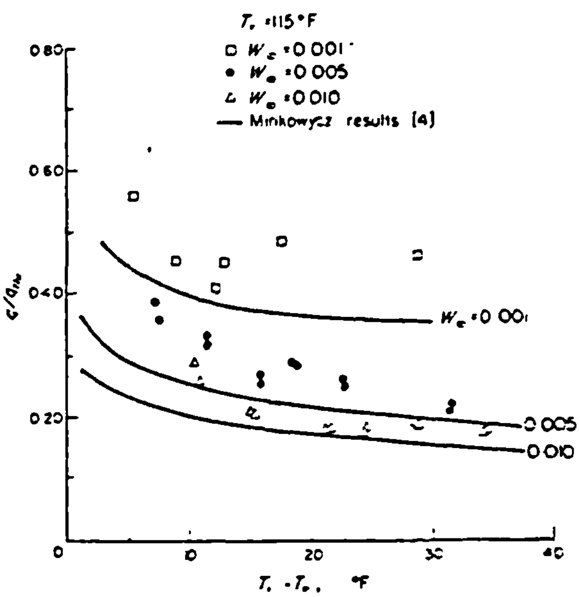

FIG. 3. Average heat flux measurements on condensing air–steam mixtures at constant vapor temperature.

(b)

Figure 2.33 Reproduced from Slegers and Seban /81 /

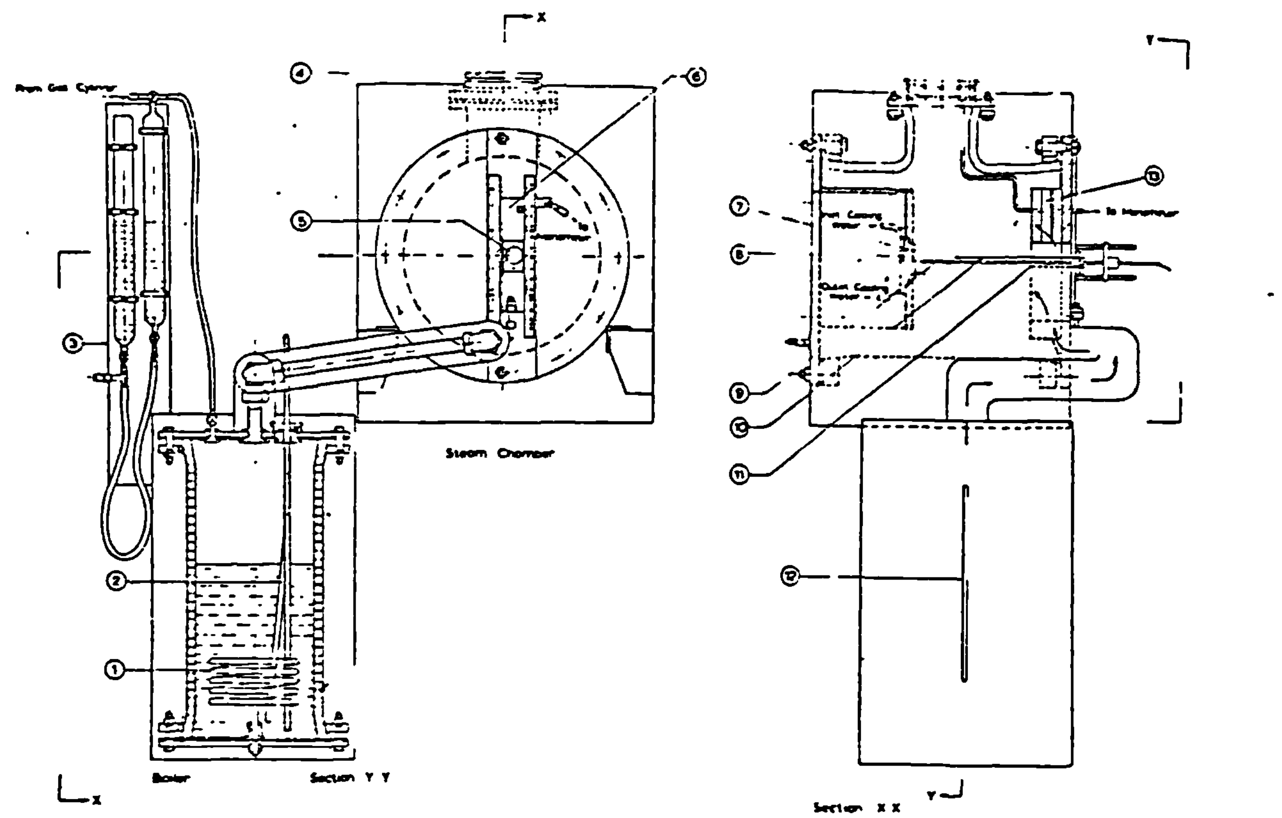

FIG 1. General assembly of the apparatus.

1. electric heater; 2. electric heater; 3 gas measuring cylinders; 4. electrically heated window; 5 electrically heated window, 6. vertically sliding plate; 7. condensing plate; 8. cooling box; 9. horizontally moveable thermocouple (see also Fig. 3 mounted on vertically sliding plate, 10 thermocouple mounted on vertically sliding plate; 11 thermocouple mounted on vertically sliding plate; 12 water level inspection slit, 13. flow straightener

Figure 2.34 (a) Reproduced from Al-Diwany and Rose /82/

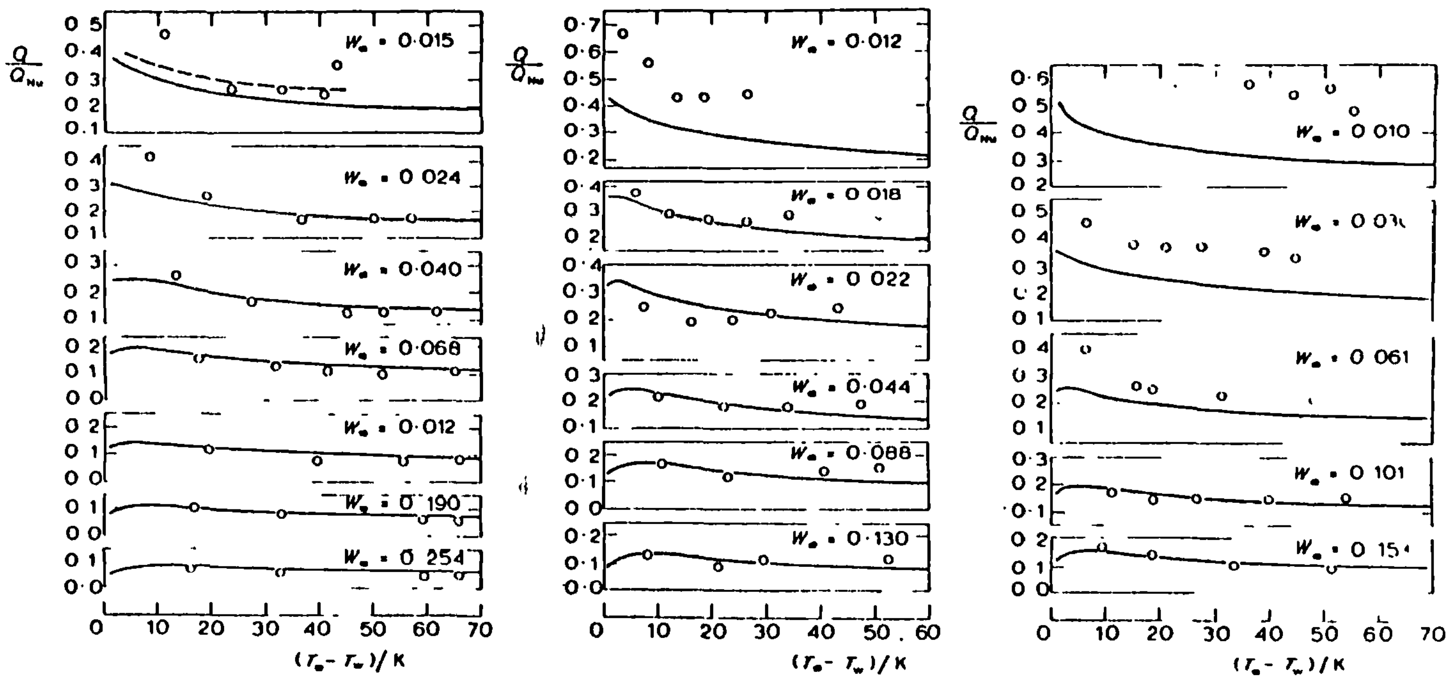

AIR

(b)

NEON

(c)

ARGON

(d)

FIG. 7. Reduction in heat transfer vs vapour-to-surface temperature difference for gases with molecular weights greater than that of water.

----- exact numerical solution [3]

——— approximate integral solution [4]

Figure 2.34 reproduced from Al–Diwany and Rose /82/ (continued)

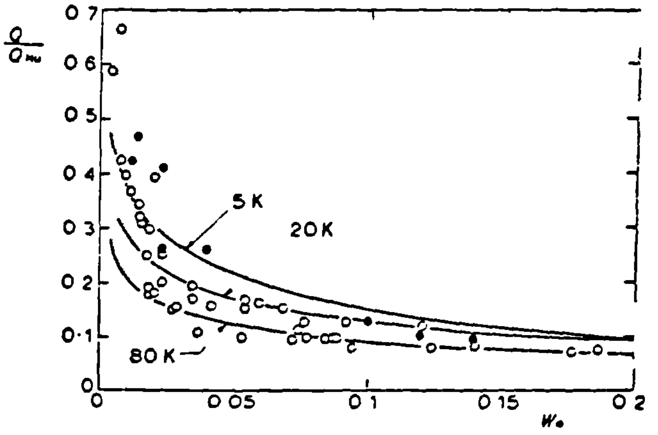

(e)

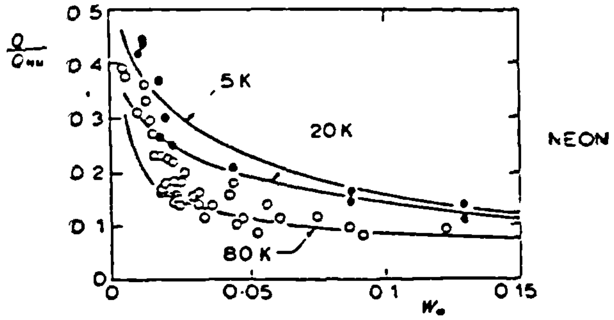

(f)

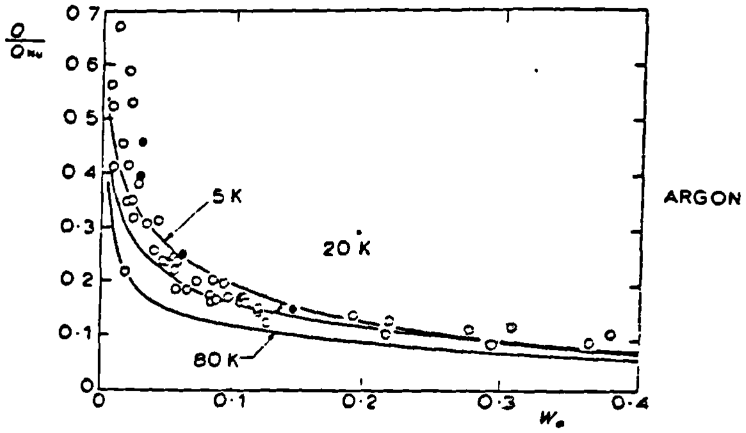

FIG. 8. Reduction in heat transfer vs non-condensing gas concentration for gases with molecular weights greater than that of water.

● $T_\infty - T_w < 20$ K
○ $T_\infty - T_w > 20$ K
—— approximate integral solution [4]

(g)

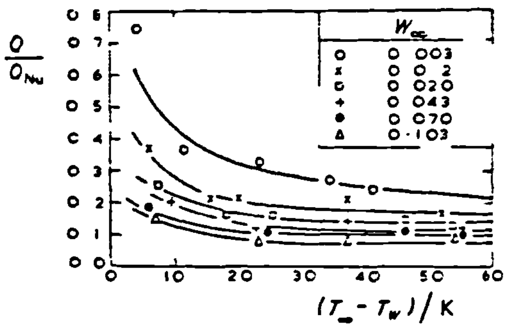

(h)

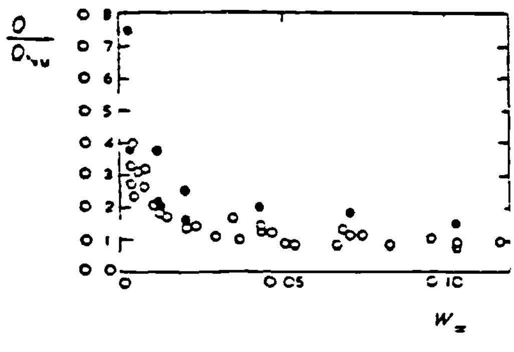

● $T_\infty - T_w < 20$ K
○ $T_\infty - T_w > 20$ K

FIG 9 Reduction in heat transfer for helium

(i)

Figure 2.34 Reproduced from Al-Diwany and Rose /82 / (continued)

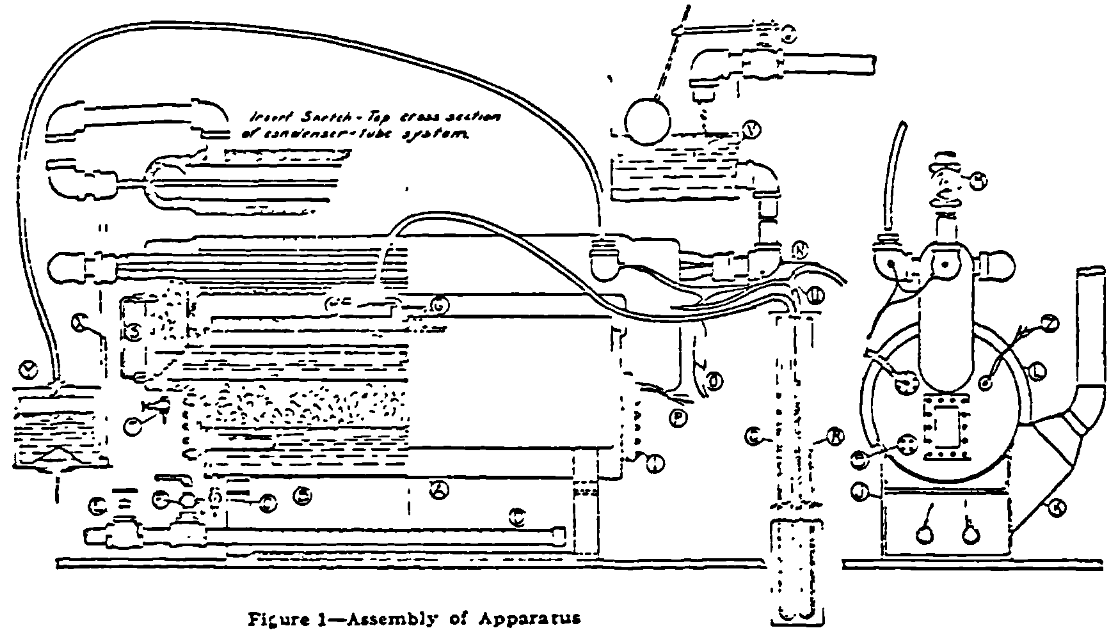

Figure 1—Assembly of Apparatus

A—Boiler body of 12-inch iron pipe
B—Electric heaters, 2 General Electric 2000-watt
C—Boiler drain valve
D—Gas heaters
E—Gas valve
F—Air valve
G—Water trap on manometer
H—Blow-off valve
I—Peep glass and hand hole packing plate
J—Iron stand for boiler
K—Hood and flue for hot gases
L—Asbestos insulation
M—Valve regulating cooling water
N—Thermometer for entering cooling water
O—Water-difference thermocouple wires
P—Tube thermocouple wires
Q—Boiler manometer
R—Evaporative space manometer
S—Water gage in evaporative space
T—Evaporative space drain valve
U—Exhaust tube for evaporative space
V—Constant-level tank
W—Float valve on city water line
X—Water orifice manometer tube
Y—Orifice chamber
Z—Standard steam thermocouple wires

Figure 2.35 Reproduced from Othmer / 78 /

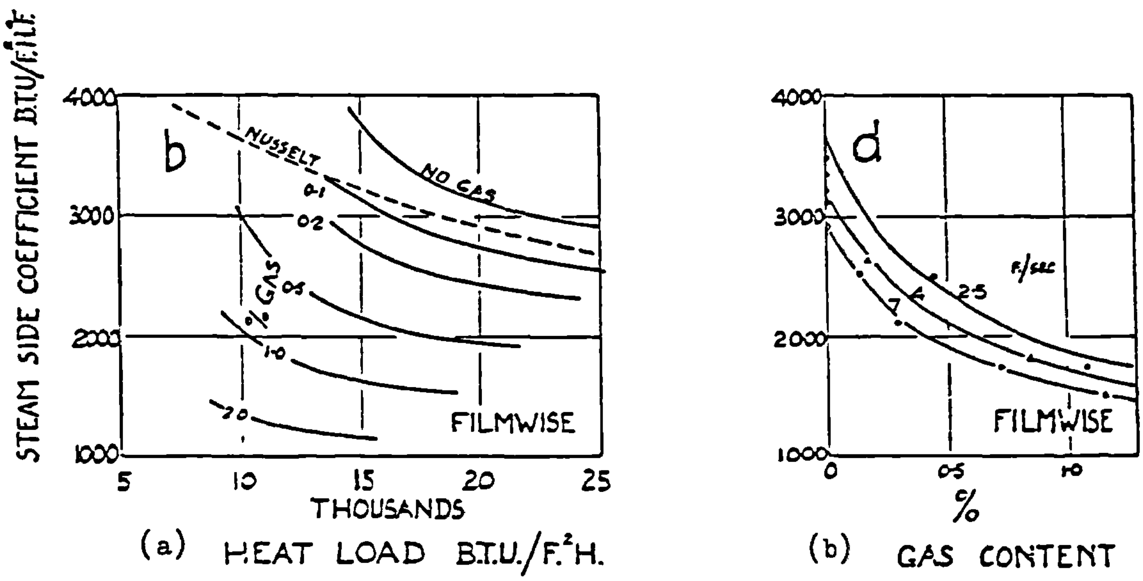

FIG. 6 – EFFECT OF GAS ON STEAM-SIDE COEFFICIENTS – 1.0 inch o.d. Copper Tube, 0.020 inch thick wall. Steam at 10 inch W. G. Gas – Nitrogen, optimum vent position. Mean Cooling Water Temperature 192 F. For Dropwise Condensation 1.0 represents 30,000 Btu/f ²h. F.

Figure 2.36 Reproduced from Hampson /83 /

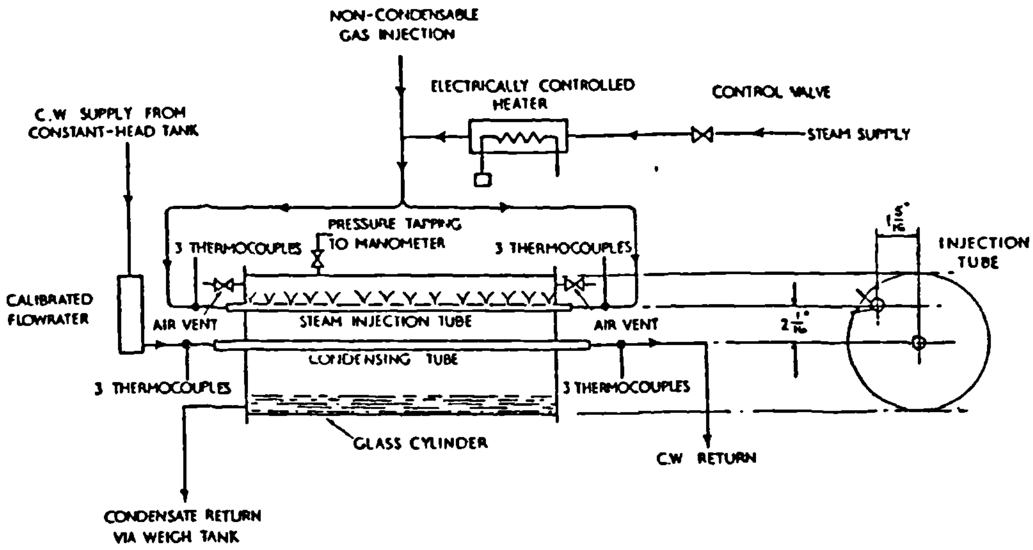

FIG 3 DIAGRAM OF APPARATUS

(a)

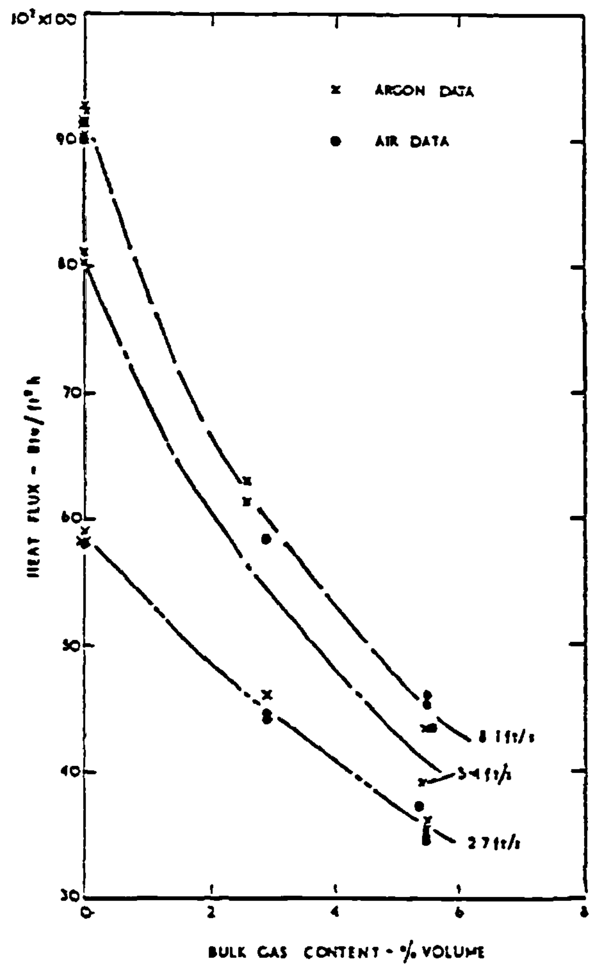

FIG 7 EFFECT OF BULK GAS CONTENT ON HEAT FLUX FOR DIFFERENT COOLANT VELOCITIES

(b)

Figure 2.37 Reproduced from Provan / 84/

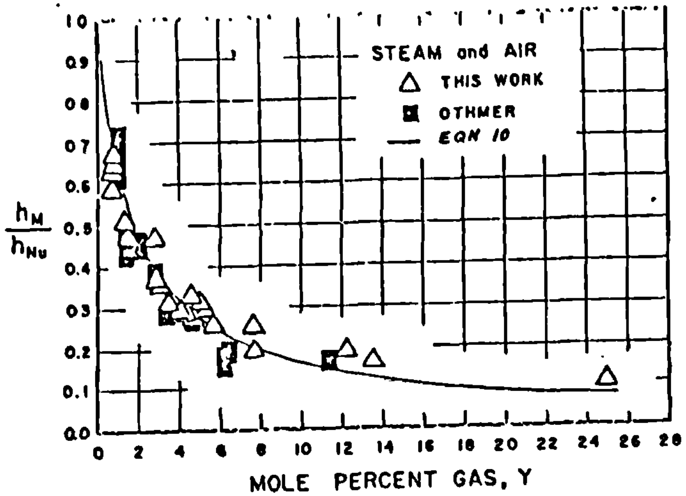

Fig. 1 Heat transfer ratio for steam and air

(a)

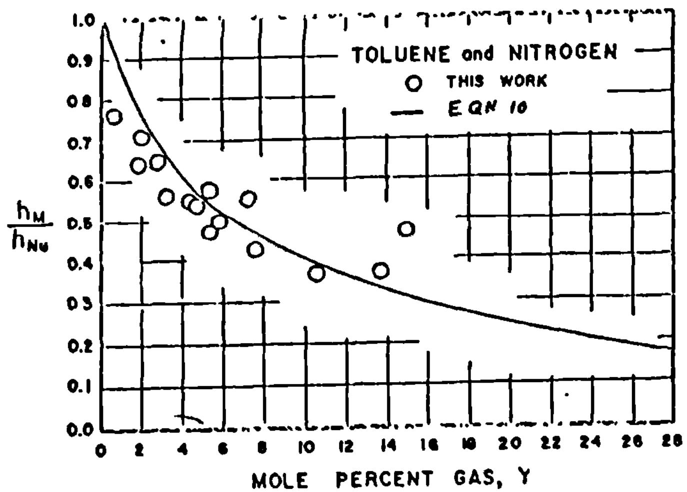

Fig. 2 Heat transfer ratio for toluene and nitrogen

(b)

Figure 2.38 Reproduced from Henderson and Marchello / 85/

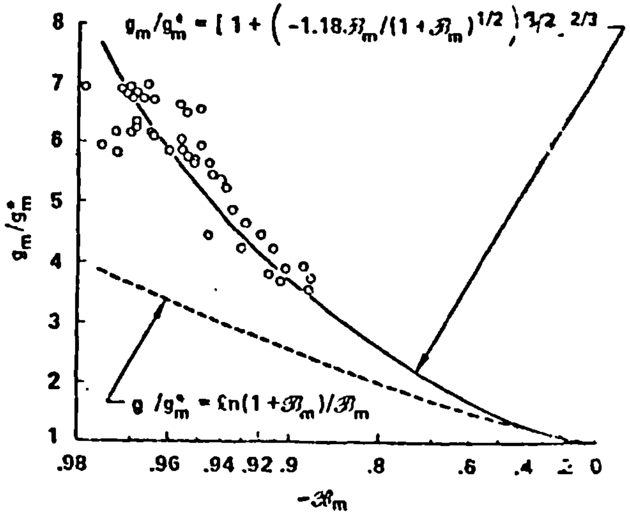

Fig. 3. Steam-Air Mixtures: Correlation of the Mass Transfer Conductance

Figure 2.39 Reproduced from Mills et. al. /76 /

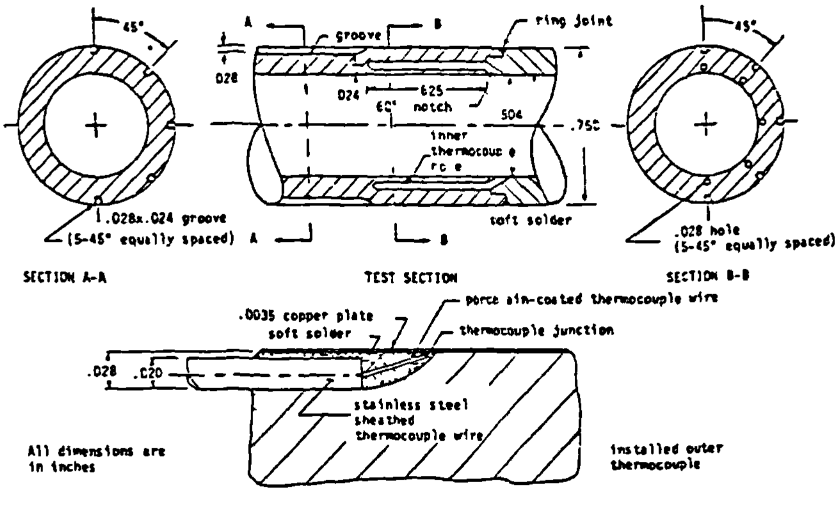

Fig. 2 Details of the heat transfer tube

(a)

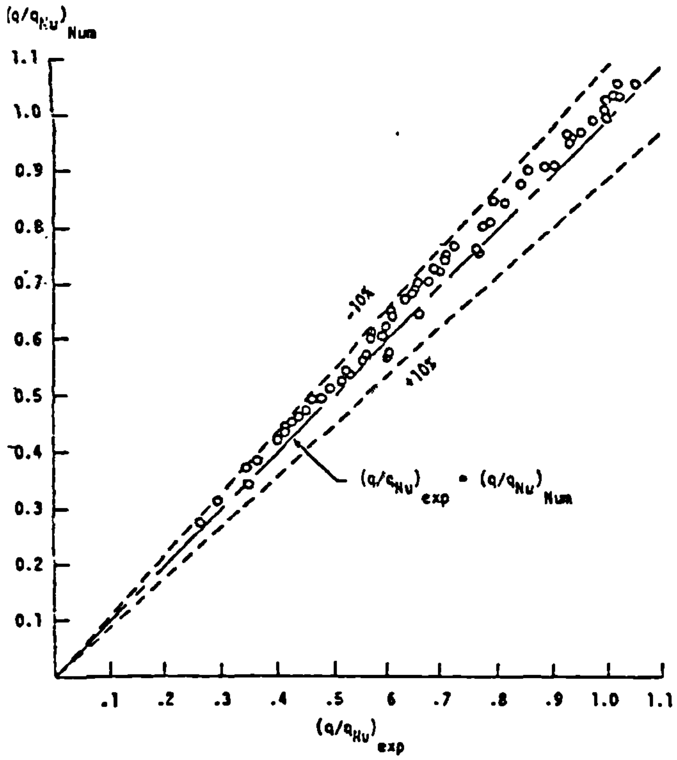

Fig. 5 Comparison of steam-air experimental stagnation point results with numerical solutions

(b)

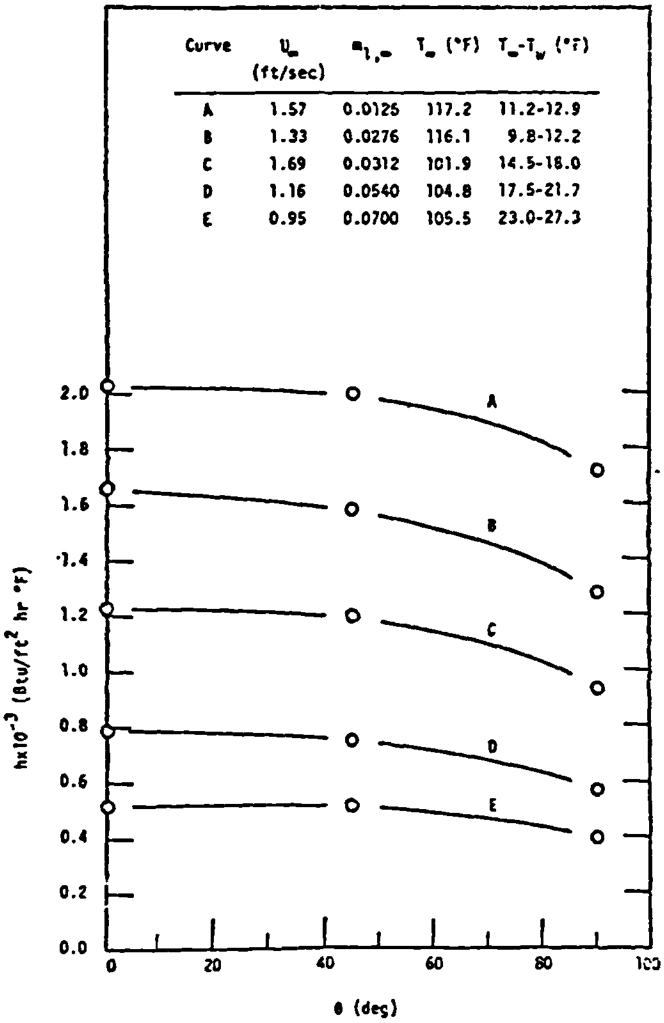

Fig. 6 Local values of heat transfer coefficient $h = q/[T_\infty - T_w]$ for steam-air

(c)

Figure 2.40 Reproduced from Rauscher et. al. /89 /

CHAPTER 3 - AIM AND SCOPE OF THE PRESENT INVESTIGATION

As discussed in Chapter 2, many of the uncertainties relating to laminar filmwise condensation heat transfer have now been resolved. However, areas of uncertainty remain. In the case of a pure vapour condensing on a horizontal tube, it appears that the effect of vapour velocity, especially at high vapour velocity and high condensation rates (i.e. low values of the parameters Pr_L/FrH and $\sqrt{Re_{TP}}/Fr\tilde{M}$) and that of the parameter RH/Pr_L are still unclear. In the case of a vapour condensing, in the presence of a non-condensing gas, on a horizontal tube, only limited experimental data (steam-air mixtures) are available. It is thus not possible to judge satisfactorily the validity of the recent theory /72 /.

The main aims of the present investigation were :-

i. to obtain reliable and accurate data for vertical downflow of pure vapours in order to help to resolve the outstanding theoretical problems; and at the same time to provide a sound basis for evaluating the condensate film resistance when studying the effect of non-condensing gas.

ii. to obtain reliable and accurate data, over a wide range of conditions, in order to evaluate the theoretical result /72 / and to provide guidance towards modification of the theory, if necessary. (In particular, it was thought that the new data might be used to obtain better values for the constants a, b and c in equation 2.51).

Two tube diameters were used. Steam and Refrigerant 113 were used as condensing fluids. Refrigerant 113 was chosen since it is relatively non-toxic and its thermophysical properties are well documented and markedly different from those of steam. Air and hydrogen were used as non-condensing gases. With these vapour-gas combinations, the practically important steam-air case was covered and at the same time, a wide range of variables was permitted, to provide a stringent check on theory. In particular, the range of Schmidt number for the vapour-gas mixtures was from about 0.05 to about 0.5. The approximate ranges of the variables covered are given in Table 3.1.

Table 3.1 Approximate overall ranges of the main parameters used in the present investigation

Mixture	P_∞ / kPa	d_o / mm	T_∞ / K	T_w / K	U_∞ / m/s	$W_{\infty 2}$ / %	$\widetilde{W}_{\infty 2}$ / %	$\dot{Q}''_{obs}$ / kW/m^2
pure steam	101	12.5	373	333 - 364	0.4 - 1.8	-	-	166 - 466
pure steam	47	12.5	353	325 - 347	1.6 - 3.3	-	-	116 - 344
pure steam	5 - 9	12.5	307 - 319	301 - 316	3.5 - 18.0	-	-	29 - 150
pure steam	101	25.25	373	322 - 364	0.4 - 1.6	-	-	126 - 412
pure steam	4 - 8	25.25	303 - 314	298 - 310	12.9 - 15.2	-	-	51 - 122
pure R-113	101 - 105	12.5	320 - 321	287 - 304	0.5 - 1.8	-	-	26 - 46
pure R-113	40 - 78	12.5	295 - 312	282 - 300	2.0 - 2.8	-	-	12 - 43
steam-air	95 - 103	12.5	366 - 373	296 - 364	0.3 - 1.8	0.5 - 24.4	0.3 - 16.8	81 - 447
steam-air	4 - 40	12.5	301 - 348	291 - 332	1.1 - 25.7	0.1 - 31.5	0.1 - 22.2	41 - 247
steam-air	99 - 101	25.25	270 - 373	301 - 355	0.8 - 1.7	0.5 - 12.4	0.3 - 8.1	106 - 371
steam-air	6 - 37	25.25	310 - 348	297 - 332	2.9 - 14.9	1.0 - 16.6	0.6 - 11.0	32 - 142
steam-hydrogen	97 - 102	12.5	362 - 373	296 - 355	0.3 - 1.8	0.1 - 5.7	0.7 - 35.1	164 - 465
steam-hydrogen	4 - 55	12.5	300 - 351	294 - 343	1.3 - 17.1	0.1 - 3.8	1.0 - 26.3	20 - 289
R-113-air	101 - 104	12.5	318 - 321	284 - 303	0.5 - 1.8	0.04 - 1.6	0.3 - 9.5	22 - 51
R-113-hydrogen	103 - 124	12.5	318 - 320	285 - 301	0.5 - 0.9	0.02 - 0.3	1.7 - 22.9	24 - 43

Of foremost importance in the present study was accuracy of measurements. The test condenser tube surface temperature was found from four thermocouples embedded in the tube wall. The heat flux was determined from the coolant mass flow rate and temperature rise and checked by collecting condensate over a measured time interval. Good agreement was found between the two values.

The vapour flow rate approaching the tube was found by accurately observing the heater input power (heater currents found from potential drops across series standard resistors). Careful preliminary tests, in which the total condensation rate (from both test and auxiliary condensers) was measured, were used to determine the 'thermal loss' between boiler and test section. These data were used in determining the vapour velocity upstream of the test condenser tube. The 'exposed length' of the tube occupied only the central portion of the test section to minimise lengthwise velocity variation. The mean velocity over the tube was obtained from the mean velocity for the test section by adopting suitable 'profiles'.

The vapour composition (vapour-gas mixture tests) was found from the vapour mass flow rate and the measured flow rate of the non-condensing gas. A second estimate was obtained from the observed (saturation) pressure and temperature. Regular checks were made to ensure that the apparatus was satisfactorily leak-tight. That this was so was shown by the close correspondence of the saturation pressure and temperature (pure vapour tests) and by the good agreement between the two composition determinations (vapour-gas mixture tests).

Special care was taken to ensure high-accuracy thermo-electric measurements (adequate isothermal immersion, lead-wire junctions at reference temperature, heavy draught-free copper switches, precision digital voltmeter (1 μV)).

The stainless-steel and glass apparatus was maintained in a very clean condition and regular observation of the test condenser tube ensured that no dropwise condensation occurred.

The present results for both pure vapours and vapour-gas mixtures are thought to have accuracy and reliability superior to earlier data. At low vapour velocities, and when using pure vapours, good agreement with the simple Nusselt theory was found, while at higher vapour velocities and when non-condensing gas was present, significant departure (as expected) from Nusselt was found. Theoretical studies of the effects of vapour velocity and non-condensing gas are examined in detail in the light of the present results.

CHAPTER 4 - APPARATUS

The apparatus was designed and built by Frydas /91 /as part of the initial phase of the present investigation, i.e. the study of forced-convection condensation of a vapour flowing vertically downwards over a horizontal tube in the presence of non-condensing gases. Minor modifications were made by the present author. For cleanliness (for the purpose of obtaining and maintaining film condensation), the whole apparatus was constructed from stainless steel and glass with neoprene gaskets and using valves with viton seals.

4.1 General Layout

The general layout of the apparatus is shown in fig. 4.1. Vapour was generated in three stainless-steel boilers. Each boiler, see fig. 4.2, was fitted with two stainless-steel sheathed 5 kW electric immersion heaters, a level-indicating tube and a closed-ended stainless-steel thermocouple pocket. A non-condensing gas could be injected at the base of the boilers. The pure vapour or vapour-gas mixture flowed vertically downwards via a diffuser and a calming section to the test section where the horizontal test condenser tube was located. Vapour and condensate from the test condenser tube passed into the auxiliary condenser (34 stainless-steel tubes, 25.4 mm o.d., 500 mm long, 11 coolant passes, see fig. 4.3) located directly beneath the test section. Non-condensing gas was removed via a vent port situated near the exit of the auxiliary condenser, while the condensate was led via a short length of glass tube to a manifold and subsequently back to the boilers. The apparatus was thermally well insulated.

Cooling water was pumped from a supply tank and was circulated via variable-aperture float-type flowmeters through both the test condenser tube and the auxiliary condenser by a centrifugal pump (7.5 kW, nominal delivery 270 kg/min. at 2900 rev/min. against a total head of 49 metres of water). Provision was made for recirculating coolant from the auxiliary condenser through the test condenser tube for the purpose of obtaining higher coolant inlet temperatures.

The non-condensing gas was metered by variable-aperture float-type flowmeters, at entry to which the pressure and temperature of the gas were measured. When testing at near (slightly above) atmospheric pressure, the gas was allowed to flow directly from the auxiliary condenser to atmosphere. When testing at sub-atmospheric pressures, the gas was extracted from the vent port via two "cold traps" in series by a vacuum pump (rotary type, swept volume of 334 litres/min.). For the case when the condensing fluid was steam, the traps were immersed in finely-ground ice while, when using Refrigerant 113, finely-ground solid carbon dioxide was used. The liquid condensed in the traps was returned continuously to the boilers. The vent rate could be controlled by a valve located at the inlet to the pump.

4.2 Test section

Fig. 4.4 shows details of the stainless-steel test section (internal diameter 152.4 mm, length 305 mm). The horizontal test condenser tube was inserted through 'O' rings contained in ptfe sleeves. The ptfe sleeves served both to insulate the tube from the test section walls and to restrict the exposed ("working") length to about 110 mm (nominal) in the central part of the test section, across which the vapour velocity was essentially uniform (see section 6.2). The test condenser tube could be rotated about its axis and the whole condensing length viewed via the observation window.

For the purpose of measuring the condensation rate on the test condenser tube (as a check on the heat flux observed from coolant measurements), a collecting tray was positioned directly beneath the tube, the condensate from which could be led (when required) out of the test section to a measuring cylinder. A valve at exit from the measuring cylinder could be temporarily closed and condensate collected over a measured time interval.

Six closed-ended stainless-steel thermocouple pockets (four upstream and two downstream of the test condenser tube) were installed in the test section. A pressure tap (internal diameter 8 mm) was provided just upstream of the test condenser tube.

4.3 Test condenser tubes

Two copper condenser tubes of different diameters were used. Following the recommendations of Fujii et. al. /49 /, four grooves, each of overall dimensions 2.06 x 1.60 mm^2 (see fig. 4.5) were machined lengthwise into the outer surface of the tubes. The grooves were orientated at 90^o to one another. One thermocouple (38 gauge twin-laid copper-constantan in fibre-glass sleeving) was placed in each groove and the junctions soldered onto the tube. Tightly-fitting copper strips (cut from the same samples as the condenser tubes) were soldered into the grooves over the thermocouples. The tubes were finally turned in a lathe to remove irregularities and finished with fine "wet-or-dry" paper. Table 4.1 below gives the specifications of the condenser tubes.

Table 4.1 Specifications of the test condenser tubes.

material	99.8 % pure copper	
length exposed to vapour (L/mm)	109.5	109.5
outside diameter (d_o/mm)	12.5	25.25
inside diameter (d_i/mm)	7.45	20.13
radial distance of thermocouple junctions location (r_{tc}/mm)	4.75	11.02
number of thermocouples	4	4

4.4 Instrumentation

4.4.1 Boiler power

The energy dissipated by each heater was obtained by measuring the potential drop across the heater terminals and the current flowing through it, see fig. 4.6. The procedure adopted in measuring the current was to connect standard resistors (nominally 10 milli-ohms, see section 6.2) in series with the heaters and measuring the potential drop across each standard resistor. The potential drop across the heater terminals and across the standard resistors were made with a precision a.c. digital voltmeter (Solartron Time Domain Analyser JM1860, accuracy ± 1 %). Variable transformers, connected to two of the heaters (in separate boilers) facilitated continuous variation of heater input power from about 6 kW to 30 kW when operating all three boilers.

4.4.2 Flow rates

4.4.2.1 Cooling water

Precision-bore variable-aperture float-type flowmeters were used to measure the coolant flow rates through the test condenser tubes. To obtain similar ranges of coolant velocity for the two tubes, two different flowmeters (nominal maximum flow rates 10 litres/min. and 70 litres/min.) were used. Equation 4.1, based on the manufacturer's specifications, gives the coolant mass flow rate, $\dot{m}_{cw}$,

$$\dot{m}_{cw} = 1.1365 \times 10^{-5}\, c_t\, k_1\, \dot{V}_{i,c} / v_f \qquad (4.1)$$

where c_t = $1.0365 - 0.00196644\, t + 0.000005252\, t^2$

t is the coolant inlet temperature in ^{o}C

k_1 =1 (for the larger flowmeter) and 0.14933 (for the smaller flowmeter)

$\dot{V}_{i,c}$ is the indicated flow rate (0 - 100)

v_f is the specific volume of the coolant at inlet to the flowmeter

The accuracy of equation 4.1 was checked /91 / by collecting and weighing. The agreement between indicated and measured flow rates was, in general, to within ± 1.0 %. Details of these measurements are given in Appendix A.

4.4.2.2 Non-condensing gas

The non-condensing gas volume flow rates were measured by variable-aperture float-type flowmeters (nominal flow rates 2.0 (0.5) 20.0 and 20 (5) 200 litres/min. air and 5 (5) 70 and 70 (10) 700 litres/min. hydrogen). The temperature and pressure of the gas at inlet to the flowmeters and the indicated volume flow rate of gas was used to determine the mass flow rate of the gas using equation 6.14.

4.4.3. Temperatures

The temperatures in the boilers, test section, test condenser tube, condensate return and coolant lines were measured using 38 guage fibre-glass insulated twin-laid copper-constantan thermocouples. Note that the coolant outlet temperature is measured at two places; one before and one after a mixing box (construction of which was based on the design given in /61/), see fig. 4.7. All thermocouples were made from the same reel. The thermo-emfs of the thermocouples were measured by a precision digital voltmeter (Solartron A200) with a sensitivity of 1 μV. Details of the thermocouple calibration are given in Appendix B.

The copper and constantan leads from the measuring junctions were soldered to thicker enamelled copper wires, which led to the selector switch. The copper-copper and copper-constantan soldered junctions so formed, were placed in closely-fitting thin-walled glass tubes. The glass tubes (one for each thermocouple) were immersed to a depth of about 300 mm in finely-ground, closely-packed, melting distilled-water ice, contained in a large vacuum-walled vessel. These arrangements (see fig. 4.8) provided the reference junctions and at the same time obviated any thermal-emf due to the thicker lead wires.

4.4.4 Pressure

Both the pressure at the test section and the pressure of the non-condensing gas at the inlet to the flowmeters were measured by mercury-filled U-tube manometers with one leg open to atmosphere. The manometers were fitted with precision steel rules and vernier scales measuring to 0.05 mm. A pressure damper (Ray Pressure Snubber, IMI Shipston Ltd., England) was incorporated in the test section manometer line to damp out fluctuations arising from "bumping" when operating at sub-atmospheric pressures.

The atmospheric pressure was measured using a Fortin barometer.

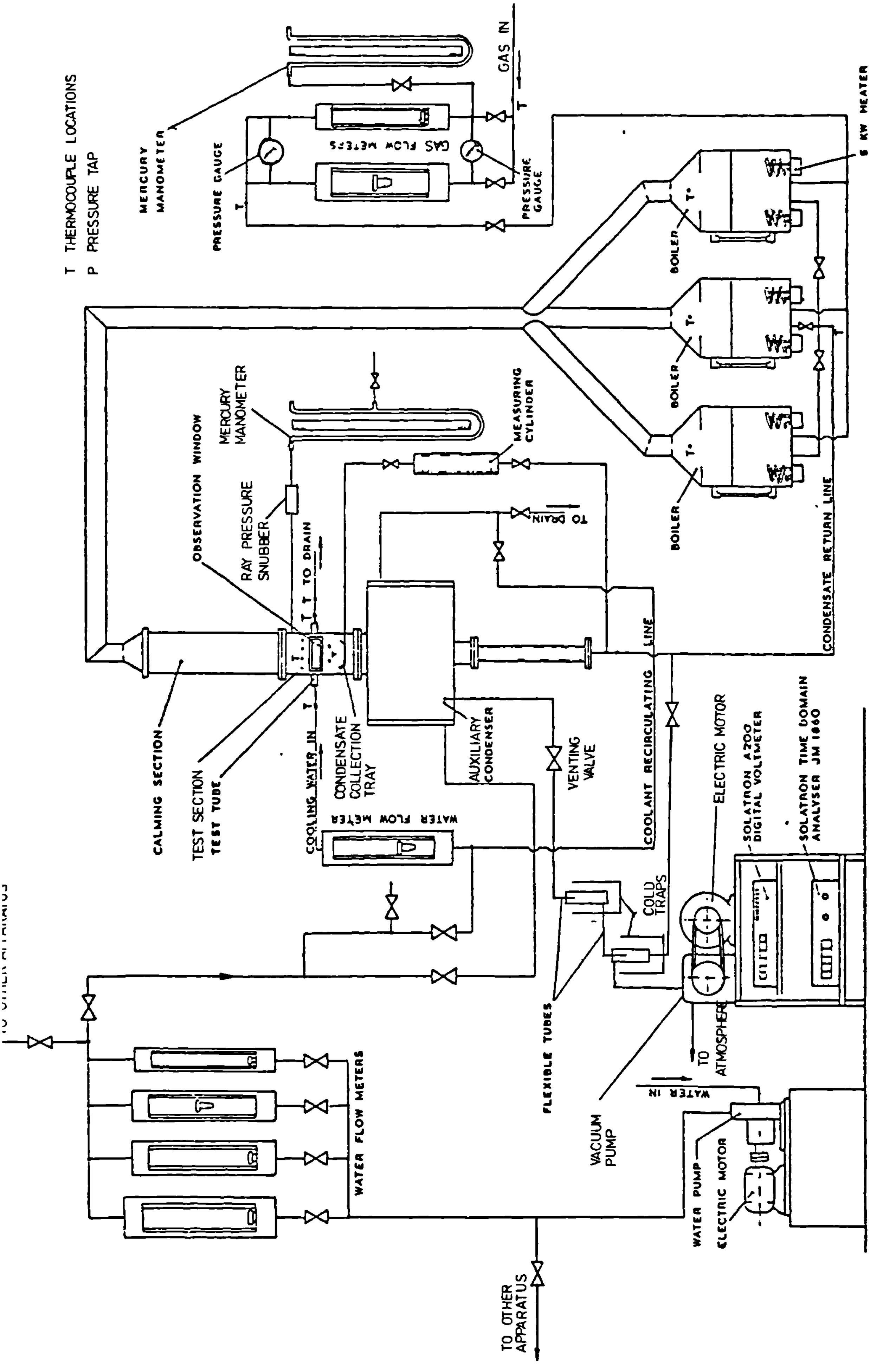

FIG. 4.1 EXPERIMENTAL APPARATUS

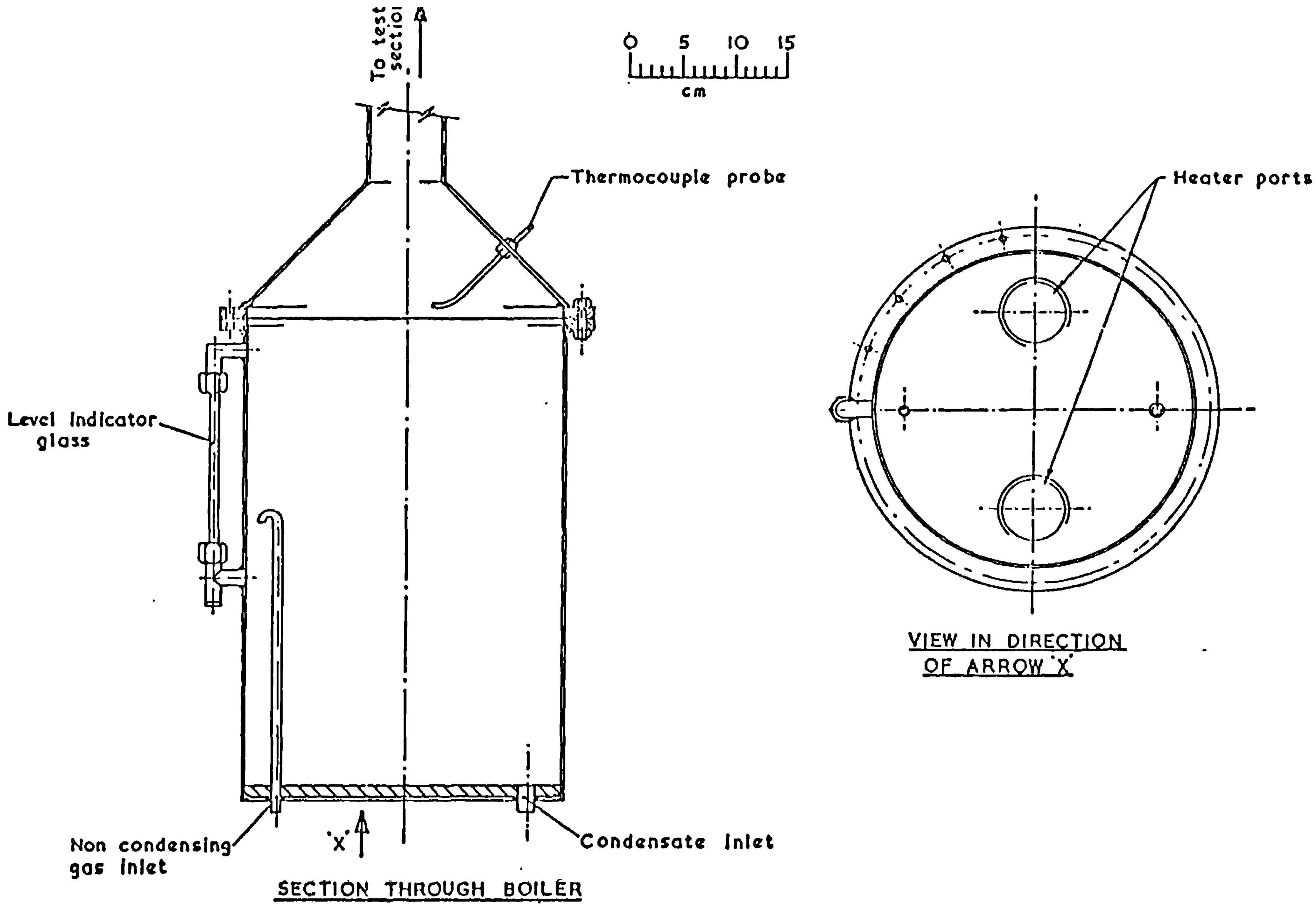

FIG. 4.2 DETAILS OF THE BOILERS

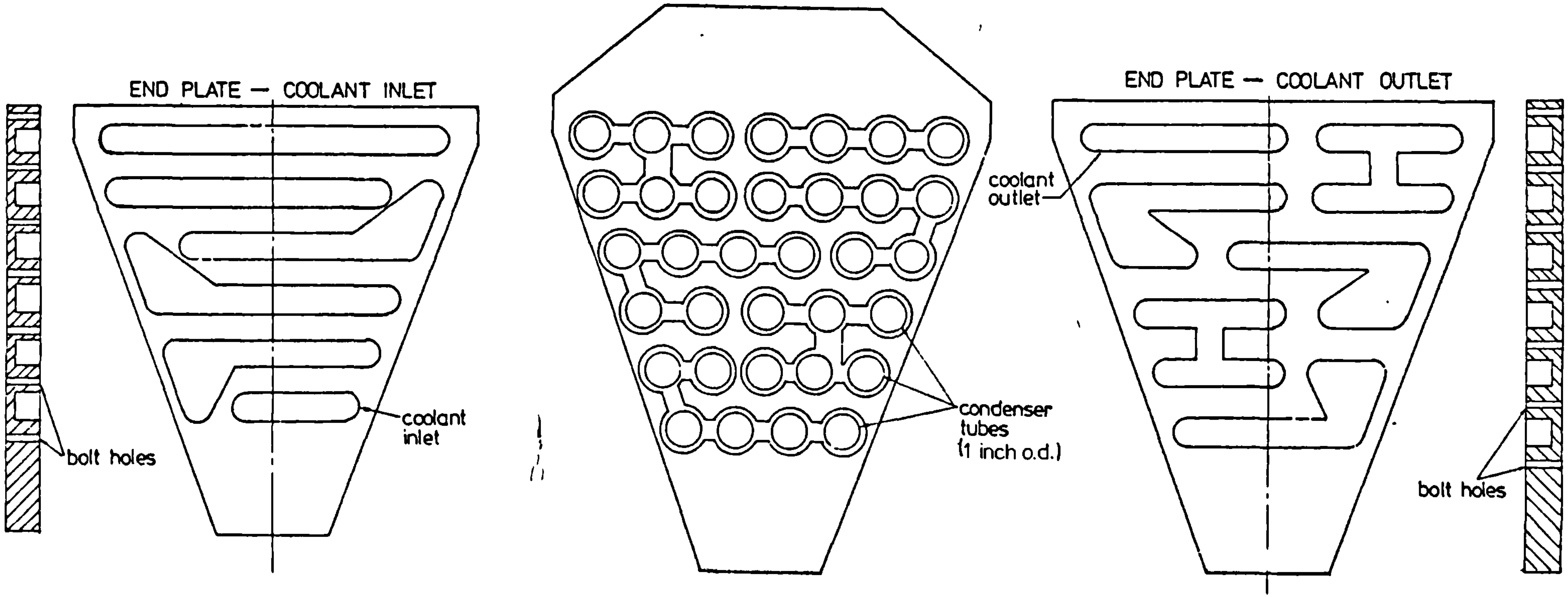

FIG. 4.3 DETAILS OF THE AUXILIARY CONDENSER

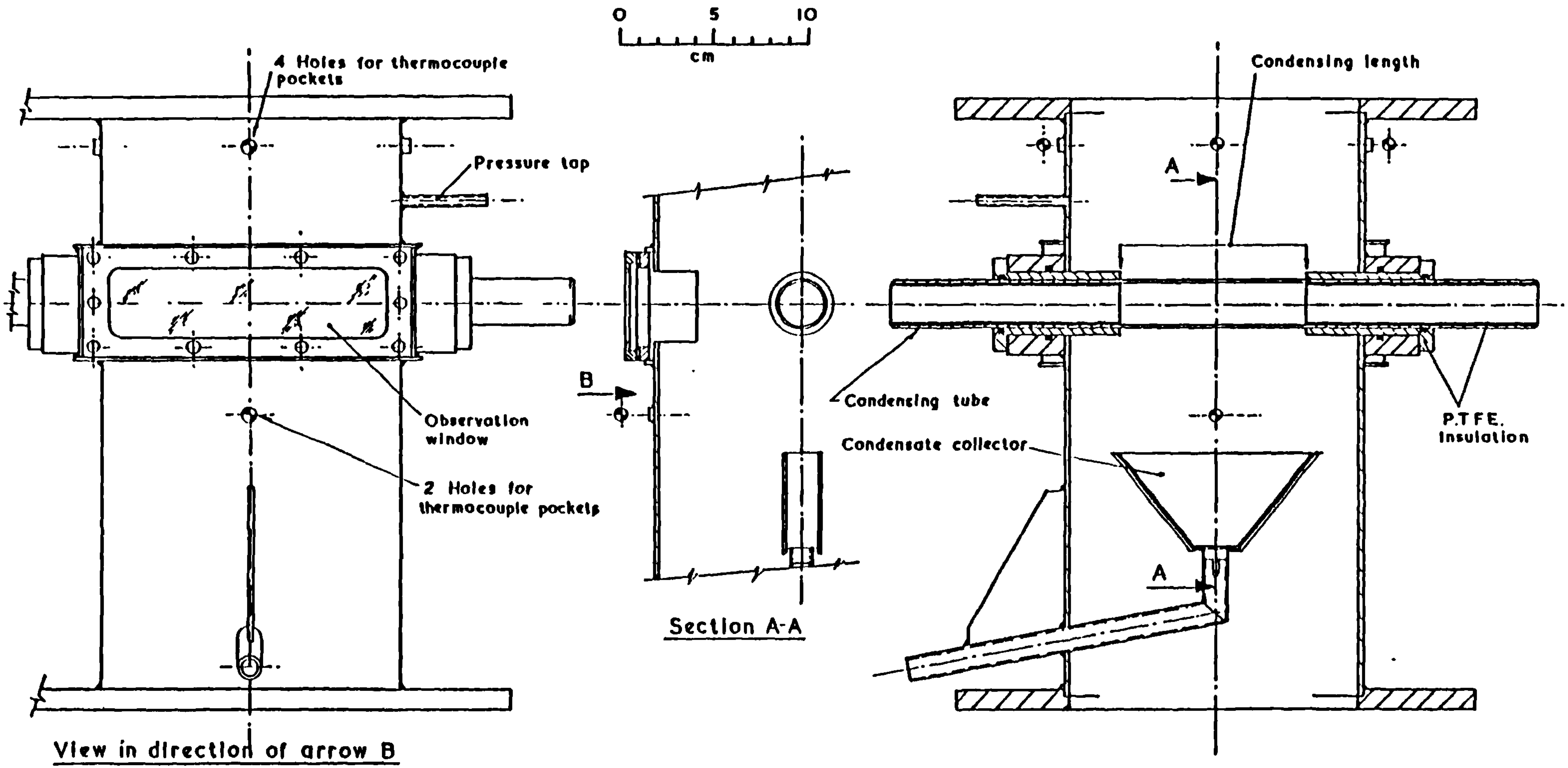

FIG. 4.4 DETAILS OF THE TEST SECTION

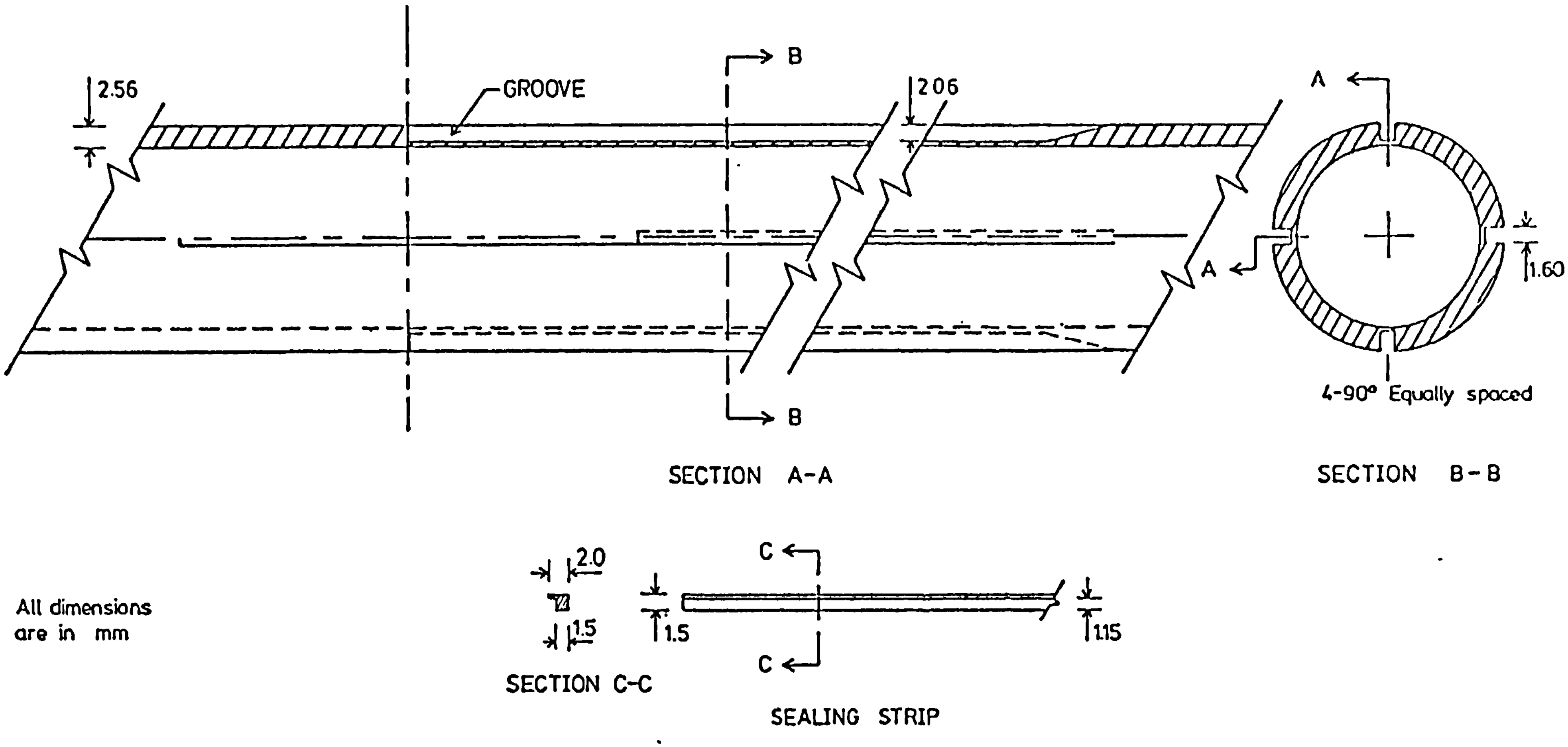

FIG. 4.5 Details of the Test Condensing Tube

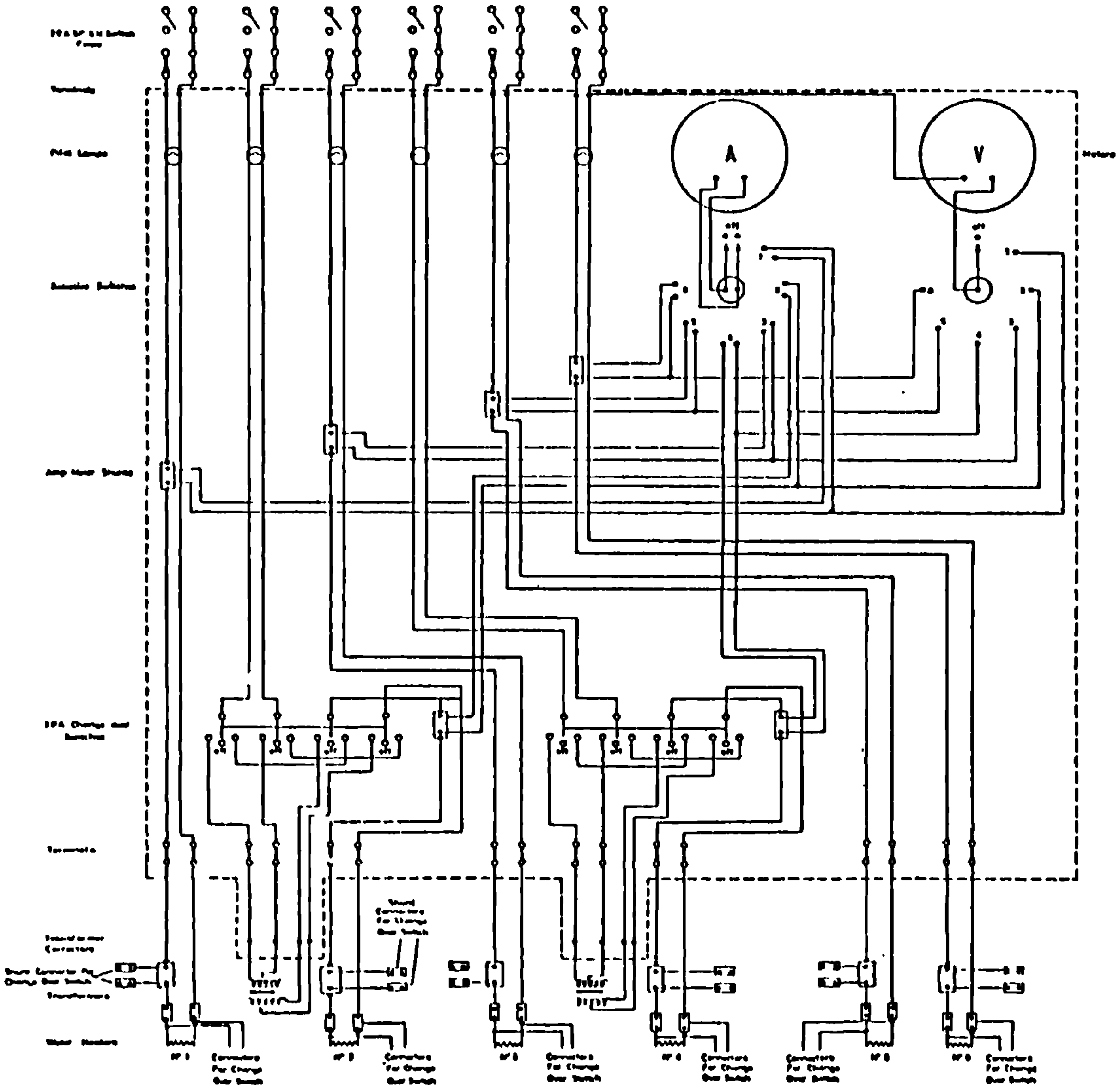

FIG 4.6 ELECTRICAL CIRCUIT FOR SUPPLYING POWER TO THE BOILERS

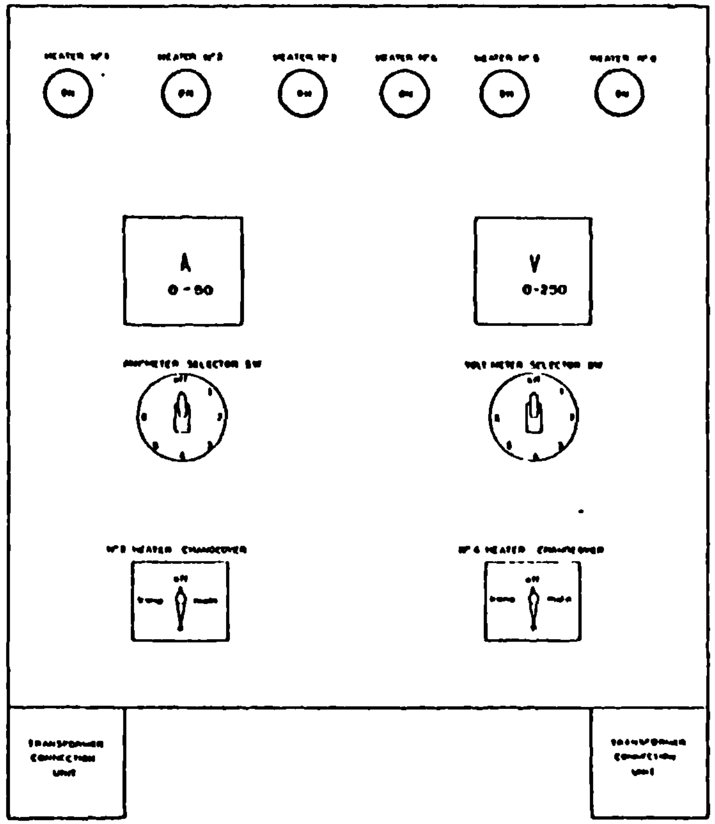

WATER HEATER PANEL FOR CONDENSATION RESEARCH LOOP

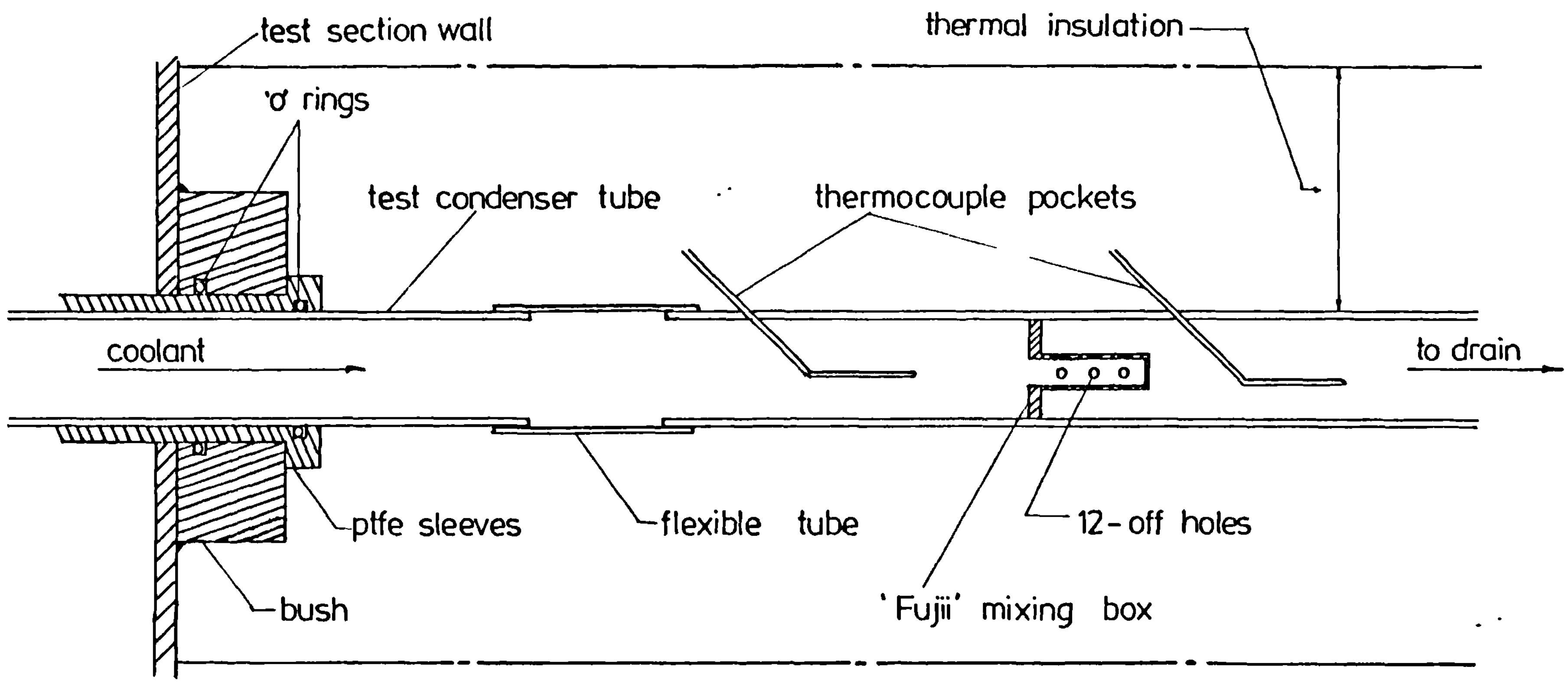

FIG. 4.7 LOCATION OF THE COOLANT OUTLET THERMOCOUPLES AND MIXING BOX

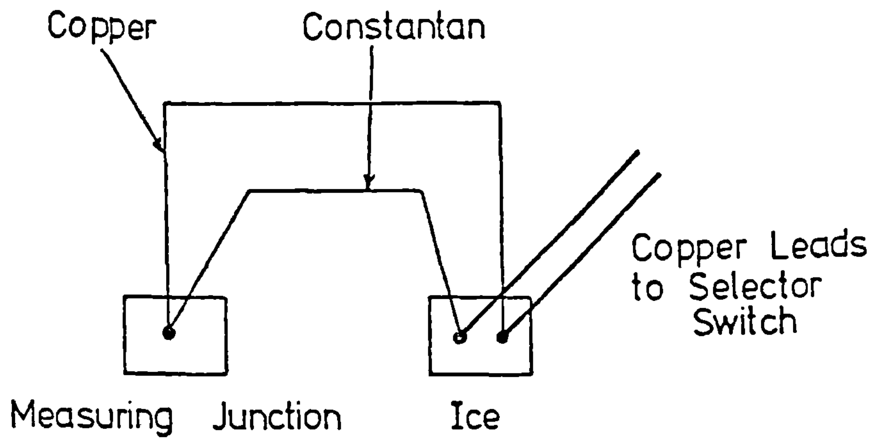

THERMOCOUPLE ARRANGEMENT

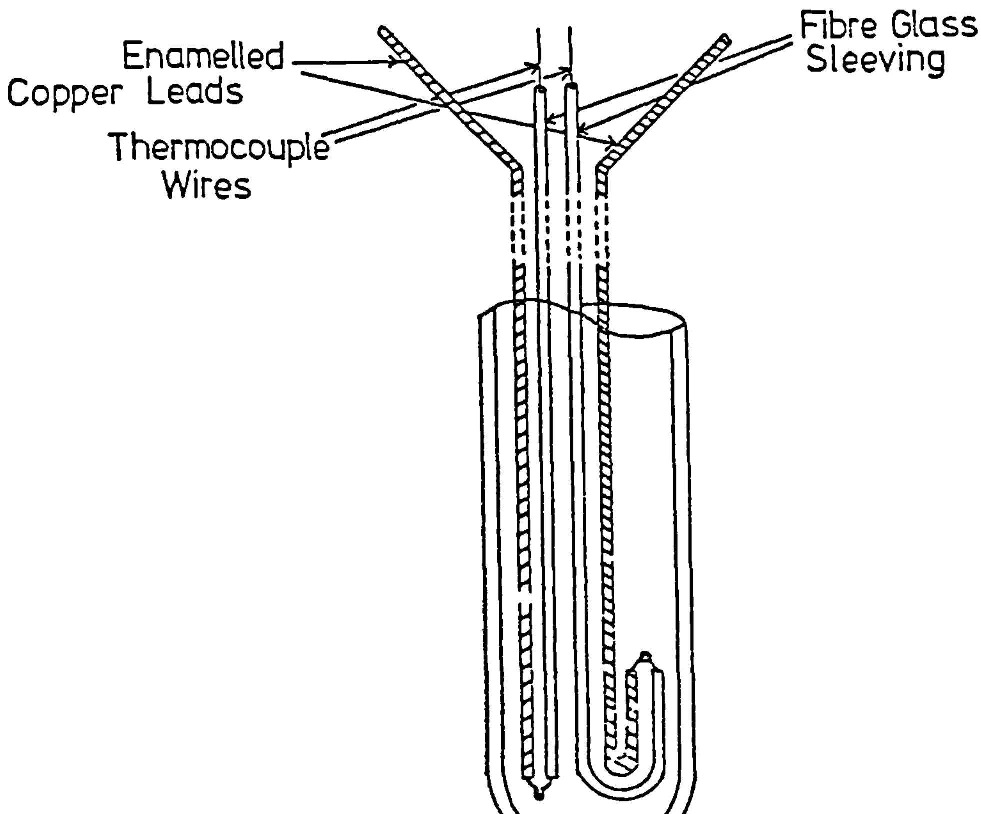

COLD JUNCTION TUBE

FIG. 4.8 THERMOCOUPLE ARRANGEMENT

CHAPTER 5 - PROCEDURES

5.1 Leak testing

Prior to carrying out tests, and periodically thereafter, the apparatus was tested for air in-leakage. To provide a criterion for judging the effects of air in-leakage on the heat-transfer measurements, an estimate was made of the leakage rate which would lead to a significant error in the measured value of the bulk air mass fraction, W_∞. This was taken as the value which would give a detectable change in W_∞ as determined from the pressure and temperature measurements using equation 6.16 (assuming saturation conditions). Taking the precision of the pressure measurement to be $\pm$ 0.1 mmHg and that of the temperature measurement to be $\pm$ 0.02 K (i.e. thermo-emf $\pm$ 1 μV), equation 6.16 could, for a pure vapour, indicate an apparent gas concentration (air) as shown in Table 5.1.

Table 5.1 Limit of estimation of air content from pressure and temperature measurements

Vapour	Pressure	Apparent air content	
	mmHg	mass fraction/ %	mole fraction /%
Steam	760	0.14	0.05
	40	0.60	0.37
R-113	760	0.06	0.39
	300	0.02	0.13

It is evident that in-leakage will be most serious when operating at low pressures and that the air concentration in the vapour resulting from a given leakage rate will be largest for the smallest vapour flow rate. Table 5.2 gives, for the lowest pressure and the lowest vapour flow rate used in the subsequent investigation, the leakage rate which would lead to a measureable air concentration.

Table 5.2 Detectable air in-leakage rate for the lowest pressure and the lowest vapour flow rate used

Vapour	Pressure	Detectable bulk air content		Lowest $\dot{m}_v$	Detectable air leakage rate‡	
	mmHg	W_∞/%	$\tilde{W}_\infty$/%	g/s	$\dot{m}_a$/(g/s)	lr/(l torr/s)
Steam	40	0.60	0.37	3	0.02	13
R-113	300	0.02	0.13	100	0.02	13

At the start of the present investigation, the apparatus was drained and evacuated. A pressure of about 2 mmHg was attained in about one hour. After continuous pumping for a further week, a pressure of about 0.2 mmHg was reached.† It was presumed that small leaks were present.

To determine the leak rate, the venting valve (see fig. 4.1) was closed and the pressure recorded. After a further 4 days, the pressure had risen to 26 mmHg indicating a leak rate of about 0.03 l torr/s. As may be seen from Table 5.2, this is clearly insignificant for the present purposes. It may further be noted that the leak rate was determined for pressures lower than the lowest used in the subsequent tests (40 mmHg).

Leak rate checks, as described above, were conducted frequently throughout the investigation and always when significant discrepancy between the gas concentration indicated by the pressure-temperature measurements and that indicated by the vapour and gas flow rates (including

‡Air leakage rate corresponding to the detectable bulk air content.

$$\mathrm{lr} = \frac{\text{pressure rise due to leakage} * \text{internal volume of apparatus}}{\text{time}}$$

(estimated internal volume of apparatus is 400 litres)

†For the vacuum pump used, the manufacturers indicated an ultimate vacuum obtainable is greater than 0.005 mmHg.

the special case of "pure" vapour, i.e. no gas was injected) was noted. When significant leakage was indicated, the following procedure was adopted to locate the leaks.

The apparatus was drained and air (from the laboratory supply line) was allowed to enter until the pressure was about 5 cmHg above that of the atmosphere. Relatively large leaks were detected by spraying soapy water in the vicinity of suspected leak points. Bubbles could be seen in the event of a substantial leak. Smaller leaks were detected using a halogen leak detector (Leybold Ltd., model no. 163-81-SU-17. This operates by detecting halogen-based compounds, in this case Refrigerant 12. The manufacturers claimed detection of leak rates of 10^{-6} l torr/s). The detector was connected in the vacuum line just before the pump (see fig. 5.1) and the apparatus was then evacuated. Refrigerant was applied by aerosol spray at points where leakage was suspected. In-leakage of the refrigerant activated either a meter or a loudspeaker. When a leak was detected, appropriate action, depending on the nature of the leak, was taken (e.g. gaskets or 'O' rings replaced, clips and bolts tightened, etc.). When it was considered that the apparatus was satisfactorily

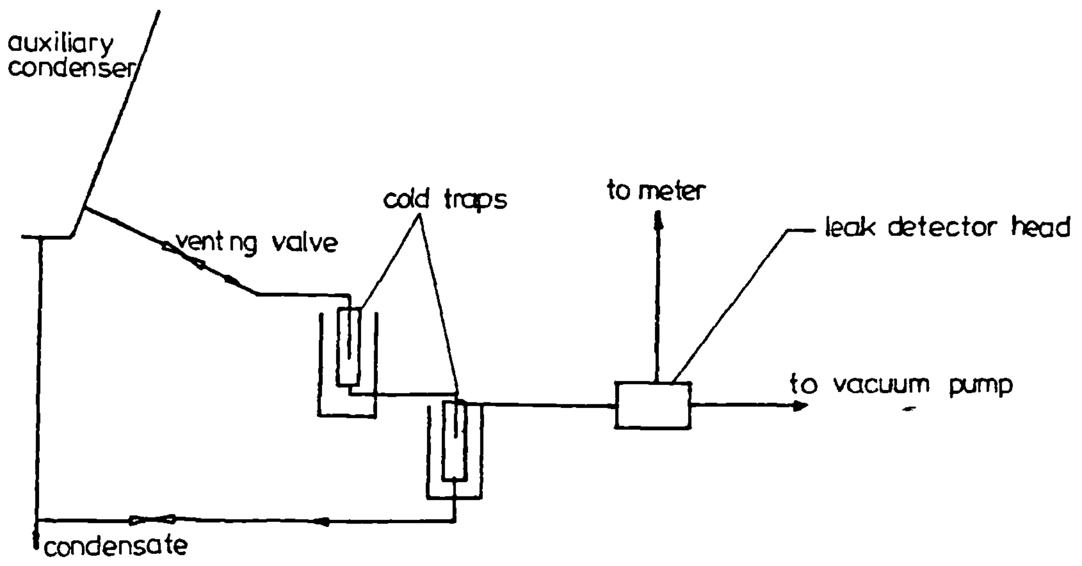

FIGURE 5.1 LOCATION OF THE LEAK DETECTOR

leak-tight, it was left overnight under vacuum and the leak rate determined by measuring the pressure rise.

Before taking further measurements, the following procedure was adopted to ensure that the apparatus would remain leak-tight under test conditions. It was filled with the test fluid and operated (i.e. boiling and condensing), without taking measurements, for a period of 8 hours a day for a week both at atmospheric pressure and at a pressure of 6 kPa for steam and 40 kPa for Refrigerant 113. The apparatus was then left overnight under vacuum with the test fluid in the boilers and the leak rate determined by measuring the pressure rise.

As noted earlier, leak-rate checks by measuring the overnight pressure rise were carried out frequently throughout the course of the investigation. In general, the leak rate was found to be less than 0.03 l torr/s, except in a few instances when significant leak rates were detected and appropriate actions taken. It may be noted that a leak rate of 0.03 l torr/s corresponds to a maximum air content of about 1×10^{-3} % (mass fraction) or 6×10^{-4} % (mole fraction) in the case of steam and 5×10^{-5} % (mass fraction) or 3×10^{-2}% (mole fraction) in the case of Refrigerant 113.

5.2 Preparation of the condensing surface

For the case when the test fluid was distilled water, Frydas /91 / found that film condensation persisted for at least four hours when the following preliminary procedure (recommended by Al-Diwany and Rose /82 /) was used. The condensing surface was first rinsed with tap water and then lightly rubbed with fine "wet or dry" paper (Grade P800) wetted with dilute sodium hydroxide solution. It was then rinsed throughly with tap water and finally with distilled water. In the present investigation, the condensing surface was cleaned using the above procedure. In addition, it was found that spraying the condensing surface with distilled water immediately after it was inserted in the test section and then allowing coolant to pass to prevent evaporation, assisted in the maintainence of film condensation. In the present work, film condensation normally persisted for the duration of a day's testing (about 8 hours).

For the case when the test fluid was Refrigerant 113, the condensing surface was lightly rubbed with fine "wet or dry" paper prior to insertion in the test section. Film condensation was always obtained.

5.3 Start up procedure

With coolant passing through the test condenser tube and the auxiliary condenser and with the venting and filling valves (see fig. 4.1) open, the boiler heaters were switched on at maximum power (about 30 kW). Upon commencement of condensation on the test condenser tube, visual observation was made to ascertain the mode of condensation. When it was established that the condensing surface was completely wetted, the coolant flow rates through the test condenser tube and the auxiliary condenser were set to low values while the apparatus was purged vigorously to the atmosphere to remove non-condensing gases. After about 20 minutes, the coolant flow rates were increased and less vigorous purging conducted for about two hours. Throughout this period, visual observations were made at regular intervals (about 15 minutes) to check that the mode of condensation was filmwise. When the process of purging was completed, the pressure and temperature in the test section were observed and checked that they corresponded to saturation values to within the accuracy of the measurements.

5.4 Test procedure

For tests at atmospheric pressure, the filling and venting valves were left open to the atmosphere. For tests at sub-atmospheric pressures, the valves were closed and the vacuum pump was connected to the venting valve via the "cold traps" (see fig. 4.1). The venting valve was gradually opened and the pressure in the test section allowed to attain its lowest value. When a steady state was reached, the valve supplying cooling water to the auxiliary condenser was fully opened and the following test procedure carried out :-

i. the ambient pressure and temperature were recorded;

ii. the heater input power was set to the nominal desired value and measured;

iii. the gas flow rate and the test condenser tube coolant flow rate were set to the desired values;

iv. the following observations were recorded :-

   a. the thermo-emfs of the thermocouples in the boilers, the test section, the test condenser tube wall, the coolant path (inlet to and outlet from the test section) and the condensate return manifold;

   b. the coolant flow rate through the test condenser tube;

   c. the test section pressure;

   d. the gas flow rate (i.e. indicated volume flow rate together with the pressure and temperature of the gas at inlet to the flowmeters).

At the end of each set of tests for a given heater input power (which could last up to one hour), the power and the ambient pressure and temperature were again recorded. The above procedure was carried out for various heater input powers, at each of which a range of gas flow rates were used and for each gas flow rate, a range of coolant flow rates were used.

When operating at atmospheric pressure, it was possible to use up to four different heater input powers in one day. At sub-atmospheric pressures, however, it was only possible to obtain sets of results for a maximum of two different heater input powers.

CHAPTER 6 - OBSERVATIONS, CALCULATIONS AND RESULTS

6.1 Visual observations

The test condenser tube was observed via the glass window at regular intervals (about 15 minutes) during all tests to ensure that the mode of condensation remained filmwise. For the case when the test fluid was water, the tube surface changed from a shiny appearance to a dull dark brown colour during the course of a day's running. When using Refrigerant 113, the surface remained bright and shiny. In both cases, however, it was observed that the condensate fell from the bottom of the tube in drops (without sideways motion along the tube) rather than as a sheet. The drops leaving the tube were more or less evenly distributed along its length. The number of drop detachment locations along the length of the tube for the case of Refrigerant 113 was about twice that for the case of water. The size of the departing drops was smaller in the case of Refrigerant 113.

6.2 Calculation of the main parameters

6.2.1 Vapour temperature in the test section (T_∞)

For all the tests (i.e. both pure vapours and vapour-gas mixtures) the vapour temperature was taken as the arithmetic mean of the temperatures recorded by the four upstream thermocouples in the test section. The difference between the highest and the lowest values of the temperatures was generally less than 0.05 K.

6.2.2 Test condenser tube outside surface temperature (T_w)

During all tests, the test condenser tube was orientated so that the four junctions of the thermocouples in the tube wall were located at angles of 45° and 135° to the vertical on either side of the forward stagnation point. Four local temperatures (T_{tc}'s) at known positions within the tube wall were thus obtained. The outside surface temperatures (T_{wo}'s) were estimated from

$$T_{wo,j} = T_{tc,j} + \dot{Q}_{cw} \ln(d_o/d_{tc})/(2\pi k_t L) \qquad j = 1,2,3,4 \qquad (6.1)$$

where $\dot{Q}_{cw}$ is the mean heat-transfer rate evaluated from coolant measurements

k_t is the thermal conductivity of the tube material (copper)

L is the exposed length of the tube

d_o is the outside diameter of the tube

d_{tc} is the thermocouple location diameter

Note: Equation 6.1 is strictly valid only for uniform radial conduction in the tube wall. However, the second term in the equation was always small ($\leqslant 2.0$ K). The range of variation of the difference in the tube wall temperatures measured at 45° and 135° from the forward stagnation point is 0.02 to 14.24.

Following the recommendations of Fujii et. al. /49 /, the value of T_w was taken as the arithmetic mean of the four values of T_{wo} around the wall of the test condenser tube.

6.2.3 Test section pressure (P_∞)

The test section pressure was obtained from the mercury-filled U-tube manometer reading, thus

$$P_\infty = P_{at} + \rho_{Hg} g h \qquad (6.2)$$

where P_{at} is the barometric pressure

ρ_{Hg} is the density of mercury

g is the gravitational acceleration

h is the difference in heights of the mercury columns

6.2.4 Heat flux on the outside surface of the test condenser tube ($\dot{Q}''_{obs}$)

The heat-transfer rate to the test condenser tube was obtained by measuring the flow rate and increase in temperature of the cooling water. The heat flux was evaluated from :

$$\dot{Q}''_{obs} = \dot{m}_{cw}\, c_{Pcw}\, (T_{out} - T_{in}) \,/\, (\pi d_o L) \qquad (6.3)$$

where $\dot{m}_{cw}$ is the mass flow rate of the coolant calculated using equation 4.1

c_{Pcw} is the specific isobaric heat capacity of the coolant, taken as c_{Pf} at $(T_{out} + T_{in}) / 2$

T_{in}, T_{out} are the coolant inlet and outlet temperatures

In view of the fact that the coolant temperature rise in certain cases is small, the reliability of the heat flux calculations based on coolant measurements was assessed by conducting preliminary tests in which the condensate from the test condenser tube was collected over measured time intervals. Measurements were made with the smaller diameter test condenser tube only and covered the whole range of coolant flow rates used in the main tests. The agreement between the two methods was, in general, better than 5 % (see Appendix C).

6.2.5 Heater input power ($\dot{Q}_h$)

The electrical power supplied to the heaters in the boilers was obtained from the measurements of the potential drops across the heater terminals and across the standard resistors connected in series with the heaters (see fig. 4.6).

$$\dot{Q}_h = \sum_{j=1}^{6} (V_j \, I_j) \tag{6.4}$$

where V_j is the potential drop across the terminals of the heater j

I_j is the current passing through the heater j

I_j was obtained from :

$$I_j = V_{r,j} / R_j \tag{6.5}$$

where $V_{r,j}$ is the potential drop across the standard resistor j

R_j is the resistance of the standard resistor j

The values of the standard resistors used in series with the corresponding heaters (see fig. 4.6) were :

R_1 = 0.009973 ohm

R_2 = 0.009964 ohm

R_3 = 0.009965 ohm

R_4 = 0.009982 ohm

$R_5 = 0.009975$ ohm

$R_6 = 0.009965$ ohm

6.2.6 Vapour mass flow rate at the test section ($\dot{m}_v$)

The vapour mass flow rate at the test section was obtained from the electrical power supply to the boiler heaters ($\dot{Q}_h$) by application of the steady flow energy equation for the condensing fluid and non-condensing gas streams. A correction for the heat transfer from the apparatus to the environment (i.e. "thermal losses") was included.

In evaluating the thermal losses (and in subsequent calculations of vapour flow rate), it is necessary to consider the apparatus from the boilers to the test section entry in two parts, i.e. referring to fig. 6.1a, that to the left of XX (boilers and vapour supply line) and that to the right of XX and upstream of the test condenser tube (calming section and test section entry). This arises from the fact that the vapour supply line to the left of XX slopes towards the boilers so that any condensate resulting from thermal losses through these walls returns to the boilers, essentially at boiler temperature, while condensate resulting from losses through the calming section and test section entry walls passes to the auxiliary condenser.

To determine the thermal losses, tests using pure steam were carried out at atmospheric pressure for various heater input powers. With coolant flowing through the test condenser tube and the auxiliary condenser, and when operating under steady conditions (the apparatus having been purged as described in section 5.3), the heater input power, the test section vapour temperatures and the ambient temperature were measured. The condensate resulting from thermal losses through the walls of the calming section and the test section entry was collected by means of a neoprene rubber channel fitted around the inside perimeter of the test section just above the test condenser tube (see figs. 6.1a and 6.2) and led to a measuring cylinder, A. By collecting the condensate over a measured time interval the condensation rate $\dot{m}_A$ could thus be determined. The remainder of the condensate (i.e. from the test condenser tube, the downstream part of the test section and the auxiliary condenser) was collected in a second measuring cylinder, B (see fig. 6.1a). Again, by collecting the condensate over a measured time interval the condensation rate $\dot{m}_B$ could be determined. When operating in this manner, the thermal losses through the walls of the boilers and the vapour supply line $(\dot{Q}^*_{loss1})$ is given by :

$$\dot{Q}^*_{loss1} = \dot{Q}_h - (\dot{m}_A + \dot{m}_B)\, h_{fg} \tag{6.6}$$

where h_{fg} is the specific enthalpy of evaporation of the vapour.

The thermal losses through the walls of the calming section and the test section entry $(\dot{Q}^*_{loss2})$ is given by :

$$\dot{Q}^*_{loss2} = \dot{m}_A\, h_{fg} \tag{6.7}$$

The results of the above tests are given in Table 6.1 and shown in fig. 6.3.

The values of the major thermal loss, $\dot{Q}^*_{loss1}$ (the surface area of the boilers and the vapour supply line is much larger than that of the calming section and the test section entry), show no clear evidence of systematic dependence on the heater input power (and hence vapour velocity). This is to be expected since the walls of the apparatus were very well insulated, so that the insulation material constitutes the major thermal resistance. Consequently, the mean value of 740 W was adopted (see fig. 6.3). The values of $\dot{Q}^{*}_{loss2}$, however, appear to show a small systematic increase with increasing heater input power as shown in fig. 6.3. The increase was thought to result from "carry-over" of liquid from the boilers, which would increase with increasing vapour velocity. Equation 6.7 would therefore overestimate the loss. By extrapolating the values of $\dot{Q}^{*}_{loss2}$ back to a heater power of 740 W (i.e. where the whole of the heater input power is "lost" through the apparatus walls to the left of XX) where the vapour velocity at section XX would be zero and hence "carry-over" of liquid would be zero, the true value of $\dot{Q}^{*}_{loss2}$ was estimated to be 160 W (see fig. 6.3). The fact that $\dot{Q}^{*}_{loss1}$ was essentially independent of $\dot{Q}_h$ would indicate that any "carry-over" effect was less than the scatter of the data.

Since the insulation constitutes the major resistance to heat transfer, the values of the actual losses, $\dot{Q}_{loss1}$ and $\dot{Q}_{loss2}$ ($\dot{Q}^{*}_{loss1}$ and $\dot{Q}^{*}_{loss2}$ are the losses determined in the tests described above), in subsequent tests are proportional to the vapour-to-ambient temperature difference. When operating at vapour temperature other than those used in the above-mentioned "loss" determinations, the losses were estimated on the basis of linear interpolation with respect to the vapour-to-ambient temperature difference between the values given in Table 6.1 and zero when operating at vapour temperature equal to ambient temperature. Thus,

$$\dot{Q}_{loss1} = \dot{Q}^{*}_{loss1} \; (T_\infty - T_{at}) \,/\, (T^{*}_\infty - T^{*}_{at})$$

$$= 9.827 \; (T_\infty - T_{at}) \;\; \text{W/K} \qquad (6.8)$$

$$\dot{Q}_{loss2} = \dot{Q}^{*}_{loss2} \, (T_\infty - T_{at}) \, / \, (T^{*}_\infty - T^{*}_{at})$$

$$= 2.125 \, (T_\infty - T_{at}) \quad W/K \qquad (6.9)$$

where T_∞, T_{at} are the vapour and ambient temperatures for the actual tests

T^{*}_∞, T^{*}_{at} are the mean of the vapour and ambient temperatures for the tests to determine $\dot{Q}^{*}_{loss1}$ and $\dot{Q}^{*}_{loss2}$.

Before indicating in detail how the losses are incorporated in the calculation of the vapour mass flow rate at the test section, it may be noted that the total losses are, in general, quite small in comparison with the total heater input power. In the worst case (i.e. smallest heater input power and highest vapour temperature used) the total loss amounts to less than 15 % of the heater input power and is itself estimated with an accuracy better than 10 % (estimation is based on the scatter of $\dot{Q}^{*}_{loss1}$, see fig. 6.3 and Table 6.1).

During the actual tests (the rubber channel in the test section was not present), all of the condensate was returned continuously to the boilers and gas was injected into the boilers and removed from the auxiliary condenser via the venting valve. With reference to fig. 6.1b, a steady flow energy balance between the inlets to the boilers (condensate return and gas inlet) and a station just upstream of the test condenser tube gives :

$$\dot{Q}_h - \dot{Q}_{loss1} - \dot{Q}_{loss2} = \dot{m}_A \, h_{f2} + \dot{m}_v \, h_{g2} + \dot{m}_n \, h_{n2} - (\dot{m}_A + \dot{m}_v) \, h_{f1} - \dot{m}_n \, h_{n0} \qquad (6.10)$$

where $\dot{m}_A$ is the condensation rate on the walls of the calming and test sections

h_{f2} is the specific enthalpy at T_∞ of the condensate on the walls of the calming and test sections

$\dot{m}_v$ is the vapour mass flow rate just upstream of the test condenser tube

h_{g2} is the specific enthalpy of the vapour at T_∞

$\dot{m}_n$ is the mass flow rate of the gas injected into the boilers

h_{n2} is the specific enthalpy of the gas at T_∞

h_{f1} is the specific enthalpy of the condensate return at entry to the boiler

h_{n0} is the specific enthalpy of the gas at entry to the boiler.

Treating the gases (air and hydrogen) as ideal and for liquid water and liquid Refrigerant 113, taking

$$h_{f2} - h_{f1} = c_P (T_\infty - T_1) \qquad (6.11)$$

equation 6.10 gives

$$\dot{m}_v = \left[\frac{1}{h_{fg} + c_P (T_\infty - T_1)}\right] \left[\dot{Q}_h - \dot{Q}_{loss1} - \dot{m}_n c_{Pn} (T_\infty - T_0) - \dot{Q}_{loss2} \left(1 + \frac{c_P' (T_\infty - T_1)}{h_{fg}}\right)\right] \qquad (6.12)$$

where h_{fg} is the specific enthalpy of evaporation taken at T_∞

c_P is the specific isobaric heat capacity of the condensate return, taken as c_{Pf} at $(T_\infty + T_1) / 2$

T_1 is the temperature of the condensate return at entry to the boiler

c_{Pn} is the specific isobaric heat capacity of the gas taken at $(T_\infty + T_0)/2$

T_0 is the temperature of gas at entry to the boiler

Equation 6.12 was used to calculate $\dot{m}_v$ in all tests using $\dot{Q}_{loss1}$ and

$\dot{Q}_{loss2}$ from equations 6.8 and 6.9 respectively.

The fact that excellent agreement was obtained throughout the present work between the gas mass fraction calculated from the vapour and gas flow rates (equation 6.15) and that calculated from the pressure and temperature measurements of the vapour-gas mixture in the test section (equation 6.16), see Appendix D and Tables 6.10 to 6.17, helps to confirm that $\dot{m}_v$ (and hence U_∞, see section 6.2.9) was accurately determined.

6.2.7 Gas mass flow rate ($\dot{m}_n$)

The flowmeters used were calibrated to read volume flow rates at the standard temperature (T_o = 288.15 K) and pressure (P_o = 760 mmHg). The gas mass flow rate was calculated from :

$$\dot{m}_n = \dot{V}\rho = \dot{V}_{ind}\sqrt{\rho\,\rho_o} \qquad (6.13)$$

where $\dot{V}$ is the actual volume flow rate of gas at the temperature (T) and pressure (P) at inlet to the flowmeters

ρ is the density of gas at temperature T and pressure P

$\dot{V}_{ind}$ is the indicated volume flow rate of gas

ρ_o is the density of gas at temperature T_o and pressure P_o

Treating the gases as ideal, equation 6.13 becomes

$$\dot{m}_n = \frac{\dot{V}_{ind}}{R_n}\left[\frac{P\,P_o}{T\,T_o}\right]^{\frac{1}{2}} \qquad (6.14)$$

where R_n is the specific ideal-gas constant of the gas.

Equation 6.14 was used to calculate the gas mass flow rate in all tests.

6.2.8 Gas mass fraction (W_∞) and gas mole fraction ($\tilde{W}_\infty$)

The gas mass fraction at entry to the test section could be calculated by two methods :-

a. from the mass flow rates of gas and vapour, thus,

$$W_{\infty 1} = \dot{m}_n / (\dot{m}_n + \dot{m}_v) \tag{6.15}$$

b. from the pressure and temperature measurements in the test section assuming saturation conditions and the Gibbs-Dalton ideal-gas mixture equations, thus,

$$W_{\infty 2} = \frac{P_\infty - P_s(T_\infty)}{P_\infty - (1 - (M_v/M_n))\; P_s(T_\infty)} \tag{6.16}$$

where $P_s(T_\infty)$ is the saturation pressure of the vapour corresponding to T_∞

M_v, M_n are the relative molecular masses of the vapour and gas respectively

The mole fraction of the gas, $\tilde{W}_\infty$, corresponding to the mass fraction, W_∞, was calculated from

$$\tilde{W}_\infty = W_\infty / (W_\infty + (1 - W_\infty)\; M_n / M_v) \tag{6.17}$$

6.2.9 Mean upstream velocity of vapour or vapour-gas mixture (U_∞)

The mean vapour velocity over the exposed length of the test condenser tube was obtained from the mass flow rate using a seventh power velocity profile for turbulent flow. (The lowest Reynolds number of the flow based on the inside diameter of the test section (d_{ic}) was generally greater than 2000). Thus,

$$U_\infty = \frac{1}{\pi (L/2)^2} \int_0^{L/2} 2 \pi r U_r \, dr \qquad (6.18)$$

where L is the exposed length of the test condenser tube ($\simeq$ 110 mm)

U_r is the vapour velocity at radius r (measured from the centre of the test section)

U_r is given by :

$$U_r = U_o \left(1 - r / (d_{ic}/2)\right)^{1/7} \qquad (6.19)$$

where d_{ic} is the inside diameter of the test section (152.4 mm)

U_o is the vapour velocity at r = 0

which gives :

$$U_\infty = 0.905 \, U_o \qquad (6.20)$$

Similarly, the mean velocity over the whole test section ($\bar{U}$) is given by :

$$\bar{U} = \frac{1}{\pi (d_{ic}/2)^2} \int_0^{d_{ic}/2} 2 \pi r U_r \, dr \qquad (6.21)$$

which gives :

$$\bar{U} = 0.817 \, U_o \qquad (6.22)$$

$\bar{U}$ is obtained from :

$$\bar{U} = (\dot{m}_v + \dot{m}_n) \, v_v / A_{ts} \qquad (6.23)$$

where A_{ts} is the cross-sectional area of the test section, $\pi d_{ic}^2/4$

v_v is the specific volume of vapour or vapour-gas mixture in the test section

Combining equations 6.20, 6.22 and 6.23, U_∞ is given by :

$$U_\infty = 1.108\ (\dot{m}_v + \dot{m}_n)\ v_v\ /\ A_{ts} \qquad (6.24)$$

Equation 6.24 was used to calculate the mean upstream velocity of vapour or vapour-gas mixture for all tests. It is of interest to note here the calculated maximum variation of velocity along the exposed length of the test condenser tube in relation to the adopted mean value. From equation 6.19, the vapour velocity at $r = L/2$, $(U_{L/2})$, is given by:

$$U_{L/2} = 0.833\ U_o \qquad (6.25)$$

Thus,

$$\frac{U_o - U_\infty}{U_\infty} = 0.105 \qquad (6.26)$$

and

$$\frac{U_{L/2} - U_\infty}{U_\infty} = 0.079 \qquad (6.27)$$

i.e. the velocity variation along the exposed length of the test condenser tube was less than 11 % of the adopted mean value.

6.3 Results

Measurements have been carried out with the following pure vapours and vapour-gas mixtures:-

i. pure steam

ii. pure Refrigerant 113

iii. steam-air

iv. steam-hydrogen

v. Refrigerant 113-air

vi. Refrigerant 113-hydrogen

Refrigerant 113 was chosen since it is relatively non-toxic and its properties well documented and are markedly different from those of steam. Moreover, there is no difficulty in maintaining filmwise condensation with this fluid. The vapour-gas combinations were chosen to give a wide range of Schmidt number (approximately 0.05 to 0.5) so as to provide a satisfactory basis for assessing the reliability of the theory /72 /.

The measurements were obtained for a wide range of vapour velocities, gas mass fractions, bulk-to-wall temperature differences, pressures and coolant flow rates. To investigate the effect of the tube diameter, measurements for steam and steam-air mixtures were obtained for two copper tubes of two different diameters. Table 6.2 gives the approximate overall ranges of the main parameters used in the tests. Full details of the results, which were calculated according to the procedure outlined in section 6.2 above, are given in Tables 6.3 to 6.17. The thermophysical equations used in the calculations are given in Appendix E. Sample calculations are given in Appendix F and a discussion of the estimation of errors in Appendix G.

6.3.1 Pure vapours

Samples of the pure vapour results are plotted on the basis of heat flux ($\dot{Q}''_{obs}$) against coolant velocity (U_{cw}) in figs. 6.4 to 6.10 and $\dot{Q}''_{obs}$ against bulk-to-wall temperature difference (ΔT) in figs. 6.11 to 6.17. In each figure, only the results for two different vapour velocities are shown. For the atmospheric-pressure tests, these corresponded to the lowest and highest values of the vapour velocity. For the sub-atmospheric-pressure tests where the pressure varies considerably within each category, the two vapour velocities corresponded to the lowest and highest values for tests performed at approximately the same pressure. It is seen from these figures that, for given values of U_{cw} and ΔT, the heat-transfer rate increases with increasing vapour velocity. This is attributed to the fact that increasing the vapour velocity increases the interfacial shear stress resulting in a thinner condensate film. Consequently, the heat-transfer rate increases.

In figs. 6.11 to 6.17, lines representing the simple Nusselt theory are also shown. In all cases, the effect of vapour velocity can be clearly seen.

6.3.2 Vapour-gas mixtures

When testing at sub-atmospheric pressures, the vacuum pump was always operated at full capacity. Thus for a given vapour flow rate, the system pressure increases with each increase in the gas flow rate injected into the boilers. Therefore, apart from the atmospheric-pressure tests, no sets of data were obtained at constant pressure. Consequently, only the results for the atmospheric-pressure tests are plotted on the basis of heat flux ($\dot{Q}''_{obs}$) against bulk gas mass fraction (W_∞) in figs. 6.18 to 6.22. As in the pure vapour case, only the results for two different vapour velocities are shown.

As anticipated, it is seen that the heat-transfer rate, for given vapour velocity, decreases with increasing bulk gas mass fraction, while, for given bulk gas mass fraction, the heat-transfer rate increases with increasing vapour velocity.

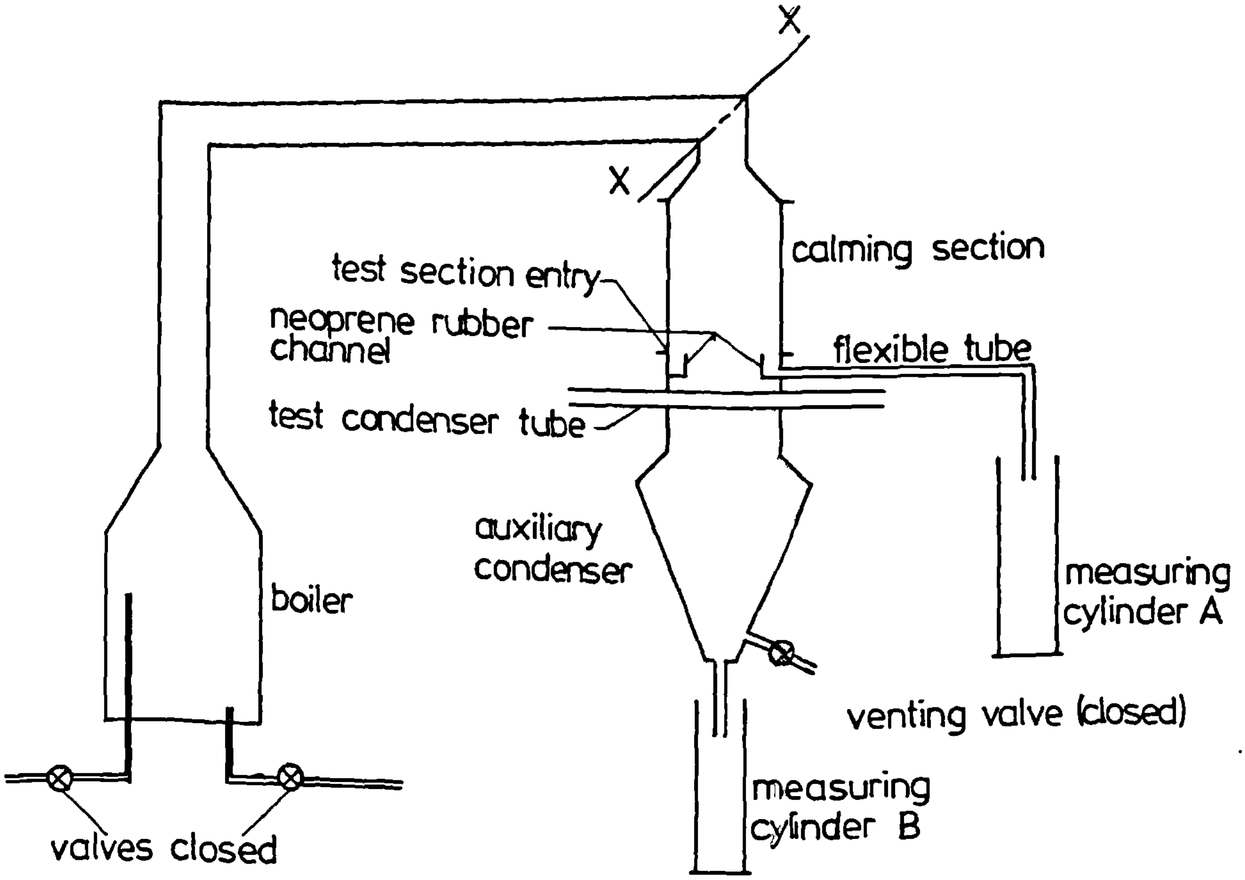

a. ARRANGEMENT OF APPARATUS FOR THERMAL LOSS TESTS

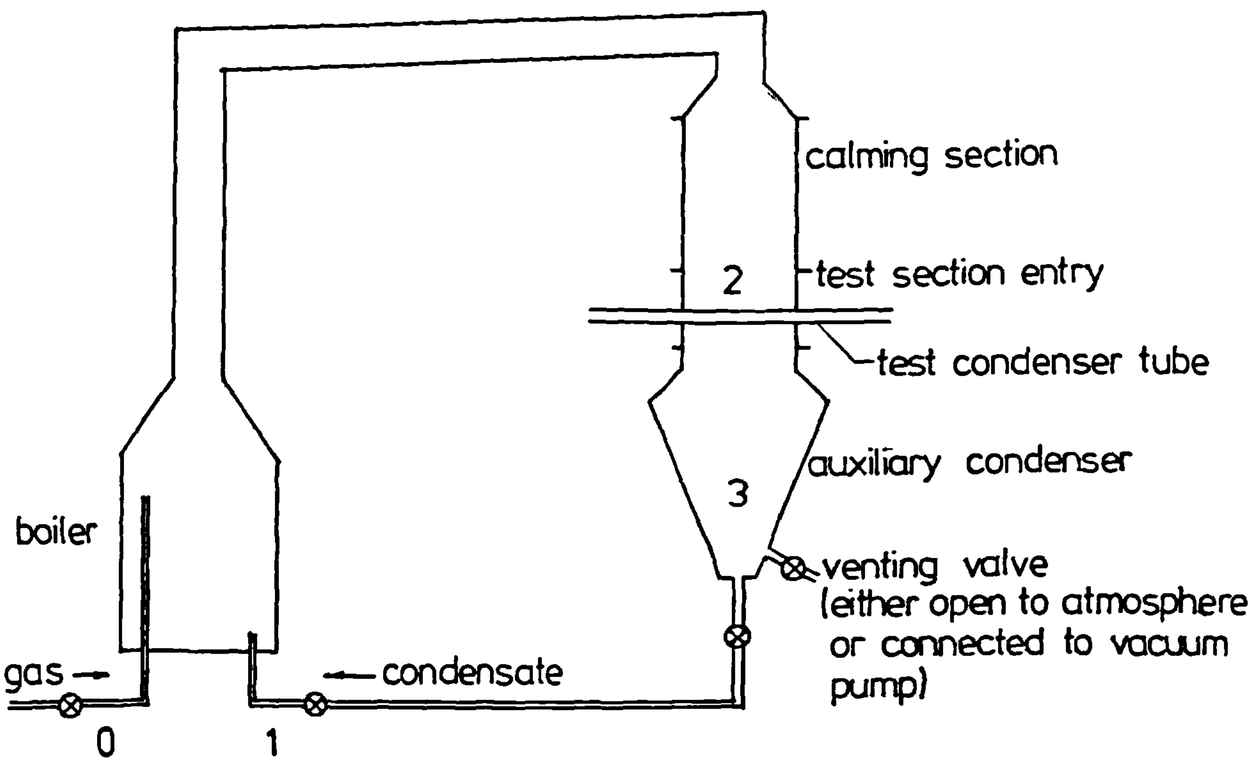

b. ARRANGEMENT OF APPARATUS FOR ACTUAL TESTS

FIGURE 6.1

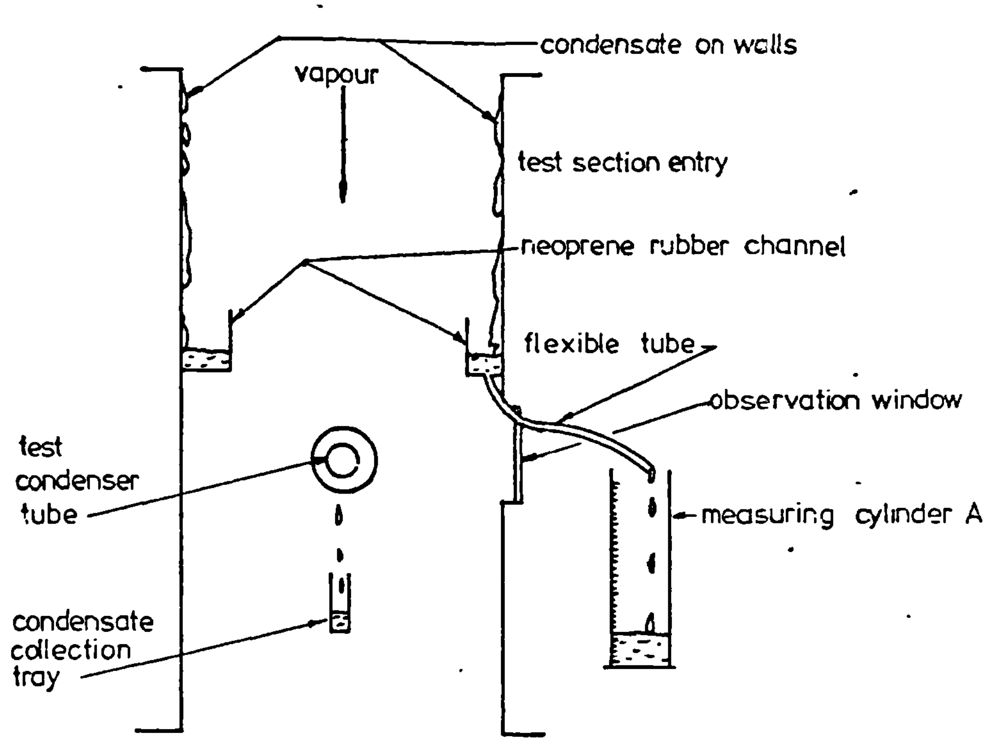

FIGURE 6.2 ARRANGEMENT OF TEST SECTION WITH NEOPRENE RUBBER CHANNEL FITTED

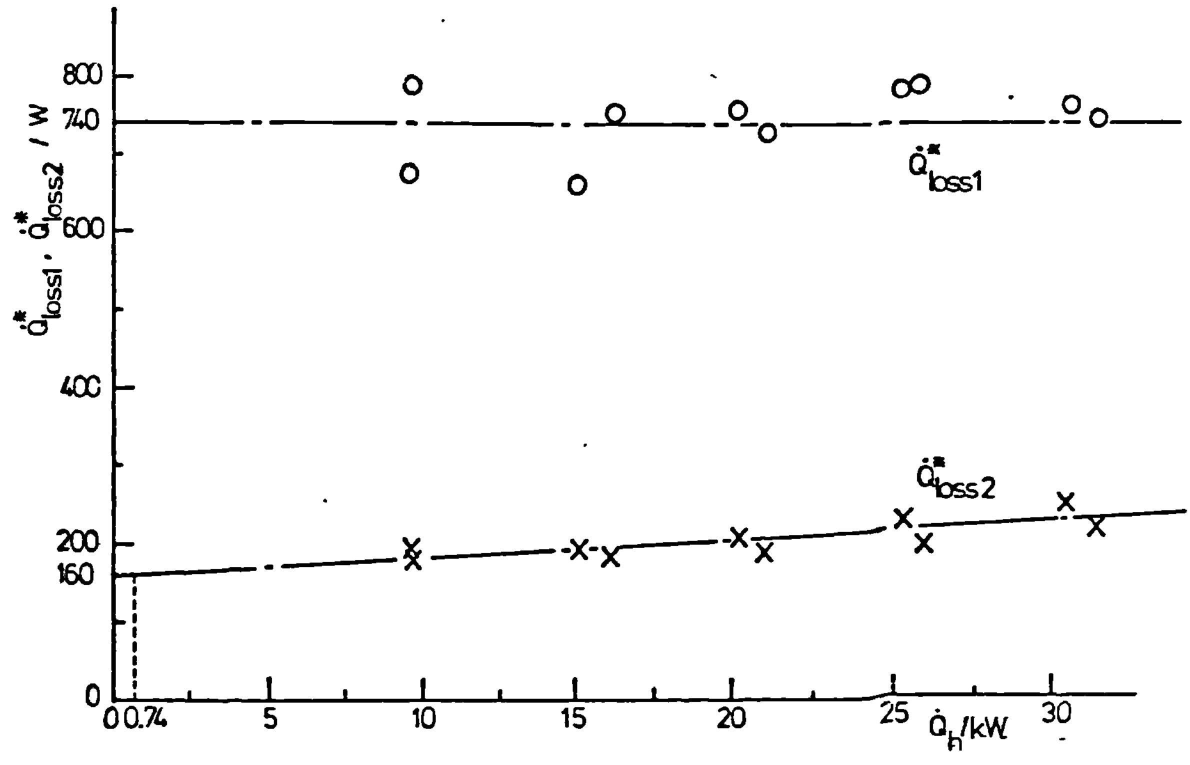

FIGURE 6.3 VARIATION OF THERMAL LOSSES ($\dot{Q}^*_{loss1}$ and $\dot{Q}^*_{loss2}$) WITH HEATER INPUT POWER ($\dot{Q}_h$)

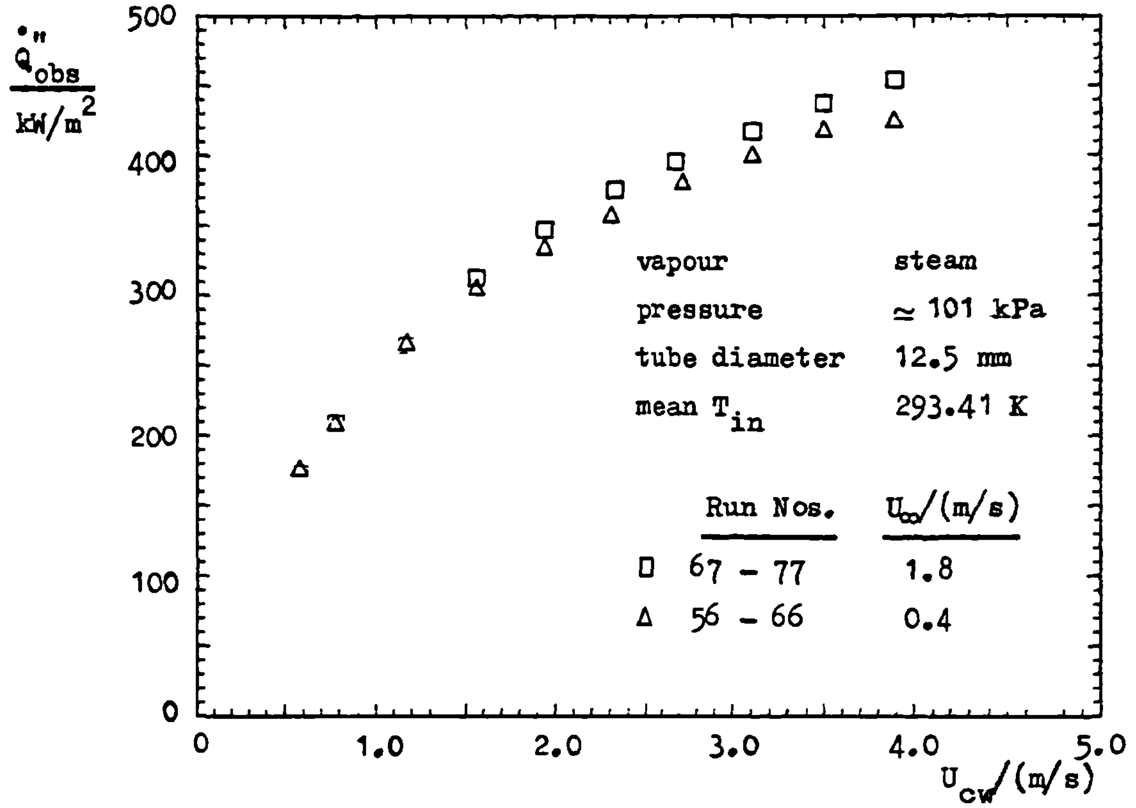

Figure 6.4 Relation between heat flux and coolant velocity: effect of vapour velocity

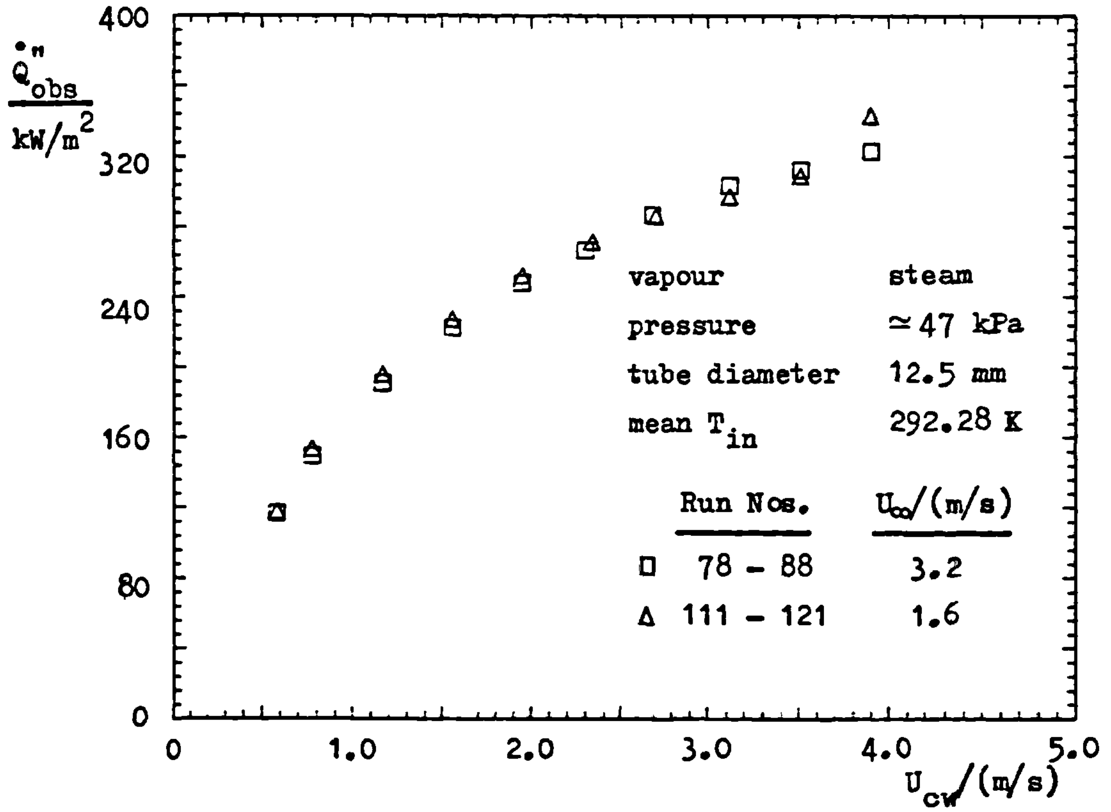

Figure 6.5 Relation between heat flux and coolant velocity: effect of vapour velocity

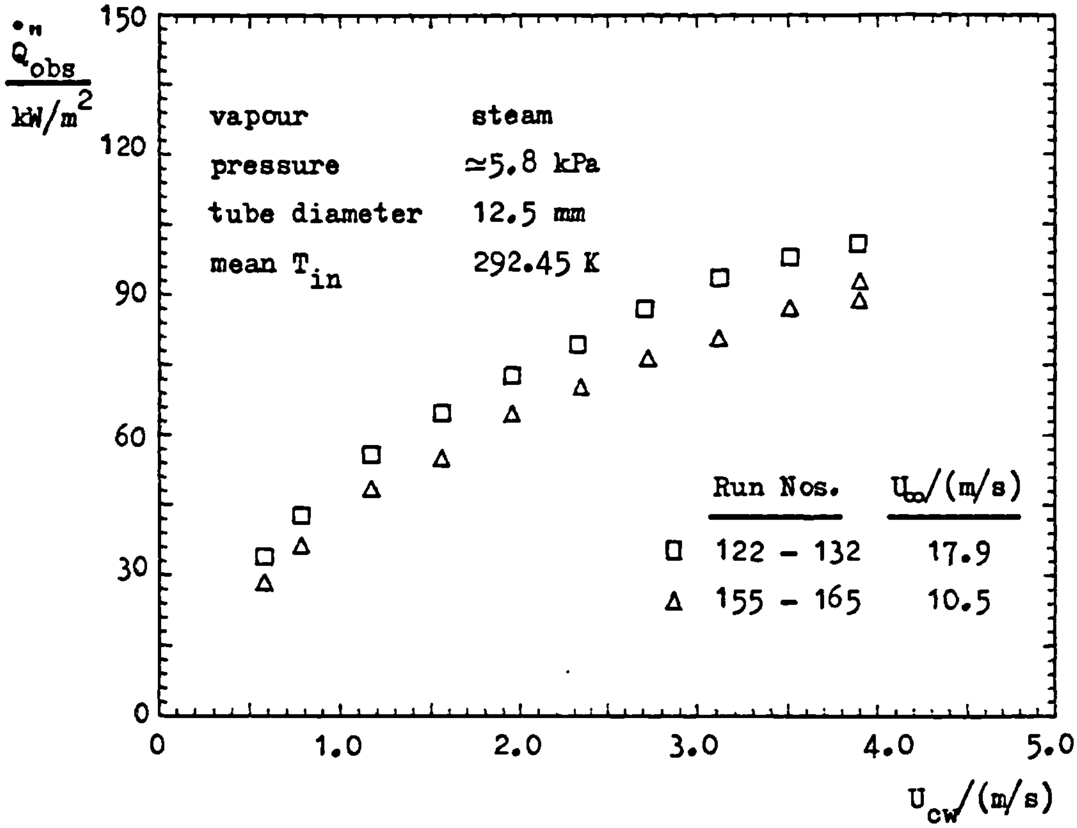

Figure 6.6 Relation between heat flux and coolant velocity: effect of vapour velocity

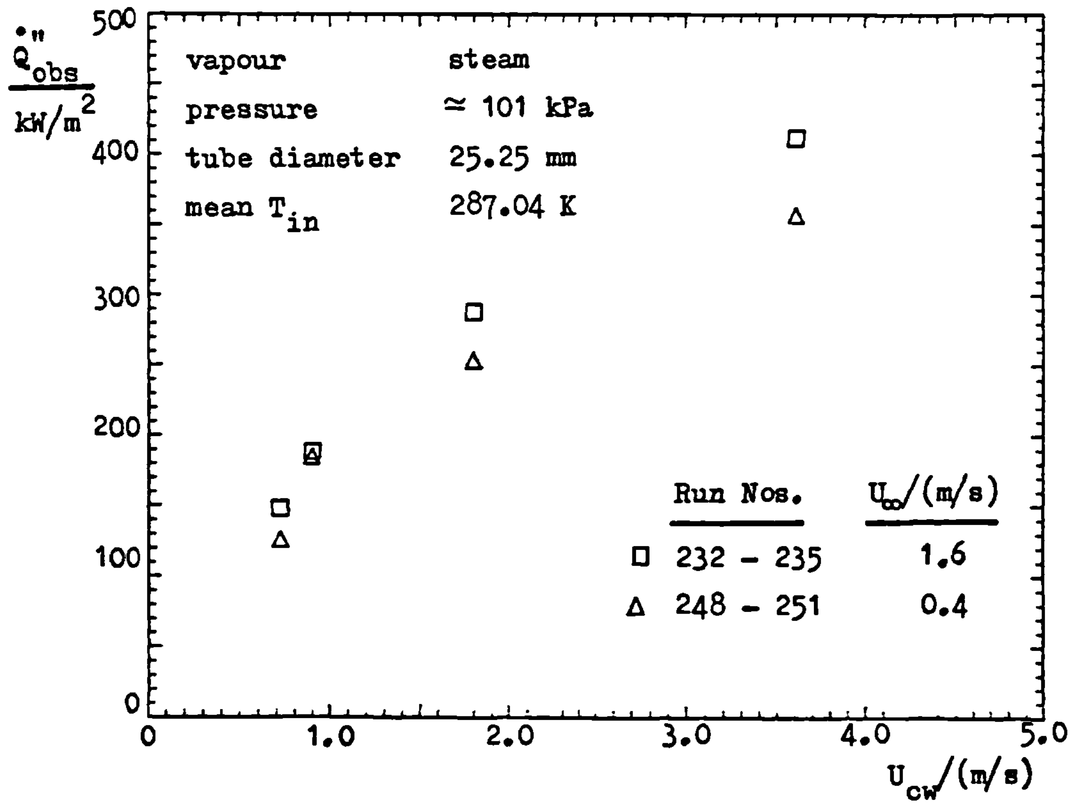

Figure 6.7 Relation between heat flux and coolant velocity: effect of vapour velocity

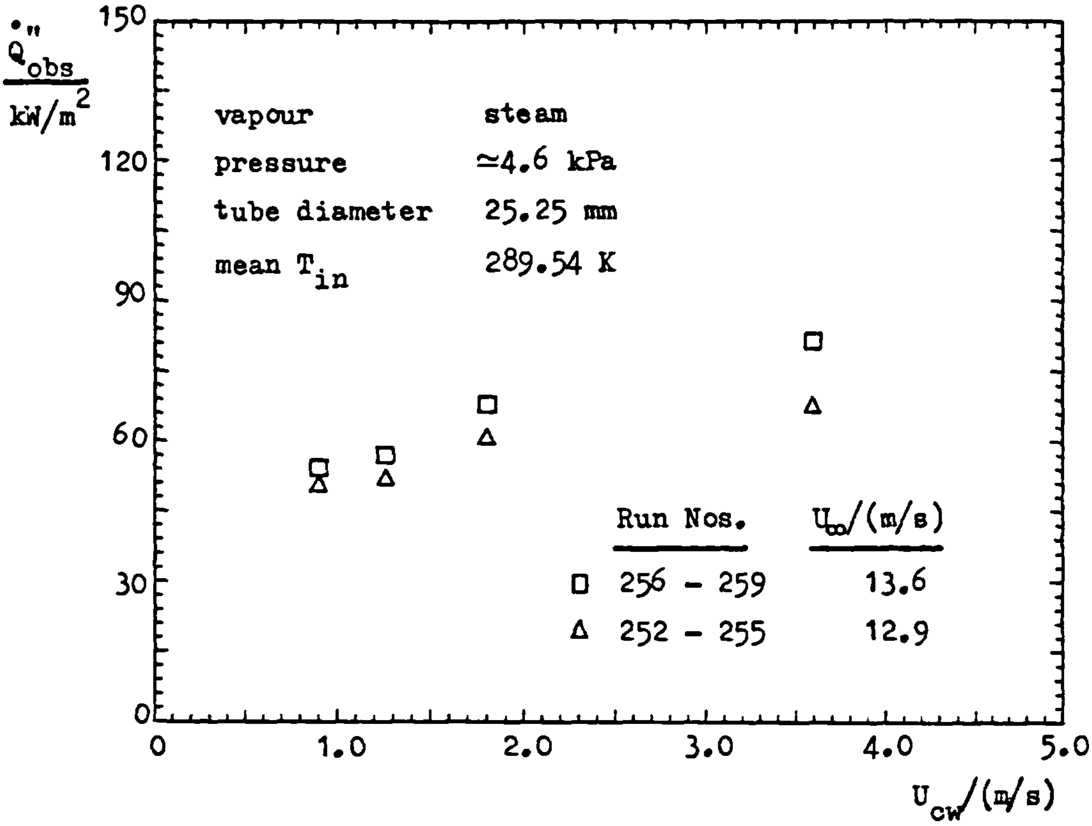

Figure 6.8 Relation between heat flux and coolant velocity: effect of vapour velocity

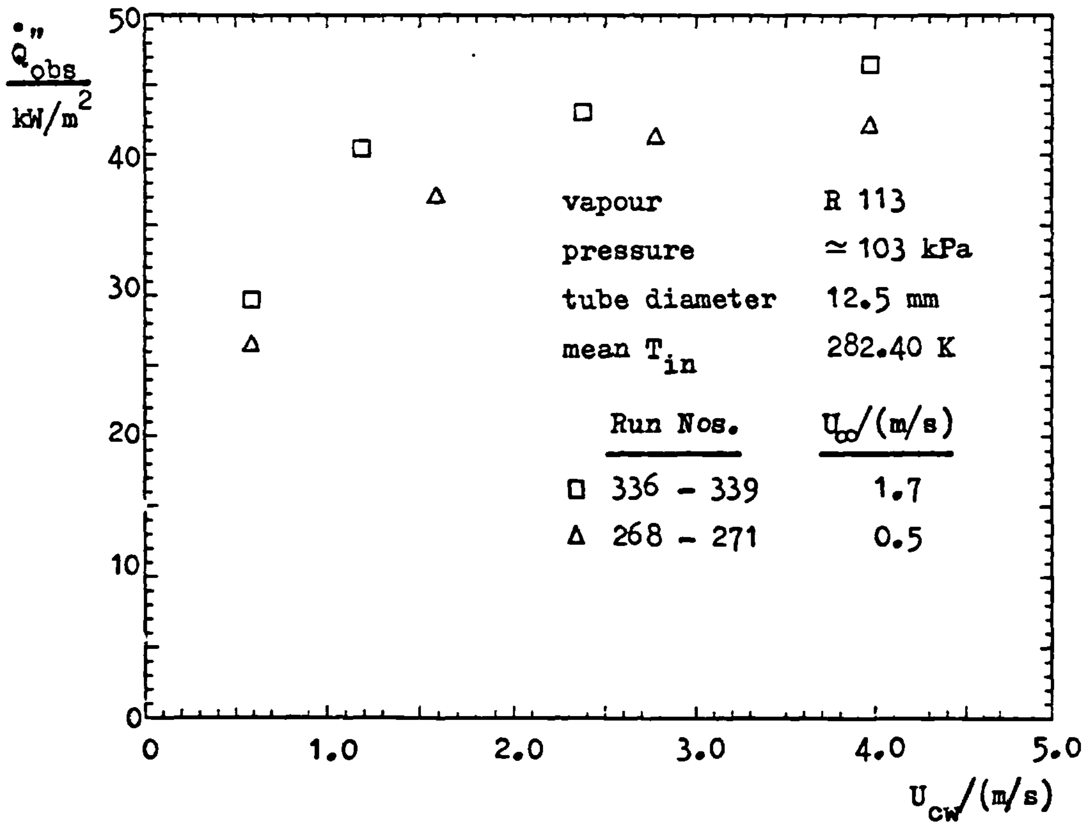

Figure 6.9 Relation between heat flux and coolant velocity: effect of vapour velocity

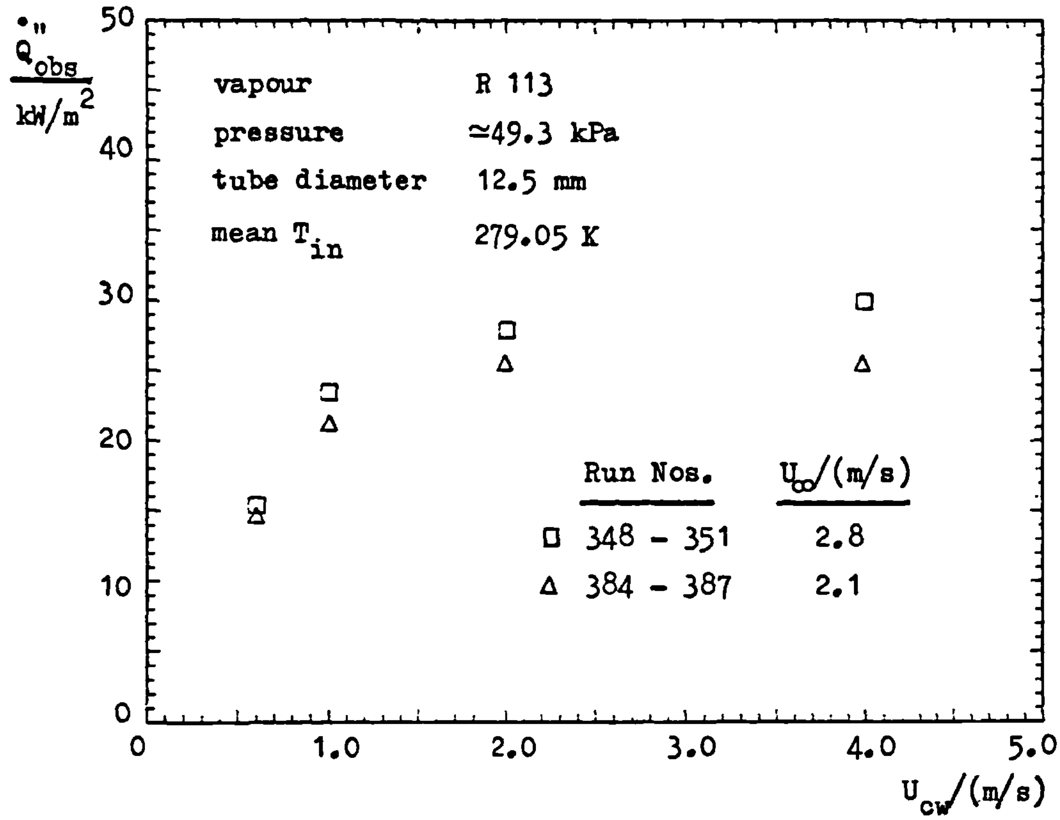

Figure 6.10 Relation between heat flux and coolant velocity: effect of vapour velocity

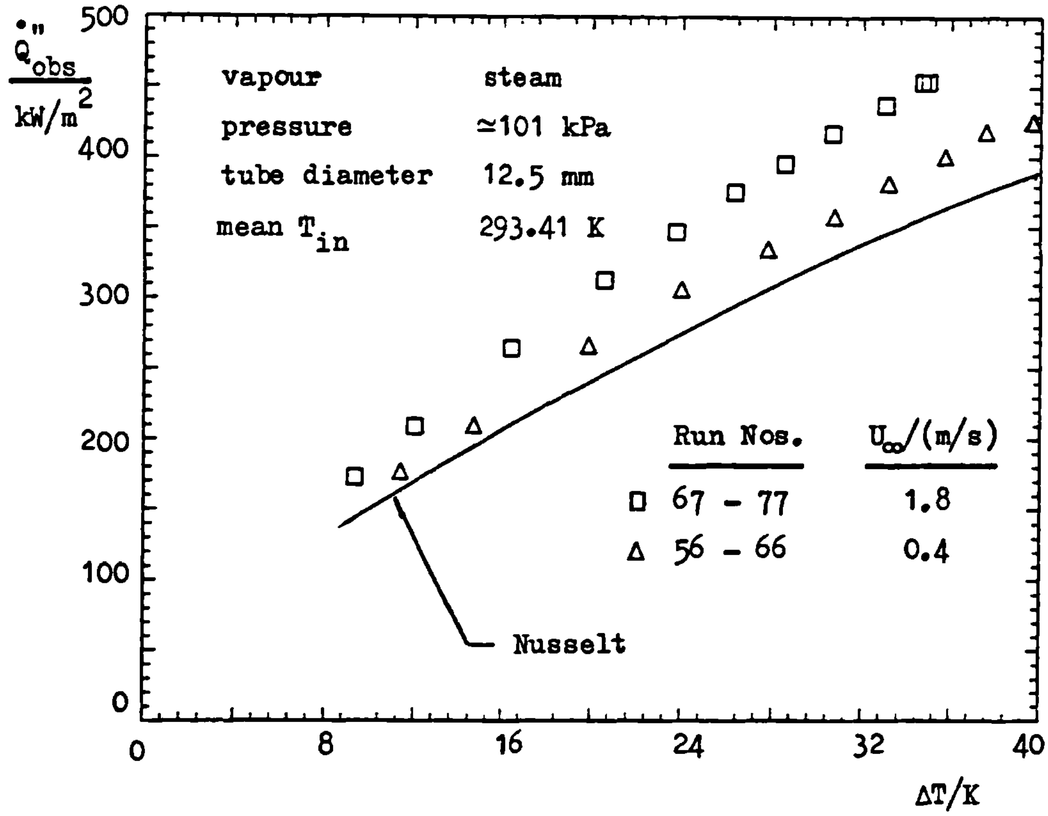

Figure 6.11 Relation between heat flux and bulk-to-wall temperature difference: effect of vapour velocity

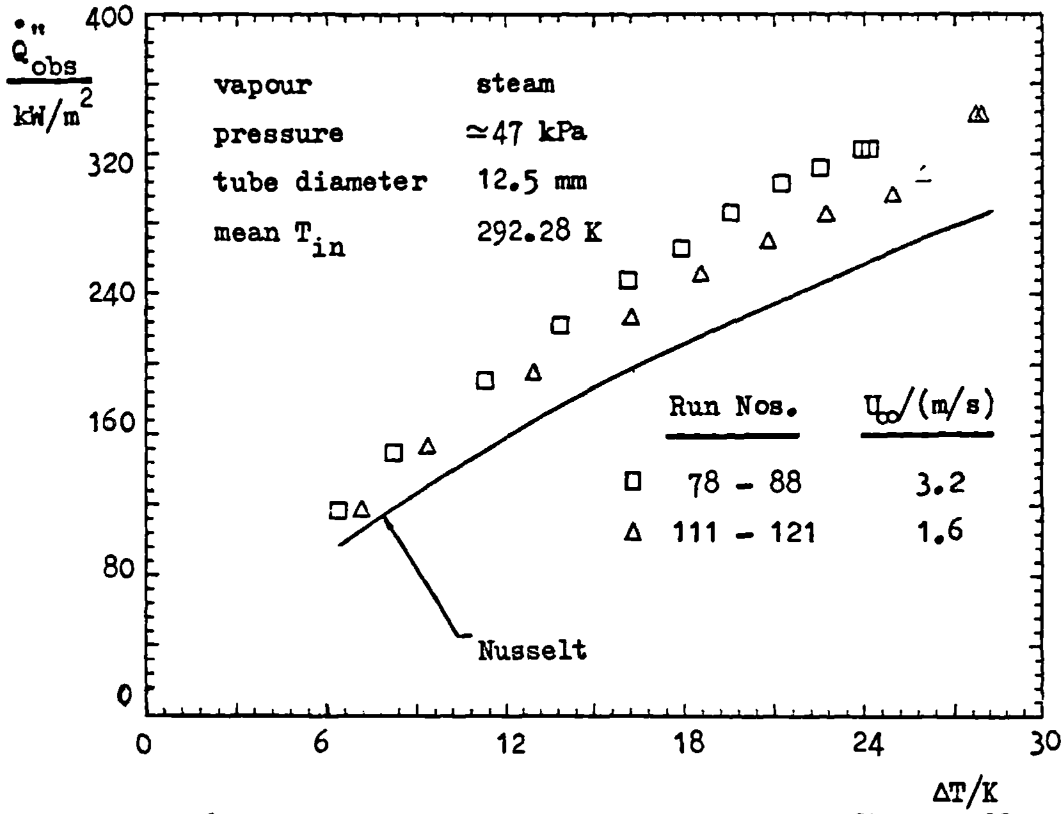

Figure 6.12 Relation between heat flux and bulk-to-wall temperature difference: effect of vapour velocity

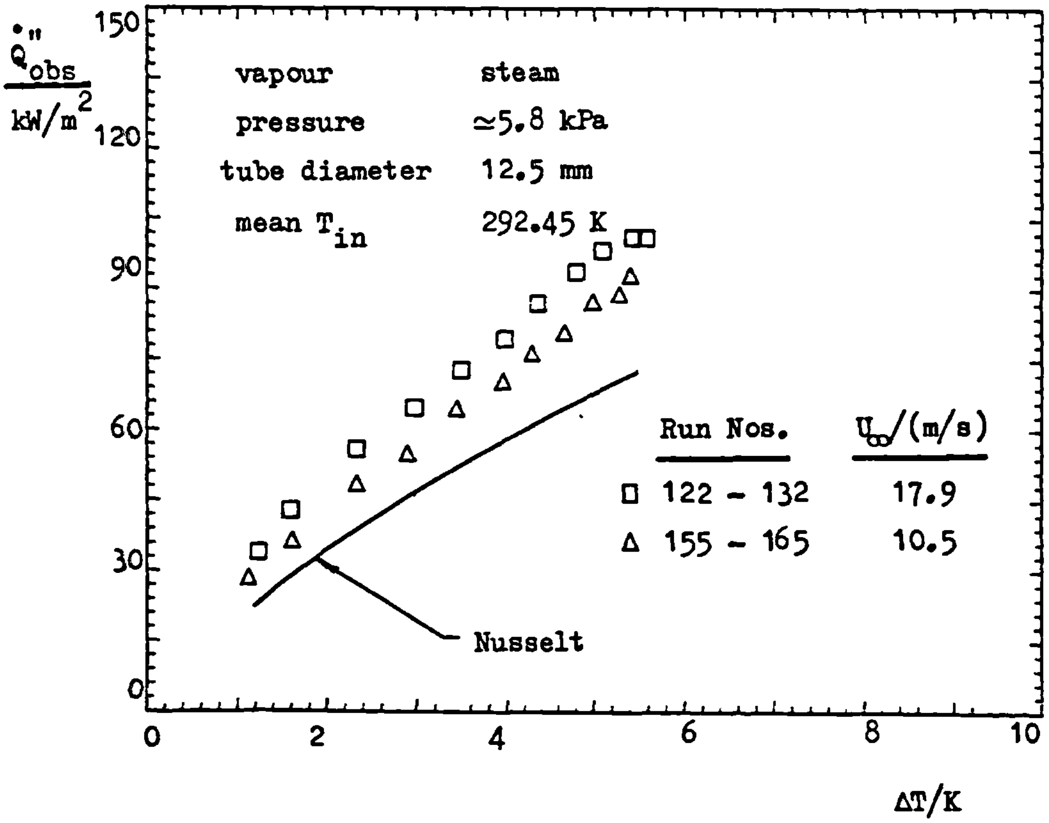

Figure 6.13 Relation between heat flux and bulk-to-wall temperature difference: effect of vapour velocity

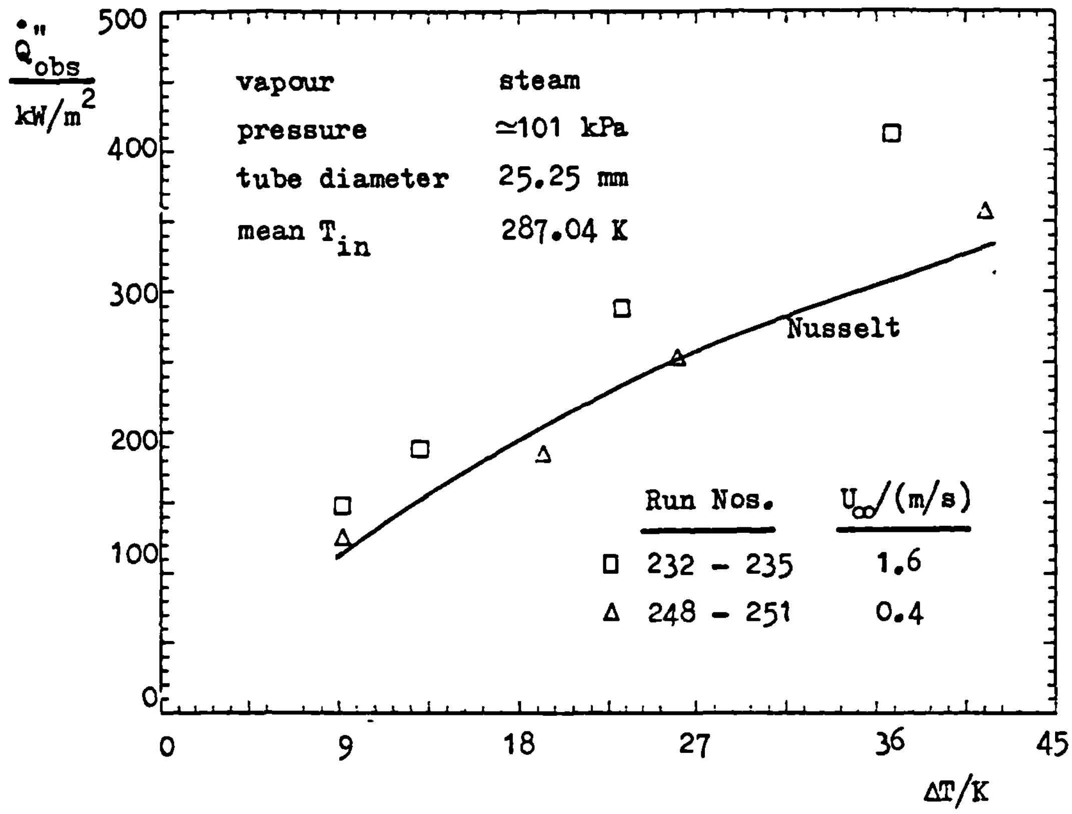

Figure 6.14 Relation between heat flux and bulk-to-wall temperature difference: effect of vapour velocity

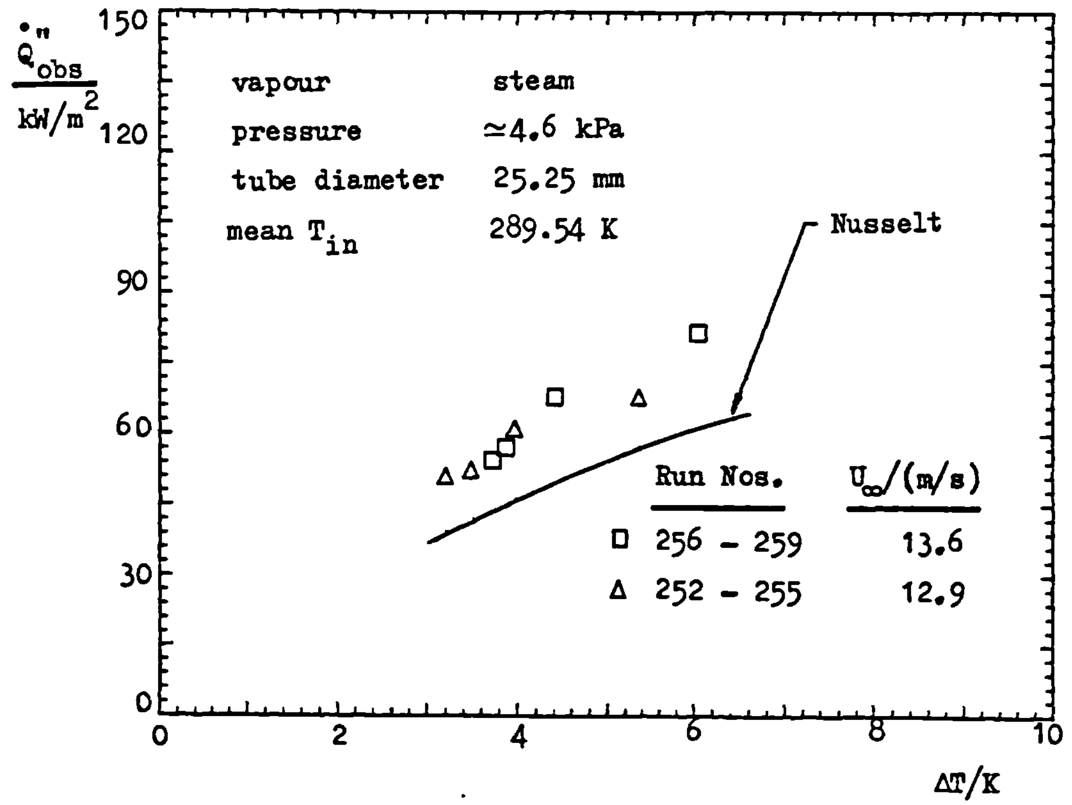

Figure 6.15 Relation between heat flux and bulk-to-wall temperature difference: effect of vapour velocity

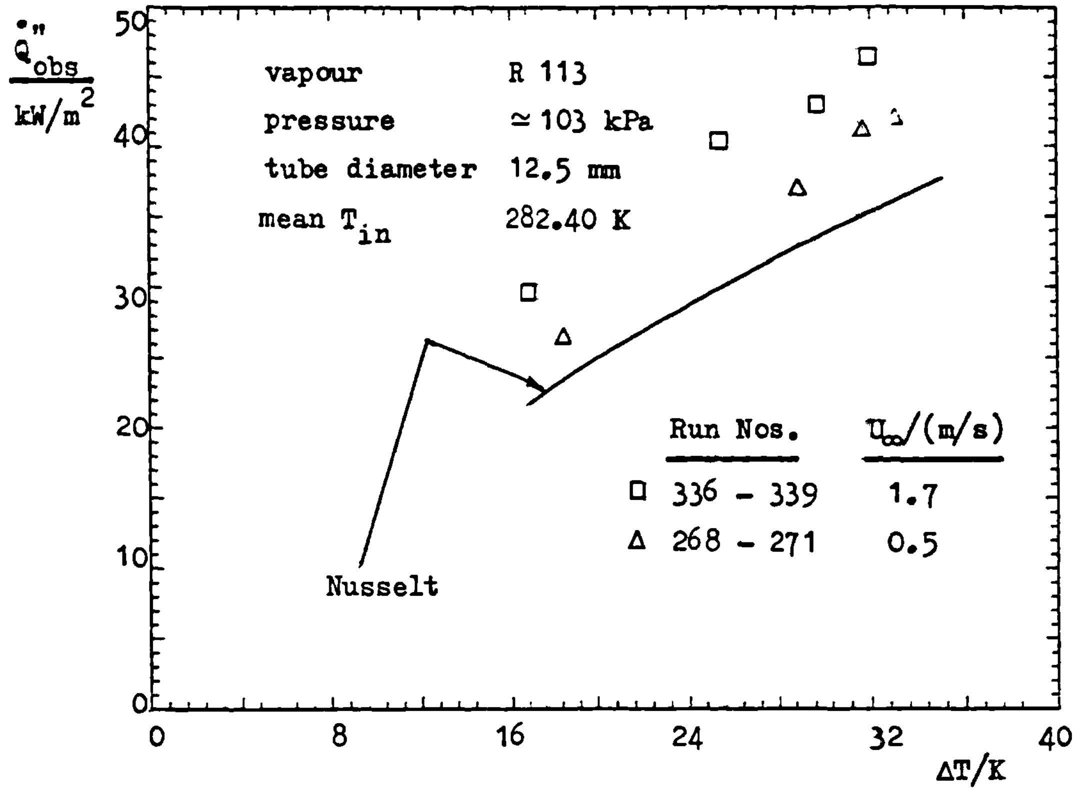

Figure 6.16 Relation between heat flux and bulk-to-wall temperature difference: effect of vapour velocity

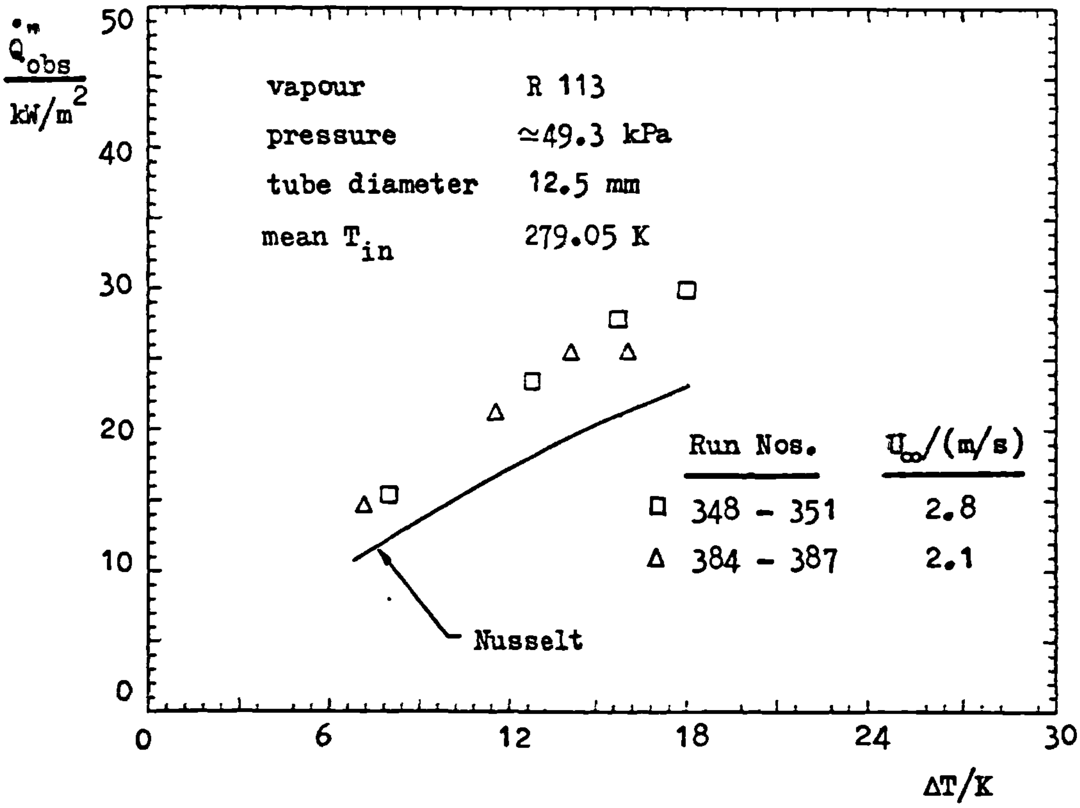

Figure 6.17 Relation between heat flux and bulk-to-wall temperature difference: effect of vapour velocity

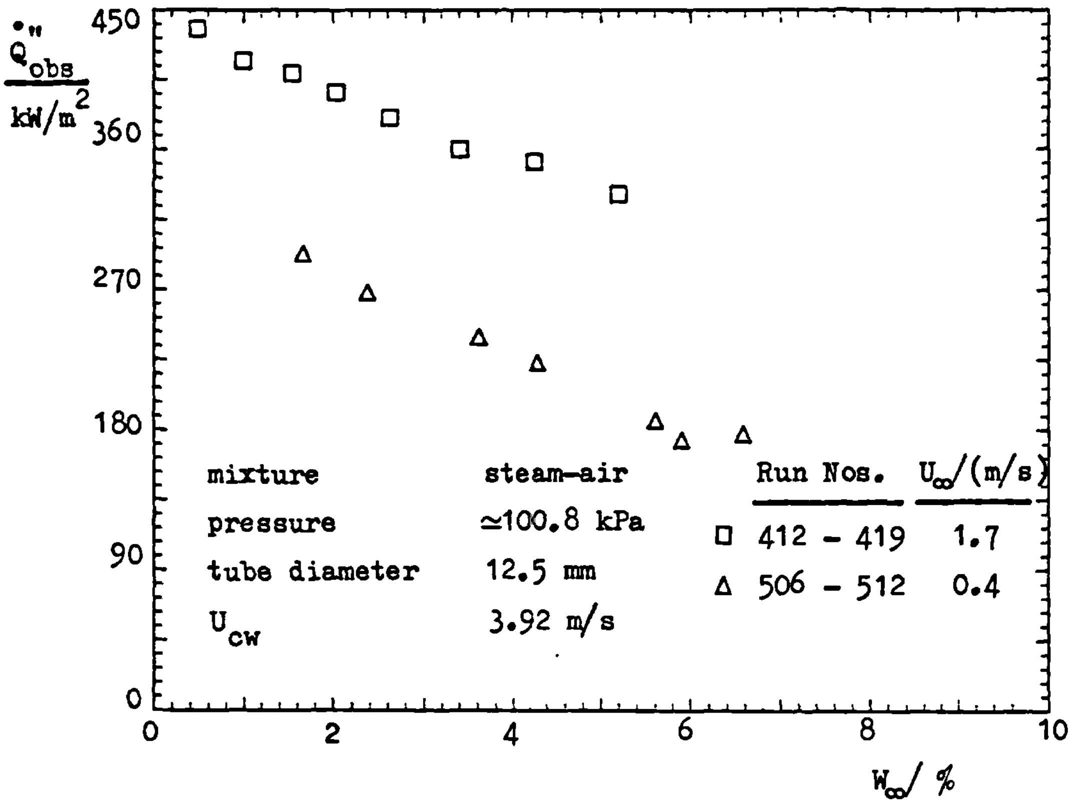

Figure 6.18 Relation between heat flux and bulk gas mass fraction: effect of vapour-gas velocity

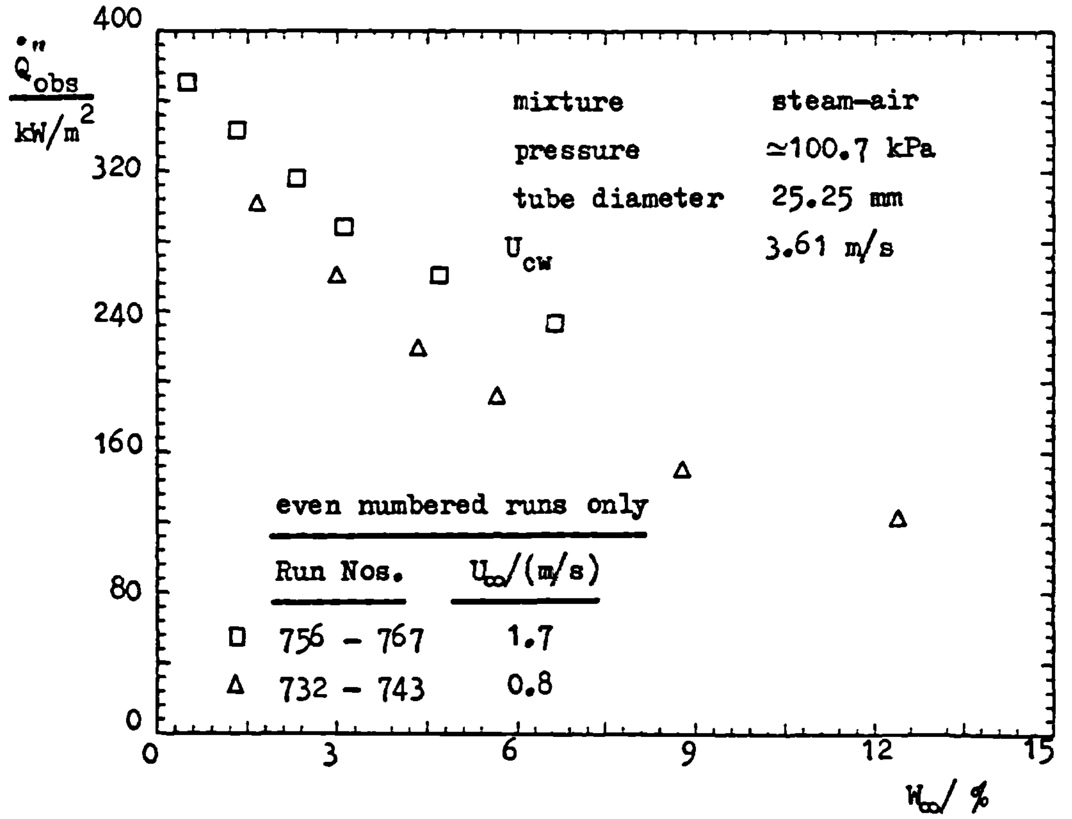

Figure 6.19 Relation between heat flux and bulk gas mass fraction: effect of vapour-gas velocity

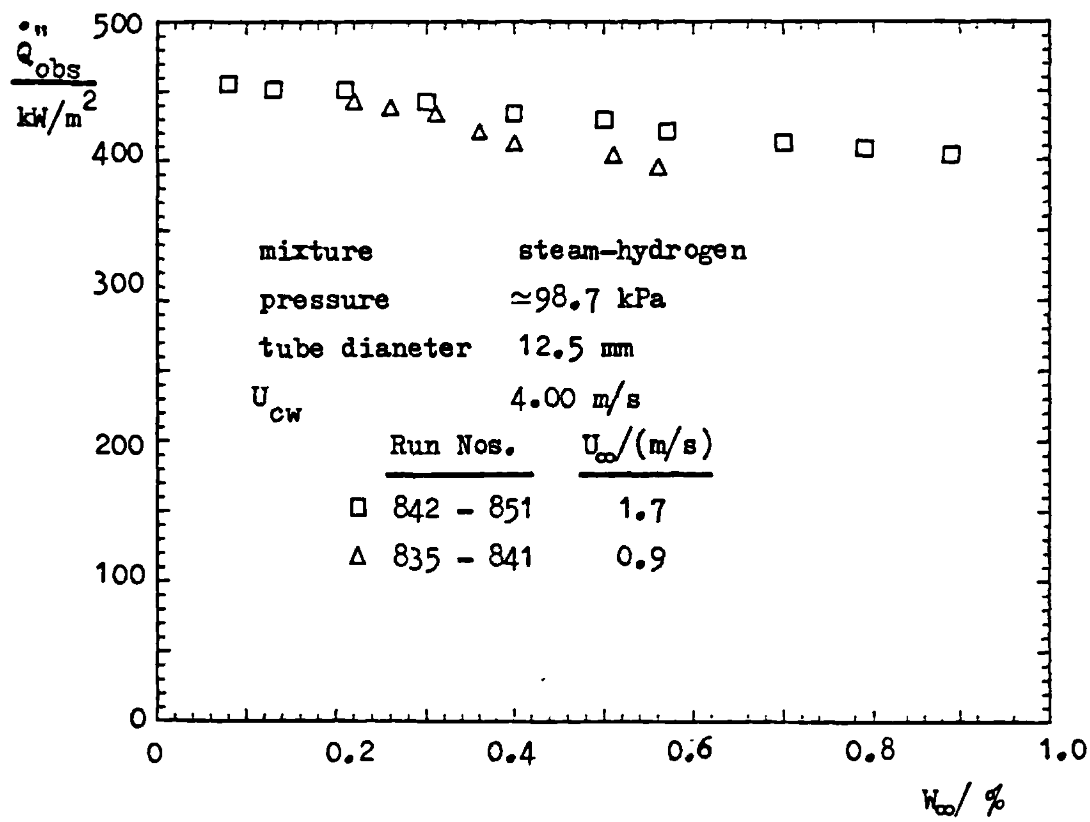

Figure 6.20 Relation between heat flux and bulk gas mass fraction: effect of vapour-gas velocity

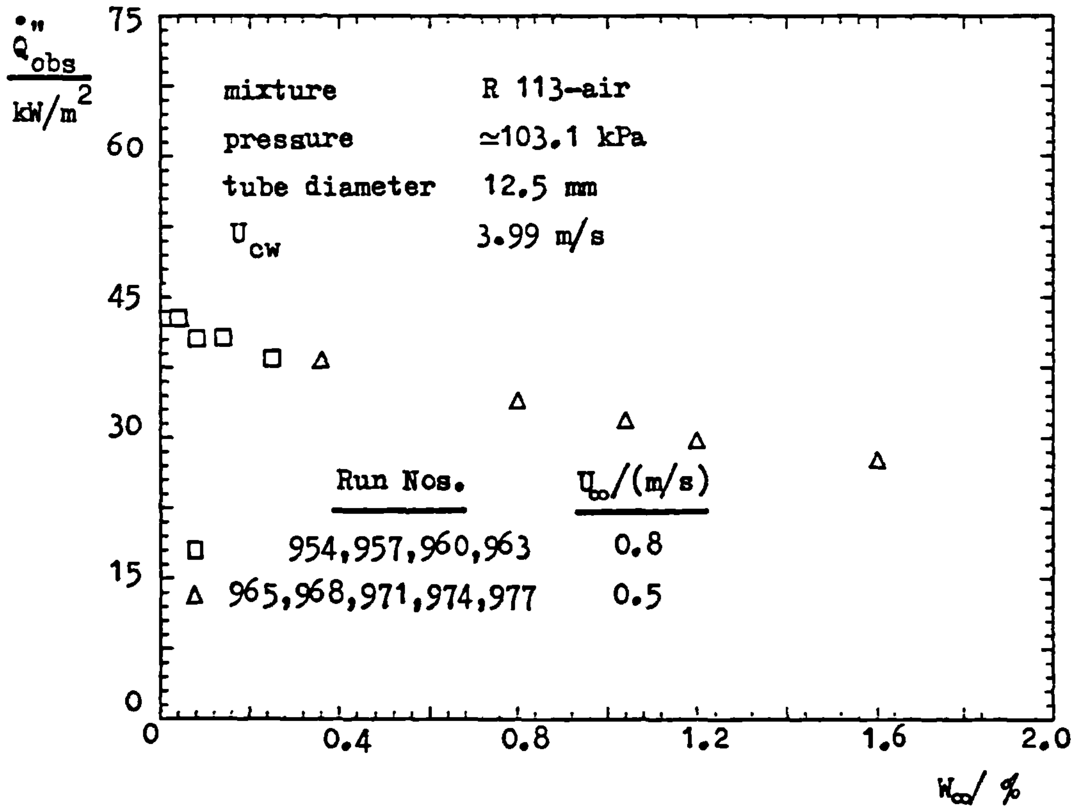

Figure 6.21 Relation between heat flux and bulk gas mass fraction: effect of vapour-gas velocity

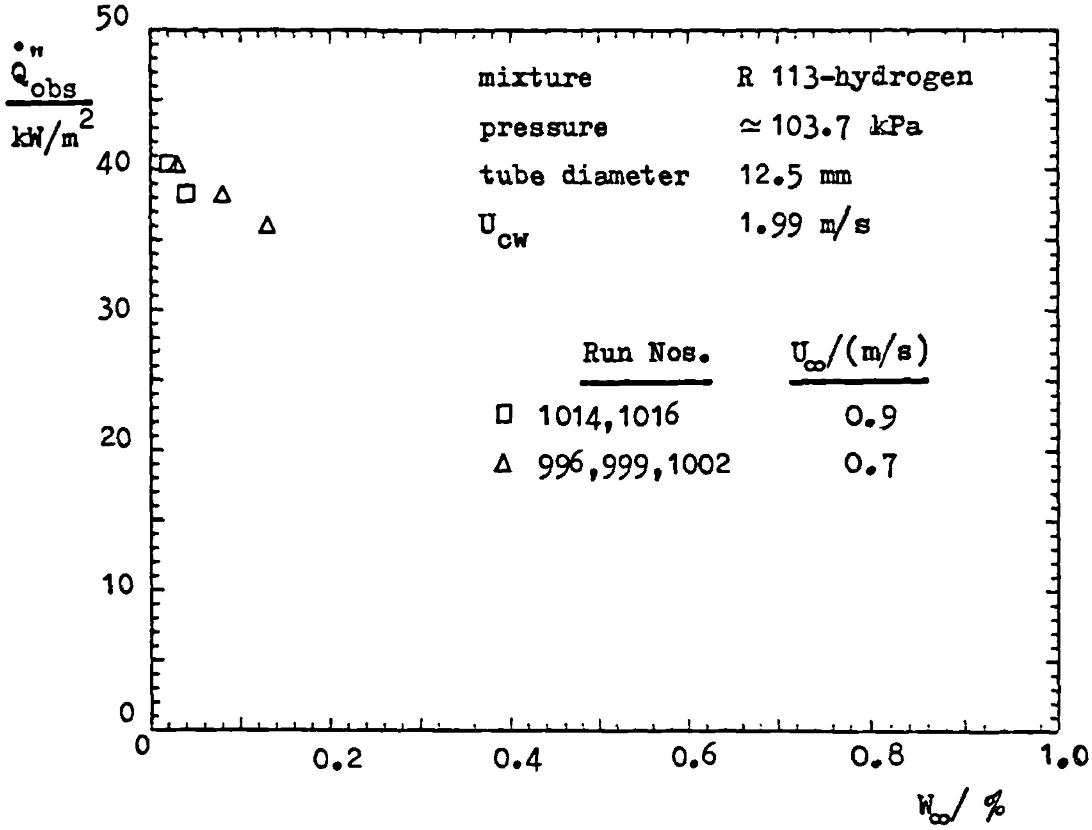

Figure 6.22 Relation between heat flux and bulk gas mass fraction: effect of vapour-gas velocity

Table 6.1 - Results of Thermal Loss Tests

$\dot{Q}_h$ W	T^*_∞ K	T^*_{at} K	$\dot{m}_A$ g/s	$\dot{m}_B$ g/s	$\dot{Q}^*_{loss1}$ W	$\dot{Q}^*_{loss2}$ W
30441.7	373.22	294.90	0.109	13.043	766.9	246.0
25103.1	373.20	295.35	0.0996	10.676	787.2	224.8
20228.9	373.28	295.65	0.0917	8.539	753.1	207.0
14953.1	373.28	295.75	0.0879	6.246	659.9	198.4
9517.1	373.31	295.95	0.0845	3.834	675.0	190.7
31335.7	372.86	299.15	0.0944	13.457	746.6	213.1
25745.4	372.88	299.75	0.0875	10.968	789.5	197.5
20910.5	372.92	300.55	0.0842	8.856	726.7	190.0
16094.9	372.88	300.15	0.0821	6.713	754.5	185.3
9601.5	372.84	300.15	0.0795	3.824	788.3	179.4

mean T^*_∞ = 373.1 K
mean T^*_{at} = 297.8 K
$\dot{Q}^*_{loss1}$ = 740 W
$\dot{Q}^*_{loss2}$ = 160 W

<u>Note</u>: $\dot{Q}^*_{loss2}$ was obtained by extrapolating back to a heater input power of 740 W, see Figure 6.3 and Section 6.2.

Table 6.2 - Approximate Overall Ranges of the Main Parameters

Mixture	P_∞ kPa	d_o mm	T_∞ K	T_w K	U_∞ m/s	$W_{\infty 2}$ %	$\tilde{W}_{\infty 2}$ %	$\dot{Q}''_{obs}$ kW/m^2
pure steam	101	12.5	373	333 - 364	0.4 - 1.8	-	-	166 - 466
pure steam	47	12.5	353	325 - 347	1.6 - 3.3	-	-	116 - 344
pure steam	5 - 9	12.5	307 - 319	301 - 316	3.5 - 18.0	-	-	29 - 150
pure steam	101	25.25	373	322 - 364	0.4 - 1.6	-	-	126 - 412
pure steam	4 - 8	25.25	303 - 314	298 - 310	12.9 - 15.2	-	-	51 - 122
pure R-113	101 - 105	12.5	320 - 321	287 - 304	0.5 - 1.8	-	-	26 - 46
pure R-113	40 - 78	12.5	295 - 312	282 - 300	2.0 - 2.8	-	-	12 - 43
steam-air	95 - 103	12.5	366 - 373	296 - 364	0.3 - 1.8	0.5 - 24.4	0.3 - 16.8	81 - 447
steam-air	4 - 40	12.5	301 - 348	291 - 332	1.1 - 25.7	0.1 - 31.5	0.1 - 22.2	41 - 247
steam-air	99 - 101	25.25	270 - 373	301 - 355	0.8 - 1.7	0.5 - 12.4	0.3 - 8.1	106 - 371
steam-air	6 - 37	25.25	310 - 348	297 - 332	2.9 - 14.9	1.0 - 16.6	0.6 - 11.0	32 - 142
steam-hydrogen	97 - 102	12.5	362 - 373	296 - 355	0.3 - 1.8	0.1 - 5.7	0.7 - 35.1	164 - 465
steam-hydrogen	4 - 55	12.5	300 - 351	294 - 343	1.3 - 17.1	0.1 - 3.8	1.0 - 26.3	20 - 289
R-113-air	101 - 104	12.5	318 - 321	284 - 303	0.5 - 1.8	0.04 - 1.6	0.3 - 9.5	22 - 51
R-113-hydrogen	103 - 124	12.5	318 - 320	285 - 301	0.5 - 0.9	0.02 - 0.3	1.7 - 22.9	24 - 43

Table 6.3 Pure vapours results

vapour steam
tube diameter 12.5 mm

Run No.	U_∞ m/s	P_∞ Pa	T_∞ K	T_w K	$\dot{Q}''_{obs}$ kW/m^2	U_{ow} m/s	T_{in} K	ΔT_{ow} K	error estimates: $\delta\dot{Q}''_{obs}/\dot{Q}''_{obs}$ %	σ_{Tw} K	$\delta U_\infty/U_\infty$ %
1	1.70	101.2	373.10	337.89	462.1	3.89	293.52	2.81	2.68	3.26	1.50
2	1.70	101.2	373.10	339.94	451.9	3.50	293.52	3.05	2.59	3.09	1.50
3	1.71	101.2	373.10	341.72	[illegible]98.5	3.11	293.52	3.33	2.59	3.06	1.50
4	1.71	101.2	373.10	343.90	413.1	2.72	293.52	3.59	2.44	3.01	1.50
5	1.71	101.2	373.10	345.21	356.5	2.33	293.52	3.61	2.43	2.71	1.50
6	1.71	101.2	373.10	349.15	359.0	1.94	293.52	4.37	2.33	2.77	1.50
7	1.71	101.2	373.10	352.56	320.7	1.56	293.52	4.67	2.25	2.19	1.50
8	1.71	101.2	373.1	356.28	250.1	1.17	293.52	5.07	2.23	1.93	1.50
9	1.71	101.[illegible]	373.10	360.92	216.9	0.78	293.55	6.59	2.14	1.51	1.50
10	1.71	101.2	373.10	363.54	179.3	0.58	293.55	7.27	2.11	1.09	1.50
11	1.70	101.2	373.10	337.96	466.2	3.89	293.5[illegible]	2.83	2.67	3.31	1.50
12	1.52	101.2	373.10	337.43	458.2	3.89	293.47	2.78	2.69	3.25	1.50
13	1.52	101.	373.10	339.[illegible]6	444.8	3.50	293.47	3.00	2.60	3.22	1.50
14	1.52	101.2	373.10	341.14	436.6	3.11	293.47	3.27	2.52	3.03	1.50
15	1.52	101.2	373.10	343.34	393.6	2.72	293.47	3.42	2.48	2.83	1.50
16	1.52	101.2	373.10	345.90	387.7	2.33	293.50	3.93	2.37	2.70	1.50
17	1.52	101.2	373.10	348.56	357.1	1.94	293.50	4.34	2.31	2.62	1.50
18	1.52	101.[illegible]	373.10	352.19	319.2	1.56	293.50	4.65	2.25	2.12	1.50
19	1.52	101.2	373.10	356.10	268.1	1.17	293.52	5.43	2.20	2.03	1.50
20	1.52	101.2	373.10	360.61	205.0	0.78	293.52	6.23	2.15	1.49	1.50
21	1.53	101.2	373.10	363.66	176.4	0.58	293.55	7.15	2.12	0.90	1.50
22	1.52	101.2	373.10	337.30	462.2	3.89	293.47	2.81	2.68	3.31	1.50
23	1.24	101.2	373.08	336.33	446.2	3.89	293.47	2.71	2.72	3.26	1.50
24	1.24	101.2	373.08	338.55	431.6	3.48	293.47	2.93	2.63	3.11	1.50
25	1.24	101.2	373.08	340.57	417.8	3.11	293.47	3.17	2.55	2.96	1.50
26	1.24	101.2	373.08	342.56	376.8	2.72	293.47	3.27	2.52	2.77	1.50
27	1.24	101.[illegible]	373.08	345.30	376.2	2.33	293.47	3.83	2.39	2.65	1.50
28	1.24	101.2	373.08	346.13	355.1	1.94	293.47	4.32	2.31	2.53	1.50
29	1.24	101.[illegible]	373.08	351.59	[illegible]17.6	1.56	293.47	4.63	2.25	2.11	1.50
30	1.24	101.[illegible]	373.08	355.99	268.1	1.17	293.50	5.43	2.20	1.80	1.50
31	1.24	101.2	373.08	360.36	2[illegible]2.6	.78	293.5[illegible]	6.16	2.16	1.45	1.50
32	1.24	101.[illegible]	373.08	363.33	178.8	0.58	293.52	7.25	2.12	0.88	1.50
33	1.24	101.[illegible]	373.08	336.85	446.2	3.89	293.45	2.71	2.72	3.11	1.50
34	0.96	101.1	373.08	335.69	450.2	3.89	293.45	2.74	2.71	3.28	1.50
35	0.96	101.1	373.08	337.97	444.9	3.50	293.45	3.00	2.60	3.14	1.50
36	0.96	101.1	373.08	340.19	421.1	3.11	293.45	3.20	2.54	3.00	1.50
37	0.96	101.1	373.08	342.25	390.9	2.72	293.45	3.39	2.48	2.80	1.50
38	0.96	101.1	373.08	344.80	383.0	2.33	293.45	3.68	2.38	2.67	1.50
39	0.96	101.1	373.08	347.63	343.2	1.94	293.45	4.17	2.33	2.36	1.50
40	0.96	101.1	373.08	351.45	314.5	1.56	293.45	4.78	2.26	2.17	1.50
41	0.96	101.1	373.08	355.47	262.1	1.17	293.47	5.31	2.21	1.86	1.50
42	0.96	101.1	373.08	360.[illegible]6	209.0	0.78	293.47	6.35	2.15	1.59	1.50
43	0.96	101.1	373.08	363.10	169.8	0.58	293.5[illegible]	6.88	2.13	1.09	1.50
44	0.96	101.1	373.08	336.14	450.3	3.89	293.42	2.74	2.71	3.16	1.50
45	0.66	101.1	373.08	335.07	436.2	3.89	293.42	2.66	2.74	3.03	1.50

Table 6.3 (continued)

Run No.	U_∞ m/s	P_∞ Pa	T_∞ K	T_w K	$\dot{Q}''_{obs}$ kW/m^2	U_{ow} m/s	T_{in} K	ΔT_{ow} K	error estimates: $\delta\dot{Q}''_{obs}/\dot{Q}''_{obs}$ %	σ_{Tw} K	$\delta U_\infty/U_\infty$ %
46	0.66	101.1	373.08	337.[illegible]2	43[illegible].5	3.50	293.42	2.91	2.64	2.96	1.50
47	0.66	101.1	373.08	336.98	417.9	3.11	293.42	3.17	2.55	2.90	1.50
48	0.66	101.1	373.08	341.[illegible]5	393.7	2.72	293.42	3.42	2.46	2.63	1.50
49	0.66	101.1	373.08	343.96	368.7	2.33	293.42	3.75	2.41	2.52	1.50
50	0.66	101.1	373.08	346.95	341.2	1.94	293.42	4.15	2.34	2.25	1.50
51	0.66	101.1	373.08	350.51	306.5	1.56	293.45	4.66	2.27	2.05	1.50
52	0.66	101.1	373.08	354.73	262.2	1.17	293.45	5.31	2.21	1.79	1.50
53	0.67	101.1	373.08	359.77	205.0	0.78	293.47	6.23	2.15	1.48	1.50
54	0.67	101.1	373.08	362.91	166.3	0.58	293.47	6.74	2.13	1.10	1.50
55	0.66	101.1	373.08	335.10	430.2	3.89	293.42	2.61	2.77	3.00	1.50
56	0.39	101.1	373.07	333.45	426.3	3.89	293.40	2.59	2.78	3.02	1.50
57	0.39	101.1	373.07	335.50	419.7	3.51	293.4[illegible]	2.83	2.67	2.91	1.50
58	0.39	101.1	373.07	337.[illegible]3	4[illegible]1.9	3.11	293.42	3.05	2.59	2.78	1.50
59	0.39	101.1	373.07	339.92	382.5	2.72	293.42	3.32	2.50	2.68	1.50
60	0.39	101.1	373.07	342.[illegible]2	358.5	2.31	293.42	3.66	2.42	2.58	1.50
61	0.39	101.1	373.07	345.30	335.2	1.94	293.42	4.07	2.35	2.23	1.50
62	0.39	101.1	373.07	349.10	306.5	1.56	293.42	4.66	2.27	2.07	1.50
63	0.39	101.1	373.07	353.2[illegible]	267.0	1.17	293.45	5.41	2.20	2.16	1.50
64	0.39	101.1	373.07	356.46	209.8	0.78	293.45	6.38	2.15	1.68	1.50
65	0.39	101.1	373.07	361.67	177.0	0.58	293.47	7.17	2.12	1.40	1.50
66	0.39	101.1	373.07	335.36	426.3	3.89	293.40	2.59	2.78	3.10	1.50
67	1.76	101.1	373.06	338.40	454.3	3.89	293.42	2.76	2.70	3.39	1.50
68	1.76	101.1	373.06	34[illegible].15	437.8	3.50	293.40	2.96	2.62	3.47	1.50
69	1.76	101.1	373.06	342.42	418.0	3.11	293.43	3.17	2.55	3.23	1.50
70	1.76	101.1	373.06	344.55	[illegible]96.4	2.68	293.4[illegible]	3.49	2.46	[illegible]	1.50
71	1.76	101.1	373.06	346.74	375.9	2.33	293.40	3.81	2.39	2.80	1.50
72	1.76	101.1	373.06	349.30	347.2	1.94	293.40	4.22	2.32	2.83	1.50
73	1.76	101.1	373.06	352.50	312.9	1.56	293.42	4.75	2.26	2.52	1.50
74	1.76	101.1	373.06	356.06	264.6	1.17	293.42	5.36	2.21	2.06	1.50
75	1.76	101.1	373.06	361.05	209.0	0.78	293.45	6.35	2.15	1.69	1.50
76	1.77	101.1	373.06	363.69	172.9	0.58	293.45	7.01	2.12	1.20	1.50
77	1.76	101.1	373.06	338.12	454.3	3.89	293.40	2.76	2.70	3.56	1.50

Table 6.4 Pure vapours results

vapour: steam
tube diameter: 12.5 mm

Run No.	U_∞ / m/s	P_∞ / Pa	T_∞ / K	T_w / K	$\dot{Q}''_{obs}$ / kW/m^2	U_{ow} / m/s	T_{in} / K	ΔT_{ow} / K	error estimates: $\delta\dot{Q}''_{obs}/\dot{Q}''_{obs}$ / %	error estimates: σ_{Tw} / K	error estimates: $\delta U_\infty/U_\infty$ / %
78	3.26	45.7	352.78	322.86	323.4	3.9	292.3[illegible]	1.96	3.24	5.37	1.50
79	3.26	46.3	352.85	33[illegible].36	[illegible]12.9	3.51	292.30	2.11	3.1[illegible]	5.49	1.50
80	3.25	47.[illegible]	352.91	331.69	303.9	3.12	292.32	2.30	2.95	5.17	1.50
81	3.25	47.	352.93	333.41	[illegible]67.1	2.69	292.32	2.52	2.82	5.01	1.50
82	3.24	47.1	353.[illegible]1	[illegible]35.13	266.8	2.[illegible]	292.37	2.74	2.71	4.77	1.50
83	3.24	47.	353.[illegible]8	336.96	248.3	1.95	292.37	3.01	2.60	4.48	1.50
84	3.23	47.4	353.14	339.28	222.7	1.56	292.37	3.36	2.49	4.13	1.50
85	3.23	47.4	353.15	341.89	191.1	1.17	292.42	3.86	2.38	3.64	1.50
86	3.23	47.5	353.18	344.94	149.9	0.76	292.42	4.54	2.28	2.97	1.50
87	3.23	47.5	353.22	346.62	116.6	0.56	292.47	4.71	2.26	2.53	1.50
88	3.21	47.6	353.26	329.10	323.3	3.9[illegible]	292.34	1.96	3.24	5.53	1.50
89	2.67	47.[illegible]	[illegible]53.25	328.[illegible]7	315.3	3.9[illegible]	292.32	1.91	3.29	5.46	1.50
90	2.67	47.5	353.2[illegible]	329.70	3[illegible]9.2	3.51	292.32	2.[illegible]8	3.12	5.18	1.50
91	2.67	47.6	353.24	331.[illegible]4	294.2	3.12	292.32	2.23	3.[illegible]1	5.09	1.50
92	2.67	47.6	353.25	332.61	[illegible]80.8	2.71	292.34	2.45	2.86	4.88	1.50
93	2.67	47.6	353.23	334.54	266.5	2.34	292.34	2.69	2.73	4.75	1.50
94	2.67	47.6	353.25	336.31	242.2	1.95	292.37	2.94	2.63	4.49	1.50
95	2.67	47.7	353.29	338.72	221.1	1.56	292.39	3.35	2.57	4.11	1.50
96	2.67	47.6	353.27	341.59	169.9	1.17	292.42	3.84	2.39	3.69	1.50
97	2.67	47.7	35[illegible].29	344.76	148.3	0.78	292.44	4.50	2.29	2.91	1.50
98	2.67	47.6	353.35	346.90	116.0	0.56	292.49	4.69	2.27	2.62	1.50
99	2.66	47.7	353.30	328.41	[illegible]19.3	3.9[illegible]	292.37	1.94	3.27	5.47	1.50
100	2.15	47.4	353.14	327.18	323.[illegible]	3.90	292.37	1.96	3.24	5.39	1.50
101	2.16	47.[illegible]	353.13	328.54	310.4	3.51	292.34	2.15	3.08	5.31	1.50
102	2.16	47.[illegible]	353.08	329.95	310.3	3.12	292.34	2.35	2.92	5.07	1.5[illegible]
103	2.16	47.[illegible]	353.[illegible]5	331.73	289.2	2.73	292.34	2.52	2.82	5.03	1.50
104	2.16	47.[illegible]	353.[illegible]6	333.48	261.1	[illegible].34	292.32	2.64	2.66	4.91	1.50
105	2.16	47.[illegible]	353.[illegible]2	335.35	260.4	1.95	292.34	3.16	2.55	4.74	1.50
106	2.16	47.[illegible]	353.[illegible]5	338.14	230.8	1.56	292.34	3.50	2.46	4.11	1.50
107	2.16	47.2	353.[illegible]6	340.05	214.4	1.17	292.37	4.13	2.34	3.75	1.50
108	2.16	47.[illegible]	353.[illegible]7	344.18	165.5	0.75	292.37	4.96	2.24	2.92	1.50
109	2.16	47.[illegible]	353.07	346.23	128.7	0.58	292.39	5.20	2.22	2.67	1.50
110	2.16	47.[illegible]	353.[illegible]4	326.43	323.5	3.9	292.25	1.96	3.24	5.34	1.50
111	1.62	47.[illegible]	352.99	325.11	343.8	3.9	292.17	2.[illegible]8	3.12	5.92	1.50
112	1.63	47.	352.91	326.97	309.4	3.51	292.17	2.38	3.12	5.20	1.50
113	1.63	47.	352.92	328.[illegible]0	297.6	3.12	292.17	2.25	2.99	5.27	1.50
114	1.63	47.	352.95	330.23	286.6	2.71	292.17	2.50	2.83	4.90	1.50
115	1.63	47.	352.95	332.18	271.5	2.34	292.2	2.74	2.71	4.89	1.50
116	1.63	47.[illegible]	352.94	334.40	252.5	1.95	292.2	3.[illegible]6	2.58	4.48	1.50
117	1.63	47.[illegible]	352.92	336.69	227.7	1.56	292.22	3.45	2.47	4.31	1.50
118	1.63	47.	352.94	339.96	196.1	1.17	292.25	3.96	2.36	3.86	1.50
119	1.63	47.[illegible]	352.96	343.61	154.0	0.78	292.25	4.67	2.27	2.98	1.50
120	1.63	47.	352.94	345.79	117.9	0.53	292.3[illegible]	4.76	2.26	2.82	1.50
121	1.63	47.	352.92	325.26	343.8	3.9[illegible]	292.17	2.[illegible]8	3.12	5.70	1.50

Table 6.5 Pure vapours results

vapour steam
tube diameter 12.5 mm

Run No.	U_∞ m/s	P_∞ Pa	T_∞ K	T_w K	$\dot{Q}''_{obs}$ kW/m^2	U_{ow} m/s	T_{in} K	ΔT_{ow} K	error estimates: $\delta\dot{Q}''_{obs}/\dot{Q}''_{obs}$ %	error estimates: σ_{Tw} K	error estimates: $\delta U_\infty/U_\infty$ %
122	17.94	6.1	309.64	304.20	101.1	3.89	292.52	0.61	8.41	1.81	1.50
123	17.94	6.1	309.64	304.55	98.3	3.51	292.52	0.66	7.81	1.71	1.50
124	17.95	6.1	309.64	304.64	93.8	3.12	292.52	0.71	7.31	1.63	1.50
125	17.99	6.1	309.59	305.[illegible]3	87.1	2.71	292.52	0.76	6.87	1.55	1.50
126	17.96	6.[illegible]	309.62	305.66	79.4	2.3[illegible]	292.52	0.81	6.49	1.43	1.50
127	17.96	6.1	309.62	306.13	72.8	1.95	292.52	0.88	6.01	1.3[illegible]	1.50
128	17.93	6.1	309.67	306.7[illegible]	64.7	1.56	292.52	0.98	5.48	1.15	1.50
129	17.86	6.1	309.74	307.42	55.8	1.17	292.52	1.13	4.86	0.94	1.50
130	17.75	6.[illegible]	309.67	30[illegible].[illegible]7	42.6	0.78	292.52	1.30	4.34	0.70	1.50
131	17.67	6.[illegible]	309.96	305.73	35.9	3.58	292.52	1.37	4.16	0.6[illegible]	1.50
132	17.58	6.[illegible]	310.06	304.49	1[illegible]1.1	3.89	292.52	0.61	8.40	1.89	1.50
133	15.92	5.9	[illegible]9.03	303.68	97.1	3.9	292.47	0.59	8.73	1.66	1.50
134	15.92	5.9	309.03	304.05	94.2	3.49	292.44	.64	8.09	1.59	1.50
135	15.92	5.9	309.03	304.31	87.4	3.17	292.44	0.66	7.61	1.53	1.50
136	15.93	5.9	309.03	304.74	82.1	2.77	292.44	0.71	7.31	1.43	1.50
137	15.93	5.9	309.03	305.11	77.7	2.34	292.44	0.76	6.68	1.34	1.50
138	15.94	5.9	309.01	305.54	70.8	1.95	292.44	0.86	6.16	1.24	1.50
139	15.94	5.9	309.01	306.10	64.7	1.56	292.44	0.98	5.46	1.06	1.50
140	15.94	5.9	3[illegible]9.01	306.79	53.4	1.17	292.47	1.08	5.05	0.84	1.50
141	15.90	5.9	309.07	307.47	40.4	0.78	292.47	1.23	4.54	0.63	1.50
142	15.90	5.9	309.07	307.99	31.5	.56	292.49	1.27	4.40	0.48	1.50
143	15.69	5.9	309.07	303.75	97.1	3.9[illegible]	292.44	0.59	8.73	1.66	1.50
144	13.54	5.5	3[illegible]7.99	302.81	89.0	[illegible].90	292.39	0.54	9.48	1.49	1.50
145	13.55	5.5	307.99	303.15	86.9	3.49	292.39	0.59	8.72	1.38	1.50
146	13.55	5.5	307.99	303.43	80.9	3.12	292.39	0.61	8.39	1.35	1.50
147	13.55	5.5	307.98	303.79	75.9	2.71	292.39	0.66	7.81	1.30	1.50
148	13.54	5.5	3[illegible]8.[illegible]0	304.17	70.4	2.34	292.39	0.71	7.31	1.20	1.50
149	13.54	5.5	[illegible]	304.64	66.8	1.95	292.39	0.81	6.49	1.17	1.50
150	13.54	5.5	[illegible]	305.16	58.3	1.56	292.39	0.88	6.01	0.93	1.50
151	13.54	5.5	308.0[illegible]	305.74	48.5	1.17	292.39	0.98	5.48	[illegible].76	1.50
152	13.54	5.5	3[illegible]8.[illegible]	306.45	37.2	0.75	292.39	1.13	4.86	0.56	1.50
153	13.54	5.5	30[illegible].[illegible]0	306.81	29.1	0.58	292.39	1.18	4.70	0.48	1.50
154	13.54	5.5	30[illegible].[illegible]	302.90	89.1	3.90	292.34	0.54	9.48	1.42	1.50
155	1[illegible].53	5.5	307.60	30[illegible].[illegible]3	89.1	3.9[illegible]	292.37	0.54	9.48	1.35	1.50
156	10.54	5.5	307.60	302.61	87.4	3.51	292.37	0.59	8.72	1.30	1.50
157	10.54	5.5	307.60	302.94	80.9	3.12	292.37	0.61	8.39	1.23	1.50
158	10.54	5.5	307.60	303.[illegible]1	76.5	2.73	292.37	0.66	7.81	1.22	1.50
159	10.52	5.5	307.63	303.68	70.4	2.34	292.37	0.71	7.31	1.12	1.50
160	10.51	5.5	307.65	304.21	64.7	1.95	292.39	0.78	6.68	1.01	1.50
161	1[illegible].51	5.5	307.65	304.75	55.0	1.56	292.39	0.83	6.32	0.88	1.50
162	10.46	5.5	307.71	305.29	48.5	1.17	292.39	0.98	5.48	0.72	1.50
163	10.48	5.5	307.71	3[illegible]6.[illegible]	36.4	.78	292.39	1.10	4.95	0.55	1.50
164	10.46	5.5	[illegible]7.71	306.59	28.5	0.58	292.39	1.15	4.78	0.45	1.50
165	10.41	5.5	3[illegible]7.65	302.45	93.1	3.9[illegible]	292.34	0.56	9.08	1.39	1.50
166	5.39	5.[illegible]	307.15	301.34	99.1	3.9	292.34	0.54	9.48	1.17	1.50
167	5.39	5.	307.15	301.66	87.4	3.51	292.34	0.59	8.72	1.13	1.50

Table 6.5 (continued)

Run No.	U_∞ (m/s)	P_∞ (Pa)	T_∞ (K)	T_w (K)	$\dot{Q}''_{obs}$ (kW/m^2)	U_{ow} (m/s)	T_{in} (K)	ΔT_{ow} (K)	error estimates: $\delta\dot{Q}''_{obs}/\dot{Q}''_{obs}$ (%)	σ_{Tw} (K)	$\delta U_\infty/U_\infty$ (%)
168	5.39	5.[illegible]	307.15	[illegible]	[illegible]	3.12	292.37	0.61	8.39	1.08	1.50
169	5.38	5.3	[illegible]7.17	30[illegible].[illegible]6	76.5	2.71	292.37	0.66	7.81	1.11	1.50
170	5.38	5.[illegible]	3[illegible]7.17	302.76	70.4	2.34	292.37	0.71	7.31	0.98	1.50
171	5.37	5.3	307.21	303.26	64.7	1.95	292.37	0.78	6.68	0.93	1.50
172	5.36	5.4	307.25	303.93	58.3	1.56	292.37	0.88	6.01	0.80	1.50
173	5.36	5.4	307.25	304.64	48.5	1.17	292.37	0.98	5.48	0.68	1.50
174	5.35	5.4	[illegible]7.29	305.41	37.2	0.78	292.37	1.13	4.86	0.53	1.50
175	5.35	5.4	307.29	[illegible]5.90	30.3	[illegible].56	292.37	1.23	4.54	0.46	1.50
176	5.34	5.4	307.33	30[illegible].42	89.1	3.9	292.34	0.54	9.48	1.14	1.50
177	17.48	6.[illegible]	31[illegible].[illegible]7	3[illegible]4.55	1[illegible]5.2	[illegible].9[illegible]	292.34	0.64	8.09	1.60	1.50
178	16.90	6.5	310.74	3[illegible]5.37	105.0	3.49	292.37	0.71	7.31	1.79	1.50
179	16.71	6.5	31[illegible].97	3[illegible]5.81	100.4	3.13	292.37	0.76	6.87	1.75	1.50
180	16.53	6.6	311.19	[illegible]6.40	95.6	2.71	292.37	[illegible].83	6.32	1.69	1.50
181	16.41	6.7	311.[illegible]4	306.95	94.7	2.53	292.37	0.88	6.01	1.55	1.50
182	16.29	6.[illegible]	311.5[illegible]	3[illegible]7.54	[illegible].9	1.95	292.37	0.96	5.46	1.44	1.50
183	16.22	6.[illegible]	311.58	3[illegible]8.22	72.8	1.56	292.37	1.1[illegible]	4.95	1.26	1.50
184	16.17	6.[illegible]	311.64	309.[illegible]	61.9	1.17	292.37	1.25	4.47	1.06	1.50
185	16.12	6.8	311.71	[illegible]9.82	46.9	0.78	292.39	1.42	4.05	0.78	1.50
186	16.07	6.9	311.77	310.45	37.0	0.52	292.39	1.50	3.91	0.58	1.50
187	15.96	6.9	311.90	3[illegible]5.73	117.4	3.9[illegible]	292.32	0.71	7.31	2.01	1.50
188	14.44	7.9	314.23	307.41	129.2	3.89	292.93	0.78	6.68	2.25	1.50
189	14.34	7.9	314.38	307.68	123.5	3.50	292.93	0.83	6.35	2.16	1.50
190	14.31	7.9	314.43	30[illegible].[illegible]1	116.3	3.11	292.91	0.88	6.01	2.08	1.50
191	14.26	7.9	314.47	308.84	111.4	2.69	292.85	0.98	5.48	1.95	1.50
192	14.29	7.9	314.47	3[illegible]9.30	104.1	2.34	292.86	1.05	5.15	1.81	1.50
193	14.32	7.9	314.43	[illegible]	92.8	1.95	292.88	1.13	4.87	1.66	1.50
194	14.32	7.9	314.43	[illegible]	83.9	1.56	292.88	1.27	4.41	1.45	1.50
195	14.32	7.9	314.43	[illegible]11.31	70.[illegible]	1.17	292.91	1.42	4.05	1.19	1.50
196	14.32	7.9	314.43	[illegible]	54.0	0.78	292.93	1.64	3.65	0.88	1.50
197	14.29	7.9	314.47	312.77	41.7	0.52	292.96	1.69	3.57	0.72	1.50
198	14.12	8.	314.71	307.67	133.3	3.89	292.86	0.81	6.53	2.31	1.50
199	13.[illegible]0	8.9	316.79	3[illegible].76	145.7	3.9	292.34	0.88	6.01	2.50	1.50
200	12.92	9.[illegible]	316.95	309.29	13[illegible].4	3.51	292.34	0.93	5.73	2.42	1.50
201	12.79	9.1	317.14	309.95	129.5	3.12	292.34	0.98	5.48	2.37	1.50
202	12.73	9.2	317.25	31[illegible].56	121.8	2.73	292.34	1.05	5.15	2.26	1.50
203	12.65	9.[illegible]	317.39	[illegible]11.[illegible]2	114.1	2.[illegible]4	292.34	1.15	4.78	2.15	1.50
204	12.61	9.[illegible]	317.45	311.90	103.1	1.95	292.34	1.25	4.47	2.02	1.50
205	12.58	9.3	317.51	312.81	93.8	1.56	292.34	1.42	4.05	1.78	1.50
206	12.56	9.[illegible]	317.55	313.75	80.1	1.17	292.74	1.62	3.68	1.54	1.50
207	12.52	9.[illegible]	317.63	314.92	61.4	0.78	292.37	1.56	3.35	1.17	1.50
208	12.36	9.5	317.68	315.92	48.5	0.52	292.44	1.96	3.24	1.03	1.50
209	11.88	[illegible].9	318.71	[illegible]	149.7	3.9[illegible]	292.32	0.91	5.86	2.75	1.50
210	9.43	9.	316.66	3[illegible]6.33	133.6	3.9[illegible]	292.3[illegible]	0.81	6.49	2.39	1.50
211	9.39	9.[illegible]	316.89	30[illegible].85	131.1	3.51	292.30	0.88	6.0[illegible]	2.36	1.50
212	9.38	9.[illegible]	316.89	309.34	123.0	3.12	292.30	0.93	5.72	2.26	1.50
213	9.38	9.	316.92	309.90	115.3	2.71	292.30	1.01	5.36	2.19	1.50
214	9.36	9.	316.95	31[illegible].48	1[illegible]9.3	2.34	292.3[illegible]	1.10	4.95	2.08	1.50
215	9.35	9.	316.97	311.18	101.1	1.95	292.32	1.23	4.54	1.95	1.50
216	9.35	9.[illegible]	316.97	[illegible]	89.0	1.56	292.37	1.35	4.21	1.71	1.50

Table 6.5 (continued)

Run No.	U_∞ / m/s	P_∞ / Pa	T_∞ / K	T_w / K	$\dot{Q}''_{obs}$ / kW/m^2	U_{ow} / m/s	T_{in} / K	ΔT_{ow} / K	error estimates: $\delta\dot{Q}''_{obs}/\dot{Q}''_{obs}$ / %	σ_{Tw} / K	$\delta U_\infty/U_\infty$ / %
217	9.[illegible]4	[illegible]	316.99	313.[illegible]2	76.4	1.17	292.39	1.54	3.81	1.53	1.50
218	9.32	9.1	317.04	314.16	58.2	0.78	292.42	1.76	3.47	1.15	1.50
219	9.31	9.1	317.08	314.99	45.4	0.52	292.49	1.84	3.38	1.02	1.50
220	9.25	9.1	317.21	308.64	137.6	3.9	292.34	0.83	6.32	2.42	1.50
221	3.58	8.5	315.87	306.17	137.6	3.9[illegible]	292.37	0.83	6.32	1.88	1.50
222	3.57	8.5	315.94	306.83	131.1	3.51	292.39	0.88	6.01	1.86	1.50
223	3.57	8.5	315.91	307.43	123.0	3.12	292.39	0.93	5.73	1.92	1.50
224	3.57	8.6	315.93	308.11	111.7	2.69	292.39	0.98	5.48	1.82	1.50
225	3.56	8.5	315.97	308.82	111.6	2.34	292.42	1.15	4.86	1.78	1.50
226	3.56	8.6	315.98	309.46	101.1	1.95	292.42	1.23	4.54	1.72	1.50
227	3.56	8.5	316.[illegible]	310.59	90.6	1.50	292.42	1.37	4.16	1.49	1.50
228	3.55	8.5	316.[illegible]9	311.57	77.6	1.17	292.44	1.57	3.76	1.43	1.50
229	3.54	8.6	316.14	312.79	60.6	0.78	292.47	1.24	3.36	1.19	1.50
230	3.54	8.5	316.10	313.06	47.3	0.50	292.52	1.91	3.29	1.07	1.50
231	3.52	8.7	316.19	306.42	129.5	3.9[illegible]	292.37	0.78	6.66	2.14	1.50

Table 6.6 Pure vapours results

vapour steam

tube diameter 25,25 mm

Run No.	U_∞ / m/s	P_∞ / Pa	T_∞ / K	T_w / K	$\dot{Q}''_{obs}$ / kW/m^2	U_{cw} / m/s	T_{in} / K	ΔT_{cw} / K	error estimates: $\delta\dot{Q}''_{obs}/\dot{Q}''_{obs}$ / %	error estimates: σ_{Tw} / K	error estimates: $\delta U_\infty/U_\infty$ / %
232	[illegible]	[illegible]	[illegible]	[illegible]	412.5	3.61	286.59	0.74	7.01	6.53	1.50
233	1.61	[illegible]	373.11	349.92	288.3	1.80	286.84	1.34	5.20	[illegible]	1.50
234	1.61	[illegible]	373.11	[illegible]	188.5	[illegible]	287.14	1.36	4.16	2.91	1.50
235	1.61	[illegible]	373.11	[illegible]	148.0	0.72	287.21	1.34	4.24	2.27	1.50
236	1.32	[illegible]	373.11	[illegible]	398.7	3.61	286.62	0.72	7.23	6.46	1.50
237	1.32	[illegible]	[illegible]	349.24	251.4	1.8	286.91	[illegible]	5.31	4.91	1.50
238	[illegible]	[illegible]	373.11	[illegible]	185.0	[illegible]	287.19	1.34	4.24	[illegible]	1.50
239	1.32	[illegible]	373.11	[illegible]	159.6	0.72	287.46	1.26	4.44	2.30	1.50
240	[illegible]	[illegible]	373.11	354.66	385.0	3.61	286.62	[illegible]	7.47	6.42	1.50
241	1.06	[illegible]	373.11	[illegible]	274.6	1.8	286.89	0.99	5.42	4.86	1.50
242	1.06	[illegible]	373.11	357.21	185.0	0.90	287.19	1.34	4.24	3.40	1.50
243	[illegible]	[illegible]	373.11	363.59	157.0	0.72	287.34	1.24	4.51	2.37	1.50
244	0.81	[illegible]	373.11	332.64	[illegible]	3.61	286.67	0.67	7.73	3.92	1.50
245	0.81	[illegible]	373.11	346.95	267.7	[illegible]	286.91	0.97	5.54	3.24	1.50
246	0.81	101.3	373.11	356.43	185.0	0.90	287.21	1.34	4.24	2.13	1.50
247	0.81	[illegible]	373.11	362.74	137.0	0.72	287.36	1.24	4.51	[illegible]	1.50
248	0.44	[illegible]	373.11	331.70	357.4	3.61	286.67	0.65	8.03	3.97	1.50
249	0.44	101.	373.11	347.05	253.9	1.80	286.94	0.92	5.81	3.19	1.50
250	0.44	[illegible]	373.11	353.94	185.0	0.90	287.24	1.34	4.24	2.54	1.50
251	0.44	[illegible]	373.11	363.69	125.8	0.72	287.66	1.14	4.83	1.98	1.50

Table 6.7 Pure vapours results

vapour steam

tube diameter 25.25 mm

Run No.	U_∞ / m/s	P_∞ / Pa	T_∞ / K	T_w / K	$\dot{Q}''_{obs}$ / kW/m^2	U_{ow} / m/s	T_{in} / K	ΔT_{ow} / K	error estimates: $\delta\dot{Q}''_{obs}/\dot{Q}''_{obs}$ / %	error estimates: σ_{Tw} / K	error estimates: $\delta U_\infty/U_\infty$ / %
252	12.85	4.	[illegible]	298.02	62.0	3.59	289.39	0.12	40.55	1.23	1.50
253	12.85	4.	303.79	299.42	61.1	1.87	289.54	0.22	22.67	0.76	1.50
254	12.87	4.	303.39	299.90	52.3	1.26	289.59	0.27	18.53	0.39	1.50
255	12.87	4.	303.39	300.19	50.9	0.93	289.69	0.37	13.66	0.21	1.50
256	13.60	4.9	305.53	299.48	81.6	3.59	289.37	0.15	23.81	1.63	1.50
257	13.60	4.9	305.53	301.11	67.9	1.80	289.49	0.25	20.36	1.02	1.50
258	13.61	4.9	305.53	301.06	57.0	1.26	289.59	0.30	17.00	0.56	1.50
259	13.63	4.9	305.53	301.50	54.3	0.90	289.66	0.39	12.82	0.31	1.50
260	14.10	6.4	310.47	302.53	118.8	3.59	289.29	0.20	25.39	2.09	1.50
261	14.10	6.4	310.47	304.87	81.6	1.80	289.59	0.33	17.00	1.46	1.50
262	14.12	6.4	310.47	305.59	71.3	1.26	289.49	0.37	13.65	0.86	1.50
263	14.13	6.4	310.47	305.77	74.7	0.90	289.54	0.54	9.43	0.43	1.50
264	15.12	7.9	314.43	305.61	122.4	3.59	289.37	0.22	22.59	2.78	1.50
265	15.11	7.9	314.43	306.62	98.3	1.80	289.41	0.32	15.71	1.89	1.50
266	15.14	7.9	314.43	309.09	85.6	1.26	289.56	0.44	11.43	1.26	1.50
267	15.16	7.9	314.43	309.68	78.1	0.90	289.64	0.57	9.04	0.58	1.50

Table 6.8 Pure vapours results

vapour Refrigerant 113
tube diameter 12.5 mm

Run No.	U_∞ m/s	P_∞ Pa	T_∞ K	T_w K	$\dot{Q}''_{obs}$ kW/m^2	U_{cw} m/s	T_{in} K	ΔT_{cw} K	error estimates: $\delta\dot{Q}''_{obs}/\dot{Q}''_{obs}$ %	error estimates: σ_{Tw} K	error estimates: $\delta U_\infty/U_\infty$ %
268	0.47	1 1.9	320.76	287.04	42.3	3.97	282.35	0.25	20.07	0.33	1.50
269	0.47	1 1.9	320.56	288.72	41.4	2.78	282.36	0.35	14.41	0.38	1.50
270	0.47	101.9	320.36	291.46	37.2	1.59	282.40	0.55	9.30	0.42	1.50
271	0.47	1 1.9	320.36	301.86	26.6	0.59	282.45	1.05	5.16	0.48	1.50
272	0.54	101.5	320.35	287.35	42.3	3.97	282.33	0.25	20.07	0.37	1.50
273	0.65	1 1.5	320.35	288.74	41.4	2.78	282.35	0.35	14.41	0.39	1.50
274	0.54	101.5	32 .35	291.54	37.2	1.59	282.40	0.55	9.30	0.43	1.50
275	0.54	101.5	320.35	301.80	26.0	0.59	282.45	1.03	5.27	0.44	1.50
276	0.61	1 2.5	320.57	287.41	42.3	3.97	282.26	0.25	20.07	0.38	1.50
277	0.61	1 2.5	320.57	288.80	41.4	2.78	282.28	0.35	14.43	0.39	1.50
278	0.61	102.5	320.57	291.54	37.2	1.59	282.33	0.55	9.30	0.45	1.50
279	0.61	1 2.5	320.57	302.04	26.6	0.59	282.38	1.05	5.16	0.45	1.50
280	0.71	1 3.4	320.79	287.45	42.3	3.97	282.25	0.25	20.06	0.41	1.50
281	.61	103.4	32 .79	288.84	41.4	2.78	282.25	0.35	14.40	0.44	1.50
282	0.61	103.4	320.79	291.68	38.9	1.59	282.28	0.58	8.91	0.47	1.50
283	0.71	1 3.4	320.79	301.97	27.2	0.59	282.40	1.08	5.06	0.71	1.50
284	0.80	104.	321.03	287.57	42.3	3.97	282.28	0.25	20.07	0.44	1.50
285	0.80	104.2	321.03	286.98	41.4	2.78	282.30	0.35	14.43	0.43	1.50
286	0.80	104.	321.03	291.82	38.9	1.59	282.33	0.58	8.91	0.49	1.50
287	0.80	1 4.	321.03	302.56	27.2	0.59	282.45	1.08	5.06	0.60	1.50
288	0.97	102.7	320.60	287.60	42.3	3.97	282.25	0.25	20.06	0.46	1.50
289	0.97	102.7	320.60	288.98	41.4	2.78	282.25	0.35	14.43	0.49	1.50
290	0.98	1 2.7	320.60	291.92	38.9	1.59	282.30	0.58	8.91	0.54	1.50
291	0.98	1 2.7	320.60	302.24	37.2	0.59	282.43	1.08	5.06	0.59	1.50
292	0.98	103.	32 .74	287.71	46.5	3.97	282.28	0.28	18.26	0.47	1.50
293	0.98	1 3.	320.74	289.10	41.4	2.78	282.31	0.35	14.40	0.52	1.50
294	0.98	103.	320.74	291.97	38.9	1.59	282.33	0.58	8.91	0.51	1.50
295	0.98	1 3.	320.74	302.60	27.9	0.59	282.45	1.10	4.96	0.62	1.50
296	0.99	1 .	320.56	287.64	46.5	3.97	282.25	0.28	18.25	0.51	1.50
297	1.00	102.5	320.56	289.05	41.4	2.78	282.26	0.35	14.40	0.49	1.50
298	1.00	1 .5	320.56	291.94	38.9	1.59	282.33	0.58	8.91	0.53	1.50
299	1.03	102.5	320.56	302.41	27.9	0.59	282.45	1.1	4.96	0.48	1.50
300	1.05	103.9	320.94	287.74	46.5	3.97	282.26	0.26	18.26	0.50	1.50
301	1.25	103.9	320.94	289.19	44.4	2.78	282.28	0.36	13.46	0.49	1.50
302	1.05	103.9	320.94	292.04	38.9	1.59	282.33	0.58	8.91	0.51	1.50
303	1.05	103.9	320.94	302.96	27.9	0.59	282.43	1.10	4.96	0.46	1.50
304	1.11	104.5	321.14	287.61	46.5	3.97	282.33	0.28	18.26	0.52	1.50
305	1.11	104.5	321.14	290.01	40.6	2.38	282.33	0.40	12.64	0.55	1.50
306	1.11	104.5	321.14	294.10	38.0	1.19	282.35	0.75	6.95	0.54	1.50
307	1.11	104.5	321.14	303.05	27.8	0.59	282.40	1.10	4.96	0.42	1.50
308	1.23	1 5.	320.68	287.67	46.5	3.97	282.20	0.28	18.26	0.54	1.50
309	1.24	105.	320.68	290.05	43.1	2.38	282.30	0.43	11.92	0.58	1.50
310	1.24	1 3.	321.68	294.16	38.0	1.19	282.35	0.75	6.95	0.57	1.50
311	1.24	1 5.	320.68	303. 9	27.6	0.59	282.51	1.10	4.96	0.49	1.50
312	1.36	105.1	321.30	288.00	46.5	3.97	282.28	0.28	18.26	0.62	1.50
313	1.38	1 5.1	321.30	290.19	43.1	2.35	282.35	0.43	11.92	0.56	1.50
314	1.37	1 5.1	321.30	294.50	39.3	1.19	282.35	0.78	6.75	0.61	1.50

Table 6.8 (continued)

Run No.	U_∞ / m/s	P_∞ / Pa	T_∞ / K	T_w / K	$\dot{Q}''_{obs}$ / kW/m^2	U_{ow} / m/s	T_{in} / K	ΔT_{ow} / K	error estimates: $\delta\dot{Q}''_{obs}/\dot{Q}''_{obs}$ / %	σ_{Tw} / K	$\delta U_\infty/U_\infty$ / %
315	1.36	103.1	321.30	303.16	29.1	0.59	282.50	1.15	4.78	0.47	1.50
316	1.25	1[illegible]4.1	321.[illegible]0	287.93	46.5	3.97	282.25	0.28	18.26	0.58	1.50
317	1.25	104.1	321.00	290.04	43.1	2.38	282.28	0.43	11.92	0.59	1.50
318	1.25	104.[illegible]	321.[illegible]	294.21	36.0	1.19	282.35	0.75	6.95	0.59	1.50
319	1.26	104.1	321.00	313.17	28.5	0.59	282.45	1.13	4.87	0.58	1.50
320	1.28	1[illegible]4.[illegible]	321.07	287.94	46.5	3.97	282.30	0.28	18.26	0.56	1.50
321	1.29	104.[illegible]	321.07	29[illegible].15	43.1	2.38	282.35	0.43	11.92	0.62	1.50
322	1.29	104.3	321.07	294.77	39.3	1.19	282.38	0.78	6.75	0.57	1.50
323	1.29	1[illegible]	321.17	303.16	29.1	0.59	282.50	1.15	4.78	0.57	1.50
324	1.32	104.9	321.24	288.[illegible]3	46.5	3.97	282.30	0.28	18.26	0.63	1.50
325	1.33	1[illegible]4.9	321.24	290.27	43.1	2.36	282.35	0.43	11.92	0.62	1.50
326	1.33	104.9	321.24	294.56	40.5	1.19	282.45	0.80	6.56	0.59	1.50
327	1.33	104.9	321.24	303.35	29.1	0.59	282.55	1.15	4.73	0.48	1.50
328	1.55	1[illegible]3.5	320.87	282.[illegible]1	46.5	3.97	282.30	0.28	18.26	0.59	1.50
329	1.55	1[illegible]3.5	320.87	290.23	43.1	2.38	282.53	0.43	11.92	0.60	1.50
330	1.55	103.5	320.87	294.56	39.3	1.19	282.40	0.78	6.75	0.63	1.50
331	1.55	1[illegible]3.5	320.87	303.37	29.1	0.59	282.50	1.15	4.78	0.59	1.50
332	1.56	1[illegible]1.2	320.16	286.[illegible]5	46.5	3.97	282.30	0.28	18.26	0.64	1.50
333	1.57	1[illegible]1.[illegible]	320.16	29[illegible].21	43.1	2.36	282.33	0.43	11.92	0.65	1.50
334	1.57	101.[illegible]	320.16	294.[illegible]9	38.0	1.19	282.38	0.75	6.95	0.64	1.50
335	1.57	101.[illegible]	320.16	312.62	26.5	0.59	282.48	1.13	4.87	0.57	1.50
336	1.65	1[illegible]4.6	321.15	286.18	46.5	3.97	282.30	0.28	18.26	0.65	1.50
337	1.66	104.5	321.15	290.53	43.1	2.38	282.35	0.43	11.92	0.65	1.50
338	1.66	104.6	321.15	294.86	40.5	1.19	282.45	0.80	6.56	0.71	1.50
339	1.66	104.6	321.14	303.55	29.1	0.59	282.53	1.15	4.78	0.66	1.50
340	1.80	101.[illegible]	320.20	2[illegible].27	46.5	3.97	282.30	0.28	18.26	0.61	1.50
341	1.81	101.[illegible]	320.20	290.44	43.1	2.36	282.35	0.43	11.92	0.71	1.50
342	1.81	101.[illegible]	320.20	294.78	40.5	1.19	282.43	0.80	6.56	0.66	1.50
343	1.81	1[illegible]1.[illegible]	32[illegible].20	30[illegible].[illegible]3	29.7	0.59	282.53	1.18	4.73	0.67	1.50

Table 6.9 Pure vapours results

vapour Refrigerant 113
tube diameter 12.5 mm

Run No.	U_∞ / m/s	P_∞ / Pa	T_∞ / K	T_w / K	$\dot{Q}''_{obs}$ / kW/m^2	U_{cw} / m/s	T_{in} / K	ΔT_{cw} / K	error estimates: $\delta\dot{Q}''_{obs}/\dot{Q}''_{obs}$ / %	error estimates: σ_{Tw} / K	error estimates: $\delta U_\infty/U_\infty$ / %
344	2.70	57.1	[illegible]4.14	283.40	34.3	3.99	278.78	0.20	24.66	0.57	1.50
345	2.70	57.1	304.14	285.[illegible]7	32.2	2.0	278.83	0.38	13.37	0.60	1.50
346	2.71	57.1	304.14	289.18	26.8	1.0	278.88	0.63	8.18	0.59	1.50
347	2.71	57.1	304.14	294.63	18.6	0.6[illegible]	278.98	0.73	7.13	0.28	1.50
348	2.77	50.5	300.96	282.99	30.0	3.99	278.83	0.18	28.39	0.52	1.50
349	2.77	50.5	30[illegible].96	285.21	27.9	2.00	279.01	0.33	15.39	0.53	1.50
350	2.77	50.5	3[illegible].96	288.20	23.6	1.[illegible]	279.21	0.55	9.24	0.50	1.50
351	2.77	50.5	[illegible]00.96	292.99	15.4	[illegible].6	279.29	0.6[illegible]	8.51	0.23	1.50
352	2.77	50.4	300.91	282.82	30.1	3.99	278.73	0.18	28.39	0.52	1.50
353	2.77	50.4	30[illegible].91	284.97	27.9	2.0	278.78	0.33	15.38	0.53	1.50
354	2.77	50.4	[illegible].91	287.92	24.7	1.00	278.83	0.58	8.85	0.52	1.50
355	2.77	50.4	3[illegible].91	292.62	16.7	0.6[illegible]	278.93	0.66	7.89	0.30	1.50
356	2.77	44.5	297.92	282.32	25.8	3.99	278.75	0.15	33.10	[illegible].47	1.50
357	2.77	44.5	297.92	284.28	23.6	2.0[illegible]	278.91	0.28	18.14	0.47	1.50
358	2.77	44.5	297.92	286.97	21.4	1.00	279.09	0.50	10.12	0.45	1.50
359	2.76	44.5	297.92	291.14	13.5	0.61	279.19	0.53	9.66	0.26	1.50
360	2.28	47.5	299.42	282.68	25.8	3.99	278.73	0.15	33.10	0.52	1.50
361	2.28	47.5	299.42	284.84	25.7	2.00	278.98	0.30	16.65	0.51	1.50
362	2.28	47.5	299.40	287.66	23.6	1.0[illegible]	279.16	0.55	9.24	[illegible].49	1.50
363	2.28	47.5	299.4[illegible]	292.16	14.1	0.6	279.21	0.55	9.24	0.24	1.50
364	1.99	40.5	295.42	283.34	25.6	3.98	279.92	0.15	33.18	0.34	1.50
365	1.99	4[illegible].5	295.42	284.46	19.2	1.99	279.94	0.23	22.17	0.35	1.50
366	1.99	40.5	295.42	286.56	17.1	1.0[illegible]	279.97	0.4[illegible]	12.58	0.32	1.50
367	1.99	40.5	295.42	290.[illegible]1	11.5	0.6[illegible]	280.02	0.45	11.22	0.24	1.50
368	2.17	50.5	30[illegible].98	283.86	29.9	3.98	279.94	0.18	25.46	0.45	1.50
369	2.17	50.5	[illegible]0.98	285.43	27.8	1.99	279.97	0.33	15.42	0.45	1.50
370	2.17	50.6	[illegible]0.98	288.73	22.4	1.00	279.99	0.53	9.68	0.43	1.50
371	2.17	50.6	300.98	293.57	14.7	0.6	280.04	0.58	8.67	0.29	1.50
372	2.28	6[illegible].7	3[illegible]5.75	284.56	34.2	3.98	279.92	0.20	24.92	0.55	1.50
373	2.28	6[illegible].7	3[illegible]5.75	287.12	34.2	1.99	279.97	0.40	12.58	0.58	1.50
374	2.28	60.7	305.75	290.57	27.7	1.00	279.99	0.65	7.90	0.54	1.50
375	2.28	60.7	3[illegible]5.75	296.27	18.6	0.63	280.07	0.73	7.14	0.37	1.50
376	2.27	75.1	311.56	285.56	42.7	3.98	279.94	0.25	19.97	0.65	1.50
377	2.27	75.1	311.56	286.52	36.3	1.99	280.02	0.43	11.86	0.66	1.50
378	2.27	75.1	311.56	292.62	33.0	1.00	280.24	0.78	6.72	0.62	1.50
379	2.27	75.1	311.56	299.62	23.0	0.61	280.27	0.90	5.88	0.41	1.50
380	2.00	44.7	297.84	28[illegible].[illegible]4	21.4	3.98	279.92	0.13	[illegible]9.79	0.41	1.50
381	2.00	44.7	297.84	285.01	21.4	1.99	279.97	0.25	19.97	0.41	1.50
382	2.00	44.7	297.84	287.44	19.2	1.0[illegible]	279.99	0.45	11.22	0.40	1.50
383	2.00	44.7	297.84	291.42	12.2	0.6[illegible]	280.07	0.48	1[illegible].65	0.26	1.50
384	2.07	48.1	299.70	283.64	25.6	3.98	279.97	0.15	33.18	0.45	1.50
385	2.07	48.1	299.70	285.53	25.6	1.99	279.99	0.30	16.68	0.46	1.50
386	2.07	48.1	299.70	286.15	21.3	1.00	280.04	0.50	10.14	0.45	1.50
387	2.[illegible]7	48.1	299.70	292.58	14.7	0.60	280.09	0.58	8.87	0.24	1.50

Table 6.9 (continued)

Run No.	U_∞ (m/s)	P_∞ (Pa)	T_∞ (K)	T_w (K)	$\dot{Q}''_{obs}$ (kW/m^2)	U_{ow} (m/s)	T_{in} (K)	ΔT_{ow} (K)	error estimates: $\delta\dot{Q}''_{obs}/\dot{Q}''_{obs}$ (%)	σ_{Tw} (K)	$\delta U_\infty/U_\infty$ (%)
388	2.12	51.7	301.55	283.85	25.6	3.98	279.92	0.15	33.18	0.48	1.50
389	2.12	51.7	301.55	285.95	25.6	1.99	279.97	0.30	16.68	0.48	1.50
390	2.12	51.7	301.55	260.69	24.4	1.00	280.02	0.53	9.68	0.47	1.50
391	2.12	51.7	301.55	293.47	15.4	0.60	280.07	0.60	6.52	0.23	1.50
392	2.21	53.9	302.62	284.78	29.9	3.98	279.94	0.18	28.46	0.50	1.50
393	2.22	53.9	302.62	260.31	29.9	1.99	279.97	0.35	14.34	0.52	1.50
394	2.21	53.9	302.62	289.32	24.5	1.00	280.02	0.58	6.87	0.48	1.50
395	2.22	53.9	302.62	294.29	16.0	0.60	280.09	0.63	8.20	0.32	1.50
396	2.21	53.8	304.92	284.45	34.2	3.98	279.94	0.20	24.92	0.54	1.50
397	2.21	58.[illegible]	304.92	286.84	29.9	1.99	279.99	0.35	14.34	0.57	1.50
398	2.21	58.8	304.92	290.[illegible]3	25.6	1.00	280.04	0.60	8.52	0.55	1.50
399	2.22	58.8	304.92	295.34	17.9	0.60	280.09	0.70	7.38	0.31	1.50
400	2.23	62.[illegible]	306.46	284.69	34.2	3.98	279.94	0.20	24.92	0.55	1.50
401	2.23	62.3	306.46	287.26	34.2	1.99	279.97	0.40	12.58	0.57	1.50
402	2.23	62.3	306.46	290.79	28.8	1.00	280.02	0.68	7.63	0.54	1.50
403	2.23	62.[illegible]	306.46	296.85	19.2	0.60	280.09	0.75	6.92	0.45	1.50
404	2.33	69.6	309.55	285.21	38.4	3.98	279.97	0.23	22.17	0.61	1.50
405	2.33	69.[illegible]	309.55	288.11	36.3	1.99	280.17	0.43	11.87	0.63	1.50
406	2.33	69.5	309.55	291.92	30.9	1.00	280.29	0.73	7.15	0.62	1.50
407	2.33	69.[illegible]	309.55	298.34	22.4	0.6	280.29	0.86	6.03	0.45	1.50
408	2.09	77.5	312.46	285.50	42.7	3.98	279.89	0.25	19.97	0.60	1.50
409	2.09	77.5	312.46	285.54	38.4	1.99	279.94	0.45	11.22	0.67	1.50
410	2.09	77.5	312.46	292.52	34.1	1.00	280.02	0.30	6.53	0.69	1.50
411	2.09	77.5	312.46	299.22	21.1	0.60	280.17	0.30	6.35	0.33	1.50

mixture steam-air

tube diameter 12.5 mm

Run No.	$W_{\infty 1}$ %	$W_{\infty 2}$ %	$\tilde{W}_{\infty 1}$ %	$\tilde{W}_{\infty 2}$ %	U_∞ m/s	P_∞ Pa	T_∞ K	T_w K	$\dot{Q}''_{obs}$ kW/m^2	U_{ow} m/s	T_{in} K	ΔT_{ow} K	error estimates: $\frac{\delta \dot{Q}''_{obs}}{\dot{Q}''_{obs}}$ %	σ_{Tw} K	$\frac{\delta U_\infty}{U_\infty}$ %	$\frac{\delta W_{\infty 1}}{W_{\infty 1}}$ %	$\frac{\delta W_{\infty 2}}{W_{\infty 2}}$ %
412	0.50	0.48	0.51	0.30	1.60	101.2	373.03	336.81	438.1	3.92	289.07	2.64	2.76	6.10	1.49	2.49	23.96
413	1.00	0.99	0.61	0.62	1.67	101.0	372.66	334.76	417.8	3.92	289.04	2.51	2.82	6.40	1.49	2.48	11.69
414	1.51	1.54	0.95	0.97	1.67	101.1	372.81	332.59	409.6	3.92	289.04	2.47	2.85	6.45	1.48	2.46	7.41
415	2.05	2.03	1.27	1.27	1.68	100.9	372.69	330.96	397.3	3.92	289.04	2.39	2.89	6.55	1.47	2.45	5.62
416	2.64	2.64	1.66	1.65	1.69	100.6	372.49	327.17	381.0	3.92	289.02	2.29	2.96	6.22	1.46	2.43	4.31
417	3.[illegible]9	3.4	2.14	2.14	1.7[illegible]	100.6	372.35	325.63	360.6	3.92	289.02	2.17	3.05	6.14	1.45	2.42	3.29
418	4.28	4.25	2.71	2.68	1.71	100.3	372.10	322.15	352.4	3.92	289.02	2.12	3.09	5.91	1.44	2.39	2.61
419	5.19	5.19	3.29	3.29	1.72	100.5	371.98	320.41	331.9	3.92	289.07	2.00	3.20	5.67	1.43	2.37	2.11
420	0.51	0.51	0.3	[illegible].32	1.73	101.8	373.20	335.49	447.2	3.92	288.60	2.69	2.73	7.63	1.49	2.49	22.57
421	1.18	1.07	0.66	0.67	1.64	101.7	373.07	333.46	426.7	3.92	288.60	2.57	2.79	8.06	1.48	2.47	10.72
422	1.55	1.53	0.97	0.96	1.64	101.7	372.98	331.37	402.2	3.92	288.57	2.42	2.88	7.96	1.48	2.46	7.47
423	2.02	2.02	1.27	1.27	1.65	101.5	372.84	329.66	385.9	3.92	288.52	2.32	2.94	7.60	1.47	2.45	5.63
424	2.68	2.70	1.69	1.69	1.66	101.3	372.67	326.45	351.8	3.92	288.52	2.30	2.96	7.69	1.46	2.43	4.18
425	3.46	3.46	2.1[illegible]	2.18	1.67	101.[illegible]	372.44	324.01	381.9	3.92	288.48	2.30	2.96	7.12	1.45	2.41	3.22
426	4.33	4.35	2.74	2.75	1.66	101.[illegible]	372.28	321.34	361.4	3.92	288.48	2.17	3.05	6.64	1.44	2.39	2.54
427	5.31	5.29	3.37	3.36	1.69	100.9	372.09	319.15	340.9	3.92	288.48	2.05	3.15	6.62	1.42	2.37	2.06
428	5.99	6.00	3.81	3.82	1.70	100.6	371.86	317.56	324.6	3.92	288.45	1.95	3.25	6.08	1.42	2.35	1.80
429	7.22	7.21	4.6[illegible]	4.61	1.7[illegible]	100.9	371.72	316.07	308.7	3.92	288.43	1.85	3.36	5.82	1.40	2.32	1.47
430	0.60	0.60	0.37	0.37	1.76	102.0	373.22	343.47	364.1	2.35	288.48	3.65	2.42	7.15	1.49	2.48	19.44
431	1.21	1.22	0.7[illegible]	0.76	1.[illegible]7	101.9	373.09	340.92	351.9	2.35	288.48	3.53	2.45	7.52	1.48	2.47	9.44
432	1.87	1.85	1.1[illegible]	1.16	1.[illegible]7	101.8	372.95	338.76	342.1	2.35	288.48	3.43	2.48	7.56	1.47	2.45	6.15
433	2.47	2.46	1.55	1.55	1.[illegible]	101.7	372.83	336.53	327.3	2.35	288.48	3.28	2.51	7.18	1.46	2.44	4.59
434	3.17	3.16	1.9[illegible]	[illegible]	1.[illegible]	1[illegible]1.5	372.63	334.11	334.7	2.35	288.45	3.35	2.49	7.22	1.45	2.42	3.52
435	4.17	4.16	2.57	2.57	1.[illegible]9	101.4	372.44	331.21	312.7	2.35	288.43	3.1[illegible]	2.56	6.88	1.44	2.40	2.73
436	5.11	5.11	[illegible]	[illegible].24	1.4[illegible]	101.[illegible]	372.23	328.80	290.6	2.35	288.45	2.91	2.64	6.90	1.43	2.37	2.14
437	6.77	6.25	3.9[illegible]	[illegible].93	1.41	101.[illegible]	371.98	324.79	27[illegible].4	2.35	288.45	2.74	2.71	6.34	1.41	2.34	1.72
438	7.48	7.46	4.7[illegible]	4.77	1.4[illegible]	101.1	371.72	322.28	256.2	2.35	288.45	2.57	2.79	5.66	1.40	2.31	1.42
439	[illegible].45	[illegible].46	[illegible].2[illegible]	[illegible].79	1.61	101.9	373.24	344.78	383.9	2.35	288.38	3.85	2.39	7.05	1.49	2.49	25.27
440	[illegible].75	[illegible].74	[illegible].47	[illegible].45	1.[illegible]1	1[illegible]1.9	373.17	343.57	374.1	2.35	288.38	3.75	2.4[illegible]	7.34	1.49	2.48	15.67
441	1.[illegible]7	1.[illegible]5	[illegible].67	[illegible].66	1.[illegible]	101.5	373.1[illegible]	342.37	359.4	2.35	288.[illegible]8	3.60	2.44	7.56	1.48	2.47	10.87
442	1.32	1.32	[illegible]	[illegible].8[illegible]	1.[illegible]	101.8	373.05	340.38	352.0	2.35	288.35	3.53	2.45	7.41	1.48	2.47	8.70

Table 6.10 (continued)

Run No.	$W_{\infty 1}$	$W_{\infty 2}$	$\tilde{W}_{\infty 1}$	$\tilde{W}_{\infty 2}$	U_∞	P_∞	T_∞	T_w	$\dot{Q}''_{obs}$	U_{ow}	T_{in}	ΔT_{ow}	error estimates: $\frac{\delta \dot{Q}''_{obs}}{\dot{Q}''_{obs}}$	σ_{Tw}	$\frac{\delta U_\infty}{U_\infty}$	$\frac{\delta W_{\infty 1}}{W_{\infty 1}}$	$\frac{\delta W_{\infty 2}}{W_{\infty 2}}$
	%	%	%	%	m/s	Pa	K	K	kW/m²	m/s	K	K	%	K	%	%	%
443	1.59	1.57	1.00	0.98	1.62	101.8	373.01	339.77	347.1	2.35	288.35	3.48	2.46	7.41	1.48	2.46	7.29
444	1.67	1.68	1.17	1.16	1.63	101.6	372.91	338.64	339.8	2.35	288.35	3.40	2.48	7.51	1.47	2.45	6.06
445	2.47	2.48	1.55	1.56	1.63	101.7	372.82	337.21	332.4	2.35	288.35	3.33	2.50	7.74	1.46	2.44	4.56
446	3.03	3.00	1.91	1.89	1.65	100.8	372.49	332.91	327.5	2.35	288.35	3.28	2.51	7.16	1.46	2.42	3.75
447	3.91	3.88	2.47	2.45	1.66	100.5	372.23	330.22	325.1	2.35	288.35	3.26	2.52	6.90	1.44	2.40	2.87
448	0.52	0.53	0.34	0.33	1.6[illegible]	102.2	373.29	359.60	213.4	0.78	288.40	6.42	2.15	4.87	1.49	2.49	21.86
449	0.79	0.78	0.45	.49	1.60	102.2	373.25	359.13	211.6	0.78	288.40	6.37	2.15	4.97	1.49	2.48	14.77
450	1.06	1.07	0.66	.67	1.61	102.1	373.17	358.53	211.0	0.78	288.38	6.34	2.15	5.08	1.48	2.47	10.76
451	1.33	1.31	0.87	.82	1.61	102.0	373.10	357.89	209.4	0.78	288.38	6.29	2.15	5.20	1.48	2.47	8.78
452	1.60	1.58	1.0	0.99	1.61	101.9	373.03	357.43	207.0	0.78	288.38	6.22	2.16	5.40	1.48	2.46	7.22
453	1.68	1.87	1.15	1.17	1.62	101.9	372.98	356.92	206.2	0.78	288.35	6.20	2.16	5.50	1.47	2.45	6.08
454	2.16	2.15	1.35	1.35	1.62	101.8	372.90	356.45	204.5	0.78	288.35	6.15	2.16	5.40	1.47	2.45	5.27
455	2.72	2.69	1.71	1.69	1.63	101.8	372.79	355.55	202.1	0.78	288.35	6.08	2.16	5.54	1.46	2.43	4.18
456	3.51	3.54	2.22	2.23	1.63	101.7	372.61	354.12	197.3	0.78	288.33	5.93	2.17	5.58	1.45	2.41	3.14
457	4.41	4.39	2.79	2.77	1.64	101.5	372.40	352.57	194.8	0.78	288.33	5.86	2.17	5.67	1.44	2.39	2.51
458	5.71	5.70	3.67	3.62	1.65	101.5	372.17	349.90	193.2	0.78	288.30	5.81	2.18	5.72	1.42	2.36	1.90
459	6.49	6.49	4.14	4.14	1.66	101.5	372.01	348.89	189.9	0.78	288.33	5.71	2.18	5.57	1.41	2.34	1.65
460	7.70	7.69	4.97	4.93	1.67	101.5	371.78	346.60	188.3	0.78	288.30	5.66	2.19	5.46	1.39	2.31	1.37
461	0.58	0.59	0.36	.37	1.66	102.7	373.43	332.58	444.2	3.93	288.03	2.67	2.74	6.70	1.49	2.49	19.46
462	0.77	0.76	.45	.43	1.67	102.7	373.39	331.58	423.7	3.93	288.03	2.54	2.80	6.96	1.49	2.48	15.09
463	1.16	1.17	0.72	.73	1.[illegible]7	102.5	373.27	329.09	407.3	3.93	288.01	2.45	2.86	7.45	1.48	2.47	9.81
464	1.54	1.54	0.97	.96	1.67	102.5	373.21	327.64	399.1	3.93	288.01	2.40	2.89	7.36	1.48	2.46	7.41
465	1.93	1.93	1.21	1.21	1.[illegible]8	102.3	373.08	325.56	378.6	3.93	288.01	2.27	2.97	6.71	1.47	2.45	5.89
466	2.33	2.31	1.46	1.45	1.68	102.2	372.99	323.47	366.3	3.93	288.01	2.20	3.03	6.81	1.47	2.44	4.89
467	2.77	2.72	1.7	1.71	1.[illegible]9	102.2	372.9[illegible]	321.71	353.9	3.93	288.01	2.13	3.09	6.62	1.46	2.43	4.13
468	3.14	3.11	1.93	1.96	1.[illegible]9	102.1	372.81	320.70	337.5	3.93	288.01	2.03	3.18	6.29	1.45	2.42	3.59
469	3.56	3.55	2.25	2.24	1.[illegible]9	102.1	372.73	319.89	333.4	3.93	288.01	2.00	3.20	6.03	1.45	2.41	3.13
470	3.98	3.9[illegible]	2.54	2.51	1.[illegible]9	102.2	372.67	316.87	325.2	3.93	288.01	1.95	3.25	6.02	1.44	2.40	2.78
471	5.1[illegible]	5.11	3.25	3.24	1.[illegible]	101.9	372.57	315.78	312.9	3.93	288.01	1.88	3.33	5.91	1.43	2.37	2.13
472	6.[illegible]8	6.4[illegible]	4.[illegible]7	4.1[illegible]	1.11	101.6	372.11	313.63	288.2	3.93	288.01	1.73	3.51	5.21	1.41	2.34	1.68
473	7.8[illegible]	7.[illegible]2	5.[illegible]	[illegible]	1.12	101.5	371.75	311.59	267.7	3.93	288.01	1.61	3.70	4.92	1.39	2.31	1.35
474	9.[illegible]	9.[illegible]	6.[illegible]	[illegible].99	1.14	101.[illegible]	371.4[illegible]	309.55	236.6	3.93	288.[illegible]5	1.43	4.02	4.41	1.37	2.27	1.11

Table 6.10 (continued)

Run No.	$W_{\infty 1}$ %	$W_{\infty 2}$ %	$\tilde{W}_{\infty 1}$ %	$\tilde{W}_{\infty 2}$ %	U_∞ m/s	P_∞ Pa	T_∞ K	T_w K	$\dot{Q}''_{obs}$ kW/m^2	U_{ow} m/s	T_{in} K	ΔT_{ow} K	error estimates: $\frac{\delta \dot{Q}''_{obs}}{\dot{Q}''_{obs}}$ %	σ_{Tw} K	$\frac{\delta U_\infty}{U_\infty}$ %	$\frac{\delta W_{\infty 1}}{W_{\infty 1}}$ %	$\frac{\delta W_{\infty 2}}{W_{\infty 2}}$ %
475	10.96	10.94	7.11	7.10	1.15	101.7	371.09	307.74	214.2	3.93	288.05	1.29	4.37	4.13	1.35	2.23	0.92
476	0.57	0.57	.36	.35	1.17	102.6	373.45	341.94	379.4	2.36	288.08	3.80	2.39	6.45	1.49	2.49	20.36
477	0.76	0.75	.49	.47	1.18	102.7	373.41	340.89	369.6	2.36	88.08	3.70	2.41	6.65	1.49	2.48	15.43
478	1.15	1.02	.7[illegible]	.64	1.[illegible]	102.5	373.30	338.93	354.9	2.36	288.08	3.55	2.45	7.02	1.48	2.47	11.25
479	1.5[illegible]	1.55	.96	.97	1.[illegible]	102.5	373.21	337.18	337.7	2.36	288.08	3.38	2.49	6.86	1.48	2.46	7.36
480	1.92	2.[illegible]6	1.20	1.29	1.[illegible]	102.5	373.12	335.80	325.4	2.36	288.08	3.26	2.52	6.96	1.47	2.45	5.51
481	2.72	2.65	1.45	1.67	1.[illegible]9	102.5	373.[illegible]1	333.58	313.2	2.36	88.08	3.13	2.56	6.84	1.47	2.44	4.25
482	2.72	3.0[illegible]	1.71	1.89	1.[illegible]9	102.5	372.95	332.76	308.2	2.36	288.08	3.09	2.57	6.69	1.46	2.43	3.73
483	3.12	3.12	1.97	[illegible].96	1.10	102.2	372.83	331.26	303.4	2.36	288.05	3.04	2.59	6.75	1.45	2.42	3.59
484	3.54	3.5[illegible]	2.23	2.2[illegible]	1.1[illegible]	102.1	372.75	330.12	293.5	2.36	288.05	2.94	2.63	6.75	1.45	2.41	3.18
485	3.97	3.94	2.51	2.49	1.10	102.0	372.62	328.05	283.7	2.36	288.05	2.84	2.66	6.73	1.44	2.40	2.81
486	5.11	5.08	3.24	[illegible].22	1.11	101.6	372.30	324.76	276.3	2.36	288.03	2.77	2.70	6.07	1.43	2.37	2.15
487	6.76	6.38	4.05	4.07	1.12	101.7	372.09	322.41	254.2	2.36	288.03	2.54	2.80	5.62	1.41	2.34	1.68
488	7.78	7.82	4.99	5.01	1.1[illegible]	101.4	371.73	320.25	237.0	2.36	288.03	2.37	2.91	5.30	1.39	2.31	1.35
489	9.75	9.25	5.9[illegible]	5.96	1.14	101.2	371.41	317.03	217.3	2.36	288.01	2.17	3.05	4.93	1.37	2.27	1.12
490	10.87	10.88	7.[illegible]5	7.06	1.15	101.4	371.12	315.29	202.5	2.36	288.01	2.03	3.18	4.66	1.35	2.23	0.93
491	0.57	0.45	[illegible].36	.28	1.[illegible]8	102.7	373.45	358.81	214.5	0.79	288.13	6.44	2.15	4.29	1.49	2.49	25.93
492	0.76	0.69	[illegible].4[illegible]	[illegible].43	1.[illegible]8	102.6	373.37	358.20	211.3	0.79	288.10	6.35	2.15	4.49	1.49	2.48	16.63
493	1.14	1.18	.7[illegible]	[illegible].73	1.[illegible]8	102.6	373.29	357.14	209.6	0.79	288.10	6.30	2.15	4.79	1.48	2.47	9.75
494	1.53	1.64	[illegible].96	[illegible].[illegible]3	1.[illegible]	102.6	373.20	356.13	208.[illegible]	0.79	288.10	6.25	2.15	4.99	1.48	2.46	6.93
495	1.92	2.26	1.2	1.42	1.[illegible]9	102.5	373.08	355.75	204.8	0.79	288.10	6.15	2.16	5.07	1.47	2.45	5.01
496	2.[illegible]1	2.72	1.45	1.71	1.[illegible]9	102.5	372.99	353.85	203.1	0.79	288.10	6.10	2.16	5.31	1.47	2.44	4.13
497	2.71	3.01	1.7[illegible]	1.90	1.09	102.5	372.94	353.30	201.5	0.79	288.10	6.05	2.16	5.36	1.46	2.43	3.72
498	3.12	3.26	1.96	[illegible].15	1.1[illegible]	102.2	372.8[illegible]	352.32	199.9	0.79	288.10	6.00	2.17	5.45	1.45	2.42	3.43
499	[illegible].54	[illegible].55	2.2[illegible]	[illegible].24	1.1[illegible]	102.1	372.73	351.74	198.[illegible]	0.79	288.10	5.96	2.17	5.35	1.45	2.41	3.14
500	3.97	[illegible].94	2.51	.49	1.1	102.1	372.65	350.29	195.8	0.79	288.10	5.88	2.17	5.62	1.44	2.40	2.81
501	4.99	5.01	3.1[illegible]	[illegible].1[illegible]	1.11	101.8	372.37	346.26	193.4	0.79	288.10	5.81	2.18	5.56	1.43	2.38	2.18
502	6.[illegible]7	6.16	3.9	.95	1.[illegible]3	101.2	371.98	344.67	186.9	0.79	288.10	5.61	2.19	5.12	1.41	2.34	1.75
503	7.65	7.78	4.9	4.98	1.[illegible]	101.5	371.77	342.87	175.4	0.79	288.10	5.27	2.21	5.31	1.39	2.31	1.35
504	9.14	9.27	5.[illegible]9	[illegible].92	1.14	101.5	371.47	340.58	167.3	0.79	288.10	5.03	2.23	4.99	1.38	2.27	1.11
505	1[illegible].71	1[illegible]	6.94	7.[illegible]	1.15	101.4	371.16	338.47	158.3	0.79	288.10	4.76	2.26	4.74	1.36	2.23	0.93
506	1.[illegible]	1.56	[illegible].1[illegible]	[illegible]	[illegible]4	101.[illegible]	372.64	319.02	293.6	3.93	266.96	1.76	3.48	5.96	1.47	2.45	6.90

Table 6.10 (continued)

Run No.	$W_{\infty1}$	$W_{\infty2}$	$\tilde{W}_{\infty1}$	$\tilde{W}_{\infty2}$	U_∞	P_∞	T_∞	T_w	$\dot{Q}''_{obs}$	U_{ow}	T_{in}	ΔT_{ow}	error estimates: $\delta\dot{Q}''_{obs}/\dot{Q}''_{obs}$	σ_{Tw}	$\delta U_\infty/U_\infty$	$\delta W_{\infty1}/W_{\infty1}$	$\delta W_{\infty2}/W_{\infty2}$
	%	%	%	%	m/s	Pa	K	K	kW/m^2	m/s	K	K	%	K	%	%	%
507	2.75	2.37	1.47	1.49	.75	101.2	372.71	316.67	268.9	3.93	286.96	1.61	3.69	5.79	1.47	2.44	4.77
508	3.44	3.61	[illegible].17	[illegible].28	0.[illegible]6	101.2	372.49	313.13	240.0	3.93	286.94	1.44	4.01	4.89	1.45	2.41	3.09
509	4.47	4.29	2.8[illegible]	2.71	0.37	100.7	372.21	310.67	223.5	3.93	286.94	1.34	4.24	4.60	1.44	2.39	2.58
510	5.90	5.9[illegible]	[illegible].76	[illegible].76	[illegible]	100.5	371.84	305.8[illegible]	173.9	3.93	286.94	1.04	5.20	3.71	1.42	2.35	1.83
511	5.65	5.61	[illegible].50	.57	0.[illegible]7	100.3	371.85	305.87	186.3	3.93	286.86	1.12	4.91	3.58	1.42	2.36	1.94
512	6.67	6.58	4.26	4.2[illegible]	0.38	10[illegible].4	371.69	303.16	178.0	3.93	286.86	1.07	5.10	3.31	1.41	2.33	1.63
513	5.14	5.01	3.26	[illegible].18	0.41	98.4	371.43	310.60	210.8	2.97	283.70	1.67	3.60	2.58	1.43	2.37	2.19
514	7.59	7.62	4.86	4.86	0.43	98.4	370.94	307.51	179.3	2.97	283.73	1.42	4.05	2.34	1.39	2.31	1.39
515	9.59	9.94	6.39	6.42	0.45	97.8	370.33	304.41	154.2	2.97	283.73	1.22	4.55	2.34	1.37	2.25	1.04
516	12.37	12.39	8.07	8.08	0.46	96.9	369.57	301.01	135.3	2.97	283.73	1.07	5.07	1.96	1.34	2.19	0.81
517	15.12	15.17	9.95	1[illegible].01	0.47	96.7	368.93	299.62	113.3	2.97	283.73	0.90	5.91	1.72	1.31	2.12	0.63
518	18.[illegible]9	18.08	12.09	12.07	0.48	96.2	368.18	298.08	1[illegible]3.9	2.97	283.73	0.82	6.39	1.63	1.28	2.05	0.51
519	21.17	21.16	14.31	14.31	0.49	95.6	367.29	296.35	94.5	2.97	283.75	0.75	6.97	1.53	1.26	1.97	0.42
520	24.35	24.22	16.6[illegible]	16.59	0.51	95.3	366.49	295.62	88.2	2.97	283.75	0.70	7.43	1.52	1.23	1.89	0.35
521	5.14	5.12	[illegible].26	[illegible].25	0.41	98.5	371.43	331.99	167.9	0.99	284.30	4.00	2.36	1.82	1.43	2.37	2.14
522	7.56	7.59	4.84	4.86	0.43	98.1	370.85	327.89	142.0	0.99	284.30	3.38	2.49	1.80	1.39	2.31	1.40
523	9.91	9.35	6.41	6.[illegible]6	[illegible].44	98.1	370.40	324.16	130.5	0.99	284.30	3.11	2.57	1.73	1.37	2.25	1.05
524	12.77	12.[illegible]3	8.[illegible]7	[illegible]	[illegible].46	96.9	369.58	319.37	114.9	0.99	284.33	2.74	2.71	1.91	1.34	2.19	0.81
525	15.1[illegible]	15.14	9.[illegible]	9.99	0.47	96.8	368.96	316.00	104.4	0.99	284.45	2.49	2.84	2.43	1.31	2.12	0.63
526	18.1[illegible]	18.[illegible]4	12.[illegible]	12.[illegible]5	[illegible]	95.9	368.08	313.45	98.0	0.99	284.75	2.34	2.93	1.84	1.28	2.05	0.51
527	21.16	21.2[illegible]	14.3[illegible]	14.34	0.49	95.9	367.39	311.6[illegible]	88.6	0.99	284.92	2.11	3.10	1.73	1.26	1.97	0.41
528	24.74	24.44	16.68	16.75	0.5[illegible]	96.[illegible]	366.65	309.81	81.3	0.99	285.05	1.94	3.26	1.27	1.23	1.89	0.34
529	2.53	2.38	1.59	1.49	[illegible]5	98.6	371.97	322.21	347.9	2.96	284.23	2.76	2.70	3.49	1.46	2.44	4.78
530	3.84	3.77	[illegible]	[illegible]	[illegible]	98.5	371.69	317.86	313.5	2.96	284.25	2.49	2.83	2.64	1.44	2.40	2.97
531	5.18	5.[illegible]	[illegible].29	[illegible]	[illegible].87	98.2	371.35	315.47	279.2	2.96	284.23	2.22	3.02	3.47	1.43	2.37	2.11
532	6.59	6.50	4.2[illegible]	4.14	0.87	97.9	371.01	312.56	235.4	2.96	284.20	1.87	3.34	3.14	1.41	2.34	1.66
533	8.18	8.18	5.25	5.25	0.88	97.6	370.6[illegible]	310.11	213.4	2.96	284.20	1.69	3.57	2.95	1.39	2.30	1.29
534	10.49	1[illegible].59	6.9[illegible]	6.86	[illegible]	97.[illegible]	37[illegible]	307.33	194.7	2.97	284.13	1.54	3.80	2.80	1.36	2.23	0.96
535	11.85	11.86	7.7	7.72	[illegible].91	96.8	369.61	305.41	179.0	2.97	284.13	1.42	4.05	2.51	1.34	2.20	0.85
536	13.55	1[illegible].9[illegible]	9.[illegible]	[illegible].13	[illegible]	96.4	369.13	303.77	169.6	2.97	[illegible]84.15	1.35	4.22	2.40	1.32	2.15	0.70
537	2.53	2.76	1.59	[illegible].42	[illegible]	96.[illegible]	371.99	343.77	246.6	1.13	284.50	5.65	2.19	1.95	1.46	2.44	5.05
538	[illegible]	3.56	2.4	.4[illegible]	[illegible].6	96.5	371.67	34[illegible].04	2[illegible]2.6	1.03	284.58	5.33	2.21	1.70	1.44	2.40	2.90

Table 6.10 (continued)

Run No.	$W_{\infty 1}$	$W_{\infty 2}$	$\tilde{W}_{\infty 1}$	$\tilde{W}_{\infty 2}$	U_∞	P_∞	T_∞	T_w	$\dot{Q}''_{obs}$	U_{ow}	T_{in}	ΔT_{ow}	error estimates: $\frac{\delta \dot{Q}''_{obs}}{\dot{Q}''_{obs}}$	σ_{Tw}	$\frac{\delta U_\infty}{U_\infty}$	$\frac{\delta W_{\infty 1}}{W_{\infty 1}}$	$\frac{\delta W_{\infty 2}}{W_{\infty 2}}$
	%	%	%	%	m/s	Pa	K	K	kW/m^2	m/s	K	K	%	K	%	%	%
539	5.19	5.20	3.29	3.30	0.87	98.2	371.35	337.28	218.4	1.03	284.75	5.01	2.24	2.28	1.43	2.37	2.11
540	6.60	6.52	4.21	4.16	0.87	97.9	371.70	334.08	197.9	1.03	284.85	4.54	2.28	2.06	1.41	2.34	1.65
541	8.21	8.27	5.27	5.31	0.88	97.6	370.58	331.17	182.8	1.03	284.92	4.19	2.33	2.75	1.[illegible]9	2.29	1.28
542	9.97	10.16	6.44	6.57	0.89	97.3	370.14	327.95	164.4	1.03	285.02	3.77	2.40	2.41	1.37	2.25	1.01
543	11.55	11.63	7.72	7.71	0.91	97.0	369.72	325.85	154.8	1.03	284.97	3.55	2.45	2.55	1.34	2.20	0.85
544	13.18	13.89	9.11	9.12	0.92	96.8	369.23	323.64	146.1	1.03	285.05	3.35	2.50	2.42	1.32	2.15	0.70
545	1.34	1.41	0.84	.88	1.58	102.6	373.25	329.49	442.1	3.97	282.55	2.62	2.76	5.04	1.48	2.47	8.11
546	1.34	1.41	0.84	.88	1.58	102.6	373.25	344.06	352.9	1.98	282.63	4.19	2.33	4.25	1.48	2.47	8.11
547	1.34	1.41	0.84	0.88	1.58	102.6	373.25	363.59	153.4	0.59	282.73	6.07	2.16	2.71	1.48	2.47	8.11
548	2.77	2.81	1.74	1.77	1.59	102.4	372.94	324.33	412.7	3.97	282.55	2.45	2.86	5.29	1.46	2.43	4.00
549	2.76	2.81	1.74	1.77	1.59	102.4	372.94	339.34	323.6	1.98	282.63	3.84	2.39	4.93	1.46	2.43	4.00
550	2.76	2.81	1.74	1.77	1.59	102.4	372.94	362.31	148.4	0.59	282.73	5.87	2.17	2.87	1.46	2.43	4.00
551	4.41	4.51	2.79	2.86	1.61	102.0	372.51	317.82	358.1	3.97	282.58	2.12	3.09	4.96	1.44	2.39	2.44
552	4.41	4.51	2.79	2.86	1.61	102.0	372.51	332.41	298.5	1.98	282.65	3.54	2.45	3.81	1.44	2.39	2.44
553	4.40	4.51	2.79	2.86	1.61	102.0	372.51	360.10	142.7	0.59	282.83	5.65	2.19	3.26	1.44	2.39	2.44
554	6.49	6.64	4.14	4.24	1.64	101.3	371.93	313.30	311.9	3.97	282.55	1.85	3.36	4.61	1.41	2.34	1.61
555	6.49	6.64	4.14	4.24	1.64	101.3	371.93	327.88	281.8	1.98	282.60	3.34	2.50	4.54	1.41	2.34	1.61
556	6.49	6.64	4.14	4.24	1.64	101.3	371.93	358.42	134.6	0.59	282.73	5.33	2.21	3.18	1.41	2.34	1.61
557	8.94	8.89	5.75	5.72	1.67	100.8	371.35	309.32	269.8	3.97	282.53	1.60	3.71	4.20	1.38	2.28	1.17
558	8.94	8.89	5.75	5.72	1.67	100.8	371.35	324.58	244.1	1.98	282.60	2.90	2.64	4.39	1.38	2.28	1.17
559	8.97	8.89	5.75	5.72	1.67	100.8	371.35	357.01	127.7	0.59	282.73	5.05	2.23	2.86	1.38	2.28	1.17
560	11.81	11.90	7.69	7.75	1.71	99.7	370.45	304.64	240.4	3.97	282.53	1.43	4.04	3.71	1.34	2.20	0.84
561	11.81	11.97	7.69	7.75	1.71	99.7	370.45	317.14	221.5	1.98	282.60	2.75	2.70	3.93	1.34	2.20	0.84
562	11.81	11.90	7.69	7.75	1.71	99.7	370.45	350.75	132.1	0.59	282.83	5.23	2.22	3.05	1.34	2.20	0.84
563	15.11	15.11	9.9	9.97	1.75	99.0	369.60	302.19	219.3	3.97	282.53	1.30	4.33	3.00	1.31	2.12	0.63
564	15.11	15.19	9.9	9.95	1.75	99.0	369.61	313.61	195.8	1.98	282.60	2.32	2.94	3.40	1.31	2.12	0.63
565	15.[illegible]1	15.11	9.9	.97	1.75	99.0	369.60	348.55	123.3	0.59	282.80	4.88	2.25	2.47	1.31	2.12	0.63
566	2.[illegible]4	2.12	1.2	1.33	1.[illegible]	102.	373.03	321.72	412.8	3.97	282.53	2.45	2.86	4.93	1.47	2.45	5.35
567	2.[illegible]4	2.12	1.2	1.33	1.73	102.3	373.03	336.90	321.6	1.98	282.63	3.82	2.39	5.01	1.47	2.45	5.35
568	2.[illegible]4	2.12	1.2	1.33	1.[illegible]4	102.	373.03	361.69	153.9	0.59	282.85	6.09	2.16	3.09	1.47	2.45	5.35
569	4.19	4.29	2.65	.71	1.[illegible]5	102.	372.56	314.55	320.3	3.97	282.55	1.90	3.31	4.62	1.44	2.40	2.57
570	4.19	4.29	2.65	.71	1.[illegible]5	102.	372.56	328.71	251.8	1.98	282.60	3.34	2.50	4.86	1.44	2.40	2.57

Table 6.10 (continued)

Run No.	$W_{\infty 1}$ (%)	$W_{\infty 2}$ (%)	$\tilde{W}_{\infty 1}$ (%)	$\tilde{W}_{\infty 2}$ (%)	U_∞ (m/s)	P_∞ (Pa)	T_∞ (K)	T_w (K)	$\dot{Q}''_{obs}$ (kW/m^2)	U_{ow} (m/s)	T_{in} (K)	ΔT_{ow} (K)	error estimates: $\frac{\delta \dot{Q}''_{obs}}{\dot{Q}''_{obs}}$ (%)	σ_{Tw} (K)	$\frac{\delta U_\infty}{U_\infty}$ (%)	$\frac{\delta W_{\infty 1}}{W_{\infty 1}}$ (%)	$\frac{\delta W_{\infty 2}}{W_{\infty 2}}$ (%)
571	4.19	4.29	2.65	2.71	1.05	102.0	372.56	358.57	142.1	0.59	282.78	5.62	2.19	3.26	1.44	2.40	2.57
572	6.62	6.65	4.22	4.24	1.07	101.3	371.93	309.02	269.8	3.97	282.53	1.60	3.71	4.04	1.41	2.33	1.61
573	6.62	6.65	4.22	4.24	1.07	101.3	371.93	322.40	250.4	1.98	282.60	2.97	2.61	3.82	1.41	2.33	1.61
574	6.61	6.65	4.22	4.24	1.07	101.3	371.93	354.41	140.9	0.59	282.75	5.57	2.19	3.32	1.41	2.33	1.61
575	9.65	9.51	6.23	6.14	1.10	100.3	371.09	303.98	240.4	3.97	282.53	1.43	4.04	3.35	1.37	2.26	1.08
576	9.65	9.51	6.23	6.14	1.10	100.3	371.09	316.38	218.9	1.98	282.60	2.60	2.78	3.70	1.37	2.26	1.08
577	9.44	9.51	6.2	6.14	1.1	100.3	371.09	350.48	132.1	0.59	282.83	5.23	2.22	3.22	1.37	2.26	1.08
578	13.14	13.18	8.6	8.63	1.12	99.8	370.21	300.80	198.3	3.97	282.53	1.18	4.70	2.94	1.33	2.17	0.74
579	13.14	13.18	8.6	8.63	1.12	99.8	370.21	311.62	187.4	1.98	282.58	2.22	3.01	3.11	1.33	2.17	0.74
580	13.14	13.18	8.6	8.63	1.12	99.8	370.21	346.19	122.7	0.59	282.80	4.86	2.25	2.74	1.33	2.17	0.74
581	17.11	16.99	11.39	11.29	1.16	98.8	369.12	298.12	168.8	3.97	282.50	1.00	5.38	2.53	1.29	2.07	0.55
582	17.11	16.99	11.38	11.29	1.16	98.6	369.12	307.88	311.1	1.98	282.60	3.69	2.42	2.96	1.29	2.07	0.55
583	17.10	16.99	11.37	11.29	1.16	98.6	369.12	342.14	113.3	0.59	282.83	4.48	2.29	2.67	1.29	2.07	0.55
584	21.43	21.47	14.5	14.53	1.21	98.1	367.94	296.31	143.5	3.97	282.50	0.85	6.21	2.31	1.25	1.96	0.41
585	21.44	21.47	14.51	14.53	1.2	98.1	367.94	305.10	141.2	1.98	282.60	1.67	3.59	2.59	1.25	1.96	0.41
586	21.43	21.47	14.51	14.53	1.2	98.1	367.94	336.15	105.2	0.59	282.83	4.16	2.33	2.52	1.25	1.96	0.41

Table 6.11 Vapour-gas mixtures results

mixture steam-air

tube diameter 12.5 mm

Run No.	$W_{\infty 1}$ %	$W_{\infty 2}$ %	$\tilde{W}_{\infty 1}$ %	$\tilde{W}_{\infty 2}$ %	U_∞ m/s	P_∞ Pa	T_∞ K	T_w K	$\dot{Q}''_{obs}$ kW/m²	U_{ow} m/s	T_{in} K	ΔT_{ow} K	error estimates: $\delta\dot{Q}''_{obs}/\dot{Q}''_{obs}$ %	σ_{Tw} K	$\delta U_\infty/U_\infty$ %	$\delta W_{\infty 1}/W_{\infty 1}$ %	$\delta W_{\infty 2}/W_{\infty 2}$ %
587	0.53	1.95	[illegible]	1.22	25.18	4.3	303.29	296.62	115.3	3.98	279.87	0.68	7.63	2.55	1.50	2.50	26.38
588	0.74	1.96	0.46	1.23	20.72	5.6	307.82	299.31	132.4	3.98	279.87	0.78	6.72	2.71	1.49	2.48	20.95
589	0.93	2.16	0.5	1.36	18.78	6.1	309.33	300.26	145.1	3.98	279.89	0.86	6.18	3.00	1.49	2.48	17.65
590	1.14	2.41	0.71	1.51	17.58	6.6	310.68	301.18	149.4	3.98	279.92	0.88	6.02	3.12	1.48	2.47	14.85
591	1.43	2.61	[illegible]	1.64	16.01	7.3	312.65	302.37	153.6	3.98	279.94	0.91	5.87	3.26	1.48	2.46	12.55
592	1.72	2.72	[illegible]	1.71	14.52	8.2	314.74	303.51	157.9	3.98	279.92	0.93	5.73	3.38	1.47	2.46	11.05
593	2.47	3.47	1.55	2.19	[illegible]	10.1	318.72	305.25	175.0	3.98	279.89	1.03	5.25	3.76	1.46	2.44	7.37
594	3.52	3.96	2.22	2.50	[illegible]	13.8	324.84	307.03	204.8	3.98	279.92	1.21	4.60	4.22	1.45	2.41	5.29
595	4.73	5.33	[illegible]	[illegible]	7.21	18.4	330.67	307.76	209.0	3.98	279.94	1.23	4.53	4.52	1.43	2.38	3.35
596	[illegible]	6.42	[illegible]	4.10	5.92	[illegible]	335.52	307.80	217.5	3.98	279.94	1.28	4.38	4.97	1.42	2.35	2.46
597	0.27	2.55	0.17	[illegible]	[illegible]	3.7	300.60	294.13	102.5	3.98	279.92	0.60	8.52	1.93	1.50	2.49	22.89
598	0.78	2.49	[illegible]	1.56	[illegible]	3.8	301.09	294.47	106.7	3.98	279.89	0.63	8.20	1.98	1.49	2.49	22.87
599	0.60	2.81	0.37	1.76	13.97	4.0	302.04	294.95	111.0	3.98	279.89	0.65	7.90	2.08	1.49	2.49	19.19
600	0.85	2.92	0.53	1.84	[illegible]	4.3	303.13	295.52	115.3	3.98	279.89	0.68	7.63	2.12	1.49	2.48	17.38
601	1.14	2.91	0.71	1.83	[illegible]	4.6	304.27	296.28	119.5	3.98	279.89	0.70	7.38	2.25	1.48	2.47	16.44
602	1.46	2.96	0.91	1.86	11.71	5.0	305.59	296.83	123.8	3.98	279.89	0.73	7.14	2.36	1.48	2.46	15.14
603	1.76	3.34	[illegible]	2.10	[illegible]	5.4	306.92	297.40	128.1	3.98	279.89	0.75	6.92	2.41	1.47	2.46	12.50
604	2.17	3.17	1.36	2.00	10.17	5.9	308.69	297.90	132.4	3.98	279.87	0.78	6.72	2.56	1.47	2.45	12.15
605	[illegible]	3.66	[illegible]	2.31	8.97	6.7	311.05	298.59	136.6	3.98	279.87	0.80	6.53	2.71	1.46	2.43	9.39
606	3.28	4.03	2.07	2.55	8.14	7.5	313.06	299.47	140.9	3.98	279.87	0.83	6.35	2.91	1.45	2.42	7.77
607	4.66	[illegible]	2.95	3.19	6.73	9.4	317.18	300.26	149.4	3.99	279.84	0.88	6.02	3.22	1.43	2.38	5.22
608	[illegible]	7.04	4.17	[illegible]	[illegible]	12.5	322.41	298.27	158.0	3.99	279.84	0.93	5.73	3.19	1.41	2.34	3.02
609	[illegible]	3.74	[illegible]	[illegible]	[illegible]	12.4	322.85	307.35	187.7	3.98	279.94	1.11	4.94	4.07	1.46	2.43	5.96
610	[illegible]	4.50	2.5	[illegible]	[illegible]	16.1	327.99	308.18	209.1	3.98	279.92	1.23	4.53	4.42	1.44	2.40	4.24
611	4.48	[illegible]	2.87	3.16	[illegible]	17.9	[illegible]	307.55	213.3	3.98	279.94	1.26	4.45	4.46	1.44	2.39	3.59
612	[illegible]	5.69	[illegible]	[illegible]	6.67	[illegible]	[illegible]	[illegible]	217.5	3.98	279.94	1.26	4.38	4.80	1.43	2.37	2.93
613	[illegible]	6.57	[illegible]	4.76	5.69	25.3	337.47	307.85	221.5	3.98	279.94	1.31	4.32	4.80	1.41	2.34	2.28
614	[illegible]	7.11	4.61	4.54	5.17	28.7	[illegible]	307.82	226.1	3.98	279.92	1.33	4.25	4.98	1.40	2.32	2.04
615	8.49	8.71	[illegible]	[illegible]	4.47	32.8	343.71	307.26	221.8	3.98	279.94	1.31	4.32	5.06	1.38	2.29	1.54
616	[illegible]	1.42	0.77	[illegible]	[illegible]	[illegible]	342.69	325.12	245.1	2.35	281.07	2.45	2.85	4.03	1.48	2.47	10.74
617	1.77	[illegible]	1.11	1.74	4.17	34.9	345.46	326.66	246.7	2.39	281.10	2.43	2.87	4.37	1.47	2.46	7.37

Table 6.11 (continued)

Run No.	$W_{\infty 1}$	$W_{\infty 2}$	$\tilde{W}_{\infty 1}$	$\tilde{W}_{\infty 2}$	U_∞	P_∞	T_e	T_w	$\dot{Q}''_{obs}$	U_{ow}	T_{in}	ΔT_{ow}	error estimates: $\frac{\delta \dot{Q}''_{obs}}{\dot{Q}''_{obs}}$	σ_{Tw}	$\frac{\delta U_\infty}{U_\infty}$	$\frac{\delta W_{\infty 1}}{W_{\infty 1}}$	$\frac{\delta W_{\infty 2}}{W_{\infty 2}}$
	%	%	%	%	m/s	Pa	K	K	kW/m^2	m/s	K	K	%	K	%	%	%
618	2.26	2.56	1.41	1.61	4.46	32.3	343.61	324.72	231.5	2.39	281.05	2.28	2.97	4.36	1.47	2.44	5.80
619	[illegible]	3.42	1.95	2.15	4.47	32.4	343.51	323.35	223.9	2.39	281.05	2.20	3.02	4.45	1.45	2.42	4.29
620	[illegible]	[illegible]	2.4	2.55	3.80	39.3	347.96	324.66	226.4	2.39	281.07	2.23	3.00	4.63	1.44	2.40	3.40
621	4.52	4.78	2.84	3.03	3.97	38.3	347.28	323.96	221.3	2.39	281.05	2.18	3.04	4.66	1.43	2.39	2.86
622	5.38	5.42	[illegible]	3.45	[illegible]	37.3	346.50	320.54	223.9	2.39	281.02	2.20	3.02	4.52	1.42	2.37	2.52
623	6.47	6.73	[illegible]	4.29	4.19	35.5	345.15	317.83	218.8	2.39	281.02	2.15	3.06	4.42	1.41	2.34	2.03
624	7.38	7.58	4.72	4.85	4.57	32.2	342.74	316.54	201.1	2.39	281.02	1.98	3.22	4.48	1.40	2.32	1.83
625	6.52	8.48	5.48	5.45	4.25	35.5	344.90	315.72	201.1	2.39	281.02	1.98	3.22	4.37	1.38	2.29	1.57
626	[illegible]	3.38	0.79	2.13	[illegible]	4.6	304.33	301.95	47.5	0.80	281.17	1.40	4.08	0.72	1.48	2.47	14.02
627	2.38	3.51	1.49	2.21	9.76	6.4	309.99	306.61	58.5	0.80	281.20	1.73	3.52	0.92	1.47	2.44	10.29
628	3.75	4.46	2.36	2.82	7.21	8.6	315.52	310.48	68.7	0.80	281.20	2.03	3.17	1.35	1.45	2.41	6.33
629	4.55	5.48	2.86	3.48	6.53	9.6	317.55	312.14	71.2	0.80	281.20	2.10	3.11	1.32	1.43	2.39	4.69
630	5.81	6.74	3.69	4.30	5.64	11.4	320.75	314.03	75.4	0.80	281.20	2.23	3.01	1.43	1.42	2.35	3.34
631	1.33	1.84	0.83	1.15	2.30	27.6	340.12	319.04	231.3	2.78	281.37	1.95	3.25	3.74	1.48	2.47	8.58
632	2.51	2.84	1.57	1.78	2.37	27.1	339.55	316.63	216.5	2.78	281.35	1.83	3.39	3.70	1.46	2.44	5.52
633	3.55	4.25	2.24	2.69	2.76	27.6	339.72	315.23	204.6	2.78	281.37	1.77	3.52	3.75	1.45	2.41	3.59
634	4.89	5.42	3.11	3.44	2.37	27.9	339.62	311.72	184.0	2.78	281.30	1.55	3.79	3.95	1.43	2.38	2.76
635	6.42	6.65	4.09	4.25	2.25	28.7	340.24	311.00	178.0	2.78	281.30	1.50	3.88	3.91	1.41	2.34	2.19
636	7.12	7.64	4.55	4.89	2.73	28.5	339.98	310.69	175.1	2.78	281.32	1.48	3.93	3.93	1.40	2.32	1.89
637	[illegible]	[illegible]	5.59	5.83	2.41	28.7	339.91	306.97	163.1	2.78	281.42	1.38	4.14	3.60	1.38	2.28	1.56
638	[illegible]	10.51	6.64	6.87	[illegible]	29.4	340.18	305.26	154.4	2.78	281.27	1.30	4.33	3.42	1.36	2.24	1.29
639	[illegible]	2.14	[illegible]	1.34	1.15	33.8	344.74	314.74	228.2	2.57	284.38	2.09	3.12	2.02	1.47	2.45	6.86
640	3.53	[illegible]	[illegible]	2.32	1.21	32.9	343.69	311.30	184.8	2.57	284.38	1.69	3.57	2.16	1.44	2.40	3.95
641	5.45	[illegible]	3.46	3.51	1.21	33.9	344.25	308.83	171.3	2.57	284.38	1.57	3.76	2.26	1.42	2.36	2.54
642	7.45	7.65	4.77	4.9	1.17	35.9	[illegible]	305.50	152.3	2.57	284.35	1.39	4.10	2.20	1.40	2.31	1.75
643	[illegible]	9.74	6.06	6.29	1.16	37.3	345.82	332.47	141.4	2.57	284.35	[illegible]	4.35	1.88	1.37	2.27	1.32
644	5.25	5.76	[illegible]	.79	[illegible]	20.1	332.47	307.49	141.1	2.61	284.00	1.27	4.41	1.84	1.43	2.37	2.83
645	7.27	7.29	4.65	4.66	1.98	18.6	330.68	304.98	124.5	2.61	284.00	1.12	4.88	1.86	1.40	2.32	2.35
646	[illegible]	10.51	[illegible]	6.81	[illegible]	18.9	330.49	301.38	113.4	2.61	[illegible]	1.07	5.28	1.79	1.36	2.25	1.55
647	11.54	11.99	[illegible]	7.61	2.21	16.7	330.05	299.03	110.7	2.61	283.98	1.00	5.40	1.67	1.35	2.21	1.33
648	[illegible]	[illegible]	[illegible]	[illegible]	[illegible]	21.2	332.47	298.03	105.2	2.61	283.98	0.95	5.64	1.56	1.33	2.17	1.06
649	[illegible]	15.72	[illegible]	[illegible]	1.74	[illegible]	335.04	298.74	99.6	2.61	283.98	[illegible]	5.92	1.70	1.31	2.12	0.85

Table 6.11 (continued)

Run No.	$W_{\omega 1}$ %	$W_{\omega 2}$ %	$\tilde{W}_{\omega 1}$ %	$\tilde{W}_{\omega 2}$ %	U_∞ m/s	P_∞ Pa	T_∞ K	T_w K	$\dot{Q}''_{obs}$ kW/m^2	U_{ow} m/s	T_{in} K	ΔT_{ow} K	$\frac{\delta \dot{Q}''_{obs}}{\dot{Q}''_{obs}}$ %	σ_{Tw} K	$\frac{\delta U_\infty}{U_\infty}$ %	$\frac{\delta W_{\omega 1}}{W_{\omega 1}}$ %	$\frac{\delta W_{\omega 2}}{W_{\omega 2}}$ %
650	0.80	2.46	0.5	1.55	19.64	5.7	308.28	301.69	116.3	3.94	286.29	0.70	7.46	1.96	1.49	2.48	16.18
651	1.46	[illegible]	0.94	1.45	14.58	7.9	[illegible]	304.98	137.0	3.94	286.32	0.82	6.42	2.37	1.48	2.46	13.08
652	2.11	2.64	1.3	1.66	11.56	10.6	319.78	307.71	161.9	3.94	286.29	0.97	5.54	2.75	1.47	2.45	9.48
653	2.96	3.51	1.86	2.21	9.77	12.9	323.58	308.36	186.8	3.94	286.29	1.17	4.90	2.97	1.46	2.43	6.23
654	3.54	[illegible]	[illegible]	1.66	8.47	15.3	327.04	310.09	203.4	3.94	286.29	1.22	4.57	3.24	1.45	2.41	4.68
655	4.42	4.46	2.8	2.82	7.74	18.3	330.69	310.76	207.5	3.94	286.29	1.24	4.50	3.40	1.44	2.39	4.03
656	5.26	5.68	3.34	3.74	6.22	21.8	334.24	310.54	207.5	3.94	286.29	1.24	4.50	3.53	1.43	2.37	2.78
657	5.87	6.39	3.77	4.07	5.65	24.3	336.61	310.60	207.5	3.94	286.27	1.24	4.50	3.69	1.42	2.35	2.43
658	7.18	7.32	4.66	4.68	4.78	30.0	341.14	308.68	215.8	3.94	286.27	1.29	4.36	3.53	1.40	2.32	1.95
659	8.64	8.65	5.56	5.56	4.16	36.4	345.40	309.31	220.0	3.94	286.24	1.32	4.30	3.64	1.38	2.28	1.52
660	8.66	8.65	5.57	5.56	[illegible]	36.4	345.40	316.18	202.3	2.40	286.32	1.98	3.22	3.77	1.38	2.28	1.52
661	8.66	8.65	5.57	5.56	[illegible]	36.4	345.40	331.87	128.2	0.79	286.49	3.84	2.39	2.34	1.38	2.28	1.52
662	7.22	7.58	4.61	4.85	4.49	32.0	342.61	330.25	129.8	0.79	286.49	3.88	2.38	2.27	1.40	2.32	1.83
663	7.22	7.58	[illegible]	4.85	4.49	32.0	342.61	317.82	199.0	2.36	286.29	1.98	3.22	3.73	1.40	2.32	1.83
664	5.55	5.97	[illegible]	3.80	[illegible]	26.4	338.51	318.02	191.6	2.36	286.27	1.91	3.29	3.49	1.42	2.36	2.54
665	5.55	5.97	[illegible]	[illegible]	5.25	26.4	338.51	329.30	115.8	0.79	286.47	3.47	2.47	2.06	1.42	2.36	2.54
666	4.58	4.74	2.9	3.00	6.15	22.0	334.59	327.19	110.0	0.79	286.49	3.29	2.51	1.84	1.43	2.39	3.49
667	4.57	4.74	2.89	[illegible]	6.17	[illegible]	334.59	316.08	194.1	2.36	286.29	1.93	3.27	3.21	1.43	2.39	3.49
668	4.69	4.5	2.97	[illegible]	[illegible]	21.1	333.71	316.72	181.6	2.36	286.29	1.81	3.41	3.16	1.43	2.38	3.67
669	4.69	[illegible]	2.97	[illegible]	6.41	21.1	333.71	326.14	105.9	0.79	286.42	3.17	2.55	1.65	1.43	2.38	3.67
670	3.43	3.95	[illegible]	[illegible]	7.69	16.9	[illegible]	[illegible]	99.3	0.79	286.47	2.97	2.61	1.55	1.45	2.41	4.76
671	3.43	3.95	[illegible]	[illegible]	[illegible]	16.9	329.10	315.40	174.2	2.36	286.24	1.74	3.51	2.93	1.45	2.41	4.76
672	0.96	2.67	[illegible]	1.65	15.51	4.9	305.41	299.14	108.0	3.94	286.14	0.65	8.00	1.54	1.49	2.48	17.05
673	0.96	2.67	[illegible]	1.68	[illegible]	4.9	305.41	300.87	82.2	2.36	286.19	0.82	6.42	1.28	1.49	2.48	17.05
674	0.96	2.67	[illegible]	1.66	15.51	4.9	305.41	303.61	41.5	0.79	286.24	1.24	4.50	0.65	1.49	2.48	17.05
675	[illegible]	2.71	[illegible]	[illegible]	[illegible]	7.5	313.19	309.97	61.4	0.79	286.39	1.83	3.38	0.89	1.47	2.45	11.81
676	[illegible]	[illegible]	[illegible]	[illegible]	[illegible]	7.5	313.19	305.70	114.6	2.36	286.24	1.14	4.81	1.77	1.47	2.45	11.81
677	[illegible]	2.71	[illegible]	1.7	[illegible]	7.5	313.19	303.12	141.2	3.94	286.17	0.84	6.25	2.05	1.47	2.45	11.81
678	[illegible]	3.90	[illegible]	[illegible]	[illegible]	10.6	319.68	315.27	157.8	3.94	286.17	0.94	5.66	2.45	1.45	2.41	6.30
679	[illegible]	[illegible]	[illegible]	[illegible]	7.91	10.6	319.68	308.98	[illegible]	2.36	286.19	1.32	4.30	2.13	1.45	2.41	6.30
[illegible]	[illegible]	[illegible]	[illegible]	[illegible]	[illegible]	10.6	319.68	314.99	71.3	0.79	[illegible]	2.13	3.08	1.21	1.45	2.41	6.30
681	[illegible]	[illegible]	[illegible]	[illegible]	[illegible]	[illegible]	[illegible]	316.85	78.7	0.79	[illegible]	2.35	2.97	1.23	1.44	2.40	4.76

Run No.	$W_{\infty 1}$	$W_{\infty 2}$	$\tilde{W}_{\infty 1}$	$\tilde{W}_{\infty 2}$	U_∞	P_∞	T_e	T_w	$\dot{Q}''_{obs}$	U_{ow}	T_{in}	ΔT_{ow}	$\delta \dot{Q}''_{obs} / \dot{Q}''_{obs}$	σ_{Tw}	$\delta U_\infty / U_\infty$	$\delta W_{\infty 1} / W_{\infty 1}$	$\delta W_{\infty 2} / W_{\infty 2}$
	%	%	%	%	m/s	Pa	K	K	kW/m^2	m/s	K	K	%	K	%	%	%
682	4.13	4.67	2.61	2.96	[illegible]	12.2	322.35	309.82	137.0	2.36	286.19	1.37	4.17	2.48	1.44	2.40	4.76
683	[illegible]	4.67	2.61	[illegible]	[illegible]	12.2	322.35	[illegible]	174.4	3.94	286.14	1.04	5.20	2.41	1.44	2.40	4.76
684	5.55	[illegible]	[illegible]	[illegible]	5.74	15.5	326.95	[illegible]	178.6	3.94	286.12	1.07	5.09	2.75	1.42	2.36	3.17
685	5.56	6.02	[illegible]	[illegible]	5.74	15.5	326.95	310.76	[illegible]	2.36	[illegible]	1.49	3.91	2.64	1.42	2.36	3.17
686	5.56	[illegible]	[illegible]	[illegible]	[illegible]	15.5	326.95	319.69	87.0	0.79	[illegible]	2.60	2.77	1.50	1.42	2.36	3.17
687	5.90	6.16	3.76	[illegible]	[illegible]	[illegible]	328.61	320.61	89.5	0.79	286.39	2.68	2.74	1.59	1.42	2.35	2.97
688	5.90	6.16	3.76	[illegible]	[illegible]	16.8	328.61	[illegible]	161.6	2.36	[illegible]	1.61	3.69	2.71	1.42	2.35	2.97
689	5.91	6.16	3.76	[illegible]	[illegible]	16.8	328.61	306.30	174.4	3.94	286.14	1.04	5.20	2.85	1.42	2.35	2.97
690	7.59	8.04	4.86	5.16	4.42	[illegible]	333.17	304.37	191.0	3.94	286.14	1.14	4.81	2.81	1.39	2.31	2.00
691	7.59	[illegible]	4.86	5.16	[illegible]	21.0	333.17	311.68	151.9	2.36	286.17	1.51	3.86	2.95	1.39	2.31	2.00
692	[illegible]	8.04	4.86	5.16	4.41	[illegible]	333.17	322.89	96.6	0.79	286.22	2.95	2.62	1.81	1.39	2.31	2.00
693	8.40	8.88	[illegible]	5.72	[illegible]	23.4	335.35	322.37	111.8	0.79	286.32	3.34	2.50	1.97	1.38	2.29	1.71
694	8.41	8.88	[illegible]	5.72	4.04	23.4	335.35	311.69	159.4	2.36	[illegible]	1.59	3.73	2.90	1.38	2.29	1.71
695	8.41	8.88	[illegible]	5.72	[illegible]	23.4	335.35	304.47	182.8	3.94	286.12	1.09	4.99	2.89	1.38	2.29	1.71
696	[illegible]	10.79	6.98	7.00	[illegible]	29.4	340.16	303.66	178.6	3.94	286.09	1.07	5.09	2.81	1.36	2.23	1.26
697	10.77	10.79	6.99	7.00	[illegible]	29.4	340.16	310.42	156.9	2.36	286.14	1.56	3.77	2.84	1.36	2.23	1.26
698	10.77	10.79	6.99	[illegible]	3.35	29.4	[illegible]	324.75	107.7	0.79	286.29	3.22	2.53	1.93	1.36	2.23	1.26
699	12.40	12.62	8.1	8.24	2.87	35.4	344.11	323.00	120.0	0.79	286.34	3.59	2.44	2.15	1.34	2.19	0.99
700	12.41	12.62	[illegible]	8.24	2.87	35.4	344.11	309.88	149.4	2.36	286.17	1.49	3.91	2.97	1.34	2.19	0.99
701	12.42	12.62	8.1	8.24	2.87	35.4	344.11	302.87	162.0	3.94	286.09	0.97	5.54	2.69	1.34	2.19	0.99
702	[illegible]	5.18	[illegible]	[illegible]	[illegible]	5.	[illegible]	296.31	67.3	3.94	286.19	0.52	9.79	1.25	1.45	2.42	8.27
703	3.74	5.18	[illegible]	[illegible]	5.13	[illegible]	305.60	298.43	77.3	2.36	286.22	0.77	6.80	1.07	1.45	2.42	8.27
704	[illegible]	5.18	[illegible]	[illegible]	5.13	[illegible]	305.60	302.37	41.5	0.79	286.24	1.24	4.50	0.66	1.45	2.42	8.27
705	[illegible]	9.51	5.35	[illegible]	[illegible]	[illegible]	312.48	305.28	52.3	0.79	286.37	1.56	3.77	1.01	1.39	2.29	3.03
706	[illegible]	9.51	[illegible]	6.13	3.65	7.6	312.48	299.16	74.8	2.36	286.24	0.74	7.00	1.36	1.39	2.29	3.03
707	[illegible]	9.51	5.35	6.13	3.65	7.6	312.48	296.23	87.2	3.94	286.22	0.52	9.79	1.28	1.39	2.29	3.03
708	9.19	9.94	5.9	[illegible]	[illegible]	[illegible]	317.91	[illegible]	91.4	3.94	286.22	0.55	9.37	1.46	1.37	2.27	2.34
709	[illegible]	9.94	[illegible]	6.43	[illegible]	[illegible]	317.91	296.43	87.2	2.36	286.22	0.87	6.09	1.40	1.37	2.27	2.34
710	[illegible]	9.94	[illegible]	[illegible]	[illegible]	[illegible]	317.91	307.69	53.0	0.79	286.24	1.89	3.32	1.09	1.37	2.27	2.34
711	12.56	[illegible]	6.2	[illegible]	[illegible]	[illegible]	321.21	307.07	63.8	0.79	286.34	1.91	[illegible]	1.32	1.34	2.19	1.51
712	12.56	[illegible]	6.2	[illegible]	[illegible]	[illegible]	321.21	298.58	79.7	2.36	286.24	0.79	6.60	1.63	1.34	2.19	1.51
713	12.56	[illegible]	6.2	[illegible]	[illegible]	[illegible]	321.21	[illegible]	[illegible]	3.94	286.19	0.52	9.79	1.44	1.34	2.19	1.51

Table 6.11 (continued)

Run No.	$W_{\infty 1}$ %	$W_{\infty 2}$ %	$\tilde{W}_{\infty 1}$ %	$\tilde{W}_{\infty 2}$ %	U_∞ m/s	P_∞ Pa	T_∞ K	T_w K	$\dot{Q}''_{obs}$ kW/m^2	U_{ow} m/s	T_{in} K	ΔT_{ow} K	error estimates: $\frac{\delta \dot{Q}''_{obs}}{\dot{Q}''_{obs}}$ %	σ_{Tw} K	$\frac{\delta U_\infty}{U_\infty}$ %	$\frac{\delta W_{\infty 1}}{W_{\infty 1}}$ %	$\frac{\delta W_{\infty 2}}{W_{\infty 2}}$ %
714	14.77	14.85	9.73	9.79	2.04	15.0	325.03	294.72	83.1	3.94	286.19	0.50	10.26	1.48	1.31	2.13	1.15
715	14.77	14.85	9.73	9.79	2.04	15.0	325.03	297.52	79.7	2.36	286.22	0.79	6.60	1.36	1.31	2.13	1.15
716	14.77	14.85	9.73	9.79	2.04	15.0	325.03	308.40	63.5	0.79	286.24	1.89	3.32	1.29	1.31	2.13	1.15
717	17.63	17.53	11.75	11.68	1.78	17.8	328.08	306.87	63.9	0.79	286.32	1.91	3.29	1.26	1.28	2.06	0.86
718	17.63	17.53	11.75	11.68	1.78	17.8	328.08	297.44	74.8	2.36	286.22	0.74	7.00	1.44	1.28	2.06	0.86
719	17.63	17.53	11.75	11.68	1.78	17.8	328.08	293.48	79.0	3.94	286.17	0.47	10.78	1.20	1.28	2.06	0.86
720	21.93	21.78	14.87	14.77	1.72	19.2	328.92	291.45	70.7	3.94	286.14	0.42	12.01	0.92	1.25	1.95	0.62
721	21.93	21.78	14.87	14.77	1.72	19.2	328.92	294.91	64.8	2.36	286.17	0.65	8.00	1.17	1.25	1.95	0.62
722	21.93	21.78	14.87	14.77	1.72	19.2	328.92	303.09	55.6	0.79	286.29	1.66	3.61	1.09	1.25	1.95	0.62
723	24.23	24.30	16.59	16.64	1.38	24.8	333.91	305.04	58.1	0.79	286.29	1.74	3.51	1.19	1.24	1.89	0.49
724	24.23	24.30	16.59	16.64	1.38	24.8	333.91	295.63	62.3	2.36	286.22	0.62	8.30	1.17	1.24	1.89	0.49
725	24.22	24.30	16.59	16.64	1.38	24.8	333.91	293.15	62.3	3.94	286.17	0.37	13.57	1.19	1.24	1.89	0.49
726	29.22	29.13	20.45	20.28	1.21	29.9	337.08	291.70	58.2	3.94	286.14	0.35	14.51	0.94	1.21	1.77	0.35
727	29.22	29.13	20.4	20.28	1.21	29.9	337.08	293.69	57.4	2.36	286.14	0.57	8.98	1.98	1.21	1.77	0.35
728	29.22	29.13	20.4	20.28	1.21	29.9	337.08	303.68	49.8	0.79	286.22	1.49	3.91	1.12	1.21	1.77	0.35
729	31.59	31.59	22.32	22.31	1.11	33.7	339.16	303.17	50.6	0.79	286.29	1.51	3.86	1.02	1.21	1.71	0.30
730	31.59	1.59	22.3	22.31	1.11	33.7	339.16	293.81	54.8	2.36	286.19	0.55	9.37	0.92	1.21	1.71	0.30
731	31.59	31.59	22.31	22.31	1.11	33.7	339.16	291.44	54.0	3.94	286.14	0.32	15.61	0.87	1.21	1.71	0.30

Table 6.12 [illegible]

mixture steam
tube diameter 25.25 mm

Run No.	$W_{\infty 1}$ %	$W_{\infty 2}$ %	$\tilde{W}_{\infty 1}$ %	$\tilde{W}_{\infty 2}$ %	U_∞ m/s	P_∞ Pa	T_∞ K	T_w K	$\dot{Q}''_{obs}$ kW/m^2	U_{ow} m/s	T_{in} K	ΔT_{ow} K	$\frac{\delta \dot{Q}''_{obs}}{\dot{Q}''_{obs}}$ %	σ_{Tw} K	$\frac{\delta U_\infty}{U_\infty}$ %	$\frac{\delta W_{\infty 1}}{W_{\infty 1}}$ %	$\frac{\delta W_{\infty 2}}{W_{\infty 2}}$ %
													error estimates				
732	1.27	1.65	.79	1.04	0.81	101.1	372.78	323.16	302.4	3.61	286.72	0.55	9.38	5.50	1.48	2.47	6.91
733	1.27	1.65	0.79	1.04	.81	101.1	372.78	353.30	161.0	0.90	287.29	1.16	4.74	2.74	1.48	2.47	6.91
734	2.54	2.99	1.6	1.88	0.82	100.9	372.53	317.55	261.1	3.61	286.74	0.47	10.79	6.12	1.46	2.44	3.75
735	2.54	2.99	1.6	1.88	0.82	100.9	372.53	351.81	151.7	0.90	287.31	1.09	5.00	3.72	1.46	2.44	3.75
736	3.86	4.34	2.44	2.75	0.82	100.6	372.18	312.26	219.9	3.61	286.74	0.40	12.75	5.73	1.44	2.40	2.54
737	3.86	4.34	2.44	2.75	0.82	100.6	372.18	345.01	150.8	0.90	287.11	1.09	5.00	4.46	1.44	2.40	2.54
738	5.22	5.64	3.32	1.58	0.83	100.3	371.83	308.59	192.5	3.61	286.74	0.35	14.53	5.70	1.43	2.37	1.93
739	5.22	5.64	3.32	.58	0.83	100.3	371.83	342.52	137.2	0.90	286.99	0.99	5.42	4.83	1.43	2.37	1.93
740	8.30	8.79	5.33	5.65	0.85	99.7	371.08	304.07	151.2	3.61	286.74	0.27	18.42	4.89	1.39	2.29	1.19
741	8.30	8.79	5.33	5.65	0.85	99.7	371.08	336.89	120.1	0.90	286.96	0.87	6.10	4.68	1.39	2.29	1.19
742	11.99	12.38	7.81	8.08	0.87	99.0	370.18	300.68	123.7	3.61	286.74	0.22	22.47	4.43	1.34	2.20	0.80
743	11.99	12.38	7.81	8.08	0.87	99.0	370.18	330.96	106.4	0.90	286.94	0.77	6.81	4.48	1.34	2.20	0.80
744	0.69	1.03	0.56	.64	1.16	100.9	372.86	328.34	343.6	3.61	286.74	0.62	8.31	5.07	1.49	2.48	11.22
745	0.69	1.03	0.56	.64	1.16	100.9	372.86	353.37	198.9	0.90	286.96	1.44	4.01	2.74	1.49	2.48	11.22
746	1.79	2.26	1.14	1.42	1.16	100.9	372.65	324.78	302.4	3.61	286.74	0.55	9.38	5.12	1.47	2.46	5.03
747	1.79	2.26	1.14	1.42	1.16	100.9	372.65	351.66	181.7	0.90	286.99	1.31	4.30	3.35	1.47	2.46	5.03
748	2.73	3.23	1.7	2.04	1.17	100.8	372.43	319.04	261.1	3.61	286.74	0.47	10.79	6.57	1.46	2.43	3.46
749	2.73	3.23	1.72	2.04	1.17	100.8	372.43	348.64	171.4	0.90	287.11	1.24	4.50	4.24	1.46	2.43	3.46
750	3.72	4.23	2.34	.68	1.17	100.7	372.22	316.11	247.4	3.61	286.74	0.45	11.37	6.27	1.45	2.41	2.61
751	3.72	4.23	2.34	.68	1.17	100.7	372.22	346.83	161.1	0.90	287.19	1.16	4.74	4.19	1.45	2.41	2.61
752	5.96	6.35	3.79	4.04	1.19	100.3	371.70	310.68	219.9	3.61	286.77	0.40	12.75	6.10	1.42	2.35	1.70
753	5.96	6.35	3.79	4.04	1.19	100.3	371.70	343.76	144.1	0.90	286.94	1.04	5.20	4.83	1.42	2.35	1.70
754	8.70	8.98	5.6	5.76	1.21	99.8	371.08	306.32	178.7	3.61	286.77	0.32	15.63	5.60	1.38	2.28	1.16
755	8.70	8.98	5.6	5.78	1.21	99.8	371.08	336.78	137.2	0.90	286.94	0.99	5.42	4.61	1.38	2.28	1.16
756	0.42	0.49	.19	.30	1.66	100.9	372.94	331.90	371.0	3.61	286.74	0.67	7.73	5.17	1.49	2.48	23.78
757	0.42	0.49	.19	.31	1.66	100.9	372.94	354.63	205.6	0.90	287.11	1.49	3.91	2.87	1.49	2.48	23.78
758	1.06	1.32	0.7	.85	1.76	101.0	372.82	328.91	343.5	3.61	286.77	0.62	8.31	5.51	1.48	2.47	8.70
759	1.06	1.32	0.7	.81	1.76	101.0	372.82	353.71	195.4	0.90	287.06	1.41	4.07	3.34	1.48	2.47	8.84
760	1.94	2.32	1.2	.46	1.76	101.1	372.67	325.93	316.1	3.61	286.77	0.57	8.99	6.06	1.47	2.45	4.88
761	1.94	2.32	1.2	.46	1.76	101.1	372.67	352.57	188.5	0.90	287.11	1.36	4.18	3.29	1.47	2.45	4.88
762	2.71	3.11	1.64	.96	1.77	101.1	372.54	323.17	288.6	3.61	286.77	0.52	9.80	6.65	1.46	2.43	3.60

Table 6.12 (continued)

Run No.	$W_{\infty 1}$ %	$W_{\infty 2}$ %	$\tilde{W}_{\infty 1}$ %	$\tilde{W}_{\infty 2}$ %	U_∞ m/s	P_∞ Pa	T_∞ K	T_w K	$\dot{Q}''_{obs}$ kW/m^2	U_{ow} m/s	T_{in} K	ΔT_{ow} K	error estimates: $\delta\dot{Q}''_{obs}/\dot{Q}''_{obs}$ %	σ_{Tw} K	$\delta U_\infty/U_\infty$ %	$\delta W_{\infty 1}/W_{\infty 1}$ %	$\delta W_{\infty 2}/W_{\infty 2}$ %
763	2.61	3.11	1.64	1.96	1.67	101.1	372.54	349.22	188.6	0.90	287.[illegible]1	1.36	4.18	3.86	1.46	2.43	3.60
764	4.[illegible]2	4.69	2.6[illegible]	[illegible].97	1.6[illegible]	100.9	372.20	318.26	261.1	3.61	286.77	0.47	10.79	6.80	1.44	2.39	2.34
765	4.21	4.69	2.6[illegible]	[illegible].97	1.[illegible]9	100.9	372.20	347.88	174.7	0.90	287.26	1.26	4.43	4.09	1.44	2.39	2.34
766	6.20	6.66	3.95	4.25	1.71	100.7	371.75	313.10	233.6	3.61	286.77	0.42	12.02	6.39	1.41	2.34	1.61
767	6.2[illegible]	6.66	3.95	4.25	1.71	100.7	371.75	341.65	167.9	0.90	287.19	1.21	4.58	9.70	1.41	2.34	1.61

Table 6.13 Vapour-gas mixtures results

mixture: steam-air
tube diameter 25.25 mm

Run No.	$W_{\infty 1}$ (%)	W_{b2} (%)	$\tilde{W}_{\infty 1}$ (%)	$\tilde{W}_{\infty 2}$ (%)	U_∞ (m/s)	P_∞ (Pa)	T_∞ (K)	T_w (K)	$\dot{Q}''_{obs}$ (kW/m^2)	U_{ow} (m/s)	T_{in} (K)	ΔT_{ow} (K)	error estimates: $\delta\dot{Q}''_{obs}/\dot{Q}''_{obs}$ (%)	σ_{Tw} (K)	$\delta U_\infty/U_\infty$ (%)	$\delta W_{\infty 1}/W_{\infty 1}$ (%)	$\delta W_{\infty 2}/W_{\infty 2}$ (%)
768	1.57	2.61	0.95	1.64	9.76	6.2	309.72	302.20	81.0	3.58	291.14	0.15	33.93	2.00	1.48	2.46	14.21
769	1.57	2.61	0.96	1.64	9.[illegible]7	6.2	309.72	307.62	32.[illegible]	1.07	291.68	0.20	25.51	0.79	1.48	2.46	14.21
770	3.03	3.59	1.91	2.26	7.[illegible]	8.4	315.08	304.12	94.5	3.58	291.12	0.17	29.10	2.63	1.46	2.42	8.13
771	3.03	3.59	1.91	2.26	7.[illegible]	8.4	315.08	311.61	44.5	1.07	291.21	0.27	18.59	1.29	1.46	2.42	8.13
772	4.36	5.77	2.75	3.67	5.92	10.6	319.42	304.09	106.0	3.58	291.12	0.20	25.48	3.15	1.44	2.39	4.15
773	4.35	5.77	2.75	3.67	5.93	10.6	319.42	314.93	44.5	1.07	291.21	0.27	18.59	1.82	1.44	2.39	4.15
774	5.72	7.12	3.63	4.55	5.17	12.7	322.73	305.37	108.0	3.58	291.12	0.20	25.48	3.61	1.42	2.36	2.96
775	5.71	7.12	3.67	4.55	5.10	12.7	322.73	316.70	52.6	1.07	291.19	0.32	15.76	2.11	1.42	2.36	2.96
776	8.57	9.64	5.51	6.22	4.74	16.8	328.13	301.10	108.3	3.58	291.09	0.20	25.48	3.78	1.38	2.29	1.81
777	8.55	9.64	5.50	6.22	4.65	16.8	328.13	319.32	56.7	1.07	291.19	0.34	14.66	2.97	1.38	2.29	1.81
778	11.14	11.97	7.23	7.80	3.42	20.6	332.12	301.21	108.0	3.58	291.12	0.20	25.48	3.56	1.35	2.22	1.28
779	11.13	11.97	7.23	7.80	3.42	20.6	332.12	320.67	56.6	1.07	291.21	0.34	14.66	3.40	1.35	2.22	1.28
780	16.77	16.84	10.83	11.18	3.11	23.8	334.47	296.66	85.0	2.51	291.12	0.22	22.67	1.89	1.30	2.09	0.80
781	16.31	16.84	10.81	11.18	3.11	23.8	334.47	313.51	68.7	1.07	291.41	0.42	12.13	3.62	1.30	2.09	0.80
782	1.33	2.45	0.83	1.54	10.65	6.3	309.64	304.32	75.5	2.51	291.29	0.20	25.49	1.80	1.48	2.47	15.15
783	1.33	2.45	0.87	1.54	10.65	6.3	309.64	307.76	32.4	1.07	291.34	0.20	25.49	0.80	1.48	2.47	15.15
784	2.62	3.42	1.65	2.16	8.[illegible]1	8.6	315.65	307.22	85.0	2.51	291.31	0.22	22.68	2.51	1.46	2.43	8.36
785	2.63	3.42	1.65	2.16	8.[illegible]	8.6	315.65	312.36	44.5	1.07	291.36	0.27	18.59	1.28	1.46	2.43	8.36
786	3.76	5.2[illegible]	2.37	3.31	6.55	11.3	320.70	308.93	93.0	2.47	291.31	0.25	20.43	3.16	1.45	2.41	4.46
787	3.76	5.2[illegible]	2.37	3.30	6.55	11.3	320.70	315.62	52.6	1.07	291.34	0.32	15.77	1.76	1.45	2.41	4.46
788	5.11	6.35	3.24	4.05	5.7[illegible]	13.3	323.84	309.97	103.8	2.51	291.31	0.27	18.59	3.56	1.43	2.37	3.25
789	5.11	6.35	3.24	4.05	5.71	13.3	323.84	317.90	56.6	1.07	291.34	0.34	14.66	2.00	1.43	2.37	3.25
790	7.65	8.23	4.87	5.28	4.75	16.4	330.32	309.62	103.8	2.51	291.31	0.27	18.59	4.60	1.39	2.31	2.07
791	7.59	8.23	4.86	5.28	4.25	16.4	330.32	320.99	56.6	1.07	291.36	0.34	14.66	2.91	1.39	2.31	2.07
792	10.35	10.9	6.7	7.07	3.51	23.9	335.49	304.62	113.7	2.51	291.29	0.30	17.06	3.94	1.36	2.24	1.35
793	10.77	10.9	6.65	7.07	3.52	23.9	335.49	322.18	76.6	1.07	291.34	0.47	10.89	3.76	1.36	2.24	1.35
794	14.13	14.58	9.[illegible]	9.61	2.92	30.[illegible]	340.15	301.77	103.8	2.51	291.29	0.27	18.59	3.24	1.32	2.15	0.88
795	14.02	14.58	9.2[illegible]	9.61	2.92	30.2	340.15	317.84	80.9	1.07	291.34	0.49	10.36	4.03	1.32	2.15	0.88
796	1.07	2.51	0.67	1.57	1[illegible]	6.7	311.17	305.35	74.5	2.47	291.07	0.25	25.48	2.05	1.48	2.47	13.94
797	1.07	2.51	0.67	1.57	1[illegible].21	6.7	311.17	309.25	32.4	1.07	291.09	0.20	25.48	0.91	1.48	2.47	13.94
798	2.15	3.[illegible]	1.75	[illegible]	1[illegible].27	9.1	316.70	309.43	83.6	2.47	291.09	0.22	22.67	2.49	1.47	2.45	8.65

Table 6.13 (continued)

Run No.	$W_{\infty 1}$	$W_{\infty 2}$	$\tilde{W}_{\infty 1}$	$\tilde{W}_{\infty 2}$	U_∞	P_∞	T_∞	T_w	$\dot{Q}''_{obs}$	U_{ow}	T_{in}	ΔT_{ow}	error estimates: $\frac{\delta \dot{Q}''_{obs}}{\dot{Q}''_{obs}}$	σ_{Tw}	$\frac{\delta U_\infty}{U_\infty}$	$\frac{\delta W_{\infty 1}}{W_{\infty 1}}$	$\frac{\delta W_{\infty 2}}{W_{\infty 2}}$
	%	%	%	%	m/s	Pa	K	K	kW/m^2	m/s	K	K	%	K	%	%	%
799	2.75	3.2[illegible]	1.35	[illegible]	1[illegible].25	9.1	316.70	315.51	44.5	1.07	291.14	0.27	18.58	1.25	1.47	2.45	8.65
810	2.89	4.21	1.81	[illegible].66	8.41	11.4	320.96	310.23	103.9	2.51	291.09	0.27	18.58	3.23	1.46	2.43	5.56
8[illegible]1	2.89	4.21	1.81	2.66	8.41	11.4	32[illegible].96	316.72	52.6	1.07	291.12	0.32	15.76	1.60	1.46	2.43	5.56
802	4.68	5.64	2.97	.59	6.46	15.5	327.07	311.79	113.4	2.51	291.09	0.30	17.05	4.12	1.43	2.38	3.40
803	4.68	5.64	2.96	.59	6.47	15.5	327.07	321.00	64.8	1.07	291.14	0.39	12.86	2.16	1.43	2.38	3.40
804	5.92	6.99	3.70	4.47	5.49	18.8	330.92	312.45	122.8	2.51	291.09	0.32	15.76	4.60	1.42	2.35	2.45
805	5.92	6.99	3.77	4.47	5.49	18.8	330.92	323.24	66.6	1.07	291.12	0.42	12.12	2.66	1.42	2.35	2.45
806	8.26	8.99	5.3[illegible]	5.79	4.11	26.5	338.15	308.70	132.3	2.51	291.09	0.34	14.65	4.72	1.39	2.29	1.61
807	8.25	8.99	5.30	5.79	4.11	26.5	338.15	324.33	89.0	1.07	291.14	0.54	9.45	4.17	1.39	2.29	1.61
808	11.[illegible]8	11.67	7.19	7.59	3.38	33.8	343.19	309.66	121.1	2.47	291.09	0.32	15.76	5.15	1.35	2.22	1.11
809	11.[illegible]8	11.67	7.2[illegible]	7.59	3.38	33.8	343.19	326.89	85.0	1.07	291.14	0.52	9.88	4.43	1.35	2.22	1.11
810	[illegible].83	1.93	[illegible].5[illegible]	1.21	14.73	8.1	314.64	308.02	94.5	2.51	291.07	0.25	20.42	2.43	1.49	2.48	15.87
811	[illegible].83	1.93	0.52	1.21	14.70	8.1	314.64	312.23	40.5	1.07	291.12	0.25	20.42	1.05	1.49	2.48	15.87
812	1.81	2.51	1.1[illegible]	1.58	11.17	11.1	320.73	312.00	102.4	2.47	291.12	0.27	18.58	3.66	1.47	2.45	9.67
813	1.81	2.51	1.1[illegible]	1.58	11.18	11.1	320.73	317.18	52.6	1.07	291.12	0.32	15.76	1.49	1.47	2.45	9.67
814	2.18	2.94	1.37	1.85	10.[illegible]4	12.2	322.54	312.38	113.4	2.51	291.09	0.30	17.05	3.26	1.47	2.45	7.76
815	2.19	2.94	1.3[illegible]	1.85	10.[illegible]	12.2	322.54	318.66	56.7	1.07	291.14	0.34	14.66	1.59	1.47	2.45	7.76
816	3.24	3.89	2.[illegible]4	[illegible].46	8.[illegible]2	15.9	327.85	314.79	132.3	2.51	291.09	0.34	14.65	4.01	1.45	2.42	4.98
817	3.24	3.89	2.[illegible]4	[illegible].46	8.[illegible]	15.9	327.85	322.48	68.8	1.07	291.12	0.42	12.12	2.08	1.45	2.42	4.98
818	4.55	4.99	2.8	[illegible].16	6.[illegible]1	21.0	333.63	317.48	132.3	2.51	291.09	0.34	14.65	4.70	1.43	2.39	3.36
819	4.58	4.99	2.9	[illegible].16	6.47	21.0	333.63	325.89	80.9	1.07	291.12	0.49	10.36	2.58	1.43	2.39	3.36
820	6.21	6.67	3.95	4.26	5.[illegible]	27.4	339.22	318.40	141.7	2.51	291.07	0.37	13.70	5.19	1.41	2.34	2.22
821	6.[illegible]3	6.67	3.97	4.26	5.17	27.4	339.22	329.15	89.0	1.07	291.12	0.54	9.45	3.27	1.41	2.34	2.22
822	8.59	9.[illegible]4	5.5	5.[illegible]	4.[illegible]8	36.7	345.56	318.01	139.7	2.47	291.09	0.37	13.70	5.78	1.38	2.29	1.45
823	8.61	9.04	5.54	5.8[illegible]	4.[illegible]7	36.7	345.56	332.13	93.1	1.07	291.12	0.57	9.06	4.07	1.38	2.28	1.45

Table 6.14 Vapour-gas mixtures results

mixture steam-hydrogen
tube diameter 12.5 mm

Run No.	$W_{\infty 1}$ %	$W_{\infty 2}$ %	$\tilde{W}_{\infty 1}$ %	$\tilde{W}_{\infty 2}$ %	U_∞ m/s	P_∞ Pa	T_∞ K	T_w K	$\dot{Q}''_{obs}$ kW/m^2	U_{ow} m/s	T_{in} K	ΔT_{ow} K	error estimates: $\delta\dot{Q}''_{obs}/\dot{Q}''_{obs}$ %	σ_{Tw} K	$\delta U_\infty/U_\infty$ %	$\delta W_{\infty 1}/W_{\infty 1}$ %	$\delta W_{\infty 2}/W_{\infty 2}$ %
824	0.07	0.14	0.61	1.21	1.62	100.4	372.56	334.86	464.9	4.00	277.47	2.72	2.71	7.28	1.50	2.50	6.03
825	0.09	0.17	0.77	1.47	1.61	100.4	372.49	334.20	460.6	4.00	277.47	2.70	2.73	7.53	1.50	2.50	4.95
826	0.1[illegible]	0.19	0.9	1.68	1.61	100.4	372.42	333.75	456.3	4.00	277.47	2.67	2.74	7.59	1.50	2.50	4.32
827	0.12	0.22	1.[illegible]	1.93	1.61	100.4	372.35	333.41	456.3	4.00	277.47	2.67	2.74	7.70	1.50	2.50	3.78
828	0.14	0.25	1.2[illegible]	[illegible].15	1.61	100.4	372.29	333.00	452.1	4.00	277.44	2.65	2.75	7.78	1.50	2.50	3.38
829	0.07	0.15	1.6[illegible]	1.28	1.6[illegible]	100.4	372.54	344.77	368.9	2.40	277.52	3.60	2.43	6.38	1.50	2.50	5.67
830	0.09	0.17	[illegible].7[illegible]	1.49	1.6[illegible]	100.4	372.48	344.45	366.3	2.40	277.52	3.58	2.44	6.46	1.50	2.50	4.88
831	0.10	0.20	0.9	1.76	1.6[illegible]	100.4	372.40	344.08	363.7	2.40	[illegible]77.52	3.55	2.45	6.43	1.50	2.50	4.14
832	0.12	0.23	1.[illegible]	1.98	1.61	100.4	372.34	343.73	358.6	2.40	277.52	3.50	2.46	6.42	1.50	2.50	3.67
833	0.14	0.25	1.2[illegible]	2.17	1.61	100.4	372.28	343.36	356.1	2.40	277.49	3.48	2.46	6.46	1.50	2.50	3.35
834	0.07	0.16	0.67	1.41	1.6[illegible]	100.4	372.50	354.66	260.9	0.80	277.55	7.65	2.10	4.78	1.50	2.50	5.14
835	0.13	0.2[illegible]	1.1[illegible]	1.92	0.89	100.2	372.30	329.70	443.7	4.00	277.34	2.60	2.78	6.94	1.50	2.50	3.80
836	0.16	0.26	1.4[illegible]	[illegible].29	0.89	100.2	372.20	328.85	439.4	4.00	277.34	2.57	2.79	7.13	1.50	2.50	3.18
837	0.19	0.31	1.67	[illegible].67	0.89	100.2	372.09	328.21	435.1	4.00	277.34	2.55	2.80	7.26	1.50	2.50	2.73
838	0.22	0.36	1.94	[illegible].11	0.9[illegible]	100.2	371.96	327.30	422.2	4.00	277.37	2.47	2.84	7.43	1.50	2.49	2.34
839	0.25	0.4[illegible]	2.21	[illegible].44	0.9[illegible]	100.3	371.88	326.71	413.6	4.00	277.37	2.42	2.87	7.42	1.50	2.49	2.12
840	0.32	0.51	2.75	4.35	0.91	100.3	371.62	325.02	405.0	4.00	277.37	2.37	2.91	7.61	1.50	2.49	1.68
841	0.38	0.56	[illegible].2[illegible]	4.79	0.91	1[illegible].3	371.50	323.99	396.4	4.00	277.37	2.32	2.94	7.75	1.49	2.49	1.52
842	0.07	0.28	0.6[illegible]	[illegible].66	1.7[illegible]	97.6	371.91	337.97	456.0	4.00	277.62	2.67	2.74	6.82	1.50	2.50	10.78
843	[illegible].1	0.13	0.9	[illegible].1	1.68	97.6	371.79	333.29	451.7	4.00	277.62	2.65	2.75	7.06	1.50	2.50	6.55
844	0.17	0.21	1.5	1.86	1.69	97.6	371.58	332.42	451.8	4.00	277.60	2.65	2.75	7.07	1.50	2.50	3.95
845	[illegible].[illegible]4	0.3[illegible]	2.[illegible]	2.59	1.7	97.6	371.37	331.45	443.2	4.00	277.60	2.65	2.78	7.19	1.50	2.49	2.83
846	0.31	0.4[illegible]	2.69	[illegible].47	1.71	97.6	371.12	330.07	434.6	4.00	277.60	2.55	2.80	7.48	1.50	2.49	2.11
847	0.38	0.5[illegible]	3.29	4.32	1.72	97.6	370.89	329.30	430.4	4.00	277.57	2.52	2.82	7.30	1.49	2.49	1.70
848	0.45	0.57	[illegible].9	4.91	1.7[illegible]	97.7	371.73	328.04	421.8	4.00	277.57	2.47	2.84	7.51	1.49	2.49	1.49
849	0.53	0.7[illegible]	4.54	5.93	1.74	97.7	37[illegible].45	327.25	413.2	4.00	277.57	2.42	2.67	7.64	1.49	2.49	1.24
850	[illegible].61	0.79	5.1[illegible]	6.65	1.75	97.[illegible]	371.27	326.38	4[illegible]9.[illegible]	4.00	277.55	2.4[illegible]	2.89	7.40	1.49	2.48	1.10
851	0.69	[illegible].59	[illegible].85	[illegible].41	1.76	98.[illegible]	371.09	325.41	404.7	4.00	277.52	2.[illegible]7	2.91	7.57	1.49	2.48	0.99
852	[illegible].42	0.4[illegible]	[illegible]	[illegible].75	[illegible]	98.4	371.26	315.71	310.3	4.00	277.44	1.82	3.40	6.53	1.49	2.49	1.95
853	1.[illegible]	1.3[illegible]	[illegible]	1[illegible].67	[illegible]3	10[illegible].4	370.31	314.75	311.3	4.01	276.74	1.82	3.40	7.12	1.48	2.47	0.68
854	1.[illegible]	1.[illegible]	[illegible].6	1[illegible].28	[illegible]5	1[illegible].4	[illegible]69.18	310.98	2[illegible]9.7	4.01	[illegible]76.74	1.69	3.56	6.69	1.48	2.46	0.51

Table 6.14 (continued)

Run No.	$W_{\infty 1}$	$W_{\infty 2}$	$\tilde{W}_{\infty 1}$	$\tilde{W}_{\infty 2}$	U_{∞}	P_{∞}	T_{∞}	T_{w}	$\dot{Q}''_{obs}$	U_{ow}	T_{in}	ΔT_{ow}	error estimates $\frac{\delta \dot{Q}''_{obs}}{\dot{Q}''_{obs}}$	σ_{Tw}	$\frac{\delta U_{\infty}}{U_{\infty}}$	$\frac{\delta W_{\infty 1}}{W_{\infty 1}}$	$\frac{\delta W_{\infty 2}}{W_{\infty 2}}$
	%	%	%	%	m/s	Pa	K	K	kW/m^2	m/s	K	K	%	K	%	%	%
855	1.89	2.34	15.37	17.66	[illegible]	102.4	368.09	307.49	268.1	4.01	276.74	1.57	3.76	6.14	1.47	2.45	0.41
856	2.57	2.94	19.15	21.31	[illegible]	103.1	[illegible]	305.19	242.2	4.01	276.76	1.42	4.06	5.78	1.46	2.44	0.34
857	3.21	3.70	22.85	25.58	0.94	103.2	365.57	302.23	216.3	4.01	276.76	1.26	4.43	5.39	1.45	2.42	0.29
858	[illegible]	4.39	25.69	29.11	0.98	104.0	364.46	299.95	194.7	4.01	276.76	1.14	4.83	4.70	1.44	2.40	0.25
859	4.73	5.23	[illegible]	[illegible]	[illegible]	102.9	362.70	297.25	177.4	4.01	276.76	1.04	5.22	4.36	1.43	2.38	0.22
860	5.78	5.71	33.7	35.09	1.16	102.6	361.81	296.41	164.5	4.01	276.74	0.96	5.57	3.89	1.42	2.37	0.21

mixture steam-hydrogen
tube diameter 12.5 mm

Run No.	$W_{\infty 1}$ %	W_{b2} %	$\tilde{W}_{\infty 1}$ %	$\tilde{W}_{\infty 2}$ %	U_∞ m/s	P_∞ Pa	T_∞ K	T_w K	$\dot{Q}''_{obs}$ kW/m^2	U_{ow} m/s	T_{in} K	ΔT_{ow} K	error estimates: $\delta\dot{Q}''_{obs}/\dot{Q}''_{obs}$ %	σ_{Tw} K	$\delta U_\infty/U_\infty$ %	$\delta W_{\infty 1}/W_{\infty 1}$ %	$\delta W_{\infty 2}/W_{\infty 2}$ %
861	0.23	0.44	2.05	2.81	6.91	3.6	299.70	293.71	83.8	3.95	284.25	0.50	10.22	0.88	1.50	2.49	10.11
862	0.49	0.61	4.27	6.82	4.72	5.6	306.89	296.43	104.7	3.95	284.25	0.62	8.27	1.27	1.49	2.49	3.80
863	0.49	0.61	4.2[illegible]	6.82	4.72	5.6	306.89	298.88	90.5	2.37	284.28	0.90	5.92	1.12	1.49	2.49	3.80
864	.49	0.81	4.2	6.82	4.72	5.6	306.89	303.29	51.9	0.79	284.33	1.54	3.81	0.73	1.49	2.49	3.80
865	.72	0.86	6.17	7.16	3.69	7.4	311.77	297.53	129.8	3.95	84.28	0.77	6.77	1.40	1.49	2.48	2.91
866	0.72	0.86	6.17	7.16	3.70	7.4	311.77	300.78	113.0	2.37	284.30	1.12	4.89	1.44	1.49	2.48	2.91
867	0.74	0.86	6.17	7.16	3.70	7.4	311.77	306.69	62.7	0.79	284.35	1.87	3.34	1.07	1.49	2.48	2.91
868	0.95	1.23	7.92	9.98	3.09	9.2	315.37	298.14	134.0	3.95	284.28	0.80	6.58	1.67	1.49	2.48	1.77
869	0.95	1.23	7.92	9.98	3.09	9.2	315.37	301.60	115.5	2.37	284.30	1.15	4.80	1.61	1.49	2.48	1.77
870	0.95	1.23	7.9[illegible]	9.98	3. 9	9.2	315.37	308.72	65.2	0.79	284.35	1.94	3.26	1.22	1.49	2.48	1.77
871	1.29	1.64	10.45	12.99	2.46	12.2	320.13	297.92	142.4	3.95	284.28	0.85	6.23	1.82	1.48	2.47	1.13
872	1.29	1.64	10.45	12.99	2.46	12.2	320.13	302.08	123.1	2.37	284.30	1.22	4.56	1.82	1.48	2.47	1.13
873	1.29	1.64	10.45	12.99	2.46	12.2	320.13	314.79	45.8	0.59	284.35	1.82	3.40	0.98	1.48	2.47	1.13
874	1.51	1.91	12.05	14.82	2.19	14.1	322.61	297.91	138.2	3.95	284.28	0.82	6.40	1.86	1.48	2.46	0.91
875	1.51	1.91	12.07	14.82	2.19	14.1	322.61	302.15	120.6	2.37	284.30	1.20	4.63	1.85	1.48	2.46	0.91
876	1.51	1.91	12.07	14.82	2.19	14.1	322.61	316.51	53.3	0.59	284.35	2.12	3.10	1.10	1.48	2.46	0.91
877	1.87	2.38	14.54	17.88	1.93	16.8	325.40	297.37	134.0	3.95	284.28	0.80	6.58	1.83	1.47	2.45	0.69
878	1.87	2.38	14.54	17.88	1.93	16.8	325.40	301.90	120.6	2.37	284.30	1.20	4.63	1.88	1.47	2.45	0.69
879	1.87	2.38	14.54	17.88	1.93	16.8	325.40	317.80	55.8	0.59	284.35	2.22	3.02	1.28	1.47	2.45	0.69
880	2.44	2.95	18.25	21.39	1.61	21.3	329.44	296.35	129.8	3.95	284.28	0.77	6.77	1.84	1.46	2.44	0.52
881	2.44	2.95	18.25	21.39	1.61	21.3	329.44	301.05	118.0	2.37	284.30	1.17	4.71	2.07	1.46	2.44	0.52
882	2.44	2.95	18.24	21.39	1.61	21.3	329.44	319.59	58.3	0.59	284.35	2.31	2.94	1.54	1.46	2.44	0.52
883	2.77	3.26	20.3	23.13	1.51	23.6	331.14	296.05	129.8	3.95	284.28	0.77	6.77	1.74	1.46	2.43	0.46
884	2.77	3.26	20.3	23.13	1.51	23.6	331.14	300.46	115.5	2.37	284.28	1.15	4.80	2.03	1.46	2.43	0.46
885	2.77	3.26	20.3	23.13	1.51	23.6	331.14	319.70	60.2	0.59	284.35	2.39	2.89	1.68	1.46	2.43	0.46
886	3.28	3.55	23.82	26.40	1.32	26.1	333.94	295.22	117.3	3.95	284.28	0.70	7.44	1.81	1.45	2.42	0.38
887	3.28	3.86	23.8[illegible]	26.40	1.32	28.1	333.94	299.69	110.5	2.37	284.30	1.10	4.98	1.88	1.45	2.42	0.38
888	3.28	3.66	23.8[illegible]	26.40	1.32	26.1	333.94	320.71	62.7	0.59	284.35	2.49	2.84	1.55	1.45	2.42	0.38
889	0.09	0.25	6.8	7.19	15.50	4.1	302.30	296.39	105.1	3.96	283.53	0.62	8.26	1.45	1.50	2.50	15.60
890	0.19	0.25	[illegible]	7.19	15.49	4.1	302.30	298.02	80.7	2.37	283.55	0.89	6.57	1.17	1.50	2.50	15.60
891	.9	0.25	[illegible]	7.19	15.49	4.1	302.30	301.56	20.2	0.59	283.58	0.80	6.57	0.31	1.50	2.50	15.60

Table 6.15 (continued)

Run No.	$W_{\infty 1}$ %	$W_{\infty 2}$ %	$\tilde{W}_{\infty 1}$ %	$\tilde{W}_{\infty 2}$ %	U_∞ m/s	P_∞ Pa	T_∞ K	T_w K	$\dot{Q}''_{obs}$ kW/m^2	U_{ow} m/s	T_{in} K	ΔT_{ow} K	error estimates: $\frac{\delta \dot{Q}''_{obs}}{\dot{Q}''_{obs}}$ %	σ_{Tw} K	$\frac{\delta U_\infty}{U_\infty}$ %	$\frac{\delta W_{\infty 1}}{W_{\infty 1}}$ %	$\frac{\delta W_{\infty 2}}{W_{\infty 2}}$ %
892	0.19	0.27	1.7	2.40	10.90	6.1	309.22	300.33	138.7	3.96	283.53	0.82	6.39	1.77	1.50	2.50	10.12
893	0.19	0.27	1.7	2.40	10.92	6.1	309.22	302.71	113.4	2.37	283.55	1.12	4.88	1.59	1.50	2.50	10.12
894	0.19	0.27	1.7	2.40	10.92	6.1	309.22	307.70	34.0	0.59	283.58	1.35	4.22	0.58	1.50	2.50	10.12
895	0.78	0.51	3.33	4.29	7.18	9.9	317.98	304.61	176.4	3.96	283.50	1.05	5.17	2.11	1.49	2.49	3.92
896	0.78	0.50	3.33	4.29	7.18	9.9	317.98	308.16	143.6	2.37	283.53	1.42	4.04	1.95	1.49	2.49	3.92
897	0.78	0.50	3.33	4.29	7.18	9.9	317.98	315.79	45.3	0.59	283.55	1.80	3.43	0.71	1.49	2.49	3.92
898	0.55	0.64	4.73	5.48	5.60	13.3	323.47	306.52	193.2	3.96	283.53	1.15	4.79	2.57	1.49	2.49	2.56
899	0.55	0.64	4.73	5.48	5.60	13.3	323.47	310.65	158.7	2.37	283.55	1.57	3.76	2.28	1.49	2.49	2.56
900	0.55	0.64	4.73	5.48	5.59	13.3	323.47	320.68	50.3	0.59	283.60	1.99	3.21	0.79	1.49	2.49	2.56
901	0.72	0.86	6.07	7.21	4.62	16.7	327.83	307.14	210.0	3.96	283.53	1.25	4.48	2.70	1.49	2.48	1.71
902	0.72	0.86	6.07	7.21	4.62	16.7	327.83	312.45	168.7	2.37	283.55	1.67	3.60	2.57	1.49	2.48	1.71
903	0.72	0.86	6.09	7.21	4.62	16.7	327.83	324.18	56.5	0.59	283.58	2.32	2.94	0.92	1.49	2.48	1.71
904	0.97	1.13	8.07	9.28	3.69	22.0	333.18	307.95	222.6	3.96	283.50	1.32	4.28	2.92	1.49	2.48	1.18
905	0.97	1.13	8.05	9.28	3.69	22.0	333.18	313.86	186.3	2.37	283.53	1.65	3.37	2.82	1.49	2.48	1.18
906	0.97	1.13	8.08	9.28	3.69	22.0	333.18	328.42	66.7	0.59	283.55	2.64	2.75	1.38	1.49	2.48	1.18
907	1.22	1.45	9.93	11.63	3.15	26.9	337.02	307.63	226.8	3.96	283.50	1.35	4.22	3.29	1.48	2.47	0.87
908	1.22	1.45	9.93	11.63	3.15	26.9	337.02	314.19	201.4	2.37	283.53	1.99	3.21	3.01	1.48	2.47	0.87
909	1.22	1.45	9.9	11.63	3.15	26.9	337.02	330.92	75.4	0.59	283.58	2.99	2.61	1.53	1.48	2.47	0.87
910	1.70	2.21	13.41	16.80	2.78	38.9	344.03	305.46	239.4	3.96	283.50	1.42	4.04	3.15	1.47	2.46	0.54
911	1.70	2.21	13.42	16.8	2.78	38.9	344.03	313.08	203.9	2.37	283.53	2.02	3.18	3.27	1.47	2.46	0.54
912	1.70	2.21	13.41	16.8	2.78	38.9	344.03	335.25	84.2	0.59	283.55	3.34	2.50	1.57	1.47	2.46	0.54
913	3. 9	3.53	22.15	24.62	1.07	56.0	350.35	299.42	210.0	3.96	283.55	1.25	4.48	2.14	1.46	2.42	0.34
914	0.11	0.19	.97	1.66	17.75	6.9	311.50	313.16	138.4	3.95	284.03	0.82	6.40	2.21	1.50	2.50	13.31
915	0.11	0.19	0.97	1.66	17.75	6.9	311.50	305.95	96.4	1.98	284.08	1.15	4.80	1.68	1.50	2.50	13.31
916	0.11	0.19	0.96	1.66	17.77	6.9	311.50	310.17	32.6	0.59	284.28	1.30	4.35	0.43	1.50	2.50	13.31
917	0.26	0.36	2.30	.16	10.14	12.2	322.33	309.31	197.0	3.95	284.05	1.17	4.71	2.88	1.50	2.49	4.65
918	.26	.36	2. [illegible]	.16	10.74	12.2	322.33	313.69	146.5	1.98	284.13	1.74	3.50	2.35	1.50	2.49	4.65
919	0.26	..6	2.31	.16	10.[illegible]9	12.2	322.33	320.08	49.5	0.59	284.35	1.97	3.23	0.87	1.50	2.49	4.65
920	0.42	0.48	3.61	4.11	7.28	18.0	330.12	312.63	236.8	3.95	284.03	1.42	4.05	3.19	1.49	2.49	2.90
921	0.42	0.48	3.6	4.11	7.19	18.0	330.12	318.43	180.0	1.98	284.08	2.14	3.07	2.68	1.49	2.49	2.90
922	.42	.43	.6	4.11	7. 9	18.	330.12	327.19	61.4	0.59	284.28	2.44	2.86	0.96	1.49	2.49	2.90
923	.62	0.75	5.	4.29	5.5[illegible]	25.[illegible]	336.94	314.85	263.9	3.95	284.05	1.57	3.76	3.62	1.49	2.48	1.65

Table 6.15 (continued)

Run No.	$W_{\infty 1}$	$W_{\infty 2}$	$\tilde{W}_{\infty 1}$	$\tilde{W}_{\infty 2}$	U_∞	P_∞	T_∞	T_w	$\dot{Q}''_{obs}$	U_{ow}	T_{in}	ΔT_{ow}	error estimates: $\frac{\delta \dot{Q}''_{obs}}{\dot{Q}''_{obs}}$	σ_{Tw}	$\frac{\delta U_\infty}{U_\infty}$	$\frac{\delta W_{\infty 1}}{W_{\infty 1}}$	$\frac{\delta W_{\infty 2}}{W_{\infty 2}}$
	%	%	%	%	m/s	Pa	K	K	kW/m^2	m/s	K	K	%	K	%	%	%
924	0.62	0.75	5.28	6.29	5.58	25.3	336.94	321.96	198.7	1.98	284.15	2.37	2.91	3.11	1.49	2.48	1.65
925	0.62	0.75	5.27	6.29	5.59	25.3	336.94	332.83	75.8	0.59	284.40	3.01	2.60	1.08	1.49	2.48	1.65
926	0.89	1.12	7.47	9.17	4.11	36.9	344.84	315.55	272.2	3.95	284.08	1.62	3.68	3.96	1.49	2.48	1.00
927	0.89	1.12	7.47	9.17	4.10	36.9	344.84	325.03	213.3	1.98	284.13	2.54	2.81	3.50	1.49	2.48	1.00
928	0.89	1.12	7.46	9.17	4.11	36.9	344.84	338.81	90.2	0.59	284.30	3.58	2.44	1.41	1.49	2.48	1.00
929	1.20	1.38	9.77	11.11	3.27	46.8	351.01	315.73	289.0	3.95	284.03	1.72	3.53	4.39	1.48	2.47	0.77
930	1.20	1.38	9.77	11.11	3.27	46.6	351.01	326.21	238.3	1.98	284.13	2.84	2.67	3.64	1.48	2.47	0.77
931	1.20	1.38	9.76	11.11	3.27	48.8	351.01	343.09	102.6	0.59	284.78	4.07	2.35	1.90	1.48	2.47	0.77

mixture Refrigerant 113–air

tube diameter 12.5 mm

Run No.	$W_{\infty 1}$ %	W_{w2} %	$\tilde{W}_{\infty 1}$ %	$\tilde{W}_{\infty 2}$ %	U_∞ m/s	P_∞ Pa	T_∞ K	T_w K	$\dot{Q}''_{obs}$ kW/m^2	U_{ow} m/s	T_{in} K	ΔT_{ow} K	error estimates: $\frac{\delta \dot{Q}''_{obs}}{\dot{Q}''_{obs}}$ %	σ_{Tw} K	$\frac{\delta U_\infty}{U_\infty}$ %	$\frac{\delta W_{\infty 1}}{W_{\infty 1}}$ %	$\frac{\delta W_{\infty 2}}{W_{w2}}$ %
932	0.05	0.05	.3	.30	1.78	103.8	320.86	285.93	51.4	3.99	279.24	0.30	16.66	0.69	1.50	2.50	23.00
933	0. 5	0.05	0.3	.31	1.78	103.8	320.86	289.48	47.1	1.99	279.29	0.55	9.24	0.74	1.50	2.50	23.00
934	0.05	0.05	0.3	.30	1.78	103.8	320.86	303.08	29.5	0.60	279.36	1.16	4.76	0.54	1.50	2.50	23.00
935	.14	0.14	.89	.88	0.62	100.7	319.78	284.78	42.8	3.99	279.24	0.25	19.94	0.40	1.50	2.50	7.77
936	0.14	0.14	0.89	0.88	0.62	100.7	319.78	287.90	40.7	1.99	279.29	0.48	10.64	0.45	1.50	2.50	7.77
937	0.14	0.14	0.89	.88	0.62	100.7	319.78	300.06	27.6	0.60	279.34	1.08	5.03	0.34	1.50	2.50	7.77
938	0.28	0.28	1.76	1.77	0.62	102.2	319.96	284.68	42.8	3.99	279.24	0.25	19.94	0.38	1.50	2.49	3.87
939	0.28	0.28	1.76	1.77	0.62	102.2	319.96	287.81	38.5	1.99	279.39	0.45	11.21	0.45	1.50	2.49	3.87
940	0.28	0.28	1.76	1.77	0.62	102.2	319.96	300.24	28.2	0.60	279.61	1.11	4.94	0.49	1.50	2.49	3.87
941	0.43	0.43	2.70	.70	0.63	101.5	319.47	284.47	42.8	3.99	279.21	0.25	19.94	0.42	1.49	2.49	2.54
942	0.43	0.43	2.69	2.70	0.63	101.5	319.47	287.49	36.4	1.99	279.29	0.43	11.85	0.45	1.49	2.49	2.54
943	0.43	0.43	2.69	2.7	0.63	101.5	319.47	299.74	26.3	0.60	279.34	1.03	5.24	0.56	1.49	2.49	2.54
944	0.58	0.57	3.66	3.56	0.64	101.5	319.19	284.37	38.6	3.99	279.26	0.23	22.14	0.41	1.49	2.49	1.93
945	0.58	0.57	3.66	3.56	0.64	101.5	319.19	287.23	36.4	1.99	279.31	0.43	11.85	0.44	1.49	2.49	1.93
946	0.58	0.57	3.66	3.56	0.64	101.5	319.19	299.27	25.7	0.60	279.46	1.01	5.35	0.54	1.49	2.49	1.93
947	0.76	0.77	4.7	4.80	0.64	102.0	318.96	284.10	38.6	3.99	279.26	0.23	22.14	0.42	1.49	2.48	1.43
948	0.76	0.77	4.71	4.80	0.64	102.0	318.96	286.93	34.3	1.99	279.31	0.40	12.57	0.45	1.49	2.48	1.43
949	0.76	0.77	4.71	4.8	0.64	102.	318.96	298.49	25.7	0.60	279.39	1.01	5.35	0.49	1.49	2.48	1.43
950	0.96	0.98	5.89	6.0	0.64	102.8	318.82	284.03	38.5	3.99	279.31	0.23	22.14	0.41	1.49	2.48	1.14
951	.96	0.98	5.86	6.	0.64	102.8	318.82	286.84	34.2	1.99	279.44	0.40	12.57	0.45	1.49	2.48	1.14
952	.96	0.98	5.8	6.	0.64	102.8	318.82	298.38	24.4	0.60	279.69	0.96	5.60	0.37	1.49	2.48	1.14
953	. 4	0.04	0.27	.26	0.82	102.8	320.59	285.17	47.1	3.99	279.29	0.28	18.15	0.45	1.50	2.50	25.94
954	. 4	0.04	.27	.26	0.82	102.8	320.59	288.46	42.8	1.99	279.34	0.50	10.13	0.45	1.50	2.50	25.94
955	0.04	0.04	0.27	.26	0.82	102.8	320.59	301.80	28.2	0.60	279.44	1.11	4.94	0.51	1.50	2.50	25.94
956	0. 8	0. 0	0.54	.54	0.82	102.3	32..34	285.15	42.9	3.99	279.29	0.25	19.95	0.48	1.50	2.50	12.58
957	0.08	0.	.54	.54	0.82	102.3	320.34	288.39	40.7	1.99	279.41	0.48	10.64	0.49	1.50	2.50	12.58
958	.08	0.08	0.5	.54	0.	102.3	320.34	301.35	26.9	0.60	279.64	1.06	5.14	0.43	1.50	2.50	12.58
959	0.17	0.14	1.	.89	0.	101.9	320.12	284.97	42.8	3.99	279.26	0.25	19.95	0.45	1.50	2.50	7.72
960	0.17	0.14	1.07	.89	0.83	101.9	320.12	288.18	40.7	1.99	279.34	0.48	10.64	0.50	1.50	2.50	7.72
961	.17	0.14	1.	.89	[illegible]	101.9	320.12	300.66	26.9	0.60	279.46	1.06	5.14	0.42	1.50	2.51	7.72
962	.25	0.25	1.6	1.61	[illegible]	[illegible]	319.98	284.91	42.8	3.99	79.29	0.25	19.95	0.48	1.50	2.49	4.26

Table 5.10 (continued)

Run No.	$W_{\infty 1}$ %	$W_{\infty 2}$ %	$\tilde{W}_{\infty 1}$ %	$\tilde{W}_{\infty 2}$ %	U_∞ m/s	P_∞ Pa	T_∞ K	T_w K	$\dot{Q}''_{obs}$ kW/m^2	U_{ow} m/s	T_{in} K	ΔT_{ow} K	$\frac{\delta \dot{Q}''_{obs}}{\dot{Q}''_{obs}}$ %	σ_{Tw} K	$\frac{\delta U_\infty}{U_\infty}$ %	$\frac{\delta W_{\infty 1}}{W_{\infty 1}}$ %	$\frac{\delta W_{\infty 2}}{W_{\infty 2}}$ %
963	0.25	0.25	1.61	1.61	0.54	102.1	319.98	288.03	38.5	1.99	279.34	0.45	11.21	0.50	1.50	2.49	4.26
964	0.25	0.25	1.6	1.61	0.53	102.1	319.98	300.73	26.3	0.60	279.41	1.03	5.24	0.55	1.50	2.49	4.26
965	0.37	0.36	2.37	2.35	0.46	104.1	320.33	285.65	38.3	3.98	280.72	0.23	22.20	0.37	1.49	2.49	2.97
966	0.38	0.36	2.38	2.35	0.46	104.1	320.33	288.55	38.3	1.99	280.77	0.45	11.24	0.36	1.49	2.49	2.97
967	0.38	0.36	2.3[illegible]	2.[illegible]	0.46	104.1	320.33	300.04	25.5	0.60	280.82	1.00	5.37	0.38	1.49	2.49	2.97
968	0.79	0.82	4.97	4.94	0.47	103.8	319.44	285.07	38.3	3.98	280.72	0.23	22.20	0.33	1.49	2.48	1.38
969	0.79	0.82	4.97	4.94	0.47	103.8	319.44	287.94	34.0	1.99	280.82	0.46	12.60	0.45	1.49	2.48	1.38
970	0.80	0.79	4.97	4.94	0.46	103.8	319.45	299.12	24.2	0.60	281.02	0.95	5.61	0.37	1.49	2.48	1.39
971	1.03	1.04	6.31	6.35	0.47	103.5	318.92	284.98	34.1	3.98	280.67	0.20	24.96	0.41	1.48	2.47	1.08
972	1.03	1.04	6.32	6.35	0.47	103.5	318.92	287.48	31.9	1.99	280.72	0.38	13.42	0.44	1.48	2.47	1.08
973	1.03	1.04	6.31	6.35	0.47	103.5	318.92	297.87	23.6	0.60	280.75	0.93	5.74	0.42	1.48	2.47	1.08
974	1.30	1.20	7.86	7.31	0.48	103.1	318.48	284.66	34.1	3.98	280.72	0.20	24.96	0.38	1.48	2.47	0.94
975	1.31	1.20	7.91	7.31	0.47	103.1	318.48	287.15	29.8	1.99	280.82	0.35	14.36	0.41	1.48	2.47	0.94
976	1.30	1.20	7.86	7.31	0.48	103.1	318.48	297.48	22.3	0.60	280.95	0.88	6.03	0.38	1.48	2.47	0.94
977	1.62	1.60	9.67	9.49	0.48	103.8	317.99	284.34	29.8	3.98	280.70	0.18	28.50	0.35	1.48	2.46	0.72
978	1.62	1.60	9.67	9.49	0.48	103.8	317.99	286.47	27.7	1.99	280.75	0.33	15.44	0.45	1.48	2.46	0.72
979	1.62	1.60	9.67	9.49	0.48	103.8	317.99	296.37	21.7	0.60	280.80	0.85	6.19	0.37	1.48	2.46	0.72
980	0.68	0.68	4.27	4.23	0.54	103.6	319.59	285.37	38.3	3.98	280.67	0.23	22.20	0.41	1.49	2.48	1.61
981	0.68	0.68	4.27	4.23	0.54	103.6	319.59	286.05	36.2	1.99	280.72	0.43	11.88	0.40	1.49	2.48	1.61
982	0.68	0.68	4.26	4.23	0.54	103.6	319.59	299.27	25.5	0.60	280.77	1.00	5.37	0.42	1.49	2.48	1.61
983	0.89	0.86	5.47	5.33	0.54	103.8	319.32	285.10	34.1	3.98	280.67	0.20	24.96	0.40	1.49	2.48	1.28
984	0.89	0.86	5.47	5.33	0.54	103.8	319.32	287.80	34.0	1.99	280.80	0.40	12.60	0.44	1.49	2.48	1.28
985	0.89	0.86	5.47	5.33	0.54	103.8	319.32	298.60	24.9	0.60	280.97	0.98	5.49	0.30	1.49	2.48	1.28
986	0.47	0.45	2.94	2.87	0.57	104.1	320.16	285.63	38.3	3.98	280.65	0.23	22.20	0.40	1.49	2.49	2.37
987	0.47	0.45	2.94	2.87	0.57	104.1	320.16	288.48	38.3	1.99	280.72	0.45	11.24	0.44	1.49	2.49	2.37
988	0.47	0.45	2.94	2.87	0.57	104.1	320.16	300.15	26.1	0.60	280.75	1.03	5.25	0.42	1.49	2.49	2.37
989	0.63	0.63	3.9[illegible]	3.97	0.58	103.6	319.74	285.45	38.3	3.98	280.65	0.23	22.20	0.39	1.49	2.48	1.72
990	0.63	0.63	3.9[illegible]	3.97	0.58	103.6	319.74	286.22	36.2	1.99	280.70	0.43	11.88	0.46	1.49	2.48	1.72
991	0.63	0.63	3.9[illegible]	.97	0.58	103.6	319.74	299.45	25.5	0.60	280.75	1.00	5.37	0.51	1.49	2.48	1.72
992	0.82	[illegible]	5.[illegible]	5.17	0.58	104.4	319.52	285.27	38.3	3.98	280.65	0.23	22.20	0.39	1.49	2.48	1.32
993	[illegible]	0.83	5.[illegible]	5.17	0.58	104.4	319.52	287.36	34.0	1.99	280.70	0.40	12.60	0.41	1.49	2.48	1.32
994	[illegible]	[illegible]	5.[illegible]7	5.17	0.58	104.4	319.52	298.96	24.9	0.60	280.60	0.98	5.49	0.36	1.49	2.48	1.32

Table 6.17 Vapour-gas mixtures results

mixture Refrigerant 113-hydrogen

tube diameter 12.5 mm

Run No.	$W_{\infty 1}$ / %	$W_{\infty 2}$ / %	$\tilde{W}_{\infty 1}$ / %	$\tilde{W}_{\infty 2}$ / %	U_{∞} / m/s	P_{∞} / Pa	T_{∞} / K	T_{w} / K	$\dot{Q}''_{obs}$ / kW/m^2	U_{ow} / m/s	T_{in} / K	ΔT_{ow} / K	error estimates: $\delta\dot{Q}''_{obs}/\dot{Q}''_{obs}$ / %	σ_{Tw} / K	$\delta U_{\infty}/U_{\infty}$ / %	$\delta W_{\infty 1}/W_{\infty 1}$ / %	$\delta W_{\infty 2}/W_{\infty 2}$ / %
995	0.14	0.03	3.27	2.65	0.66	102.7	319.83	285.98	42.5	3.98	280.80	0.25	20.01	0.37	1.50	2.50	2.59
996	0.14	0.03	3.27	2.64	0.66	102.7	319.83	288.99	41.4	1.99	280.85	0.48	10.67	0.39	1.50	2.50	2.60
997	0.14	0.03	3.26	2.65	0.66	102.7	319.83	301.04	26.1	0.60	280.90	1.03	5.26	0.53	1.50	2.50	2.59
998	0.17	0.08	6.49	6.64	0.67	103.6	318.84	285.75	38.3	3.98	280.80	0.23	22.21	0.36	1.50	2.50	1.04
999	0.17	0.08	6.48	6.64	0.67	103.6	318.84	288.60	38.3	1.99	280.82	0.45	11.24	0.38	1.50	2.50	1.04
1000	0.17	0.08	6.49	6.64	0.67	103.6	318.84	300.32	24.9	0.60	280.90	0.98	5.49	0.49	1.50	2.50	1.04
1001	0.12	0.13	9.74	10.66	0.69	105.8	318.16	285.44	38.3	3.98	280.77	0.23	22.21	0.35	1.50	2.50	0.65
1002	0.12	0.13	9.81	10.66	0.68	105.8	318.16	288.46	36.1	1.99	280.92	0.43	11.88	0.40	1.50	2.50	0.65
1003	0.12	0.13	9.76	10.66	0.69	105.8	318.16	299.49	24.2	0.60	281.05	0.95	5.61	0.45	1.50	2.50	0.65
1004	0.03	0.02	2.84	2.09	0.76	102.9	320.04	286.18	42.5	3.98	280.80	0.25	20.01	0.39	1.50	2.50	3.29
1005	0.03	0.02	2.84	2.09	0.76	102.9	320.04	289.16	40.4	1.99	280.82	0.46	10.67	0.41	1.50	2.50	3.29
1006	0.03	0.02	2.84	2.09	0.76	102.9	320.04	300.75	26.1	0.60	280.87	1.07	5.26	0.56	1.50	2.50	3.29
1007	0.06	0.07	5.64	6.01	0.77	104.2	319.21	285.92	42.6	3.98	280.77	0.25	20.01	0.37	1.50	2.50	1.15
1008	0.06	0.07	5.59	6.01	0.78	104.2	319.21	288.82	38.3	1.99	280.82	0.45	11.24	0.42	1.50	2.50	1.15
1009	0.06	0.07	5.6[illegible]	6.01	0.77	104.2	319.21	300.37	23.6	0.60	280.87	0.93	5.74	0.54	1.50	2.50	1.15
1010	0.10	0.11	8.5[illegible]	9.44	0.78	107.4	319.00	285.72	42.6	3.98	280.77	0.25	20.01	0.39	1.50	2.50	0.73
1011	0.10	0.11	8.61	9.44	0.77	107.4	319.0	288.66	38.3	1.99	280.80	0.45	11.24	0.45	1.50	2.50	0.73
1012	0.10	0.11	8.5	9.44	0.78	107.4	319.00	299.93	25.5	0.60	280.92	1.00	5.37	0.51	1.50	2.50	0.73
1013	0.13	0.02	2.53	1.68	0.85	102.9	320.17	286.20	42.5	3.98	280.80	0.25	20.01	0.41	1.50	2.50	4.07
1014	0.1[illegible]	0.02	2.5[illegible]	1.68	0.85	102.9	320.17	289.23	40.4	1.99	280.82	0.48	10.67	0.44	1.50	2.50	4.07
1015	0.13	0.02	2.52	1.94	0.85	103.1	320.17	300.47	27.4	0.60	280.87	1.08	5.05	0.43	1.50	2.50	3.54
1016	0.06	0.04	5.01	7.54	0.86	103.4	319.75	286.00	42.6	3.98	280.77	0.25	20.01	0.41	1.50	2.50	1.94
1017	0.[illegible]6	0.04	5.[illegible]	.54	0.86	103.4	319.75	288.93	38.3	1.99	280.82	0.45	11.24	0.42	1.50	2.50	1.94
1018	0.06	0.14	5.02	7.54	0.86	103.4	319.75	300.63	26.8	0.60	280.87	1.05	5.15	0.58	1.50	2.50	1.94
1019	0.34	0.32	23.94	27.84	0.46	123.[illegible]	318.33	287.14	29.8	1.99	280.90	0.35	14.36	0.41	1.49	2.49	0.30

CHAPTER 7 - DISCUSSION

7.1 Pure vapours

7.1.1 Comparison of the present results with earlier measurements and with theory

The present results are examined below in the light of the recent observations for steam of Nobbs and Mayhew /42, 43 / and Fujii et. al. /50, 60 / and for Refrigerant 21 of Gogonin and Dorokhov /59 /. Comparisons are also made with the theoretical studies of Shekriladze and Gomelauri /24 / and Fujii and co-workers /49 - 52 / and the correlations of Fujii et. al. /50, 51 /. The very high vapour velocity data of Nicol and co-workers /37 - 40 / are discussed in section 7.1.2.

As was seen in Chapter 2, the theoretical solutions based on the assumption of uniform wall surface temperature /24, 49 - 51/† tended to predict higher heat-transfer coefficients (particularly at high condensation rates and high vapour velocities) than those found in recent observations /37 - 40, 42, 43, 50, 60 / (see figs. 2.10b, 2.12b, 2.13f and 2.13h). The data of Gogonin and Dorokhov /59 / are in the region of very low vapour velocities ($\leqslant$ 0.56 m/s) and the deviation from Nusselt is small. More recent theoretical results based on the assumption of uniform wall heat flux /50, 51/† and an overall vapour-to-coolant analysis‡ /52 / were in better agreement with the observations of Fujii et. al. /50, 60 / and Nobbs /42 / (see figs. 2.13g, 2.13i and 2.14). However,

† Both /50, 51 / contain errors, see Chapter 2 and Lee and Rose /92 /.

‡ The theoretical solutions obtained in /52/ were, for practical purposes, the same as those based on the uniform heat flux condition /50, 51/ (see /92/ for corrected results of /50,51/).

Lee and Rose /92 / showed that the uniform-wall-heat-flux based solutions and the overall vapour-to-coolant solutions are unsatisfactory. No comparisons are made with the latter theories.

The analyses /49 - 51 / indicated that the vapour-side heat-transfer coefficient could be expressed as a relation between three dimensionless parameters. Two of these may be considered as primary parameters in the sense that for the ranges of variables covered by the available experimental data, the third parameter has a relatively much weaker effect. Moreover, the data themselves, when plotted on the basis of the primary parameters, apparently indicate weak dependence on the third parameter. In the more recent theoretical solutions /50 - 52 /, closed-form expressions relating the dominating parameters were not given. Fujii et. al. /50, 60/ have, however, provided semi-empirical correlations, based on their theoretical solutions, of their experimental results (steam only). These correlating equations (see equations 2.42 to 2.45) are rewritten here:-

(i) based on the main dimensionless parameters arising from the uniform wall surface temperature analysis:-

$$Nu/\sqrt{Re_{TP}} = 0.96\ (Pr_L/FrH)^{0.2} \qquad (7.1)$$

$$\text{for } 0.03 < Pr_L/FrH < 600$$

while for $Pr_L/FrH > 600$, Fujii et. al. indicated that the Nusselt equation is adequate,

$$\left.\begin{aligned} &Nu = 0.728\ (Ga\ Pr_L/H)^{\frac{1}{4}} \\ \text{or}\quad & \\ &Nu/\sqrt{Re_{TP}} = 0.728\ (Pr_L/FrH)^{\frac{1}{4}} \end{aligned}\right\} \qquad (7.2)$$

(ii) based on the main dimensionless parameters arising from the uniform wall heat flux analysis:-

$$Nu/\sqrt{Re_{TP}} = (\sqrt{Re_{TP}}/Fr\widetilde{M})^{0.26} \qquad (7.3)$$

$$\text{for } 0.06 < \sqrt{Re_{TP}}/Fr\widetilde{M} < 200$$

while for $\sqrt{Re_{TP}}/Fr\widetilde{M} > 200$, they indicated that the zero-vapour velocity "Nusselt-type" uniform wall heat flux equation /21/ be used,

$$\left.\begin{aligned} &Nu = 0.615\ (Ga/\widetilde{M})^{\frac{1}{5}} \\ \text{or} \\ &Nu/\sqrt{Re_{TP}} = 0.615\ (\sqrt{Re_{TP}}/Fr\widetilde{M})^{\frac{1}{5}} \end{aligned}\right\} \qquad (7.4)$$

In equations 7.1 to 7.4,

Nu is the average Nusselt number, $\dot{Q}'' d_o/k_L\Delta T$

Re_{TP} is the two-phase Reynolds number, $U_\infty d_o \rho_L/\mu_L$

Pr_L is the condensate Prandtl number, $\mu_L c_{PL}/k_L$

Fr is the Froude number, U_∞^2/gd_o

H is the phase change number, $c_{PL}\Delta T/h_{fg}$

Ga is Galileo number, gd_o^3/μ_L^2

$\widetilde{M}$ is a dimensionless number, $\dot{Q}'' d_o/\mu_L h_{fg}$

The present results are plotted in figs. 7.1 to 7.7 on the basis of

$Nu/\sqrt{Re_{TP}}$ against Pr_L/FrH and in figs. 7.8 to 7.14 on the basis of $Nu/\sqrt{Re_{TP}}$ against $\sqrt{Re_{TP}}/Fr\tilde{M}$ (Note that low values of the abscissae correspond to high vapour velocities and high condensation rates). A separate graph is given for each of the two fluids, for each of the two tube diameters and for each vapour pressure used. Following Minkowcyz and Sparrow /66 /, the condensate film properties (except h_{fg} which was evaluated at T_i) were evaluated at the reference temperature, T_r, where

$$T_r = T_w + \tfrac{1}{3}(T_i - T_w) \qquad (7.5)$$

where T_w is the (arithmetic mean) outside surface temperature of the test condenser tube;

T_i is the condensate surface temperature ($= T_\infty$ for pure vapours).

Lines representing equations 7.1 to 7.4 are included in the relevant figures.

It can be seen from figs. 7.1 to 7.14 that the present results both for steam and for Refrigerant 113 agree satisfactorily with those calculated using equations 7.1 and 7.3. In view of the fact that the correlating equations 7.1 and 7.3 were based on steam data only, the agreement with the present data for Refrigerant 113 provides good support for the theoretical basis for the correlations (see Chapter 2).

For the present data, it may be noted that, for both fluids, the results obtained when operating the apparatus at sub-atmospheric pressures showed more scatter than those for atmospheric pressure. This is thought to be due to the fact that the overall vapour-to-coolant temperature difference ($T_{\infty} - T_{ow}$) is considerably smaller for the lower pressure tests. Thus for these tests, the heat-transfer rate is smaller leading to a smaller coolant temperature rise and consequent increase in uncertainty in the measured heat flux. The higher scatter of the Refrigerant 11_ low-pressure data reflects the higher vapour-side thermal resistance and consequent lower heat-transfer rate obtained with this fluid.

In figs. 7.15 and 7.16, all of the present results are shown together with those of Nobbs /42 /, Fujii et. al. /50, 60 / and Gogonin and Dorokhov /59 / and are compared with the equations 7.1 and 7.3. It may be seen that the data of the four separate investigations are in quite good general agreement with each other and, taken together, are reasonably well represented by equations 7.1 and 7.3. The data of Gogonin and Dorokhov /59 / are for very low vapour velocities ($\leqslant 0.56$ m/s) and the deviation from the Nusselt prediction is small. The results of Fujii et. al. are rather more scattered than those of the present work and Nobbs. Towards the lower end of the range of Pr_L/FrH ($\leqslant$ about 1.0; fig. 7.15) and of $\sqrt{Re_{TP}}/Fr\tilde{M}$ ($\leqslant$ about 1.0; fig. 7.16), the values of $Nu/\sqrt{Re_{TP}}$ found by Nobbs are generally higher than those of Fujii, while the present values fall roughly between the two. It may be noted that in the above-mentioned ranges, the present data are those for steam at low pressures comparable with those used by Fujii while the data of Nobbs are for atmospheric pressure and higher condensation rates.

In fig. 7.17, the data shown in fig. 7.15 are compared with the theoretical equations of Shekriladze and Gomelauri /24/ and Fujii et. al. /49/, both based on a uniform wall surface temperature analysis and exclude the possibility of separation of the vapour boundary layer (see Chapter 2). (Note that the Shekriladze result is essentially the limiting case of that of Fujii for $RH/Pr_L \rightarrow \infty$ and for practical purpose for RH/Pr_L greater than about 10, see fig. 2.12). The theoretical lines of Fujii et. al. /49 / are plotted for the extreme values of the parameter RH/Pr_L of the experimental data.

There is clear evidence from all four data sets /42, 43, 50, 59, 60 and present / that, except at higher values of Pr_L/FrH (> about 1.0), the above-mentioned theoretical results over-predict the Nusselt number, the discrepancy increasing as the parameter Pr_L/FrH decreases, i.e. as the heat flux and vapour velocity increases.

7.1.2 Considerations relating to the very high vapour velocities

As noted earlier, the data of Nicol and co-workers /37 - 40 /, which extend to significantly higher vapour velocities than those used by Nobbs and Mayhew /42, 43 /, Fujii et. al. /50, 60 /, Gogonin and Dorokhov /59 / and in the present work, indicate markedly lower heat-transfer coefficients than found by the latter workers. This is illustrated in figs. 7.18 and 7.19 plotted on the basis of $Nu/\sqrt{Re_{TP}}$ against Pr_L/FrH and $Nu/\sqrt{Re_{TP}}$ against $\sqrt{Re_{TP}}/Fr\tilde{M}$ respectively. For the ranges of Pr_L/FrH and $\sqrt{Re_{TP}}/Fr\tilde{M}$ where the data of Wallace /38 / overlap those of the other investigators, it can be seen that Wallace's results are clearly lower than those of Nobbs /42 / and the present work and just within the lower bound of the scatter of the data of Fujii et. al. /50, 60/.

It may be noted that in the case of Wallace's investigation, the steam was sampled and the air concentration determined /38 / (see Chapter 2).

When the temperature drop in the vapour-gas boundary layer, determined on the basis of the equation of Rose /72/ (see section 7.2 and Chapter 2), is subtracted from the observed vapour-to-wall temperature difference, and the parameters in figs. 7.18 and 7.19 reevaluated on this basis, somewhat higher values of the Nusselt number are obtained as may be seen in figs. 7.20 and 7.21. The fact that substantial amounts of air (up to about 5 % by mass) has a relatively small effect on the results is due to the very high vapour velocities used.

It may be seen that the reevaluated values of Wallace's /38/ data lie closer to the extrapolated Fujii correlations and appear to blend reasonably well with the results of Fujii and those of the present work while still lying significantly below those of Nobbs and Mayhew. Again, it may be significant to note that the measurements of Wallace /38/ were taken at sub-atmospheric pressures (as were those of Fujii et. al. /50, 60/ and the present work for $Pr_L/FrH <$ about 1.0 while those of Nobbs /42/ were for atmospheric pressure).

Fig. 7.22 shows the same sets of data as fig. 7.20 together with the theoretical lines of Nusselt /2/, Shekriladze and Gomelauri /24/ (no vapour boundary-layer separation case) and Fujii et. al. /49/ (for values of the parameter $RH/Pr_L = 0.5$, $RH/Pr_L = 1.0$ and $RH/Pr_L = 7.0$; the approximate range covered in the experimental data). It is clear that the results of Wallace /38/ (after allowance for the effects of air as indicated above) are well below the uniform-wall-surface-temperature solutions /24, 49/

It has been seen that the correlations of Fujii et. al. /50, 60/ for steam (equations 7.1 and 7.3) are in broad general agreement with the steam data (which in the case of Wallace /38 / extended to well beyond the ranges of the correlations) and also the present data for Refrigerant 113. It should be noted that these correlations suggest that the values of $Nu/\sqrt{Re_{TP}}$ decreases monotonically with decreasing values of Pr_L/FrH. However, it would seem evident that for sufficiently high vapour velocities (i.e. sufficiently low values of Pr_L/FrH), the parameter $Nu/\sqrt{Re_{TP}}$ should approach a constant value where the effect of vapour drag completely overwhelms that of gravity in the manner indicated by the uniform wall surface temperature analyses of Shekriladze and Gomelauri /24/ and Fujii et. al. /49 - 51 /.

It was seen in Chapter 2 that the analysis of Shekriladze and Gomelauri /24/ gives a conservative estimate of $Nu/\sqrt{Re_{TP}}$ (with respect to the analysis of Fujii et. al. /49/) since the former used the asymptotic value of the shear stress on the condensate surface which is less than the actual value. For the case when separation of the vapour boundary layer was neglected, the theory of Shekriladze and Gomelauri predicted a limiting value of $Nu/\sqrt{Re_{TP}}$ of about 0.9. By making the additional conservative approximations that the vapour boundary layer separates at $\phi_s = 82^\circ$ (earliest possible value for flow without suction) and that the heat transfer beyond the separation point is negligible, Shekriladze and Gomelauri obtained a (triply) conservative estimate of $Nu/\sqrt{Re_{TP}}$ of about 0.59. On this basis, Shekriladze and Gomelauri suggested that their equation of $Nu/\sqrt{Re_{TP}}$ as a function of Pr_L/FrH be multiplied by $0.59/0.9 \simeq 0.65$ to allow for vapour boundary layer separation. However, the result in the zero vapour velocity limit is then 65 % that of the Nusselt value which is clearly unsatisfactory. Attention has been drawn to this fact by Butterworth /47 / who suggested that the factor 0.65 be applied to the forced-convection solution before blending with the Nusselt result in the manner adopted by Shekriladze and Gomelauri. This gives:-

$$Nu/\sqrt{Re_{TP}} = 0.416 \left[1 + (1 + 9.467\ Pr_L/FrH)^{\frac{1}{2}}\right]^{\frac{1}{2}} \qquad (7.6)$$

Equation 7.6 is compared with the data of Wallace /38 / (with the temperature drop across the vapour-gas layer accounted for by the method of Rose /72 /), Nobbs /42 /, Fujii et. al. /50, 60 /, Gogonin and Dorokhov /59 / and the present results in fig. 7.23. With the exception of the results of Wallace and a few of the relatively widely-scattered points of Fujii et. al., the bulk of the data supports the contention that equation 7.6 is indeed conservative.

To summarise, there is apparently good evidence (both theoretical and experimental) that equation 7.6 should be conservative. However, the work of Wallace suggests that at low values of Pr_L/FrH (i.e. high vapour velocities and high condensation rates) this is not the case. This issue evidently needs to be resolved.

7.1.3 Alternative method of displaying the experimental and theoretical results

As noted above, the variables used as co-ordinates for displaying the results arose from theoretical considerations. They do not, however, readily convey information relating to the effect of vapour velocity on the rate of heat transfer. For this purpose, the experimental /38,42,50,59,60 and present / and theoretical /24,49 / results and the correlations of Fujii et. al. /50, 60/ have been replotted in figs. 7.24 and 7.25 on the basis outlined below.

It was seen in Chapter 2 that the "Nusselt theory" (based on both the uniform wall surface temperature /2 / and the uniform wall heat flux / 21 /) is sufficiently accurate for predicting filmwise condensation heat transfer of a stationary vapour on a horizontal tube. Thus, by dividing the value of the Nusselt number for the case when the vapour is moving by the corresponding value (i.e. for the same ΔT or for the same $\dot{Q}''$) obtained from the "Nusselt theory", the effect of vapour velocity is indicated by the divergence of the result from unity.

The Nusselt numbers for the stationary vapour case are:

$$Nu_{Nu} = 0.728\ (Ga\ Pr_L/H)^{\frac{1}{4}} \tag{7.7a}$$

for the case of uniform wall surface temperature, and

$$Nu_{Nu} = 0.615\ (Ga/\tilde{M})^{\frac{1}{5}} \tag{7.7b}$$

for the case of uniform wall heat flux.

For the moving vapour case, the uniform-wall-temperature analysis of Fujii et. al. /49/ indicated that

$$\frac{Nu}{\sqrt{Re_{TP}}} = \phi_1\left[\frac{Pr_L}{FrH}, \frac{RH}{Pr_L}\right]$$

Thus,

$$\frac{Nu}{Nu_{Nu}} = \frac{\sqrt{Re_{TP}}\ \phi_1(Pr_L/FrH,\ RH/Pr_L)}{0.728\ (Ga\ Pr_L/H)^{\frac{1}{4}}}$$

i.e. $$\frac{Nu}{Nu_{Nu}} = \frac{\phi_1(Pr_L/FrH\ ,\ RH/Pr_L)}{0.728\ (Pr_L/FrH)^{\frac{1}{4}}} \qquad (7.8)$$

Similarly, the equations of Fujii et. al. /50, 60/ and Shekriladze and Gomelauri /24 / can be normalised thus :

$$\frac{Nu}{Nu_{Nu}} = \frac{\phi_2\ (Pr_L/FrH)}{0.728\ (Pr_L/FrH)^{\frac{1}{4}}} \qquad (7.9)$$

Note that in equations 7.8 and 7.9,

$$\frac{Nu}{Nu_{Nu}} = \frac{\dot{Q}''}{\dot{Q}''_{Nu}} \qquad (7.10)$$

where $\dot{Q}''_{Nu}$ is the mean heat flux given by the simple Nusselt theory /2 / for the same ΔT as that used when evaluating the mean $\dot{Q}''$ for the case of the moving vapour.

Similarly, for the uniform-wall-heat-flux case, the correlation of Fujii et. al. /50, 60 / indicated that

$$\frac{Nu}{\sqrt{Re_{TP}}} = \phi_3 \left(\sqrt{Re_{TP}}/Fr\tilde{M}\right)$$

Thus,

$$\frac{Nu}{Nu_{Nu}} = \frac{\sqrt{Re_{TP}}\,\phi_3\left(\sqrt{Re_{TP}}/Fr\tilde{M}\right)}{0.615\,(Ga/\tilde{M})^{\frac{1}{3}}}$$

i.e.

$$\frac{Nu}{Nu_{Nu}} = \frac{\phi_3\left(\sqrt{Re_{TP}}/Fr\tilde{M}\right)}{0.615\left(\sqrt{Re_{TP}}/Fr\tilde{M}\right)^{\frac{1}{3}}} \qquad (7.11)$$

Note that in equation 7.11,

$$\frac{Nu}{Nu_{Nu}} = \frac{\Delta T_{Nu,Q}}{\Delta T} \qquad (7.12)$$

where $\Delta T_{Nu,Q}$ is the mean temperature drop across the condensate film given by the uniform wall heat flux "Nusselt" theory /21 / for the same $\dot{Q}''$ as that used when evaluating the mean ΔT for the case of the moving vapour.

In figs. 7.24 and 7.25, the curves for the theoretical equations and correlations were plotted as indicated above. The experimental points in fig. 7.24 were plotted on the same basis as the curves for equations 7.8 and 7.9 while those in fig.7.25 were plotted on the same basis as the curve for equation 7.11. In these figures, reciprocals of the parameters $Pr_L/Fr\tilde{H}$ and $\sqrt{Re_{TP}}/Fr\tilde{M}$ have been used as abscissae so that increasing values of the abscissae correspond to increasing values of vapour velocity (and increasing ΔT in the case of $Fr\tilde{H}/Pr_L$ and increasing $\dot{Q}''$ in the case of $Fr\tilde{M}/\sqrt{Re_{TP}}$). The conclusions drawn earlier in sections 7.11 and 7.12 may again be deduced from figs. 7.24 and 7.25.

7.2 Vapour-gas mixtures

The present results (four different vapour-gas mixtures (steam-air, steam-hydrogen, Refrigerant 113-air and Refrigerant 113-hydrogen), two tube diameters (12.5 mm and 25.25 mm) and a range of pressures) are examined in the light of recent observations for steam-air mixtures of Mills et. al. /76 /, Fujii et. al. /52, 77 / and the empirical correlation (for steam-air mixtures only) of Berman /87,90/, the semi-empirical correlation of Mills et. al. /76 / (based on the theoretical analysis of Acrivos /88 / for boundary-layer flow with strong suction and using data for steam-air mixtures only) and the theoretical equation of Rose /72 /. For steam-air mixtures, it was seen in Chapter 2 that Rose's equations 2.53 are in satisfactory agreement with Berman's correlation, see fig. 2.32, (except for $W_i/W_\infty \rightarrow 1$ where the latter behaves incorrectly).

According to the theory of Rose /72 /, the dimensionless quantity $Sh/\sqrt{Re_v}$ is related to the far-to-near gas mass fraction ($\omega = W_\infty/W_i$) and the Schmidt number (Sc) thus,

$$Sh/\sqrt{Re_v} = \left[1 + 2.28Sc^{\frac{1}{3}}\,(\omega^{-1} - 1)^{\frac{1}{2}} - 1\right]/(2 - 2\omega) \qquad (7.13)$$

where Sh is the Sherwood number, $\dot{m}''\, d_o/\rho_v D\,(1 - \omega)$

Re_v is the gas-phase Reynolds number, $U_\infty d_o \rho_v / \mu_v$

$\dot{m}''$ is the condensation flux

D is the binary diffusion coefficient

The semi-empirical correlation of Mills et. al. /76 / contains the vapour Reynolds number (Re_v) as an additional parameter. Figs. 7.26 show the comparison (on the basis of $Sh/\sqrt{Re_v}$ against $1/\omega$) of the equations of Rose and Mills for a wide range of Schmidt number which includes the range covered in the present work. For each Schmidt number where experimental data is available, the ranges of Re_v used in calculating the Mills prediction are those used in the experiments. For the cases where no experimental data is available, the ranges of Re_v chosen are from 100 to 10000. Also shown in the figure are the approximate ranges covered in the present investigation. It is evident that the equation of Rose /72 / and Mills et. al. /76 / (i.e. equations 2.53 and 2.56 respectively; equation 2.53c is rewritten here as equation 7.13) are in satisfactory agreement, for the range of the experimental data, figs. 7.26. The present results are therefore compared only with the equation of Rose.

In order to make comparisons relating to the vapour-gas layer only (i.e. excluding the effect of the condensate film), an estimate must be made of the effective thermal resistance of (or mean temperature drop across) the condensate layer so that this may be subtracted from the overall resistance (or overall temperature drop) between the bulk vapour and the condenser tube outside wall. In the present work, the semi-empirical correlation of Fujii et. al. /50, 60/ based on the uniform wall heat flux theory (i.e. equation 7.3) has been used for the condensate film. As was seen in section 7.1, this equation is in very good agreement with the present results for pure steam and pure Refrigerant 113 (see figs. 7.8 to 7.14). In calculating the mean temperature drop across the condensate film, an iterative procedure was used. Starting with a guessed interfacial temperature (T_i) the heat flux calculated from equation 7.3 for the condensate film was determined. Using an iterative procedure, the calculation was repeated (at each step the new estimate of the interfacial temperature, T_i, was used) until the heat flux given by equation 7.3 for the condensate film differed from the observed value by less than 1 kW/m^2 (which is 0.005 % of the lowest observed heat flux), see Appendix F. Having found the interfacial temperature, the values of $Sh/\sqrt{Re_v}$ and ω can then be evaluated as indicated in Appendix F.

On the basis of equation 7.13, the steam-air data of Mills et. al. /76 /, Fujii et. al. /52, 77 / and the present work (steam-air mixtures) for which the Schmidt number is essentially constant (approximately 0.5), may be compared on a single graph, fig.7.27. As will be seen later, these data extend from those cases where the dominant resistance is that of the condensate film (lowest gas concentrations and highest vapour velocities) to those where the gas-phase resistance is the controlling factor. It is clear from the figure that the range of W_i/W_∞ (i.e. $1/\omega$) extends approximately from 2 to 40 and that the agreement between the observed and calculated values is excellent over the whole range. This lends strong support to equation 7.13. It may be noted that the measurements of Mills et. al. /76 / are for relatively low vapour velocities (< 1.0 m/s) while those of Fujii et. al. /52, 77/ extend to higher vapour velocities (2 to 48 m/s). Both measurements were obtained at sub-atmospheric pressures and for only one tube. The range of vapour velocities used in the present work is from 0.3 to 25.7 m/s. The present data were obtained with two tubes of different diameters and for both atmospheric and sub-atmospheric pressures.

In the above and subsequent comparisons (except where stated), the properties of the vapour-gas mixture and those of the condensate film have been calculated on the following basis. For the vapour-gas layer, the density and viscosity were taken as the arithmetic means of their values at, and remote from, the vapour-condensate interface; the densities being evaluated on the basis of ideal-gas mixtures and the viscosities by the method of Wilke /92a/, see Appendix E. The diffusion coefficient was taken at $(T_\infty + T_i)/2$. The properties of the condensate film were evaluated as for the pure vapour cases, see section 7.11.

Besides the steam-air mixtures, three other vapour-gas combinations (steam-hydrogen, Refrigerant 113-air and Refrigerant 113-hydrogen) were used in the present investigation. In order to test the theory /72 / for a wide range of parameters, these vapour-gas combinations were chosen so that the relevant thermophysical properties would be markedly different from those of steam-air mixtures. Thus the theoretical predictions using equation 7.13 for the four different vapour-gas combinations differed widely. In particular, the Schmidt number for the above mixtures are approximately 0.5, 0.2, 0.2 and 0.05 respectively.

The different vapour-gas combinations and test conditions used are summarised in Table 7.1. It may be seen from the Table that the vapour-gas combinations fall predominantly into three Schmidt number ranges. On this basis, the theoretical results (equation 7.13) have been evaluated for values of Sc = 0.5, 0.2 and 0.05, and are compared with the relevant experimental results in figs. 7.28 to 7.35. A separate graph is given for each of the four vapour-gas combinations, for each of the two tube diameters and for each pressure used. It is evident that in all cases, the theory correctly predicts the relationship between $Sh/\sqrt{Re_v}$ and ω ($= W_\infty/W_i$) and the dependence of this relationship on the Schmidt number.

Since the Schmidt numbers used in the present investigation fall predominantly into three narrow ranges, a comparison for each range was made on the relation between $Sh/\sqrt{Re_v}$ and $1/\omega$, figs. 7.36 to 7.38. On each graph, all of the present data (for the relevant Schmidt number) together with the steam-air data of Fujii et. al. /52, 77 / and Mills et. al. /76 / ($Sc \simeq 0.5$) are included. In fig. 7.39, all the data given in figs. 7.36 to 7.38 are shown together. It is clear that in all cases, the measurements are in good agreement with each other and with theory /72 /.

As may be seen in Table 7.1, the Schmidt number varied somewhat for each individual data set. A more detailed comparison is therefore given in Tables 7.2 to 7.9 and in figs. 7.40 to 7.43 (corresponding to figs. 7.36 to 7.39) which are plotted on the basis of calculated heat flux against observed heat flux. The calculated heat flux was determined on the basis of coupling equation 7.3 (condensate film) with equation 7.13 (vapour-gas layer) in the following manner. Starting with a guessed interfacial temperature (T_i), the heat fluxes given by equations 7.3 (condensate film) and 7.13 (vapour-gas layer) were determined. Using an iterative procedure, the calculation was repeated (at each step the new estimate of the interfacial temperature, T_i, was used) until the difference in the heat flux given by equation 7.3 and that given by equation 7.13 was less than 1 W/m^2 (which is 0.005 % of the lowest observed heat flux), see

Appendix F. The value of T_i thus found showed that the results extend from those cases where $(T_i - T_w) >> (T_\infty - T_i)$, (i.e. the condensate film is the dominant resistance to heat transfer), to those cases where $(T_i - T_w) << (T_\infty - T_i)$, (i.e. the vapour-gas layer is the dominant resistance to heat transfer). As expected, it is evident that in all cases, the agreement between the observed and calculated heat fluxes is excellent (within ± 10 %).

As noted in Chapter 3, one of the aims of the present investigation was to determine, on the basis of the experimental measurements, improved values of the constants a, b and c (see equation 2.51, Chapter 2) which in the theory of Rose /72 / was provisionally set to unity in each case. In view of the excellent agreement between theory and experiment, it is recommended that the adopted values a = b = c = 1 be retained.

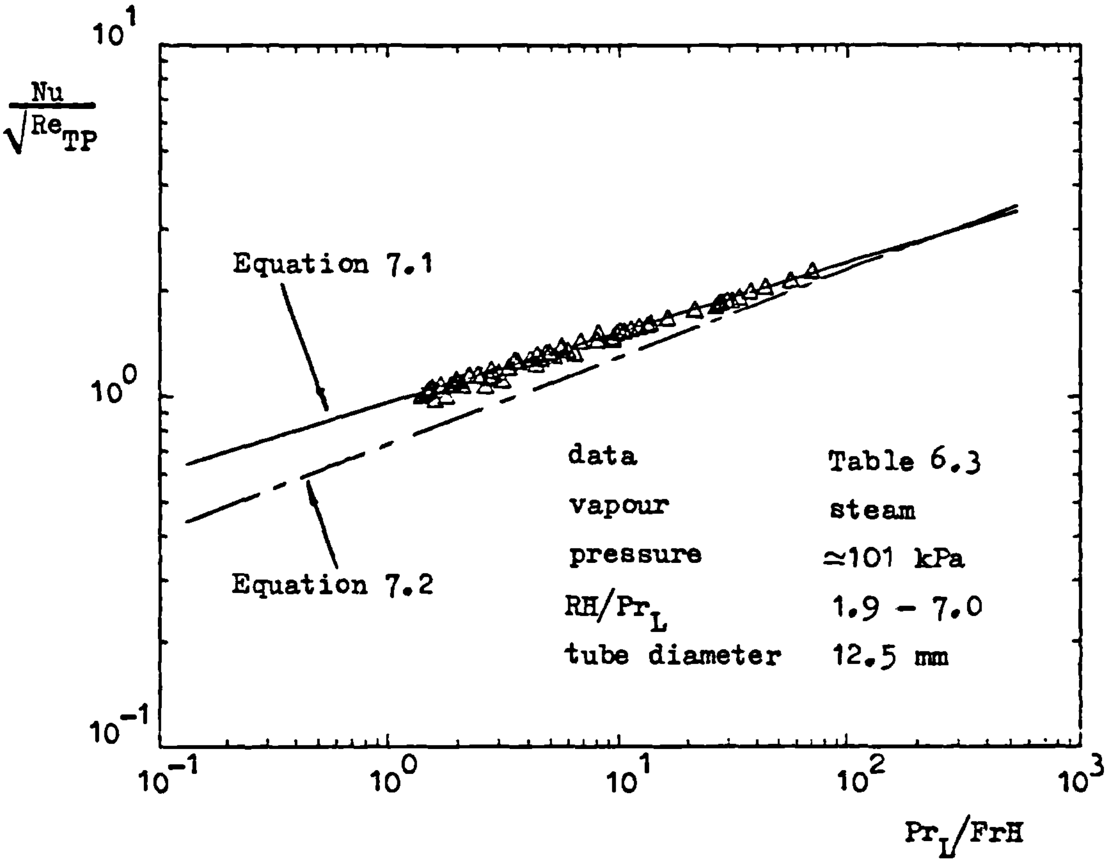

Figure 7.1 Comparison of present results with the correlation of Fujii et. al. /50, 60/

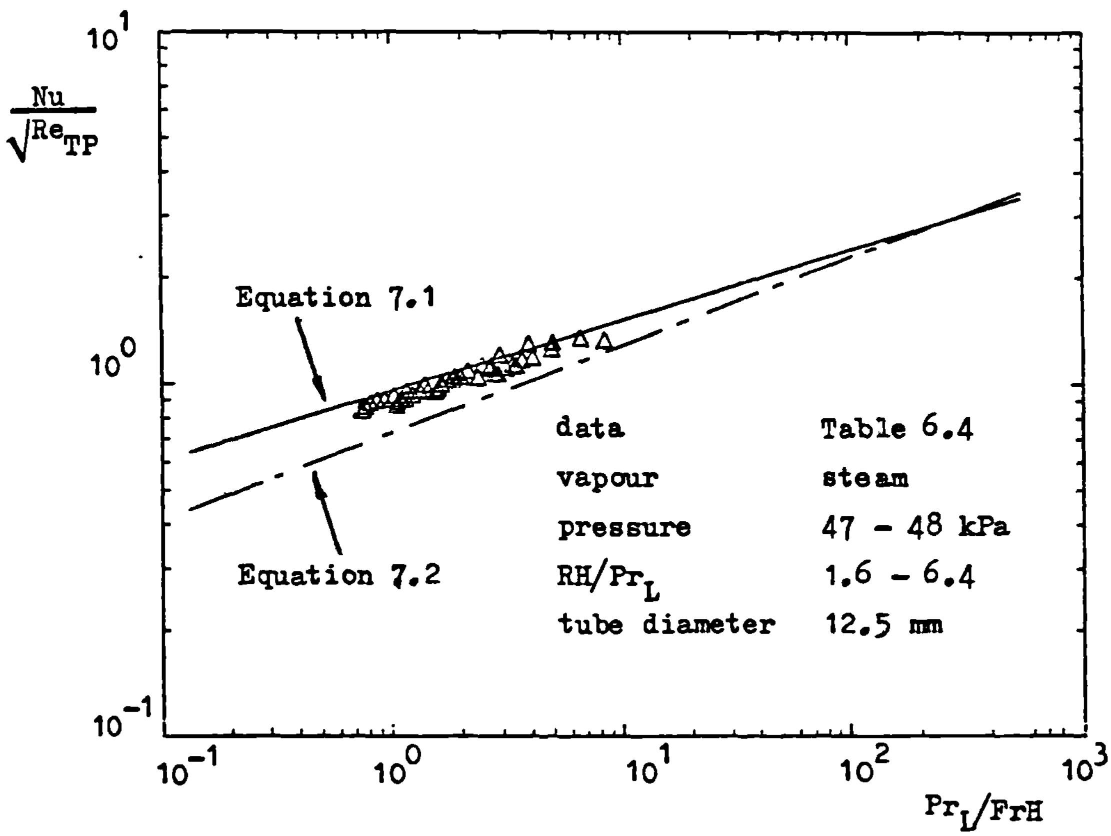

Figure 7.2 Comparison of present results with the correlation of Fujii et. al. /50, 60/

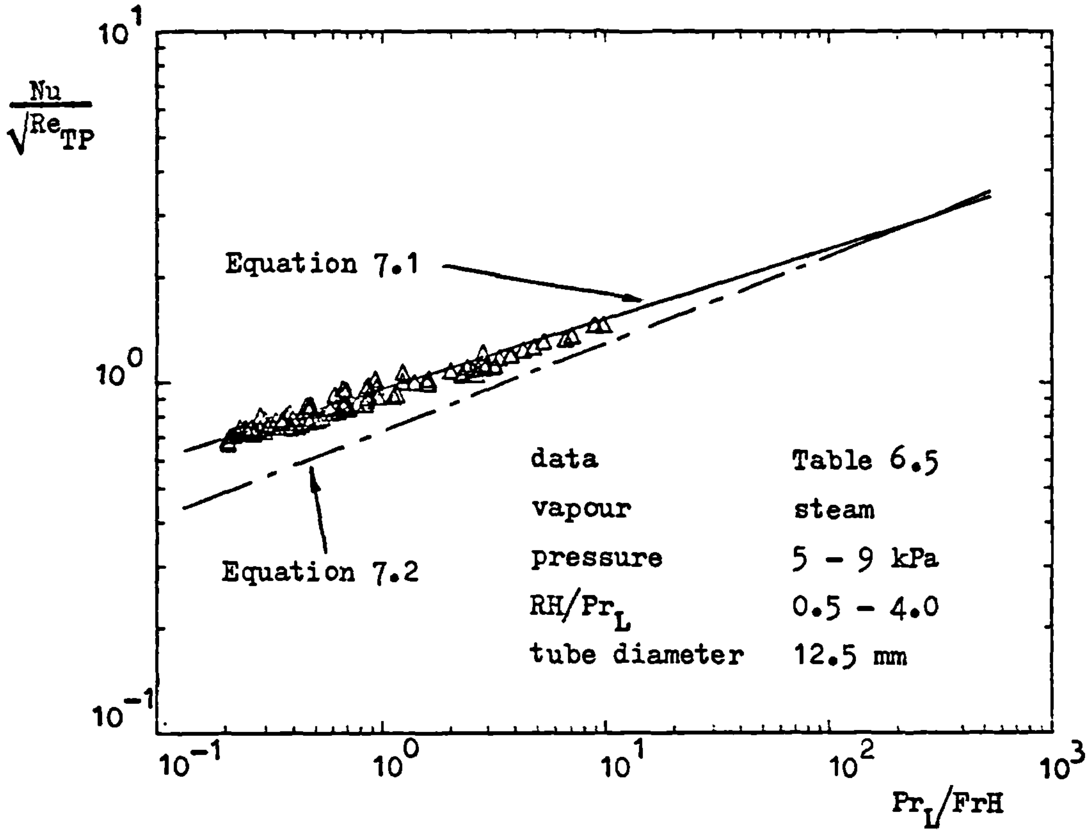

Figure 7.3 Comparison of present results with the correlation of Fujii et. al. /50, 60/

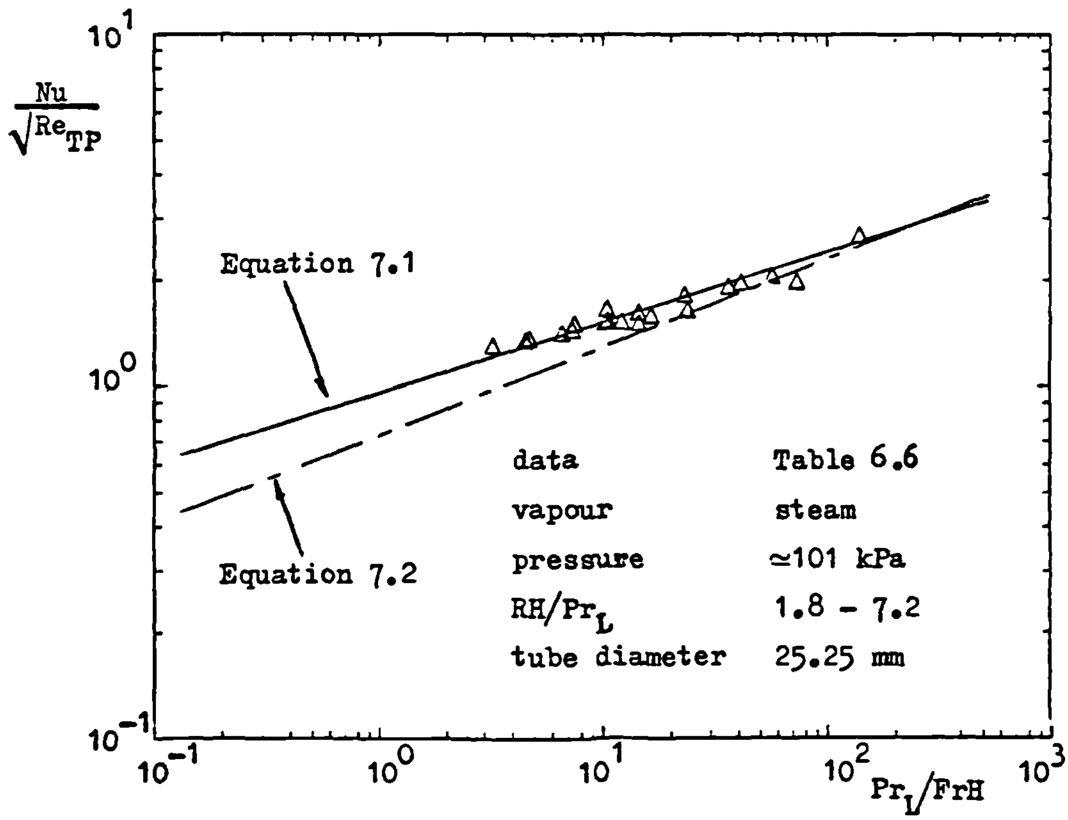

Figure 7.4 Comparison of present results with the correlation of Fujii et. al. /50, 60/

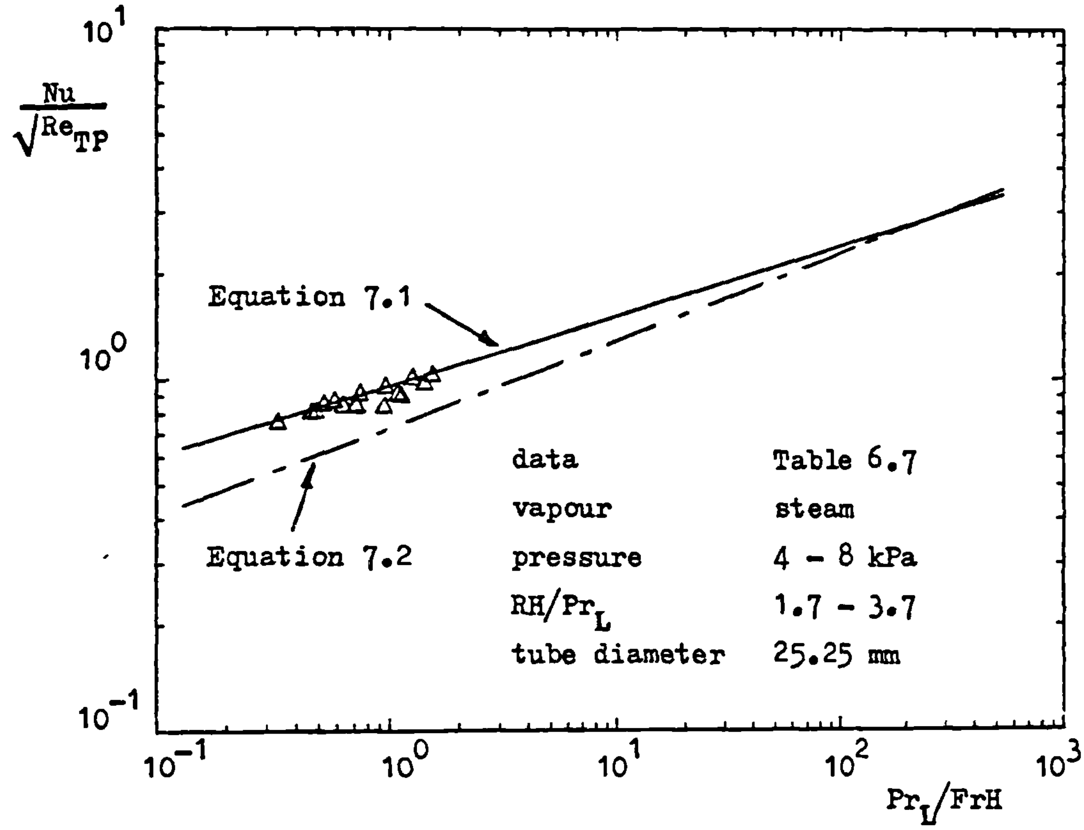

Figure 7.5 Comparison of present results with the correlation of Fujii et. al. /50, 60/

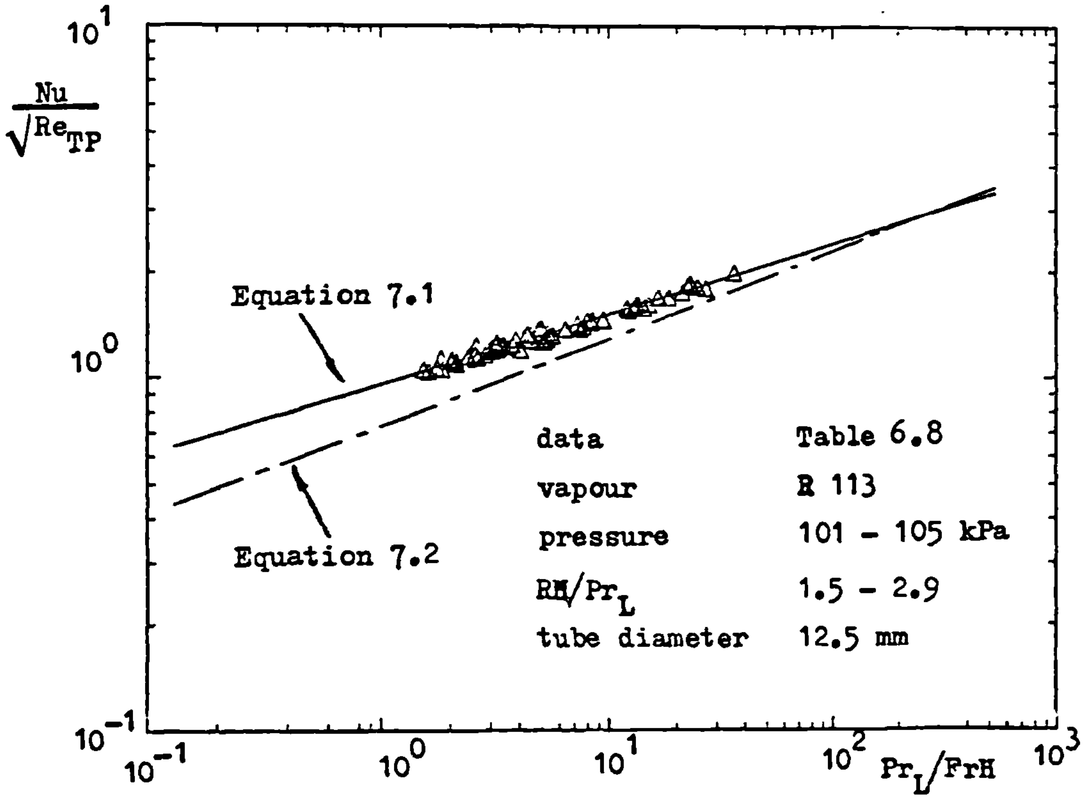

Figure 7.6 Comparison of present results with the correlation of Fujii et. al. /50, 60/

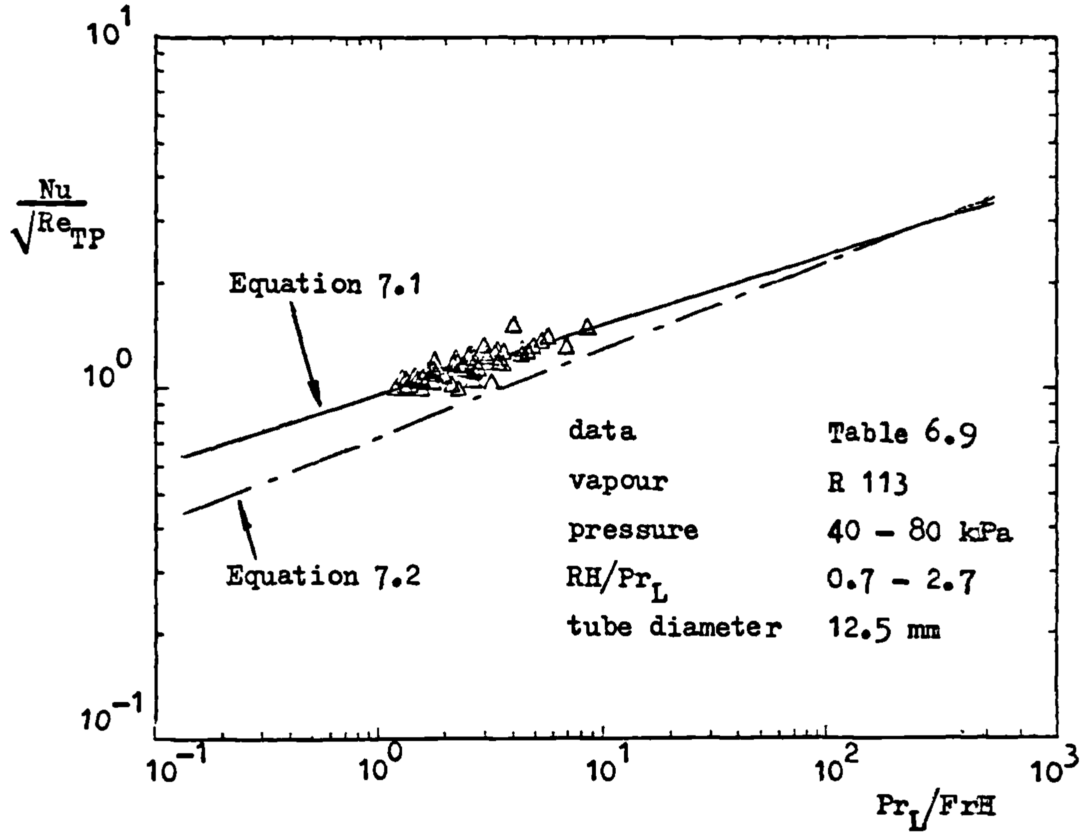

Figure 7.7 Comparison of the present results with the correlation of Fujii et. al. /50, 60/

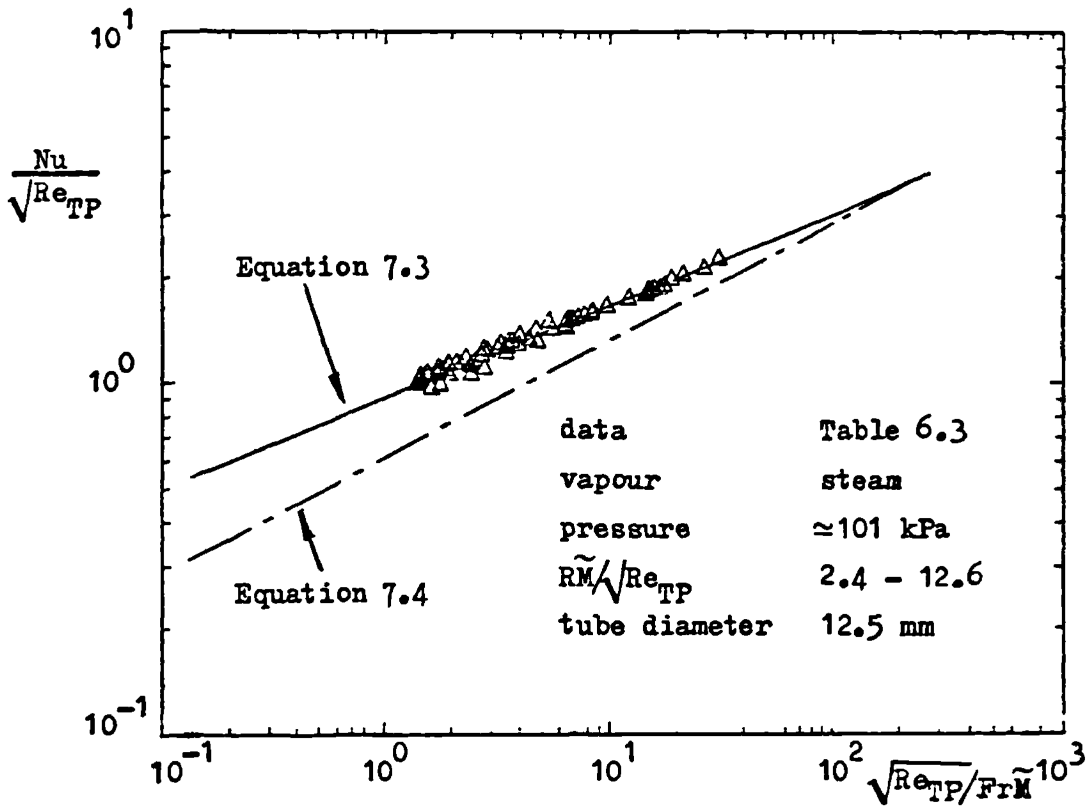

Figure 7.8 Comparison of present results with the correlation of Fujii et. al. /50, 60/

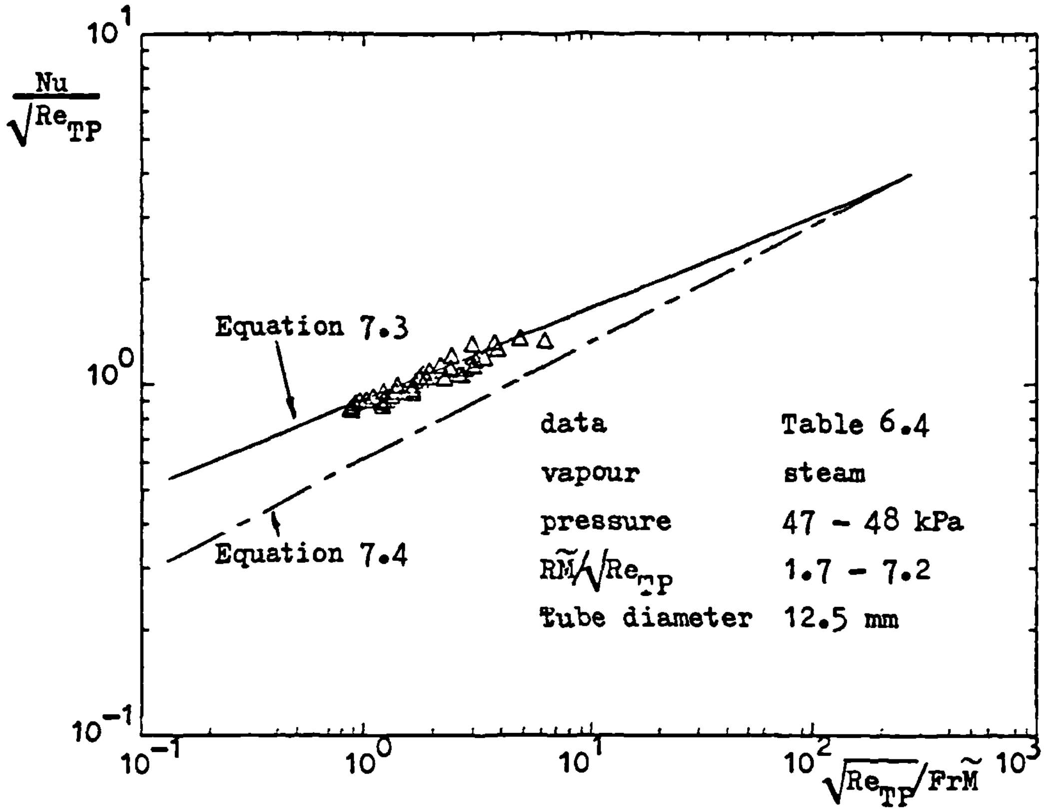

Figure 7.9 Comparison of present results with the correlation of Fujii et. al. /50, 60/

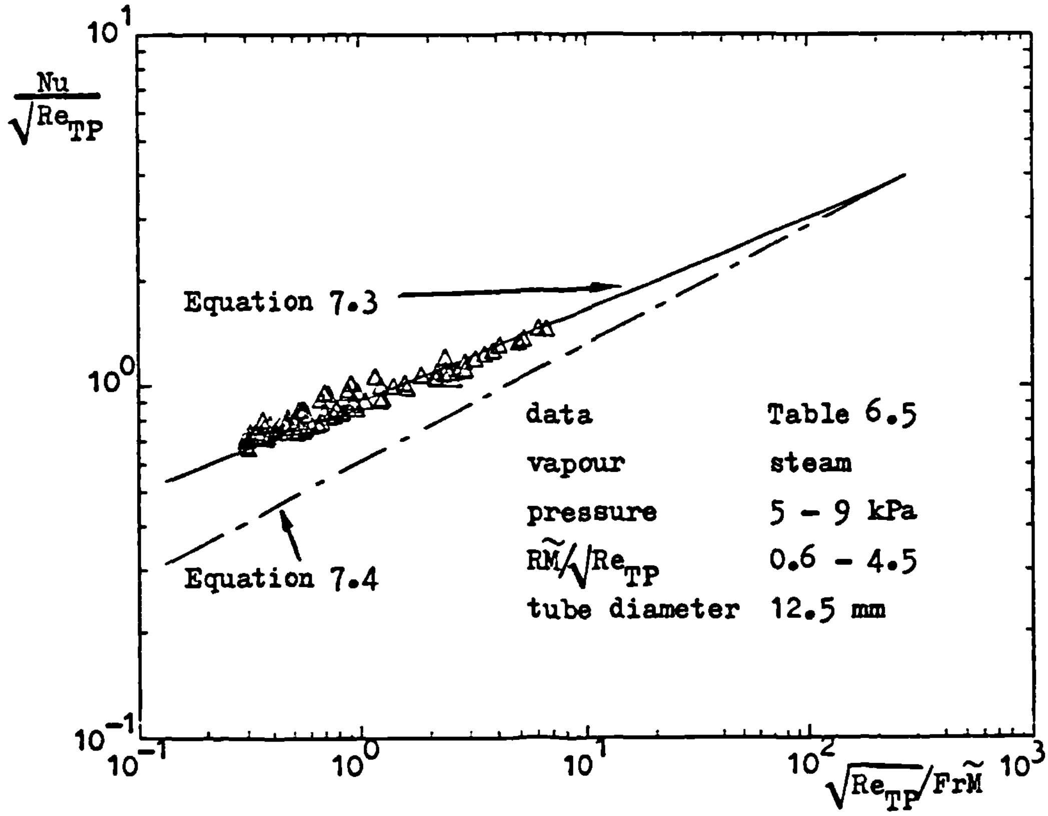

Figure 7.10 Comparison of present results with the correlation of Fujii et. al. /50, 60/

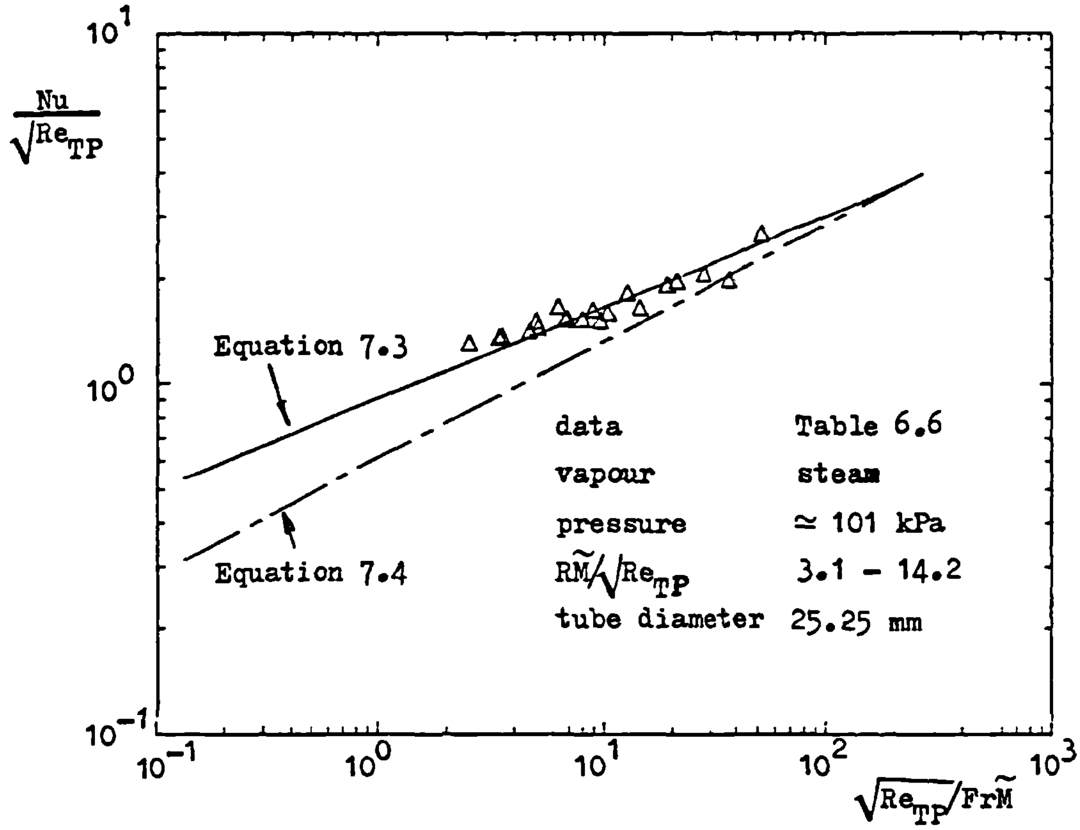

Figure 7.11 Comparison of present results with the correlation of Fujii et. al. /50, 60/

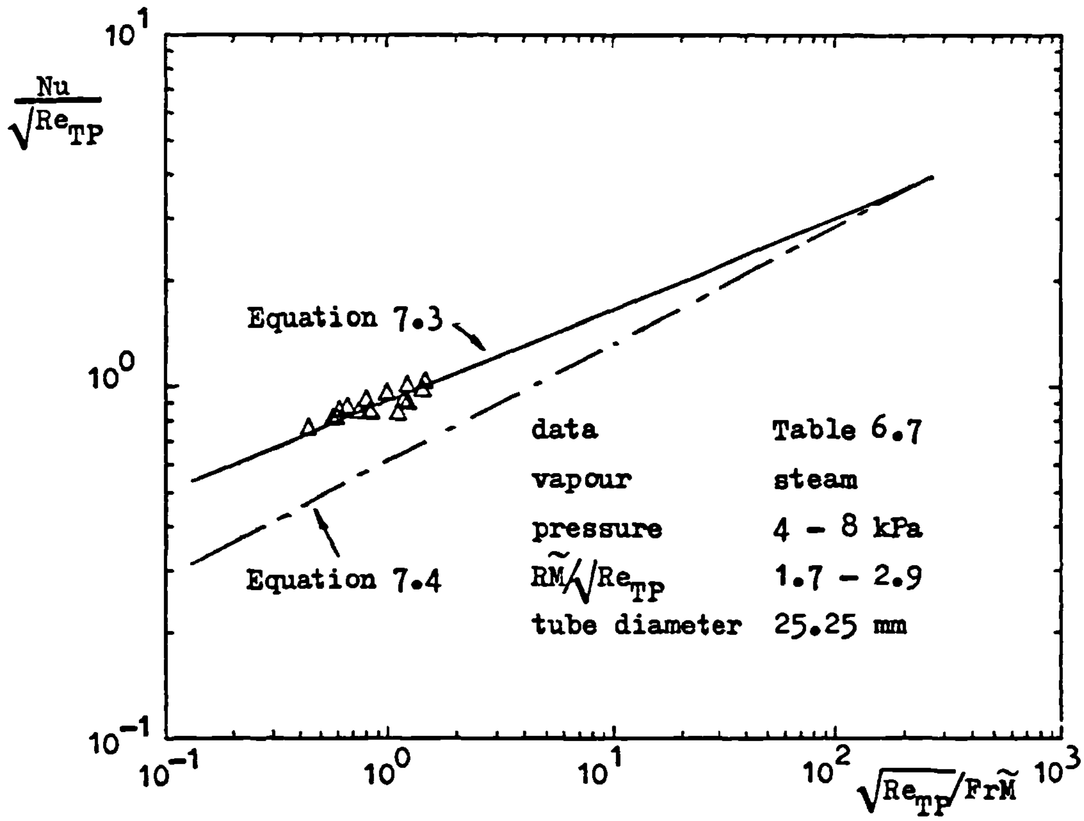

Figure 7.12 Comparison of present results with the correlation of Fujii et. al. /50, 60/

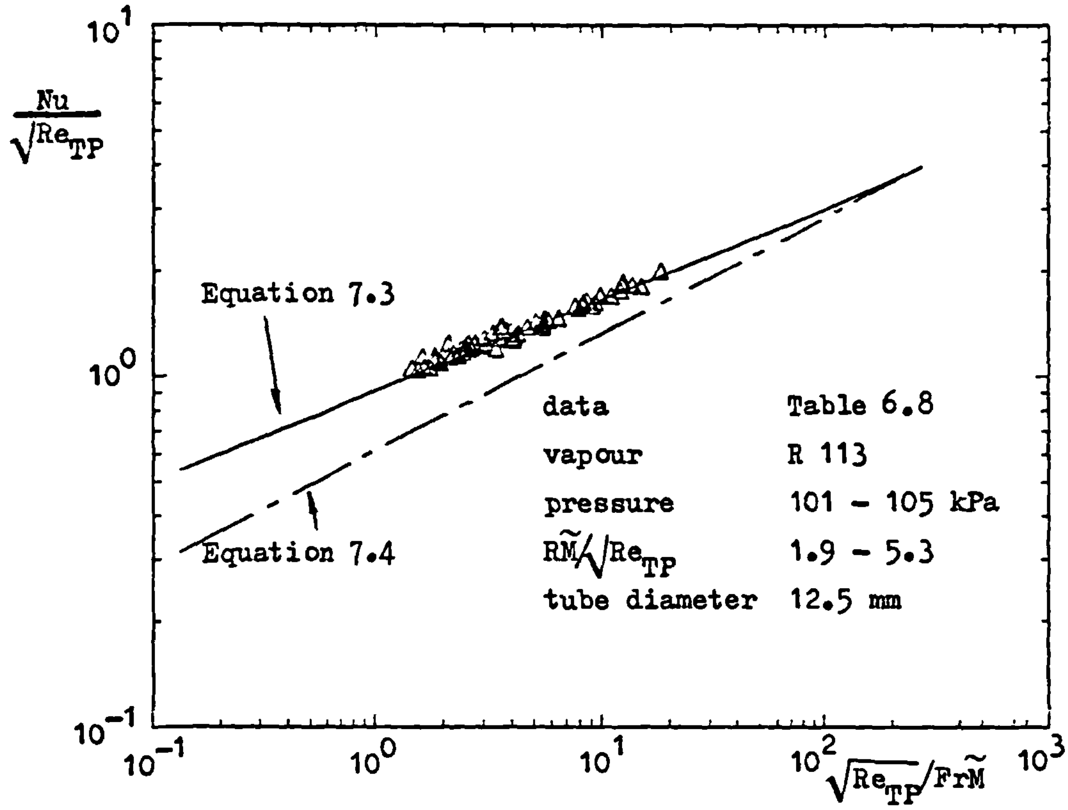

Figure 7.13 Comparison of present results with the correlation of Fujii et. al. /50, 60/

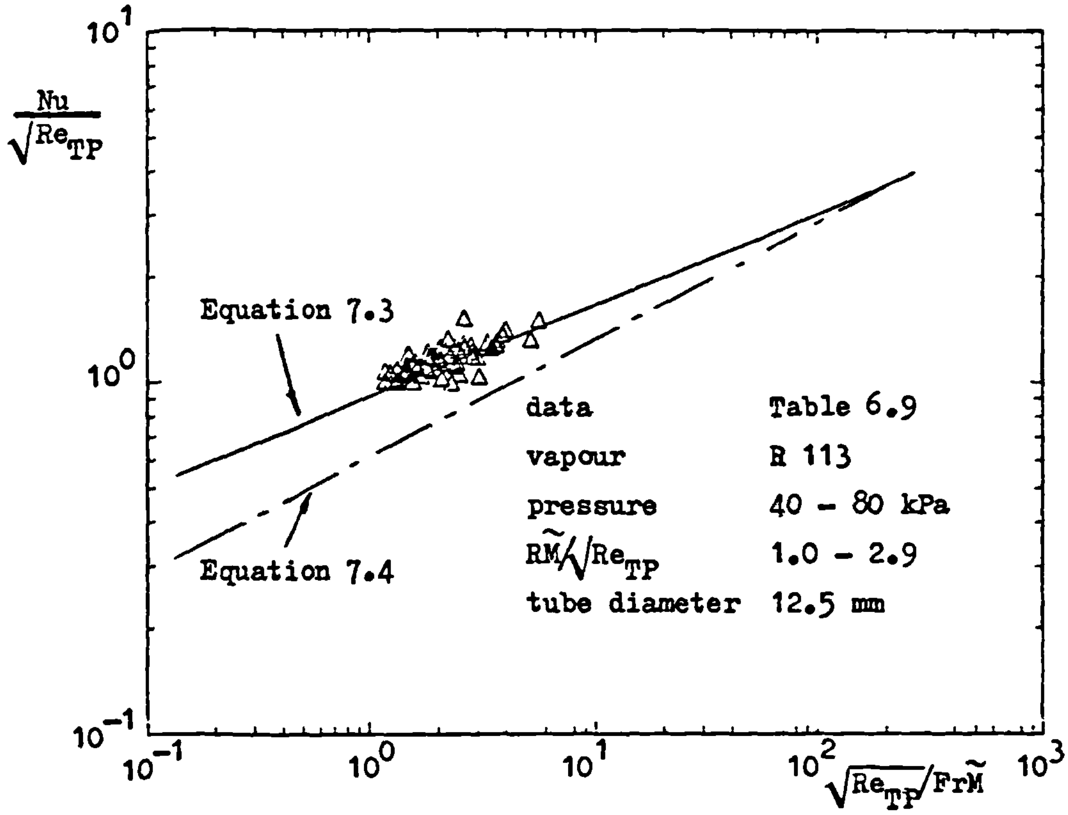

Figure 7.14 Comparison of present results with the correlation of Fujii et. al. /50, 60/

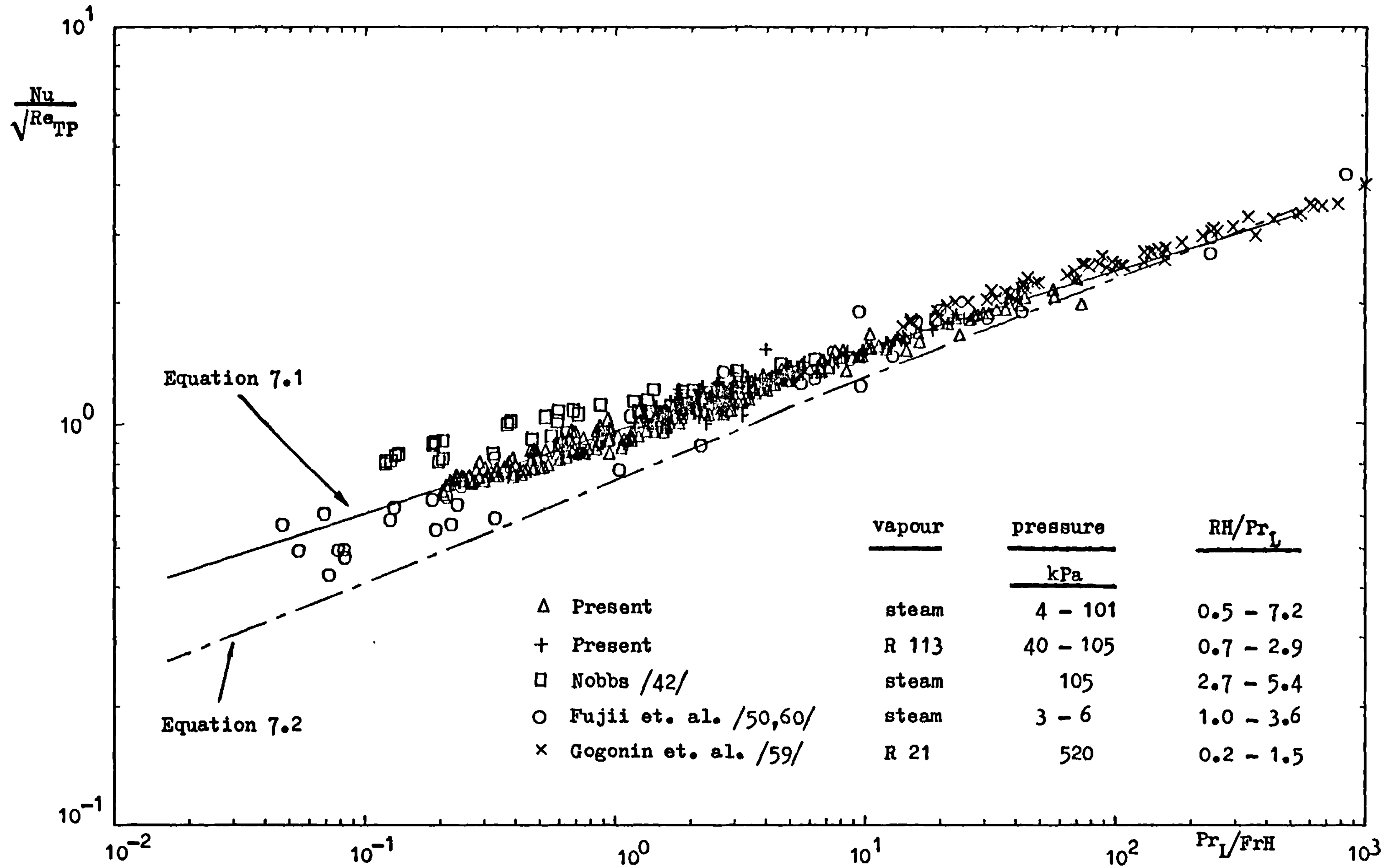

Figure 7.15 Comparison of present results and those of Nobbs /42 /, Fujii et. al. /50, 60/ and Gogonin et. al. /59 / with the correlation of Fujii et. al. /50,60/

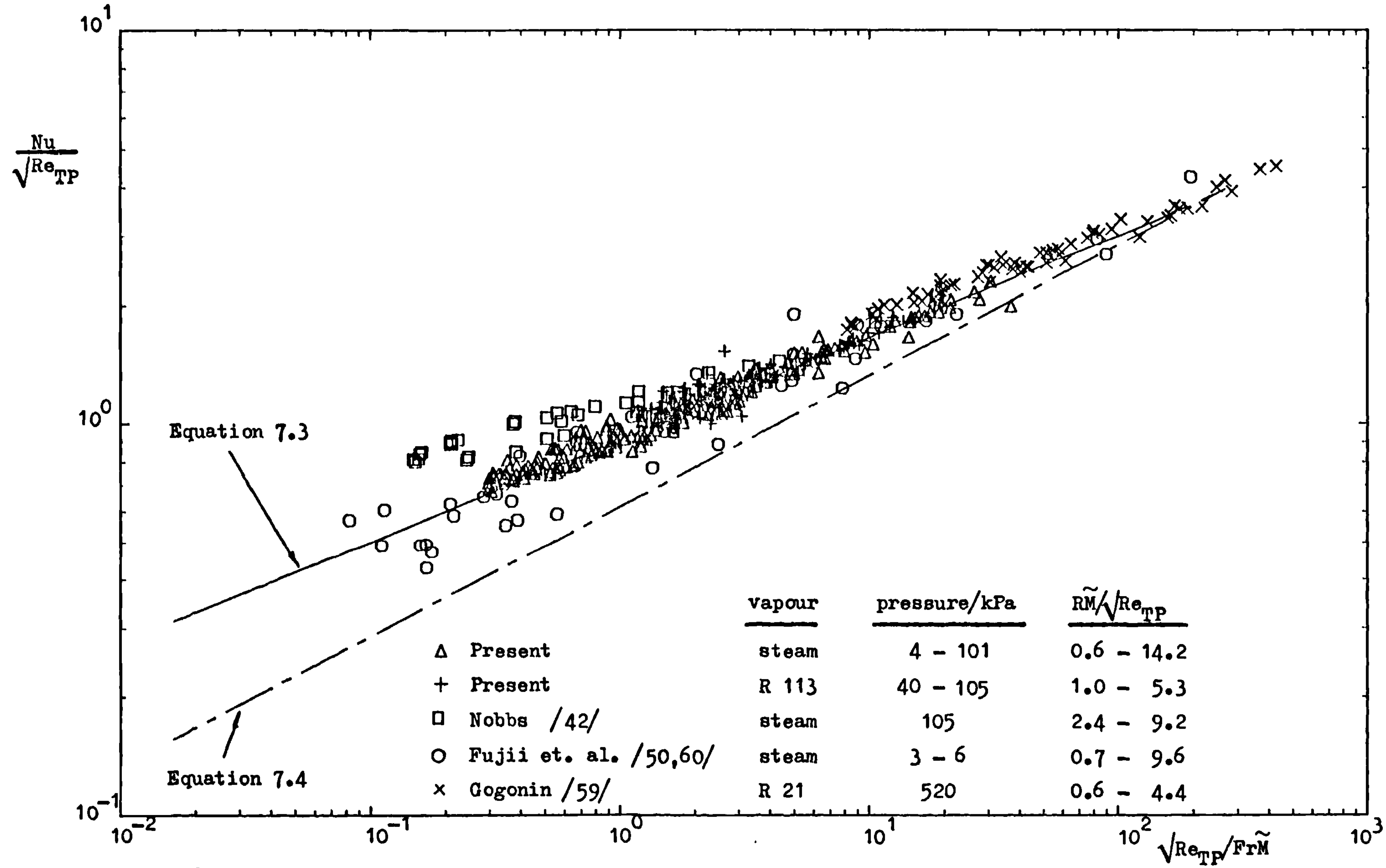

Figure 7.16 Comparison of present results and those of Nobbs /42 /, Fujii et. al. /50,60/ and Gogonin et. al. /59 / with the correlation of Fujii et. al. /50,60/

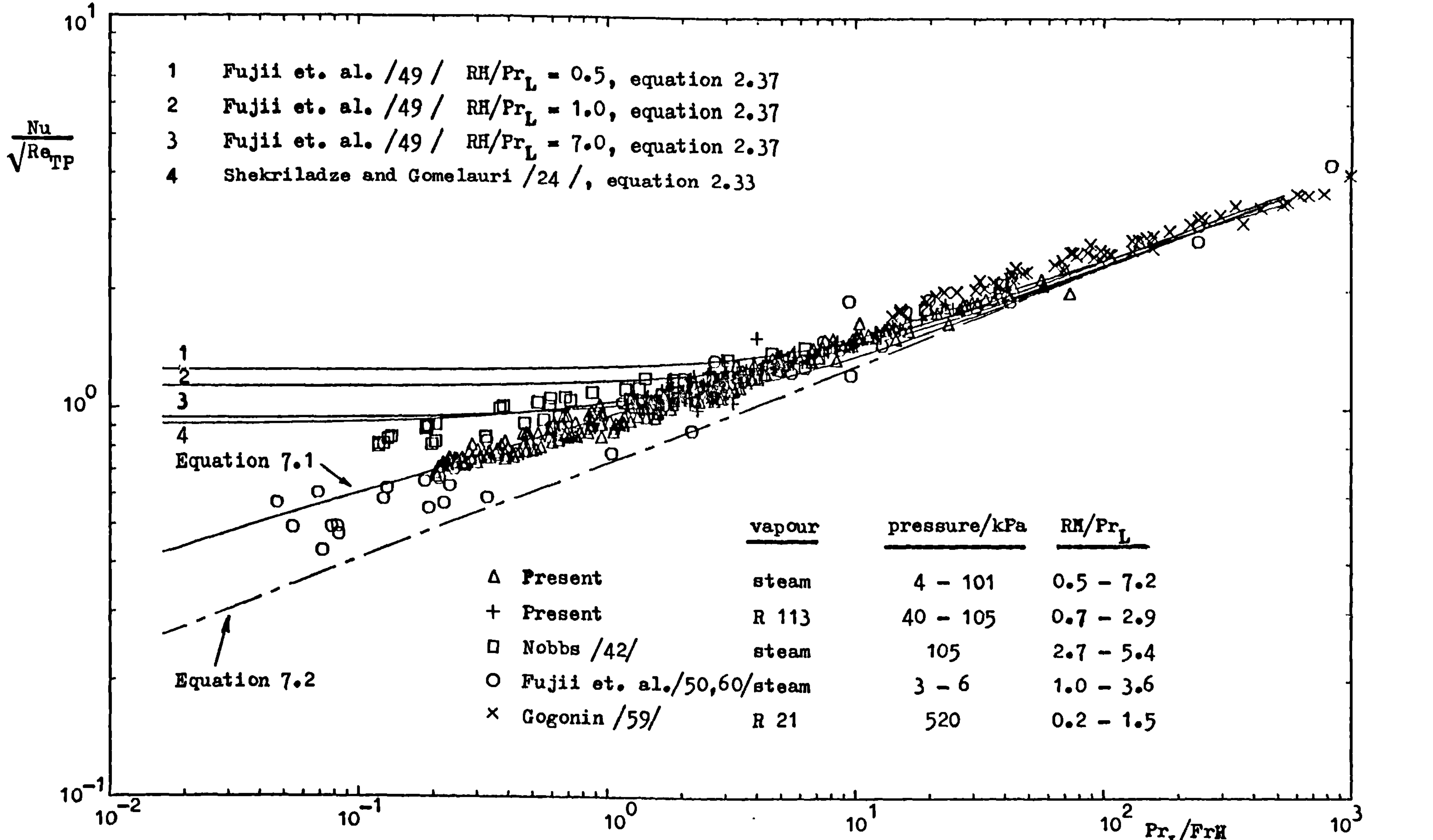

Figure 7.17 Comparison of present results and those of Nobbs /42 /, Fujii et. al. /50,60/ and Gogonin et. al. /59 / with the correlations of Fujii et. al. /50,60/ and the theories of Fujii et. al. /49 / and Shekriladze and Gomelauri /24 /

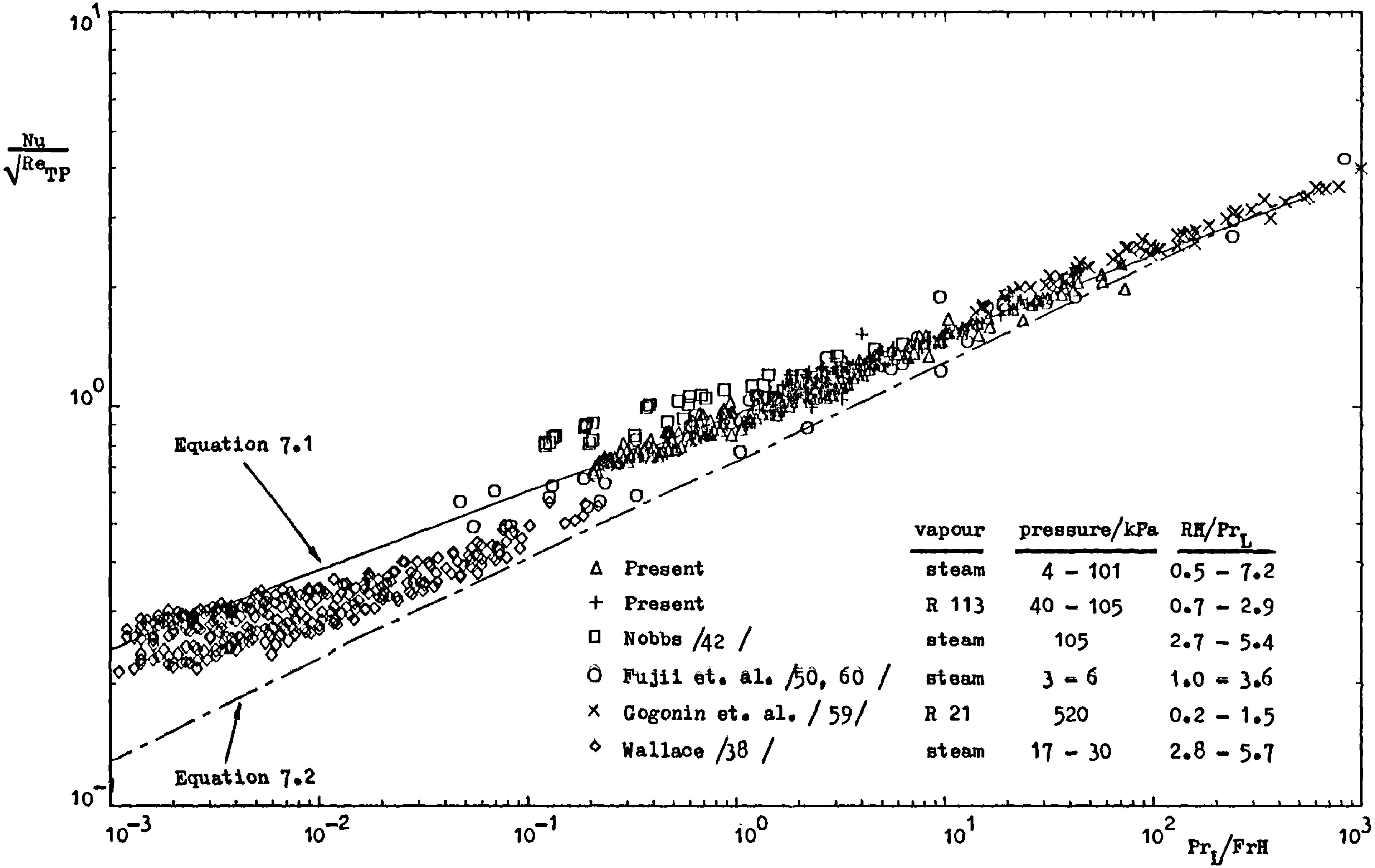

Figure 7.18 Comparison of present results and those of Nobbs /42 /, Fujii et. al. /50, 60/, Gogonin et. al. /59 / and Wallace /38 / with the correlation of Fujii et. al. / 50, 60/

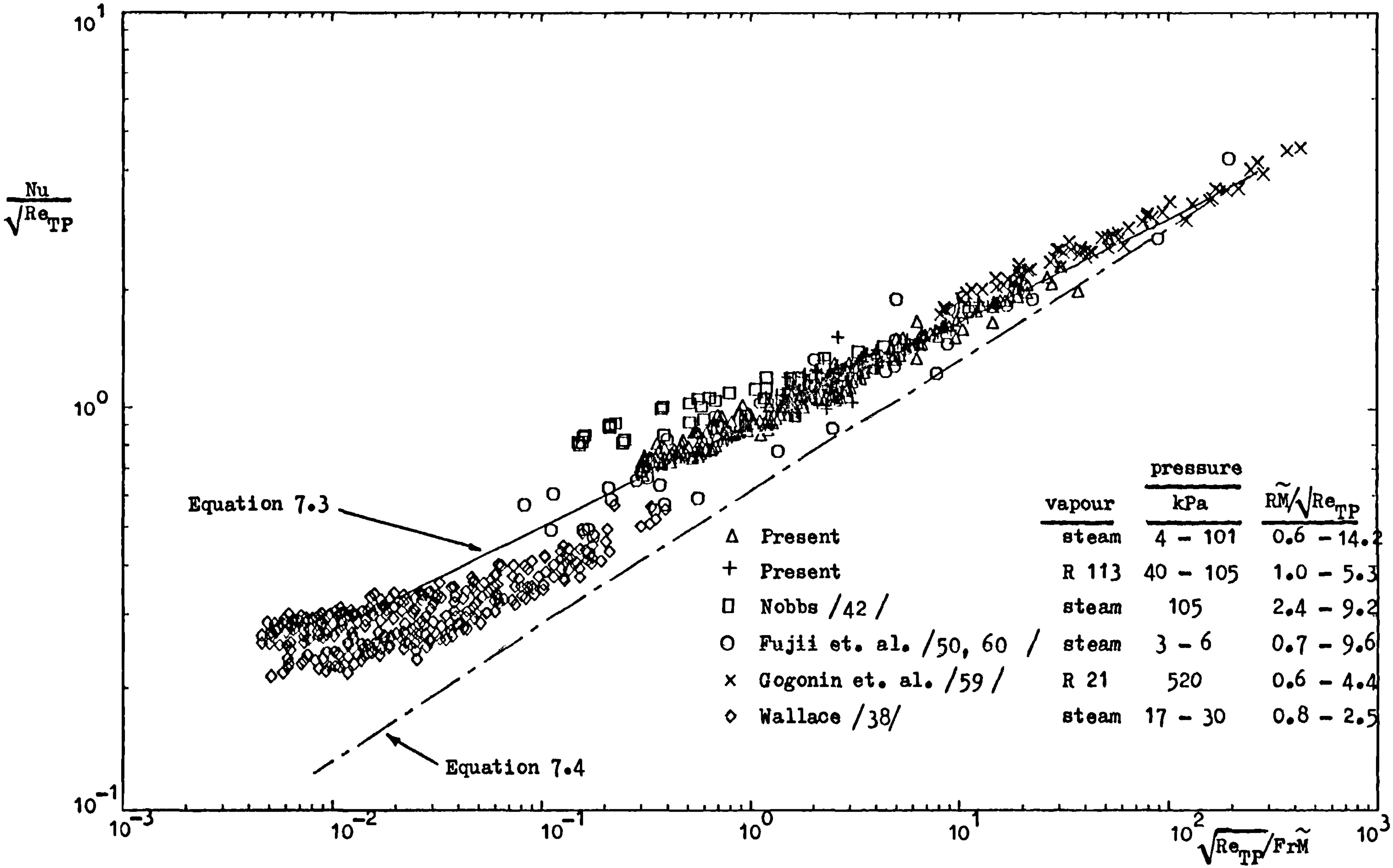

Figure 7.19 Comparison of present results and those of Nobbs /42/, Fujii et. al. /50,60/, Gogonin et. al. /59/ and Wallace /38/ with the correlation of Fujii et. al. /50,60/

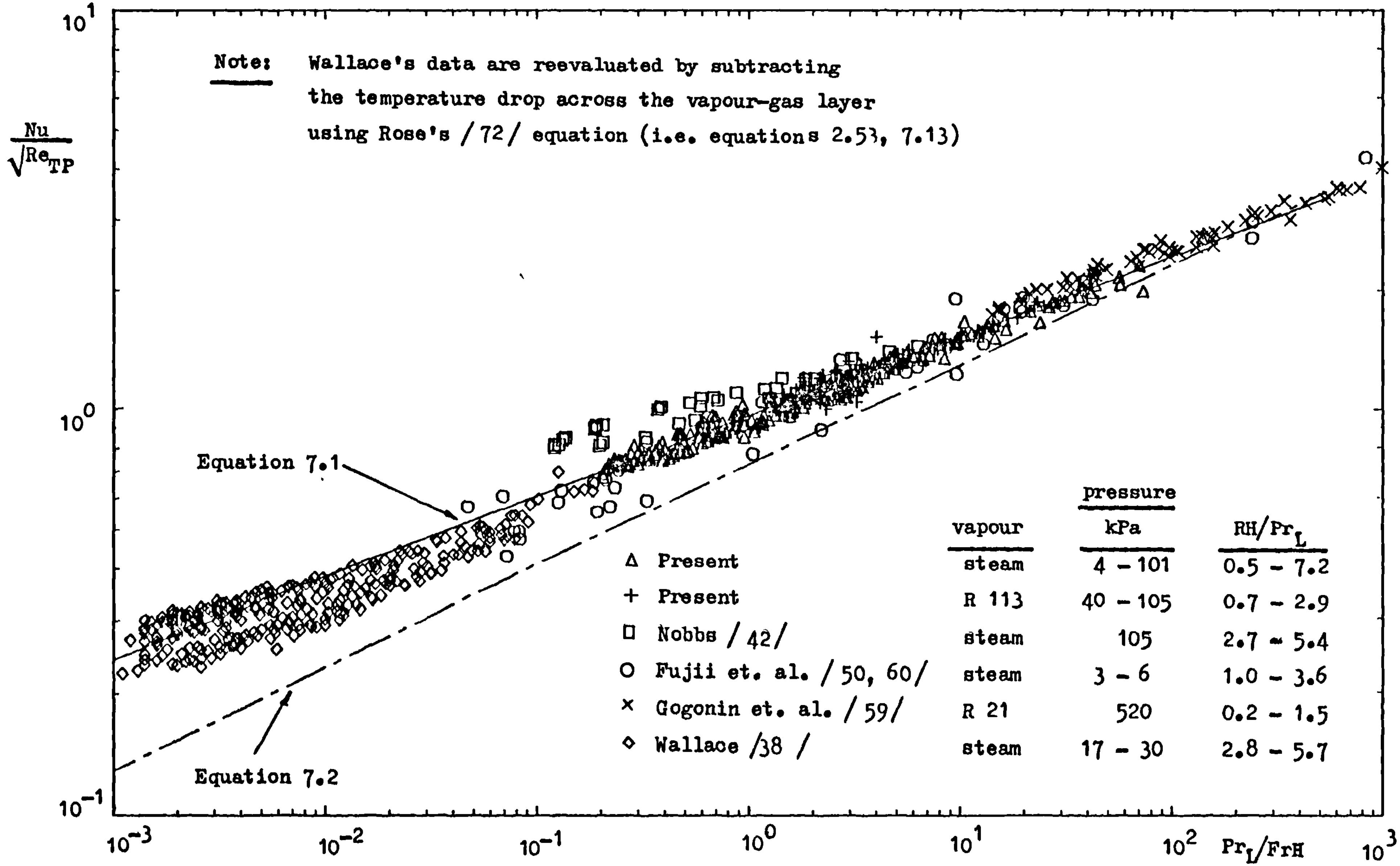

Figure 7.20 Comparison of present results and Nobbs /42/, Fujii et. al. /50,60 /, Gogonin et. al. /59/ and reevaluated Wallace /38/ with the correlation of Fujii et. al. /50, 60/

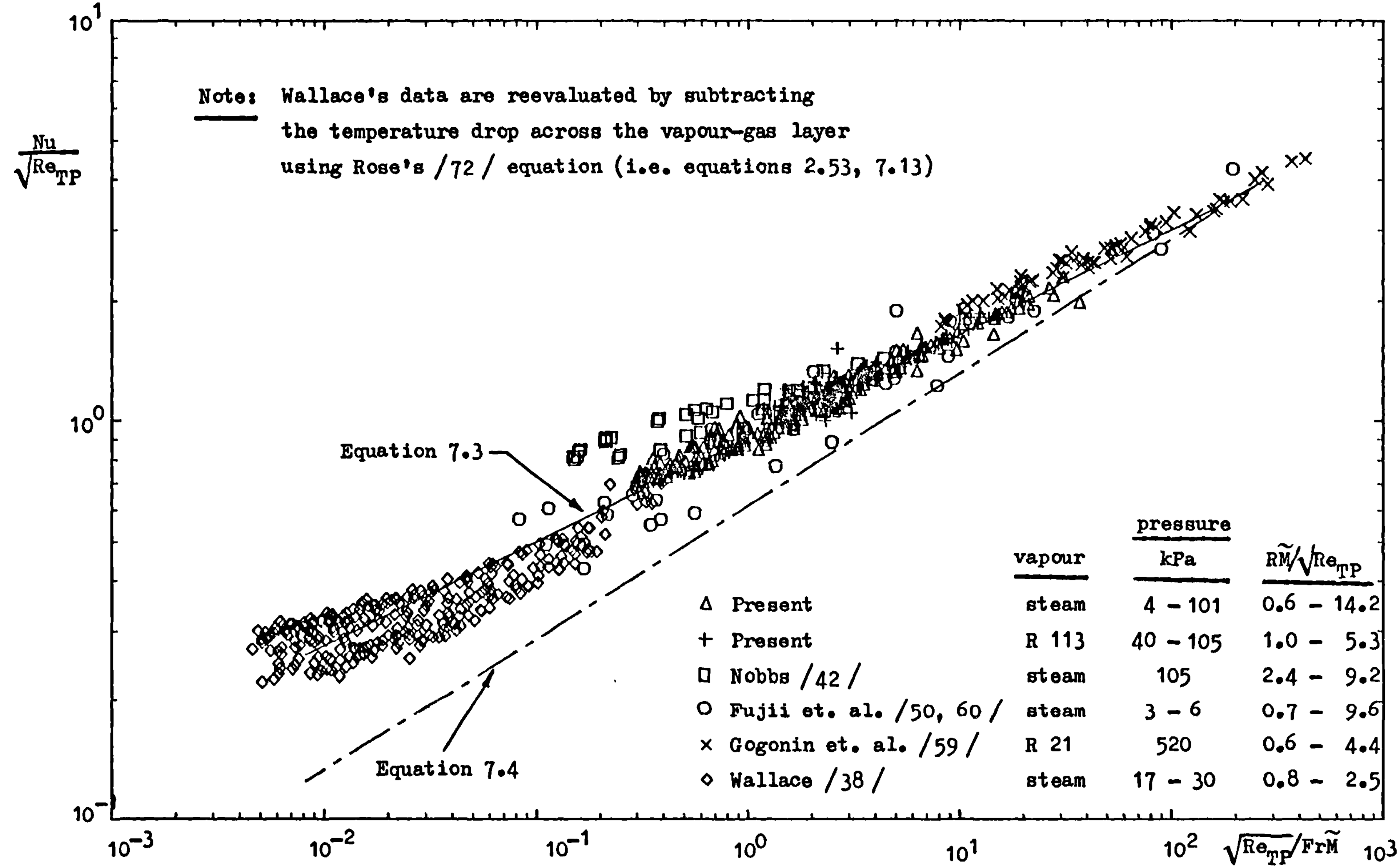

Figure 7.21 Comparison of present results and those of Nobbs /42 /, Fujii et. al. /50, 60/, Gogonin et. al. /59 / and reevaluated Wallace /38 / with the correlation of Fujii et. al /50,60 /

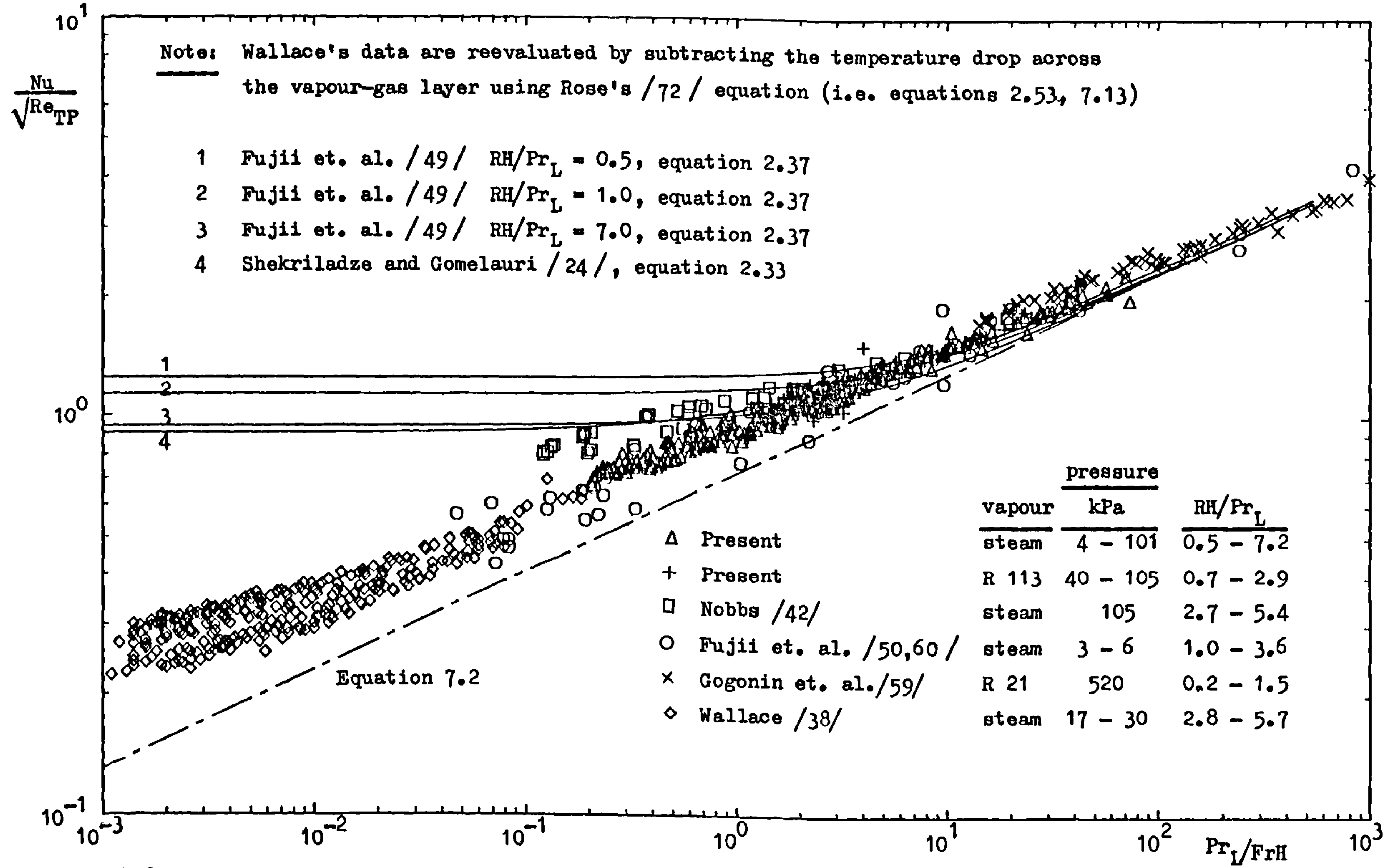

Figure 7.22 Comparison of present results and those of Nobbs /42/, Fujii et. al. /50,60/, Gogonin et. al. /59/ and reevaluated Wallace /38/ with the correlation of Fujii et. al. /50,60/

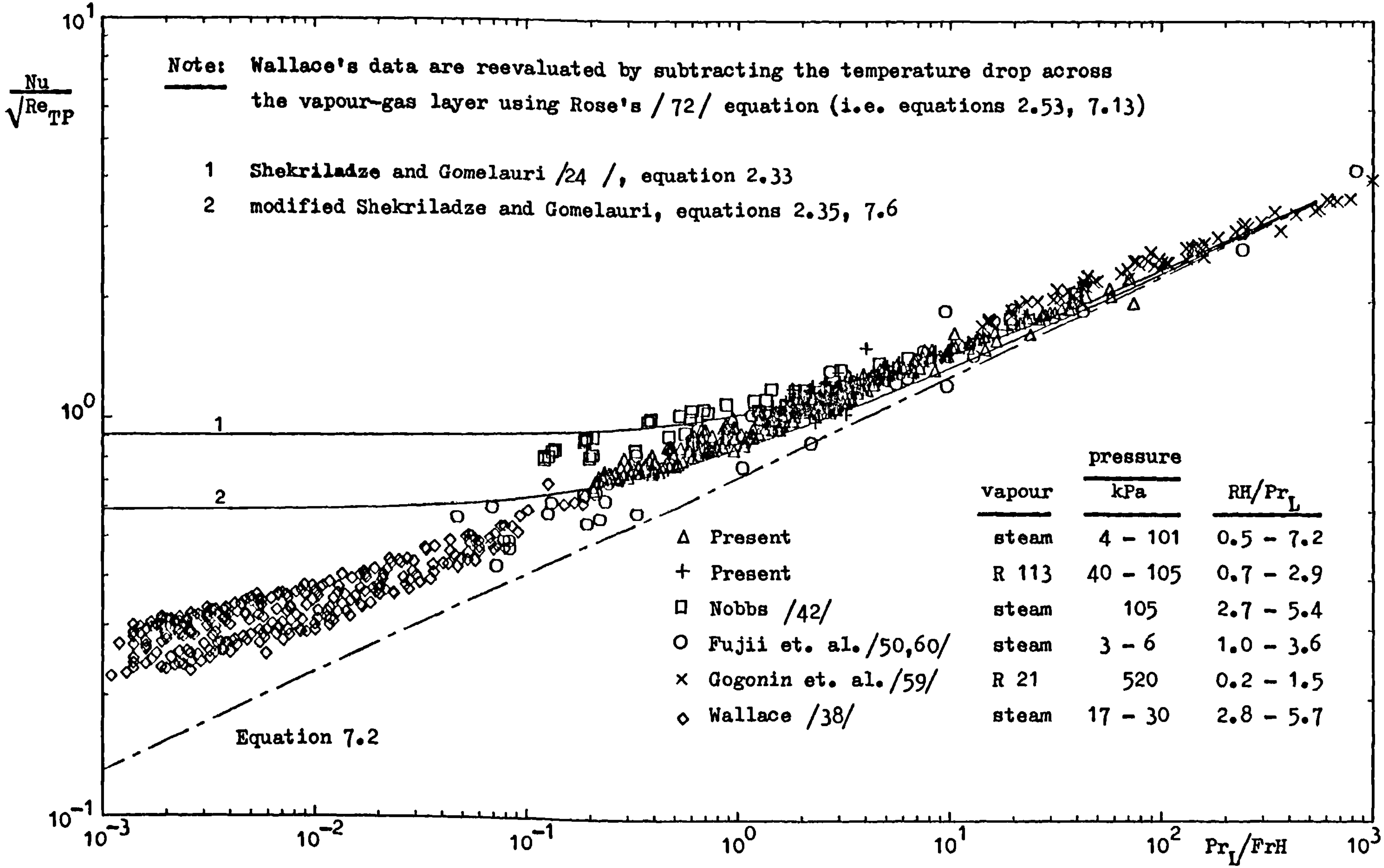

Figure 7.23 Comparison of present results and those of Nobbs / 42 /, Fujii et. al. /50, 60/, Gogonin et. al. /59 / and reevaluated Wallace /38 / with the original and modified theory of Shekriladze and Gomelauri /24 /

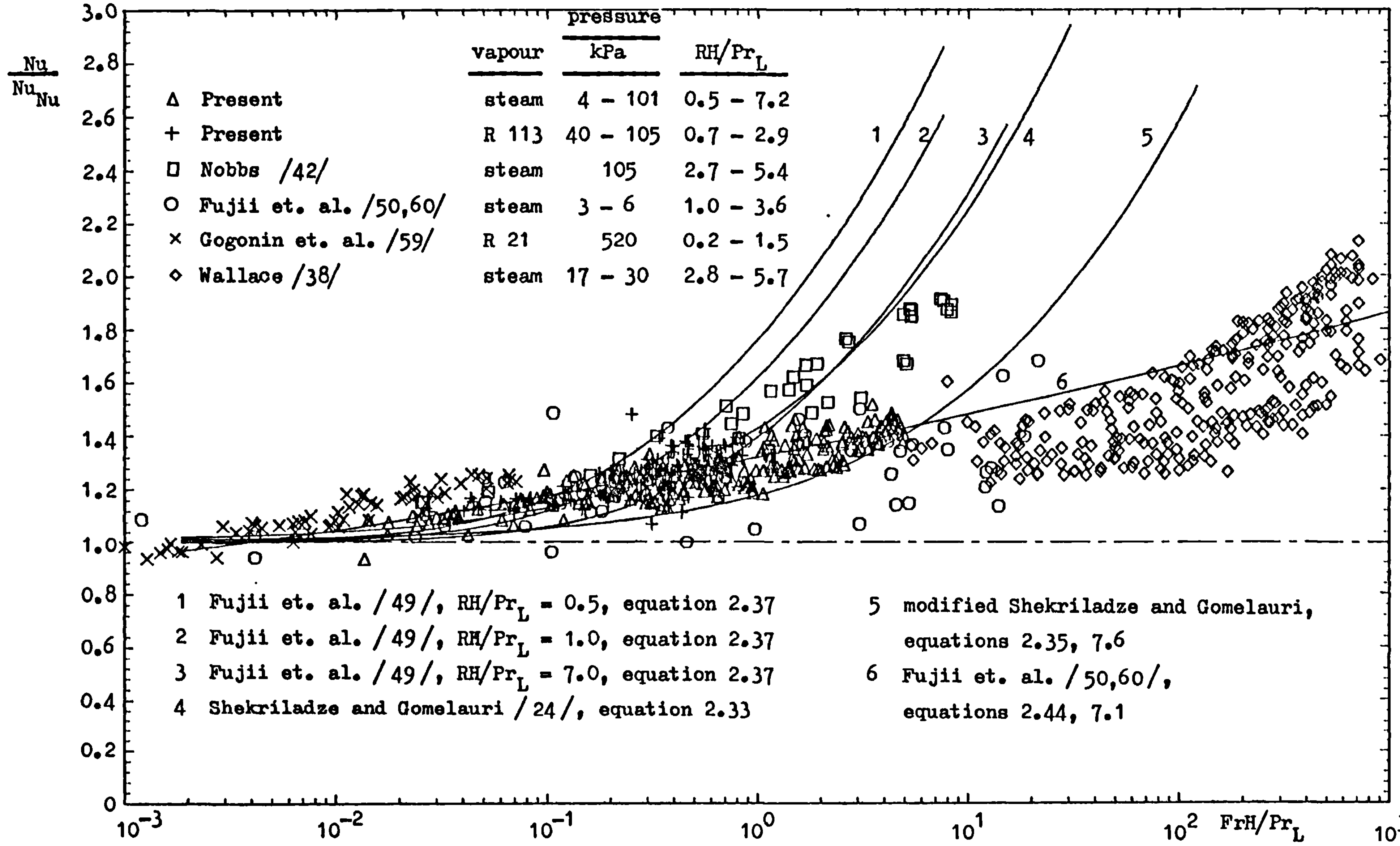

Figure 7.24 Comparison of present results and those of Nobbs /42 /, Fujii et. al. /50, 60/, Gogonin et. al. /59 / and reevaluated Wallace /38 / with the correlation of Fujii et. al. /50, 60/, the theories of Fujii et. al. /49 / and Shekriladze et. al. /24 /; all normalised by the Nusselt value

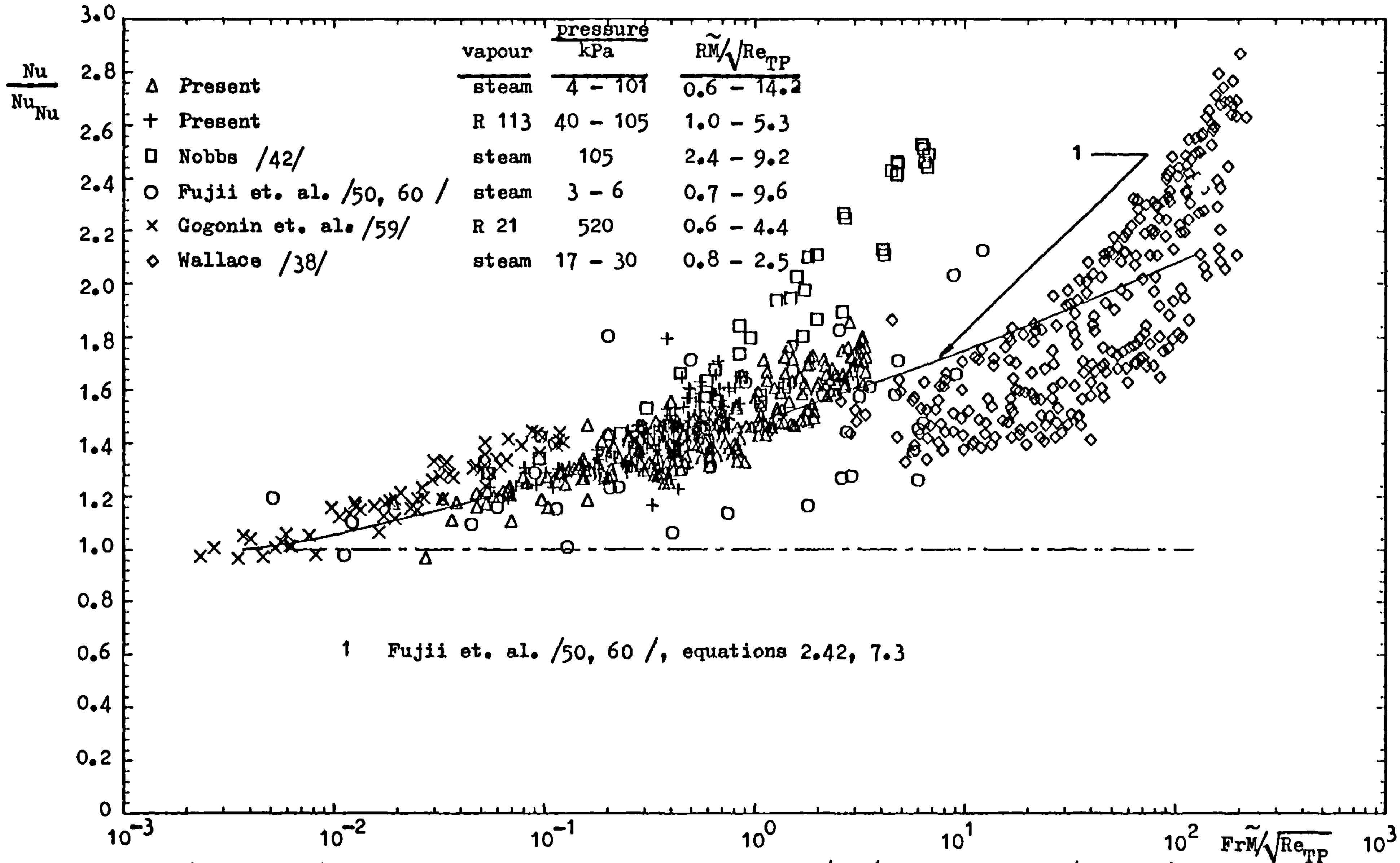

Figure 7.25 Comparison of present results and those of Nobbs /42 /, Fujii et. al. /50, 60 /, Gogonin et. al. /59 / and reevaluated Wallace /38 / with the correlation of Fujii et. al. /50, 60 /; all normalised by the Nusselt value

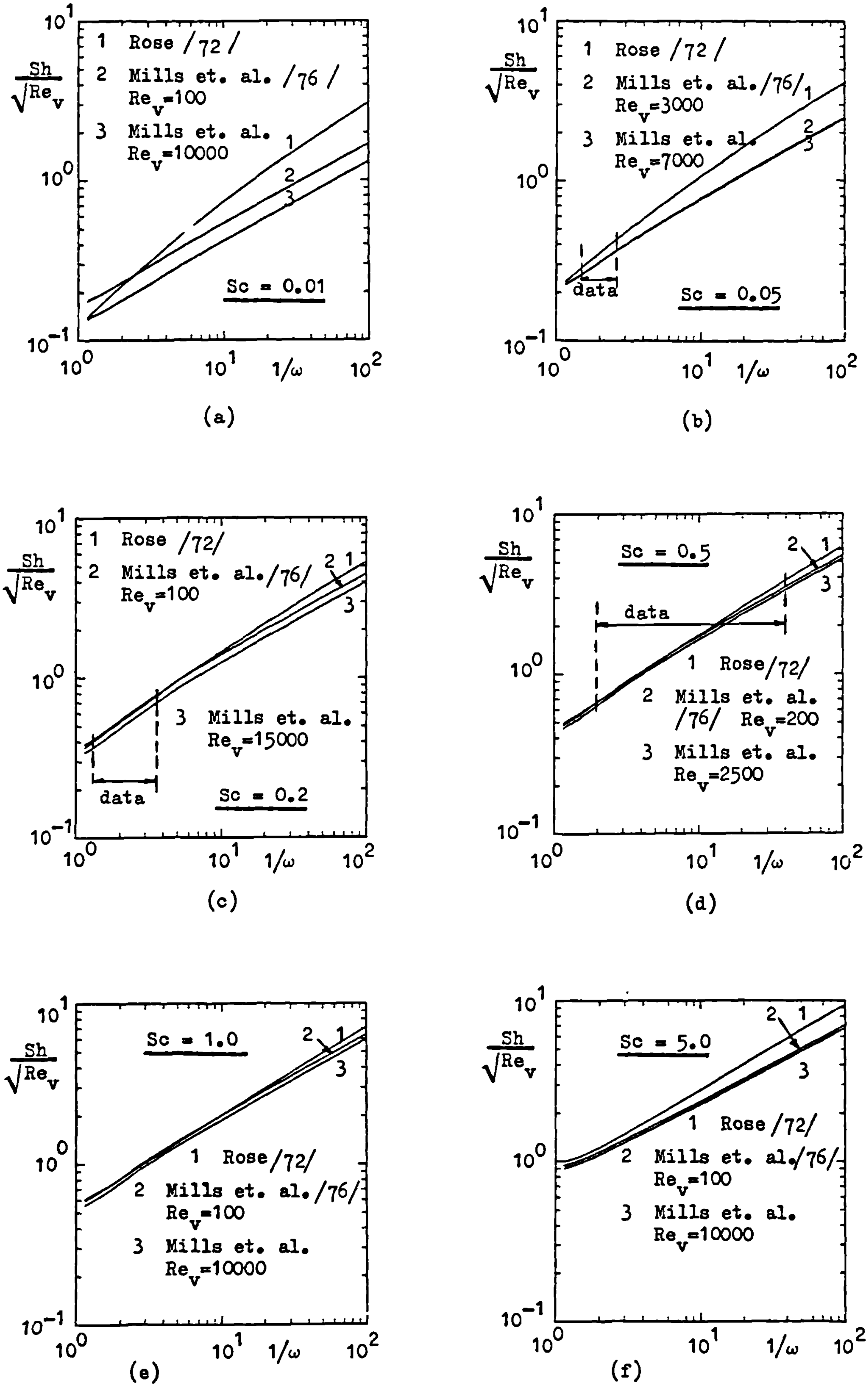

Figure 7.26 Comparison of the semi-empirical equation of Mills et. al. /76/ with the theoretical equation of Rose /72 /

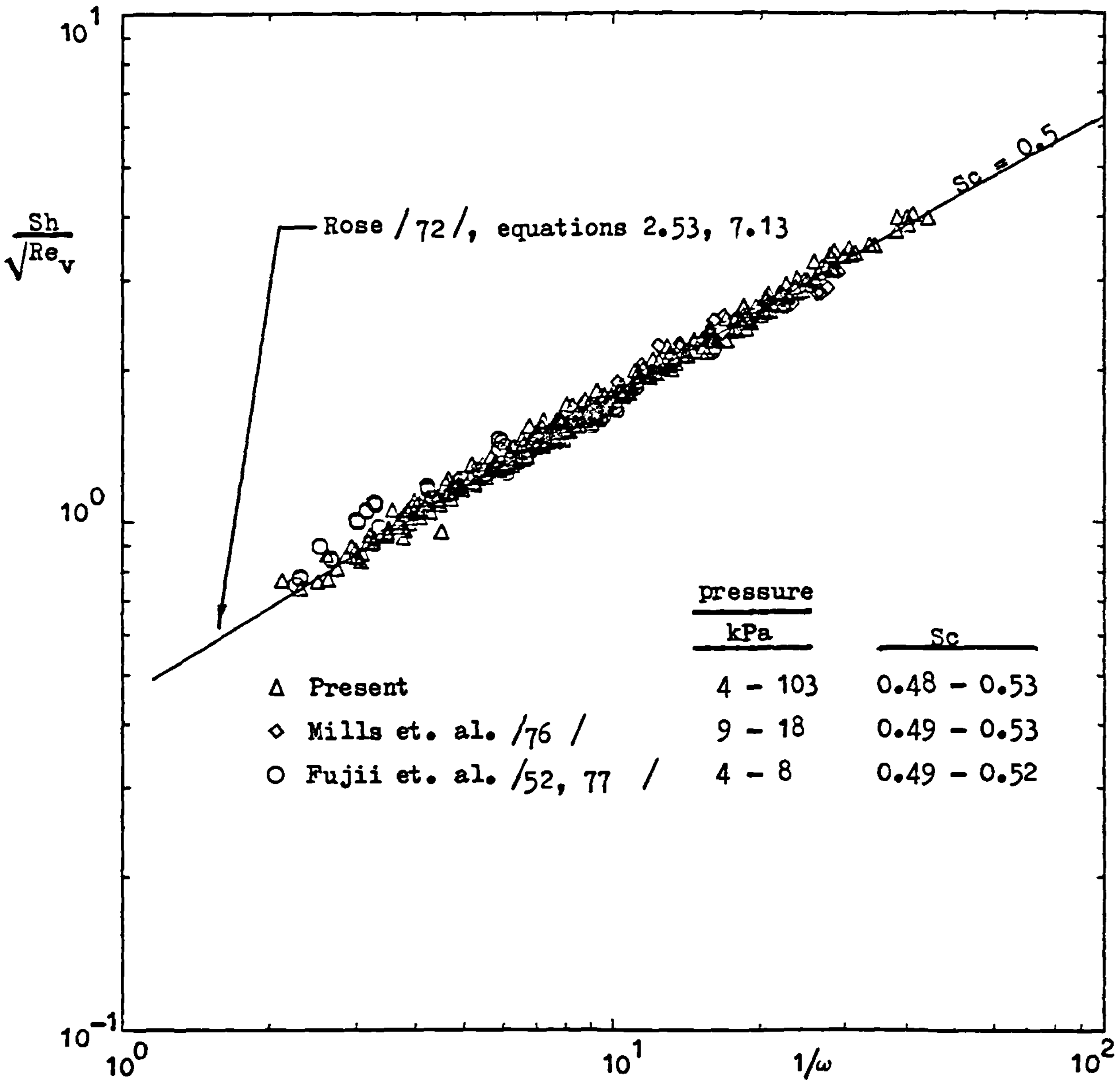

Figure 7.27 Comparison of the results for steam-air mixtures of Mills et. al. /76 /, Fujii et. al. /52, 77 / and the present work with the theory of Rose /72 /

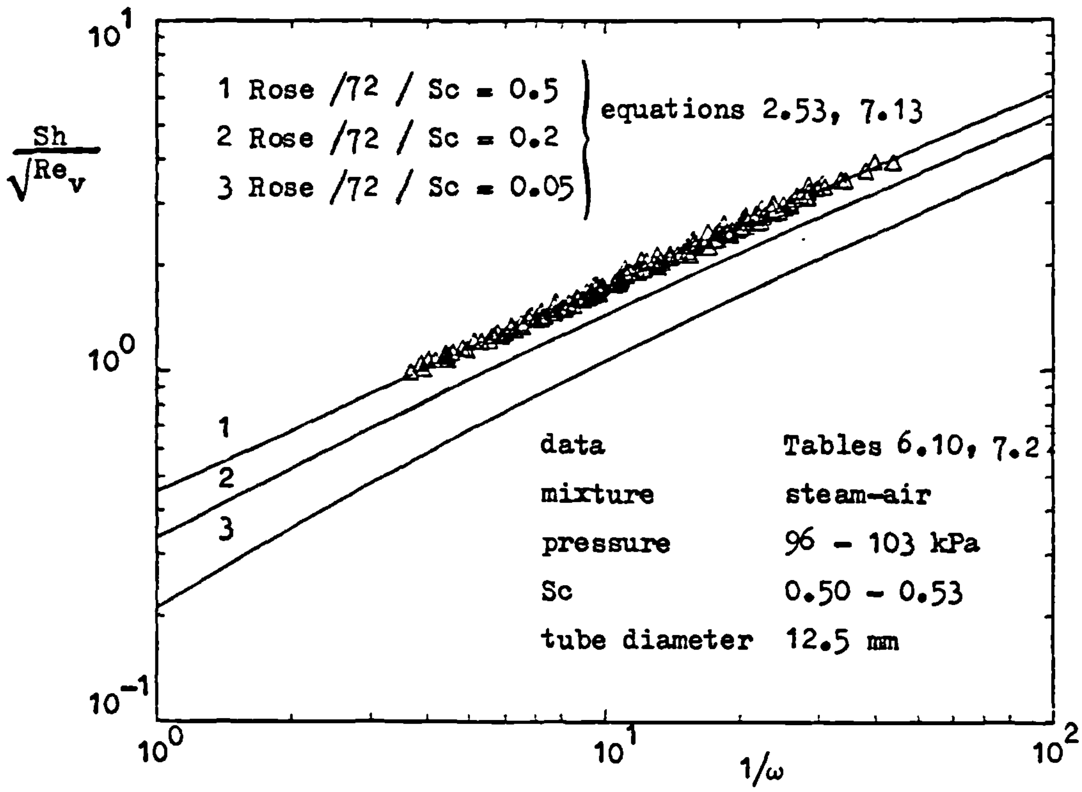

Figure 7.28 Comparison of present results with the theory of Rose /72/

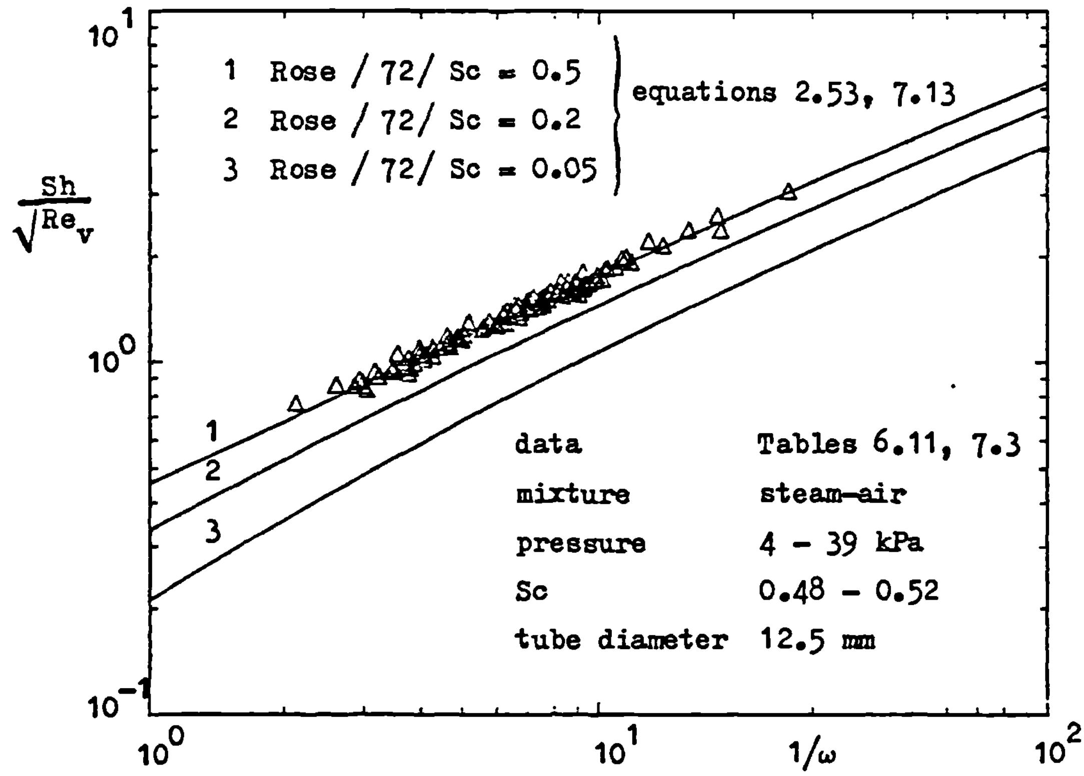

Figure 7.29 Comparison of present results with the theory of Rose /72/

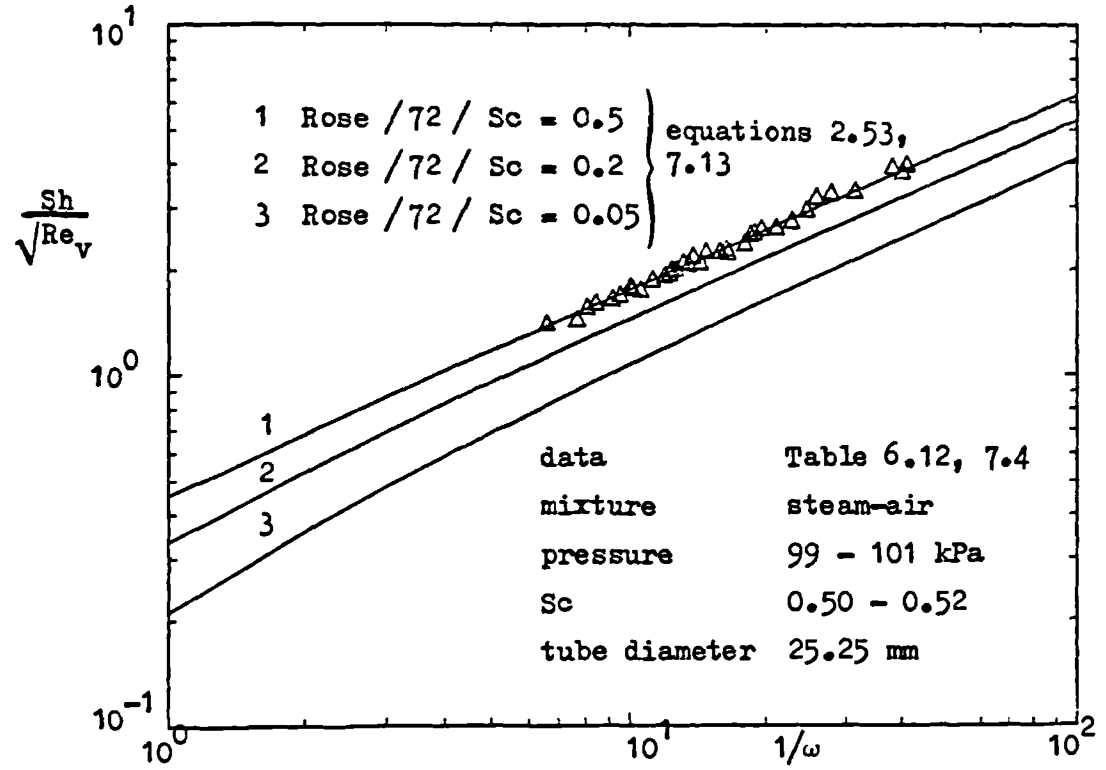

Figure 7.30 Comparison of present results with the theory of Rose /72/

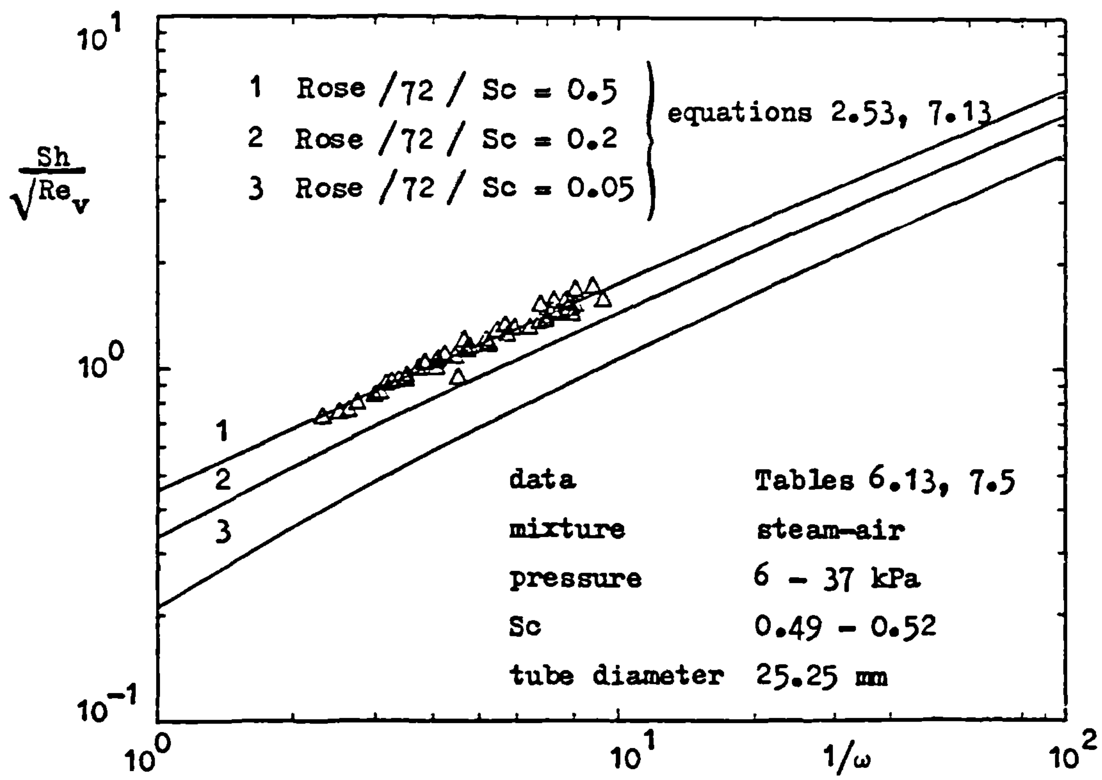

Figure 7.31 Comparison of present results with the theory of Rose /72/

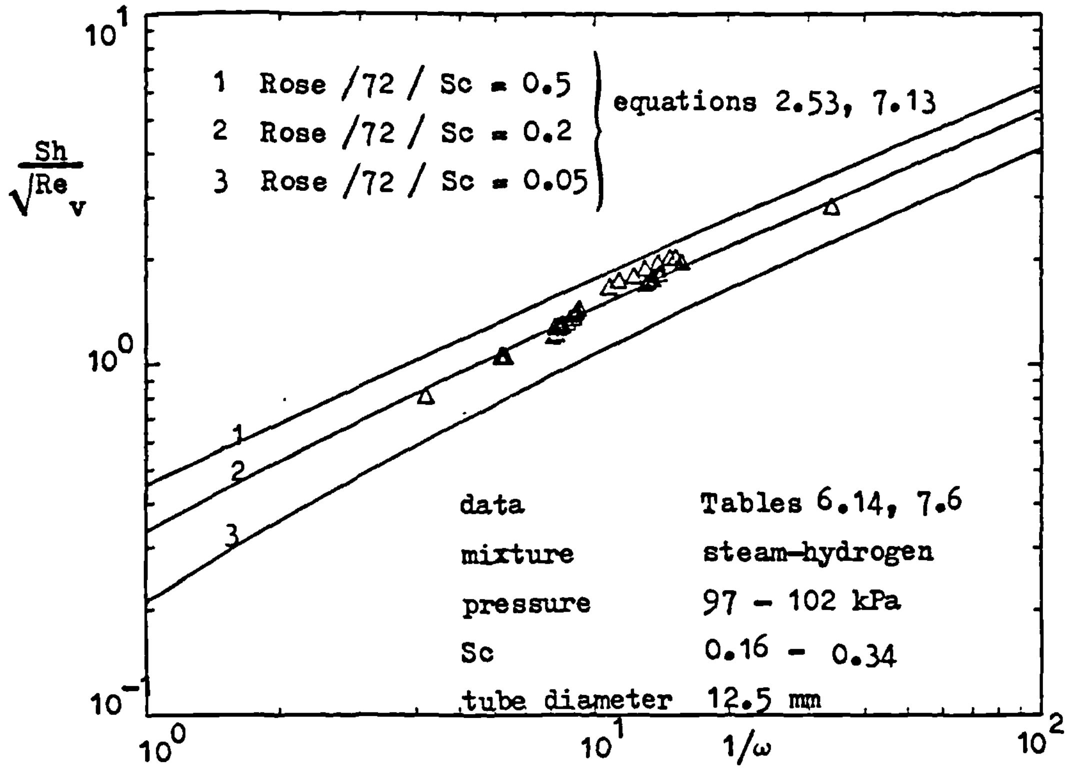

Figure 7.32 Comparison of present results with the theory of Rose /72/

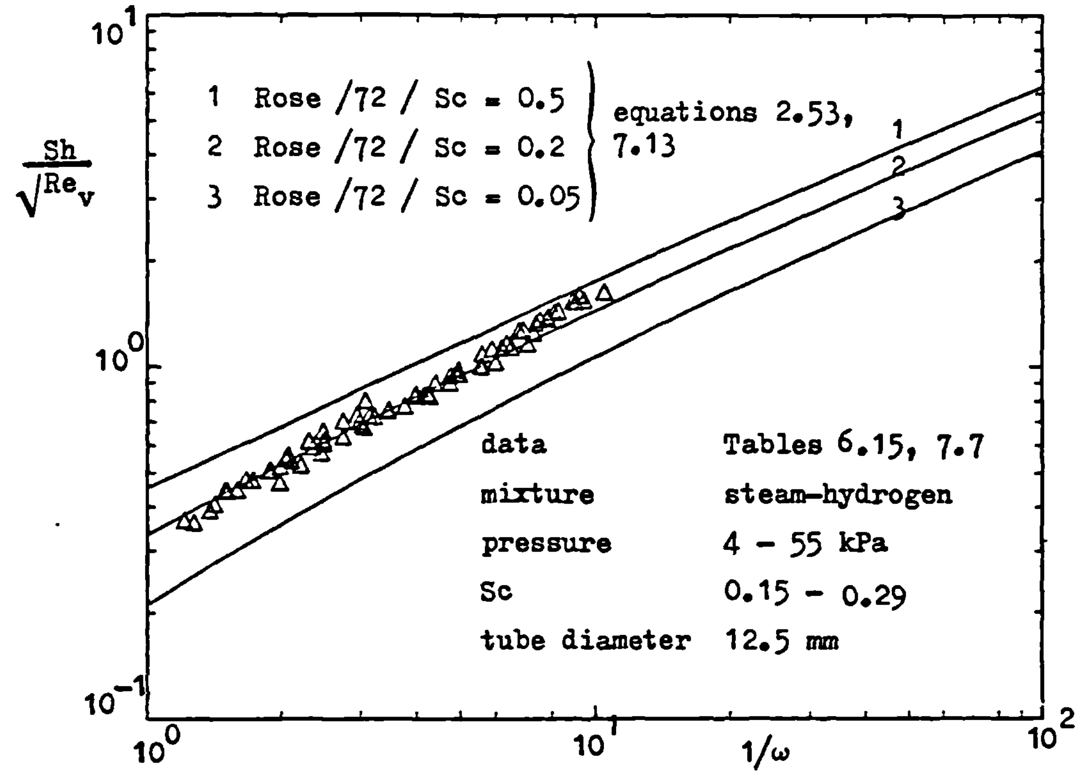

Figure 7.33 Comparison of present results with the theory of Rose /72/

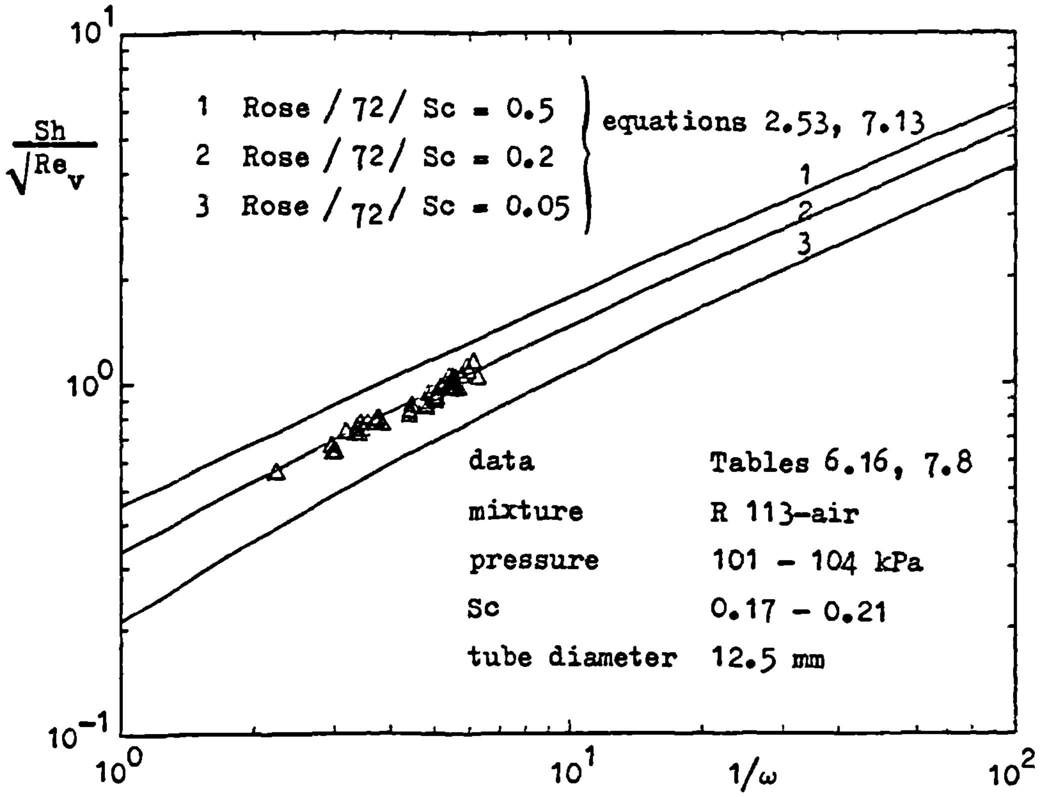

Figure 7.34 Comparison of present results with the theory of Rose /72/

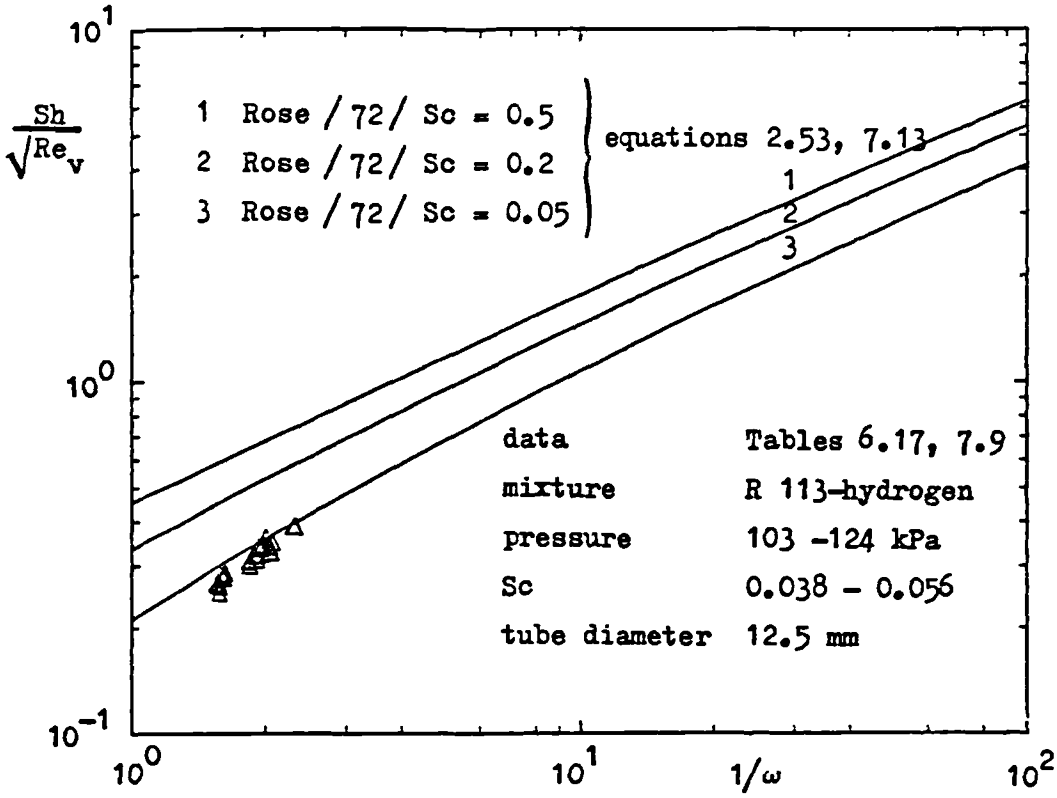

Figure 7.35 Comparison of present results with the theory of Rose /72/

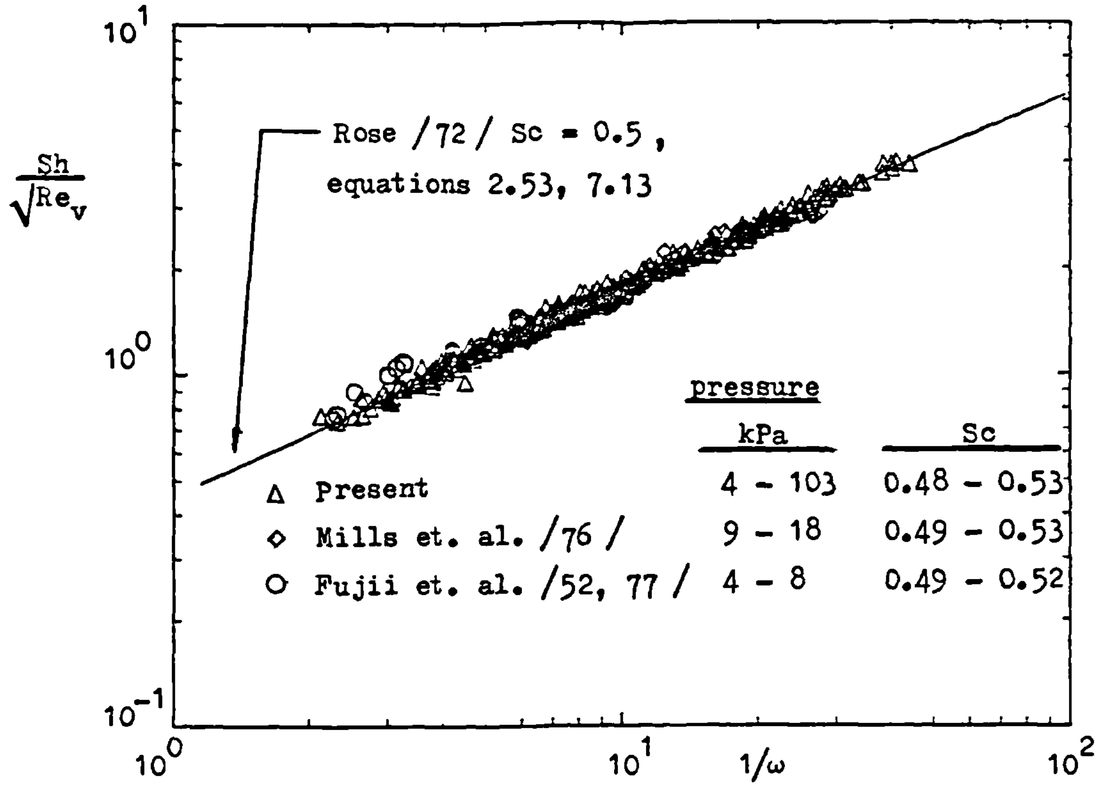

Figure 7.36 Comparison of steam-air results on the basis of $Sh/\sqrt{Re_v}$ and $1/\omega$

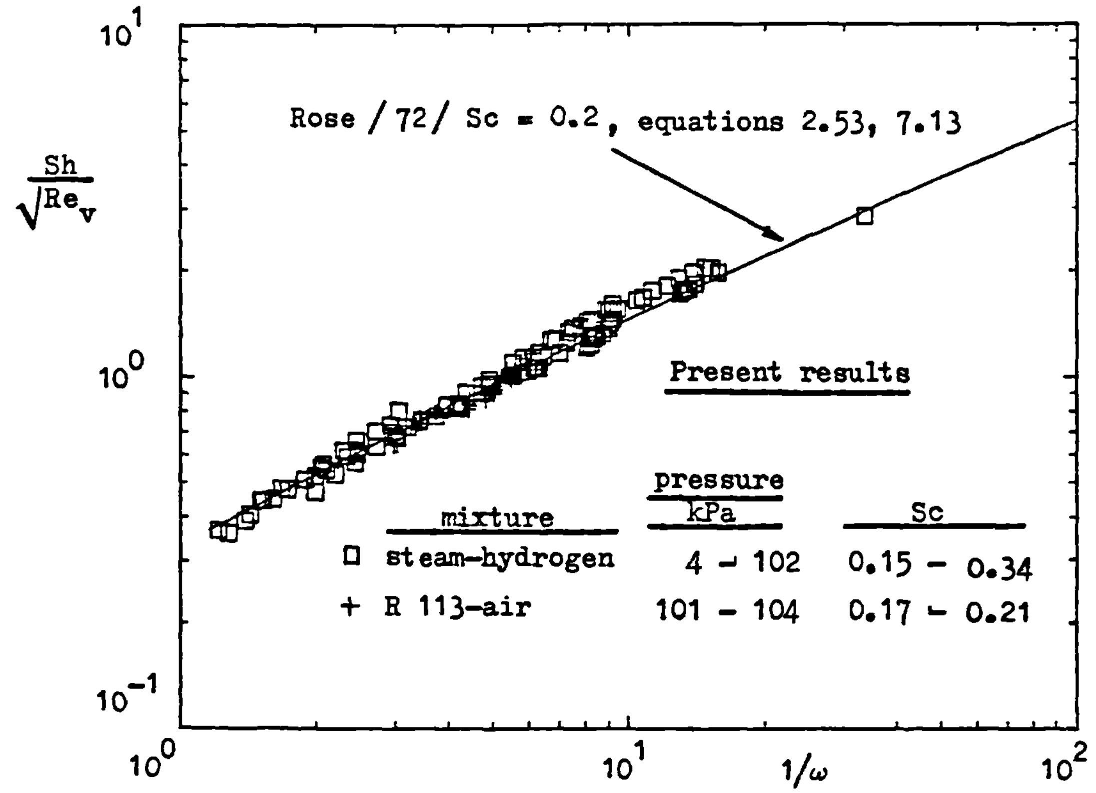

Figure 7.37 Comparison of steam-hydrogen and R 113-air results on the basis of $Sh/\sqrt{Re_v}$ and $1/\omega$

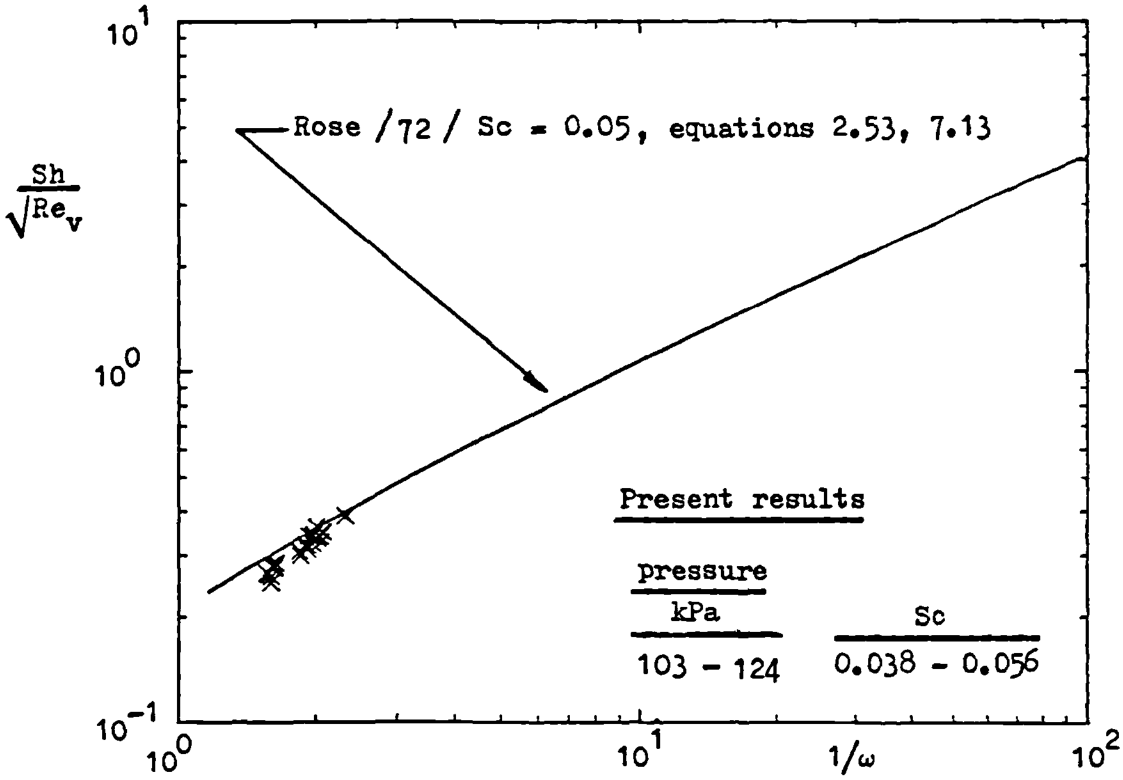

Figure 7.38 Comparison of R 113-hydrogen results on the basis of $Sh/\sqrt{Re_v}$ and $1/\omega$

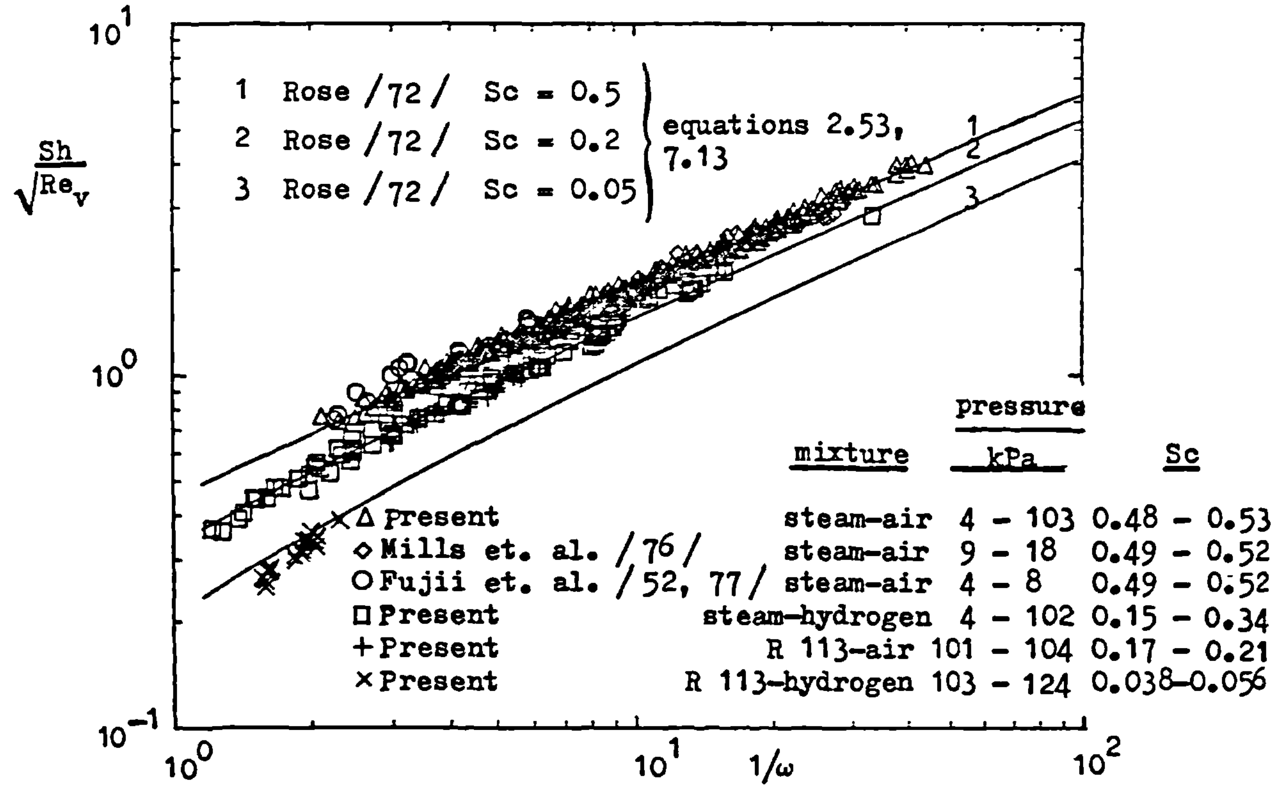

Figure 7.39 Comparison of vapour-gas results on the basis of $Sh/\sqrt{Re_v}$ and $1/\omega$

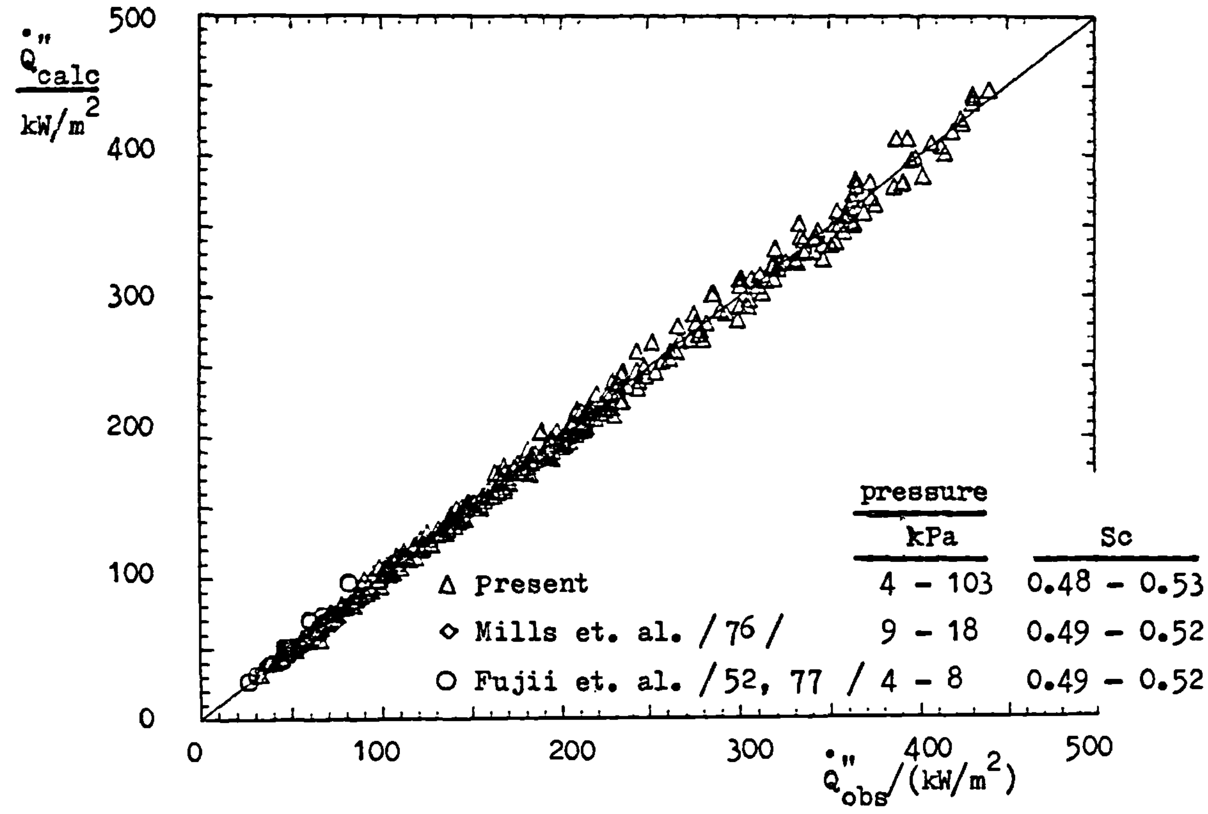

Figure 7.40 Comparison of steam results on the basis of calculated and observed heat fluxes

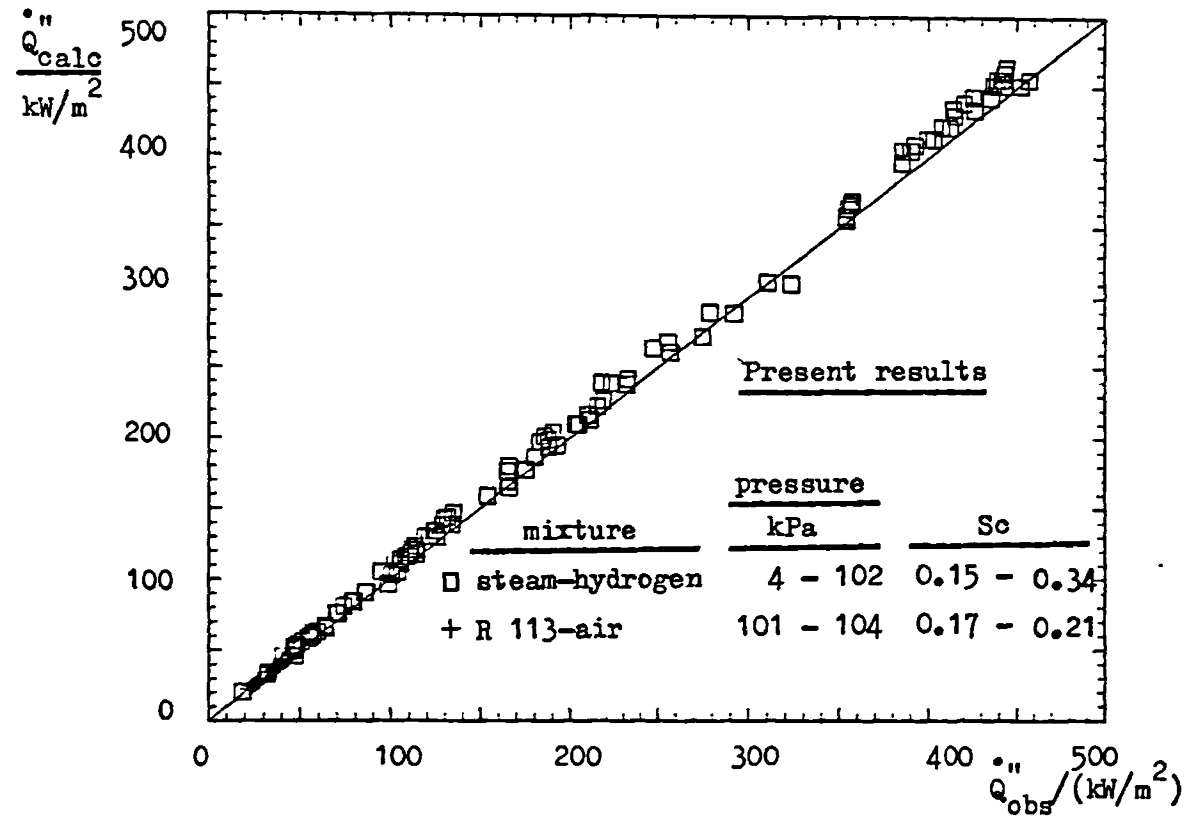

Figure 7.41 Comparison of steam-hydrogen and R 113-air results on the basis of calculated and observed heat fluxes

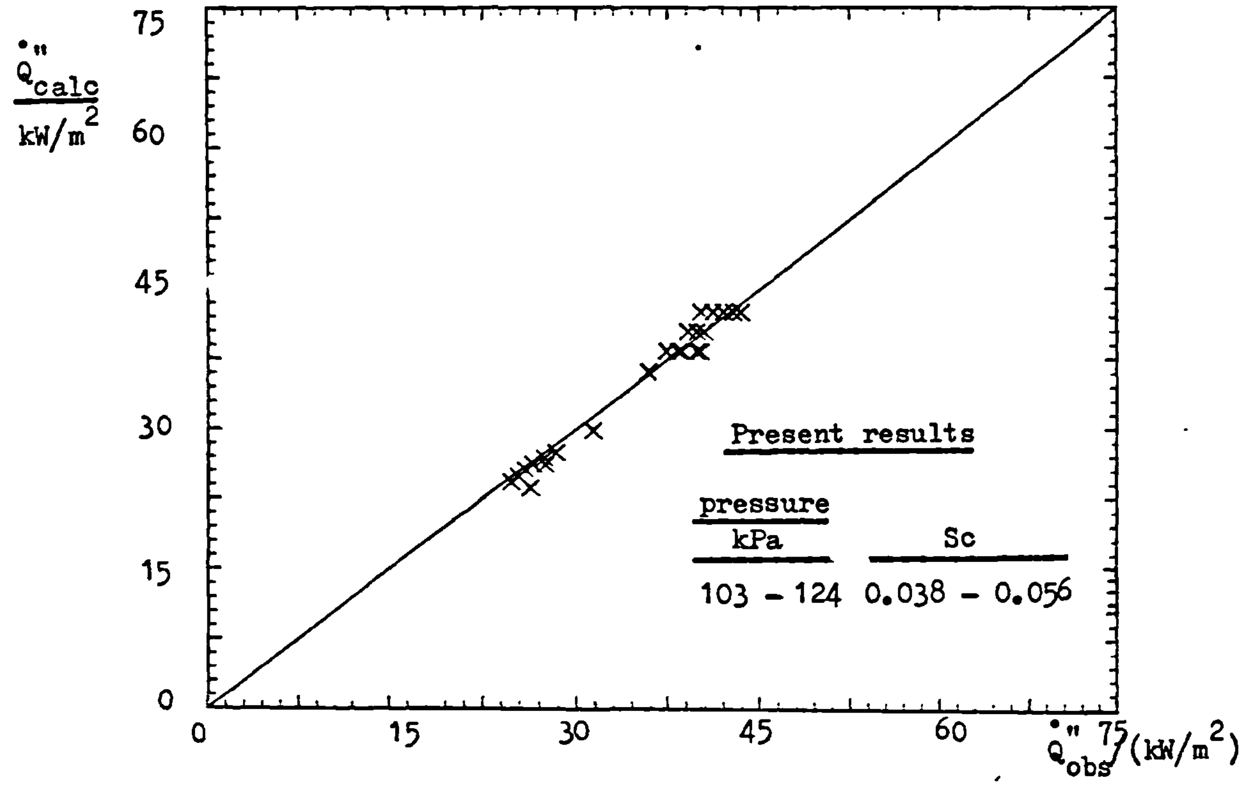

Figure 7.42 Comparison of R 113-hydrogen results on the basis of calculated and observed heat fluxes

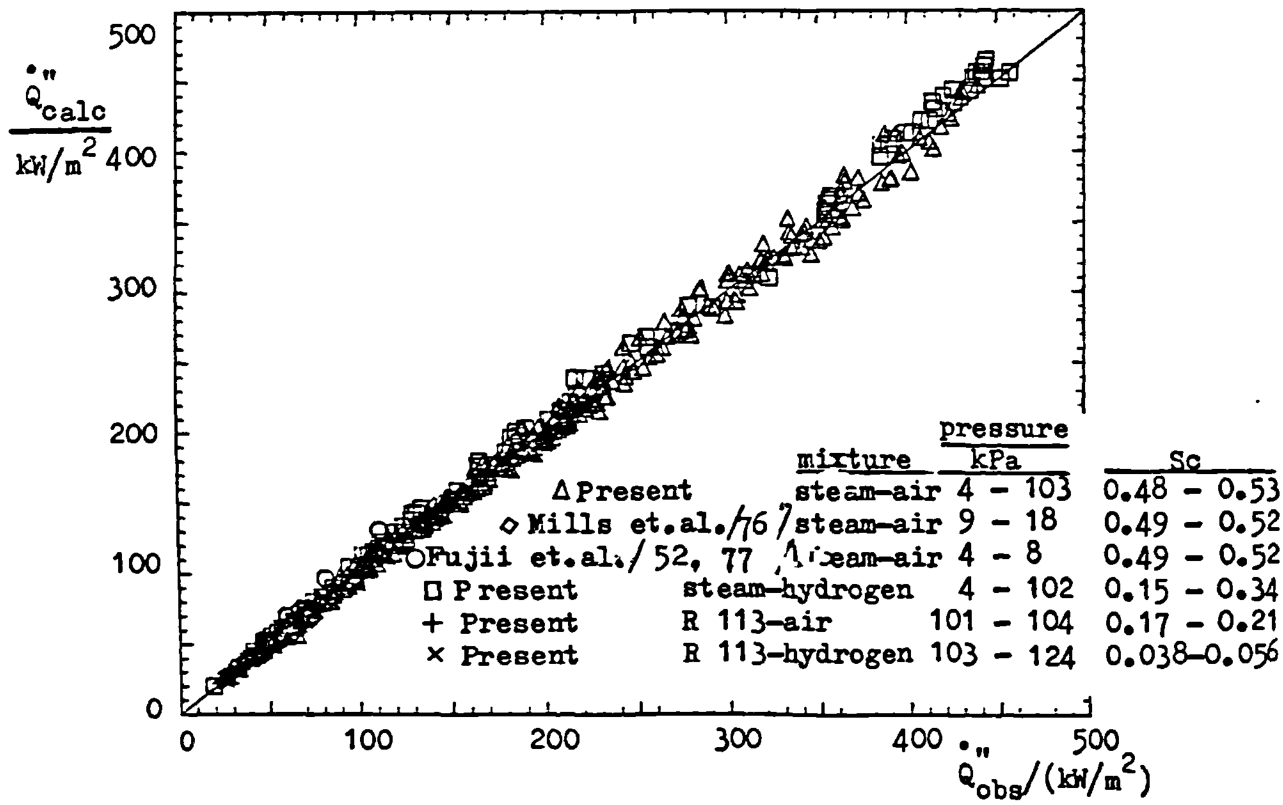

Figure 7.43 Comparison of vapour-gas results on the basis of calculated and observed heat fluxes

Table 7.1 Summary of vapour-gas mixture results

mixture	d_o / mm	P_∞ / kPa	$W_{\infty 2}$ / %	$Sh/\sqrt{Re_v}$	$1/\omega$	So
steam-air	12.5	95 - 103	0.5 - 24.4	0.99 - 4.17	3.18 - 44.69	0.50 - 0.53
steam-air	12.5	4 - 40	0.1 - 31.5	0.84 - 3.52	1.02 - 24.32	0.48 - 0.52
steam-air	25.25	99 - 101	0.5 - 12.4	1.42 - 4.07	6.56 - 42.38	0.50 - 0.52
steam-air	25.25	6 - 37	1.0 - 16.6	0.93 - 2.74	1.18 - 7.89	0.49 - 0.52
steam-hydrogen	12.5	97 - 102	0.1 - 5.7	0.87 - 2.90	3.25 - 36.85	0.16 - 0.34
steam-hydrogen	12.5	4 - 55	0.1 - 3.8	0.53 - 3.57	1.07 - 10.19	0.15 - 0.29
Refrigerant 113-air	12.5	101 - 104	0.04- 1.6	0.52 - 1.48	1.07 - 14.24	0.17 - 0.21
Refrigerant 113-hydrogen	12.5	103 - 124	0.02- 0.3	0.15 - 1.58	1.12 - 3.65	0.038-0.056

mixture steam-air
tube diameter 12.5 mm

Run No.	$W_{\infty 2}$ %	$\tilde{W}_{\infty 2}$ %	U_∞ m/s	P_∞ Pa	T_∞ K	T_w K	$\dot{Q}''_{obs}$ kW/m²	coupled condensate film and gas layer equations: $\dot{Q}''_{calc}$ kW/m²	$T_\infty - T_i$ K	$T_i - T_w$ K	gas layer only (condensate film resistance accounted by equation 7.3): $\frac{Sh}{\sqrt{Re_v}}$	$\frac{1}{\Phi}$	W_i %	$T_\infty - T_i$ K	$T_i - T_w$ K	Sc
412	[illegible]	[illegible]	1.66	[illegible]	[illegible]	[illegible]	428.1	[illegible]	2.56	[illegible]	[illegible]	21.66	10.49	1.87	34.35	0.52
413	[illegible]	[illegible]	1.67	[illegible]	[illegible]	[illegible]	417.8	419.3	5.19	32.93	3.02	26.63	26.27	.34	32.78	0.52
414	1.54	0.97	1.67	[illegible]	[illegible]	332.59	409.6	407.3	8.05	32.16	2.90	23.14	35.73	7.84	32.38	0.52
415	[illegible]	1.27	1.68	[illegible]	372.69	[illegible]	397.3	395.8	10.36	31.35	2.76	21.48	43.51	10.25	31.48	0.52
416	2.62	1.65	1.69	[illegible]	372.49	327.17	381.0	391.1	13.78	31.54	2.55	21.07	55.24	14.73	30.59	0.52
417	3.40	2.14	1.7	[illegible]	372.35	325.6[illegible]	360.6	369.8	15.95	29.77	2.37	18.21	61.89	17.83	28.89	0.52
418	4.25	2.68	1.71	[illegible]	372.10	322.15	352.4	356.2	20.90	29.05	2.27	16.03	68.08	21.26	28.69	0.52
419	5.19	3.29	1.72	100.5	371.98	320.41	331.9	336.1	24.17	27.41	2.11	14.08	73.08	24.57	27.00	0.52
420	0.51	0.32	1.6[illegible]	101.8	373.20	335.49	447.2	439.9	2.87	34.84	3.39	23.54	12.08	2.19	35.52	0.52
421	1.07	0.67	1.64	101.7	[illegible]	333.48	426.7	424.2	5.90	33.69	3.10	25.72	27.59	5.67	33.92	0.52
422	1.53	0.96	1.64	101.7	372.98	331.37	402.2	415.1	8.41	33.19	2.81	27.04	41.40	9.63	31.97	0.52
423	[illegible]	1.27	1.65	[illegible]	372.64	329.66	385.9	402.5	10.89	32.28	2.64	24.50	49.51	12.46	30.71	0.52
424	2.70	1.69	1.66	[illegible]	372.67	326.25	381.8	391.7	14.57	31.85	2.56	21.13	56.96	15.53	30.90	0.52
425	3.46	2.18	1.67	[illegible]	372.44	324.01	381.9	372.9	18.01	[illegible]	2.55	17.49	60.57	17.14	31.28	0.52
426	[illegible]	2.75	1.6[illegible]	[illegible]	372.28	321.34	361.4	354.8	21.81	29.13	2.35	15.62	67.91	21.17	29.77	0.52
427	[illegible]	3.36	1.65	[illegible]	372.19	319.15	340.9	335.7	25.28	27.65	2.18	13.86	73.35	24.78	28.15	0.52
428	[illegible]	3.82	1.7	100.6	371.66	317.58	324.6	322.6	27.65	26.63	2.05	12.80	76.79	27.46	26.82	0.52
429	7.21	4.61	1.7	[illegible]	371.74	316.07	[illegible]	300.9	30.90	24.76	1.94	11.08	79.91	30.19	25.46	0.52
430	[illegible]	[illegible]	[illegible]	[illegible]	373.22	343.47	364.1	361.9	2.77	26.98	3.00	23.43	13.94	2.57	27.18	0.52
431	[illegible]	0.76	[illegible]	[illegible]	373.39	[illegible]	351.9	353.0	5.67	26.50	2.81	23.10	28.10	5.78	26.39	0.52
432	1.95	1.16	1.37	[illegible]	372.95	338.7[illegible]	342.1	341.2	8.49	25.70	2.67	20.41	37.78	8.42	25.77	0.52
433	2.46	1.55	[illegible]	[illegible]	372.63	336.5[illegible]	327.3	331.7	11.17	25.12	2.49	19.24	47.38	11.58	24.72	0.52
434	[illegible]	[illegible]	1.39	101.5	372.63	334.11	334.7	32[illegible].1	14.16	24.36	2.54	16.01	50.92	12.82	25.70	0.52
435	4.06	2.57	1.39	[illegible]	372.44	331.21	312.7	307.2	17.68	23.55	2.30	14.98	60.82	17.17	24.05	0.52
436	5.11	[illegible]	[illegible]	[illegible]	[illegible]	[illegible]	290.6	[illegible]	21.16	[illegible]	2.09	13.33	68.04	21.12	22.31	0.52
437	[illegible]	[illegible]	1.41	[illegible]	371.98	324.79	273.4	278.1	25.51	21.67	1.92	12.01	75.04	25.95	21.23	0.52
438	7.46	4.77	1.4	[illegible]	371.72	[illegible]	256.2	262.3	28.93	[illegible]	1.77	10.63	79.27	29.51	19.94	0.52
439	[illegible]	[illegible]	[illegible]	[illegible]	373.24	344.78	[illegible]	365.4	1.84	26.61	4.17	3.18	1.46	0.18	28.28	0.51
440	[illegible]	[illegible]	[illegible]	[illegible]	373.17	[illegible]	[illegible]	363.2	2.99	26.61	2.91	15.62	11.52	2.04	27.56	0.52
441	[illegible]	[illegible]	[illegible]	[illegible]	[illegible]	342.37	359.4	359.5	4.31	26.42	2.69	20.96	22.18	4.33	26.41	0.52
442	[illegible]	[illegible]	[illegible]	[illegible]	[illegible]	[illegible]	[illegible]	363.9	5.59	[illegible]	2.56	23.84	31.41	6.65	26.02	0.52

Table [illegible] (continued)

Run No.	$W_{\infty 2}$ %	$\tilde{W}_{\infty 2}$ %	U_∞ m/s	P_∞ Pa	T_∞ K	T_w K	$\dot{Q}''_{obs}$ kW/m^2	coupled condensate film and gas layer equations: $\dot{Q}''_{calc}$ kW/m^2	$T_\infty - T_i$ K	$T_i - T_w$ K	gas layer only (condensate film resistance accounted by equation 7.3): $\frac{Sh}{\sqrt{Re_v}}$	$\frac{1}{\psi}$	W_i %	$T_\infty - T_i$ K	$T_i - T_w$ K	Sc
443	1.57	0.98	1.62	101.8	373.31	339.77	347.1	358.4	6.58	26.66	2.50	22.23	34.86	7.59	25.65	0.52
444	1.68	1.18	1.63	101.6	372.91	338.64	339.8	352.9	7.87	26.40	2.42	21.32	40.06	9.13	25.13	0.52
445	2.48	1.56	1.6	101.7	372.82	337.21	332.4	341.9	10.10	25.50	2.34	18.46	45.72	1[illegible].96	24.65	0.52
446	[illegible]	1.89	1.65	[illegible]	372.49	332.91	327.5	346.9	13.04	24.53	2.24	18.54	55.55	14.81	24.76	0.52
447	[illegible]	2.45	1.65	[illegible]	[illegible]	[illegible]	325.1	332.4	16.44	25.57	2.19	15.66	60.70	17.12	24.89	0.52
448	0.53	0.33	1.6	[illegible]	373.29	[illegible]	213.4	212.8	0.85	[illegible]	1.77	9.37	4.96	0.80	12.89	0.52
449	0.78	0.49	1.6	102.2	373.25	359.13	211.8	212.6	1.26	12.85	1.73	10.16	7.94	1.32	12.79	0.52
450	1.17	0.67	1.61	102.1	373.17	358.57	211.0	212.7	1.75	12.89	1.71	10.29	10.99	1.88	12.76	0.52
451	1.31	0.82	1.61	102.0	373.10	357.89	209.4	214.3	2.18	13.04	1.67	11.04	14.42	2.54	12.67	0.52
452	1.58	0.99	1.61	101.9	373.03	357.43	207.0	213.0	2.64	12.96	1.64	10.86	17.17	3.09	12.51	0.52
453	1.87	1.17	1.62	101.9	372.98	356.92	206.2	212.2	3.13	12.94	1.63	10.49	19.61	3.58	12.48	0.52
454	2.15	1.35	1.62	101.8	372.90	356.45	204.5	210.9	3.60	12.86	1.61	10.18	21.93	4.07	12.38	0.52
455	2.69	1.69	1.6	101.8	372.79	355.55	202.1	208.8	4.50	12.74	1.58	9.69	26.12	5.00	12.24	0.52
456	3.54	2.23	1.6	101.7	372.61	354.12	197.3	205.5	5.92	12.57	1.53	9.17	32.47	6.54	11.95	0.52
457	4.39	2.77	1.64	101.5	372.4[illegible]	352.57	194.8	203.0	7.37	12.46	1.49	8.64	37.89	7.99	11.84	0.52
458	5.70	3.62	1.65	101.5	372.17	349.9[illegible]	193.2	200.9	9.82	12.45	1.46	8.05	45.84	10.41	11.86	0.52
459	6.49	4.14	1.66	101.5	372.01	346.89	189.9	195.9	10.99	12.12	1.43	7.55	49.02	11.45	11.66	0.52
460	7.69	4.93	1.67	101.5	371.78	346.6[illegible]	188.3	192.8	13.17	12.01	1.40	7.09	54.57	13.51	11.67	0.52
461	0.59	0.37	1.0[illegible]	102.7	373.43	332.5[illegible]	444.2	43[illegible].8	4.79	36.06	4.05	30.49	18.10	3.47	37.38	0.52
462	0.76	0.48	1.07	102.7	373.39	331.58	423.7	425.2	6.13	35.68	3.73	38.84	29.68	6.28	35.53	0.52
463	1.17	0.73	1.0[illegible]	102.5	373.27	329.[illegible]	407.3	412.0	9.29	34.88	3.48	35.70	41.74	9.82	34.35	0.52
464	1.54	0.96	[illegible]	102.5	373.21	327.64	399.1	396.1	11.88	33.69	3.36	30.81	47.43	11.78	33.79	0.52
465	1.93	1.21	1.0[illegible]	102.3	373.[illegible]8	325.56	378.6	386.3	14.63	32.89	3.10	29.19	56.35	15.41	32.11	0.52
466	2.[illegible]1	1.45	1.0	102.2	372.99	323.47	366.3	376.[illegible]	17.28	32.24	2.94	26.91	62.25	18.27	31.26	0.52
467	2.72	1.71	1.0[illegible]	102.2	372.90	321.71	353.9	364.[illegible]	19.84	[illegible]1.34	2.80	24.55	66.88	20.85	30.33	0.52
468	[illegible]	1.96	[illegible]	[illegible]	372.[illegible]1	[illegible]	337.5	351.4	21.87	[illegible].24	2.64	22.69	70.68	23.27	28.84	0.52
469	[illegible].55	2.24	[illegible]	102.1	[illegible]72.73	319.[illegible]9	333.4	337.6	23.86	2[illegible].98	2.59	20.32	72.20	24.28	28.56	0.52
470	[illegible].98	2.51	[illegible]	[illegible]	372.67	31[illegible].87	325.2	326.2	25.80	28.00	2.51	18.69	74.40	25.90	27.90	0.52
471	5.11	[illegible].24	1.1	101.9	372.[illegible]7	[illegible]	312.9	3[illegible]1.[illegible]	30.63	25.96	2.39	15.38	78.68	29.42	27.17	0.52
472	6.4	4.[illegible]	[illegible].1	[illegible]	372.[illegible]1	[illegible]	288.2	275.7	34.77	2[illegible].72	2.17	12.93	82.74	33.48	25.00	0.51
473	7.[illegible]	5.[illegible]1	1.1	101.5	371.75	311.59	267.7	252.6	38.50	21.66	2.0[illegible]	10.96	85.68	36.96	23.21	0.51
474	9.[illegible]9	5.[illegible]9	1.1[illegible]	[illegible]	371.4[illegible]	[illegible]9.55	2[illegible]8.8	23[illegible]	41.67	19.97	1.76	9.54	88.65	41.30	20.55	0.51

Table 7.2 (continued)

Run No.	$W_{\infty 2}$	$\tilde{W}_{\infty 2}$	U_∞	P_∞	T_∞	T_w	$\dot{Q}''_{obs}$	coupled condensate film and gas layer equations: $\dot{Q}''_{calc}$	$T_\infty - T_i$	$T_i - T_w$	gas layer only (condensate film resistance accounted by equation 7.3): $\frac{Sh}{\sqrt{Re_v}}$	$\frac{1}{\psi}$	W_i	$T_\infty - T_i$	$T_i - T_w$	Sc
	%	%	m/s	Pa	K	K	kW/m^2	kW/m^2	K	K			%	K	K	
475	10.94	7.10	1.15	1 1.3	371.09	307.74	214.2	214.9	45.00	18.35	1.57	8.30	90.79	45.08	18.28	0.51
476	0.57	0.35	1.07	1 2.8	373.45	341.94	379.4	365.4	3.31	[illegible]	3.56	19.75	11.20	2.01	29.50	0.52
477	0.75	0.47	[illegible]	1 2.7	373.41	341.89	369.6	363.2	4.39	26.13	3.36	26.23	19.60	.79	28.73	0.52
478	1.12	0.64	[illegible]	1 2.5	373.30	338.91	354.9	361.8	6.10	28.27	3.11	30.91	31.57	6.75	27.61	0.52
479	1.55	0.97	[illegible]	1 2.5	373.21	337.16	337.7	346.5	8.97	27.06	2.89	26.96	41.83	9.79	26.25	0.52
480	2. 6	1.29	[illegible]	1 2.5	373.12	335.60	325.4	331.9	11.44	25.88	2.75	2 .51	48.38	12.04	25.28	0.52
481	2.45	1.67	1. 9	1 2.5	373.01	332.56	313.2	319.7	14.40	25.03	2.60	21.04	55.76	15.01	24.42	0.52
482	3. 7	1.89	1.09	1 2.5	372.95	332.76	308.2	311.1	15.67	24.32	2.54	19.41	58.28	16.13	24.06	0.52
483	3.12	1.96	1.1	1 2.2	372.83	331.26	303.4	313.4	16.83	24.73	2.46	19.76	61.61	17.78	23.78	0.52
484	3.50	2.27	1.1	1 2.1	372.75	330.12	293.5	305.7	18.47	24.15	2.36	18.60	65.06	19.62	23.00	0.52
485	3.94	2.49	1.1	[illegible]	372.62	328.05	283.7	299.8	20.69	2 .87	2.24	17.62	69.37	22.22	22.34	0.52
486	5. 8	3.22	1.11	1 1.6	372.30	324.76	276.3	279.9	25.13	27.40	2.16	14.61	74.16	25.48	22.06	0.52
487	6. 8	4.07	1.1	1 1.7	372.09	322.41	254.2	258.3	29.05	2 .63	1.96	12.38	78.95	29.44	20.24	0.52
488	7.82	5.01	1.13	1 1.4	371.73	320.25	237.0	237.9	32.55	18.93	1.81	10.52	82.27	32.64	18.84	0.52
489	9.25	5.96	1.14	1 1.2	371.41	317.07	217.3	223.3	36.47	17.92	1.64	9.30	85.95	37.05	17.33	0.51
490	10.88	7.36	1.15	1 1.4	371.12	315.29	202.5	206.5	39.35	16.49	1.52	8.08	87.91	39.73	16.10	0.51
491	0.45	0.28	1.0	1 2.7	373.45	358.81	214.5	215.2	1.01	13.63	2.07	14.06	6.28	1.06	13.58	0.52
492	0.69	0.43	1.0	1 2.6	373.37	358.23	211.3	214.3	1.57	13.60	2.02	14.91	10.35	1.81	13.36	0.52
493	1.18	0.73	1.0	1 2.6	373. 9	357.14	209.6	212.0	2.67	13.47	1.99	13.40	15.76	2.85	13.29	0.52
494	1.64	1.03	1.0	1 2.6	373.20	356.13	208.0	209.5	3.74	13.33	1.96	12.51	20.57	3.85	13.22	0.52
495	2. 6	1.42	[illegible]	1 2.5	373. 6	355.25	204.8	202.8	4.98	13.85	1.93	11.11	25.08	4.82	13.01	0.52
496	2.72	1.71	1.0	1 .5	372.99	353.8	203.1	2 .6	6.17	13.30	1.89	11.28	30.67	6.20	12.96	0.52
497	3. 1	1.90	1. 9	1 2.5	372.94	353.30	201.5	201.5	6.78	12.86	1.86	10.93	32.93	6.78	12.86	0.52
498	3. 6	2. 5	1.1	1 2.2	372.80	352.32	199.9	202.7	7.47	1 .01	1.83	11.12	36.23	7.70	12.78	0.52
499	3.55	2.24	1.1	1 2.1	372.73	351.74	198.3	20 .9	8.09	12.89	1.80	10.82	38.37	8.30	12.68	0.52
500	3.94	2.49	1.1	[illegible]	372.65	350.29	195.8	202.3	9.26	13.09	1.75	10.93	43.10	9.78	12.57	0.52
501	5. 1	3.18	1.1	[illegible]	372.37	348.2	193.4	195.3	11.53	12.64	1.72	9.75	48.87	11.68	12.49	0.52
502	6.16	3.9	1.1	1 1.	371.98	344.67	186.9	193.4	14.61	12.70	1.61	9.33	57.52	15.14	12.18	0.52
503	7.78	4.93	1.1	1 1.5	371.77	342.87	175.4	18 .1	17.17	11.74	1.51	8.08	62.82	17.54	11.37	0.52
504	9. 7	5.98	1.14	1 1.5	371.47	34 .	167.3	171.5	19.71	11.17	1.43	7.29	67.61	20.05	10.84	0.52
505	1 .82	7. 2	1.15	1 1.4	371.16	33 .47	158.3	163.1	22. 7	1 .62	1.34	6.62	71.64	22.45	10.23	0.52
506	1.44	1. 4	[illegible]	1 1.	372. 4	19.	293.6	3 .8	25.18	2 .64	3.94	44.69	74.04	26.00	27.83	0.52

Table 7.2 (continued)

Run No.	$W_{\infty 2}$	$\tilde{W}_{\infty 2}$	U_∞	P_∞	T_∞	T_w	$\dot{Q}''_{obs}$	coupled condensate film and gas layer equations: $\dot{Q}''_{calc}$	$T_\infty - T_i$	$T_i - T_w$	gas layer only (condensate film resistance accounted by equation 7.3): $\frac{Sh}{\sqrt{Re_v}}$	$\frac{1}{\omega}$	W_i	$T_\infty - T_i$	$T_i - T_w$	Sc
	%	%	m/s	Pa	K	K	kW/m²	kW/m²	K	K			%	K	K	
507	2.37	1.49	0.35	101.2	372.71	316.67	268.9	268.0	30.74	25.30	3.50	33.49	79.45	30.64	25.40	0.51
508	3.61	2.28	0.36	101.2	372.49	313.13	240.0	229.3	37.88	21.48	3.03	23.53	84.90	36.68	22.68	0.51
509	4.79	2.71	0.37	100.7	372.21	310.67	223.5	216.1	41.23	21.31	2.75	20.41	87.57	40.41	21.13	0.51
510	5.9	3.76	0.35	100.5	371.84	305.80	173.9	162.7	48.69	17.35	2.15	15.65	92.40	49.69	15.35	0.50
511	5.61	3.57	.37	100.2	371.85	305.87	186.3	191.6	47.71	15.27	2.26	16.36	91.81	48.31	17.67	0.50
512	6.58	4.20	0.38	100.4	371.69	303.16	178.0	179.2	51.31	17.22	2.13	14.15	93.11	51.45	17.08	0.50
513	5. 1	3.18	0.41	98.4	371.43	31 .61	210.8	206.3	41.83	19.01	2.50	17.62	88.30	41.34	19.50	0.51
514	7.62	4.88	0.4	98.4	370.94	307.51	179.3	168.5	48.21	15.22	2.09	12.00	91.48	47.03	16.40	0.51
515	9.94	6.42	0.45	97.8	370.33	304.41	154.2	148.2	52.61	13.31	1.77	9.42	93.60	51.96	13.96	0.50
516	12.39	8.08	0.46	96.9	369.57	301.01	135.3	131.5	56.74	11.83	1.55	7.68	95.10	56.31	12.25	0.50
517	15.17	10.01	0.47	96.7	368.93	299.62	113.3	115.8	59.07	11.24	1.31	6.33	95.99	59.33	9.97	0.50
518	18.78	12.07	0.48	96.2	368.16	298.08	103.9	103.3	61.09	9.01	1.22	5.34	96.49	61.02	9.08	0.50
519	21.16	14.31	0.49	95.6	367.29	296.35	94.5	92.7	62.94	8.00	1.13	4.58	96.96	62.75	8.19	0.50
520	24.22	16.59	0.51	95.3	366.49	295.62	88.2	83.8	63.76	7.11	1.08	4.01	97.18	63.31	7.56	0.50
521	5.12	3.25	0.41	98.5	371.43	331.99	167.9	171.1	26.38	13.06	2.16	14.80	75.79	26.67	12.76	0.52
522	7.59	4.86	0.43	98.1	370.85	327.89	142.0	146.4	31.95	11.01	1.78	10.82	82.13	32.35	10.61	0.52
523	9.85	6.36	0.44	98.0	370.40	324.16	130.5	131.4	36.38	9.86	1.62	8.71	85.75	36.47	9.77	0.51
524	12.33	8.05	0.46	96.9	369.58	319.37	114.9	119.0	41.23	8.99	1.41	7.24	89.32	41.60	8.61	0.51
525	15.14	9.99	0.47	96.6	368.96	316.00	104.4	106.5	44.93	8.03	1.29	6.04	91.36	45.13	7.83	0.51
526	18.04	12.15	0.45	95.9	368.06	313.45	98.0	95.8	47.47	7.16	1.22	5.13	92.55	47.26	7.37	0.51
527	21.10	14.34	0.49	95.9	367.39	311.60	88.6	86.1	49.43	6.35	1.12	4.41	93.53	49.19	6.59	0.51
528	24.44	16.75	0.5	96.0	366.65	309.81	81.3	77.9	51.15	5.69	1.05	3.86	94.31	50.84	6.00	0.51
529	2.38	1.49	0.85	98.6	371.97	322.21	347.9	343.9	19.80	29.96	3.17	27.12	64.51	19.40	30.37	0.52
530	3.77	2.38	0.86	98.5	371.69	317.86	313.5	301.8	27.47	26.36	2.76	19.90	74.98	26.25	27.57	0.52
531	5.[illegible]	3.[illegible]	0.87	98.2	371.35	315.47	279.2	266.7	32.79	21.10	2.41	15.56	80.93	31.50	24.38	0.51
532	6.50	4.14	0.87	97.9	371.01	312.56	235.4	244.3	37.24	21.21	1.99	13.31	86.49	38.16	20.29	0.51
533	8.18	5.25	0.8	97.6	370.60	310.11	213.4	219.6	41.49	18.99	1.79	10.89	89.13	42.13	18.36	0.51
534	10.59	6.86	0.9	97.7	37 .76	3 7.7	194.7	192.7	46.15	16.57	1.63	8.62	91.79	45.95	16.77	0.51
535	11.16	7.72	.9	96.6	369.61	305.41	179.0	181.7	48.54	15.66	1.50	7.81	92.62	48.81	15.39	0.51
536	13.90	9.13	0.9	96.4	369.13	303.77	169.6	165.7	51.17	14.19	1.43	6.73	93.50	50.77	14.59	0.51
537	2.36	1.47	.8	98.6	371.99	34 .7	240.6	254.6	9.83	10.45	2.44	19.73	44.57	10.53	17.74	0.52
538	[illegible]	2.43	[illegible]	[illegible]	371.67	34 . 4	232.6	228.6	15.15	10.48	2.25	14.53	56.02	14.81	16.82	0.52

Table 7.2 (continued)

Run No.	$W_{\infty 2}$	$\tilde{W}_{\infty 2}$	U_{∞}	P_{∞}	T_{∞}	T_w	$\dot{Q}''_{obs}$	coupled condensate film and gas layer equations $\dot{Q}''_{calc}$	$T_{\infty}-T_i$	T_i-T_w	gas layer only (condensate film resistance accounted by equation 7.3) $\frac{Sh}{\sqrt{Re_v}}$	$\frac{1}{\omega}$	W_i	$T_{\infty}-T_i$	T_i-T_w	Sc
	%	%	m/s	Pa	K	K	kW/m^2	kW/m^2	K	K			%	K	K	
539	5.20	3.30	0.87	98.2	371.75	337.28	218.4	211.4	18.90	15.17	2.08	12.20	63.45	18.28	15.79	0.52
540	6.52	4.16	0.87	97.9	371.00	334.0[illegible]	197.9	199.1	22.58	14.34	1.84	10.88	70.96	22.68	14.24	0.52
541	8.27	5.31	[illegible].8[illegible]	97.6	370.58	331.17	182.8	162.9	26.28	1[illegible].13	1.68	9.21	76.09	26.29	13.13	0.52
542	1[illegible].16	6.57	[illegible].89	97.3	37[illegible].14	327.95	164.4	169.9	30.06	12.14	1.50	7.96	80.88	30.44	11.75	0.52
543	11.83	7.71	0.91	97.0	369.72	325.85	154.8	157.7	32.58	11.30	1.41	7.04	83.31	32.84	11.04	0.52
544	13.89	9.12	0.94	96.5	369.23	323.64	146.1	145.6	35.21	1[illegible].38	1.34	6.15	85.46	35.16	10.42	0.52
545	1.41	0.88	1.55	1[illegible]2.6	37[illegible].75	329.40	44[illegible].1	431.4	8.52	35.24	3.21	24.39	34.39	7.49	36.27	0.52
546	1.41	0.68	1.55	1[illegible]2.6	373.25	344.06	352.9	333.5	5.21	24.98	2.75	13.43	18.94	3.52	25.68	0.52
547	1.41	0.88	1.55	102.6	373.25	363.59	153.4	151.7	1.36	8.30	1.37	5.76	8.12	1.25	8.42	0.52
548	2.81	1.77	1.59	102.4	372.94	324.33	412.7	393.9	15.05	32.56	2.84	19.25	54.07	14.23	34.39	0.52
549	2.81	1.77	1.59	1[illegible]2.4	372.94	339.34	323.6	318.7	10.39	24.21	2.34	15.31	42.99	9.95	23.65	0.52
550	2.81	1.77	1.59	102.4	372.94	362.31	148.4	146.5	2.65	7.98	1.31	5.55	15.58	2.52	8.11	0.52
551	4.51	2.86	1.61	102.0	372.51	317.83	358.1	358.3	24.41	[illegible].28	2.32	16.10	72.66	24.44	30.25	0.52
552	4.51	2.86	1.61	1[illegible]2.[illegible]	372.51	332.41	298.5	306.1	17.17	22.93	2.04	13.80	62.25	17.86	22.24	0.52
553	4.51	2.86	1.61	102.0	372.51	360.10	142.7	146.0	4.40	8.01	1.21	5.75	25.95	4.63	7.79	0.52
554	6.64	4.24	1.64	1[illegible]1.3	371.93	313.3	311.9	315.2	31.85	26.78	1.96	12.30	81.67	32.19	26.45	0.52
555	6.64	4.24	1.64	1[illegible]1.3	371.93	327.88	261.8	276.6	23.26	2[illegible].80	1.89	10.68	70.96	22.78	21.27	0.52
556	6.64	4.24	1.64	1[illegible]1.3	371.93	358.42	134.6	136.6	6.09	7.42	1.15	5.03	33.39	6.22	7.28	0.52
557	8.89	5.72	1.67	100.8	371.75	309.7[illegible]	269.8	280.8	38.04	[illegible].99	1.66	9.82	87.32	39.15	22.89	0.51
558	8.89	5.72	1.67	1[illegible].8	371.35	324.56	244.1	249.4	28.29	18.69	1.60	8.84	78.60	28.57	18.21	0.52
559	8.89	5.72	1.67	1[illegible].8	371.35	357.[illegible]1	127.7	127.[illegible]	7.55	6.83	1.10	4.40	39.10	7.50	6.85	0.52
560	11.90	7.75	1.71	99.7	370.45	304.64	240.4	245.0	44.69	21.11	1.47	7.64	90.97	45.16	20.65	0.51
561	11.90	7.75	1.71	99.7	370.45	317.14	231.5	226.4	35.87	17.44	1.49	7.16	85.20	35.39	17.92	0.52
562	11.90	7.75	1.71	99.7	370.45	35[illegible].75	132.1	135.6	12.12	7.58	1.07	4.53	53.94	12.37	7.33	0.52
563	15.11	9.97	1.75	99.0	369.60	302.19	219.3	214.3	49.07	18.34	1.36	6.14	92.72	48.57	18.84	0.51
564	15.09	9.95	1.75	[illegible]	369.61	312.61	195.8	201.1	40.52	15.47	1.26	5.92	89.24	41.01	14.98	0.51
565	15.11	9.97	1.75	99.0	369.60	346.55	123.[illegible]	124.2	14.25	6.85	1.02	3.94	59.49	14.25	6.79	0.53
566	2.12	1.37	1.[illegible]	1[illegible]	373.[illegible]	321.76	412.8	387.7	17.38	3[illegible].94	3.48	25.99	55.08	14.80	36.52	0.52
567	2.12	1.33	1.0[illegible]	1[illegible]2.3	373.03	336.9[illegible]	321.6	319.0	11.49	24.65	2.61	21.85	46.31	11.25	24.88	0.52
568	2.12	1.37	1.[illegible]	1[illegible]2.[illegible]	373.[illegible]	361.69	157.9	148.2	2.84	[illegible].51	1.62	6.86	14.55	2.43	8.92	0.52
569	4.[illegible]9	2.71	1.[illegible]	1[illegible]2.0	372.56	314.55	32[illegible]	322.0	29.49	28.52	2.48	18.37	78.77	29.67	28.34	0.52
570	4.[illegible]9	2.71	1.[illegible]	1[illegible]	372.56	32[illegible].71	281.8	282.7	21.58	2[illegible].27	2.30	16.00	68.62	21.66	22.19	0.52

Table 7.2 (continued)

Run No.	$W_{\infty 2}$	$\tilde{W}_{\infty 2}$	U_∞	P_∞	T_∞	T_w	$\dot{Q}''_{obs}$	coupled condensate film and gas layer equations			gas layer only (condensate film resistance accounted by equation 7.3)					
								$\dot{Q}''_{calc}$	$T_\infty - T_i$	$T_i - T_w$	$\frac{Sh}{\sqrt{Re_v}}$	$\frac{1}{\omega}$	W_i	$T_\infty - T_i$	$T_i - T_w$	Sc
	%	%	m/s	Pa	K	K	kW/m²	kW/m²	K	K			%	K	K	
571	4.19	2.71	1.05	102.0	372.56	358.57	142.1	143.0	5.75	8.24	1.43	7.07	30.33	5.82	8.17	0.52
572	6.65	4.24	1.07	101.3	371.93	309.02	269.8	275.3	38.51	24.39	2.02	13.07	86.85	38.88	24.02	0.51
573	6.65	4.24	1.07	101.3	371.93	322.4	250.4	247.9	29.80	19.73	1.98	11.91	79.15	29.56	19.97	0.52
574	6.65	4.24	1.07	101.3	371.93	354.41	140.9	141.1	9.29	8.23	1.37	6.50	43.22	9.30	8.22	0.52
575	9.51	6.14	1.1	101.3	371.09	302.98	240.4	232.4	46.24	21.87	1.78	9.55	90.84	45.39	21.73	0.51
576	9.51	6.14	1.1	100.3	371.09	316.38	218.9	215.7	37.38	17.34	1.69	9.04	86.04	37.07	17.64	0.51
577	9.51	6.14	1.10	100.3	371.09	350.48	132.1	132.6	12.87	7.74	1.27	5.68	54.04	12.90	7.71	0.52
578	13.18	8.63	1.14	99.8	370.21	300.81	196.3	194.3	52.13	17.28	1.47	7.11	93.68	51.71	17.70	0.51
579	13.18	8.63	1.12	99.8	370.21	311.62	187.4	183.6	43.84	14.74	1.45	6.85	90.29	43.47	15.12	0.51
580	13.18	8.63	1.11	99.8	370.21	346.19	122.7	121.8	16.92	7.10	1.17	4.83	63.64	16.86	7.17	0.52
581	16.99	11.29	1.16	98.8	369.12	298.12	168.8	166.7	56.33	14.68	1.27	5.61	95.25	56.10	14.90	0.50
582	16.99	11.29	1.16	98.6	369.12	307.88	311.1	159.1	48.52	12.72	2.61	4.95	84.18	32.92	28.32	0.51
583	16.99	11.29	1.16	98.6	369.12	342.14	113.3	111.7	20.50	6.49	1.08	4.16	70.66	20.38	6.61	0.53
584	21.47	14.53	1.2	98.1	367.94	296.31	143.5	142.2	59.35	12.28	1.11	4.48	96.24	59.21	12.42	0.50
585	21.47	14.53	1.2	98.1	367.94	305.11	141.2	136.6	52.06	10.78	1.13	4.39	94.28	51.62	11.22	0.51
586	21.47	14.53	1.2	98.1	367.94	336.15	105.2	103.9	25.66	6.12	0.99	3.65	78.40	25.57	6.21	0.53

Table 7.3 Vapour-gas mixtures results

mixture steam-air
tube diameter 12.5 mm

Run No.	$W_{\infty 2}$	$\tilde{W}_{\infty 2}$	U_∞	P_∞	T_∞	T_w	$\dot{Q}''_{obs}$	coupled condensate film and gas layer equations: $\dot{Q}''_{calc}$	$T_\infty - T_i$	$T_i - T_w$	gas layer only (condensate film resistance accounted by equation 7.3): $\frac{Sh}{\sqrt{Re_v}}$	$\frac{1}{\psi}$	W_i	$T_\infty - T_i$	$T_i - T_w$	Sc
	%	%	m/s	Pa	K	K	kW/m²	kW/m²	K	K			%	K	K	
587	1.95	1.72	25.1	4.3	303.29	295.62	115.3	102.4	0.76	5.91	-	-	-	-	-	-
588	1.96	1.73	20.2	5.6	307.82	299.31	132.4	124.0	1.04	7.46	1.64	2.83	5.55	0.42	8.08	0.48
589	2.16	1.76	18.7[illegible]	6.1	309.33	301.28	145.1	126.9	1.24	7.61	-	-	-	-	-	-
590	2.41	1.51	17.59	6.5	311.65	301.1[illegible]	149.4	132.3	1.45	8.06	3.36	1.55	3.73	0.16	9.35	0.49
591	2.61	1.54	16.[illegible]	7.[illegible]	312.65	302.37	153.6	139.0	1.73	8.56	1.85	2.89	7.55	0.62	9.67	0.49
592	2.72	1.71	14.52	8.2	314.74	303.51	157.9	147.8	2.01	9.22	1.59	4.46	12.13	1.23	10.00	0.49
593	3.47	2.19	12.0[illegible]	1[illegible].1	318.72	305.25	175.0	162.0	3.11	10.36	1.65	5.26	18.24	2.09	11.38	0.49
594	3.96	2.50	9.26	13.8	324.84	307.03	204.8	191.6	4.93	12.88	1.76	7.08	28.01	3.85	13.96	0.50
595	5.30	3.36	7.21	18.4	330.67	307.76	209.0	208.3	8.34	14.56	1.65	8.83	46.77	8.29	14.61	0.51
596	6.42	4.12	5.92	23.2	335.52	307.8	217.5	218.9	11.95	15.77	1.64	8.99	57.73	12.07	15.65	0.51
597	2.55	1.60	15.05	3.7	300.60	294.13	102.5	86.5	1.27	5.20	-	-	-	-	-	-
598	2.49	1.56	14.7[illegible]	3.8	301.39	294.47	106.7	88.4	1.28	5.34	-	-	-	-	-	-
599	2.81	1.76	13.97	4.0	302.14	294.95	111.0	91.2	1.53	5.55	-	-	-	-	-	-
600	2.92	1.84	13.26	4.7	303.13	295.52	115.3	95.5	1.73	5.88	3.52	1.58	4.60	0.19	7.41	0.48
601	2.91	1.83	12.50	4.6	304.27	296.28	119.5	99.2	1.84	6.15	3.07	1.76	5.14	0.26	7.74	0.48
602	2.96	1.86	11.71	5.0	305.59	296.83	123.8	105.8	2.09	6.67	2.09	2.89	8.56	0.67	8.09	0.48
603	3.34	2.10	10.94	5.4	306.92	297.4[illegible]	128.1	109.6	2.55	6.97	1.94	3.59	11.98	1.07	8.45	0.49
604	3.[illegible]7	2.[illegible]0	10.[illegible]7	5.9	308.69	297.90	132.4	121.1	2.86	7.92	1.73	5.69	18.07	1.95	8.83	0.49
605	3.66	2.31	8.97	6.7	311.[illegible]5	298.59	136.6	129.5	3.81	8.65	1.67	7.19	26.29	3.23	9.23	0.49
606	4.[illegible]3	2.55	8.14	7.5	313.08	299.47	14[illegible].9	134.[illegible]	4.57	9.05	1.69	7.61	30.66	4.01	9.61	0.50
607	5.[illegible]	[illegible].19	6.7	9.4	317.12	3[illegible].26	149.4	144.3	6.90	10.02	1.70	8.39	42.23	6.46	10.45	0.50
608	7.[illegible]4	4.50	5.2[illegible]	12.5	322.41	298.27	158.[illegible]	155.5	12.67	11.47	1.67	8.77	61.77	12.45	11.70	0.51
609	3.74	2.36	10.49	12.4	322.35	307.35	187.7	177.7	3.91	11.58	1.64	6.46	24.13	3.12	12.38	0.50
610	4.50	2.85	8.[illegible]5	15.1	327.99	308.1[illegible]	209.1	200.9	6.15	1[illegible].67	1.70	7.93	35.70	5.47	14.34	0.50
611	5.[illegible]1	3.18	7.6	[illegible]7.9	33[illegible].15	307.55	213.3	21[illegible].0	7.8[illegible]	14.81	1.67	8.89	44.57	7.69	14.91	0.51
612	5.69	3.42	6.67	[illegible].9	333.39	30[illegible].49	217.5	216.6	9.6[illegible]	15.29	1.66	8.88	50.53	9.53	15.37	0.51
613	6.67	4.26	5.6[illegible]	[illegible]5.[illegible]	337.42	[illegible]7.85	221.6	226.4	13.[illegible]8	16.5[illegible]	1.62	9.14	60.06	13.49	16.09	0.51
614	7.11	4.54	5.1	[illegible]6.7	340.72	307.8[illegible]	226.1	232.6	15.16	17.24	1.61	9.22	65.51	15.75	16.65	0.51
615	8.71	5.6[illegible]	4.47	[illegible]3.8	343.71	307.26	221.6	226.7	19.42	17.03	1.54	8.34	72.60	19.86	16.58	0.52
616	1.72	[illegible]	4.6	[illegible]	[illegible]42.69	325.1	245.1	231.[illegible]	2.35	15.22	2.17	6.56	9.33	1.22	16.36	0.50
617	1.[illegible]	1.24	4.17	[illegible]4.9	345.46	32[illegible].46	246.7	23[illegible].7	3.43	15.37	2.08	8.03	15.91	2.30	16.50	0.51

Table 7.3 (continued)

Run No.	$W_{\infty 2}$ %	$\tilde{W}_{\infty 2}$ %	U_∞ m/s	P_∞ Pa	T_∞ K	T_w K	$\dot{Q}''_{obs}$ kW/m²	coupled condensate film and gas layer equations: $\dot{Q}''_{calc}$ kW/m²	$T_b - T_i$ K	$T_i - T_w$ K	gas layer only (condensate film resistance accounted by equation 7.3): $\frac{Sh}{\sqrt{Re_v}}$	$\frac{1}{\psi}$	W_i %	$T_b - T_i$ K	$T_i - T_w$ K	So
618	2.56	1.61	4.46	32.3	343.61	324.72	231.5	223.3	4.20	14.70	1.89	9.00	23.01	3.54	15.36	0.51
619	3.42	2.15	4.47	32.4	343.51	323.35	223.9	219.6	5.63	14.54	1.78	9.29	31.74	5.29	14.88	0.51
620	4.[illegible]4	2.55	3.8	29.3	347.96	324.66	226.4	231.6	7.66	15.65	1.72	10.44	42.17	8.09	15.22	0.51
621	4.76	3.03	3.9	18.3	347.28	323.96	221.3	220.9	8.52	14.79	1.69	9.21	44.01	8.49	14.83	0.51
622	5.42	3.45	4.0	7.3	346.5	322.54	223.9	226.4	10.40	15.56	1.67	9.41	51.07	10.61	15.35	0.51
623	6.73	4.29	4.19	75.5	345.15	317.83	218.8	215.9	12.43	14.89	1.63	8.35	56.14	12.18	15.14	0.51
624	7.58	4.85	4.57	74.2	342.74	316.54	201.1	201.1	12.53	17.66	1.51	7.64	57.86	12.54	13.66	0.52
625	8.46	5.45	4.25	75.5	344.90	315.72	201.1	204.2	15.06	14.12	1.47	7.55	64.08	15.33	13.85	0.52
626	3.78	2.13	12.34	4.6	304.33	301.95	47.5	39.1	0.56	1.83	4.38	1.14	3.84	0.05	2.33	0.48
627	3.51	2.21	9.36	6.4	309.99	306.61	58.5	51.2	0.86	2.52	1.34	1.93	6.79	0.40	2.98	0.49
628	4.46	2.82	7.21	8.6	315.52	310.48	68.7	65.6	1.63	3.42	1.05	3.36	14.95	1.43	3.62	0.49
629	5.48	3.48	6.57	9.6	317.55	312.14	71.2	65.1	2.04	5.37	1.12	3.12	17.07	1.64	3.77	0.50
630	6.74	4.30	5.64	11.4	320.75	314.03	75.4	70.9	2.97	[illegible].76	1.09	3.57	24.05	2.67	4.05	0.50
631	1.84	1.15	2.3	27.6	340.12	31[illegible].04	231.3	214.0	5.50	15.58	2.71	13.64	25.07	3.97	17.11	0.51
632	2.64	1.78	2.37	27.1	339.55	316.67	216.5	203.1	8.09	14.82	2.43	13.64	38.69	6.90	16.01	0.51
633	4.25	2.69	2.36	27.6	339.72	315.23	204.6	185.5	11.07	17.42	2.27	11.31	48.13	9.37	15.12	0.51
634	5.42	3.44	2.37	27.9	339.82	311.72	184.0	182.8	14.57	13.53	1.93	11.50	62.30	14.45	13.65	0.51
635	6.65	4.25	2.35	28.7	340.24	311.00	178.0	171.4	16.64	12.60	1.85	9.92	65.98	16.05	13.19	0.51
636	7.64	4.89	2.3	28.5	339.98	31[illegible].69	175.1	161.1	17.59	11.70	1.83	8.76	66.92	16.35	12.94	0.51
637	9.[illegible]5	5.83	2.41	28.7	339.91	306.97	163.1	157.5	21.22	11.72	1.65	8.26	74.74	20.71	12.23	0.52
638	10.41	6.87	2.4	9.4	340.16	305.26	154.4	149.2	23.79	11.13	1.55	7.41	78.56	23.32	11.60	0.52
639	2.14	1.[illegible]4	1.15	32.8	344.74	314.74	228.2	221.1	12.01	17.99	3.10	24.32	52.06	11.31	18.69	0.51
640	3.68	2.32	1.21	32.9	343.89	311.30	184.8	191.6	17.16	15.44	2.38	18.46	67.85	17.81	14.78	0.51
641	5.52	3.51	1.21	33.9	344.[illegible]5	308.83	171.3	167.2	22.07	17.36	2.16	13.51	74.57	21.67	13.75	0.51
642	7.65	4.9[illegible]	1.17	35.9	345.30	305.3[illegible]	152.3	150.1	27.90	12.10	1.87	10.73	82.11	27.68	12.32	0.51
643	9.74	6.29	1.16	37.3	345.32	3[illegible]2.47	141.4	136.3	32.31	11.35	1.71	8.83	86.02	31.80	11.56	0.51
644	5.96	3.79	1.86	[illegible].1	332.47	307.49	141.1	135.3	15.[illegible]2	9.96	1.95	10.77	64.16	14.50	10.48	0.51
645	7.[illegible]9	4.66	1.9	[illegible]6.6	330.68	304.95	124.5	124.2	16.6[illegible]	9.10	1.72	9.50	69.23	16.57	9.13	0.51
646	10.51	6.81	2.06	18.9	330.49	301.35	113.4	110.3	21.03	8.09	1.52	7.32	76.95	20.74	8.37	0.52
647	11.99	7.81	2.21	18.7	330.05	299.[illegible]	110.7	107.2	23.09	7.94	1.45	6.67	80.02	22.78	8.25	0.52
648	13.87	9.11	2.	1.2	332.47	298.[illegible]	105.2	102.6	26.76	7.67	1.36	6.06	84.03	26.52	7.91	0.52
649	15.[illegible]2	1[illegible].41	1.74	15.[illegible]	335.94	29[illegible].[illegible]4	99.6	96.2	30.25	7.36	1.27	5.53	86.88	30.11	7.49	0.52

Table 7.3 (continued)

Run No.	$W_{\infty 2}$ %	$\tilde{W}_{\infty 2}$ %	U_∞ m/s	P_∞ Pa	T_∞ K	T_w K	$\dot{Q}''_{obs}$ kW/m²	coupled condensate film and gas layer equations: $\dot{Q}''_{calc}$ kW/m²	$T_\infty - T_i$ K	$T_i - T_w$ K	gas layer only (condensate film resistance accounted by equation 7.3): $\frac{Sh}{\sqrt{Re_v}}$	$\frac{1}{\omega}$	W_i %	$T_\infty - T_i$ K	$T_i - T_w$ K	Sc
550	2.46	1.55	19.64	5.7	308.28	301.69	116.3	100.2	0.96	5.62	-	-	-	-	-	-
551	2.77	1.49	14.9	7.9	314.10	304.98	137.0	129.5	1.40	7.71	1.46	3.82	9.06	0.85	8.26	0.49
552	2.64	1.66	11.56	10.6	319.78	307.71	161.9	157.7	2.21	9.86	1.49	6.14	16.21	1.89	10.18	0.49
553	3.51	2.21	9.77	12.9	323.58	308.36	186.8	176.9	3.73	11.49	1.66	6.52	22.91	2.94	12.28	0.50
554	4.20	2.66	8.4	15.3	327.4	310.39	203.4	183.1	4.93	12.01	1.82	5.94	24.99	3.30	13.64	0.50
555	4.46	2.82	7.24	18.3	330.69	310.76	207.5	201.1	6.32	13.61	1.70	8.22	36.65	5.80	14.13	0.50
556	5.18	3.74	6.2	21.8	334.24	310.54	207.5	206.1	9.44	14.27	1.62	8.47	49.78	9.32	14.38	0.51
557	6.39	4.07	5.65	24.3	336.60	311.6	207.5	211.4	11.14	14.86	1.58	8.75	55.89	11.47	14.53	0.51
558	7.32	4.68	4.78	30.0	341.14	308.68	215.8	227.6	15.66	16.80	1.55	9.20	67.29	16.71	15.75	0.52
559	8.65	5.56	4.06	36.4	345.40	309.31	220.0	223.8	19.44	16.65	1.55	8.34	72.13	19.78	16.31	0.52
560	8.45	5.56	4.06	36.4	345.40	316.18	202.3	200.7	15.38	13.85	1.50	7.38	63.85	15.24	13.98	0.52
561	8.65	5.56	4.05	36.4	345.40	331.87	128.2	126.4	6.51	7.03	1.13	4.51	39.04	6.39	7.15	0.51
562	7.55	4.55	4.49	[illegible]	342.51	331.25	129.8	125.2	5.43	6.94	1.18	4.45	33.75	5.11	7.26	0.51
563	7.56	4.65	4.49	32.0	342.61	317.87	199.0	193.3	11.87	12.92	1.54	7.25	54.93	11.40	13.39	0.51
564	5.97	3.80	5.25	26.4	338.51	318.02	191.6	188.1	8.22	12.27	1.54	7.43	44.36	7.94	12.55	0.51
565	5.97	3.80	5.25	26.4	338.51	329.3	115.8	110.6	3.33	5.88	1.14	3.91	23.33	2.99	6.23	0.51
566	4.74	3.0	6.15	22.0	334.59	327.19	110.0	100.6	2.19	5.21	1.21	3.14	14.88	1.58	5.83	0.50
567	4.74	3.0	6.17	22.0	334.59	316.08	194.1	189.3	6.18	12.33	1.60	7.63	36.17	5.81	12.71	0.51
568	4.60	2.91	6.4	21.1	333.71	316.72	181.6	180.6	5.46	11.54	1.51	7.48	34.38	5.38	11.62	0.51
569	4.60	2.91	6.41	21.1	333.71	326.14	105.9	103.1	2.18	5.39	1.08	3.76	17.29	2.00	5.57	0.50
570	3.95	2.50	7.69	16.9	329.10	323.22	99.3	86.1	1.45	4.43	1.35	2.29	9.06	0.73	5.15	0.50
571	3.95	2.5	7.7	16.9	329.10	315.4	174.2	161.5	3.74	8.96	1.59	5.47	21.60	2.77	10.93	0.50
572	2.67	1.68	15.5	4.9	305.41	299.14	108.0	89.1	1.15	5.12	-	-	-	-	-	-
573	2.67	1.66	15.5	4.9	305.41	300.87	82.2	70.0	0.81	3.73	-	-	-	-	-	-
574	2.67	1.68	15.51	4.9	305.41	303.61	41.5	34.3	0.31	1.49	-	-	-	-	-	-
575	2.71	1.72	11.71	7.5	313.19	309.97	61.4	54.7	0.60	2.62	1.60	1.58	4.28	0.19	3.02	0.49
576	2.71	1.70	11.7	7.5	313.19	305.7	114.6	102.9	1.51	5.96	1.65	2.95	7.98	0.66	6.83	0.49
577	2.71	1.70	11.7	7.5	313.19	303.12	141.2	127.2	2.12	7.95	1.79	3.95	10.70	1.32	9.04	0.49
578	3.90	2.46	7.9	11.6	319.68	305.27	157.8	151.7	4.41	10.00	1.64	7.44	29.03	3.91	10.50	0.50
579	3.90	2.46	7.9	[illegible]	319.68	308.9	132.0	124.2	3.13	7.57	1.48	5.45	21.26	2.54	8.16	0.50
580	[illegible]	2.46	[illegible]	[illegible]	319.68	314.9	71.3	68.5	1.25	3.44	1.00	3.01	11.75	1.07	3.62	0.49
581	4.7	2.96	[illegible]	[illegible]	322.75	316.85	78.7	74.0	1.71	3.78	1.07	3.12	14.57	1.41	4.08	0.50

Table 7.3 (continued)

Run No.	$W_{\infty 2}$ %	$\tilde{W}_{\infty 2}$ %	U_∞ m/s	P_∞ Pa	T_∞ K	T_w K	$\dot{Q}''_{obs}$ kW/m^2	coupled condensate film and gas layer equations: $\dot{Q}''_{calc}$ kW/m^2	$T_\infty - T_i$ K	$T_i - T_w$ K	gas layer only (condensate film resistance accounted by equation 7.3): $\frac{Sh}{\sqrt{Re_v}}$	$\frac{1}{\psi}$	W_i %	$T_\infty - T_i$ K	$T_i - T_w$ K	Sc
682	4.67	2.96	7.01	12.2	322.35	309.82	137.0	132.1	4.31	8.22	1.46	6.28	29.30	3.94	8.59	0.50
683	4.67	2.96	7.01	12.2	322.35	303.92	174.4	169.1	6.71	11.71	1.72	8.62	40.24	6.27	12.16	0.50
684	6.12	3.83	5.74	15.5	326.95	305.83	178.6	169.2	9.35	11.77	1.72	8.10	48.77	8.55	12.57	0.51
685	6.12	3.83	5.74	15.5	326.95	310.78	149.4	144.0	6.90	9.27	1.51	6.81	40.99	6.47	9.70	0.51
686	6.12	3.83	5.74	15.5	326.95	319.69	87.0	84.3	2.82	4.45	1.07	3.77	22.71	2.64	4.62	0.50
687	6.16	3.92	5.36	16.8	328.61	320.61	89.5	89.7	3.20	4.80	1.05	4.18	25.73	3.21	4.79	0.50
688	6.16	3.92	5.36	16.8	328.61	308.90	161.8	161.3	8.81	10.90	1.56	8.00	49.24	8.77	10.94	0.51
689	6.16	3.92	5.36	16.8	328.61	306.30	174.4	173.3	10.15	12.16	1.64	8.67	53.37	10.05	12.26	0.51
690	8.04	5.16	4.41	21.0	333.17	304.37	191.0	178.3	15.74	13.06	1.73	8.07	64.84	14.60	14.20	0.51
691	8.04	5.16	4.41	21.0	333.17	311.68	151.9	152.4	11.35	10.14	1.44	7.09	57.00	11.39	10.10	0.51
692	8.04	5.16	4.41	21.0	333.17	322.89	98.6	96.4	4.99	5.28	1.11	4.26	34.27	4.84	5.43	0.51
693	8.88	5.72	4.04	23.4	335.35	322.37	111.8	107.7	6.84	6.14	1.20	4.66	41.40	6.55	6.43	0.51
694	8.88	5.72	4.04	23.4	335.35	311.69	159.4	153.6	13.32	10.34	1.49	6.82	60.60	12.84	10.82	0.51
695	8.88	5.72	4.04	23.4	335.35	304.47	182.8	176.2	17.89	12.99	1.62	7.88	70.01	17.30	13.58	0.51
696	10.79	7.00	3.35	29.4	341.16	303.66	178.6	173.2	23.44	14.06	1.52	7.24	78.11	22.94	13.56	0.52
697	10.79	7.00	3.35	29.4	340.16	310.42	156.9	157.4	18.76	10.98	1.39	6.68	72.10	18.80	10.94	0.52
698	10.79	7.00	3.35	29.4	340.16	324.75	107.7	109.4	9.12	6.29	1.11	4.69	50.65	9.25	6.16	0.52
699	12.62	8.24	2.87	35.4	344.11	323.00	120.0	121.0	13.78	7.33	1.16	4.95	62.45	13.86	7.26	0.52
700	12.62	8.24	2.87	35.4	344.11	309.88	149.4	154.4	23.28	10.95	1.29	6.23	78.66	23.71	10.52	0.52
701	12.62	8.24	2.87	35.4	344.11	302.87	162.0	167.2	28.42	12.82	1.34	6.67	84.16	28.90	12.34	0.52
702	5.18	3.29	5.1	5.0	305.60	296.31	87.3	75.6	4.45	4.84	1.67	5.75	29.80	3.52	5.78	0.49
703	5.18	3.29	5.1	5.0	305.60	298.43	77.3	63.9	3.33	3.84	1.62	4.31	22.35	2.31	4.86	0.49
704	5.18	3.29	5.1	5.0	305.60	302.37	41.5	36.5	1.40	1.83	1.09	2.66	13.76	1.08	2.16	0.49
705	9.51	6.17	3.65	7.6	312.46	305.28	54.3	49.0	4.52	2.68	1.08	3.76	35.73	4.29	2.90	0.50
706	9.51	6.17	3.65	7.6	312.46	299.16	74.8	71.5	8.76	4.55	1.33	5.59	53.13	8.51	4.81	0.51
707	9.51	6.13	3.65	7.6	312.46	296.23	87.2	79.8	10.66	5.37	1.50	6.18	58.71	10.25	6.00	0.51
708	9.94	6.43	4.81	10.1	317.91	295.72	91.4	90.7	15.68	6.51	1.46	7.12	70.76	15.62	6.57	0.51
709	9.94	6.43	4.81	10.1	317.91	298.43	67.2	85.2	13.63	5.86	1.43	6.65	66.10	13.45	6.03	0.51
710	9.94	6.43	4.81	10.1	317.91	307.69	63.0	59.4	6.79	3.43	1.20	4.52	44.95	6.53	3.69	0.51
711	13.02	8.52	2.4	12.2	321.21	307.07	65.8	61.5	10.46	3.66	1.15	4.48	58.37	10.30	3.83	0.51
712	13.02	8.52	2.4	12.2	321.21	298.58	79.7	78.4	17.27	5.36	1.29	5.66	73.67	17.15	5.48	0.51
713	13.02	8.52	2.4	12.2	321.21	295.20	87.3	83.4	20.01	6.00	1.38	5.97	77.70	19.67	6.34	0.51

Table 7.3 (continued)

Run No.	$W_{\infty 2}$ %	$\tilde{W}_{\infty 2}$ %	U_{∞} m/s	P_{∞} Pa	T_{∞} K	T_w K	$\dot{Q}''_{obs}$ kW/m^2	coupled condensate film and gas layer equations: $\dot{Q}''_{calc}$ kW/m^2	$T_{\infty}-T_i$ K	T_i-T_w K	gas layer only (condensate film resistance accounted by equation 7.3): $\frac{Sh}{\sqrt{Re_v}}$	$\frac{1}{\psi}$	W_i %	$T_{\infty}-T_i$ K	T_i-T_w K	Sc
714	14.85	9.79	[illegible]	15.0	325.03	294.72	83.1	81.6	24.32	[illegible]	1.28	5.59	83.04	24.20	6.11	0.52
715	14.75	9.79	[illegible]	15.0	325.03	297.52	79.7	76.6	21.97	5.54	1.25	5.41	80.30	21.87	5.64	0.52
716	14.85	9.79	2.04	15.0	325.03	308.40	63.0	51.8	12.93	3.70	1.11	4.36	64.71	12.83	3.80	0.52
717	17.53	11.68	1.76	17.8	328.08	306.87	63.9	62.6	17.34	3.87	1.09	4.19	73.52	17.24	3.97	0.52
718	17.53	11.68	1.76	17.8	328.08	297.44	74.8	73.7	25.45	5.19	1.17	4.80	84.11	25.36	5.29	0.52
719	17.53	11.65	1.76	17.8	328.08	293.48	79.0	77.2	28.87	5.73	1.20	4.97	87.16	28.71	5.89	0.52
720	21.78	14.77	1.72	19.2	328.92	291.45	70.7	68.3	32.41	5.06	1.09	4.13	89.99	32.19	5.27	0.52
721	21.78	14.77	1.72	19.2	328.92	294.91	64.8	66.0	29.34	4.67	1.02	4.04	88.08	29.44	4.57	0.52
722	21.78	14.77	1.72	19.2	328.92	303.09	55.6	59.0	22.08	3.74	0.93	3.74	81.40	22.35	3.47	0.52
723	24.30	16.64	1.38	[illegible]	333.91	305.04	58.1	56.6	25.30	3.58	0.97	3.46	84.00	25.18	3.69	0.52
724	24.30	16.64	1.36	24.8	333.91	295.63	62.3	63.2	33.79	4.49	0.98	3.73	90.59	33.86	4.42	0.52
725	24.30	16.64	1.36	24.8	333.91	293.15	62.3	64.5	36.02	4.74	0.96	3.78	91.88	36.22	4.54	0.52
726	[illegible]	20.28	1.21	29.9	337.08	291.71	58.2	58.1	41.09	4.29	0.91	3.24	94.01	41.09	4.29	0.52
727	29.03	20.23	1.21	29.9	337.08	293.69	57.4	57.3	39.27	4.12	0.91	3.21	93.28	39.26	4.13	0.52
728	29.03	20.28	1.21	29.9	337.08	303.68	49.8	52.2	30.08	[illegible]	0.84	3.04	88.38	30.27	3.13	0.52
729	31.59	22.31	1.11	33.7	339.16	303.17	50.6	49.9	32.80	3.18	0.86	2.85	90.00	32.74	3.24	0.52
730	31.59	22.31	1.11	33.7	339.16	293.81	54.8	54.0	41.48	3.86	0.88	2.98	94.09	41.41	3.94	0.52
731	31.59	22.31	1.11	33.7	339.16	291.44	54.0	54.9	43.67	4.04	0.86	3.00	94.89	43.75	3.97	0.52

Dashes denote that the temperature drop across the condensate film, calculated using equation 7.3, corresponding to the observed heat flux is greater than the measured temperature drop ($T_{\infty} - T_w$).

mixture steam-air

tube diameter 25.25 mm

Run No.	$W_{\infty 2}$ %	$\tilde{W}_{\infty 2}$ %	U_∞ m/s	P_∞ Pa	T_∞ K	T_w K	$\dot{Q}''_{obs}$ kW/m^2	coupled condensate film and gas layer equations: $\dot{Q}''_{calc}$ kW/m^2	$T_\infty - T_i$ K	$T_i - T_w$ K	gas layer only (condensate film resistance accounted by equation 7.3): $\frac{Sh}{\sqrt{Re_v}}$	$\frac{1}{\phi}$	W_i %	$T_\infty - T_i$ K	$T_i - T_w$ K	Sc
732	1.65	[illegible]	[illegible]	[illegible]	372.78	323.16	302.4	286.5	16.82	[illegible]	4.02	35.79	59.19	16.78	32.84	0.52
733	1.65	[illegible]	[illegible]	[illegible]	372.78	[illegible]	161.0	165.1	6.08	[illegible]	2.39	18.78	31.06	6.49	12.99	0.52
734	2.99	1.86	[illegible]	[illegible]	372.50	317.55	261.1	243.5	28.66	26.29	3.29	25.00	74.84	26.38	28.57	0.52
735	2.99	1.88	[illegible]	[illegible]	372.50	[illegible]	[illegible]	144.6	9.25	11.43	2.23	13.09	39.20	8.65	12.04	0.52
736	4.24	2.75	[illegible]	[illegible]	372.18	312.26	219.9	214.6	36.46	23.46	2.66	19.42	84.34	35.77	24.15	0.51
737	[illegible]	2.75	[illegible]	[illegible]	372.18	[illegible]	150.8	147.3	15.07	[illegible]	2.12	12.87	55.89	14.71	12.45	0.52
738	5.64	3.58	[illegible]	[illegible]	371.83	308.59	192.5	193.1	42.01	21.23	2.28	15.74	88.74	42.09	21.15	0.51
739	5.64	3.58	0.83	100.3	371.83	342.57	137.2	137.0	18.12	11.19	1.89	11.21	63.17	18.10	11.21	0.52
740	8.79	5.65	0.85	99.7	371.08	304.07	151.2	155.3	50.08	16.93	1.76	10.58	92.98	50.61	16.40	0.50
741	8.79	5.65	0.85	99.7	371.08	336.89	[illegible]	116.7	24.55	9.64	1.62	8.40	73.79	24.41	9.79	0.52
742	12.38	8.08	0.87	99.0	370.18	[illegible]	123.7	128.3	55.68	13.81	1.45	7.68	95.03	56.27	13.22	0.50
743	[illegible]	[illegible]	0.87	[illegible]	370.18	330.96	106.4	104.1	30.75	[illegible]	1.42	6.56	81.29	30.52	8.70	0.52
744	[illegible]	0.64	1.16	[illegible]	372.86	328.34	343.6	[illegible]	9.98	34.55	4.07	37.56	38.59	8.80	35.72	0.52
745	[illegible]	0.64	1.16	[illegible]	372.86	353.37	198.9	195.8	3.58	15.91	2.56	17.07	17.54	3.26	16.23	0.52
746	2.26	1.42	1.16	100.9	372.65	324.76	302.4	285.5	18.61	29.26	3.40	26.12	58.93	16.54	31.33	0.52
747	2.26	1.42	1.16	[illegible]	372.65	351.66	181.7	175.9	6.94	14.04	2.30	13.74	31.00	6.36	14.63	0.52
748	[illegible]	2.04	1.17	[illegible]	372.43	319.04	261.1	265.6	25.57	27.81	2.77	23.05	74.56	26.10	27.28	0.52
749	[illegible]	[illegible]	1.17	[illegible]	372.43	348.64	171.4	171.4	10.00	13.80	2.10	13.43	43.43	10.00	13.79	0.52
750	4.23	2.68	1.17	[illegible]	[illegible]	316.11	247.4	243.5	30.55	25.57	2.58	16.72	79.21	30.05	26.07	0.52
751	4.23	2.68	1.17	[illegible]	372.22	346.83	161.1	162.3	12.40	13.00	1.94	11.98	50.68	12.51	12.88	0.52
752	[illegible]	[illegible]	1.19	[illegible]	371.70	[illegible]	219.9	206.8	38.92	22.10	2.24	13.54	85.92	37.51	23.51	0.51
753	[illegible]	[illegible]	1.19	[illegible]	371.70	343.76	144.1	145.0	16.47	11.47	1.71	9.54	60.51	16.56	11.38	0.52
754	8.98	5.78	1.21	99.8	[illegible]	306.32	178.7	177.9	45.92	18.84	1.78	10.13	91.00	45.81	18.95	0.51
755	8.98	5.78	1.21	99.6	[illegible]	336.76	137.2	136.4	23.26	11.03	1.57	8.04	72.21	23.18	11.11	0.52
756	[illegible]	[illegible]	[illegible]	[illegible]	372.94	[illegible]	371.0	373.1	3.82	37.22	3.82	42.38	20.69	4.07	36.97	0.52
757	[illegible]	[illegible]	1.66	[illegible]	372.94	354.63	205.6	213.3	[illegible]	16.92	2.20	24.17	11.80	2.14	16.17	0.52
758	[illegible]	[illegible]	[illegible]	[illegible]	372.82	[illegible]	343.5	342.8	9.70	34.21	3.39	31.26	41.28	9.62	34.29	0.52
759	[illegible]	0.61	[illegible]	[illegible]	372.82	352.71	195.4	199.8	3.44	15.67	2.10	15.73	20.44	3.87	15.24	0.52
760	[illegible]	1.46	1.6	[illegible]	372.67	[illegible]	316.1	311.5	15.69	31.05	3.01	24.12	55.99	15.14	31.60	0.52
761	[illegible]	1.46	[illegible]	[illegible]	372.67	352.57	188.5	166.0	5.69	14.41	[illegible]	11.90	27.62	5.45	14.66	0.52
762	[illegible]	1.96	[illegible]	[illegible]	372.54	323.17	[illegible]	293.2	20.21	29.36	2.65	21.38	66.54	20.54	28.83	0.52

Table 7.4 (continued)

Run No.	$W_{\infty 2}$	$\tilde{W}_{\infty 2}$	U_∞	P_∞	T_∞	T_w	$\dot{Q}''_{obs}$	coupled condensate film and gas layer equations: $\dot{Q}''_{calc}$	$T_\infty - T_i$	$T_i - T_w$	gas layer only (condensate film resistance accounted by equation 7.3): $\frac{Sh}{\sqrt{Re_v}}$	$\frac{1}{\omega}$	W_i	$T_\infty - T_i$	$T_i - T_w$	Sc
	%	%	m/s	Pa	K	K	kW/m^2	kW/m^2	K	K			%	K	K	
763	3.11	1.96	1.67	[illegible]	372.54	349.22	188.6	190.3	8.27	15.05	1.96	12.39	38.57	8.43	14.89	0.52
764	4.59	2.97	1.6	[illegible]	372.2[illegible]	318.26	261.1	262.6	27.39	26.55	2.32	16.32	76.60	27.56	26.38	0.52
765	4.59	2.97	1.69	[illegible]	372.20	347.86	174.7	171.5	11.01	13.32	1.81	9.83	46.17	10.70	13.62	0.52
766	6.66	4.25	1.71	[illegible]	371.75	313.1[illegible]	233.6	233.2	34.80	23.86	2.02	12.60	83.87	34.74	23.92	0.52
767	6.66	4.25	1.71	10[illegible].7	371.75	341.65	167.9	169.2	16.60	17.50	1.64	9.16	60.94	16.73	13.38	0.52

Table 7.5 Vapour–gas mixtures results

mixture steam–air

tube diameter 25.25 mm

Run No.	$W_{\infty 2}$ (%)	$\tilde{W}_{\infty 2}$ (%)	U_∞ (m/s)	P_∞ (Pa)	T_∞ (K)	T_w (K)	$\dot{Q}''_{obs}$ (kW/m²)	coupled condensate film and gas layer equations: $\dot{Q}''_{calc}$ (kW/m²)	$T_\infty - T_i$ (K)	$T_i - T_w$ (K)	gas layer only (condensate film resistance accounted by equation 7.3): $\frac{Sh}{\sqrt{Re_v}}$	$\frac{1}{\psi}$	W_i (%)	$T_\infty - T_i$ (K)	$T_i - T_w$ (K)	Sc
768	2.61	1.64	9.36	6.2	339.72	302.2	81.0	76.0	1.96	5.56	1.54	5.52	14.43	1.51	6.01	0.49
769	2.61	1.64	9.37	6.2	339.72	[illegible]	32.3	29.5	0.48	1.62	1.08	1.91	5.00	0.29	1.82	0.49
770	3.59	2.26	7.3	8.4	315.08	304.12	94.5	91.7	3.69	7.07	1.63	7.78	27.90	3.62	7.34	0.50
771	3.59	2.26	7.3	8.4	315.[illegible]8	311.61	44.5	40.5	1.07	2.39	1.11	2.66	9.54	0.77	2.69	0.49
772	5.77	3.67	5.9[illegible]	10.6	319.42	304.[illegible]	108.0	96.3	7.63	7.69	1.79	7.33	42.25	6.47	8.85	0.50
773	5.77	3.67	5.9[illegible]	10.6	319.42	314.95	44.5	42.5	1.96	2.53	0.99	3.16	18.24	1.81	2.68	0.50
774	7.12	4.55	5.1	12.7	322.73	305.37	108.0	94.7	9.79	7.57	1.75	7.00	49.85	8.47	8.89	0.51
775	7.12	4.55	5.1	12.7	322.73	316.7[illegible]	52.6	48.3	3.06	2.97	1.10	3.43	24.44	2.72	3.31	0.50
776	9.64	6.22	4.04	16.8	328.13	301.1[illegible]	106.0	102.7	18.12	8.92	1.59	7.49	72.16	17.56	9.48	0.51
777	9.64	6.22	4.05	16.8	328.13	319.32	56.7	54.3	5.35	3.46	1.08	3.88	37.43	5.17	3.65	0.51
778	11.97	7.80	3.4[illegible]	20.6	332.12	301.21	108.0	96.8	22.48	8.43	1.56	6.49	77.65	21.27	9.64	0.52
779	11.97	7.80	3.4[illegible]	20.6	332.12	320.67	56.6	57.1	7.74	3.71	1.02	4.01	47.99	7.77	3.68	0.51
780	16.84	11.18	3.11	23.8	334.47	296.66	85.0	85.3	30.18	7.62	1.20	5.19	87.29	30.20	7.59	0.52
781	16.84	11.18	3.11	23.8	334.47	313.51	68.7	65.7	16.23	4.73	1.11	4.15	69.87	15.96	5.00	0.52
782	2.45	1.54	10.85	6.3	309.84	304.32	75.5	63.6	1.22	4.30	2.74	1.68	4.13	0.20	5.32	0.49
783	2.45	1.54	10.85	6.3	309.84	307.76	32.4	3[illegible].5	0.42	1.65	0.97	1.97	4.82	0.28	1.79	0.49
784	3.42	2.16	8.[illegible]	8.6	315.65	307.[illegible]	85.0	80.2	2.58	5.74	1.46	5.53	18.94	2.16	6.17	0.49
785	3.42	2.16	8.5	8.6	315.65	312.3[illegible]	44.5	40.7	0.92	2.36	1.08	2.46	8.43	0.65	2.64	0.49
786	5.20	3.30	6.55	11.5	320.70	308.9[illegible]	93.[illegible]	89.4	5.12	6.65	1.49	6.56	34.12	4.78	6.98	0.50
787	5.20	3.30	6.55	11.5	320.70	315.8[illegible]	52.6	48.7	1.93	2.95	1.08	3.18	16.57	1.63	3.24	0.50
788	6.75	4.[illegible]5	5.7	13.3	323.84	309.97	103.6	92.1	6.93	6.94	1.64	6.14	39.02	5.83	8.04	0.50
789	6.75	4.05	5.7[illegible]	13.3	323.84	317.9[illegible]	56.6	52.4	2.71	3.23	1.10	3.44	21.83	2.79	3.55	0.50
790	8.[illegible]3	5.28	4.3[illegible]	18.4	330.32	309.62	103.8	10[illegible].7	12.40	8.30	1.47	7.33	60.30	12.39	8.31	0.51
791	8.23	5.28	4.35	18.4	330.32	32[illegible].95	56.6	64.1	5.15	4.17	0.94	4.70	38.70	5.75	3.57	0.51
792	10.9[illegible]	7.[illegible]7	3.5[illegible]	[illegible]3.9	335.49	304.6[illegible]	113.[illegible]	10[illegible].3	21.41	9.46	1.50	7.01	76.39	23.99	9.88	0.52
793	10.9[illegible]	7.[illegible]7	3.5[illegible]	23.9	335.49	322.[illegible]	76.8	70.1	8.67	4.74	1.24	4.40	47.92	8.10	5.31	0.51
794	14.56	9.6[illegible]	2.9[illegible]	30.[illegible]	340.15	301.73	103.8	101.1	29.42	[illegible].00	1.33	5.85	85.25	29.12	9.30	0.52
795	14.56	9.60	[illegible].9	[illegible]	340.15	317.84	80.9	79.0	16.52	5.79	1.17	4.72	68.84	16.35	5.96	0.52
796	2.51	1.57	13.2[illegible]	6.7	311.17	305.[illegible]5	74.5	69.4	1.98	4.64	1.35	3.40	8.53	0.75	5.07	0.49
797	2.51	1.57	1[illegible]	6.7	311.17	[illegible]9.[illegible]5	32.4	29.8	0.36	1.56	1.09	1.62	4.[illegible]7	0.19	1.73	0.49
798	[illegible]	[illegible]	[illegible]	[illegible]	316.7[illegible]	3[illegible].4	8[illegible].8	78.6	1.89	5.37	1.[illegible]6	4.36	13.92	1.45	5.82	0.49

Table 7.5 (continued)

Run No.	$W_{\infty 2}$ %	$\tilde{W}_{\infty 2}$ %	U_∞ m/s	P_∞ Pa	T_∞ K	T_w K	$\dot{Q}''_{obs}$ kW/m^2	coupled condensate film and gas layer equations: $\dot{Q}''_{calc}$ kW/m^2	$T_\infty-T_i$ K	T_i-T_w K	gas layer only (condensate film resistance accounted by equation 7.3): $\frac{Sh}{\sqrt{Re_v}}$	$\frac{1}{\phi}$	W_i %	$T_\infty-T_i$ K	T_i-T_w K	Sc
799	3.22	2.01	11.25	9.1	316.70	313.51	44.5	42.6	0.77	2.42	0.93	2.53	8.08	0.63	2.56	0.49
800	4.21	2.66	6.41	11.4	320.96	310.2.	103.9	96.7	3.68	7.05	1.53	5.74	24.17	3.02	7.71	0.50
801	4.21	2.66	6.41	11.4	321.96	316.72	52.6	49.8	1.31	3.93	1.00	2.89	12.18	1.10	3.14	0.50
802	5.64	3.59	6.45	15.5	327.07	311.79	113.4	111.2	6.77	8.51	1.52	7.29	41.14	6.57	8.71	0.51
803	5.64	3.59	6.47	15.5	327.07	321.0.	64.8	59.7	2.41	3.65	1.12	3.33	18.81	2.02	4.05	0.50
804	6.99	4.47	5.47	18.8	330.92	312.45	122.8	114.8	9.51	8.96	1.60	7.01	49.04	8.74	9.73	0.51
805	6.99	4.47	5.49	18.8	330.92	323.24	68.8	65.3	3.58	4.09	1.10	3.80	26.56	3.31	4.37	0.51
806	8.99	5.79	4.11	26.5	338.15	308.70	132.3	131.6	18.18	11.27	1.55	7.89	70.90	18.11	11.34	0.52
807	8.99	5.79	4.11	26.5	338.15	324.3.	89.0	86.3	7.89	5.93	1.23	5.00	44.96	7.65	6.17	0.51
808	11.67	7.59	3.38	33.8	343.19	309.66	121.1	122.0	23.13	10.40	1.39	6.69	78.07	23.23	10.31	0.52
809	11.67	7.59	3.3.	33.8	343.19	326.89	85.0	83.6	10.58	5.72	1.15	4.62	53.97	10.46	5.84	0.52
810	1.93	1.21	14.7.	8.1	314.64	308.0.	94.5	83.4	0.98	5.63	7.13	1.18	2.27	0.04	6.57	0.49
811	1.93	1.21	14.7	8.1	314.64	312.2.	40.5	38.6	0.33	2.08	0.99	1.86	3.59	0.20	2.20	0.49
812	2.51	1.58	11.17	11.1	320.73	312.0.	102.4	99.4	1.75	6.97	1.38	5.32	13.38	1.49	7.23	0.49
813	2.51	1.58	11.18	11.1	320.73	317.18	52.6	50.9	0.65	2.91	0.95	2.60	6.53	0.53	3.03	0.49
814	2.94	1.85	10.34	12.2	322.54	312.38	113.4	108.1	2.39	7.77	1.50	5.56	16.35	1.91	8.24	0.50
815	2.94	1.85	10.3.	12.2	322.54	318.66	56.7	53.2	0.82	3.06	1.06	2.43	7.14	0.56	3.31	0.49
816	3.89	2.46	8.2	15.9	327.85	314.7.	132.3	121.4	4.05	9.02	1.68	5.98	23.25	3.05	10.02	0.50
817	3.89	2.46	8.2.	15.9	327.85	322.4.	68.8	64.6	1.49	.89	1.10	3.08	11.98	1.17	4.21	0.50
818	4.99	3.16	6.51	21.0	333.63	317.48	132.3	130.6	6.24	9.91	1.53	7.55	37.64	6.08	10.07	0.51
819	4.99	3.16	6.47	21.0	333.63	325.89	80.9	79.2	2.72	5.02	1.12	4.19	20.89	2.58	5.16	0.50
820	6.67	4.26	5.2	27.4	339.22	318.4	141.7	137.8	10.05	1..77	1.57	7.53	50.25	9.67	11.15	0.51
821	6.67	4.26	5.07	7.4	339.22	329.15	89.0	86.7	4.45	5.63	1.16	4.48	29.90	4.26	5.82	0.51
822	9. 4	5.52	4.1.	36.7	345.56	318.01	139.7	141.1	16.14	11.42	1.45	7.30	66.02	16.28	11.28	0.52
823	9. 4	5.82	4..7	36.7	345.56	332.13	93.1	92.5	7.28	6.15	1.14	4.68	42.28	7.23	6.20	0.52

Table 7.6 Vapour–gas mixtures results

mixture steam–hydrogen
tube diameter 12.5 mm

Run No.	$W_{\infty 2}$ %	$\tilde{W}_{\infty 2}$ %	U_∞ m/s	P_∞ Pa	T_∞ K	T_w K	$\dot{Q}''_{obs}$ kW/m^2	coupled condensate film and gas layer equations: $\dot{Q}''_{calc}$ kW/m^2	$T_\infty - T_i$ K	$T_i - T_w$ K	gas layer only (condensate film resistance accounted by equation 7.3): $\frac{Sh}{\sqrt{Re_v}}$	$\frac{1}{\psi}$	W_i %	$T_b - T_i$ K	$T_i - T_w$ K	Sc
824	[illegible].14	1.21	1.6	100.4	372.56	334.86	464.9	444.2	2.32	35.38	2.07	2.08	0.28	0.36	37.34	0.16
825	0.17	1.47	1.61	100.4	372.49	334.2	460.6	443.0	2.87	35.42	1.46	3.96	0.66	1.19	37.09	0.16
826	0.19	1.68	1.6[illegible]	1[illegible]0.4	372.42	3[illegible].75	456.3	441.7	3.30	35.37	1.37	5.16	0.99	1.90	36.77	0.16
827	[illegible].22	1.93	1.61	1[illegible].4	372.75	3[illegible].41	456.3	439.0	3.77	35.18	1.39	5.07	1.11	2.12	36.83	0.16
828	0.25	2.15	1.61	1[illegible].4	372.29	333.[illegible]	452.1	437.2	4.21	35.07	1.35	5.86	1.44	2.79	36.50	0.17
829	0.15	1.28	1.6[illegible]	1[illegible].4	372.54	344.77	368.9	357.5	1.80	25.98	1.25	3.25	0.47	0.80	26.98	0.16
830	[illegible].17	1.49	1.6	1[illegible].4	372.46	344.45	366.3	356.7	2.09	25.94	1.16	4.04	0.68	1.24	26.79	0.16
831	0.20	1.76	1.6	1[illegible].4	372.40	344.08	363.7	355.3	2.47	25.85	1.12	4.60	0.92	1.72	26.60	0.16
832	[illegible].23	1.98	1.61	1[illegible].4	372.34	343.73	358.6	354.4	2.79	25.81	1.08	5.54	1.25	2.41	26.19	0.16
833	[illegible].25	2.17	1.61	1[illegible].4	372.28	343.36	356.1	354.4	3.07	25.85	1.06	6.04	1.50	2.91	26.01	0.17
834	0.16	1.41	1.6	1[illegible].4	372.5[illegible]	354.66	260.9	257.5	1.24	16.61	0.87	3.48	0.56	0.96	16.88	0.16
835	0.22	1.92	[illegible]	1[illegible]	372.[illegible]	329.7[illegible]	443.7	425.8	5.81	[illegible].79	1.71	8.93	1.95	3.97	38.63	0.17
836	[illegible].26	2.29	[illegible].89	1[illegible]	372.20	328.65	439.4	420.5	6.93	36.41	1.72	9.48	2.48	4.99	38.36	0.17
837	0.31	2.67	[illegible].89	1[illegible]	372.[illegible]9	326.21	435.1	414.4	7.99	35.89	1.74	9.68	2.96	5.85	38.03	0.17
838	0.36	3.11	0.9[illegible]	100.2	371.96	327.3	422.2	407.9	9.26	35.40	1.73	11.23	4.02	7.78	36.88	0.18
839	0.40	3.44	0.9[illegible]	1[illegible]0.3	371.86	326.71	413.6	403.1	10.15	35.01	1.74	12.03	4.77	9.05	36.11	0.18
840	0.51	4.35	[illegible].91	100.2	371.62	325.[illegible]	405.0	390.3	12.60	34.00	1.78	12.02	6.08	11.05	35.55	0.19
841	0.56	4.79	[illegible].91	100.[illegible]	371.50	325.99	396.4	385.5	13.81	3[illegible].70	1.80	12.78	7.15	12.66	34.85	0.19
842	[illegible]8	0.65	1.7[illegible]	97.6	371.91	333.97	456.0	457.5	1.31	36.63	1.20	6.87	0.68	1.45	36.48	0.16
843	0.12	1.12	1.6[illegible]	97.6	371.79	333.[illegible]	451.7	452.6	2.17	36.32	1.23	8.54	1.08	2.25	36.24	0.16
844	[illegible].21	1.86	1.65	97.6	371.58	332.4[illegible]	451.8	443.1	3.58	35.57	1.30	6.61	1.40	2.76	36.39	0.16
845	[illegible]	2.59	1.7[illegible]	97.6	371.77	331.75	443.2	435.6	4.99	35.03	1.30	7.37	2.19	4.26	35.76	0.17
846	[illegible].40	3.47	1.71	97.6	371.12	3[illegible]7	434.6	426.7	6.65	34.40	1.32	7.76	3.11	5.89	35.16	0.17
847	[illegible].50	4.32	1.7[illegible]	97.6	370.[illegible]9	329.3	43[illegible].4	415.6	8.14	35.45	1.36	7.28	3.66	6.72	34.87	0.18
848	[illegible].57	4.91	1.77	97.7	370.73	328.04	421.8	412.7	9.29	35.40	1.36	8.14	4.67	8.42	34.28	0.18
849	[illegible].7	5.93	1.74	97.7	37[illegible].45	327.25	41[illegible].2	399.5	10.95	3[illegible].25	1.39	7.91	5.54	9.63	33.57	0.19
850	[illegible].79	6.65	1.7[illegible]	97.6	37[illegible].27	326.[illegible]	409.[illegible]	392.5	12.17	31.73	1.41	7.88	6.23	10.58	33.31	0.19
851	[illegible].89	7.4[illegible]	1.76	98.[illegible]	37[illegible]9	325.4[illegible]	4[illegible]4.7	385.[illegible]	13.44	31.24	1.43	7.89	7.01	11.61	33.07	0.20
852	[illegible].47	7.75	[illegible].2[illegible]	98.4	371.26	315.71	31[illegible]	323.6	22.92	3[illegible].63	2.96	36.85	16.00	24.47	31.08	0.22
853	1.[illegible]	13.47	[illegible]	1[illegible].4	[illegible].31	[illegible]4.75	311.[illegible]	31[illegible].7	27.59	27.97	1.96	15.72	20.72	27.51	28.05	0.24
854	1.[illegible]	14.[illegible]	[illegible]	1[illegible].4	36[illegible]	[illegible]	[illegible]9.7	279.4	32.93	25.26	2.00	14.55	26.62	31.82	26.38	0.25

Table 7.6 (continued)

Run No.	$W_{\infty 2}$ %	$\tilde{W}_{\infty 2}$ %	U_∞ m/s	P_∞ Pa	T_∞ K	T_w K	$\dot{Q}''_{obs}$ kW/m^2	coupled condensate film and gas layer equations: $\dot{Q}''_{calc}$ kW/m^2	$T_\infty - T_i$ K	$T_i - T_w$ K	gas layer only (condensate film resistance accounted by equation 7.3): $\frac{Sh}{\sqrt{Re_v}}$	$\frac{1}{\phi}$	W_i %	$T_\infty - T_i$ K	$T_i - T_w$ K	Sc
855	[illegible]	17.66	[illegible]	[illegible]	368.09	307.49	268.1	256.4	37.25	23.35	2.01	14.06	32.96	35.97	24.63	0.27
856	2.94	21.31	[illegible]	[illegible]	367.03	305.19	242.2	232.9	40.69	21.15	1.95	13.38	39.37	39.68	22.16	0.28
857	[illegible]	25.56	0.94	[illegible]	365.57	[illegible]	216.3	209.8	[illegible]	19.05	1.88	12.63	46.81	43.58	19.76	0.30
858	[illegible]	29.11	[illegible]	[illegible]	364.46	299.95	194.7	193.0	46.99	17.52	1.80	12.09	53.10	46.79	17.72	0.31
859	5.23	[illegible]	1.03	[illegible]	362.70	297.25	177.4	175.6	49.49	15.95	1.74	11.25	58.82	49.29	16.15	0.33
860	5.71	[illegible]	[illegible]	[illegible]	361.81	296.41	164.5	166.4	50.37	15.03	1.67	10.82	61.75	50.58	14.82	0.34

mixture steam-hydrogen
tube diameter 12.5 mm

Run No.	$W_{\infty 2}$ %	$\tilde{W}_{\infty 2}$ %	U_∞ m/s	P_∞ Pa	T_∞ K	T_w K	$\dot{Q}''_{obs}$ kW/m^2	coupled condensate film and gas layer equations: $\dot{Q}''_{calc}$ kW/m^2	$T_\infty - T_i$ K	$T_i - T_w$ K	gas layer only (condensate film resistance accounted by equation 7.3): $\frac{Sh}{\sqrt{Re_v}}$	$\frac{1}{\phi}$	W_i %	$T_\infty - T_i$ K	$T_i - T_w$ K	Sc
861	0.44	3.81	6.91	3.6	299.70	293.71	83.8	75.0	1.22	4.77	1.01	1.81	0.80	0.52	5.47	0.15
862	.81	6.82	4.7	5.6	306.89	296.47	104.7	100.0	3.57	6.89	0.87	3.79	3.07	3.17	7.29	0.17
863	.81	6.82	4.7[illegible]	5.6	306.89	298.8[illegible]	90.5	82.4	2.72	5.29	0.83	2.77	2.25	2.07	5.94	0.16
864	0.81	6.82	4.7[illegible]	5.6	306.89	303.29	51.9	44.7	1.24	2.37	0.75	1.63	1.32	0.76	2.85	0.16
865	0.86	7.16	3.69	7.4	311.77	297.53	129.8	122.4	5.27	6.97	1.04	4.84	4.14	4.60	9.64	0.17
866	0.86	7.16	3.7[illegible]	7.4	311.77	300.76	113.0	102.3	4.03	6.97	0.96	3.51	3.00	3.12	7.88	0.17
867	0.86	7.16	3.7[illegible]	7.4	311.77	306.69	62.7	57.6	1.85	[illegible].23	0.67	2.15	1.84	1.49	3.59	0.16
868	1.23	9.98	3.[illegible]9	9.2	315.37	298.14	134.0	123.1	8.08	9.14	1.15	5.34	6.55	7.08	10.15	0.19
869	1.23	9.98	3.[illegible]9	9.2	315.37	301.6[illegible]	115.5	106.0	6.40	7.36	1.01	4.30	5.27	5.58	8.19	0.18
870	1.23	9.98	3.09	9.2	315.37	308.72	65.2	62.6	3.05	3.59	0.65	2.59	3.17	2.86	3.78	0.17
871	1.64	12.99	2.46	12.2	320.13	297.92	142.4	127.9	12.36	9.85	1.33	6.41	10.54	10.99	11.22	0.21
872	1.64	12.99	2.46	12.2	320.13	302.08	123.1	112.3	9.99	6.06	1.14	5.25	8.63	9.02	9.03	0.20
873	1.64	12.99	2.46	12.2	320.13	314.79	45.8	46.7	2.92	2.42	0.53	2.22	3.65	2.98	2.36	0.18
874	1.91	14.87	2.1[illegible]	14.1	322.61	297.91	138.2	127.3	14.79	9.91	1.37	7.14	13.64	13.74	10.96	0.22
875	1.91	14.82	2.19	14.1	322.61	302.15	120.6	113.4	12.21	8.26	1.17	5.93	11.31	11.56	8.91	0.21
876	1.91	14.82	2.19	14.1	322.61	316.51	53.3	48.1	3.59	2.51	0.65	2.15	4.11	3.25	2.86	0.18
877	2.38	17.88	1.9	16.8	325.40	297.37	134.0	123.2	18.32	9.71	1.44	7.66	18.21	17.27	10.75	0.24
878	2.38	17.88	1.9	16.8	325.40	301.90	120.6	110.7	15.35	8.15	1.27	6.25	14.87	14.45	9.05	0.23
879	2.38	17.88	1.9	16.8	325.40	317.5[illegible]	55.8	50.6	4.91	2.69	0.68	2.34	5.57	4.56	3.04	0.19
880	2.95	21.39	1.61	21.[illegible]	329.44	296.[illegible]5	129.8	121.0	23.31	9.77	1.53	8.58	25.36	22.43	10.65	0.26
881	2.95	21.39	1.61	21.[illegible]	329.44	301.[illegible]5	118.0	11[illegible].4	20.04	8.34	1.36	7.17	21.18	19.33	9.06	0.25
882	2.95	21.39	1.61	21.[illegible]	329.44	319.59	58.3	54.1	6.91	2.94	0.71	2.64	7.79	6.63	3.23	0.21
883	3.26	23.13	1.5	23.6	331.14	296.[illegible]5	129.8	118.6	25.45	9.64	1.59	8.68	28.27	24.33	10.77	0.27
884	3.26	23.13	1.5	23.6	331.14	30[illegible].46	115.5	109.4	22.31	8.37	1.39	7.55	24.61	21.73	8.95	0.26
885	3.26	23.13	1.5	23.6	331.14	319.7	60.2	56.9	8.29	3.15	0.74	2.87	9.34	8.06	3.38	0.22
886	3.86	26.4[illegible]	1.32	28.1	333.94	295.22	117.3	113.8	29.35	9.37	1.55	9.27	35.77	29.00	9.72	0.29
887	3.86	26.43	1.3[illegible]	28.1	333.94	299.89	110.5	1[illegible]5.4	25.91	8.14	1.43	7.87	30.35	25.42	8.63	0.28
888	3.86	26.43	1.3[illegible]	28.1	333.94	32[illegible].7[illegible]	62.7	56.7	10.07	3.15	0.81	2.96	11.41	9.65	3.58	0.23
889	0.25	[illegible].19	15.5	4.1	302.7[illegible]	296.39	105.1	91.4	0.49	5.42	-	-	-	-	-	-
890	0.25	[illegible].19	15.46	4.1	302.30	298.0[illegible]	80.7	71.2	0.36	.92	-	-	-	-	-	-
891	.25	2.19	15.4[illegible]	4.1	30[illegible]	[illegible].56	20.2	17.8	0.36	[illegible].67	-	-	-	-	-	-

Table 7.7 (continued)

Run No.	$W_{\infty 2}$ %	$\tilde{W}_{\infty 2}$ %	U_∞ m/s	P_∞ Pa	T_∞ K	T_w K	$\dot{Q}''_{obs}$ kW/m^2	coupled condensate film and gas layer equations: $\dot{Q}''_{calc}$ kW/m^2	$T_\infty - T_i$ K	$T_i - T_w$ K	gas layer only (condensate film resistance accounted by equation 7.3): $\frac{Sh}{\sqrt{Re_v}}$	$\frac{1}{\omega}$	W_i %	$T_\infty - T_i$ K	$T_i - T_w$ K	Sc
892	0.27	2.40	10.91	6.1	309.22	300.33	138.7	125.9	0.85	8.04	-	-	-	-	-	-
893	0.27	2.40	10.92	6.1	309.22	302.71	113.4	99.5	0.63	5.88	-	-	-	-	-	-
894	0.27	2.40	10.97	6.1	309.22	307.70	34.0	31.8	0.17	1.35	1.07	1.11	0.31	0.05	1.47	0.15
895	0.50	4.29	7.18	9.9	317.98	304.61	176.4	162.3	2.32	11.04	1.03	2.40	1.20	1.14	12.22	0.16
896	0.50	4.29	7.18	9.9	317.98	308.16	143.6	129.5	1.70	8.12	1.14	1.73	0.87	0.61	9.21	0.15
897	0.50	4.29	7.18	9.9	317.98	315.79	45.3	40.3	0.41	1.78	1.11	1.16	0.58	0.13	2.06	0.15
898	0.64	5.48	5.6	13.3	323.47	306.52	193.2	185.9	3.79	13.16	0.93	4.05	2.61	3.16	13.79	0.17
899	0.64	5.48	5.6	13.3	323.47	310.65	158.7	152.3	2.85	9.97	0.82	3.22	2.08	2.34	10.48	0.16
900	0.64	5.48	5.59	13.3	323.47	320.68	50.3	47.0	0.66	2.13	0.57	1.42	0.92	0.47	2.32	0.16
901	0.86	7.21	4.62	16.7	327.83	307.14	210.0	201.3	5.98	14.71	1.03	4.86	4.19	5.21	15.48	0.18
902	0.86	7.21	4.62	16.7	327.83	312.45	168.7	164.0	4.41	10.98	0.86	3.90	3.36	4.02	11.36	0.17
903	0.86	7.21	4.62	16.7	327.83	324.18	58.5	54.9	1.08	2.57	0.55	1.58	1.36	0.86	2.79	0.16
904	1.13	9.28	3.69	22.0	333.18	307.95	222.6	213.8	9.12	16.10	1.14	5.89	6.67	8.32	16.90	0.19
905	1.13	9.28	3.69	22.0	333.18	313.86	186.3	179.2	6.92	12.40	0.97	4.56	5.16	6.32	13.00	0.18
906	1.13	9.28	3.69	22.0	333.18	328.42	66.7	62.9	1.72	3.04	0.55	1.76	1.99	1.49	3.27	0.17
907	1.45	11.63	3.15	26.9	337.02	307.63	226.8	217.4	12.64	16.75	1.25	6.72	9.76	11.77	17.62	0.21
908	1.45	11.63	3.15	26.9	337.02	314.19	201.4	185.1	9.75	13.08	1.10	4.78	6.94	8.34	14.50	0.19
909	1.45	11.63	3.15	26.9	337.02	331.92	75.4	70.5	2.59	3.51	0.59	1.91	2.77	2.28	3.82	0.18
910	2.21	16.80	2.37	38.9	344.03	305.46	239.4	217.0	21.05	17.52	1.52	7.78	17.20	18.86	19.70	0.24
911	2.21	16.80	2.37	38.9	344.03	313.08	203.9	194.0	16.91	14.03	1.27	6.30	13.92	15.65	15.29	0.23
912	2.21	16.80	2.37	38.9	344.03	335.25	84.2	76.6	4.75	4.03	0.63	2.19	4.85	4.39	4.39	0.19
913	3.53	24.62	1.87	56.0	350.75	299.44	210.0	204.6	33.28	17.64	1.63	10.19	35.92	32.73	18.20	0.28
914	0.19	1.66	17.05	6.9	311.50	303.18	138.4	131.6	0.44	7.88	-	-	-	-	-	-
915	0.19	1.66	17.05	6.9	311.50	305.95	96.4	96.6	0.30	5.24	0.47	2.03	0.38	0.31	5.23	0.15
916	0.19	1.66	17.07	6.9	311.50	310.17	32.6	31.4	0.08	1.24	1.20	1.07	0.20	0.02	1.30	0.15
917	0.36	3.16	10.74	12.2	322.33	309.21	197.3	181.0	1.36	11.66	3.57	1.16	0.42	0.10	12.92	0.15
918	0.36	3.16	10.74	12.2	322.33	314.69	146.5	135.4	0.91	7.73	-	-	-	-	-	-
919	0.36	3.16	[illegible]	12.2	322.33	320.05	49.5	46.6	0.27	1.98	0.82	1.17	0.43	0.11	2.14	0.15
920	0.48	4.11	7.36	[illegible]	330.12	312.63	238.8	221.3	2.46	15.03	1.11	2.19	1.04	1.01	16.48	0.16
921	0.48	4.11	[illegible]	18.0	330.12	318.47	180.0	164.9	1.65	10.03	1.20	1.59	0.76	0.51	11.17	0.16
922	0.48	4.11	[illegible]	[illegible]	330.12	327.19	61.4	56.4	0.45	1.46	0.93	1.19	0.57	0.17	2.76	0.15
923	0.75	[illegible]	[illegible]	[illegible]	336.94	314.55	263.9	246.4	4.75	17.34	1.01	3.48	2.60	3.26	18.83	0.17

Table 7.7 (continued)

Run No.	$W_{\infty 2}$ %	$\tilde{W}_{\infty 2}$ %	U_∞ m/s	P_∞ Pa	T_∞ K	T_w K	$\dot{Q}''_{obs}$ kW/m^2	coupled condensate film and gas layer equations: $\dot{Q}''_{calc}$ kW/m^2	$T_\infty - T_i$ K	$T_i - T_w$ K	gas layer only (condensate film resistance accounted by equation 7.3): $\frac{Sh}{\sqrt{Re_v}}$	$\frac{1}{\omega}$	W_i %	$T_\infty - T_i$ K	$T_i - T_w$ K	Sc
924	0.75	6.29	5.50	25.3	336.94	321.96	198.7	187.0	3.21	11.77	0.83	2.72	2.03	2.31	12.67	0.17
925	0.75	6.29	5.54	25.3	336.94	332.83	75.8	69.3	0.93	3.18	0.68	1.39	1.04	0.55	3.56	0.16
926	1.12	9.17	4.1	76.9	344.84	315.55	272.2	274.2	9.01	20.28 -	1.04	6.08	6.80	9.19	20.10	0.19
927	1.12	9.17	4.11	76.9	344.84	325.33	213.3	210.5	6.04	13.77	0.84	4.01	4.48	5.82	14.00	0.18
928	1.12	9.17	4.11	6.9	344.84	338.81	90.2	86.0	1.87	4.16	0.55	1.77	1.98	1.62	4.41	0.17
929	1.38	11.11	3.27	48.8	351.01	315.73	289.0	291.7	12.94	22.33	1.17	7.17	9.89	13.19	22.09	0.21
930	1.38	11.11	3.27	48.8	351.01	326.21	238.3	232.1	9.02	15.77	0.96	4.64	6.40	8.50	16.29	0.19
931	1.38	11.11	3.27	48.8	351.01	347.09	102.6	100.2	2.88	5.04	0.55	2.05	2.82	2.73	5.19	0.18

Dashes denote that the temperature drop across the condensate film, calculated using equation 7.3, corresponding to the observed heat flux is greater than the measured temperature drop ($T_\infty - T_w$)

Table 7.8 Vapour-gas mixtures results

mixture Refrigerant 113-air
tube diameter 12.5 mm

Run No.	W_{a2} %	$\tilde{W}_{a2}$ %	U_a m/s	P_a Pa	T_a K	T_w K	$\dot{Q}''_{obs}$ kW/m^2	coupled condensate film and gas layer equations: $\dot{Q}''_{calc}$ kW/m^2	T_a-T_i K	T_i-T_w K	gas layer only (condensate film resistance accounted by equation 7.3): $\frac{Sh}{\sqrt{Re_v}}$	$\frac{1}{\omega}$	W_i %	T_a-T_i K	T_i-T_w K	Sc
932	[illegible]	0.30	1.76	[illegible]	320.86	265.97	51.4	47.6	0.21	[illegible]	-	-	-	-	-	-
933	[illegible]	[illegible]	1.76	[illegible]	320.86	289.46	47.1	43.6	0.19	[illegible]	-	-	-	-	-	-
934	[illegible]	0.30	1.76	[illegible]	320.86	[illegible]	29.5	28.1	0.11	17.67	-	-	-	-	-	-
935	0.14	0.88	[illegible]	[illegible]	319.78	284.76	42.6	42.6	1.17	[illegible]	1.03	4.41	0.61	0.88	34.11	0.17
936	0.14	0.88	[illegible]	[illegible]	319.78	287.90	40.7	39.6	1.05	[illegible]	-	-	-	-	-	-
937	0.14	0.38	0.63	[illegible]	319.78	300.00	27.6	27.3	0.63	19.15	0.84	2.52	0.35	0.40	19.38	0.17
938	0.28	1.77	0.62	[illegible]	319.96	284.66	42.8	41.7	2.31	32.97	1.16	3.27	0.91	1.18	34.11	0.17
939	0.28	1.77	0.63	102.2	319.96	287.81	38.5	38.8	2.08	[illegible]	0.90	5.69	1.58	2.38	29.76	0.18
940	0.28	1.77	0.63	102.2	319.96	300.24	28.2	26.6	1.22	18.49	-	-	-	-	-	-
941	0.43	2.70	0.63	101.5	319.47	284.47	42.8	40.3	3.42	31.58	1.48	2.21	0.94	0.96	34.05	0.17
942	0.43	2.70	0.63	101.5	319.47	287.49	36.4	37.7	3.09	28.90	0.87	6.72	2.87	4.29	27.69	0.18
943	0.43	2.70	0.63	101.5	319.47	299.74	26.3	25.9	1.83	17.90	0.76	2.92	1.25	1.51	18.22	0.17
944	0.57	3.56	0.64	101.5	319.19	284.37	38.6	39.2	4.40	[illegible]	0.96	6.10	3.46	5.00	29.82	0.19
945	0.57	3.56	0.64	101.5	319.19	287.23	36.4	36.7	3.99	27.97	0.92	5.35	3.03	4.30	27.66	0.19
946	0.57	3.56	0.64	101.5	319.19	299.77	25.7	25.5	2.39	17.53	0.73	3.22	1.83	2.27	17.64	0.18
947	0.77	4.80	0.64	[illegible]	318.96	[illegible]	38.6	37.6	5.78	29.08	1.02	4.84	3.74	5.07	29.79	0.19
948	0.77	4.80	0.64	102.0	318.96	286.93	34.3	35.5	5.25	26.78	0.89	5.96	4.60	6.41	25.63	0.20
949	0.77	[illegible]	0.64	[illegible]	318.96	298.49	25.7	25.2	3.22	17.25	0.76	3.07	2.37	2.82	17.65	0.18
950	0.98	6.00	0.64	[illegible]	[illegible]	[illegible]	[illegible]	36.5	7.03	27.76	1.09	4.04	3.95	5.03	29.75	0.19
951	0.98	6.00	0.64	[illegible]	[illegible]	285.84	34.2	34.2	6.39	25.59	0.94	4.95	4.84	6.40	25.58	0.20
952	0.98	6.00	0.64	[illegible]	318.82	298.38	24.4	24.4	3.92	16.52	0.72	3.33	3.26	3.93	16.51	0.19
953	[illegible]	0.26	0.82	[illegible]	320.59	265.17	47.1	44.9	0.30	[illegible]	-	-	-	-	-	-
954	[illegible]	0.26	0.87	102.6	320.59	282.46	42.8	41.6	0.27	31.86	-	-	-	-	-	-
955	[illegible]	0.26	0.82	102.8	320.59	301.8	28.2	27.4	0.15	[illegible]	-	-	-	-	-	-
956	[illegible]	0.54	[illegible]	[illegible]	320.34	265.15	42.8	44.3	0.61	[illegible]	0.76	14.24	1.20	2.08	[illegible]	0.17
957	[illegible]	0.54	[illegible]	[illegible]	320.34	288.39	40.7	41.2	0.55	[illegible]	0.75	7.63	0.64	1.06	30.89	0.17
958	[illegible]	0.54	[illegible]	[illegible]	[illegible]	[illegible]	26.9	27.5	0.32	[illegible]	0.52	5.90	[illegible]	0.78	18.21	0.17
959	0.14	0.89	[illegible]	101.9	320.12	284.97	42.8	43.9	1.06	34.16	0.79	9.09	1.25	2.07	33.08	0.17
960	0.14	0.89	0.87	101.9	320.12	[illegible]	40.7	40.9	0.89	[illegible]	0.81	5.14	0.71	1.07	30.87	0.17
961	[illegible]	[illegible]	[illegible]	101.9	320.12	[illegible]	26.9	27.8	0.53	[illegible]	0.53	5.69	0.78	1.21	18.24	0.17
962	[illegible]	1.61	[illegible]	[illegible]	[illegible]	[illegible]	42.8	43.1	1.77	[illegible]	0.87	5.40	1.36	2.04	33.03	0.17

Table 7.8 (continued)

Run No.	$W_{\infty 2}$	$\tilde{W}_{\infty 2}$	U_∞	P_∞	T_∞	T_w	$\dot{Q}''_{obs}$	coupled condensate film and gas layer equations: $\dot{Q}''_{calc}$	$T_\infty - T_i$	$T_i - T_w$	gas layer only (condensate film resistance accounted by equation 7.3): $\frac{Sh}{\sqrt{Re_v}}$	$\frac{1}{\psi}$	W_i	$T_\infty - T_i$	$T_i - T_w$	Sc
	%	%	m/s	Pa	K	K	kW/m^2	kW/m^2	K	K			%	K	K	
963	0.25	1.61	0.84	102.1	319.98	288.65	38.5	40.1	1.60	31.35	0.75	7.81	1.97	3.11	28.84	0.18
964	0.25	1.61	0.83	102.1	319.98	300.73	26.3	27.1	0.94	16.32	0.56	4.39	1.10	1.58	17.67	0.17
965	0.36	2.30	0.46	104.1	320.33	285.65	38.3	38.9	3.43	31.25	1.04	7.26	2.62	4.04	30.65	0.18
966	0.36	2.30	0.46	104.1	320.33	288.55	38.3	36.4	3.11	28.67	1.30	2.85	1.03	1.25	30.53	0.17
967	0.36	2.30	0.46	104.1	320.33	300.14	25.5	25.8	1.89	18.40	0.75	4.19	1.52	2.12	18.17	0.18
968	0.80	4.94	0.47	103.8	319.44	285.07	38.3	35.3	6.80	27.57	1.24	3.76	2.99	3.83	30.54	0.19
969	0.80	4.94	0.47	103.8	319.44	287.94	34.0	33.1	6.15	25.35	1.05	4.85	3.86	5.24	26.27	0.19
970	0.79	4.92	0.46	103.8	319.45	299.12	24.2	23.7	3.78	16.55	0.81	3.41	2.70	3.35	16.97	0.19
971	1.04	6.35	0.47	103.5	318.92	284.98	34.1	33.4	8.30	25.65	1.09	5.52	5.73	7.62	26.33	0.20
972	1.04	6.35	0.47	103.5	318.92	287.48	31.9	31.5	7.60	23.84	1.03	5.27	5.47	7.24	24.21	0.20
973	1.04	6.35	0.47	103.5	318.92	297.87	23.6	23.3	4.87	16.19	0.80	3.63	3.76	4.63	16.42	0.19
974	1.20	7.31	0.46	103.1	318.48	284.66	34.1	32.3	9.25	24.58	1.13	4.90	5.90	7.56	26.27	0.21
975	1.20	7.31	0.47	103.1	318.48	287.15	29.8	30.5	8.50	24.83	0.99	5.84	7.03	9.15	22.18	0.21
976	1.20	7.31	0.46	103.1	318.48	297.48	22.3	22.6	5.44	15.57	0.77	3.88	4.66	5.73	15.28	0.20
977	1.60	9.49	0.45	103.8	317.99	284.34	29.8	30.0	11.29	22.36	1.06	5.81	9.28	11.44	22.22	0.23
978	1.60	9.49	0.48	103.8	317.99	286.87	27.7	26.6	10.48	21.04	0.98	5.76	9.19	11.33	20.19	0.23
979	1.60	9.49	0.48	103.8	317.99	296.37	21.7	21.7	6.90	14.72	0.80	3.71	5.91	6.89	14.73	0.21
980	0.68	4.23	0.54	103.6	319.59	285.37	38.3	36.9	5.46	28.74	1.09	4.49	3.05	4.14	30.08	0.19
981	0.68	4.23	0.54	103.6	319.59	288.15	36.2	34.7	4.99	26.54	1.05	4.03	2.73	3.62	27.91	0.18
982	0.68	4.23	0.54	103.6	319.59	299.27	25.5	24.8	3.08	17.23	0.81	3.03	2.06	2.47	17.84	0.18
983	0.56	5.33	0.54	103.8	319.32	285.13	34.1	35.7	6.77	27.49	0.97	6.89	5.95	8.26	25.95	0.20
984	0.56	5.33	0.54	103.8	319.32	287.8	34.0	33.6	6.12	25.79	0.99	4.89	4.22	5.67	25.84	0.19
985	0.56	5.33	0.54	103.8	319.72	298.63	24.9	24.4	3.86	16.86	0.79	3.29	2.84	3.46	17.25	0.19
986	0.45	2.87	0.57	104.1	320.16	285.63	38.3	39.2	3.73	31.80	0.96	6.77	3.08	4.62	29.91	0.19
987	0.45	2.87	0.57	104.1	320.16	286.48	38.3	36.8	3.38	28.30	1.10	3.27	1.49	1.89	29.78	0.18
988	0.45	2.87	0.57	104.1	320.16	300.15	26.1	25.8	2.05	17.96	0.77	3.07	1.40	1.73	18.28	0.18
989	0.63	3.97	0.56	103.8	319.74	285.45	38.3	37.8	4.98	25.31	1.02	5.01	3.18	4.44	29.86	0.19
990	0.63	3.97	0.5	103.8	319.74	288.22	36.2	35.4	4.53	26.99	0.99	4.42	2.81	3.82	27.70	0.18
991	0.63	3.97	0.55	103.8	319.74	299.45	25.5	25.3	2.80	17.49	0.76	3.28	2.08	2.59	17.70	0.18
992	[illegible]	5.17	0.56	104.4	319.54	285.27	38.3	36.4	6.30	27.95	1.10	4.07	3.40	4.42	29.82	0.19
993	[illegible]	5.17	0.55	104.4	319.52	287.86	34.0	34.3	5.76	25.89	0.94	5.26	4.39	6.00	25.66	0.20
994	[illegible]	5.17	0.5	104.4	319.54	296.96	24.9	24.7	3.59	16.95	0.75	3.33	2.78	3.41	17.13	0.19

Table 7.9 Vapour-gas mixtures results

mixture: Refrigerant 113-hydrogen
tube diameter: 12.5 mm

Run No.	$W_{\infty 2}$ %	$\tilde{W}_{\infty 2}$ %	U_∞ m/s	P_∞ Pa	T_∞ K	T_w K	$\dot{Q}''_{obs}$ kW/m^2	coupled condensate film and gas layer equations: $\dot{Q}''_{calc}$ kW/m^2	$T_\infty - T_i$ K	$T_i - T_w$ K	gas layer only (condensate film resistance accounted by equation 7.3): $\frac{Sh}{\sqrt{Re_v}}$	$\frac{1}{\psi}$	W_i %	$T_\infty - T_i$ K	$T_i - T_w$ K	Sc
995	0.03	2.65	0.65	102.7	319.83	285.98	42.5	42.0	0.81	33.04	0.69	1.33	0.04	0.26	33.59	0.04
996	0.03	2.64	0.64	102.7	319.83	288.99	40.4	39.1	0.74	30.09	–	–	–	–	–	–
997	0.03	2.65	0.66	102.7	319.83	301.04	26.1	26.5	0.48	18.31	0.21	2.05	0.06	0.81	17.98	0.04
998	0.08	6.64	0.67	103.6	318.84	285.75	38.3	40.1	1.99	31.11	0.26	3.06	0.23	3.73	29.36	0.04
999	0.08	6.64	0.67	103.6	318.84	288.60	38.3	37.4	1.83	28.41	0.48	1.52	0.12	1.00	29.24	0.04
1000	0.08	6.64	0.67	103.6	318.84	300.34	24.9	25.4	1.19	17.33	0.23	1.89	0.14	1.68	16.84	0.04
1001	0.13	10.66	0.69	105.6	318.16	285.44	38.3	38.6	3.15	29.58	0.34	2.18	0.28	3.44	29.28	0.04
1002	0.13	10.66	0.68	105.6	318.16	288.46	36.1	35.8	2.89	26.81	0.37	1.86	0.24	2.55	27.16	0.04
1003	0.13	10.66	0.69	105.6	318.16	299.49	24.2	24.8	1.91	16.76	0.25	1.81	0.23	2.41	16.26	0.04
1004	0.02	2.09	0.76	102.9	320.04	286.18	42.5	42.7	0.60	33.27	0.28	2.30	0.05	0.79	33.08	0.04
1005	0.02	2.09	0.76	102.9	320.04	289.16	40.4	39.8	0.55	30.34	–	–	–	–	–	–
1006	0.02	2.09	0.76	102.9	320.04	300.75	26.1	27.5	0.37	18.93	0.14	3.63	0.08	1.58	17.72	0.04
1007	0.07	6.01	0.77	104.2	319.21	285.92	42.6	41.1	1.69	31.60	1.09	1.18	0.08	0.31	32.98	0.04
1008	0.07	6.01	0.76	104.2	319.21	288.82	38.3	38.3	1.55	28.84	0.32	1.93	0.13	1.61	28.78	0.04
1009	0.07	6.01	0.77	104.2	319.21	300.37	23.6	26.3	1.03	17.81	0.15	2.99	0.21	3.30	15.54	0.04
1010	0.11	9.44	0.76	107.4	319.00	285.72	42.6	40.1	2.66	30.62	1.58	1.12	0.13	0.34	32.94	0.04
1011	0.11	9.44	0.77	107.4	319.00	288.66	38.3	37.3	2.47	27.87	0.45	1.56	0.17	1.51	28.83	0.04
1012	0.11	9.44	[illegible]	107.4	319.00	299.93	25.5	25.9	1.63	17.45	0.25	1.73	0.19	1.96	17.11	0.04
1013	0.02	1.68	[illegible]	102.9	320.17	286.2[illegible]	42.5	43.4	0.46	33.51	0.21	3.65	0.07	1.29	32.67	0.04
1014	0.02	1.68	0.85	102.9	320.17	289.23	40.4	40.4	0.42	30.51	0.32	1.81	0.03	0.40	30.53	0.04
1015	0.02	1.94	0.85	103.1	320.17	30[illegible].47	27.4	28.3	0.33	19.37	0.15	2.99	0.06	1.12	18.58	0.04
1016	0.04	3.54	0.86	[illegible]	319.75	286.[illegible]	42.6	42.8	0.95	32.81	0.29	2.12	0.08	1.15	32.61	0.04
1017	0.04	3.54	[illegible]	[illegible]	319.75	288.95	38.3	39.8	0.88	29.94	0.20	3.33	0.13	2.33	28.49	0.04
1018	0.04	3.54	0.86	103.4	319.75	30[illegible].63	26.8	27.4	0.58	18.54	0.19	2.09	0.08	1.12	18.00	0.04
1019	[illegible]	12.54	[illegible]	[illegible]	318.73	287.14	29.8	31.3	7.53	2[illegible].67	0.37	2.61	0.83	8.96	22.23	0.06

Dashes denote that the temperature drop across the condensate film, calculated using equation 7.3, corresponding to the observed heat flux is greater than the measured temperature drop $(T_\infty - T_w)$

CHAPTER 8 – CONCLUDING REMARKS

In recent years significant progress has been made towards the theoretical understanding of forced convection condensation on a horizontal tube, notably by Shekriladze and Gomelauri /24 / and Fujii and co-workers /49 – 52 /. Comparison with limited experimental data (mostly for steam) however, is inconclusive.

In the present work, further data for vertical downward flow of pure vapours condensing on a horizontal tube have been obtained with a view to shedding further light on the problem. Measurements have been made for a wide range of conditions of vapour velocity, pressure, vapour-to-wall temperature difference and heat flux. Tests have been performed with two different fluids (steam and Refrigerant 113) and using two tubes of different diameters. Special attention has been given to accuracy in the determination of vapour velocity, vapour and condensing tube surface temperatures and the heat-transfer rate. Care has been taken to ensure that the results were not affected by the presence of non-condensing gases in the vapour nor by the occurence of dropwise condensation on the tube.

Theory /49 – 52 / indicates that the vapour-side heat-transfer coefficient is given by an equation of the form :

$$Nu/\sqrt{Re_{TP}} = \psi_1 \left(Pr_L/FrH \, , \; RH/Pr_L \right)$$

For the experimental ranges which have been used to date, the predicted dependence on the RH/Pr_L parameter is of similar magnitude to, or less than, the scatter of the data. So essentially, for these data we have,

$$Nu/\sqrt{Re_{TP}} = \psi_2 \left(Pr_L/FrH \right)$$

as indicated by the approximate theory of Shekriladze and Gomelauri /24/.

The present results for steam are in broad general agreement with the results of other workers /37 - 40, 42, 43, 50, 59, 60 /. They are significantly less scattered than the results of Fujii et. al. /50, 60 / but they agree well with Fujii's correlations /50, 60 / of his own steam data. All of the data are in good accord with the Nusselt theory at low vapour velocity. Where deviation from Nusselt theory becomes more evident (sufficiently small values of Pr_L/FrH), the Nusselt numbers found in the present work are somewhat lower than those found by Nobbs and Mayhew /42, 43 /. It may be significant that the Nobbs and Mayhew data were obtained at around atmospheric pressure whereas the present results, for similar values of Pr_L/FrH, were obtained at sub-atmospheric pressures.

At moderate vapour velocities, these data sets (Nobbs and Mayhew /42, 43 /, Fujii /50, 60 / and present) are in good general agreement with theory but show significant deviation from theory at the low Pr_L/FrH (high vapour velocities and high condensation rates) end of the data; the Nobbs results being in closest agreement with theory.

Apart from the results of Gogonin and Dorokhov /59 / for Refrigerant 21, the present results for Refrigerant 113 are the only non-steam data which seem to be available. The data of Gogonin and Dorokhov are for very low vapour velocities where the predicted deviation from Nusselt is small so that these results shed little light on the problem. The present results for Refrigerant 113 cover a similar range of Pr_L/FrH to the steam data /42, 43, 50, 60 and present / and on the basis of a $Nu/\sqrt{Re_{TP}}$ - Pr_L/FrH plot are in good agreement with the latter. It is of interest to note that the present Refrigerant 113 results are in very good agreement with Fujii's correlation of his data for steam, providing evidence that, while the theory may be imperfect, the parameters used (arising from the theory and which are used in the correlation, i.e. $Nu/\sqrt{Re_{TP}}$ and Pr_L/FrH) are the important ones.

Only one set of data /37 - 40 / exists for very low values of Pr_L/FrH (i.e. high vapour velocities and high condensation rates). These data indicate Nusselt numbers well below the theoretical predictions, but not too far below a linear extrapolation of the lower-vapour-velocity results /42, 43, 50, 59, 60 and present /. What would appear to be a very conservative modification of the theory /24, 47 / is indeed seen to be conservative with respect to most of the data with the of those for the highest vapour velocities which gave significantly lower heat-transfer coefficients.

In conclusion, it would appear that the theory is generally satisfactory for moderate vapour velocities but that for higher values, considerable doubt exists. It is not clear at this point which factors ignored in the theory would lead to the prediction of lower vapour-side heat-transfer coefficient at high vapour velocity. It would seem that further high-accuracy data for the high-velocity region are needed, including results for fluids other than steam.

Prior to the present work, few experimental data /52, 76, 77, 87, 90 / were available for forced convection condensation on a horizontal tube in the presence of a non-condensing gas. These data were all for the case of condensation of steam in the presence of air. An approximate theoretical treatment of this problem /72 / was in good agreement with this limited data. The purpose of the present investigation of this problem was to provide data for different vapour-gas combinations in order to provide a more stringent check on the theory. In particular, vapour-gas combinations have been chosen to give a wide range of Schmidt number.

Measurements have been made for steam-air, steam-hydrogen, Refrigerant 113-air and Refrigerant 113-hydrogen mixtures for a wide range of bulk gas mass fraction, vapour velocity, pressure, vapour-to-wall temperature and heat-transfer flux. The Schmidt number for the above vapour-gas combinations ranged approximately from 0.05 to 0.5. As in the case of the pure vapour investigation, special care was taken to obtain high-accuracy measurements and to ensure that the results were not affected by the occurrence of dropwise condensation. The gas content was determined by two independent methods which agreed closely for all tests. Since one of the methods involved the vapour flow rate, this provides verification of the measurement of the latter and hence of the vapour velocity in both the pure vapour and the vapour-gas investigations.

For the purpose of comparison with theory /72 /, it is necessary to determine the temperature drop across the condensate film. It was the original intention that the present data for the pure vapour case would be used for this purpose. In view of the excellent agreement between the correlation of Fujii's steam data /50, 60 / and the present results for steam and Refrigerant 113, the correlation was used to evaluate the temperature drop across the condensate film when treating the vapour-gas results. It may also be noted that for the ranges of the vapour velocity used, the correlation and theory /49 - 52 / do not differ greatly, so that it is considered that the condensate thermal resistance was determined with good accuracy. For most of the data, the temperature drop in the vapour (required for comparison with the theory for the vapour-gas boundary layer) was a substantial proportion of the measured vapour-to-wall temperature difference.

The present results were found to be in good agreement with the earlier steam-air data and with theory. The precision of the measurements was such as to show a clear Schmidt number dependence in line with the theoretical prediction. It is of interest to note that, for the ranges used in the present investigation, the semi-empirical equation of Mills et. al. /76 / (based on steam-air mixture data) is in satisfactory agreement with the theoretical equation of Rose /72 /. The correlation of Berman and Fuks /87, 90 / for steam-air mixtures agrees well with both of the above except at very high gas mass fractions which are outside the range of the data used in obtaining the correlation.

APPENDIX A

Check on the coolant flow rate calibration

Each flowmeter was calibrated in turn by collecting and weighing and the results were tabulated in Tables A.1 and A.2 below.

Table A.1 Large metering tube (nominal maximum volume flow rate 68.19 l/min.)

water collected / kg	time / s	indicated volume flow rate, $\dot{V}_{i,c}$, %	water mass flow rate, $\dot{m}_{cw}$ / (kg / s): from collecting and weighing	equation 4.1	percent difference
inlet temperature T_{in} = 279.65 K					
26.50	150	15.0	0.177	0.175	1.1
41.50	120	29.6	0.345	0.345	0.0
57.40	120	41.0	0.478	0.478	0.0
51.90	90	50.0	0.577	0.583	-1.0
61.80	89	60.0	0.697	0.699	-0.3
64.10	75	74.0	0.859	0.862	-0.3
103.50	89	100.0	1.163	1.165	-0.2
inlet temperature T_{in} = 293.15 K					
27.00	150	16.0	0.180	0.182	-1.0
41.04	120	30.0	0.342	0.340	0.6
61.45	120	45.0	0.512	0.511	0.2
68.02	80	75.0	0.850	0.851	-0.1

Table A.2 Small metering tube (nominal maximum volume flow rate 10.18 l/min.)

water collected / kg	time / s	indicated volume flow rate, $\dot{V}_{i,o}$, %	water mass flow rate, $\dot{m}_{cw}$ / (kg / s): from collecting and weighing	equation 4.1	percent difference
inlet temperature T_{in} = 279.65 K					
6.00	180	19.0	0.033	0.033	0.0
9.00	180	29.0	0.050	0.050	0.0
13.05	180	41.0	0.073	0.071	2.7
15.95	180	50.5	0.089	0.088	1.1
16.00	150	61.0	0.107	0.106	0.9
14.70	120	70.0	0.123	0.122	0.8
17.10	120	82.0	0.143	0.143	0.0
20.10	120	95.0	0.168	0.166	1.2
inlet temperature T_{in} = 293.15 K					
4.80	185	15.0	0.026	0.025	3.8
10.62	180	35.0	0.059	0.059	0.0
15.28	180	50.0	0.085	0.085	0.0
15.13	120	75.0	0.126	0.127	-0.8
19.40	120	95.0	0.162	0.161	0.6

APPENDIX B

Calibration of the thermocouples

All thermocouples used in the investigation were made from the same reel of twin-laid copper-constantan wire. Two thermocouples were calibrated simultaneously, one taken from the beginning of the reel and one after cutting the wires to be used for the investigation. The thermocouples were calibrated against a platinum resistance thermometer calibrated by the National Physical Laboratory (U.K.) (accuracy better than 0.001 K). The "cold" junctions were placed in 300 mm long glass tubes which were immersed in finely-ground, closely-packed, melting distilled-water ice. The "hot" junctions were wound round the resistance thermometer bulb.

A constant temperature oil bath, designed and built in Queen Mary College by Dr. M.R. Nightingale, was used for the calibration. The oil bath was constructed of brass with dimensions 760 x 380 x 250 mm^3 and placed in a wooden box with the interspace filled with granules of expanded vermiculite insulation. An impeller driven by an electric motor was used to rapidly circulate the oil first through a 90 mm diameter "Tufnel" cylinder that served to provide a near-isothermal enclosure where all measurements were made. At the entrance of the "isothermal" enclosure, a resistance thermometer provided the signal to operate an automatic temperature controller, the output of which was fed to the bath heater. (The controller was of model 1053 A with resistance thermometer type 1080 A supplied by the Hallikainan Instruments Division of Elliott Process Instruments Limited, Century Works, London).

Over periods of several hours, changes in the oil-bath temperature did not exceed 0.005 K and over periods of several minutes the changes were not more than 0.002 K. Within the "isothermal" enclosure of the oil bath, temperature gradients were less than 0.001 K in 100 mm. A typical calibration "point" was obtained in two minutes.

The calibration temperatures ranged from 283.15 K to 373.15 K in steps of approximately 10 K. At each temperature, the thermo-emf of each thermocouple was noted and the temperature of the resistance thermometer (with resistance of approximately 25 ohms at 273.15 K) was found using a current of approximately 1 mA, which was small enough to avoid significant heating effect in the thermometer. As the thermocouple and thermometer readings were taken within two minutes of each other, temperature changes in the oil bath introduced negligible error in the calibration. The thermo-emfs of the two thermocouple differed, at most, by 0.5 μV (corresponding to about 0.01 K). The calibration data (see Table B.1) were fitted using the "least squares" method resulting a in the following equation:-

$$T = 273.0995 + 2.5518496 \times 10^{-2}\, e - 6.6119645 \times 10^{-7}\, e^2 + 2.6750257 \times 10^{-11}\, e^3 \qquad (B.1)$$

where T is the thermodynamic temperature /K

e is the thermo-emf /μV.

The mean and maximum deviation from the above equation were 0.003 K and 0.01 K respectively. Table B.1 gives the temperature recorded by the resistance thermometer, the values of the thermo-emfs produced by the thermocouples and temperatures calculated using equation B.1.

Table B.1 Thermocouple calibration

Resistance Thermometer	Thermo-emfs		Equation B.1 with $e = (e_1 + e_2)/2$	
T_{obs} / K	e_1 / μV	e_2 / μV	T_{calc} / K	$T_{obs} - T_{calc}$ / K
288.131	397.00	397.50	283.13	0.00
293.082	798.70	799.15	293.08	0.00
303.154	1213.65	1214.05	303.15	0.00
313.213	1636.85	1637.05	313.22	-0.01
323.079	2059.20	2059.55	323.08	0.00
332.746	2480.80	2481.15	332.75	0.00
343.146	2942.40	2942.45	343.14	0.01
353.117	3392.85	3392.90	353.11	0.01
363.100	3851.45	3851.35	363.10	0.00
373.232	4323.75	4323.35	373.23	0.00

APPENDIX C

Check on the heat transfer rate through the test condenser tube to the coolant based on the coolant measurements

Tests, covering the whole range of coolant flow rates used in the main tests, were carried out where the heat transfer rate was obtained using two methods:-

a. from measurements of the condensation rate, $\dot{m}_{c1}$, on the outside of the test condenser tube by collecting the condensate over a measured time interval:

$$\dot{Q}_a = \dot{m}_{c1} \, h_{fg} \tag{C.1}$$

where $\dot{Q}_a$ is the heat transfer rate

h_{fg} is the specific enthalpy of evaporation taken at T_∞

b. from measurements of the cooling water mass flow rate and the temperature increase:

$$\dot{Q}_b = \dot{Q}_{cw} = \dot{m}_{cw} \, c_P \, (T_{out} - T_{in}) \tag{C.2}$$

where $\dot{Q}_b$, $\dot{Q}_{cw}$ are the heat transfer rates

$\dot{m}_{cw}$ is the mass flow rate of the coolant calculated using equation 4.1

c_P is the specific isobaric heat capacity of the coolant, taken as c_{Pf} at $(T_{in} + T_{out})/2$

T_{in}, T_{out} are the coolant inlet and outlet temperatures.

The results of the heat transfer rate calculated using equations C.1 and C.2 are tabulated in Table C.1. It may be noted that the agreement between the two different results are generally better than ± 5 %. Further, the two measurements of the cooling water outlet temperature (see also section 4.4.3) agree with each other to better than 0.02 K (i.e. corresponding to a thermo-emf of 1 μV).

Table C.1 Comparison of the heat transfer rates calculated from equations C.1 and C.2

vapour : steam

T_∞ / K	$\dot{m}_{cw}$ / kg/s	ΔT_{cw} † / K	$\dot{m}_{co}$ ‡ / l	time / s	Heat transfer rate /W equation C.1	C.2	percent difference
373.11	0.172	2.75	300	350.8	1924	1977	2.8
373.11	0.026	6.54	150	460.5	733	704	-3.9
373.11	0.172	2.73	325	384.0	1904	1960	2.9
373.11	0.026	6.54	175	577.0	682	704	3.2
373.11	0.172	2.68	300	359.8	1876	1924	2.6
373.11	0.026	6.44	150	465.4	725	694	-4.3
373.11	0.172	2.63	300	360.0	1875	1888	0.7
373.11	0.026	6.37	200	650.3	692	686	-0.9
373.11	0.172	2.58	300	379.9	1776	1853	4.3
373.11	0.026	6.29	175	569.2	692	678	-2.0
304.32	0.172	0.60	150	813.9	446	431	-3.4
304.32	0.026	1.99	50	569.0	213	215	1.0
304.20	0.172	0.60	175	953.7	444	431	-3.0
304.20	0.026	1.99	100	1125.0	215	215	0.0
305.56	0.172	0.62	200	1071.7	451	449	-0.6
305.56	0.026	2.41	100	905.5	267	260	-2.5

Table C.1 (continued)

vapour : Refrigerant 113

T_∞ / K	$\dot{m}_{cw}$ / kg/s	ΔT_{cw}† / K	$\dot{m}_{co}$‡ / l	time / s	Heat transfer rate /W equation C.1	C.2	percent difference
321.22	0.173	0.25	500	635.3	182	183	0.8
321.22	0.026	1.05	325	638.3	117	115	-2.0
321.26	0.173	0.25	400	522.3	177	183	3.6
321.26	0.026	1.05	300	603.0	115	115	0.0
321.77	0.173	0.28	400	476.1	194	201	4.0
321.77	0.026	1.18	300	506.9	136	129	-5.6
321.13	0.026	1.15	400	725.3	127	126	-0.9
321.12	0.173	0.28	450	513.5	202	201	-0.3
321.11	0.173	0.28	350	386.0	209	201	-3.6
321.11	0.026	1.18	300	531.3	130	129	-1.0
321.63	0.173	0.30	400	430.7	214	220	2.8
321.63	0.026	1.20	400	671.1	137	131	-4.2

† ΔT_{cw} is the coolant temperature rise

‡ $\dot{m}_{co}$ is the condensate collected in the time indicated

APPENDIX D

Sample comparisons of the two methods of determining the gas mass fraction

The symbols used in this appendix are:-

$W_{\infty 1}$ bulk gas mass fraction calculated from vapour and gas mass flow rates, see equation 6.15

$W_{\infty 2}$ bulk gas mass fraction calculated from pressure and temperature measurements in the test section, see equation 6.16

Table D.1 Sample comparisons of $W_{\infty 1}$ and $W_{\infty 2}$

Steam-air mixtures

$W_{\infty 1}$	$W_{\infty 2}$
0.50	0.48
1.43	1.57
2.05	2.03
3.52	3.46
4.73	4.95
6.29	6.40
7.20	6.91
8.52	8.35
10.26	10.43
12.42	12.49
14.77	14.46
17.63	17.22
21.93	21.52
24.23	24.12
29.22	28.90

Steam-hydrogen mixtures

$W_{\infty 1}$	$W_{\infty 2}$
0.09	0.11
0.19	0.18
0.38	0.44
0.45	0.57
0.72	0.83
1.22	1.32
2.57	2.94
3.21	3.70
4.73	5.23
5.38	5.71

R 113-air mixtures

$W_{\infty 1}$	$W_{\infty 2}$
0.05	0.05
0.29	0.28
0.42	0.43
0.58	0.57
1.03	1.04
1.30	1.20
1.62	1.60

R 113-hydrogen mixtures

$W_{\infty 1}$	$W_{\infty 2}$
0.04	0.03
0.06	0.07
0.12	0.13
0.34	0.32

In view of the excellent agreement between the two methods of determining the bulk gas mass fraction (see Table D.1) over the whole range of bulk gas mass fraction used in the tests, the results tabulated in Tables 6.10 to 6.17 and Tables 7.2 to 7.9 have been obtained only for $W_{\infty 2}$. It may be noted that the results obtained when using $W_{\infty 1}$ are generally within ± 3 % of those given in the Tables.

APPENDIX E

Thermophysical properties of the test fluids

E.1 Symbols and units

The symbols and units used in this appendix are given below:-

c_P	specific isobaric heat capacity / (J/kg K)
c_{Pf}	specific isobaric heat capacity of saturated liquid / (J/kg K)
D	binary diffusion coefficient / (m^2/s)
h_{fg}	specific enthalpy of evaporation / (J/kg)
k_f	thermal conductivity of saturated liquid / (W/m K)
k_t	thermal conductivity of copper / (W/m K)
M	relative molecular mass / (kg/kmol)
P	pressure / Pa
P_c	critical pressure / Pa
P_s	saturation pressure / Pa
R	specific ideal-gas constant / (J/kg K)
T	thermodynamic temperature / K
T_c	critical temperature / K
T_s	saturation temperature / K
t	Celsius temperature/ K, (T - 273.15)
v_f	specific volume of saturated liquid / (m^3/kg)
v_g	specific volume of saturated vapour / (m^3/kg)
ϵ_o	interaction energy parameter / J
κ	Boltzmann's constant / (J/K), 1.3805×10^{-23}

μ dynamic viscosity / (kg/m s)

μ_f dynamic viscosity of saturated liquid / (kg/m s)

μ_g dynamic viscosity of saturated vapour / (kg/m s)

μ_v dynamic viscosity of vapour or vapour-gas mixture / (kg/m s)

ρ density / (kg/m^3)

ρ_{Hg} density of liquid mercury / (kg/m^3)

ρ_v density of vapour or vapour-gas mixture / (kg/m^3)

$\sum v_i$ diffusion volume

σ interaction molecular distance parameter / Å

Ω_D collision intergral

E.2 Properties of Water Substance

The following equations were used in all calculations in the present thesis:-

specific isobaric heat capacity of saturated liquid (c_{Pf})

$$c_{Pf} = 4215 - 2.229\ t + 0.03772\ t^2 - 1.536 \times 10^{-4}\ t^3 \qquad \text{(E.2.1)}$$

(ref. /42/)

specific enthalpy of evaporation (h_{fg})

$$h_{fg} = 3468920 - 5707.4\ T + 11.5562\ T^2 - 0.0133103\ T^3 \qquad \text{(E.2.2)}$$

(ref. / 93 /)

thermal conductivity of saturated liquid (k_f)

$$k_f = -0.92247 + 2.8395\,(T/273.15) - 1.8007\,(T/273.15)^2 + 0.52577\,(T/273.15)^3 - 0.07344\,(T/273.15)^4 \qquad (E.2.3)$$

(ref. /94/)

relative molecular mass ("molecular weight") (M)

$$M = 18.015$$

(ref. / 95 /)

saturation pressure (P_s)

$$P_s = 10^6 \times \exp\left\{A_1 + A_2/T_R + A_3 \ln(T_R) + A_4 T_R + A_5 (T_R)^2 + A_6 (T_R)^3 + A_7 (T_R)^4 + A_8 (T_R)^5 + A_9 (T_R)^6 + A_{10} (T_R)^7 + A_{11} (T_R)^8\right\} \qquad (E.2.4)$$

where $T_R = T/1000$

$A_1 = 15.49217901$

$A_2 = -5.6783717693$

$A_3 = 1.4597584637$

$A_4 = 13.877000608$

$A_5 = -80.887673591$

$A_6 = 123.56883468$

$A_7 = -188.321212064$

$A_8 = 660.91763485$

$A_9 = -1382.4740091$

$A_{10} = 1300.1040184$

$A_{11} = -449.39571976$

(ref. / 93 /)

specific ideal-gas constant (R)

R = 461.51

specific volume of saturated liquid (v_f)

$$v_f = 9.9917 \times 10^{-4} + t(6.5 \times 10^{-8} + 3.83333 \times 10^{-9}\, t) \qquad (E.2.5)$$

(ref. / 93 /)

specific volume of saturated vapour (v_g)

$$v_g = \frac{B_2}{[1 + \sqrt{\{1 + 2B_1\, B_2\}}]} \qquad (E.2.6)$$

where $B_1 = \dfrac{0.0015}{1 + 0.0001T} - 0.000942\sqrt{\dfrac{1}{X_1}}\; e^{(X_1 + X_2)}$

$- 0.0004882\, X_f$

$B_2 = 2\, P_s/RT$

$X_1 = 1500/T$

$X_2 = 2.5 \ln (1 - e^{-X_1})$

(ref. / 96 /)

dynamic viscosity of saturated liquid (μ_f)

$$\mu_f = 0.00002414 \times 10^J \qquad (E.2.7)$$

where J = 247.8 / (T - 140)

(ref. /94 /)

dynamic viscosity of saturated vapour (μ_g)

$$\mu_g = - 4.478415 \times 10^{-6} + T(5.0216 \times 10^{-8} - 1.579 \times 10^{-11}T) \qquad (E.2.8)$$

(ref. / 93 /)

diffusion volumes

(used in the estimation of diffusion coefficient for steam-hydrogen mixtures)

$$\sum v_i = 12.7 \qquad (E.2.9)$$

(ref. / 97 /)

Properties of water substance given in the above equations for temperature range 275 - 375 K are tabulated in Table E.1.

E.3 Properties of Refrigerant 113 (trichlorotrifluoroethane)

The following equations were used in all calculations in the present thesis:-

specific isobaric heat capacity of saturated liquid (c_{Pf})

$$c_{Pf} = 929 + 1.03\ t \qquad (E.3.1)$$

(ref. / 98 /)

specific enthalpy of evaporation (h_{fg})

$$h_{fg} = (1.611 - 0.0031\ t) \times 10^5 \qquad (E.3.2)$$

(ref. / 98 /)

thermal conductivity of saturated liquid (k_f)

$$k_f = 0.0802 - 0.000203\ t \qquad (E.3.3)$$

(ref. / 98 /)

relative molecular mass ("molecular weight") (M)

$$M = 187.38$$

(ref. / 99 /)

saturation pressure (P_s)

$$P_s = 3.413 \times 10^6 \times 10^J \qquad \text{(E.3.4)}$$

where $J = - J_1\ (2.8 + 0.1\ (1 + 185\ J_1^{5.8})^{0.2})$

$J_1 = (T_c - T_s)/T_s$

$T_c = 487.25$ K

(ref. / 98 /)

specific ideal-gas constant (R)

R = 44.371

specific volume of saturated liquid (v_f)

$$v_f = (0.617 + 0.000647\ t^{1.1}) \times 10^{-3} \qquad \text{(E.3.5)}$$

(ref. / 98 /)

specific volume of saturated vapour (v_g)

$$v_g = RT/(\,P_s \;\cdot\; (1 + 0.636\ (P_s/P_c)^{0.816})) \qquad \text{(E.3.6)}$$

where P_c = 3.413 MPa

(ref. / 98/)

dynamic viscosity of saturated liquid (μ_f)

$$\mu_f = 1.34 \times 10^{-5} \times 10^{J} \qquad (E.3.7)$$

where J = 503/(t + 271)

(ref. /98 /)

dynamic viscosity of saturated vapour (μ_g)

$$\mu_g = (0.920 + 0.003\ t) \times 10^{-5} \qquad (E.3.8)$$

(ref. /98 /)

Lennard-Jones potentials (σ and ϵ_o/κ)

(used in the estimation of the diffusion coefficient of Refrigerant 113 -air and Refrigerant 113-hydrogen mixtures)

$$\sigma = 5.730$$

$$\frac{\epsilon_o}{\kappa} = 360.75$$

(ref. /100 /)

Properties of Refrigerant 113 given in the above equations for the temperature range 275 - 325 K are tabulated in Table E.2.

E.4 Properties of air

The following equations were used in all calculations in the present thesis:-

specific isobaric heat capacity (c_p)

$c_p = 1005$

(ref. /101 /)

relative molecular mass ("molecular weight") (M)

$M = 28.96$

(ref. /101 /)

specific ideal-gas constant (R)

$R = 287.1$

dynamic viscosity (μ)

$$\mu = (5.26 + 0.044\ T) \times 10^{-6} \qquad (E.4.1)$$

(ref. / 93 /)

density (ρ)

$$\rho = P/RT \tag{E.4.2}$$

Lennard-Jones potentials (σ and ϵ_o/κ)

(used in the estimation of the diffusion coefficient of Refrigerant 113-air mixture)

$$\sigma = 3.711$$

$$\epsilon_o/\kappa = 78.6$$

(ref. / 100/)

Properties of air given in the above equations for the temperature range 275 - 375 K are tabulated in Table E.3.

E.5 Properties of hydrogen

The following equations were used in all calculations in the present thesis:-

specific isobaric heat capacity (c_p)

$$c_p = (27297.94 + 3.2657\ T + 502.42 \times 10^5/T^2)/2.016 \tag{E.5.1}$$

(ref. / 102/)

relative molecular mass ("molecular weight") (M)

M = 2.016

(ref. / 103/)

specific ideal-gas constant (R)

R = 4124.157

dynamic viscosity (μ)

$$\mu = 841.1 \times 10^{-8} \times 0.1017 \left\{\frac{T^{3/2}}{T + 19.55}\right\} \left\{\frac{T + 650.39}{T + 1175.9}\right\} \qquad (E.5.2)$$

(ref. /104 /)

density (ρ)

$$\rho = P/RT \qquad (E.5.3)$$

Lennard-Jones potentials (σ and ϵ_0/κ)

(used in the estimation of the diffusion coefficient of Refrigerant 113-hydrogen mixture)

σ = 2.827

ϵ_0/κ = 59.7

(ref. / 100 /)

diffusion volumes

(used in the estimation of the diffusion coefficient of steam-hydrogen mixture)

$\sum v_i = 7.07$

(ref. /97 /)

Properties of hydrogen given in the above equations for the temperature range 275 - 375 K are tabulated in Table E.3.

E.6 Mixture properties

The following equations were used in all calculations in the present thesis:-

Diffusion coefficient (D)

steam-air

$$D = 7.65 \times 10^{-5} \frac{T^{11/6}}{P} \qquad \text{(E.6.1)}$$

(ref. /105 /)

steam-hydrogen

The method of Fuller et. al. / 97 / was used to estimate the diffusion coefficient for steam-hydrogen mixture.

$$D = \frac{101325 \times 10^{-7} \, (T)^{1.75} \left[\frac{1}{M_1} + \frac{1}{M_2}\right]^{\frac{1}{2}}}{P\left[(\sum_1 v_i)^{\frac{1}{3}} + (\sum_2 v_i)^{\frac{1}{3}}\right]^2} \tag{E.6.2}$$

where M_1, M_2 are the relative molecular masses of steam and hydrogen respectively

$\sum_1 v_i, \sum_2 v_i$ the diffusion volumes of steam and hydrogen respectively

Substituting the values for M_1, M_2, $\sum_1 v_i$ and $\sum_2 v_i$ gives,

$$D = 4.1614 \times 10^{-4} \, (T)^{1.75} / P \tag{E.6.3}$$

R 113-air

The recommendations of Reid and Sherwood /100 / were used to estimate the diffusion coefficient of R 113-air and R 113-hydrogen mixtures.

$$D = \frac{0.01883 \, T^{3/2} \quad [(M_1 + M_2)/M_1 \, M_2]^{\frac{1}{2}}}{P \, \sigma^2 \quad \Omega_D} \tag{E.6.4}$$

where M_1, M_2 are the relative molecular masses of the pure constituents 1 and 2 respectively

σ is the Lennard-Jones force constant for the mixture

Ω_D is the collision integral

(Note: Ω_D depends only on the dimensionless ratio $\kappa T/\epsilon_o$, κ being Boltzmann's constant. Values of Ω_D as a function of $\kappa T/\epsilon_o$ are given in Table E.4 (reproduced from Table 11 - 1 of / 100 /).

The values of ϵ_o/κ and σ for the mixture are estimated from the Lennard-Jones potentials for the pure constituents using the following combining rules.

$$\frac{\epsilon_o}{\kappa} = \sqrt{\left\{ \left[\frac{\epsilon_o}{\kappa}\right]_1 \left[\frac{\epsilon_o}{\kappa}\right]_2 \right\}} \tag{E.6.5}$$

$$\sigma = (\sigma_1 + \sigma_2)/2 \tag{E.6.6}$$

Using the values of ϵ_o/κ and σ for R 113 and air, equations E.6.5 and E.6.6 give,

$$\epsilon_o/\kappa = 168.389$$

$$\sigma = 4.7205$$

For T = 321 K,

$$\kappa T/\epsilon_o = 1.9063$$

and from Table E.4, by linear interpolation,

$$\Omega_D = 1.09274$$

Substituting the values of σ , Ω_D and the relative molecular masses of R 113 and air into equation E.6.4 gives, the following equation for the diffusion coefficient for R 113-air mixtures,

$$D = 1.5438 \times 10^{-4}\ T^{3/2}\ /P \qquad (E.6.7)$$

R 113-hydrogen

Using the values of ϵ_o/κ and σ for R 113 and hydrogen, equations E.6.5 and E.6.6 give,

$$\epsilon_o\ /\kappa\ = 146.754$$

$$\sigma\ = 4.2785$$

For T = 321 K,

$$\kappa T/\epsilon_o\ = 2.18733$$

and from Table E.4, by linear interpolation,

$$\Omega_D = 1.0430$$

Substituting the values of σ , Ω_D and the relative molecular masses of R 113 and hydrogen into equation E.6.4 gives the following equation for the diffusion coefficient for R 113-hydrogen mixtures.

$$D = 6.982 \times 10^{-4}\ T^{3/2}\ /P \qquad (E.6.8)$$

dynamic viscosity (μ_v)

$$\mu_v = (\mu_1/(1 + \phi_1)) + (\mu_2/(1 + \phi_2)) \qquad \text{(E.6.9)}$$

where μ_1, μ_2 are the dynamic viscosity of the pure constituents 1 and 2 respectively

$$\phi_1 = \frac{(\tilde{W}_2/\tilde{W}_1)\left[1 + [(\mu_1/\mu_2)(\varrho_2/\varrho_1)]^{\frac{1}{2}}(M_1/M_2)^{\frac{1}{4}}\right]^2}{(4/\sqrt{2})[1 + (M_1/M_2)]^{\frac{1}{2}}}$$

$$\phi_2 = \frac{(\tilde{W}_1/\tilde{W}_2)\left[1 + [(\mu_2/\mu_1)(\varrho_1/\varrho_2)]^{\frac{1}{2}}(M_2/M_1)^{\frac{1}{4}}\right]^2}{(4/\sqrt{2})[1 + (M_2/M_1)]^{\frac{1}{2}}}$$

$\tilde{W}_1$, $\tilde{W}_2$ are the mole fractions of constituents 1 and 2 respectively

ϱ_1, ϱ_2 are the density of pure constituents 1 and 2 respectively at the temperature and total pressure of the mixture

M_1, M_2 are the relative molecular masses of pure constituents 1 and 2 respectively

(ref. /92a/)

density (ϱ_v)

Applying the Gibbs-Dalton Law of partial volumes, the mixture density is taken to be the sum of the partial densities of the constituents at the temperature of the mixture. Thus,

$$\varrho_v = \sum_{i=1}^{n} \varrho_i \qquad \text{(E.6.10)}$$

where n is the number of constituents in the mixture.

E.7 Thermal conductivity of copper (k_t)

$$k_t = 438.643 - 0.1306926\ T + 4.540943 \times 10^{-5}\ T^2 \qquad (E.7.1)$$

(ref. / 4/)

Thermal conductivity of copper given in the above equation for the temperature range 275 to 375 K is tabulated in Table E.3.

E.8. Density of liquid mercury (ρ_{Hg})

$$\rho_{Hg} = (6.98392 \times 10^{-5} + 1.40194 \times 10^{-8}\ T - 2.2775 \times 10^{-12}\ T^2 + 2.70871 \times 10^{-15}\ T^3)^{-1} \qquad (E.8.1)$$

(ref. / 4 /)

Density of liquid mercury given in the above equation for the temperature range 275 to 375 K is tabulated in Table E.3.

Table E.1 Thermophysical Properties of Water Substance

T K	c_{pf} kJ/kg K	h_{fg} MJ/kg	k_f W/m K	P_s Pa	$v_f \times 10^3$ m^3/kg	v_g m^3/kg	$\mu_f \times 10^3$ kg/m s	$\mu_g \times 10^6$ kg/m s
275	4.211	2.497	0.572	698	0.999	181.79	1.653	8.137
280	4.202	2.485	0.581	991	1.000	130.36	1.421	8.344
285	4.194	2.473	0.590	1387	1.000	94.74	1.235	8.551
290	4.188	2.461	0.598	1917	1.001	69.73	1.083	8.756
295	4.183	2.449	0.606	2618	1.002	51.95	0.958	8.961
300	4.180	2.437	0.614	3532	1.004	39.14	0.854	9.165
305	4.178	2.426	0.621	4713	1.005	29.81	0.767	9.369
310	4.177	2.414	0.627	6223	1.007	22.94	0.692	9.571
315	4.177	2.402	0.634	8135	1.009	17.82	0.629	9.773
320	4.178	2.390	0.640	10533	1.011	13.97	0.575	9.974
325	4.180	2.378	0.645	13516	1.013	11.05	0.527	10.170
330	4.182	2.366	0.650	17194	1.015	8.816	0.486	10.370
335	4.185	2.353	0.655	21694	1.018	7.088	0.450	10.570
340	4.189	2.341	0.660	27160	1.021	5.741	0.419	10.770
345	4.193	2.329	0.664	33749	1.024	4.683	0.390	10.970
350	4.197	2.316	0.668	41641	1.027	3.846	0.365	11.160
355	4.201	2.304	0.671	51031	1.030	3.179	0.343	11.360
360	4.206	2.291	0.674	62135	1.034	2.644	0.323	11.550
365	4.210	2.278	0.677	75190	1.037	2.212	0.305	11.750
370	4.214	2.265	0.679	90452	1.041	1.861	0.288	11.940
375	4.217	2.252	0.681	108201	1.046	1.574	0.274	12.130

Table E.2 Thermophysical Properties of Refrigerant 113

T K	c_{Pf} J/kg K	h_{fg} kJ/kg	$k_f \times 10^3$ W/m K	P_s Pa	$v_f \times 10^3$ m^3/kg	v_g m^3/kg	$\mu_f \times 10^3$ kg/m s	$\mu_g \times 10^6$ kg/m s
275	930.9	160.5	79.8	16392	0.618	0.738	0.935	9.256
280	936.1	159.0	78.8	20755	0.622	0.593	0.866	9.406
285	941.2	157.4	77.8	26023	0.627	0.480	0.804	9.556
290	946.4	155.9	76.8	32328	0.631	0.393	0.749	9.706
295	951.5	154.3	75.8	39813	0.636	0.323	0.699	9.856
300	956.7	152.8	74.7	48630	0.641	0.268	0.654	10.010
305	961.8	151.2	73.7	58940	0.646	0.224	0.614	10.160
310	967.0	149.7	72.7	70914	0.651	0.189	0.577	10.310
315	972.1	148.1	71.7	84729	0.656	0.160	0.543	10.460
320	977.3	146.6	70.7	100572	0.662	0.136	0.512	10.610
325	982.4	145.0	69.7	118632	0.667	0.117	0.484	10.760

Table E.3 Properties of air, hydrogen, copper and mercury

	air	hydrogen		copper	mercury
T	$\mu \times 10^6$	c_p	$\mu \times 10^6$	k_t	ρ_{Hg}
K	kg/m s	kJ/kg K	kg/m s	W/m K	Mg/m^3
275	126.26	14.32	8.447	406.1	13.59
280	128.46	14.31	8.550	405.6	13.58
285	130.66	14.31	8.653	405.1	13.57
290	132.86	14.31	8.755	404.6	13.55
295	135.06	14.31	8.856	404.0	13.54
300	137.26	14.30	8.957	403.5	13.53
305	139.46	14.30	9.057	403.0	13.52
310	141.66	14.30	9.157	402.5	13.51
315	143.86	14.30	9.256	402.0	14.49
320	146.06	14.30	9.355	401.5	13.48
325	148.26	14.30	9.453	401.0	13.47
330	150.46	14.30	9.551	400.5	13.46
335	152.66	14.31	9.648	400.0	13.44
340	154.86	14.31	9.745	399.5	13.43
345	157.06	14.31	9.841	399.0	13.42
350	159.26	14.31	9.937	398.5	13.41
355	161.46	14.31	10.030	398.0	13.40
360	163.66	14.32	10.130	397.5	13.38
365	165.86	14.32	10.220	397.0	13.37
370	168.06	14.32	10.320	396.5	13.36
375	170.26	14.33	10.410	396.0	13.35

Table E.4 Reproduced from Reid and Sherwood /100 /

TABLE 11-1. VALUES OF THE COLLISION INTEGRAL Ω_D BASED ON THE LENNARD-JONES POTENTIAL†

kT/ϵ_0‡	Ω_D‡	kT/ϵ_0	Ω_D	kT/ϵ_0	Ω_D
0 30	2.662	1.65	1.153	4 0	0.8836
0.35	2 476	1.70	1.140	4 1	0.8788
0.40	2.318	1.75	1.128	4.2	0.8740
0.45	2.184	1.80	1.116	4.3	0.8694
0 50	2 066	1.85	1.105	4 4	0.8652
0 55	1.966	1.90	1.094	4 5	0 8610
0.60	1.877	1 95	1.084	4 6	0 8568
0 65	1.798	2 00	1.075	4.7	0.8530
0.70	1.729	2.1	1.057	4.8	0.8492
0 75	1.667	2.2	1.041	4.9	0.8456
0.80	1.612	2.3	1.026	5.0	0.8422
0 85	1.562	2.4	1.012	6	0.8124
0 90	1.517	2.5	0.9996	7	0.7896
0 95	1.476	2.6	0.9878	8	0.7712
1 00	1.439	2.7	0.9770	9	0.7556
1.05	1.406	2.8	0.9672	10	0.7424
1.10	1.375	2.9	0.9576	20	0.6640
1.15	1.346	3.0	0.9490	30	0.6232
1.20	1.320	3.1	0.9406	40	0.5960
1.25	1.296	3.2	0.9328	50	0.5756
1.30	1.273	3.3	0.9256	60	0.5596
1.35	1.253	3.4	0.9186	70	0.5464
1.40	1.233	3.5	0.9120	80	0.5352
1.45	1.215	3.6	0.9058	90	0.5256
1.50	1.198	3.7	0.8998	100	0.5130
1.55	1.182	3.8	0.8942	200	0.4644
1.60	1.167	3.9	0.8888	400	0.4170

† From J. O Hirschfelder, C. F. Curtiss, and R. B. Bird, "Molecular Theory of Gases and Liquids," John Wiley & Sons, Inc., New York, 1954.

‡ Hirschfelder uses the symbols T^* for kT/ϵ_0 and $\Omega^{(1,1)*}$ in place of Ω_D.

APPENDIX F

Sample calculations

F.1 Pure vapours

The experimental point chosen to illustrate the method of calculation for pure vapours is run number 1. The measured values are:-

vapour velocity, U_∞	1.70 m/s
bulk saturation pressure, P_∞	101.2 kPa
bulk saturation temperature, T_∞	373.10 K
mean wall outside temperature, T_w	337.89 K
coolant mass flow rate, $\dot{m}_{cw}$	0.169 kg/s
coolant inlet temperature, T_{in}	293.52 K
coolant temperature rise, ΔT_{cw}	2.81 K
exposed length of the test condenser tube, L	109.5 mm
outside diameter of the test condenser tube, d_o	12.5 mm

Calculation of the observed heat flux and Nusselt number

The mean coolant temperature, T_{cw}, is

$$T_{cw} = T_{in} + 0.5\,\Delta T_{cw} = 294.93\text{ K}$$

The rate of heat transfer to the coolant is calculated from equation C.2 as

$$\dot{Q}_{cw} = \dot{m}_{cw}\, c_{Pcw}\, \Delta T_{cw}$$

$$= 0.169 \times 4183.0 \times 2.81 = 1986.5\text{ W}$$

The area of heat transfer, A_{tt}, is

$$A_{tt} = \pi d_o L = 0.0043 \text{ m}^2$$

Thus the observed heat flux, $\dot{Q}''_{obs}$, and the Nusselt number, Nu, are

$$\dot{Q}''_{obs} = \dot{Q}_{cw}/A_{tt} = 462.0 \text{ kW/m}^2$$

$$Nu = \dot{Q}''_{obs} \, d_o / (k_L \, \Delta T) = 245.9$$

Calculation of the predicted heat flux and Nusselt number

The reference temperature, T_r, used to calculate the condensate film properties is calculated from equation 7.5 as

$$T_r = T_w + \tfrac{1}{3} \Delta T = 349.63 \text{ K}$$

The properties of the condensate film calculated at T_r are:-

density, ρ_L	974.1 kg/m^3
dynamic viscosity, μ_L	3.67×10^{-4} kg/(m s)
specific isobaric heat capacity, c_{PL}	4196.8 J/kg
thermal conductivity, k_L	0.667 W/(m K)

The specific enthalpy of evaporation, h_{fg}, is calculated at T_∞, thus,

$$h_{fg} = 2.257 \text{ MJ/kg}$$

The properties of the vapour calculated at T_∞ are:-

density, ρ_v 0.60 kg/m^3

dynamic viscosity, μ_v 12.0×10^{-6} kg/(m s)

The values of the dimensionless parameters, Pr_L, Fr, Re_{TP}, M, $\tilde{M}$ and R follows

condensate Prandtl number, Pr_L	2.3
Froude number, Fr	23.6
two-phase Reynolds number, Re_{TP}	56454
phase change number, M	0.0655
$\rho\mu$ - ratio, R	223.0
$\tilde{M}$	6.969
Pr_L/FrM	1.5
RM/Pr_L	6.3
$\sqrt{Re_{TP}}/Fr\tilde{M}$	1.4
$R\tilde{M}/\sqrt{Re_{TP}}$	6.5

The predicted heat fluxes and Nusselt numbers are given in Table F.1 below.

Table F.1 Predicted heat fluxes and Nusselt numbers for run number 1

Theory/Correlation	Equation no.	Calculated values: $\dot{Q}''_{calc}$ kW/m^2	Calculated values: Nu	$\dot{Q}''_{obs}/\dot{Q}''_{calc}$
Nusselt /2 /	2.2	359.4	191.3	1.285
Shekriladze /24/	2.33	484.7	258.0	0.953
Fujii et. al. /49 /	2.37	468.2	249.2	0.987
Fujii et. al. /50,60/	2.42, 7.3	464.3	247.1	0.995
Fujii et. al. /50,60/	2.44, 7.1	450.0	239.5	1.027

F.2 Vapour-gas mixtures

The experimental point chosen to illustrate the method of calculation for vapour-gas mixtures is run number 412. The measured values are:-

gas mass fraction, $W_{\infty 2}$	0.48 %
vapour velocity, U_∞	1.66 m/s
bulk saturation pressure, P_∞	101.2 kPa
bulk saturation temperature, T_∞	373.03 K
mean wall outside temperature, T_w	336.81 K
coolant mass flow rate, $\dot{m}_{cw}$	0.169 kg/s
coolant inlet temperature, T_{in}	289.07 K
coolant temperature rise, ΔT_{cw}	2.64 K
exposed length of the test condenser tube, L	109.5 mm
outside diameter of the test condenser tube, d_o	12.5 mm

Calculation of the observed heat flux

The mean coolant temperature, T_{cw}, is

$$T_{cw} = T_{in} + 0.5 \ \Delta T_{cw} = 290.39 \text{ K}$$

The rate of heat transfer to the coolant is calculated from equation C.2 as

$$\dot{Q}_{cw} = 0.169 \times 4187.3 \times 2.64 = 1884.0 \text{ W}$$

and the observed heat flux, $\dot{Q}''_{obs}$, is

$$\dot{Q}''_{obs} = \dot{Q}_{cw} / A_{tt} = 1884.0/0.0043 = 438.0 \text{ kW/m}^2$$

Calculation of the values of $Sh/\sqrt{Re_v}$ and ω

It was seen in Chapter 7 that the condensate film resistance is satisfactorily represented by equation 7.3. This equation is therefore used in the present calculations to estimate the temperature drop, corresponding to the observed heat flux, across the condensate film. Starting with a guessed interfacial temperature (T_i) the heat flux calculated from equation 7.3 was determined. Using an iterative procedure, the calculation was repeated (at each step the new estimate of the interfacial temperature, T_i, was used) until the heat flux given by equation 7.3 for the condensate film differed from the observed value by less than 1 W/m^2 (which is 0.005 % of the lowest observed heat flux). Table F.2 below gives the results of the calculations.

Table F.2 Results of iterations to obtain the interfacial temperature corresponding to the observed heat flux and mean tube wall temperature (using equation 7.3)

T_i/K	heat flux given by equation 7.3 $\dot{Q}''/(kW/m^2)$	$\dot{Q}'' - \dot{Q}''_{obs}$ (W/m^2)
373.03	458272.8	20137.1
354.92	257163.4	-180972.4
363.98	359817.9	-78317.9
368.51	409435.8	-28700.0
370.77	433940.1	-4194.7
371.90	446126.6	7990.9
371.34	440038.5	1902.8
371.05	436990.6	-1145.1
371.19	438514.9	379.2
371.12	437752.8	-382.9
371.16	438133.9	1.8
371.18	438324.4	188.7
371.17	438229.2	93.4

Table F.2 (continued)

T_i/K	heat flux given by equation 7.3 $\dot{Q}''/(kW/m^2)$	$\dot{Q}'' - \dot{Q}''_{obs}$ (W/m^2)
371.16	438181.5	45.8
371.16	438157.7	22.0
371.16	438145.8	10.1
371.16	438139.9	4.1
371.16	438136.9	1.1
371.16	438135.4	0.4

When the interfacial temperature has been evaluated, the values of $Sh/\sqrt{Re_v}$ and ω can be determined as follows. The interfacial gas mass fraction is calculated from equation 6.16 as

$$\text{interfacial gas mass fraction, } W_i = 10.49\ \%$$

and therefore,

$$\omega = W_\infty / W_i = 0.05$$

The Sherwood number, Sh, is given by

$$Sh = \dot{m}'' d_o / (\rho_v D (1 - \omega))$$

$$= \dot{Q}''_{obs} d_o / (h_{fg} \rho_v D (1 - \omega))$$

and the vapour Reynolds number, Re_v, by

$$Re_v = \rho_v d_o U_\infty / \mu_v$$

The specific enthalpy of evaporation, h_{fg}, is calculated at T_i, thus,

$$h_{fg} = 2.262 \text{ MJ/kg}$$

The density and dynamic viscosity of the vapour are taken as the mean of their values at T_i and T_∞, thus,

$$\text{density,} \quad \rho_v = (0.62 + 0.60)/2 = 0.61 \text{ kg/m}^3$$

$$\text{dynamic viscosity,} \quad \mu_v = (0.000013 + 0.000012)/2$$
$$= 0.0000125 \text{ kg/m s}$$

The diffusion coefficient is calculated (using equation E.6.1) at $(T_i + T_\infty)/2$ as

$$\text{diffusion coefficient, } D = 0.000039 \text{ m}^2/\text{s}$$

The value of $Sh/\sqrt{Re_v}$ is thus

$$Sh/\sqrt{Re_v} = 3.31$$

The values of $Sh/\sqrt{Re_v}$ and ω found using the above calculation procedure are tabulated in Tables 7.2 to 7.9 of Chapter 7.

Calculation of the predicted (coupled condensate film and vapour-gas layer equations) heat flux ($\dot{Q}''_{calc}$)

The predicted (or calculated) heat flux was determined on the basis of coupling equation 7.3 (for the condensate film) with equation 7.13 (for the vapour-gas layer) in the following manner. Starting with a guessed interfacial temperature (T_i), the heat fluxes given by equations 7.3 and 7.13 were determined respectively. Using an iterative procedure, the calculation (at each step the new estimate of the interfacial temperature , T_i, was used) until the difference in the heat flux given by equation 7.3 and that given by equation 7.13 was less than 1 W/m^2 (which is 0.005 % of the lowest observed heat flux). Table F.3 below gives the results of the the calculations.

Table F.3 Results of iterations to obtain the calculated heat flux

	heat flux/(W/m^2)		
	equation 7.3	equation 7.13	$(\dot{Q}''_{calc1} - \dot{Q}''_{calc2})$
T_i/K	$\dot{Q}''_{calc1}$	$\dot{Q}''_{calc2}$	W/m^2
354.92	258075.0	1120713.0	-862637.9
363.97	360285.9	821888.9	-461603.1
368.50	409512.6	583215.3	-173702.7
370.76	433779.2	403315.0	30464.2
369.63	421672.2	501893.7	-80221.5
370.20	427732.1	455346.3	-27614.2
370.48	430757.3	430121.5	635.7
370.34	429245.1	442916.4	-13671.3
370.41	430001.3	436566.3	-6565.0
370.44	430379.3	433356.0	-2976.7
370.46	430568.3	431741.8	-1173.5
370.47	430662.8	430932.4	-269.7
370.47	430710.0	430527.2	182.9
370.47	430686.4	430729.8	-43.4
370.47	430698.2	430628.5	69.7
370.47	430692.3	430679.2	13.1
370.47	430689.3	430704.5	-15.2
370.47	430690.8	430691.8	-1.0
370.47	430691.6	430685.5	6.0
370.47	430691.2	430688.7	2.5
370.47	430691.0	430690.3	0.7

The interfacial temperature, T_i, thus found can then be used to evaluate the respective temperature drops across the condensate film and the vapour-gas layer. The temperature drops thus found indicate the relative magnitude of the resistance to heat transfer of the condensate film to that of the vapour-gas layer. The calculated heat flux and the temperature drops across the condensate film and the vapour-gas layer are tabulated in Tables 7.2 to 7.9 of Chapter 7.

APPENDIX G

Estimation of errors

The important quantities measured during the present investigation are the heat flux ($\dot{Q}''_{obs}$), the bulk-to-wall temperature difference (ΔT), the vapour velocity (U_∞) and the gas mass fraction (W_∞). Error estimates in these quantities are obtained as follows:-

Heat flux

The heat flux was calculated from coolant measurements, thus,

$$\dot{Q}''_{obs} = \dot{m}_{cw}\, c_{Pcw}\, \Delta T_{cw}/A_{tt} \qquad (G.1)$$

where $\dot{m}_{cw}$ is the coolant flow rate

c_{Pcw} is the specific isobaric heat capacity of the coolant, taken as c_{Pf} at the mean coolant temperature

ΔT_{cw} is the coolant temperature rise

A_{tt} is the exposed area of the test condenser tube

Taking the limits of error in $\dot{m}_{cw}$ and ΔT_{cw} as 2 % and 0.05 K (corresponding to a thermo-emf of about 2 μV) respectively, the relative error $\delta\dot{Q}''_{obs}/\dot{Q}''_{obs}$ was estimated, see /106 /, as:-

$$\delta\dot{Q}''_{obs}/\dot{Q}''_{obs} = \left\{0.02^2 + (0.05/\Delta T_{cw})^2\right\}^{\frac{1}{2}} \qquad (G.2)$$

where ΔT_{cw} varies between 0.12 and 7.27.

The values of the percent error in heat flux, calculated using equation G.1, are tabulated in Tables 6.3 to 6.17 and ranged approximately from 2.1 to 40.6. However, condensate collection tests (see Appendix C) indicated that the above estimates are conservative.

Bulk-to-wall temperature difference

Taking the present thermocouple calibration, thermoelectric measuring techniques and precautions to ensure adequate isothermal immersion of both thermocouple junctions into consideration, it was estimated that all temperatures were measured with an accuracy of about ± 0.02 K (corresponding to a thermo-emf of about 1 μV). Thus, in general, the bulk-to-wall temperature difference (ΔT) was measured with an accuracy of about ± 0.05 K. The value of ΔT depended on the mean outside wall temperature which was taken as the mean of the four local and radially-extrpolated outside wall temperatures which, in some cases, vary considerably. As a guide to the "reliability" of the quoted values of ΔT, the standard deviation (σ_{Tw}) of the four local outside wall temperatures from the mean value is suggested thus,

$$\sigma_{Tw} = \sqrt{\frac{1}{4} \sum_{j=1}^{4} (T_{wo,j} - T_w)^2} \qquad (G.3)$$

where $T_{wo,j}$ is the local outside wall temperature

T_w is the mean outside wall temperature, $= \frac{1}{4}\left[\sum_{j=1}^{4}\left\{T_{wo,j}\right\}\right]$

The values of σ_{Tw} calculated using equation G.3 are tabulated in Tables 6.3 to 6.17 and ranged approximately from 0.2 K to 8.1 K.

Vapour velocity

The mean vapour velocity (U_∞) over the exposed length of the test condenser tube was obtained from the mass flow rates using a seventh power velocity profile for turbulent flow, see section 6.2. The resulting equation for U_∞ is,

$$U_\infty = 1.108\,((\dot{m}_v + \dot{m}_n)/A_{ts})\,v_v \qquad (G.4)$$

where $\dot{m}_v$ is the mass flow rate of vapour

$\dot{m}_n$ is the mass flow rate of non-condensing gas

v_v is the specific volume of vapour-gas mixture

A_{ts} is the cross-sectional area of the test section

Taking the limits of error on $\dot{m}_v$ and $\dot{m}_n$ as 1.5 % (see section 6.2) and 2 % respectively, the relative error $\delta U_\infty/U_\infty$ was estimated, see / 106 /, as:-

$$\delta U_\infty/U_\infty = \frac{\{(0.015\,\dot{m}_v)^2 + (0.02\cdot\dot{m}_n)^2\}^{\frac{1}{2}}}{\{\dot{m}_v + \dot{m}_n\}} \qquad (G.5)$$

The values of the percent error in vapour velocity, calculated using equation G.5, are tabulated in Tables 6.3 to 6.17 and ranged approximately from 1.2 to 1.5.

Gas mass fraction

In the present work, the gas mass fraction has been evaluated by two methods:-

a. from the vapour and gas mass flow rates (see equation 6.15),

$$W_{\infty 1} = \dot{m}_n / (\dot{m}_n + \dot{m}_v) \qquad (G.6)$$

b. from the pressure and temperature measurements of the vapour-gas mixture at the test section (see equation 6.16),

$$W_{\infty 2} = \frac{P_\infty - P_s(T_\infty)}{P_\infty - (1 - M_v/M_n)\, P_s(T_\infty)} \qquad (G.7)$$

For $W_{\infty 1}$, taking the limits of error in $\dot{m}_n$ and $\dot{m}_v$ as ± 2 % and ± 1.5 % respectively, the relative error $\delta W_{\infty 1}/W_{\infty 1}$ was estimated, see /106 /, as:-

$$\frac{\delta W_{\infty 1}}{W_{\infty 1}} = \frac{1}{W_{\infty 1}} \left\{ \left[\frac{\partial W_{\infty 1}}{\partial \dot{m}_n}\, \delta \dot{m}_n \right]^2 + \left[\frac{\partial W_{\infty 1}}{\partial \dot{m}_v}\, \delta \dot{m}_v \right]^2 \right\}^{\frac{1}{2}}$$

$$\text{i.e.} \quad \frac{\delta W_{\infty 1}}{W_{\infty 1}} = 0.025\, \dot{m}_v / (\dot{m}_v + \dot{m}_n) \qquad (G.8)$$

Similarly, for $W_{\infty 2}$, taking the limits of error in P_∞ and P_s to be ± 13.3 Pa and ± $(P_s(T_\infty + 0.02) - P_s(T_\infty))$ respectively, the relative error $\delta W_{\infty 2}/W_{\infty 2}$ was estimated as:-

$$\frac{\delta W_{\infty 2}}{W_{\infty 2}} = \frac{1}{W_{\infty 2}} \left\{ \left[\frac{\partial W_{\infty 2}}{\partial P_\infty}\, \delta P_\infty \right]^2 + \left[\frac{\partial W_{\infty 2}}{\partial P_s}\, \delta P_s \right]^2 \right\}^{\frac{1}{2}}$$

$$\text{i.e.} \quad \frac{\delta W_{\infty 2}}{W_{\infty 2}} = \left[\frac{1}{W_{\infty 2}\, (P_\infty - (1 - M_v/M_n) P_s(T_\infty))^2} \right] \Big\{ (13.3\, P_s(T_\infty) \times M_v/M_n)^2 + (P_\infty\, M_v/M_n\, (P_s(T_\infty + 0.02) - P_s(T_\infty)))^2 \Big\}^{\frac{1}{2}}$$

(G.9)

The values of the precent errors $\delta W_{\varpi 1}/W_{\varpi 1}$ (equation G.8) and $\delta W_{\varpi 2}/W_{\varpi 2}$ (equation G.9) are tabulated in Tables 6.10 to 6.17 and ranged approximately from 1.7 to 2.5 and from 0.3 to 26.4 respectively. However, the good agreement between the two measurements of the gas mass fraction throughout the present work suggests that the above estimates are conservative. In view of this, the results tabulated in Tables 6.10 to 6.17 and in Tables 7.2 to 7.9 have been obtained only for the gas mass fraction $W_{\varpi 2}$. It may be noted that the results obtained when using the gas mass fraction $W_{\varpi 1}$ differed, in general, from those given in the Tables by about ± 3 %.

REFERENCES

1. W. Nusselt
Die oberflachen kondensation des wasserdampfes
Z. des Vereines Deutscher Ing., 60, 541 - 546, 1916

2. W. Nusselt
Die oberflachen kondensation des wasserdampfes
Z. des Vereines Deutscher Ing., 60, 569 - 575, 1916

3. S.A. Stylianou
Heat transfer during dropwise condensation of steam and ethanediol
PhD Thesis, Queen Mary College, University of London, 1980

4. J. Niknejad
An investigation of heat transfer during filmwise and dropwise condensation of mercury
PhD Thesis, Queen Mary College, University of London, 1979

5. R. Wilmshurst
Heat transfer during dropwise condensation of steam, ethane 1, 2 diol, aniline and nitrobenzene
PhD Thesis, Queen Mary College, University of London, 1979

6. I. Tanasawa
Dropwise condensation - The way to practical applications
Proc. 6th Int. Heat Transfer Conf., Toronto, Vol. 6, Paper KS - 28, 393 - 405, 1978

7. J.W. Rose
Studies of interphase mass transfer via liquid metal condensation experiments
Proc. 2nd Multi-phase Flow and Heat Transfer Symposium Workshop, Miami Beach, 1979

8. W.H. McAdams
Heat Transmission, 3rd ed.
McGraw-Hill Book Co., 1954

9. A.F. Mills and R.A. Seban
The condensation coefficient of water
Int. J. Heat Mass Transfer, 10, 1815 - 1827, 1967

10. L. Slegers and R.A. Seban
Nusselt condensation of n-butyl alcohol
Int. J. Heat Mass Transfer, 12, 237 - 239, 1969

11. B.S. Magal
Film condensation of saturated steam on a horizontal tube
Ind. J. Tech., 10, 370 - 376, 1972

12. D.K. Chung
Verification of Nusselt theory of condensation on a horizontal tube
MSc Thesis, University of California, Los Angeles, 1972

13. L.A. Bromley
Heat transfer in condensation - Effect of heat capacity of condensate
Ind. Eng. Chem., 44, 12, 2966 - 2969, 1952

14. W.M. Rohsenow
Heat transfer and temperature distribution in laminar-film condensation
Trans. ASME, 78, 1645 - 1648, 1956

15. Discussion in /14 /

16. E.M. Sparrow and J.L. Gregg
A boundary-layer treatment of laminar-film condensation
Trans. ASME, 81, 13 - 18, 1959

17. E.M. Sparrow and J.L. Gregg
Laminar condensation heat transfer on a horizontal cylinder
Trans. ASME, 81, 291 - 296, 1959

18. J.C.Y. Koh, E.M. Sparrow and J.P. Hartnett
The two phase boundary layer in laminar film condensation
Int. J. Heat Mass Transfer, 2, 69 - 82, 1961

19. M.M. Chen
An analytical study of laminar film condensation:
Part 1 - Flat plates
Trans. ASME, 83, 48 - 54, 1961

20. M.M. Chen
An analytical study of laminar film condensation:
Part 2 - Single and multiple horizontal tubes
Trans. ASME, 83, 55 - 60, 1961

21. T. Fujii, H. Uehara and K. Oda
Filmwise condensation on a surface with uniform heat flux
and body force convection
Heat Transfer - Japan Research, 1, 4, 76 - 83, 1972

22. R.D. Cess
Laminar film condensation on a flat plate in the absence
of body force
Z. Agnew Math. Phys., 11, 426 - 433, 1960

23. J.C.Y. Koh
Film condensation in a forced-convection boundary-layer flow
Int. J. Heat Mass Transfer, 5, 941 - 954, 1962

24. I.G. Shekriladze and V.I. Gomelauri
Theoretical study of laminar film condesation of flowing vapour
Int. J. Heat Mass Transfer, 9, 581 - 591, 1966

25. Y.R. Mayhew, D.J. Griffiths and J.W. Phillips
Effect of vapour drag on laminar film condensation
on a vertical surface
Proc. Instn. Mech. Engrs., 180, 280 - 289, 1965 - 1966

26. Y.R. Mayhew and J.K. Aggarwal
Laminar film condensation with vapour drag on a flat surface
Int. J. Heat Mass Transfer, 16, 1944 - 1949, 1973

27. V. South III and V.E. Denny
The vapour shear boundary condition for laminar film
condensation
Trans. ASME, 94, 248 - 249, 1972

28. V.E. Denny and A.F. Mills
Nonsimilar solutions for laminar film condensation on a
vertical surface
Int. J. Heat Mass Transfer, 12, 965 - 979, 1969

29. V.E. Denny, A.F. Mills and V.J. Jusionis
Laminar film condensation from a steam - air mixture undergoing forced flow down a vertical surface
Trans. ASME, 93, 297 - 304, 1971

30. V.E. Denny and V. South III
Effects of forced flow, non - condensables and variable properties on film condensation of pure and binary vapors at the forward stagnation point of a horizontal cylinder
Int. J. Heat Mass Transfer, 15, 2133 - 2142, 1972

31. K. Asano, Y. Nakano and M. Inaba
Forced convection film condensation of vapours in the presence of noncondensable gas on a small vertical flat plate
J. Chem. Eng. Japan, 12, 3, 196 - 202, 1979

32. H.R. Jacobs
An integral treatment of combined body force and forced convection in laminar film condensation
Int. J. Heat Mass Transfer, 9, 637 - 648, 1966

33. T. Fujii and H. Uehara
Laminar filmwise condensation on a vertical surface
Int. J. Heat Mass Transfer, 15, 217 - 233, 1972

34. H. Schlichting
Boundary Layer Theory, 6th edition
McGraw-Hill, New York, 1968

35. H. Honda and T. Fujii
Effect of the direction of on-coming vapour on laminar filmwise condensation on a horizontal cylinder
Proc. 5th Int. Heat Transfer Conf., Tokyo,
Vol 3, 299 - 303, 1974

36. S. Sugawara, I Michiyoshi and T. Minamiyama
The condensation of vapour flowing normal to a horizontal pipe
Proc. 6th Japanese Nat. Congress Appl. Mech., 385 - 388, 1956

37. A.A. Nicol and D.J. Wallace
The influence of vapour shear force on condensation on a cylinder
Symp. on Multi-Phase Flow Systems, Inst. Chem. Engrs., Symp. Series No. 38, 1 - 19, 1974

38. D.J. Wallace
A study of the influence of vapour velocity upon condensation on a horizontal tube
PhD Thesis, University of Strathclyde, Glasgow, 1975

39. A.A. Nicol and D.J. Wallace
Condensation with appreciable vapour velocity and variable wall temperature
Symp. on Steam Turbine Condensers, N.E.L. Report No. 619, 27 - 38, 1976

40. A.A. Nicol, A. Bryce and A.S.A. Ahmed
Condensation of a horizontally flowing vapour on a horizontal cylinder normal to the vapour stream
Proc. 6th Int. Heat Transfer Conf., Toronto, Vol. 2, Paper CS - 4, 401 - 406, 1978

41. K. Heimenz
Die grentzschicht an einem in den gleichförmigen Flüssigkeitstrom eingetanchten geraden Kreiszylinder
Dinglers Polytechnisches Journal, 326, 321 - 324, 344 - 348, 372 - 376, 391 - 393, 1911

42. D.W. Nobbs
The effect of downward vapour velocity and inundation on the condensation rates on horizontal tubes and tube banks
PhD Thesis, University of Bristol, 1975

43. D.W. Nobbs and Y.R. Mayhew
Effect of downward vapour velocity and inundation on condensation rates on horizontal tube banks
Symp. on Steam Turbine Condensers, N.E.L. Report No. 619, 39 - 52, 1976

44. L. Prandtl
See H. Schlichting /34 /, page 376

45. M.G. Morsy
Skin friction and form pressure loss in tube bank condensers
Proc. Instn. Mech. Engrs., 189, 49 - 75, 1975

46. L.D. Berman and Yu. A. Tumanov
Investigation of the heat transfer in the condensation of moving steam on a horizontal tube
Teploenergetika, 9, 10, 77 - 83, 1962
(N.E.L. Translation No. 1460)

47. D. Butterworth
Developments in the design of shell and tube condensers
ASME Paper No. 77 - WA / HT - 24, 1977

48. V.E. Denny and A.F. Mills
Laminar film condensation of a flowing vapour on a horizontal cylinder at normal gravity
Trans. ASME, 91, 495 - 501, 1969

49. T. Fujii, H. Uehara and C. Kurata
Laminar filmwise condensation of flowing vapour on a horizontal cylinder
Int. J. Heat Mass Transfer, 15, 235 - 246, 1972

50. T. Fujii, H. Honda and K. Oda
Condensation of steam on a horizontal tube - the influence of oncoming velocity and thermal condition at the tube wall
Condensation Heat Transfer, The 18th Nat. Heat Transfer Conf., San Diego, California, 35 - 43, 1979

51. T. Fujii and H. Honda
Forced condensation on a horizontal tube (1st Report) - Theoretical treatment (In Japanese)
Trans. Japan Soc. Mech. Engrs., 46, 401B, 95 - 102, 1980

52. T. Fujii
Vapour shear and condensate inundation
Power condenser heat transfer technology, ed. P.J. Marto and R.H. nunn, 193 - 223, Hemisphere, 1981

53. E. Truckenbrodt
Ein einfaches Näherungs versfahren zerm Beredinen der laminaren Reibung sschicht mit Absaugung
Forschung Ing. - Wes., 22, 147 - 157, 1956

54. R.M. Terril
Laminar boundary-layer flow near separation with and without suction
Phil. Trans. Roy. Soc. London, Series A, 253, 55 - 100, 1960

55. T. Fujii
Private communications, 1980

56. D.G. Hurley and B. Thwaites
An experimental investigation of the boundary-layer on a porous circular cylinder
ARC R & M No. 2829, 1951

57. A. Roshko
A new hodograph for free-streamline theory
NACA TN 3168, 1954

58. M. Hiwada, M. Niwa, I. Mabuchi and M. Kumada
Effects of a tunnel blockage on local mass transfer from a column cylinder in cross flow (In Japanese)
Trans. Japan Soc. Mech. Engrs., 42, 2481 - 2491, 1976

59. I.I. Gogonin and A.R. Dorokhov
Heat transfer from condensing Freon - 21 vapor moving over a horizontal tube
Heat Transfer - Soviet Research, 3, 6, 157 - 161, 1971

60. T. Fujii, H. Honda and K. Oda
Forced convection condensation on a horizontal tube (2nd Report) - Experiments for horizontal flow of low pressure steam (In Japanese)
Trans. Japan Soc. Mech. Engrs., 46, 401B, 103 - 110, 1980

61. T. Fujii, H. Uehara, K. Hirata and K. Oda
Heat transfer and flow resistance in condensation of low pressure steam flowing through tube banks
Int. J. Heat Mass Transfer, 15, 249 - 260, 1972

62. L.D. Berman
Heat transfer with condensation of moving vapour on a horizontal tube
Thermal Engg., 20, 8, 103 - 105, 1973

63. L.D. Berman
Influence of vapour velocity on heat transfer with filmwise condensation on a horizontal tube
Thermal Engineering, 26, 5, 274 - 278, 1979

64. E.M. Sparrow and E.R.G. Eckert
Effects of superheated vapour and noncondensable gases on laminar film condensation
AIChE Journal, 7, 3, 473 - 477, 1961

65. E.M. Sparrow and S.H. Lin
Condensation heat transfer in the presence of a noncondensable gas
Trans. ASME, 86, 430 - 436, 1964

66. W.J. Minkowycz and E.M. Sparrow
Condensation heat transfer in the presence of noncondensables, interfacial resistance, superheating, variable properties and diffusion
Int. J. Heat Mass Transfer, 9, 1125 - 1144, 1966

67. J.W. Rose
Condensation of a vapour in the presence of a non-condensing gas
Int. J. Heat Mass Transfer, 12, 233 - 237, 1969

68. E.M. Sparrow, W.J. Minkowycz and M. Saddy
Forced convection condensation in the presence of noncondensables and interfacial resistance
Int. J. Heat Mass Transfer, 10, 1829 - 1845, 1967

69. W.J. Minkowycz and E.M. Sparrow
The effect of superheating on condensation heat transfer in a forced convection boundary layer flow
Int. J. Heat Mass Transfer, 12, 147 - 154, 1969

70. J.C.Y. Koh
Laminar film condensation of condensible gases and gaseous mixtures on a flat plate
Proc. 4th U.S.A. Nat. Cong. Appl. Mech., 2, 1327 - 1336, 1962

71. T. Fujii, H. Uehara, K. Mihara and Y. Kato
Forced convection condensation in the presence of non-condensables - a theoretical treatment for two-phase laminar boundary layer (In Japanese)
University of Kyushu Research Institute of Industrial Science, Report No. 66, 53 - 80, 1977

72. J.W. Rose
Approximate equations for forced - convection condensation in the presence of a non - condensing gas on a flat plate and horizontal tube
Int. J. Heat Mass Transfer, 23, 539 - 546, 1980

73. J.W. Rose
Boundary-layer flow with transpiration on an isothermal flat plate
Int. J. Heat Mass Transfer, 22, 1243 - 1244, 1979

74. T. Fujii
Private communications, 1978

74a. J.W. Rose
Boundary - layer theory results for condensation from vapour - gas mixtures
HTFS Research Symp., Paper RS 338, Oxford, 1980

75. V.E. Denny and V.J. Jusionis
Effects of non-condensable gas and forced flow on laminar film condensation
Int. J. Heat Mass Transfer, 15, 315 - 326, 1972

76. A.F. Mills, C. Tan and D.K. Chung
Experimental study of condensation from steam - air mixtures flowing over a horizontal tube : overall condensation rates
Proc. 5th Int. Heat Transfer Conf., Tokyo , Vol. 5, Paper CT1.5, 20 - 23, 1974

77. T. Fujii, H. Honda, K. Oda and S. Kawano
Forced convection condensation from steam - air mixture on a horizontal tube, (In Japanese)
Proc. 16th Japanese Heat Transfer Symposium, Paper C103, 331 - 333, 1979

78. D.J. Othmer
The condensation of steam
Ind. Eng. Chem., 21, 6, 576 - 583, 1929

79. H. Hampson
The condensation of steam on a metal surface
Proc. General Discussion on Heat Transfer, Instn. Mech. Engrs., 58 - 61, 1951

80. W.W. Akers, S.H. Davies and J.E. Crawford
Condensation of a vapour in the presence of a non-condensing gas
Chem. Eng. Prog. Symp. Series, 56, 30, 139 - 144, 1960

81. L. Slegers and R.A. Seban
Laminar film condensation of steam containing small concentrations of air
Int. J. Heat Mass Transfer, 13, 1941 - 1947, 1970

82. H.K. Al-Diwany and J.W. Rose
Free convection film condensation of steam in the presence of non-condensing gases
Int. J. Heat Mass Transfer, 16, 1359 - 1369, 1973

83. H. Hampson
The condensation of steam on a tube with filmwise or dropwise condensation in the presence of a non-condensing gas
Int. Dev. Heat Transfer, 2, 310 - 318, 1961

84. T.F. Provan
Effect of vapour superheat and non-condensable gas on the performance of a horizontal single-tube condenser
NEL Report No. 219, 1966

85. C.L. Henderson and J.M. Marchello
Film condensation in the presence of a non-condensable gas
Trans. ASME, 91, 447-450, 1969

86. C.G. Kirkbride
Heat transmission by condensing pure and mixed substances on horizontal tubes
Ind. Eng. Chem., 25, 1324 - 1331, 1933

87. L.D. Berman and S.N. Fuks
Mass exchange in horizontal tube condenser with steam containing air
Teploenergetika, 5, 8, 66 - 74, 1958
(C.E. Translation No. 1423)

88. A. Acrivos
Mass transfer in laminar boundary layer flows with interfacial velocities
AIChE Journal, 6, 3, 410 - 414, 1960

89. J.W. Rauscher, A.F. Mills and V.E. Denny
Experimental study of film condensation from steam-air mixtures flowing downward over a horizontal tube
Trans. ASME, 96, 83 - 88, 1974

90. L.D. Berman
Determining the mass transfer coefficient in calculations on condensation of steam containing air
Thermal Engg., 16, 10, 95 - 99, 1969

91. C.P. Frydas
PhD Thesis (in preparation), Queen Mary College, London University, 1981

92. W.C. Lee and J.W. Rose
Film condensation on a horizontal tube - effect of vapour velocity
submitted to the 7th Int. Heat Transfer Conf., Munich, 1982

92a. C.R. Wilke
A viscosity equation for gas mixtures
J. Chem. Phys., 18, 4, 517 - 519, 1950

93. J.R. Cooper
Private communications, 1978

94. International Skeleton Tables of the Thermodynamic Properties of Water Substance, October 1963
(Supplementary Release on Transport Properties), November 1964
The 6th Int. Conf. on Properties of Steam

95. J.R. Cooper and E.J. Le Fevre
Thermophysical Properties of Water Substance
Edward Arnold (Pub.) Ltd., 1969

96. E.J. Le Fevre, M.R. Nightingale and J.W. Rose
The second virial coefficient of ordinary water substance : a new correlation
J. Mech. Sci., 17, 5, 243 - 251, 1975

97. E.N. Fuller, P.D. Schettler and J.C. Giddings
A new method for prediction of binary gas-phase diffusion coefficients
Ind. Eng. Chem., 58, 5, 18 - 27, 1966

98. T. Fujii, S. Nozu and H. Honda
Expressions of thermodynamic and transport properties of Refrigerants R-11, R-12, R-22 and R-113 (In Japanese)
University of Kyushu, Res. Inst. Ind. Sci., Report 67, 43 - 59, 1978

99. "Freon Fluorocarbons" Technical Bulletin B-2
E.I. du Pont de Nemours and Co.

100. R.C. Reid and T.K. Sherwood
The Properties of Gases and Liquids, 2nd. ed.,
McGraw Hill Book Co., New York, 1966

101. Y.R. Mayhew and G.F.C. Rogers
Thermodynamic and Transport Properties of Fluids, 2nd. ed.,
Blackwell, Oxford, 1974

102. G.V. Sansonov, ed.
Handbook of the Physiochemical Properties of the Elements, English edition
Oldbourne, London, 1968

103. R.C. Weast, ed.
CRC Handbook of Chemistry and Physics
CRC Press, Inc., Cleveland, Ohio, 1977

104. H.W. Wooley, R.B. Scott and F.G Brickwedde
Compilation of thermal properties of hydrogen in its various
isotopic and ortho-para modifications
J. of Research, Nat. Bureau of Standards, 41, 379 - 475, 1948

105. T. Fujii, Y. Kato and K. Mihara
Expression of transport and thermodynamic properties of air,
steam and water (In Japanese)
University of Kyushu, Res. Inst. Ind. Sci., Report 66,
81 - 95, 1977

106 J. Topping
Errors of observation and their treatment, 4th ed.,
Chapman and Hall, London, 1972